Delft University of Technology Ingenieursbureau Amsterdam

Application of Ultra High Performance Concrete in the new Leiden Bridge

Graduation committee:

- Prof.dr.ir. D.A Hordijk, Delft University of Technology
- Dr.ir. C. van der Veen, Delft University of Technology
- Ir. A.D. Reitsema, Delft University of Technology
- Dr.ir. M.A.N. Hendriks, Delft University of Technology
- Ir. A. Quansah, Ingenieursbureau Amsterdam

Antonio Paškvalin

Preface

This report presents the final result of the master thesis that is performed to obtain the diploma of the Master Structural Engineering at the faculty of Civil Engineering and Geosciences at the Delft University of Technology. This thesis has been done in collaboration with Ingenieursbureau Amsterdam. During the past months a study has been performed on the application of Ultra High Performance Concrete in the new Leiden Bridge.

I would like to express my gratitude to all the members of my committee. First of all I like to thank Professor Dick Hordijk for helping me establish a contact with Ingenieursbureau Amsterdam. I would like to thank Ingenieursbureau Amsterdam for giving me the opportunity to perform my thesis at their firm and for the excitement of us working together during my master thesis.

I would also like to thank Cor van der Veen and Max Hendriks for their support during the thesis.

Special gratitude goes to Andrew Quansah and Albert Reistema for their enthusiastic daily support during my thesis. They were truly helpful during the make of this thesis and bringing me on new ideas that could make this thesis even better.

Antonio Paskvalin

Delft, 17 February 2015

Reading guide

Chapter 1 gives an introduction and problem description of the thesis. The method of approach of the thesis is also discussed. Chapter 2 deals with the current Leiden Bridge. It gives a general overview of the bridge and also discussed are some technical aspects of the bridge. Besides this the demands and constraints for the new bridge are dealt with as well. Chapter 3 deals with the first design for the new Leiden Bridge and that is the design in normal strength concrete. Chapter 4 gives a short introduction to Ultra High Performance concrete and gives the learning points from the literature study. Also an elaboration of the transition from normal strength to Ultra High Performance concrete is given. Chapter 5 deals with the design in Ultra-High performance concrete. Chapter 6 discusses the design in High performance concrete. This design fills the 'grey area' between normal and Ultra-high performance concrete. Chapter 7 contains the optimization process for the design in UHPC. In this chapter an attempt is made to reduce the amount of material used in the UHPC design and to make the UHPC design as slender as possible. Then chapter 8 brings all the designs together, and comparisons are made between each other concerning multiple aspects, such as structural performance and material use. Chapter 9 discusses the construction of the new bridge. In the final chapters a conclusion is made based on the findings during the study and further recommendations are given as well.

Summary

In the Netherlands there are a number of bridges across the country that are at the end of their life span. These bridges cannot keep up with the ever increasing traffic intensity and therefore they do not suffice anymore structurally wise.

The same applies for the Leiden Bridge, which is located in the crowded centre of Amsterdam, the capital of the Netherlands. This old traffic bridge, which was built in the early 20th century, has deteriorated quite a lot in the past years. The municipality of Amsterdam has decided to replace the bridge with a new one. This will bring a lot of challenges with it as there are some strict demands for the new bridge. First of all it is required that the architectural view of the bridge remains the same. For the structure specifically this means that the construction height needs to remain the same as the current height. Another important requirement is that the construction of the bridge causes as less hindrance as possible. This mostly holds true for the trams crossing the bridge. It is preferred that the tram service is halted as short as possible during construction.

With these requirements as the basis for the new bridge, three designs are developed. The main dimensions for the bridge are a box girder with a construction height of 600mm (maximum allowed height is 650mm) and a single span of 24m. The designs should be structurally safe while having these dimensions. Next to structural safety it is desired to develop a bridge that is as slender as possible. A single span is chosen instead of two spans (which the current bridge has), because it is preferred that the intermediate pier of the current bridge remains unused and a single span would prove a bigger challenge and also a more slender bridge. The three designs are: a Normal Strength Concrete C50/60 design (NSC), an Ultra High performance Concrete C170/200 design (UHPC) and a High Performance Concrete C90/105 design (HPC) in that order.

The NSC does not meet the requirements regarding safety and is uneconomical. It is found that there is not enough fatigue resistance and the high needed amount of prestressing steel and reinforcement will result in fitting issues of it all in the girder. Required is a much thicker structure of 800mm, which in the case of the Leiden Bridge is not allowed.

It was expected that a design in normal strength concrete would most likely not be achievable, therefore a design is made in Ultra High Performance Concrete. UHPC is a fairly new type of concrete, which is much stronger, more ductile and has a better durability than normal and high strength concrete. The better properties are mostly due to the very dense matrix and inclusion of steel fibres. Using UHPC could very well lead to a structural safe and achievable design.

The UHPC design proves that indeed this is the case. The design has more than enough resistance in both the ULS and SLS. The same also holds true for the fatigue resistance, in spite of the very slender design, which gave a higher probability of fatigue resistance issues. The design has a lot of additional capacity so there is room for optimization. Sizing optimization has been performed, where the goal was to achieve a thinner and more slender beam. This was achieved by being able to reduce the construction height down to 550 mm and also to make a beam that varies in height over the length of the beam. It is unfortunately a known fact that producing UHPC is very expensive. Therefore another design is made in High Performance concrete.

The HPC design uses high strength concrete, but steel fibres are included as well, hence the name High Performance concrete. This will result in a similar behaviour to that of UHPC, only HPC is cheaper to produce, but the strength is lower. The HPC design fulfils the safety requirements and is achievable.

Comparison of all the mentioned designs shows that the designs that can be made are the HPC and UHPC design. The UHPC design results in the lightest and most slender structure, but also the one that is the most expensive, even after optimization. The HPC design would be most realistic choice for the Leiden Bridge. It is achievable and cheaper than UHPC. Furthermore it has enough durability to result in a maintenance free life span of 100 years. There are a lot of old bridges just like the Leiden bridge in Amsterdam and other cities as well and the HPC design (and the UHPC design for that matter) will bring great structural and economic benefits, since a lot of money will be saved in the future on maintenance and on replacing the substructure as well.

Furthermore it is recommended to not ignore the benefits UHPC brings, even though it is not the best choice for the Leiden Bridge. UHPC has the best mechanical and durability properties and for other applications, especially bridges with long spans, UHPC will most likely be the most economical choice. If a chance is given to UHPC and if it is considered as a realistic design alternative, it could be applied more often in the future, which would result in strong, durable and maintenance free bridges that could last for years to come.

Table of contents

Chapter 1 Introduction

In the Netherlands a time period has commenced, where a lot of old bridges across the country do not suffice anymore structurally wise. This is also the case in Amsterdam. Amsterdam is known for its old historical central district. In the central district are a lot of bridges to be found, which date back from the beginning of the 20th century.

This is also the case for the bridge that is going to be dealt with in this master thesis, namely the Leiden Bridge. The Leiden Bridge is a traffic bridge, which serves as an important crossing for vehicles, public transportation (including trams and buses), cyclists and pedestrians. The bridge, which can be found right next to the famous Leiden square, was originally an old wooden bridge, which was then replaced by a stone arch bridge. And this stone bridge has been replaced by the current bridge back in 1925. Nowadays the bridge has deteriorated quite a lot, so the municipality of Amsterdam has decided to replace the bridge by a new one.

1.1 Problem description

As said the Leiden Bridge is going to have to be replaced with a new bridge. When making a new design for the bridge there are a couple of requirements that need to be taken into account. First of all it is demanded that the appearance of the bridge remains exactly the same as the current one. So the construction height of the bridge has to stay the same. One of the reasons is because trams pass the bridge and it is important that the rail alignment stays unaltered. Not only the construction height has to stay the same, the architecture needs to remain intact as well, especially since the bridge is a listed national monument.

Second, the Leiden Bridge is located in an area of the city which is very dense and crowded most of the time. This means a lot of traffic, pedestrians, etc. cross the bridge. So it is a very important connection point in that area. This means that during construction of the new bridge the hindrance has to stay a short as possible, so the construction time needs to be very short, as closing the bridge costs a lot of money and is a large nuisance for the bridge users.

In short when making a new bridge design it is important to keep the construction height the same as the current height and it is important that the design causes as less traffic hindrance as possible. But besides this, it is also important that the bridge has a high durability and a long life span.

The current bridge's superstructure consists of steel girders and a concrete deck. A new design could be a composite structure like the current one or maybe a bridge made only out of concrete. These materials however don't have a very long life span and one has to think that there are a lot of bridges that need replacement and in the long term it is very important that all these bridges need as less maintenance as possible. So a solution would be, instead of using steel or ordinary concrete, to use Ultra high performance concrete (UHPC).

1.2 Research Objective

The main objective of this thesis is to research if UHPC can be a realistic solution for the Leiden Bridge. More specifically the objective is to find out if using UHPC as a design solution, while taking the strict demands given by the municipality of Amsterdam into account, will lead to a structure that is economically, structurally and execution wise more feasible than using other materials. The result of this research should show that UHPC is indeed a feasible solution for a bridge design and it should encourage a broader use of UHPC in the Netherlands. Especially since there is a high need for new and durable materials to use in old and soon to be replaced bridges.

The research objective can be formulated in a main research question which is:
"Is it possible to make a bridge design in UHPC for the Leiden Bridge, while meeting the strict demands given by the city's municipality, which can act, not only for the Leiden Bridge but also eventually in general cases, as a serious alternative next to other types of concrete?"

1.3 Research scope

This research's main focus will lie on the constructive design of the superstructure of the Leiden Bridge. A design is going to be made based on the criterion that the construction height must stay the same as the current height. Here the focus will be to make the bridge's superstructure as slender as possible, while being able to suffice to all structural requirements. While making decisions on the bridge design the criterion of as less hindrance as possible is also going to be taken account. So a bridge design that has the fastest and easiest method of construction will be chosen.

1.4 Method of approach

In Figure 1-1 the method of approach of the master thesis is shown in a flowchart. The steps will be discussed more in detail in the following.

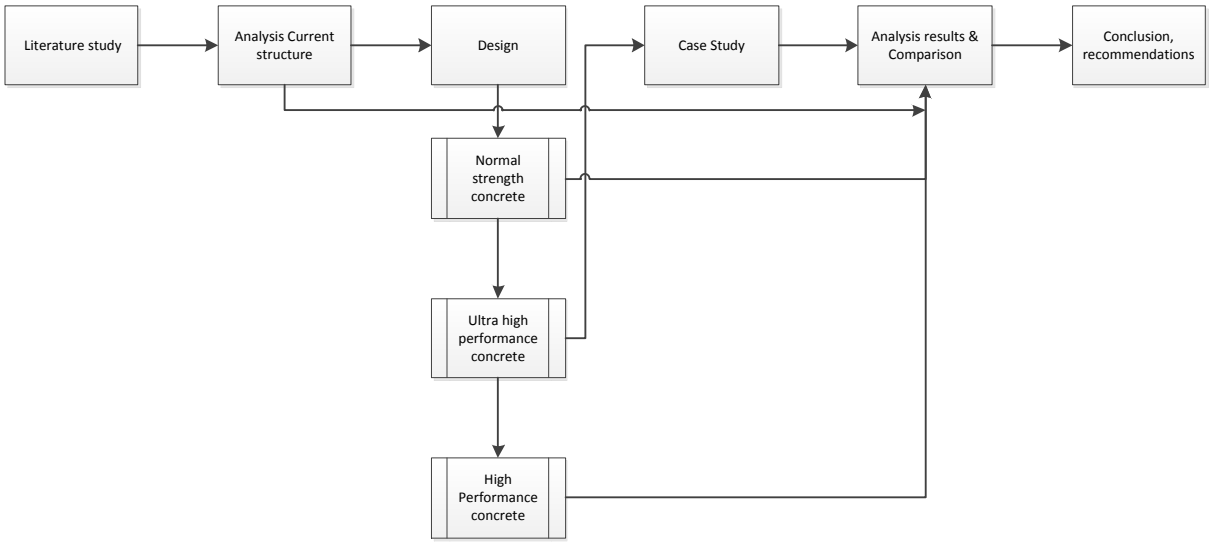

Figure 1-1: Flowchart method of approach

Before the main design study a literature study has to be made in order to gain more knowledge about the unknown subject that is UHPC. The emphasis of the literature study lies on:

- The characteristics of UHPC (mixture, mechanical properties, durability, costs)
- Performed researches with focus on application on bridges
- Reference projects
- Calculation methods for UHPC.
- Structural optimization methods

When the literature study is completed, an analysis is going to be made of the current structure. Here the focus will lie on the structure itself (geometry, material use, etc.). The demands and constraints will be looked at further and with these appropriate choices will be made for the type of bridge and the construction method that will be used for the new design.
After the analysis of the current structure a new design will be made for the Leiden Bridge.

Before making a design in UHPC a design in normal strength concrete (C50/60) will be made first. This will be done to find out if it is perhaps possible to make the new bridge with a more often used material. After the design in normal strength concrete a design will be made in UHPC. In a later stage the UHPC design will be optimized further to try to make better use of the material.
Lastly a design in high performance concrete will be made as well. High performance concrete here is defined as high strength concrete (C90/105) with the inclusion of steel fibres. After each design is finished and checked on structural performance, a short conclusion will be made for each design to see if the design is suitable for the Leiden Bridge, based on its safety. Afterwards the designs are going to be compared to each other. The main comparisons will be the structural performance, material use, environmental impact and costs. And lastly the construction of the new bridge is also looked at.

Based on the work done and the findings in the thesis, conclusions will be made and further recommendations will be given for future purposes.

Chapter 2 Leiden Bridge

2.1 General

The Leiden Bridge is a traffic bridge located in the centre of Amsterdam. The bridge crosses the Singelcanal and it connects Leiden Square with Stadhouderskade. The bridge serves as an important connection between the old city centre and the 19th century part of the city. In Figure 2-1 a map is shown, which indicates where the bridge is located. The bridge is located in a popular and crowded area, where the traffic flow is very intense. Leiden Bridge serves as a main route and connection for traffic, especially for pedestrians, cyclists and trams in that area. Moreover a tram and bus station is located on the bridge, which serves as a stopping point for multiple different lines, so public transportation frequently stops on and passes over the bridge.

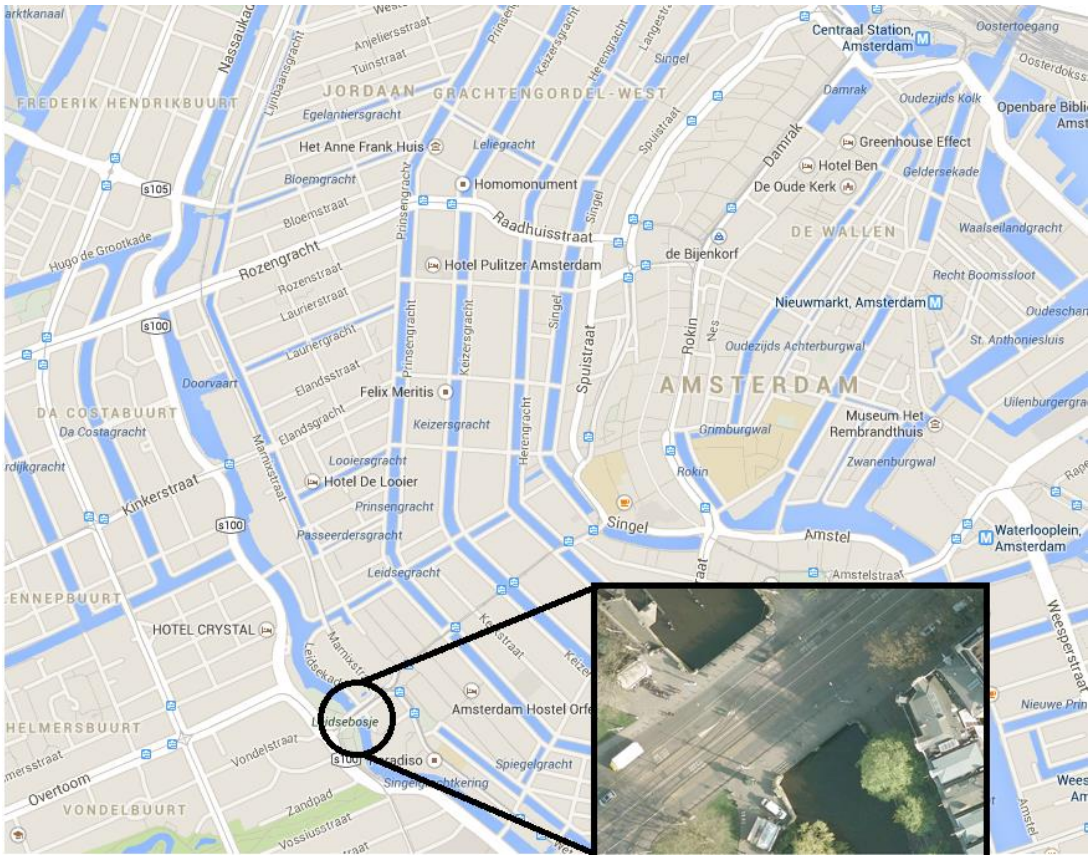

Figure 2-1: Location of Leiden Bridge in Amsterdam

2.2 History

Until 1830 the Leiden Bridge was actually an old wooden draw bridge. Due to deterioration the wooden bridge was replaced by a fixed bridge. In 1860 after the demolition of the Leiden Gate, the Leiden barrier was built, in which the fixed bridge was incorporated. This barrier was mostly made out of stone. Then in 1874 it was decided by the municipality to demolish the barrier and build a new bridge together with a sluice. This bridge was completed in 1877. Because of the coming of the electric trams it was necessary to strengthen the bridge, which happened in 1903. In 1925 it became necessary again to strengthen and widen the bridge due to increased traffic flow. The bridge was partially demolished and rebuild again in its current state. The new bridge was designed by Architect P.L. Kramer. Eventually the bridge was widened from 20 to 30 meters, which is now the current width of the bridge. The natural stone ornaments (such as the lion heads) on the side of the bridges were also designed in 1925. Same goes for the steel railings. So most parts on the existing bridge come from the renovation in 1925.

The sluice was initially right under the bridge, but the sluice had to be relocated to the north side of the bridge in 1987, because maintenance of the sluice became too complicated. For reference the old situation back in the 19th century is seen in Figure 2-2.

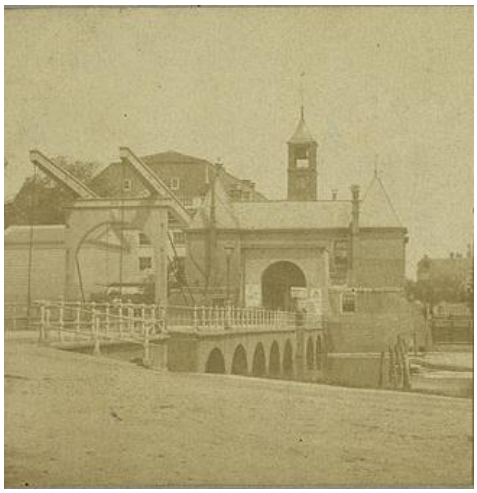

Figure 2-2: Old Leiden bridge, with in background the Leiden Gate

2.3 Specification bridge structure

2.3.1 General dimensions and bridge function

The total length of the bridge is 21m and the bridge has one intermediate support so the bridge consists of two spans. Under the bridge are two passageways with a width of 9m each. The total width of the bridge is 29.5m.

As already mentioned earlier the bridge serves as a traffic bridge that is used by cars, public transportation, pedestrians and cyclists. The bridge is arranged in such a way, that each mode of transportation has its own lane. The current road layout of the bridge is seen in Figure 2-3. The layout is such that the heaviest loads are on the inside (tram, bus) and the lightest loads on the outside (pedestrians, cyclists). This layout will initially also be used for the new design. But the client possesses the option to change the road layout according to his needs. This means that during design of the new bridge it is necessary that the road layout with the most negative impact on the structure (most likely were traffic lanes are the closest to the edges) is taken into account.

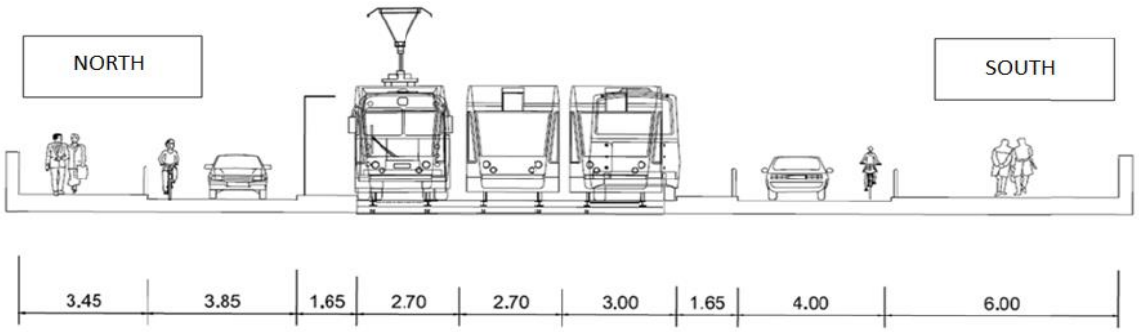

Figure 2-3: Road layout Leiden Bridge

2.3.2 Superstructure

The superstructure of the Leiden Bridge is a composite structure that consists of steel girders with a concrete cast in situ deck. However the concrete and steel are not connected with dowels, so it's technically not a true composite bridge. The structure, because it was widened in the past, consists of an old midsection part and the widened parts. The steel girders are stiffened with steel diagonals in the mid-section, which serve as diaphragms.

The steel profiles for the girders are INP 425 in the mid-section and INP360 and HEB300 in the widened parts. All steel profiles have a steel quality of S235. There are two spans over the whole bridge length and the girders are simply supported. The steel girders are 10m long each.

The concrete deck consists of concrete with strength class C30/37 and thickness of 140mm. The concrete is reinforced with steel bars with quality FeB220. The reinforcement net consists of ϕ8-110 mm in both longitudinal (x) and transversal (y) direction in the concrete deck. The concrete cover is 30mm. The reinforcement scheme is seen in Figure 2-4. The area of the reinforcement is 456mm^2/m. Assumed is that the bars have a length equal to the length of the direction in which they are placed.

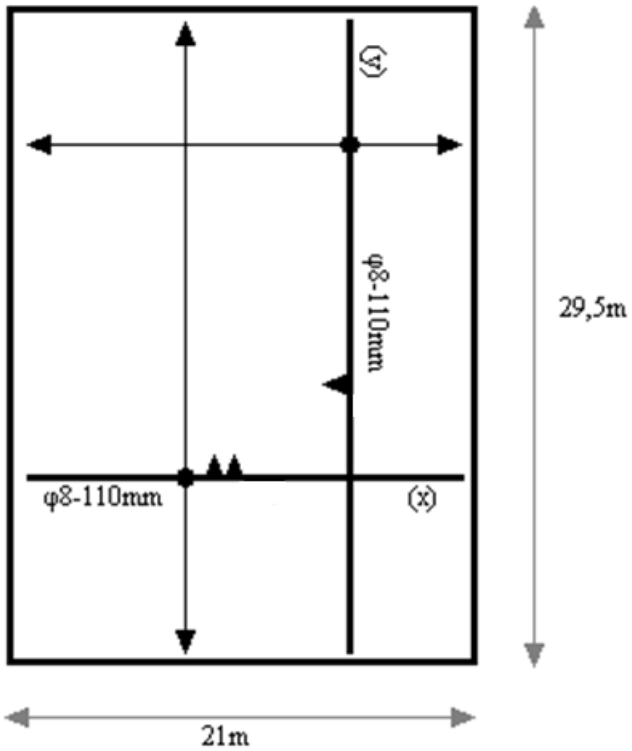

Figure 2-4: Reinforcement scheme

In Figure 2-5 the cross section of the bridge in transverse direction is seen. One can see that the section of the wider parts differs from the midsection, as described. Furthermore, on the sides of the superstructure, natural stone elements and steel railings are located. These only serve for aesthetical purposes. When the demands and constraints of the new design are discussed, it will become clear that this architecture may not be replaced.

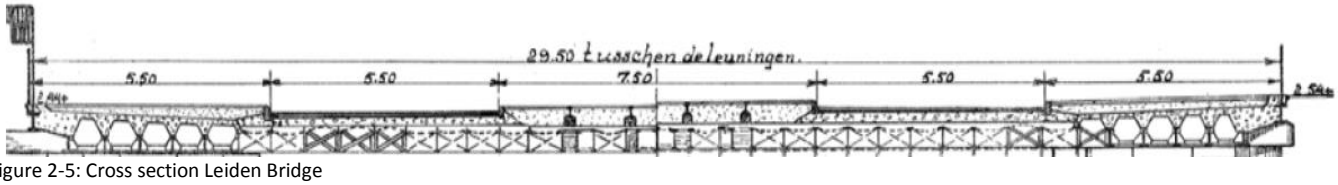

Figure 2-5: Cross section Leiden Bridge

With the discussed material an estimation of total amount of each material can be determined. Besides steel and concrete, pavement and asphalt is also found on the bridge on top of an extra thickening layer. These will not be taken into consideration as they will also be placed on the new bridge and they do not have a structural purpose per se. The same holds true for the stone ornaments and steel railings. So only the amount of steel and reinforced concrete will be determined.

In Table 2-1 the amount of material used in the current bridge is shown. These estimated amounts of the material used can later be compared with the material use in the new design. The amount of material here is based on the quantification made in [6].

Table 2-1: List of the amount of materials used

Concrete	*height [m]*	*width [m]*	*length [m]*	*volume [m^3]*	*density [kg/m^3]*	*mass [kg]*
C30/37	0,14	29,5	21	86,73	2400	2,1E+05
Steel (S235)	*Amount girders [-]*	*Area section [m^2]*	*length [m]*	*volume [m^3]*	*density [kg/m^3]*	*mass [kg]*
HEB 300	4	0,01491	10	0,5964	7850	4,7E+03
INP 360	20	0,0097	10	1,94	7850	1,5E+04
INP 425	62	0,0132	10	8,184	7850	6,4E+04
Reinforcement steel	*Area section [m^2/m]*	*length in direction [m]*	*length bar [m]*	*volume [m^3]*	*density [kg/m^3]*	*mass [kg]*
Feb220 ϕ8-110mm (x)	0,000456	29,5	21	0,282492	7850	2,2E+03
Feb220 ϕ8-110mm (y)	0,000456	21	29,5	0,282492	7850	2,2E+03

Total amount of:	*[tons]*
Concrete	208,2
Steel	84,2
Reinforcement	4,4

2.3.3 Substructure

The substructure consists of two abutments and one intermediate pier. The substructure at the old midsection differs from the substructure at the widened section.

Midsection

At the abutments and the pier of the mid-section the steel girders are supported by natural stone elements. The abutments and pier are made out of masonry bricks. The abutments have a thickness of 1.75m and the pier a thickness of 1.5m. The substructure lies on an 80mm thick wooden floor, which is supported by wooden piles.

Widened section

The substructure is almost the same as in the midsection. At the abutments and the pier of the mid-section the steel girders are supported by natural stone elements. The abutments and pier are made out of masonry bricks. At the widened section however the abutments have a thickness of 1.21m instead of 1.75m. The pier thickness stayed the same with 1.5m. The substructure lies on a 300 mm thick unreinforced concrete floor, which is supported by wooden piles.

2.4 Recent inspection and recalculation results

Leiden Bridge is a very old bridge so it was important to perform inspections on the bridge to see if the bridge could still function properly. The most recent inspection showed that there are some issues with the bridge. It was clear that the bridge was too heavy loaded; a lot of cracks were found in the walls. The steel girders were in good state generally speaking, but at the supports the steel thickness has been halved due to severe corrosion. Also the masonry works on the abutments and on the pier were in bad condition. Furthermore, leakages were also discovered in the structure.

The bridge has been recalculated as well [6]. The recalculation was based on NEN 8700 and the Eurocode. The structure had to be reviewed to see if the rejection level given in NEN 8700 is satisfied. In the recalculation assumed was consequence class 2 (CC2), where the minimum requirement is a rest life span of one year and a reference period of 15 years.

The results of the recalculation showed that the steel girders in the midsection do not suffice on moment capacity. The same holds true for the concrete deck for the moment capacity in transverse direction. Also the abutments and the pier do not suffice structurally. In a lot of the piles the capacity has been exceeded. With these findings it was concluded that the current structure of the Leiden Bridge did not fulfil the requirements according to the rejection level stated in NEN 8700.
Based on the inspection and recalculation results it is advised to strengthen or replace the Leiden Bridge. The latter case will be studied further in this research.

2.5 Product design specification

For the renovation of the Leiden Bridge there are a lot of factors that need to be taken into account when designing the new bridge.
A product design specification specifically for the bridge has been formulated by the municipality of Amsterdam [2]. Here all the demands and constraints by different stakeholders are described. The relevant demands and constraints are going to be summed up in the following.

Functional demands:

- The bridge must keep the status of National monument after renovation.
- Preservation of monumental parts goes before repair and repair goes before replacement of monumental parts.
- The intermediate pier may not be removed, as it is a monumental part.
- As result of maintenance the unavailability of the bridge is allowed to be 4 hours/year at maximum.
- The boat passage width of the bridge is 2x9.0m of which 2x4.5 navigable.
- The minimal life span for new constructions per part are:
    - Concrete structures: 100 years
    - Foundation structures: 100 years
    - Steel work: 100 years
    - Preservation: 10 years
    - Natural stone: 100 years
    - Bearings: 25 years
    - Joints: 25 years
    - Asphalt: 10 years
- Sections of the bridge which are kept after the renovation need to have the following rest life span:
    - Existing structures with function:
        - Intermediate pier: 25 years
        - Fly walls: 25 years
    - Existing structures without function:
        - Intermediate pier: 50 years
        - Abutments: 50 years
        - Fly walls: 25 years

Design demands:

- The full bridge deck width, including the cycle and pedestrian lanes, must be dimensioned on traffic loads according to the Eurocode.
- The architectural view of the bridge (side view, railing and vertical alignment of the edge of the bridge may not be altered.
- The reference period of the structure is 100 years.
- The traffic intensity over the structure is 7000 trucks per direction per year.
- The traffic intensity over the structure is 30 tram movements per hour per direction.
- The railings must be earthed in the bridge.

Demands for execution:

- During construction the bridge may not be fully closed for waterway traffic
- Slow traffic will be transferred to a temporary bridge.
- The bridge will be closed for vehicular traffic during construction.
- The tram exploitation can be closed for a maximum of 4 weeks straight in order to replace the bridge deck under the tram rails.

These were the relevant demands concerning the bridge design. To summarize these demands, the most important demands that absolutely need to be taken into account are:

- The architectural view needs to remain unaltered. For the bridge design this will mean that the construction height will stay the same as the current height. And it will mean that the intermediate pier must remain in its place. (However it does not have to be used structurally wise).
- There has to be as less traffic disruption as possible. Especially for the public transport, because restricting its access for a long time can bring high costs.

2.6 Preliminary design new Leiden Bridge

For the new design in UHPC, suitable choices have to be made, namely the type of bridge and the construction method. During the literature study (Appendix A) the types of bridges, the construction methods and such were documented. With the gathered information and the given demands and constraints the appropriate choices for the new design can be made.
In Table 2-2 a list is given with the choices for each subject concerning bridges in general, which were intensively discussed in the literature study. From these available choices the ones most suitable for the Leiden Bridge should be picked. Not all bridge types are mentioned, because it is obvious that a couple of bridge types (such as an arch or cable stayed bridge) are definitely out of the question.

Table 2-2: List of available choices

Bridge types	**Construction methods**	**Structural systems**	**Bearing types**
Solid deck bridge	*Prefab or in situ in combination with:*	Simply supported	Elastomeric
Girder bridge	Lifting, hoisting	Simply supported with continuous slab	Pot
Box beam bridge	Stationary falsework	Full continuity	Sliding
Mono box bridge	Travelling falsework	Integral bridge	
	Span-by-span method		
	Cantilever method		
	Incremental launching method		

Because there are a lot of strict demands and boundaries there is not much freedom in choosing a certain design for the new bridge. So it is easy to eliminate certain solutions, which are given in Table 2-2, beforehand without going into detail with the demands of the Leiden Bridge.

Bridge types
First of all, the bridge will only be 24 meters long and because of the relatively high width of the bridge a mono box bridge is not suitable to use for the new design. Concerning the bridge types, realistic solutions are:

- Solid deck bridge (massive plate, or in-filled beams)
- Girder bridge (I or inverted T)
- Box-beam bridge

Construction method

The limiting length of the bridge also eliminates a couple of construction methods. First of all the cantilever method and the incremental launching method are not suitable for the execution.
Not only because it is expensive and not profitable to use these methods for such short lengths, but also because there is limiting space to build up the construction sites required for these methods.
The span-by-span method is not very suitable for the Leiden Bridge, because there are two spans at max (for the UHPC design only one span is allowed). So using this method here is highly unprofitable. Same goes for travelling falsework.
Realistic construction methods for the Leiden Bridge are:

- Lifting or hoisting
- Stationary falsework

Lifting and hoisting usually happens with prefab elements and the falsework is used in combination with in situ concrete. Now considering the fact that a fast construction is required and that the bridge cannot be closed for a long time, the fastest construction method would be using prefab girders and then lifting them in place. This will save much more time compared to setting up falsework and then pouring the concrete on site. In the later stages of the design study a deeper look in the actual execution will be made after calculations of the bridge designs have been performed.

Structural system

As for the structural systems depending on the amount of spans, all systems stated in Table 2-2 are realistic solutions. If there is only one span, then only a simply supported or an integral bridge can be used.

Bearings

The type of bearing is influenced by the total amount of forces working on the supports. So a suited bearing is chosen after calculations have been performed. However it can be stated that sliding bearings will not be used. These are only feasible when dealing with large span bridges on which large forces and rotations are exerted and for small bridge like the Leiden Bridge sliding bearings are too expensive.

2.7 Required construction height

Earlier, the demands and constraints were presented. The most important ones were that the architectural view (so basically the construction height) of the new bridge must stay the same as the current one and also that the construction of the bridge should cause as less hindrance as possible. The current construction height varies between 500 and 600 mm. This is purely the structural height without pavement, asphalt and such. Governing for the new bridge will be the side view of the bridge and also the alignment of the tram route. Mentioned already were the materials used in the bridge. In Figure 2-6 the layers of material used on the bridge over the width are shown.

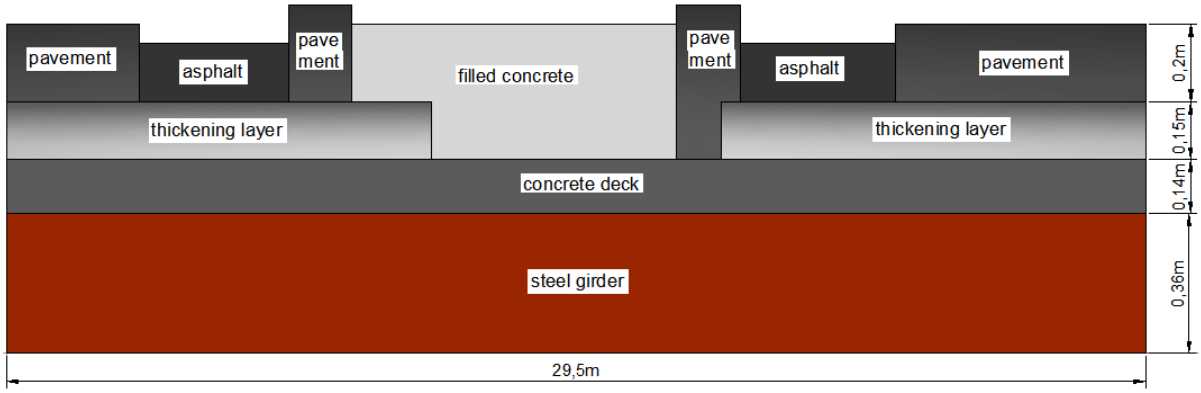

Figure 2-6: Bridge layers across the width

When looking to the side of the current bridge, the bridge height consists of the steel girder, concrete deck, a thickening layer and the pavement. For the new design the thickness of these extra layers also has to be taken into account. So looking more closely at the outskirts of the bridge one finds INP360 steel girders. On top of that there is the concrete deck. Then as extra layers one finds a thickened layer of concrete with a thickness of 150 mm and on top of the thickened layer the pavement of 200 mm thick is located.
So in total this gives a side view height of around 850 mm. In the centre, where the tram tracks are located, the height from the bottom of the steel girder to the top of the rail profile is also 850mm. Here the height of the rail profile (h=180 mm) needs to be taken into account, when choosing an appropriate height for the concrete girder. Considering these restrictions the height of the new bridge girders has to stay in the range of 600-650mm. As initial height 600mm is taken to make the bridge more slender.

2.8 Conclusion

In summary, the Leiden Bridge is an old bridge that has a monumental value to Amsterdam. The bridge consists of steel girders and a concrete deck. The current bridge is due to replacement. The bridge does not suffice according to the norms and the bridge has deteriorated visually as well.

The bridge will be replaced and for the new bridge a lot of strict demands have been given.
The most important demands are:

- The architectural view needs to remain unaltered. For the bridge design this will mean that the construction height will stay the same as the current height. And it will mean that the intermediate pier must remain in its place. (However it does not have to be used structurally wise).
- There has to be as less traffic disruption as possible. Especially for the public transport, because restricting its access for a long time can bring high costs.

The determined allowed construction height for the bridge is 600mm. The realistic bridge types for the new bridge are: Solid deck bridge, Inverted-T bridge or box-beam bridge. The bridge will most likely consist of prefabricated elements, which will be hoisted in position. The new design must have the required construction height and it has to be determined, which bridge type is the most suitable to achieve this goal.

Chapter 3 Bridge design in C50/60

3.1 General

In this chapter the design in normal strength concrete C50/60 will be discussed. The goal of this calculation is to examine if it is possible to design the Leiden Bridge in C50/60. This means that the bridge has to be structurally safe and it also has to meet the requirements given by the municipality of Amsterdam. First the dimensions and properties of the concrete and of the box beam girder will be determined. Then the calculation model of the bridge will be presented. With the loads and the model the internal forces will be determined. This will be done with SCIA Engineer. After the results from SCIA are obtained the structure will be checked in the Ultimate Limit State (ULS) if it can resist the loads working on the bridge. For the calculation in C50/60 the safety check will only be limited to the ULS. More detailed calculations can be found in Appendix D.

3.2 Determining h_{min}

Three possible bridge types were considered the most realistic for the new Leiden Bridge. Since prefab girders will be used, it is helpful to consult various girder producers to obtain the available girder sizes. First the minimum height needed for the span has to be calculated with a rule of thumb. The requirement is to construct a new bridge, which only contains one single span. The reason for this is that it is required that the intermediate pier stays intact. It may not be removed due to its monumental value. But the intermediate pier has deteriorated quite a lot which makes it nearly impossible to include it in the new structure. So for the design in C50/60 (and for all other designs as well) a one span bridge will be designed. So the bridge will be a one span girder bridge of 24 meters. In Table 3-1 the minimum construction height for each type of girder is determined. Also the minimum height for a two span bridge is shown.

Table 3-1: Minimum heights for the new design

	Slenderness ratio (λ)	h_{min} for l=12m [m]	h_{min} for l=24m [m]
Solid deck bridge	20 - 25	480 - 600	960 - 1200
inverted T/I - girder	20 - 28	429 - 600	858 - 1200
Box beam girder	28 - 32	375 - 429	750 - 858

From the results it becomes clear that building the bridge with only one span with C50/60 would not meet the height requirements. When the most slender bridge type is used (box beam) the minimum height will be around 750mm. So actually for a bridge in normal strength concrete C50/60 the best bet would be to build the bridge in two spans, concerning the construction height. However if two spans are considered only a solid deck bridge would be appropriate, since box and inverted T girders are not produced for such short spans. A solid deck bridge could be used, as its minimum height is the maximum required construction height, but as already explained a two span bridge is not an option because of the very weak intermediate pier. Now if one would ignore the limited construction height a box beam bridge would be the best option for a C50/60 one span bridge. Using this girder will give the most slender bridge and an additional deck will not be necessary.

Looking at the determined limits of h_{min} and the available girder heights produced by manufacturers, a box beam girder with h=800mm (λ =30) should be used for the C50/60 design.
It is however much wiser to investigate if the bridge could be made in C50/60 concrete, while also using a girder with a height of 600mm (λ=40). To achieve the goal of the research, this height has to be used for the UHPC design, so it will be much better to also design the bridge in C50/60 with a girder of 600mm thick. This will result in a better comparison later with the UHPC design. So for the design a height of 600 mm will be used and not the recommended height of 800 mm.

3.3 Material Properties

The concrete and steel material properties are based on NEN-EN-1992-1-1. The volumetric weight of the concrete is 25 kN/m^3. In appendix D.3 all the properties are found.

Additional assumptions	
Environmental class	XD1
Concrete cover	45 mm
φ shear reinforcement	12 mm
φ longitudinal reinforcement	10 mm
Maximum aggregate size d_g	32mm

3.4 Bridge dimensions and cross sectional properties

Box beam girders are used for the bridge design. Manufacturers do not produce box girders of 600 mm so a modified box girder of h=600 mm will be used instead, of which the properties will be determined with hand calculations. This basically means that the same dimensions will be used except for the total height of the beam. The cross section of one box beam girder is seen Figure 3-1. The web and flange thicknesses are based on values given by Spanbeton BV. Same goes for the width.

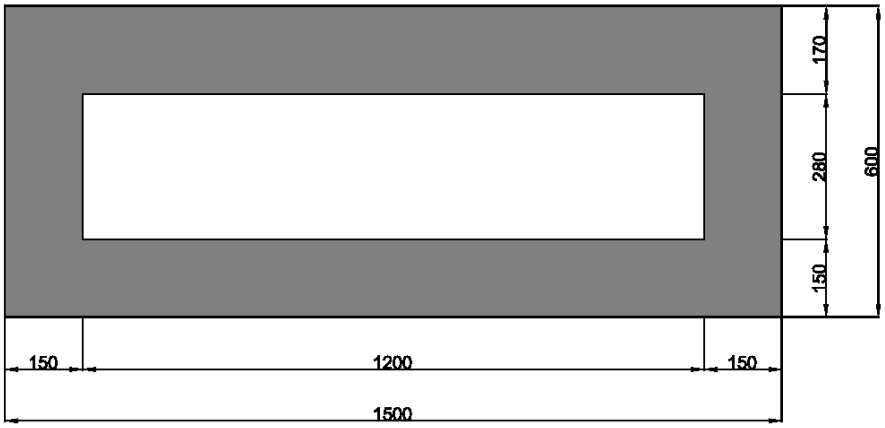

Figure 3-1: Cross section of one box beam girder [m]

In Table 3-2 the dimensions and cross sectional properties of one girder are shown.

Table 3-2: Dimensions and cross sectional properties of box girder

L	*Span*	24 m
H	*Height girder*	0.6 m
B	*Width girder*	1.5 m
b_{web}	*Web thickness*	0.15 m
$h_{top,fl}$	*Top flange thickness*	0.17 m
$h_{bot,fl}$	*Bottom flange thickness*	0.15 m
A_c	*Cross sectional area*	0.564 m^2
z_t	*Distance top fibre to c.a.*	0.294 m
z_b	*Distance bottom fibre to c.a.*	0.306 m
I_c	*Moment of Inertia*	0.025 m^4
$W_{c,t}$	*Section Modulus top fibre*	0.084 m^3
$W_{c,b}$	*Section Modulus bottom fibre*	0.081 m^3

3.5 Load cases and combinations

Before the SCIA Engineer model is presented, the loads have to be determined first. There are a lot of different loads that will work on the bridge. And these loads will not occur exclusively. Therefore it is important to determine all the load cases and load combinations for the bridge. The load cases and combinations are all described extensively in appendix B.

Basically the following load cases will occur on the bridge:

Permanent loads:	
LC1: Self-weight girders (not included in SCIA)	A_c*25 kN/m
LC2: Dead load	
– Pavement	4.6 kN/m^2
– Asphalt	4.8 kN/m^2
– Concrete filling around tram rails	3.5 kN/m^2
LC3: Steel railing and natural stone elements (Edge Load)	2.0 kN/m^2
Variable loads:	
LC4&5: Traffic loads with presence of trams (UDL & tandem axle)	Conform Load Model 1
LC6&7: Traffic loads with absence of trams (UDL & tandem axle)	Conform Load Model 1
LC8: Tram-axle loads (No UDL specified for tram loads)	Conform GVB
LC9: Pedestrian loads over whole width (crowd loading)	5.0 kN/m^2
LC10: Pedestrian loads on designed locations.	5.0 kN/m^2

In total there are four main load combinations:

- Combination 1: Traffic loads in the presence of tram loading, where the traffic loads are the leading variable load. (1 LM1 TS + 2 tram TS)
- Combination 2: Traffic loads in the presence of tram loading, where the tram loading is the leading variable load. (1 LM1 TS + 2 tram TS)
- Combination 3: Traffic loads in absence of tram loading. (3 LM1 TS)
- Combination 4: Crowd loading

In Table 3-3 the load combinations are presented with the load factors[1] used in the ULS situation

Table 3-3: Load combinations with ULS load factors

	Load cases	Ψ	γ	CO1	CO2	CO3	CO4
LC1	Self-weight	1	1.2	1.2	1.2	1.2	1.2
LC2	Dead load (pavement, asphalt, tram rails)	1	1.2	1.2	1.2	1.2	1.2
LC3	Edge loads (railing, stone elements)	1	1.2	1.2	1.2	1.2	1.2
LC4	Traffic loads| UDL| Tram present	0.8	1.35	1.35	1.08		
LC5	Traffic loads| TS| Tram present	0.8	1.35	1.35	1.08		
LC6	Traffic load| UDL| Tram absent	0.8	1.35			1.35	
LC7	Traffic loads| TS| Tram absent	0.8	1.35			1.35	
LC8	Tram loading| TS	0.8	1.45	1.16	1.45		
LC9	Pedestrian loads| Crowd loading	0.8	1.35				1.35
LC10	Pedestrian loads| Loads on designated locations	0.8	1.35	1.08	1.08	1.08	

[1] In hindsight it was found out that the wrong load factors were used for the permanent loads. The load factors should be 1.4, which belong to CC3. This will not impact the results found later in the report as the conclusions made about the design remain the same. This goes for all three the designs.

3.6 Calculation model

The bridge is modelled in SCIA Engineer as a 2D orthotropic plate. This way the transverse action of all girders combined can be modelled in a good way. With this model the internal forces caused by the loads on the bridge will be determined. The self-weight will be left out, because the 2D model will be inputted as a plate. So the self-weight calculated will not be correct. Using the correct orthotropic parameters will still give the correct internal forces. Furthermore in SCIA, results in 2D are usually given per meter width. So the governing internal forces can easily be transformed to give results for one girder. Then adding the self-weight of one girder, which can easily be determined by hand, will result in the total internal forces in one girder. With these internal forces a safety check can be performed for one girder. The aforementioned orthotropic parameters are calculated with a Mathcad sheet, which can be found in appendix D.6.

The bridge is modelled as a simply supported bridge. In reality the amount of supports on each side will be the same as the amount of girders. Each girder is 1.5m wide. The bridge is 30m wide, so this results in a total of 20 girders. So in the model 20 internal nodes are placed on each side, which represent the location of the supports. The locations of the support in the model are determined by taking the centre location of each girder (right in the middle). In Figure 3-2 the SCIA model is shown.

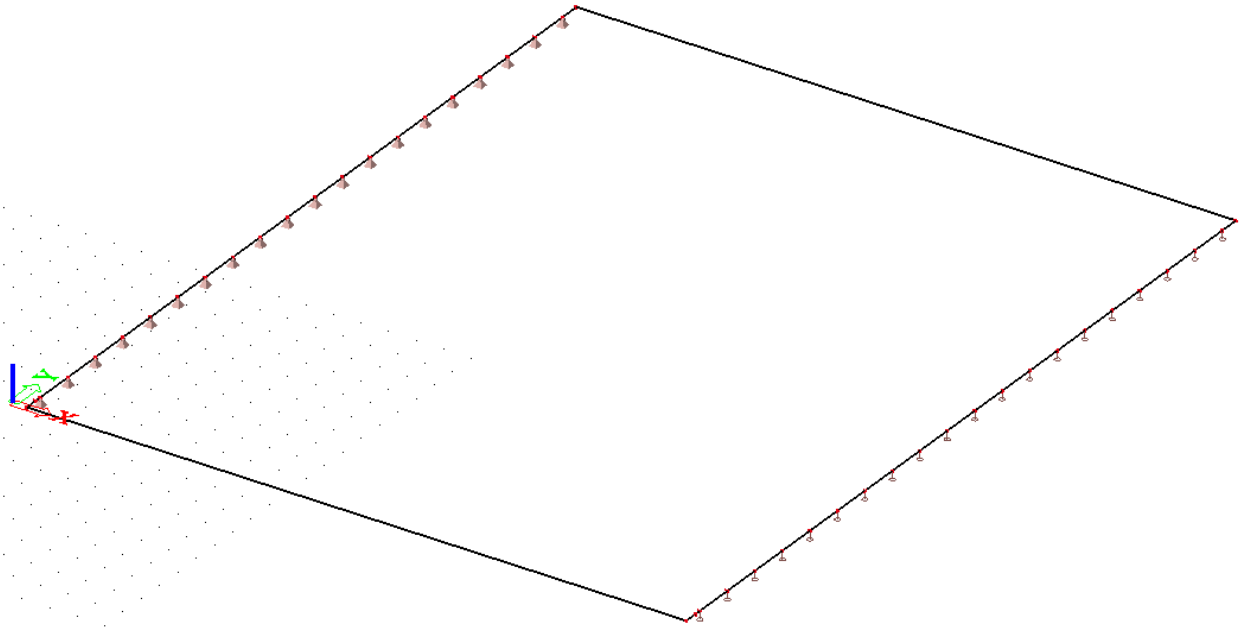

Figure 3-2: SCIA 2D model of C50/60

Because vehicles and trams constantly cross the bridge, these are defined as variable loads. In the model the traffic and tram loads are defined as mobile loads. Because they are defined as mobile loads the program can determine at which position of the load, across the length of the bridge, is the governing one for the bending moments, Shear force etc. These mobile loads will be combined with the other, static loads to determine the maximum internal forces on the bridge.
A full report on the model (such as coordinates, loads, etc.) and also the results from the model can be found in the engineering report in appendix D.

3.7 Results SCIA Engineer

Presented here are the internal forces necessary to perform the safety checks in ULS. The results are all from the ULS. The results for vx are taken from a section made near the supports. A section there is used, because of very high peak values occurring right at the internal nodes which represent the supports. These are likely caused by singularities in the calculations. Therefore a section is placed just outside the peak area to give more realistic results for the shear force.

For bending moment resistance check:
mxD^-: 1602.82 kNm/m

For shear and [torsion + shear] safety check
mxy: 344.75 kNm/m (When torsion is governing)
172.3 kNm/m (When shear is governing)

vx: 220.76 kN/m (When torsion is governing)
645.0 kN/m (When shear is governing)

The values given by SCIA are per meters width. These values have to be recalculated to represent the forces on one girder. The width of one girder is 1.5m:

For bending moment resistance check:
mxD^-: 2404.24 kNm

For torsion + shear safety check
mxy: 517.13 kNm (When torsion is governing)
258.39 kNm (When shear is governing)

vx: 331.14 kN (When torsion is governing)
967.5 kN (When shear is governing)

These last presented values will be used for the safety checks. However these values are only based on the loads working on the bridge. Here nor self-weight nor prestressing is included. These have to be added separately. This will be done in the following, where also the amount of prestressing will be determined.

3.8 Tendon profile and prestress force

The beams will consist of pre-tensioned strands, as the beams are prefabricated. The tendon profile is shown in Figure 3-3. The tendon consists of straight and kinked strands. The kinked strands cause an upward force P_u at the deviation points. This point is at a distance 'a' from the support. The kinked strands are placed in the webs. The strands will be placed as high as possible to ensure a high upward force. This force slightly reduces the total shear force. Most of the strands will be placed in the bottom flange. This means that the fictitious tendon (or the gravity point) does not coincide with the neutral axis (dashed line). So these will create a moment at the heads due to eccentricity, so a capacity check at the support has to be made to make sure the structure can take the moments.

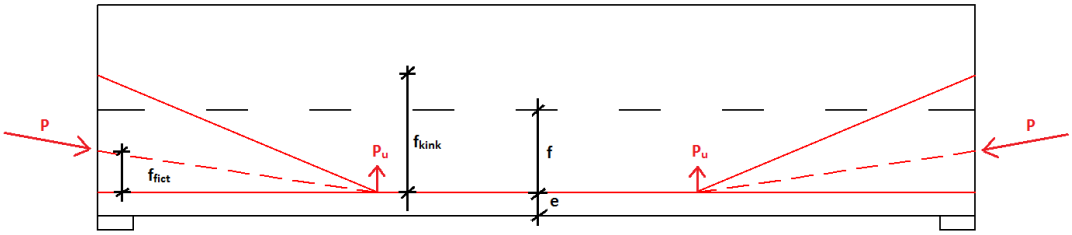

Figure 3-3: Tendon profile pre-tensioned strands

Distance strands from bottom fibre:	e = 0.093mm
Amount of kinked strands per web:	6 strands
Drape of all strands:	$f = z_b - e = 0.213m$
Distance deviation points from supports:	$a = (1/3)*L = 8m$
Drape of kinked strands:	$f_{kink} = 0.276m$
Upward prestress force:	$P_u = P_{kink} * \sin \alpha_{kink} \approx P_{kink} * (f_{kink}/a)$ or $P*(f_{fict}/a)$
Bending moment in mid span:	$M_{p,mid} = P*f$

The prestress force is determined by taking a couple of requirements into account that concern stresses in the concrete. These requirements need to be applied in the governing cross section (cross section with highest bending moment). Here that is in the middle of the beam. These requirements are:

$$t = 0 \text{ at top fibre: } -\frac{P_{m0}}{A_c} + \frac{M_{p,0}}{W_{ct}} - \frac{M_g}{W_{ct}} \leq 0$$

$$t = 0 \text{ at bottom fibre: } -\frac{P_{m0}}{A_c} - \frac{M_{p,0}}{W_{cb}} + \frac{M_g}{W_{cb}} \geq -0.6 * f_{ck}$$

$$t = \infty \text{ at bottom fibre: } -\frac{P_{m\infty}}{A_c} - \frac{M_{p,\infty}}{W_{cb}} + \frac{M_{tot}}{W_{cb}} \leq 0$$

Assumed is a total loss of 20% so $P_{m\infty} = 0.8*P_{m0}$

The moment due to static loads (self-weight + dead load) is:
$M_g = 1481.3kNm$
The moment due to the variable loads is:
$M_q = 1417.6$ kNm
This results in a total moment of:
$M_{tot} = 2898.9$ kNm
The moments and requirements result in a minimum amount of 53 strands, which have a total cross sectional area of $53*139 = 7367mm^2$. This results in a force of $P_{m0} = 10276.97$ kN.
The moment caused by the prestressing force is:
$M_{p\infty} = P_{m\infty}*f = 1754.13kNm$
The stress caused by the prestress force during $t=\infty$ in the concrete is:
$\sigma_{cp} = 0.8*P_{mo}/A_c = 14.58$ N/mm^2.

The prestress force delivers a vertical force at the deviators P_u, which is equal to: $P_{u0} = P_{m0}*(f_{fict}/a) = 80.38kN$. $P_u = 64.30kN$.
As can be expected the fictitious drape is low because the gravity point is very close to the bottom flange, due to the high amount of strands there. The gravity point is at a distance of $f-f_{fict} = 0.151m$ from the neutral axis. This basically means the moment due to prestressing isn't zero anywhere.

A more detailed calculation of the amount of prestressing strands is found in appendix D.8.

3.9 Bending moment resistance

It is a requirement that the bending moment resistance is higher than the design bending moment: $M_{Rd} > M_{Ed}$.

$M_{Ed} = \gamma_g * M_g + \gamma_q * M_q - \gamma_p * M_p$

It is possible that the eventual governing design bending moment is found at the construction stage (t=0) and perhaps at the support, because the prestressing causes a moment there.. So the bending moment will be determined for the whole span at multiple stages: These stages and the moments are:

- t=0 only self weight: $M_{Ed} = M_{self} - M_p$
- t=0 permanent loads: $M_{Ed} = M_{perm} - M_p$
- t=∞ all loads + torsion: $M_{Ed} = M_{perm} + M_{var} - M_p$

In Figure 3-4 the moment lines are shown, for multiple stages. The governing M_{Ed} = 1868.343 kNm. The moment at the support is 1549.62 kNm. Technically right at the support the prestress force is also zero. The force has a certain transmission length, where after the force is fully transferred in the concrete.

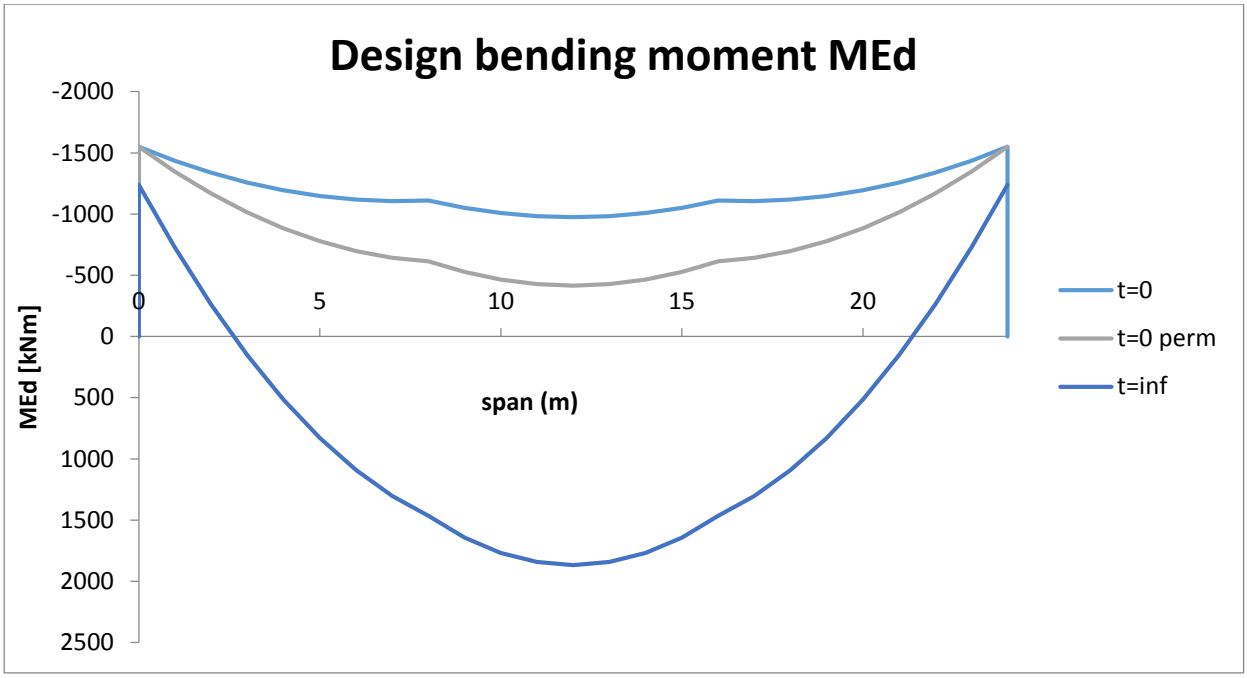

Figure 3-4: Design bending moment at multiple stages

The design bending moment needs to be lower than the moment capacity. To determine M_{Rd} one has to assume equilibrium of internal forces in the cross section and with that assumption determine M_{Rd} (see Figure 3-5): $N_c = P_{m\infty} + \Delta N_p + N_s$.

The last term N_s is removed, as there is no bending reinforcement applied. If by any chance the height of the compressive zone x_u exceeds the the top flange thickness, then Figure 3-6 is used to find a new equilibrium and determine the moment capacity.

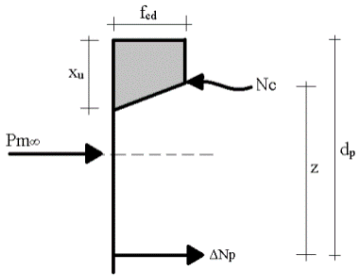

Figure 3-5: Equilibrium of internal forces

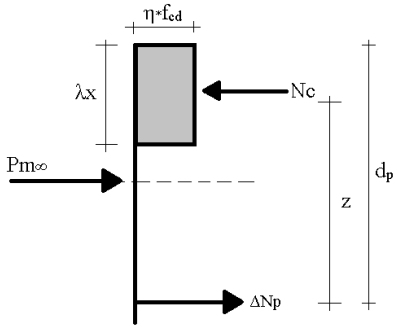

Figure 3-6: Rectangular stress strain relationship

For the height of the compressive zone found is:
λx = 489.48mm

The moment capacity M_{Rd}:
M_{Rd} = $P_{m\infty}*z_t + \Delta N_p*d_p - N_{c,flange}* h_{top,fl} - N_{c,web} * (\lambda x - 0.5(\lambda x - h_{top,fl}))$ = **2403.85 kNm**

Unity check: $M_{Ed}/M_{rd} = 0.778 \rightarrow$OK

A more detailed calculation is found in appendix D.9.

3.10 Rotational capacity

The bending moment resistance suffices. But it is also important that the structure has enough rotational capacity in order to give enough warning before failure. For this the following requirement has to be met[2]:

$x_u/d \leq 0.471$

With x_u = 489.48:

$x_u/d = 0.96 > 0.471 \rightarrow$ NOT OK

The results show that even though the bending moment resistance is sufficient the compression zone height is very high. This is caused by the amount of prestress that is applied. This shows that the used cross section is too small to be able to resist the loads working on the bridge and requires a high amount of strands. What could be done is to use a thicker cross section instead. But because of the requirements, that state that the cross section height is limited, this option is not possible.

It is however allowed to fictively reduce the amount of prestressing until M_{Rd} is just above M_{Ed} and then calculate the rotational capacity. After a few iterations the prestressing has to be fictively reduced to A_p = 5700mm^2. Here xu/d = 0.46, which is just below the max requirement. M_{Ed}/M_{Rd} = 0.778. The moment resistance stays around the same value as earlier and is actually even higher (new M_{Rd} = 2400kNm). This is because the height of the compression zone which decreases due to less prestressing. Therefore the internal arm becomes higher. This arm compensates the reduction in prestressing force and thus keeps M_{Rd} around the same value as before.

[2] NEN-EN-1992-1-1 Dutch NB cl.5.5

3.11 Shear and Torsion resistance

The detailed calculations are found in appendix D.11

3.11.1 Shear

It is a requirement that the shear resistance is higher then the design shear force:
$V_{Rd}>V_d$
The design shear force is the sum of the shear force caused by bending moments and the shear force caused by torsional moments:
$V_d = V_{Ed} + V_{Td}$
Two cases have to be investigated, of which the most governing one will be used:

Situation 1. Location of highest torsional moment in structure
Situation 2. Location of highest shear force in structure

For both locations the internal forces were calculated and the results were presented in paragraph 3.7. These were:
Mxy = TEd:

Situation 1. 517.13 kNm --> V_{Td} = 191.53 kN
Situation 2. 258.39 kNm --> V_{Td} = 95.7 kN

Vx (without self-weight and prestressing):

Situation 1. 331.14 kN
Situation 2. 967.51 kN

The shear force V_{Td} due to T_{Ed} is calculated with: $V_{Td} = h_m * T_{Ed}/(2*A_k)$.

The governing total shear force taken from SCIA is the one where the sum of V_x and V_{Td} is the largest. This is the case for situation 2, where V_{Ed} = 1063.21 kN. The shear force over the length of the beam needs to be determined at multiple stages. These stages and the shear forces are:

- t=0 only self weight: $V_{Ed} = V_{self} - P_{u0}$
- t=0 permanent loads: $V_{Ed} = V_{perm} - P_{u0}$
- t=∞ all loads + torsion: $V_{Ed} = V_{perm} + V_{var} - P_{u\infty}$

For t=∞ the shear force is added with V_{Td}. Assumed is that V_{Td} is constant over the length of the beam. The shear force line is seen in Figure 3-7.

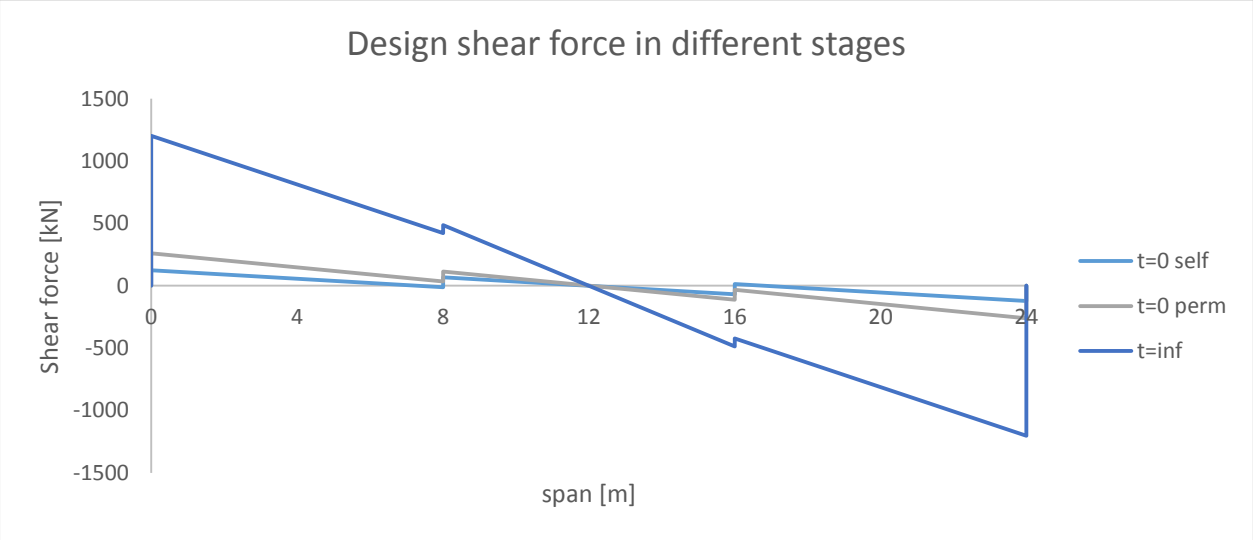

Figure 3-7: Shear force line at multiple stages

The governing shear force V_{Ed} = 1201.94 kN at t=∞. The shear resistance has to be high enough to resist this force.

For determining the shear resistance two areas in the beam have to be considered: the cracked and uncracked area. In the cracked area if no shear reinforcement is applied the design shear force has to be smaller than the shear resistance of the concrete ($V_{Rd,c}$)[3]:
$V_{Rd,c}$ = (v_{min} + k_1*σ_{cp})*b_w*d = **411 kN**

For the uncracked area it is a requirement that the principal tensile stress is smaller than the design value of the concrete tensile strenght (f_{ctd}). This requirement[4] leads to:
$V_{Rd,c}$ = [I/(d*S)]*[(f_{ctd})^2+ α_l*fctd* σ_{cp}]$^{0.5}$

The first crack that causes failure is at a distance of l_x = 400 mm from the end (100mm + H/2 see Figure 3-8).

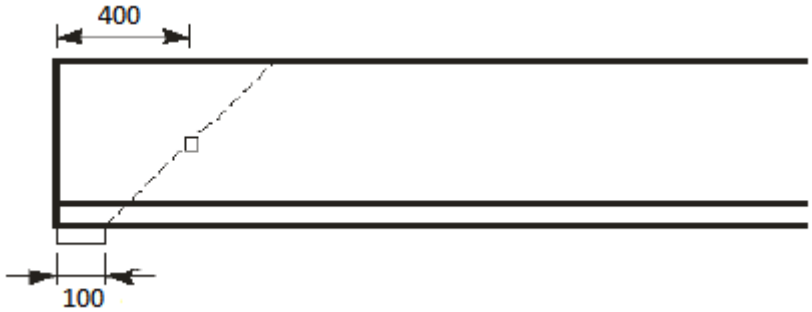

Figure 3-8: Location of first crack

Because the strands are bonded by anchorage, there is a certain transmission length where the strands become fully prestressed. This transmission length is calculated according to EN 1992-1-1 cl. 8.10.2.2) and is: $l_{pt,2}$ = 935.8mm. So before the prestress force is fully transferred there is a reduced shear resistance (taken into account by α_l = l_x/l_{pt} = 0.43). This results in:
$V_{Rd,c}$ = 691.54 kN
Then when the prestressing is fully transferred the shear resistance becomes (α_l = 1):
$V_{Rd,c}$ = 983.43 kN

The governing shear resistance is the one in the cracked area. This resistance has to be checked if it can resist the shear force at location l_x. V_{Ed}(l_x) = 1162.92 kN

UC= V_{Ed}/$V_{Rd,c}$ = 1162.92/411.1 = 2.83 → NOT OK!

It is obvious that the shear resistance does not suffice at all. So shear reinforcement has to be applied. In total applied is φ12-75 which is equal to A_s = 6030 mm^2/m. This is a lot of required shear reinforcement, caused by low shear resistance.

The stirrups have to be placed until 8.6m from the supports. Normally hammerheads are applied at the supports, which are around 1m long (their extra added weight not taken into account in the calculations as the influence is minimal in this case). So at these locations the shear capacity does suffice, because of the solid cross section. But there is still 7.6m left where the concrete does not have enough shear reinforcement and it is not wise to make a solid cross section over that length, because this will only result in more weight and therefore higher internal forces (and more prestressing strands as well). So in short the required amount of shear reinforcement still has to be applied in the required areas outside of the hammerheads.

[3] NEN-EN 1992-1-1 cl 6.2.2(1)
[4] NEN-EN 1992-1-1 cl 6.2.2(2)

3.11.2 Shear + torsion

It is also required that the combination of shear forces and torsional moments is verified. The structure should be able to resist these forces. The requirement for this states[5]:

$T_{Ed}/T_{Rd,max} + V_{Ed}/V_{Rd,max} \leq 1.0$

The requirement means that the capacity of the concrete struts has to be sufficient to resist the loads on the structure. Here the two previous situations are going to be investigated as well.

First $T_{Rd,max}$[6] and $V_{Rd,max}$[7] have to be determined:

$\mathbf{T_{Rd,max}} = 2*\nu*\alpha_{cw}*f_{cd}*A_k*t_{ef}*\sin\theta\cos\theta$ = **1782.98 kNm**

$\mathbf{V_{Rd,max}} = \alpha_{cw}*b_w*z*\nu*f_{cd}/(\cot\theta+\tan\theta)$ = **1369.98 kNm**

Unity check:

Situation 1: $T_{Ed}/T_{Rd,max} + V_{Ed}/V_{Rd,max}$ = 517.13/1783 + 469.87/1370 = 0.633 → OK

Situation 2: $T_{Ed}/T_{Rd,max} + V_{Ed}/V_{Rd,max}$ = 258.39/1783 + 1106.2/1370 = 0.952 → OK

For both situations the concrete struts suffice. However situation 2 is close to failure.

The required torsional reinforcement[8] is is divided over the flanges and webs and placed in two layers (total of 3772mm^2):

Per flange: $A_s = T_{Ed}/(2*h_m*f_{yd})$ = 1350 mm^2 → 9φ10 per layer (divided over the whole flange).

Per web: $A_s = T_{Ed}/(2*b_m*f_{yd})$ = 440 mm^2 → 3φ10 per layer (divided over the web)

3.12 Fitting of prestressing and reinforcement

The calculated amount of prestressing strands and (shear) reinforcement has to be fitted in the cross section of the box girder. In Figure 3-9 and Figure 3-10 the cross section at the mid and end span respectively are shown (measurements in millimetres). In practice the cross section at the support is a hammerhead, which means that the cross section is a solid concrete section. But for fitting of the reinforcement and prestressing the extra solid part is neglected. There are 53 strands in total of which 12 are located in the webs (6 strands per web) and 41 in the bottom flange. Longitudinal reinforcement is placed in two layers in the cross section (3φ10 per layer in the webs and 9φ10 per layer in the flanges). In the webs there is also shear reinforcement of diameter 12 mm and in the flanges transverse reinforcement is placed as well. Assumed for this is a diameter of 12 mm. (Detailed calculation of transverse reinforcement is left out in this chapter).

[5] NEN-EN-1992-1-1 cl. 6.3.2(4)
[6] NEN-EN-1992-1-1 formula 6.30
[7] NEN-EN-1992-1-1 formula 6.9
[8] Determined with NEN-EN-1992-1-1 formula 6.28

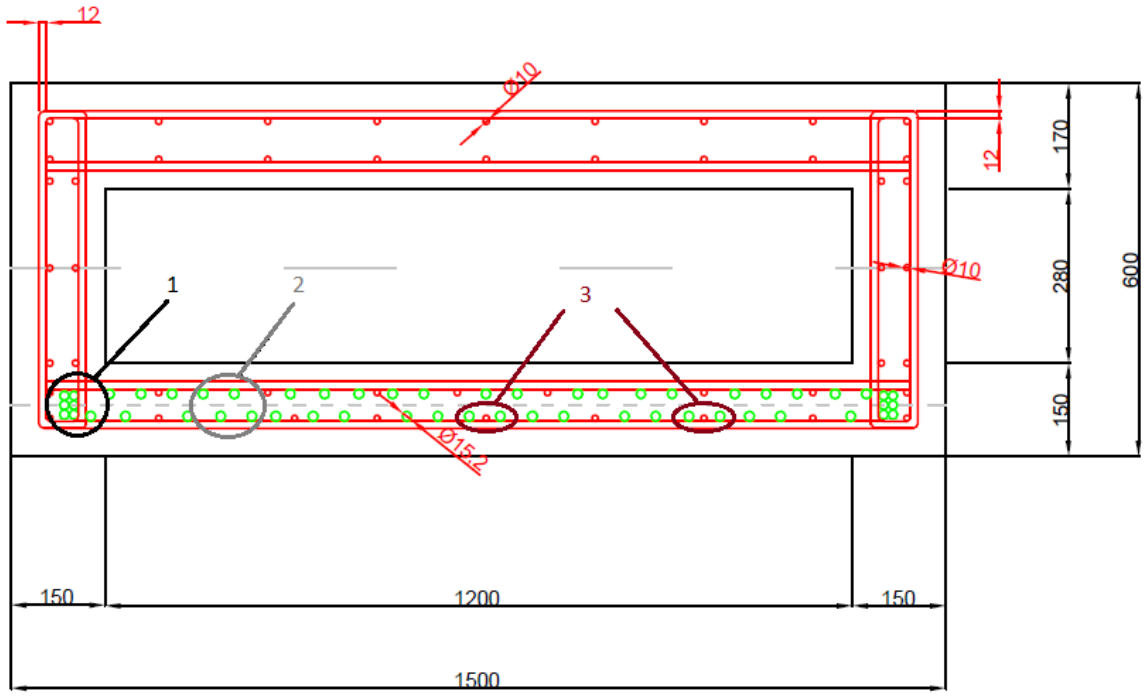

Figure 3-9: C50/60 cross section mid span

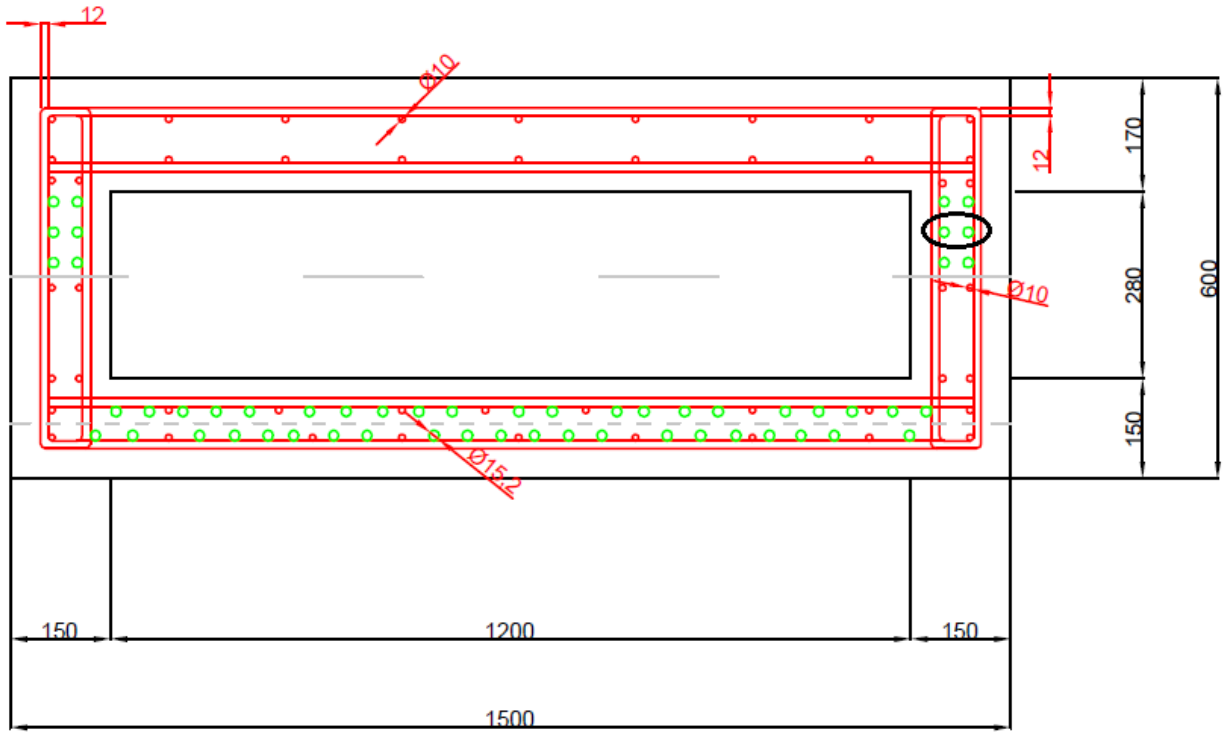

Figure 3-10: C50/60 cross section end span

In general it can be stated that the reinforcement and prestressing strands can (with effort) be fitted in the box girder. However there are some areas of concern that have to do with spacing between prestressing strands and reinforcement bars. These areas of concern have been marked in Figure 3-9. Number 1 shows that there is a high concentration of the strands located in the web at the mid span. These are placed here in order to coincide with the gravity point of all the strands in the mid span.

But due to transverse and shear reinforcement the strands have to be placed right next to each other in order for them not to cause eccentricities. This placement could be very difficult to construct.

Number 2 has to do with the spacing between prestressing strands. The distance between the centres of the strands has to be at least $D_{g,max} + \varphi_{strand}$ which is 47 mm. Horizontally this requirement is met. Vertically as well since the strands are not placed directly under each other. Diagonally however the centre spacing is 43.5mm, which is lower the minimum requirement. The difference is not very high so this spacing is rather acceptable.

Number 3 concerns the spacing between reinforcement bar and prestressing strand. The centre spacing between bar and strand in the second layer of reinforcement in the flange is rather low. Here it could be possible that aggregates get stuck between the bar and the strand causing a local weak point. So in theory the spacing should be enlarged so that the area between the bar and strand is at least $D_{g,max}$. In the first layer this issue exist as well, but here it is more acceptable, since gravity will make sure the aggregates don't get stuck there.

In Figure 3-10 there is an issue point at the anchorage location of the strands. The vertical spacing is sufficient. The horizontal distance between the strands (required 47mm) is 35.8 mm, which leaves only 20.6mm gap between the strands. The maximum aggregate is 32mm so depending on the method of concrete pouring there is a chance that aggregate gets stuck between the strands. This will negatively impact the concrete quality in the box girder. Furthermore all these above mentioned issue points could also result in problems concerning bursting and splitting. The spacing requirements that are given by the Eurocode are also there to prevent these two from occurring. So with the spacings lower than recommended, more reinforcement will probably be necessary in order to prevent bursting and splitting.

Looking back at these issues, the most straight forward solution (which could also solve the problems concerning structural safety) is to increase the construction height. This would lead to a smaller amount of required strands and also less reinforcement bars. But as already mentioned a couple of times, increasing the construction height is not an option. So what could be done instead is somehow shifting a couple of strands or bars to try to solve the issue points mentioned. This could prove a very complicated job to perform. If all the spacing requirements are strictly followed then it would be nearly impossible to fit all the required strands and reinforcement.

3.13 Capacity check at point of full transfer of prestress force

When looking at the support, most of the prestressing strands are concentrated in the bottom flange, while a couple are located in the webs (6 per web). So the gravity point of all strands will not coincide with the neutral axis of the box girder. This means that the strands will cause a moment here. At time of construction (t=0) this moment could possibly cause failure as there are no variable loads present. Because of the required transfer length of the prestress forces there are no moments caused by the strands directly at the supports, since the force is not fully transferred yet. But at the end of the transfer length, the moment capacity will have to be checked, because here the prestress force is fully transferred and a moment is caused by the eccentricity of the strands. This check will be performed here. The transfer length is l_{pt} = 779.86 mm. So the cross section at a distance of 779.86 mm from the support will be checked.

The design bending moment at l_{pt} is: $M_{Ed,lpt}$ = 1781.57 kNm

At l_{pt} the situation is as in Figure 3-11 is presented. The compression zone is at the bottom side. The torsion reinforcement ($A_{s,top}$ = $A_{s,bot}$ = 1350mm^2) is also taken into account, as it benefits the moment capacity.

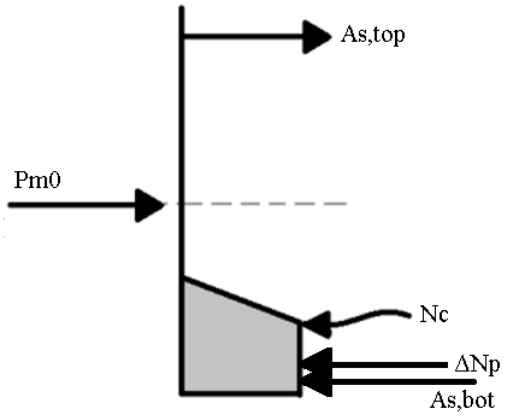

Figure 3-11: Cross section at l_{pt}

For equilibrium of the internal forces the following equation stands: P_{m0} + A_s,bot = N_c + ΔN_p +$A_{s,bot}$. Solving this equation results in a compression zone height of x_u = 232.53mm. Then if the moment around the point of the resultant of N_c is taken the moment capacity becomes: **$M_{Rd,lpt}$ = 2488.9 kNm**

Unity Check: $M_{Ed,lpt}/M_{Rd}$ = 1781.6/2488.9 = 0.716 → OK

The structure is safe. No extra longitudinal reinforcement is required.

A more detailed calculation is found in appendix D.12.

3.14 Conclusion

A design in concrete strength C50/60 has been developed. With the given requirements an appropriate bridge type and a construction thickness have been chosen. The bridge design has been tested on the working loads and checked if it is structurally safe. The calculations showed that the structure has enough bending moment resistance (UC=0.778). However the rotational capacity is very low and does not suffice at all according to the requirements (x_u/d = 0.96; should be lower than 0.47). This means that the structure will not give any warning before failure. The low rotational capacity is likely caused by the use of a construction thickness that is too low in combination with a high amount of prestressing. The internal forces are so high, that a lot of prestressing is needed, which causes a very high compression zone. And besides that also a high compressive stress is caused by the prestressing. This again benefits the bending moment resistance and reduces the design bending moment, which is why the bending moment resistance suffices.

Furthermore the shear resistance of the structure is significantly low (UC=2.83) even with the inclusion of the high compressive stress of the prestressing. This means that a high amount of shear reinforcement has to be applied to handle the shear forces (A_{sw} = 6030mm^2). Also necessary is reinforcement to resist the torsional moments (A_s = 3772 mm^2). The concrete struts do suffice according to the requirements (UC=0.95). But also here the limits are being reached.

The reinforcement and prestressing strands hardly fit in the cross section. Because of the amount of strands and reinforcement the execution of the box beam will prove to be rather difficult, because of bars and strands being relatively close to each other. Furthermore there are a couple of area of concerns regarding the spacing of strands and reinforcement bars. These could cause problems during the pouring of concrete, which could negatively impact the concrete quality. So basically it is a very complicated and tedious job to be able to fit the reinforcement and prestressing, while meeting the detailing requirements.

The problems arising in this design could be solved by using a higher construction thickness. If for example a thickness of 750 or 800mm is used, which is what the thickness should be for this span and this concrete class, than most of the issues would be solved. This is not an option however considering the stated architectural requirements. Therefore it can be concluded that a bridge design in C50/60 is not a good option if the design demands have to be taken into account. The results from the calculations show that the design is not economical, due to the high amount of prestressing and reinforcement. Instead of using C50/60 a higher concrete class should be used. Since the aim of this research is to see if UHPC can provide a realistic design for the Leiden Bridge, UHPC will be the higher concrete class that will be investigated further.

3.15 Summary

Also added are results if H=800mm would be used

H=600mm

Amount of strands:	53ϕ15.2 strands	
Total losses in strands:	20%	
Slenderness ratio, λ	40	
Bending moment capacity, M_{Rd}:	M_{Rd} = 2403.85 kNm	UC = 0.778
Rotational capacity: x_u/d	x_u/d = 0.965	UC = 2.049
Shear capacity V_{Rd}:	$V_{Rd,c}$ = 411.08 kN	UC = 2.829
Shear reinforcement	A_{sw} = 6030 mm^2	
Torsion reinforcement:	A_s = 3772 mm^2	
Capacity concrete at hammerhead:	$M_{Rd,head}$ = 2488.9 kNm	UC = 0.716

H=800mm

Amount of strands:	38ϕ15.2 strands	
Total losses in strands:	20%	
Slenderness ratio, λ	30	
Bending moment capacity, M_{Rd}:	M_{Rd} = 3296.2 kNm	UC = 0.572
Rotational capacity: x_u/d	x_u/d = 0.207	UC = 0.433
Shear capacity V_{Rd}:	$V_{Rd,c}$ = 400.28 kN	UC = 2.82
Shear reinforcement	A_{sw} = 4110 mm^2	
Torsion reinforcement:	A_s = 2828 mm^2	
Capacity concrete at hammerhead:	$M_{Rd,head}$ = 2785.81 kNm	UC = 0.514

Note: Using H=800 mm still does not result in a high shear capacity, but the amount of strands and reinforcement is greatly reduced and the design would therefore be more economical and easier to construct (concerning fitting everything).

Chapter 4 Ultra High Performance Concrete

4.1 General information

Ultra High Performance concrete, or in short UHPC, is a fairly new type of concrete, which on multiple aspects differs from normal and also high strength concrete. First of all UHPC only contains fine materials, where usually the maximum size of the aggregates is 2mm. Normal strength concrete usually has sizes that go up to 32mm, while high strength concrete sticks around 8mm. Also UHPC has a water cement ratio that is lower than 0.2. Furthermore steel fibres are included in the mixture of UHPC. These provide a higher tensile strength and a better ductility than normal and high strength concrete. Finally UHPC is more durable than other types of concrete, because the use of only fine material results in a very dense matrix, which provides great protection against environmental threats. All these aspects result in UHPC having a very high strength (compressive strength up to 200 MPa and tensile strengths around 8 to 9 MPa. These high compressive and tensile strengths, could prove beneficial in developing a design for the new Leiden Bridge. Together with the great durability properties, UHPC could result in a structure that has a long life span, is maintenance free and has great structural performance. In the following paragraphs the main learning points from the literature study will be given and also an elaboration on why UHPC would prove to be a better option than normal strength concrete.

4.2 Summary literature study

An extensive literature study has been performed to get a better understanding of UHPC. The complete report of the literature study is found in Appendix A. Here all information concerning the properties of UHPC can be found, as well as completed project that utilised UHPC. All the important findings are collected here for future quick reference. The points mentioned in this paragraph are considered the most useful findings of the literature study for the main research.

- ***Advantages UHPC***
    - High strength properties
    - Great ductility
    - Outstanding durability and sustainability
    - No need for mild and shear reinforcement
    - Very slender structures possible.

- ***Disadvantages UHPC***
    - UHPC is more expensive that ordinary concrete (Slender materials so less concrete necessary)
    - Longer production times due to longer mixing (optimize mixture packing)
    - Steel fibres decrease workability (use more short fibres and finer materials)
    - Hard to control orientation of steel fibres (Use horizontal casting)
    - Worse fire resistance than ordinary concrete (use PVA fibres)
    - High early shrinkage and creep (can be controlled and reduced by using steam based curing)
    - Possibility of insufficient resistance against dynamic loads due to higher slenderness.

Concerning application of UHPC

- Through the years UHPC has successfully been applied in structures both structurally and architecturally wise.
- In a couple of projects the newly developed Pi-girder has been used, which optimally used the UHPC material properties.
- UHPC will provide the lightest structures compared to conventional concrete and steel

- The high slenderness that can be achieved with UHPC could possibly lead to dynamic behaviour issues, which need to be resolved, with dampers.
- Modular UHPC segments can be used in structures for a faster execution.
- The older bridge projects haven't used fully optimized UHPC girders, but existing girders that were slightly modified.

Concerning researches on UHPC

- In general UHPC has better material properties (structural, durability) than normal strength and high strength concrete.
- Box sections provide highest span-to-depth ratio and girder sections save most material volume per span length.
- Using UHPC in bridge structures will require a lesser amount of girders compared to HSC and smaller sections as well. Both will lead to a concrete volume reduction. Using less and smaller girders can result in an increase in prestressing cables per girder.
- Besides volume reduction, using UHPC over HSC results in a high increase in span length.
- UHPC has higher material and production costs than normal concrete. However when the complete life cycle is considered, UHPC becomes cheaper (after 100+ years), due to the longer life span and less maintenance needs.
- Researchers concluded that further optimization is required for the use of UHPC in structures. Options for optimization can be:
    - Optimizing cross section (construction height, web/flange thickness)
    - Optimising amount of girders
    - Optimizing concrete composition and production process

Concerning design in UHPC

- The steel fibres provide a high ductility. This allows for the use of the tensile capacity of UHPC.
- The consideration of the high tensile capacity leads to a better bending moment and shear resistance.
- The length and amount of the steel fibres will have a positive influence on crack propagation and distribution, by resulting in well distributed micro cracks.

4.3 Transition from C50/60 to C170/200

The results of the design in C50/60 showed some complications with the design. The moment capacity met the requirements. The rotational capacity at first did not suffice, but with fictively reducing the prestressing the rotational capacity can be made to meet the requirements. This does not change the fact that a high amount of prestressing is required: 53 strands of 15.2 mm are needed, and all of these have to be fitted in the cross section.

The shear capacity did not suffice. A lot of shear reinforcement is required to be able to resist the design shear force. Reinforcement is also necessary to resist the torsion moment.
All the prestressing strands and all the required reinforcement need to be fitted in the cross section. The problem here is that there will be hardly any room to fit all of this. Especially if a fairly high cover is required (c=45 mm). This covers reduces the area left for the strands and bars. It was shown that all the reinforcement and strands can just barely be fitted in and still there are a certain issue points left. And using and fitting all of this reinforcement and prestressing could cost a lot of money and it will be difficult to construct such a box beam full with steel.

So it is safe to say that a design in C50/60 is not a realistic option. To be able to make a design that meets the safety requirements and that is also less difficult to construct, it is wise to use concrete with a higher strength. But it is important to realise if it is possible to, in this case, reduce the amount of prestressing needed and to reduce the amount of shear reinforcement needed, by providing enough concrete strength to resist the design shear force.

To solve the problems arising with the design in C50/60 it is therefore an option to use UHPC. UHPC has a much higher strength than C50/60. The biggest difference is that UHPC has a high tensile strength, which is caused by the addition of steel fibres in the concrete. These fibres also provide a high ductility (strain limits around at least 5‰ compared to around 0.15‰ for ordinary concrete) and tension capacity. Therefore it is allowed to take the tension capacity into account during calculations. In the literature study it was shown with an example calculation that the shear resistance for UHPC is much higher than that for C50/60. The higher resistance is not only because of a higher concrete strength (from f_{ck} = 50 MPa to f_{ck} =170MPa), but especially because of the positive contribution of the steel fibres.

This high shear capacity of UHPC may prove to be very useful. It is very likely that UHPC can resist the shear forces found working on the Leiden Bridge. This will result in the exclusion of shear reinforcement. Also a big reduction of torsion reinforcement is most likely, since the tensile strength of UHPC is much higher than that of C50/60 (from f_{ctk}=2.9 MPa to f_{ctk}= 8 MPa). The researches discussed in the literature study also showed that with UHPC shear and passive reinforcement can be excluded from the cross section.

This is also most likely the reason why it is better to jump straight to UHPC instead of high strength concrete. Using for example C90/105 will give a safer structure, but the composition of the mixture for C90/105 (where no steel fibres are used as in UHPC) does not provide a significant better tensile capacity as is with UHPC. Therefore according to the Eurocode, also with C90/105 only the compression capacity may be taken into account for certain calculations. So even when using C90/105 instead of C50/60 it is most likely that the shear capacity will still not suffice. Most of the shear capacity in the C50/60 design comes from the prestressing stress σ_{cp} (around 75%). The increase of the compressive strength from 60 to 90 MPa will not result in the unity check to drop from above 2 to below 1. Most likely the UC will stay around 2.0 and therefore still a large amount of shear and (perhaps also torsional) reinforcement will be necessary to apply in the structure. So again there will be a problem with fitting everything in the structure, since there is no reduction in the amount of prestressing strands.

The exclusion of shear and passive reinforcement when using UHPC results in extra space for prestressing strands. Furthermore with UHPC it is possible to make lighter structures. For example the box girder can be made smaller and more slender. This reduces the dead load and thus decreases the amount of prestressing needed. So with UHPC there is a higher chance that all the required prestressing can be fitted in the structure.

Besides the aforementioned structural advantages of UHPC, another advantage of UHPC is the high durability. The very dense matrix structure results in a good protection against environmental threats such as carbonation, chloride, ASR etc. This provides a high durability compared to normal concrete and high strength concrete (which is denser than normal strength concrete, but not as dense to require such a high durability as UHPC does) and thus less maintenance needs. A structure in UHPC can easily fulfil a life span of 100 years without barely any maintenance. This is a great advantage over normal concrete, because it can save a lot of maintenance costs. And for the Leiden Bridge it is important that the bridge is closed as less a possible for maintenance. So with UHPC the bridge hardly has to be maintained.

Another advantage of the durability is that the cover for the reinforcement may be reduced (according to the AFGC recommendations), because of the dense matrix. Reducing the cover is also beneficial for fitting the prestressing besides the exclusion of shear and passive reinforcement.

With the mentioned structural benefits from and the great durability that UHPC brings, there is a high probability that a safe and feasible design can be made for the Leiden Bridge. This however will have to be proven. Therefore in the next chapter a design is going to be developed and calculated in UHPC C170/200.

Chapter 5 Bridge design in UHPC C170/200

5.1 General

In Chapter 4 it was already elaborated that using UHPC gives a high probability that the issues found in the C50/60 design could be solved. In this chapter a design in UHPC C170/200 is going to be developed and calculated in order to research if UHPC can indeed make a better, more realistic design for the Leiden Bridge. This calculation will be more profound than the calculation of the C50/60 design. First a design for the girder is going to be made along with its cross-sectional and material properties. Then the loads are going to be defined. Afterwards a SCIA model is going to be developed. With this model the forces caused by the loads will be determined. Then with these results a design calculation will be performed in both ULS (moment and shear capacity) and SLS (crack width, deflection and fatigue). Based on the results of the design calculation a conclusion will be made. Detailed calculations of this chapter can be found in appendix E.

5.2 Design of UHPC Box girder

In order to optimally make use of UHPC the current box beam girder design can be modified. There are multiple options for modifying the existing girder.

Option 1: Only adjusting the webs and flanges

An option could be to keep everything as it is in the current design, but only modifying the flange and web thicknesses, by decreasing their size. In this way the beam can be made more slender and the number of required beams (20 beams over the whole width) will stay the same.

Option 2: Lower width of the beam

It is also possible to lower the width of the box girder from 1.5m to 1.0m. Since new formwork will be necessary to develop box girders with a thickness below 700mm (which is the current minimum height produced), then the width might as well be altered too. And with this the web and flange thicknesses could also be modified. In this way the beam becomes lighter and more slender than the current box beams. The number of beams would logically increase (from 20 to 30 beams), but more beams also result in a higher overall stiffness of the structure. And a high stiffness is important in this case, because more slender structures become more susceptible to fatigue, which is in this case caused by trams and vehicles. Also more beams lead to a longer construction time, but the lighter and smaller beams are easier to transport.

Option 3: Increase spacing between the beams in combination with modifying the geometry

Another possibility is to increase the distance between the box beams, so that less beams are required over the whole width. Besides the increase in spacing, the beams can be made smaller in size as well. So for example box girders with a width of 1.0m can be placed with a centre spacing of 1.5m. In this way a lot of concrete material can be saved. But it will become necessary to increase the width of the joints between the girders. In the example mentioned it means that the joints go from around 50 mm to 500 mm in width. These joints are usually cast in situ. So when the joints are large it will take a lot of time to pour the concrete and let the concrete harden. But required is a fast construction method so using large joints is very negative concerning the construction time. Moreover, increasing the spacing and thus reducing the number of required girders results in a lower overall stiffness. And already mentioned is that a high stiffness is important. There is also the fact that each beam will have to take up more forces, so there is a chance that the loads become too high for one girder.

Looking at the three options it becomes clear that in this case it is best to consider the first two options. Option three has the benefit of saving material, but in this case a fast execution is more important than saving material. Same goes for a higher stiffness of the structure. And there is a possible chance that a girder cannot take the higher loads resulting from the increased spacing.
The second option has the benefit over the first one that the beam becomes lighter and more slender and also that the overall stiffness will increase due to the increase in the number of beams.

Some issues in the C50/60 design were that the shear capacity did not meet the requirements and that a lot of prestressing was required. Also a high amount of reinforcement was necessary. When using smaller beams, this will mean less prestressing, but also less space to fit prestressing. So relatively speaking going from a width of 1.5m to 1.0m does not change the issue in prestressing a lot. However with UHPC a smaller cover can be used due to the high density of the concrete. A smaller cover benefits the prestressing in a way that the eccentricity from the strands with reference to the bottom fibre decreases so the arm of the prestress force increases. This results in a smaller amount of required prestressing. Then there's the high probability that shear and also (a high amount of) longitudinal reinforcement is not needed, as already mentioned earlier in Chapter 4. This only gives more space for the fitting of the prestressing strands.

Considering the advantages and disadvantages and the issues found in the C50/60 design it will be chosen to use option 2. So a beam with a smaller width (1.0m) and with decreased thicknesses of the webs and flanges. Using this option gives a higher overall stiffness and lighter beams.

Another option that could be investigated is the use of an integral bridge. If the problem of too much prestressing and with that a difficulty to fit all the strands still occurs, it can be an option to use an integral bridge design. Here the substructure is integrated with the superstructure. This basically means that the supports are fixed instead of simply supported. This will result in lower field moments and thus a smaller amount of strands required. However now, with the fixed supports, there will be also moments present at the supports, so it is necessary to use enough reinforcement at the supports to resist these moments. Furthermore a restriction is caused for deformation and rotation. So temperature changes and imposed deformations will have to be taken into account. These will lead to internal forces, as the deformations are restricted by the fixed supports. The construction time for the superstructure is longer that when simply supported, because the monolithic connection has to be made in situ. But the advantage is that the sub- and superstructure can be constructed together instead of separately.

For the design however a simply supported structure will still be used, as it is easier to design and construct. However should this design not be possible to make, a step to an integral bridge has to be done.

5.3 Material properties

The concrete properties values are based on the recommended values in the AFGC Recommendations 2013 and also on an article in Cement magazine, which deals with UHPC calculations [4]. There are multiple UHPC mixtures available, which result in different material properties. This article is based on a UHPC mixture produced by Ductal and it used the AFGC to give specific values for certain parameters in order to give designers the ability to perform calculations for a UHPC design. The assumptions made in the article and also the mixture will be used in this thesis as well. The steel properties are based on NEN-EN-1992-1-1. All properties are found in appendix E.2.

5.4 Cross sectional properties

In paragraph 5.2 possible options for a box girder design have been discussed. There it is concluded that the main dimension would be a height of 600 mm and a width of 1000 mm. The flanges and webs are slightly reduced in size compared to the design in C50/60. The cross section of the UPHC box girder can be seen in Figure 5-1.

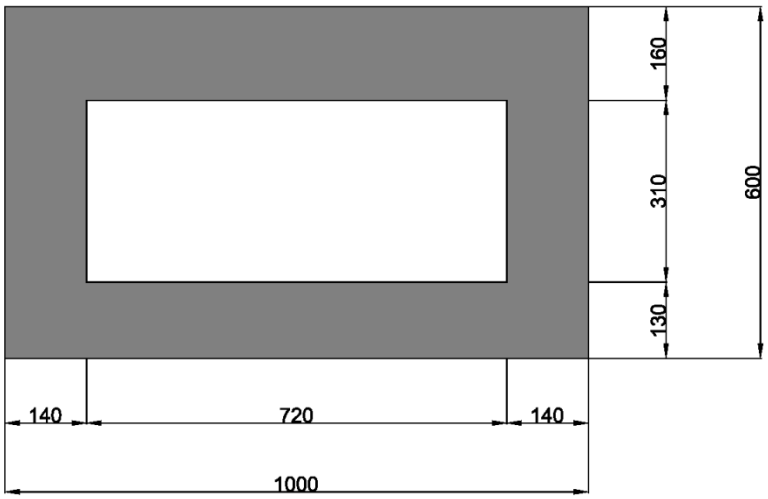

Figure 5-1: Cross section UPHC box girder

In Table 5-1 the dimensions and cross sectional properties of one girder are shown.

Table 5-1: Dimensions and cross sectional properties of box girder

L	*Span*	24 m
H	*Height girder*	0.6 m
B	*Width girder*	1.0 m
b_{web}	*Web thickness*	0.14 m
$h_{top,fl}$	*Top flange thickness*	0.16 m
$h_{bot,fl}$	*Bottom flange thickness*	0.13 m
A_c	*Cross sectional area*	0.377 m^2
z_t	*Distance top fibre to c.a.*	0.291 m
z_b	*Distance bottom fibre to c.a.*	0.309 m
I_c	*Moment of Inertia*	0.0161 m^4
$W_{c,t}$	*Section Modulus top fibre*	0.0554 m^3
$W_{c,b}$	*Section Modulus bottom fibre*	0.0522 m^3

5.5 Exposure class and concrete cover

The exposure class for superstructures in bridges is set by the AFGC Recommendations to be XC4[9]. For the inside of the box girder the exposure class can be set to XC1, since the inside is not as exposed as the outside of the girder.
The cover can also be determined conform the AFGC Recommendations[10]. Here basically the same method is used as in NEN-EN-1992-1-1, only with a couple of modifications. The most notable one is the reduction of all values given for the minimum cover. The values are divided by √5, which takes into account the diffusion coefficient of UHPC. This is due to the fact that UHPC has a much better durability than ordinary concrete, due to the very dense matrix. So the cover does not have to be as high as for ordinary concrete.

The nominal cover is $c_{nom} = c_{min} + \Delta c_{dev}$ (with Δc_{dev} = 5 mm) = 35.4mm for both the inner and outer perimeter of the box girder.

5.6 Load cases and load combinations

Before the SCIA Engineer model is presented, the loads have to be determined first. There are a lot of different loads that will work on the bridge. And these loads will not occur exclusively. Therefore it is important to determine all the load cases and load combinations for the bridge. The load cases and combinations are all described extensively in appendix B.

Basically the following load cases will occur on the bridge:

Permanent loads:	
LC1: Self-weight girders (not included in SCIA)	A_c*25 kN/m
LC2: Dead load	
– Pavement	4.6 kN/m^2
– Asphalt	4.8 kN/m^2
– Concrete filling around tram rails	3.5 kN/m^2
LC3: Steel railing and natural stone elements (Edge Load)	2.0 kN/m^2
Variable loads:	
LC4&5: Traffic loads with presence of trams (UDL & tandem axle)	Conform Load Model 1
LC6&7: Traffic loads with absence of trams (UDL & tandem axle)	Conform Load Model 1
LC8: Tram-axle loads (No UDL specified for tram loads)	Conform GVB
LC9: Pedestrian loads over whole width (crowd loading)	5.0 kN/m^2
LC10: Pedestrian loads on designed locations.	5.0 kN/m^2

In total there are four main load combinations:

- Combination 1: Traffic loads in the presence of tram loading, where the traffic loads are the leading variable load. (1 LM1 TS + 2 tram TS)
- Combination 2: Traffic loads in the presence of tram loading, where the tram loading is the leading variable load. (1 LM1 TS + 2 tram TS)
- Combination 3: Traffic loads in absence of tram loading. (3 LM1 TS)
- Combination 4: Crowd loading
- Combination 5: Governing transverse moment

[9] AFGC2013 paragraph 2.3 section 4.2
[10] AFGC2013 paragraph 2.3 section 4.4

In Table 5-2 the load combinations are presented with the load factors used in the ULS situation.

Table 5-2: Load combinations with ULS load factors

	Load cases	Ψ	γ	CO1	CO2	CO3&5	CO4
LC1	Self-weight	1	1.2	1.2	1.2	1.2	1.2
LC2	Dead load (pavement, asphalt, tram rails)	1	1.2	1.2	1.2	1.2	1.2
LC3	Edge loads (railing, stone elements)	1	1.2	1.2	1.2	1.2	1.2
LC4	Traffic loads| UDL| Tram present	0.8	1.35	1.35	1.08		
LC5	Traffic loads| TS| Tram present	0.8	1.35	1.35	1.08		
LC6	Traffic load| UDL| Tram absent	0.8	1.35			1.35	
LC7	Traffic loads| TS| Tram absent	0.8	1.35			1.35	
LC8	Tram loading| TS	0.8	1.45	1.16	1.45		
LC9	Pedestrian loads| Crowd loading	0.8	1.35				1.35
LC10	Pedestrian loads| Loads on designated locations	0.8	1.35	1.08	1.08	1.08	

5.7 SCIA calculation model

As with the earlier C50/60 design, the UHPC bridge is modelled in SCIA Engineer as a 2D orthotropic plate. This way the transverse action of all girders combined can be modelled in a good way. With this model the internal forces caused by the loads on the bridge will be determined. The self-weight will be left out, because the 2D model will be inputted as a plate. So the self-weight calculated will not be correct. Using the correct orthotropic parameters will still give the correct internal forces, caused by loads other than the self-weight. Furthermore in SCIA, results in 2D are usually given per meter width. So the governing internal forces can easily be transformed to give results for one girder. But in this case the girder has a width of 1 meter so the results from SCIA are directly the correct moments for one box beam. When the self-weight is added of one girder, which can easily be determined by hand, the total internal forces in one girder can be determined. With these internal forces a safety check can be performed for one girder. The aforementioned orthotropic parameters are calculated with a Mathcad sheet, which can be found in appendix E.6.

The bridge is modelled as a simply supported bridge. In reality the amount of supports on each side will be the same as the amount of girders. Each girder is 1.0m wide. The bridge is 30m wide, so this results in a total of 30 girders. So in the model 30 internal nodes are placed on each side, which represent the location of the supports. The locations of the support in the model are determined by taking the centre location of each girder (right in the middle). All supports are fixed in the vertical Z direction. On X=0, one support, which is located in the middle of the transverse (Y) span, is also fixed in X and Y direction, while the support parallel to this one is fixed in Y direction. This provides stability in the structure and it will not cause strange results, which could occur if on one side of the span all support nodes are made fixed in all directions. But in this case only vertical loads are applied so the additional fixations in X and Y direction on one side would not influence the results. In Figure 5-2 the SCIA model is shown.

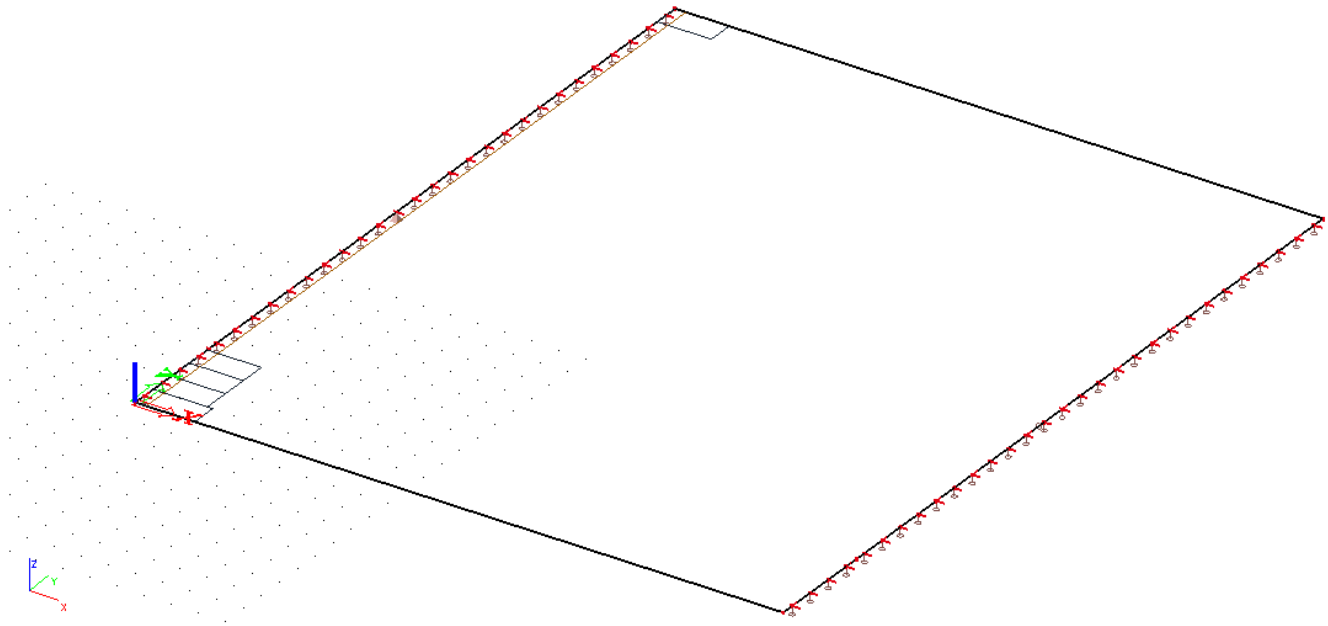

Figure 5-2: SCIA 2D model of C170/200

Because vehicles and trams constantly cross the bridge, these are defined as variable loads. In the model the traffic and tram loads are defined as mobile loads. Because they are defined as mobile loads the program can determine at which position of the load, across the length of the bridge, is the governing one for the bending moments, Shear force etc. These mobile loads will be combined with the other, static loads to determine the maximum internal forces on the bridge.

Furthermore, a section is placed close to the support and an averaging strip is placed at the location where the highest shear forces could be present. This is necessary, because the support nodes will result in very high unrealistic values for the shear force. The strip will average the peak points out over a certain length (which is taken 4d according to RBK 1.1) to give more realistic values. Then a section is placed at a distance d from the support edge, in order to not take a certain value right at the edge. The combination of a section and an averaging strip will provide a shear force value that is realistic and can be used for further calculations.

A full report on the model (such as coordinates, loads, etc.) and also the results from the model can be found in the engineering report in appendix E.

5.8 Results SCIA Engineer

Presented here are the internal forces necessary to perform the safety checks in ULS. The results are all from the ULS:

For bending moment resistance check:
mxD^-: 1712.15 kNm/m

For shear and [torsion + shear] safety check
mxy: 317.09 kNm/m (When torsion is governing)
116.75 kNm/m (When shear is governing)

vx: 235.94 kN/m (When torsion is governing)
584.56 kN/m (When shear is governing)
For transverse moment check
myD^-: 332.06 kNm/m
myD^+ 303.09 kNm/m

The presented values will be used for the safety checks. However these values are only based on the loads working on the bridge. Here no self-weight and no prestressing is included yet. These have to be added separately.

5.9 Prestress tendon profile

The beams will consist of pre-tensioned strands, as the beams are prefabricated. The tendon profile is shown in Figure 5-3. The tendon consists of straight and kinked strands. The kinked strands cause an upward force P_u at the deviation points. This point is at a distance 'a' from the support. The kinked strands are placed in the webs. The strands will be placed as high as possible to ensure a high upward force. This force slightly reduces the total shear force. Most of the strands will be placed in the bottom flange. This means that the fictitious tendon (or the gravity point) does not coincide with the neutral axis (dashed line). So these will create a moment at the heads due to eccentricity, so a capacity check at the support has to be made to make sure the structure can take the moments.

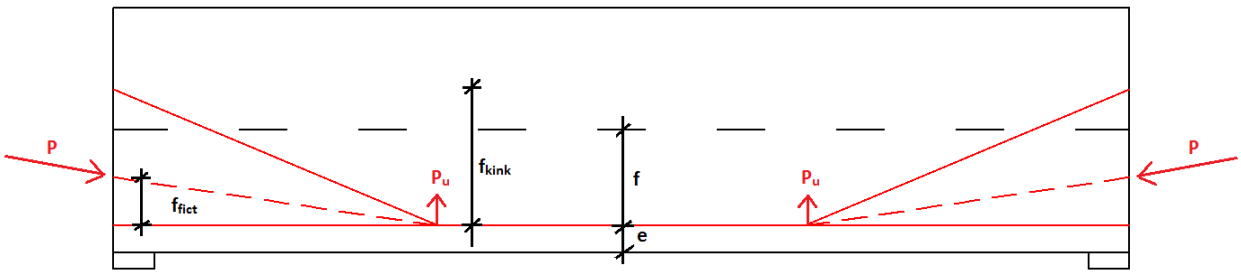

Figure 5-3: Tendon profile pre-tensioned strands

Distance strands from bottom fibre:	e = 0.066mm
Amount of kinked strands per web:	4 strands
Drape of all strands:	$f = z_b - e = 0.243m$
Distance deviation points from supports:	$a = (1/3)*L = 8m$
Drape of kinked strands:	$f_{kink} = 0.0343m$
Upward prestress force:	$P_u = P_{kink} * \sin \alpha_{kink} \approx P_{kink} * (f_{kink}/a)$ or $P*(f_{fict}/a)$
Bending moment in mid span:	$M_{p,mid} = P*f$

The prestress force is determined by taking a couple of requirements into account that concern stresses in the concrete. These requirements need to be applied in the governing cross section (cross section with highest bending moment). Here that is in the middle of the beam. These requirements are the same as the requirements used in paragraph 3.8:

$$t = 0 \text{ at top fibre: } -\frac{P_{m0}}{A_c} + \frac{M_{p,0}}{W_{ct}} - \frac{M_g}{W_{ct}} \leq 0$$

$$t = 0 \text{ at bottom fibre: } -\frac{P_{m0}}{A_c} - \frac{M_{p,0}}{W_{cb}} + \frac{M_g}{W_{cb}} \geq -0.6 * f_{ck}$$

$$t = \infty \text{ at bottom fibre: } -\frac{P_{m\infty}}{A_c} - \frac{M_{p,\infty}}{W_{cb}} + \frac{M_{tot}}{W_{cb}} \leq 0$$

Assumed is a total loss of 20% so $P_{m\infty} = 0.8*P_{m0}$. After the prestress force is determined with the three requirements, the actual losses (direct and time dependent losses) have to be determined and checked if the assumption of a 20% loss is on the safe side.

The moment due to all static loads now becomes:
$M_g = 1020.53$ kNm
The moment due to the variable loads is:
$M_q = 1027.95$ kNm
This results in a total moment of:
$M_{tot} = 2048.48$ kNm

The moments and requirements result in a minimum amount of 35 strands, which have a total cross sectional area of $35*139 = 4685$ mm^2. This results in a force of $P_{m0} = 6786.675$ kN.
The moment caused by the prestressing force is:
$M_{p\infty} = P_{m\infty}*f = 1319.79$ kNm
The stress caused by the prestress force during $t=\infty$ in the concrete is:
$\sigma_{cp} = 0.8*P_{mo}/A_c = 14.41$ N/mm^2.

A more detailed calculation of the prestressing force is found in appendix E.8 and E.9

5.10 Prestressing Losses

The required amount of strands and also the resulting prestress force are determined. Now the actual losses have to be determined. The percentage of the total losses should be lower than the assumed losses of 20%, so that the determined prestress force is on the save side. If this is not the case the amount of strands has to be determined again with the correct percentage of losses.
The losses can be divided in direct and time dependent losses.

5.10.1 Direct losses

For pre-tensioned strands the elastic shortening is part of the direct losses. When the strands are released after tensioning the strands will shorten elastically. The result is that the stresses and forces in these strands decrease. Also occurring is concentrated friction at the kink points of the strands but these can be neglected when looking at the big picture.

5.10.1.1 Losses due to elastic deformation

The loss of force in one strand due to elastic shortening is[11]:

$$\Delta P_{el} = A_p * E_p * \frac{\Delta\sigma_c(t)}{E_{cm}(t)}$$

And $\Delta\sigma_c(t)$ being the variation of stress at the centre of gravity of the strands at time t:

$$\Delta\sigma_c(t) = \frac{P_{m0}}{A_c} * [1 + \frac{e_p^2 * A_c}{I_c}]$$

To compensate the loss in forces due to elastic shortening it is allowed to overstress the strands, provided that the stress stays under the maximum allowed stress $\sigma_{p,max}$ = 1488 N/mm^2.
The extra stress per strand needed to compensate the loss is: $\sigma_{extra} = \Delta P_{el}/A_p$ = 4.78 N/mm^2. So the total stress applied becomes $\sigma_{pm0} + \sigma_{extra}$ = 1399.78 N/mm^2 which is far below the maximum allowed stress.

5.10.2 Time dependent losses

Certain losses appear during the life span of the structure. These are shrinkage and creep of the concrete and relaxation of the strands. All these losses can be combined in one formula[12] which is given in NEN-EN-1992-1-1:

$$\Delta P_{c+s+r} = A_p \Delta\sigma_{p,c+s+r} = A_p \frac{\varepsilon_{cs} E_p + 0{,}8\Delta\sigma_{pr} + \frac{E_p}{E_{cm}} \varphi(t,t_0).\sigma_{c,QP}}{1 + \frac{E_p}{E_{cm}} \frac{A_p}{A_c}(1 + \frac{A_c}{I_c} z_{cp}^2)[1 + 0{,}8\,\varphi(t,t_0)]}$$

The shrinkage strain and creep-coefficient are not allowed to be determined conform the Eurocode, because UHPC behaves differently than ordinary concrete. There is not yet one uniform method to determine the shrinkage and creep. Therefore the AFGC recommendations give recommended values for shrinkage and creep to use in calculations[13]. The values that are recommended are:

	Shrinkage strain	**Creep coefficient**
Without heat treatment:	Total shrinkage of $\varepsilon_{cs} = \varepsilon_{cd} + \varepsilon_{ca}$ = 550 + 150 = 700*10^{-6}	Φ(t,t0) = 0.8
Type 1 heat treatment:	Total shrinkage of ε_{cs} = 550*10^{-6}	Φ(t,t0) = 0.4
Type 2 heat treatment:	Only autogenous shrinkage of ε_{ca} = 550*10^{-6} during treatment. Afterwards no shrinkage	Φ(t,t0) = 0.2

One thing that can be noticed is that the shrinkage for UHPC is pretty high compared to other types of concrete. This is caused by the high autogenous shrinkage that is again caused by a very low water cement ratio. The heat treatments result in most of the shrinkage happening early on so that during the serviceability stage of the structure there is hardly to no shrinkage occurring. Assumed is that at least type1 heat treatment is going to be used, as heat treatment should actually be a part of producing UHPC. In Appendix C more information can be found about shrinkage and creep in UHPC.

[11] NEN-EN-1992-1-1 formula 5.44
[12] NEN-EN-1992-1-1 formula 5.46
[13] AFGC 2013 paragraph 1.9

When all the parameters are filled in the formula for the time dependent losses the total stress loss due to time dependent losses becomes: $\Delta\sigma_{p,c+s+r}$ = 170.58 N/mm^2. This is **12.23%** of σ_{pm0}, which is below the assumed loss of 20% so the assumption was on the safe side.

*Remark: When no heat treatment is used shrinkage becomes 700*10^{-6} and the creep factor 0.8. With these values the total losses would be around 16%, which is still lower than the assumed 20%.*

Because the actual losses are smaller than the assumed loss, the losses will be set to 16%. Putting it to 16% results in a smaller amount of strands, while still taking unforeseen losses (such as friction at the deviators) into account and also the fact that no heat treatment could be applied. With the losses being 16% the new minimum required amount strands becomes 33 (instead of 35).
The total area of the strands is now: A_p = 4587 mm^2 (Pm0 = 6398.87 kN).
The prestress force delivers a vertical force at the deviators P_u, which is equal to: $P_{u0} = P_{m0}*(f_{fict}/a)$ = 66.53kN and $P_{u\infty}$=55.88kN.

5.11 Bending moment capacity

The full calculation is found in appendix E.11

5.11.1 Hand calculation

It is a requirement that the bending moment resistance is higher than the design bending moment: $M_{Rd} > M_{Ed}$.

$M_{Ed} = \gamma_g * M_g + \gamma_q * M_q - \gamma_p * M_p$

It is possible that the eventual governing design bending moment is found at the construction stage (t=0) and perhaps at the support, because the prestressing causes a moment there.. So the bending moment will be determined for the whole span at multiple stages: These stages and the bending moments are:

- t=0 only self weight: $M_{Ed} = M_{self} - M_p$
- t=0 permanent loads: $M_{Ed} = M_{perm} - M_p$
- t=∞ all loads + torsion: $M_{Ed} = M_{perm} + M_{var} - M_p$

In Figure 5-4 the moment lines are shown, for multiple stages. The governing M_{Ed} = 1259.62 kNm. The moment at the support is 1023.26 kNm. Technically right at the support the prestress force is also zero. The force has a certain transmission length, where after the force is fully transferred in the concrete.

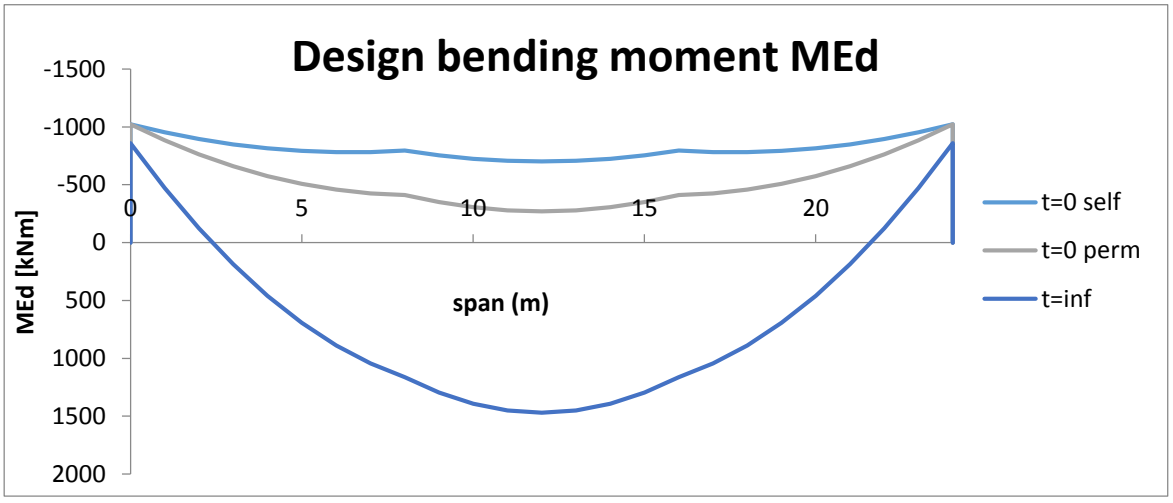

Figure 5-4: Design bending moment at multiple stages

The moment capacity should be high enough to resist the determined $M_{Ed.}$ When the moment capacity of a UHPC structure needs to be determined, a slight different approach has to be taken than when ordinary concrete is used. The main difference is the inclusion of the tensile capacity of UHPC. This gives an additional internal tensile force in the structure. To determine M_{Rd} one has to assume equilibrium of internal forces in the cross section and with that assumption determine M_{Rd}. The general case of internal forces is seen in Figure 5-5.

For equilibrium the following statement needs to hold true: $N_c - N_t = P_{m\infty} + \Delta N_p + N_s$. The last term N_s is removed, as there is no bending reinforcement applied.

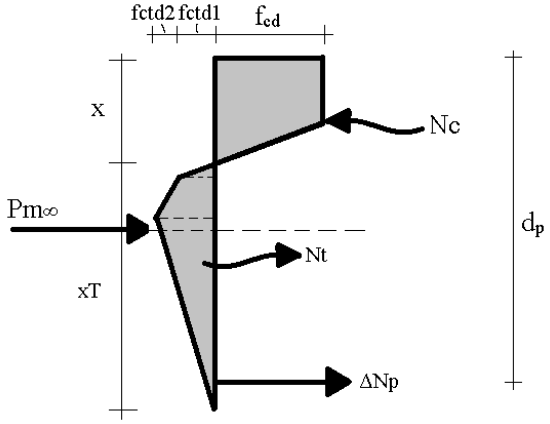

Figure 5-5: Equilibrium of internal forces

The stress-strain relationship assumed for the calculations is seen in Figure 5-6. The stress strain diagram is based on the derived diagram in Cement article “Rekenmodel VVUHSB” [4]. The diagram in the article is again derived from the one in the AFGC Recommendations. Same goes for the values for the strain limits:

ε_{c3} = 2.3‰

ε_{cu3} = 2.6‰

$\varepsilon_{ct} = f_{ctd,1}/E_c$ =0.10667 ‰

$\varepsilon_{u0,3} = \varepsilon_{ct}$ + w0.3(=0.3mm)/ l_c(=2H/3) = 0.85667‰

$\varepsilon_{ctu} = l_f$ (=13mm)/4l_c = 8.125‰

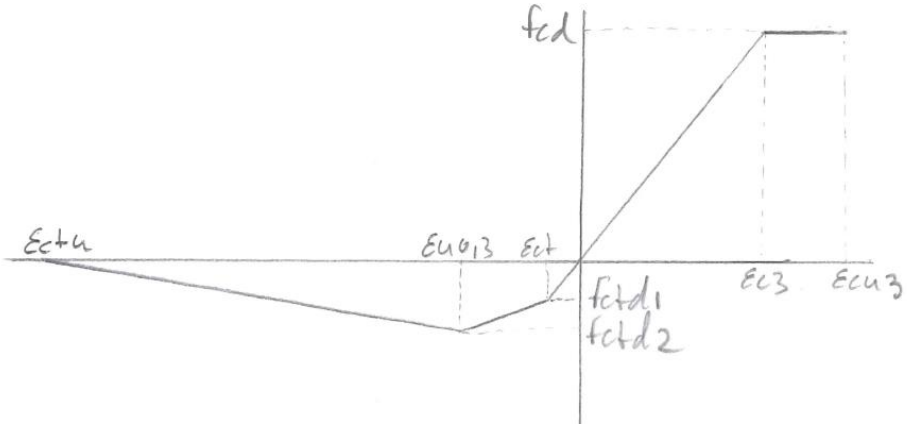

Figure 5-6: Stress diagram UHPC

Because a box girder is used, the width is not constant over the height. It is therefore possible that the compression zone and tension zone do not have a uniform width over their height. Multiple situations can occur of how the zones are divided over the height of the section. These derivations can be found in appendix H. The moment capacity, while taking the multiple situations into account, has been determined with a maple sheet, which is found in appendix E.11.1.

The moment capacity is:
M_{Rd} = 2319 kNm with x = 143.69mm

Unity Check: M_{Ed}/M_{Rd} = 1259.62/2319 = 0.543 → OK
The moment capacity is more than enough to resist the working moments on the structure.

5.11.2 Parametric study Moment capacity

For determining the moment capacity it was assumed that the ultimate tensile strain limit (ε_{ctu}) is reached. In reality this is often not the case for UHPC structures. It is also possible that during a stage of loading, where the ultimate compressive strain limit (ε_{cu3}) is not yet reached, that the total tensile capacity is higher than when ε_{cu3} reached. This could possibly result in a higher moment capacity. So it is necessary to perform a parametric study, where at different stages of loading (so basically at different values of the compressive strain ε_c) the moment capacity is determined. For this a Maple sheet is developed which is found in appendix E.11.2. The sheet is based on the following procedure:

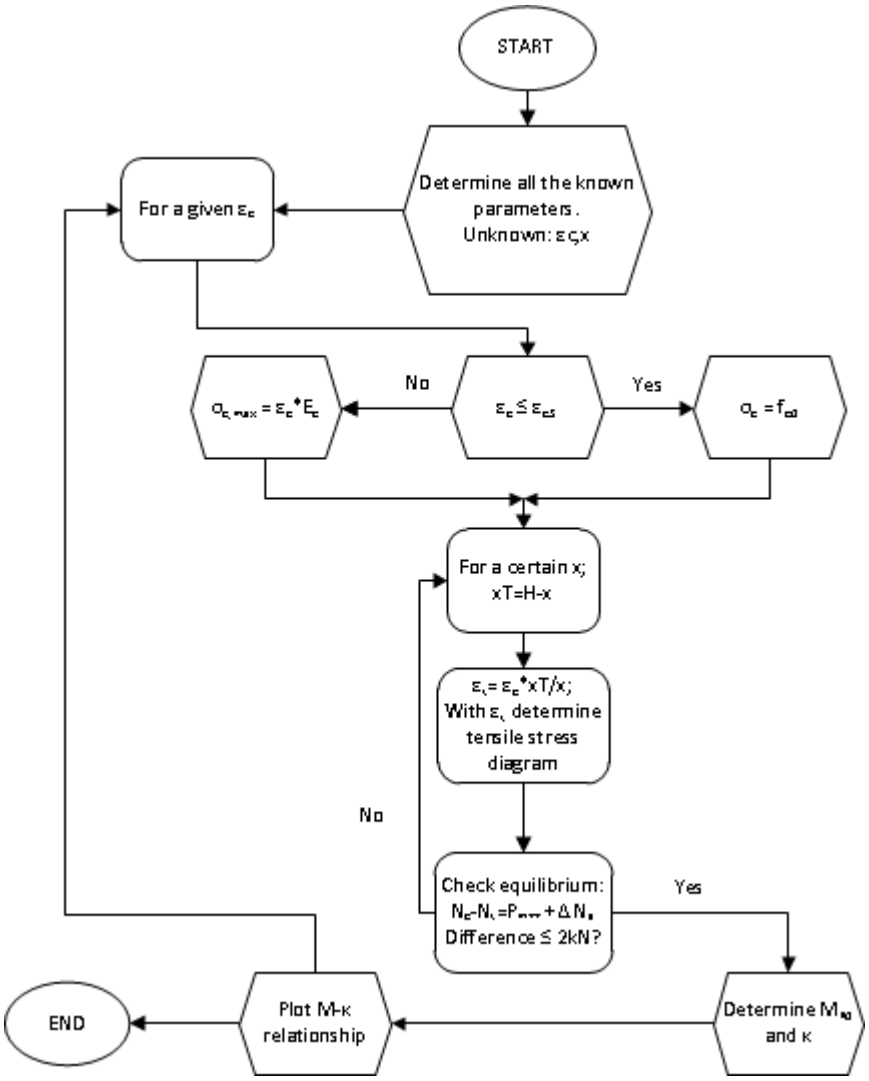

So a certain value for ε_c is assigned. With this value a check needs to be made if the strain limit ε_{c3} is reached. On basis of this check the maximum compressive stress for the given ε_c can be determined. Then with trial and error the correct x needs to be determined. Assigning a value for x will subsequently determine the tension zone height xT and thus the tensile strain ε_t in the bottom fibre. This tensile strain will determine the tensile stress diagram.
That is done by checking if $\varepsilon_t \leq \varepsilon_{ct}$ or $\varepsilon_{ct} \leq \varepsilon_t \leq \varepsilon_{u0,3}$ or $\varepsilon_{u0,3} \leq \varepsilon_t \leq \varepsilon_{ctu}$. With the tensile strain in one of these three areas, the stress diagram changes accordingly. The internal forces are determined and checked if they are in equilibrium. In this case that will be where the difference between the compression and tension forces is equal or lower than 2 kN. This will still give an accurate x value, while keeping the calculation time low.

The results of the procedure are shown in an M-κ diagram, which is seen in Figure 5-7.

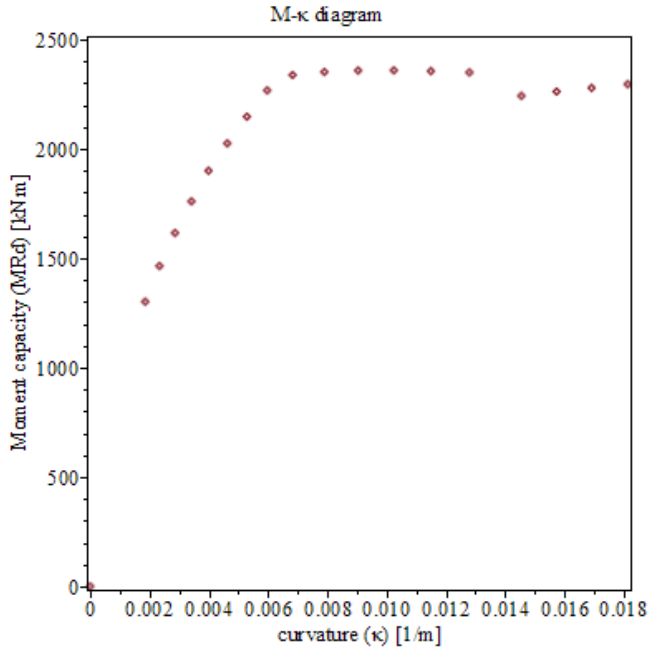

Figure 5-7: M-κ diagram UHPC

The highest moment capacity is found at ε_c = 2.0‰. Here a moment capacity of **M_{Rd} = 2358.5 kNm** is found and x_u of 195.2 mm The value for M_{Rd} determined in the parametric study is around 39 kNm higher than the value calculated earlier, where assumed was that $\varepsilon_c = \varepsilon_{c3}$ and $\varepsilon_t = \varepsilon_{ctu}$. In the parametric study the moment capacity for $\varepsilon_c = \varepsilon_{cu3}$ = 2.6‰ was M_{Rd} = 2295.3 kNm. The difference between this value and the earlier determined value is around 1.0% so the procedure of the parametric study is pretty accurate.

The new unity check: UC = 1259.62 / 2358.5 = 0.534 → OK

The structure would already be one the safe side even without the new determined M_{Rd}. Now the structure is even safer concerning the moment capacity (not much safer though as the increase in moment is only 39 kNm).

It has to be remarked that in the parametric study it was not possible to find equilibrium below ε_c = 0.9‰. This is most likely because there is already a prestressing force and the internal compressive force is not able to compensate for this force, due to the low maximum compressive stress at a certain low ε_c value. In theory a compressive zone larger than the total height of the structure would be necessary, which is not possible in reality of course. In reality the pretress force already causes a certain strain in the structure. So the strain does not start at zero but at a value higher.

Another remark has to be made on the fact that the maximum moment capacity is reached earlier then when the compressive strain limit is reached. So in reality, when the bridge is loaded high enough, the bridge will most likely fail due to yielding of the prestressing strands, as the compressive limit has not been reached yet.

It also can be seen that in Figure 5-7 around $\kappa = 0.014\ m^{-1}$ there is a sudden drop in moment capacity. This most likely has to do with the fact that at the compressive strain that occurs around this curvature the compressive zone is for the first time completely in the top flange. So this probably causes an increase in the compression force and therefore the moment capacity decreases. Afterwards there is a rise in moment capacity again, because the compression zone keeps decreasing, while the tension zone increases.

Furthermore it is also possible that strain softening occurs instead of strain hardening. This can occur for example if during (not carefully) pouring of the concrete the positioning of the steel fibres is very negatively impacting the tensile behaviour. The stress diagram changes, which results in no strength increase between ε_{ct} and $\varepsilon_{u0,3}$ (Figure 5-8).

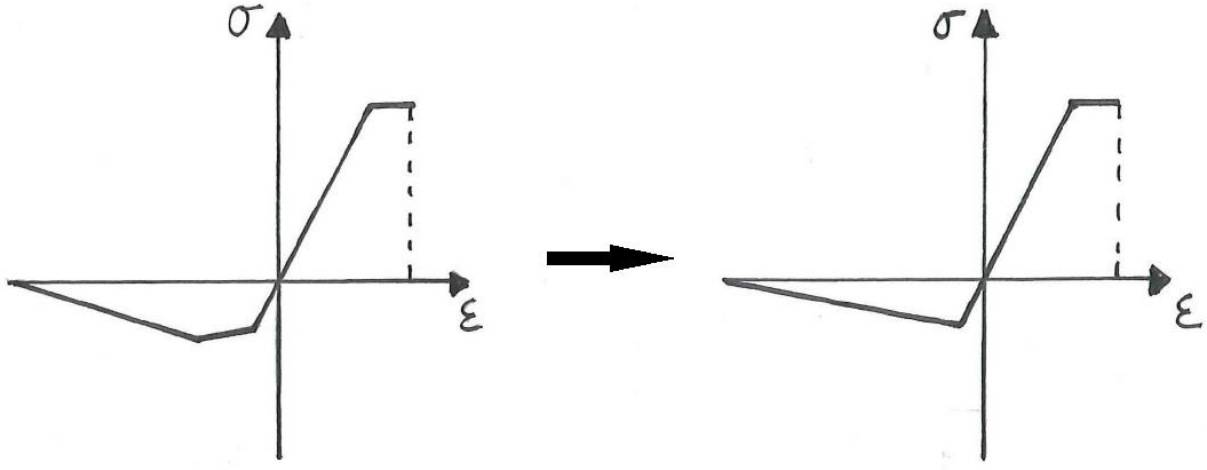

Figure 5-8: From strain hardening to strain softening

The tensile capacity decreases, which subsequently leads to a decrease in moment capacity.
For this design in case of softening the moment capacity becomes M_{Rd} = 2259 kNm (determined in appendix E.11.2). In the original case M_{Rd} = 2319 kNm. The reduction in capacity is 60 kNm. This is not a dramatic decrease in moment capacity. This is most likely due to the fact that the prestressing provides the largest contribution in moment capacity, so a decrease in tensile capacity will not have a large influence in this case. And the moment capacity in softening is still much higher than the design bending moment M_{Ed}.

Remark: Because the difference in results from the hand calculation and parametric study is not high, the hand calculation method will be used in further calculations (optimization or other designs). This is allowed because the parametric study has shown that in reality a higher moment capacity can be found if it is not assumed that the maximum tensile strain is reached

5.12 Rotational capacity

The bending moment resistance suffices. But it is also important that the structure has enough rotational capacity in order to give enough warning before failure. For this the following requirement has to be met[14]:

$x_u/d \leq 0.497$

With x = 195.21 (result from parametric study. Hand calculation results in a lower x)

$x/d = 0.365 < 0.497$

So the structure has enough rotational capacity

5.13 Shear and torsion capacity

The detailed calculations are found in appendix E.13

5.13.1 Shear

It is a requirement that the shear resistance is higher then the design shear force:
$V_{Rd} > V_d$
The design shear force is the sum of the shear force caused by bending moments and the shear force caused by torsional moments:
$V_d = V_{Ed} + V_{Td}$
Two cases have to be investigated, of which the most governing one will be used:

Situation 1. Location of highest torsional moment in structure
Situation 2. Location of highest shear force in structure

For both locations the internal forces were calculated and the results were presented in paragraph 5.8. These were:
Mxy = T_{Ed}:

Situation 1. 317.09 kNm --> V_{Td} = 184.35 kN
Situation 2. 116.75 kNm --> V_{Td} = 67.88 kN

Vx (without self-weight and prestressing):

Situation 1. 235.94 kN
Situation 2. 584.56 kN

The shear force V_{Td} due to T_{Ed} is calculated with: $V_{Td} = h_m * T_{Ed}/(2*A_k)$.

The governing total shear force taken from SCIA is the one where the sum of V_x and V_{Td} is the largest. This is the case for situation 2, where V_{Ed} = 652.44 kN. The shear force over the length of the beam needs to be determined at multiple stages. These stage and the shear forces are:

- t=0 only self weight: $V_{Ed} = V_{self} - P_{u0}$
- t=0 permanent loads: $V_{Ed} = V_{perm} - P_{u0}$
- t=∞ all loads + torsion: $V_{Ed} = V_{perm} + V_{var} - P_{u\infty}$

For t=∞ the shear force is added with V_{Td}. Assumed is that V_{Td} is constant over the length of the beam. The shear force lines are seen in Figure 5-9.

[14] NEN-EN-1992-1-1 Dutch NB cl.5.5

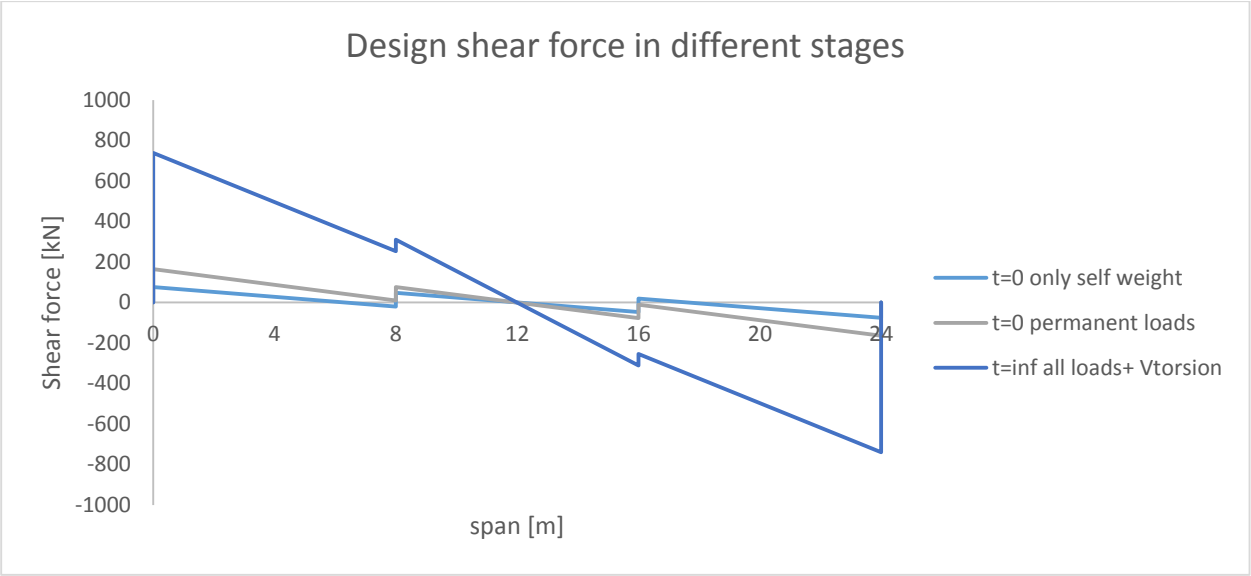

Figure 5-9: Shear force line at multiple stages

The governing shear force V_{Ed} = 738.9 kN at t=∞. The shear resistance has to be high enough to resist this force.

The shear resistance for a UHPC structure is determined in a different way than the resistance for a NSC structure. This is mainly due to the inclusion of steel fibres in UHPC. AFGC gives a procedure to determine the shear resistance. It states that the shear resistance is equal to the smaller values of the two parameters V_{Rd} (tensile resistance of ties in concrete) and $V_{Rd,max}$ (resistance of compressive struts).

$V_{Rd} = V_{Rd,c} + V_{Rd,f} + V_{Rd,s}$

Where:
$V_{Rd,c}$ = the contribution of the concrete to the shear capacity
$V_{Rd,f}$ = the contribution of the steel fibres to the shear capacity
$V_{Rd,s}$ = the contribution of the shear reinforcement to the shear capacity

Because of the behaviour of the steel fibres in tension, it is allowed to view it seperately from the concrete, as if it is serving as reinforcement. Shear reinforcement will not be applied (unless the shear capacity is not enough to resist the design shear force), so $V_{Rd} = V_{Rd,c} + V_{Rd,f}$.

For a prestressed section the shear resistance $V_{Rd,c}$ is[15]:
$V_{Rd,c}$ = $0.24*(1/\gamma_{cf}\gamma_E)*k*f_{ck}^{1/2} * b_w*z$ = **351.53 kN**

The contribution of the steel fibres can be determined with[16]:
$V_{Rd,f} = A_{fv}*\sigma_{Rd,f}/\tan\theta$ = 1088.71 kN which is much higher than $V_{Rd,c}$.

Now with both terms determined the shear capacity can be determined:
V_{Rd} = 1440.24 kN

Unity Check: V_{Ed}/V_{Rd} = 738.9/1440.24 = 0.513→ OK

[15] AFGC2013 paragrapgh 2.4 section 6.2(1)
[16] AFGC2013 paragrapgh 2.4 section 6.2(2)

However V_{Ed} is larger than the concrete contribution $V_{Rd,c}$. Theoretically this part may not be taken into account because the concrete capacity is exceeded. So only the contribution of steel fibres may be taken into account (this assumption will hold true during other design stages as well). Now for the unity check:

Unity Check = 738.9/1088.71 = 0.679 → OK

The shear capacity is more than enough to resist the design shear force, also if only $V_{Rd,f}$ is taken into account. It is obvious that the steel fibres contribute the most to the shear capacity. Moreover, the structure would not have enough capacity were it not for the steel fibres. So the inclusion of steel fibres works very positively for the shear resistance.

However it is possible that the concrete shows strain softening behaviour instead of strain hardening (Figure 5-8). If there would be strain softening, then the new shear capacity (without the concrete part) becomes:

V_{Rd} = 830.24 kN and UC = 0.89.

The change from strain hardening to softening has a large influence on the shear capacity. More than for the moment capacity. The reduction is around 250 kN, which is quite a lot. But in spite of the large decrease, there is still enough capacity to resist the design shear force, as the unity check shows.

5.13.2 Torsion

There should be enough torsional resistance in the structure against working torsion moments:
$T_{Ed} \leq T_{Rd}$
If this is not the case reinforcement has to be applied. The torsion resistance can be determined with:
$T_{Rd} = f_{ctd,1} * t_{ef} * 2 * A_k$

The result is: **T_{Rd} = 542.6 kNm**

Unity Check: T_{Ed}/T_{Rd} = 317.09/542.6 = 0.584 → OK

The torsional moment resistance (without taking the effect of the fibres into account) is sufficient to resist the working torsional moments, so no torsional reinforcement needs to be applied.

5.13.3 Shear + torsion

It is also required that the combination of shear forces and torsional moments is verified. The structure should be able to resist these forces. The requirement for this states:
$T_{Ed}/T_{Rd,max} + V_{Ed}/V_{Rd,max} \leq 1.0$
The requirement means that the capacity of the concrete struts has to be sufficient to resist the loads on the structure. Here the two previous situations (shear governing or torsion governing) are going to be investigated as well.

First $T_{Rd,max}$[17] and $V_{Rd,max}$[18] have to be determined:
$T_{Rd,max} = 2 * 1.14 * (\alpha_{cc}/\gamma_c) * f_{ck}^{2/3} * 2A_k * t_{ef} * \sin\theta\cos\theta$ = 1747 kNm
$V_{Rd,max} = 2 * 1.14 * (\alpha_{cc}/\gamma_c) * b_w * z * f_{ck}^{2/3} / (\cot\theta + \tan\theta)$ = 2311 kNm

[17] AFGC2013 paragrapgh 2.4 section 6.3.2(4)
[18] AFGC2013 paragrapgh 2.4 section 6.2(4)

Unity check:
Situation 1: $T_{Ed}/T_{Rd,max} + V_{Ed}/V_{Rd,max}$ = 317.09/1747 + 322.41/2311 = 0.321 → OK
Situation 2: $T_{Ed}/T_{Rd,max} + V_{Ed}/V_{Rd,max}$ = 116.75/1747 + 671.02/2311 = 0.357 → OK
For both situations the concrete struts suffice.

5.13.4 Shear resistance according to Model Code

In the recent version of the fib Model Code for Concrete Structures (MC2010) the determination of the shear resistance (both V_{Rd} and $V_{Rd,max}$) is done in a different way than how it is described in the Eurocode. Also described is the determination of the shear resistance, when steel fibres are included in the concrete. It is wise to compare the results from the Model Code with the results from AFGC. Usually the Model Code is considered more reliable than a certain guideline such as the AFGC.
According to paragraph 7.7.3.2 of MC2010 the shear resistance is determined with:

$$V_{Rd,F} = \frac{1}{\gamma_F}\left(k_v\sqrt{f_{ck}} + k_f f_{Ftuk}\cot\theta\right) z * b_w$$

The term $k_v * \sqrt{f_{ck}}$ represents the contribution of the concrete and the term $k_f * f_{Ftuk} * \cot\theta$ represents the contribution of the steel fibres.
k_f=0.8
f_{Ftuk} is the ultimate residual tensile strength(formula 5.6-6 in MC2010):
$f_{Ftuk} = 0.45f_{R1} – (w_u/CMOD_3)(0.45f_{R1}-0.5f_{R3}+0.2f_{R1})$
where f_{R1} and f_{R3} are determined with experiments. Since it is not possible to perform experiments it is safe to assumed that $f_{Ftuk} = f_{ctk}$ if the concrete shows strain hardening behaviour.

The term for the steel fibres is pretty much the same as in AFGC ($=\sigma_{Rd,f}/\tan\theta$). Only the residual stresses are defined differently. The factor k_f=0.8 is already incorporated in $\sigma_{Rd,f}$ as 1/K = 1/1.25=0.8. Moreover if for $\sigma_{Rd,f}$ is assumed f_{ctk} than the result for the steel fibre contribution would be the same for AFGC and MC2010. The main difference lies in the concrete part.

*Note: In paragraph 5.13.1 $\sigma_{Rd,f}$ is determined the way it is because f_{ctk} and σ(w=0.3) are both known values. However the terms necessary for determining f_{Ftuk} are not known and not possible to determine for this thesis. Therefore in the Model Code formula $f_{Ftuk} = f_{ctk}$. If in paragraph 5.13.1 $\sigma_{Rd,f}$ would be set to [1/(K*γf)]*fctk then obivously $V_{Rd,f}$ would be lower and the results of both methods for the steel fibre part would be the same.*

If assumed is $f_{Ftuk} = f_{ctk} = 8N/mm^2$ then the shear capacity becomes:
$V_{Rd,F}$ = 1188.93 kN.

The total shear resistance according to AFGC was: V_{Rd} = 1440.24 kN

The total value according to AFGC is higher because of the higher concrete part. If in MC2010 the fibre part would be left out then only the concrete part would remain and: $V_{Rd,c}$ = 269.74 kN.
And AFGC: $V_{Rd,c}$ = 351.53 kN. So around 70 kN higher. This is most likely due to the k factor in AFGC which directly takes the compression force of prestressing into account.
However in paragraph 5.13.1 it is assumed eventually that when $V_{Ed} > V_{Rd,c}$ then $V_{Rd} = V_{Rd,f} + V_{Rd,s}$ instead of $V_{Rd,c} + V_{Rd,f} + V_{Rd,s}$ (if additional shear reinforcemeent would be used).

In the Model Code however is stated that (if shear reinforcement would be used) $V_{Rd} = V_{Rd,F} + V_{Rd,s}$. This means that:
MC2010 => V_{Rd} = 1188.93kN
AFGC => V_{Rd} = 1088.71 kN

So considering the assumptions made the model code would in this case provide a higher shear resistance than the AFGC. So the result from AFGC is on the safe side.

$V_{Rd,max}$ is calculated in a different way as well in MC2010. The maximum shear resistance is determined with[19]:

$$\mathbf{V_{Rd,max}} = k_c \frac{f_{ck}}{\gamma_c} b_w z * \sin\theta\cos\theta = \mathbf{2393.5\ kN}$$

This value is close to the $V_{Rd,max}$ calculated according to AFGC (=2311 kN). The one from AFGC is slightly lower, because θ is taken 30 (minimum acccording to AFGC) instead of 32 (minimum according to the model code). So AFGC gives a reliable result (if assumed is that the Model Code gives the most reliable result).

To make it clear for further design steps (optmization) the AFGC will still be used for determination of the shear resistance

5.14 Transverse direction (moments)

5.14.1 Design transverse moment

Transverse moments also occur in the structure. It is necessary to validate if the box girder can resist these moments. Transverse prestressing strands, which are placed in the top flange, can benefit the transverse moment capacity. These strands are also necessary to connect all the box girders together in order for the bridge to have transverse action. Only the top flange can contribute to the transverse moment capacity, together with the joints. Assumed is that a tendon of 7φ15.7 strands with quality Y1860H are used which are placed with a centre spacing of 1000 mm. The governing section is in the joint: The joint is not made of UHPC and it has no other reinforcement in the concrete, except for the transverse prestressing. It has to be verified if the joint can resist the design transverse moment. Assumed is that the joint is made of C90/105. For box girders made out of normal or high strength concrete, a concrete strength of C35/45 is used usually, but here it is chosen to make the joint out of high strength concrete, because the bridge itself is made out of UHPC. This way the difference in strength between box girder and joint will not be too high. The joint will have a thickness of 250 mm.

It is expected that the highest transverse moment is located right around the middle of the bridge. The highest moment should be found for the combination, where the loads are placed to give the highest transverse moments. In SCIA the result for the transverse moment myD^- was 322.06 kNm. However this (quite large) moment is found near the corners of the bridge. This can be explained by the fact that SCIA calculates myD^- by stating: $myD^- = my + |mxy|$. As the results showed in paragraph 5.8, mxy = 317.09 kNm. This results in a high myD^-, which occurs in the same area as the highest torsional moment mxy. But the problem is that SCIA does not link the torsional moments with the given orthotropic parameters. For a box girder the stiffness is much higher in the longitudinal direction than in the transverse direction. So this also means that mxy ≠ myx. Therefore a factor K should be applied based on the orthotropy of a box girder:

$K_x = 2*D_{xy}/(D_{xy}+D_{yx})$
$K_y = 2*D_{yx}/(D_{xy}+D_{yx})$

This has been done in the Mathcad sheet for determining the orthotropic parameters. The resulting factors are:
$K_x = 1.948$
$K_y = 0.052$

[19] MC2010 formula 7.3-26

To calculate myD^- the following is used: $myD^- = my + K_y*mxy$. Finding m_y in the same node as where the highest mxy is and then applying the factor will lead to $myD^- = 34.53$ kNm. This is much lower than the given value of 322.06 kNm. If this procedure would be applied all over the structure one would find the highest myD^- in the middle of the bridge as expected. Here m_y is the largest and mxy is very low in value.
SCIA gives a value of $myD^- = 113.68$ kNm/m. This is the value that will be used for determining if the transverse moment capacity ($M_{Rd,y}$) is sufficient. The moment on the box girder is the sum of the global and local transverse moments. The local transverse moment is the result of the force of a single axle load from Load Model 1.
$M_{Ed,y} = myD^-*B_{centre,spacing}$=113.68 kNm. This is the global transverse moment. The global moment in the SLS state is: M_{SLS} =85.74 kNm.

The local moment is: $M_{Ed,local}$ = 46.84 kNm and $M_{SLS,local}$ = 26.05 kNm.

Because the placement of the axle loads for the local effects usually do not coincide with the placement of the axle loads for the global effects, the local effect may be reduced. A reduction of 25% is assumed. This results in a total transverse moment of:
ULS: $M_{Ed,tot}$ = 113.68+0.75*46.84 = 148.81 kNm
SLS: $M_{SLS,tot}$ = 85.74 +0.75*34.73 = 111.79 kNm

The transverse capacity is determined where the following equilibrium needs to hold true:
$N_c = P_{m\infty}$

The moment capacity becomes: **$M_{Rd,joint}$ = 140 kNm**

Unity Check: $M_{Ed,tot}/M_{Rd,joint}$ = 148.81/140 = 1.06 → NOT OK

There is not enough capacity. Increasing the thickness of the joint to 270mm results in a moment capacity of $M_{Rd,joint}$ = 152.45 kNm and UC=0.976. Now there is enough capacity.

For joints it is also important that there are no tensile stresses at the height of the prestressing strands. At this location the joint has to remain in compression at all times. This holds true for the SLS state. The stress at the height of the strands is:
σ = -4.61N/mm^2 so there is compression.

At the location of the duct the concrete has to be thickened internally to be able to fit the anchor and for enough space for the duct itself.

A more detailed calculation is found in appendix E.14.

5.15 Fitting of prestressing strands

The amount of strands has already been determined. The total amount is 33 strands. Four strands are placed in each web. This means there are 25 strands left to fit in the bottom flange. The area available in the bottom flange is 720mm (H-2*b_{web}). The strands will be placed in 2 layers of 13 and 12 strands. The determined cover (for inner and outer perimeter of box girder c=35.4mm) and the eccentricity need to be taken into account, when fitting the concrete. In the mid span the distance of the gravity point with regards to the bottom fibre should be the same as the determined eccentricity.

In Figure 5-10 and Figure 5-11 the cross section of the end span and mid span are shown respectively. In reality there is a hammerhead at the end span, but in the figure the extra solid part is left out. The horizontal and vertical centre-to-centre spacing are sufficient according to requirements ($2\varphi_{strand} + \varphi_{strand}$ in both directions). No further issues are present.

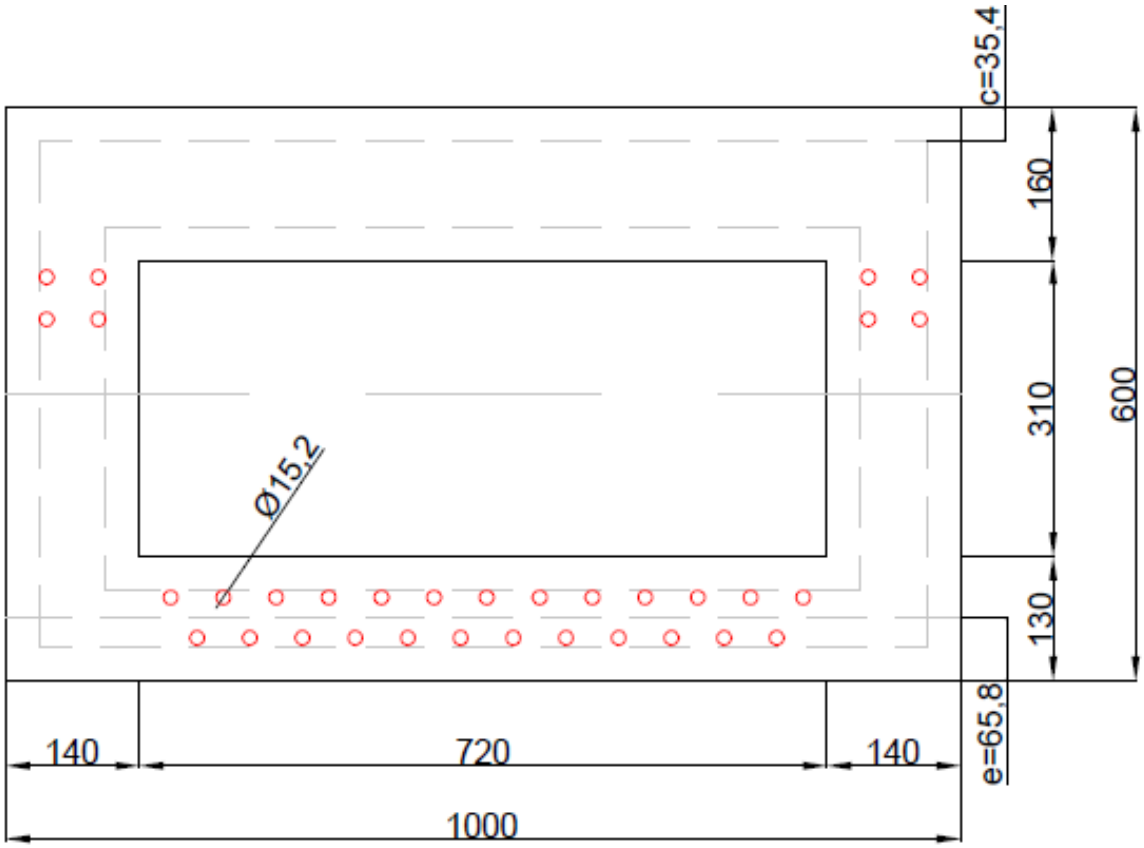

Figure 5-10: UHPC cross section at end span

In the mid span the strands meet the centre-to-centre spacing requirements for the centre to centre spacing in both horizontal and vertical direction. For the 25 strands in the bottom flange the diagonal centre-to-centre spacing is sufficient as well. No further issues are found in the mid span as well.

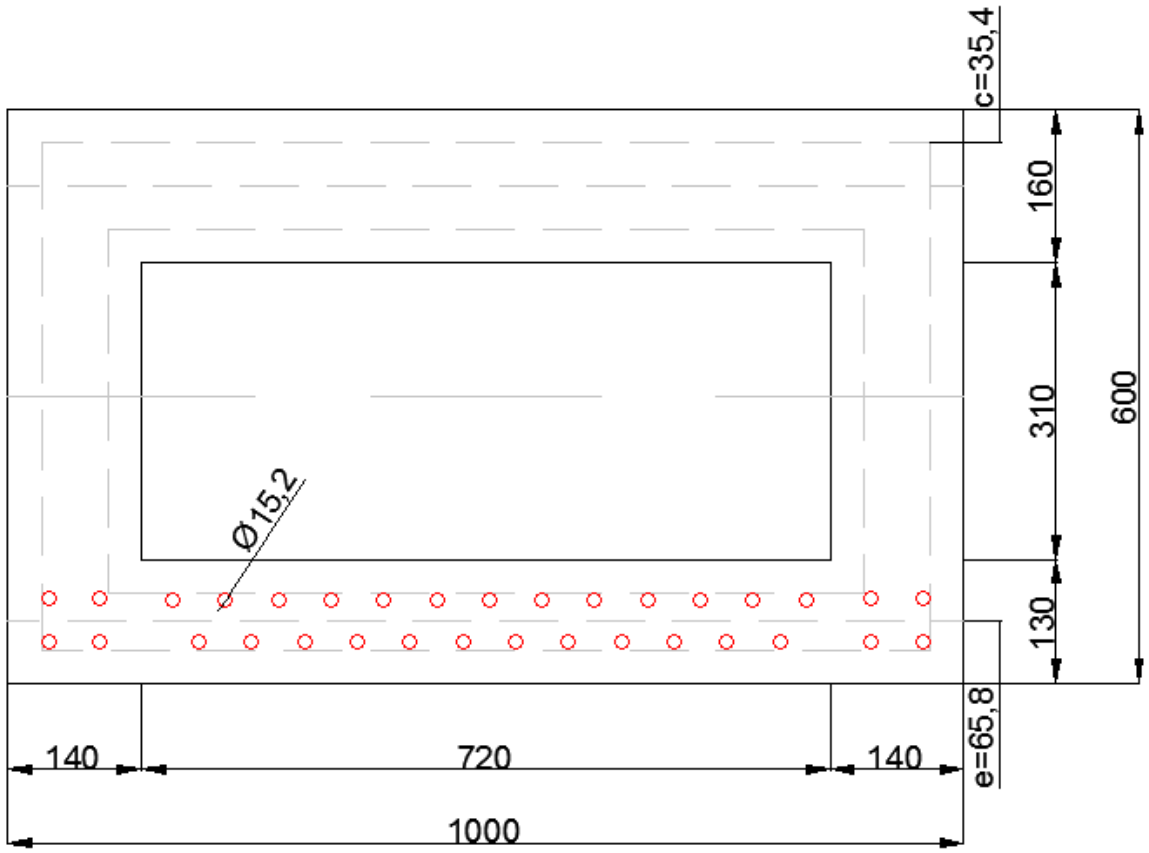

Figure 5-11: UHPC cross section at mid span

It can be concluded that all the prestressing strands can fit in the cross section without much complications. This is thanks to the low cover that is required for UHPC and especially because there is no passive reinforcement present (shear and longitudinal reinforcement).

5.16 Capacity check of hammerhead

Because most of the strands are located in the bottom flange, the gravity point of strands will fall outside the neutral axis and cause an eccentric moment at the hammerheads. Since the moment due to static loading is very low close to the support it is necessary to see if there is enough capacity to resists the eccentric moment caused by the strands. The governing location is there where the strands have reached their full force and that is at the end of the transition at a distance of l_{pt} from the supports. The check should be performed at time of construction (t=0), as variable loads are not yet presented here to slightly counter balance the eccentric moment. Already was found that indeed at this stage the moment at the end support is the highest. This transmission length is calculated according to EN 1992-1-1 cl. 8.10.2.2 while taking into account the changes given in the AFGC AFGC2013 paragraph 2.6 section 8.10.2:

l_{pt} = 639.5 mm.

The design bending moment at l_{pt} is: $M_{Ed,lpt}$ = 1189 kNm.

At l_{pt} the situation is as in Figure 5-12 is presented. The compression zone is at the bottom side. The height of the compression zone has to be determined. Then the moment capacity can be calculated. The moment capacity $M_{Rd,head}$ should be higher than the design moment M_{Ed}.

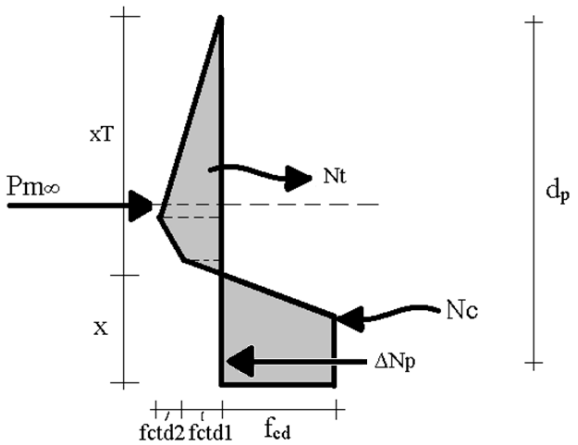

Figure 5-12: Internal forces at hammerhead

For equilibrium of the internal forces the following equation stands: $P_{m0} + N_t = N_c + \Delta N_p$. Solving this equation results in a compression zone height of x_u = 131.08 mm. Then if the moment around the point of the resultant of N_c is taken a moment capacity of **$M_{Rd,lpt}$ = 2145.1kNm** is found.

Unity Check: $M_{Ed,lpt}/M_{Rd}$ = 1189/2145 = 0.55 → OK

A more detailed calculation is found in appendix E.15.

5.17 Detailing

The prestress force in pre-tensioned steel is introduced by bonding. There is a certain transmission length (here l_{pt} = 532.91mm) where after the prestress force is fully transferred. Inside the transmission length the bond stresses can cause tensile stresses. In pre-tensioned steel three types of tensile stresses can occur (Figure 5-13):

- Bursting stresses
- Splitting stresses
- Spalling stresses

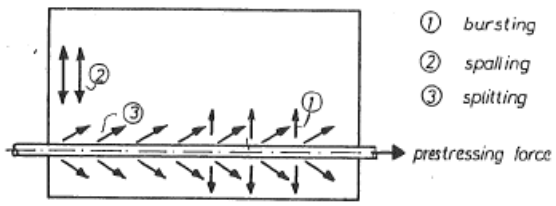

Figure 5-13: Types of tensile stresses

The bursting and splitting stresses are prevented if the cover and distance between strands is at least 2φ. That is the case here so these two types of stresses are prevented. To determine the spalling stresses a graphical method by Den Uijl [9] can be used (Figure 5-14).

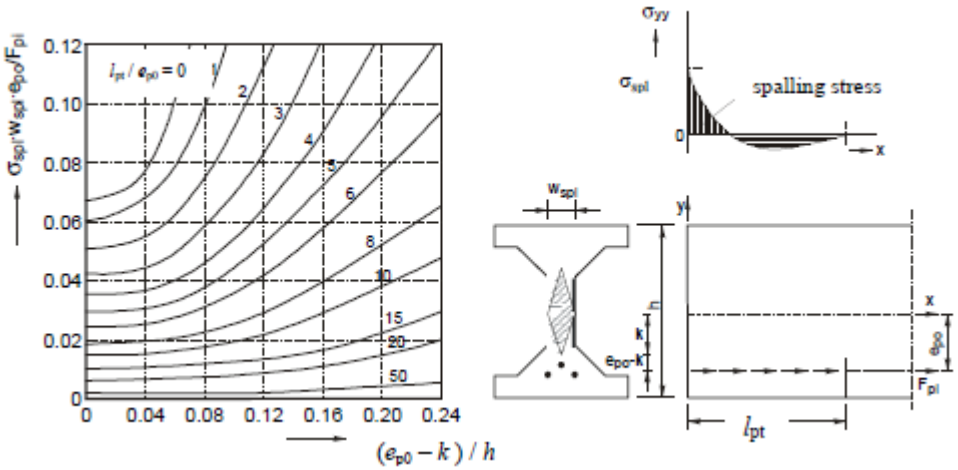

Figure 5-14: Graphical method by Den Uijl for determining the spalling stresses

A spalling stress of σ_{spl} **= 1.68 N/mm²** is found

The spalling stress is lower than the tensile strength (lower than both f_{ctd} and f_{ctk}), so no spalling reinforcement is needed in the structure.

Appendix E.16 gives a more detailed calculation.

5.18 Crack width verification

In order for a structure not to be verified for crack width, it is necessary that the maximum moments in SLS (M_{max}) do not exceed the cracking moment (M_{cr}). And it is also necessary that the tensile strength of the concrete is not exceeded anywhere in the structure. The frequent factor ψ1 has to be applied for the variable loads (is 0.8 for UDL, TS and pedestrian load).
M_{max} = 536.3 kNm
The cracking moment M_{cr} is determined with:
$M_{cr} = W_b*(f_{ctm} + P_{m\infty}/A_c)$. = 1162.86 kNm.

Unity Check: M_{max}/M_{cr} = 536.3/1162.86 = 0.447 → OK
The maximum moments in the SLS do not exceed the cracking moment.

Now the stresses in the structure in the SLS have to be checked. This is done with the same expressions used to determine the amount of strands:

t = 0 at top fibre: $\sigma_c = -\frac{P_{m0}}{A_c} + \frac{M_{p,0}}{W_{ct}} - \frac{M_g}{W_{ct}}$: σ_c = -1.76 N/mm²

t = 0 at bottom fibre: $\sigma_c = -\frac{P_{m0}}{A_c} - \frac{M_{p,0}}{W_{cb}} + \frac{M_g}{W_{cb}}$: σ_c = -33.14 N/mm²

t = ∞ at bottom fibre: $\sigma_c = -\frac{P_{m\infty}}{A_c} - \frac{M_{p,\infty}}{W_{cb}} + \frac{M_g + \psi 1 * M_q}{W_{cb}}$: σ_c = -4.0 N/mm²

The structure is in all three situations completely under compression. So crack formation is not possible. These results are expected, since the prestressing is determined with assuming a fully prestressed beam.

The cracking moment is not exceeded and no tensile stresses occur at the construction and user stage in the SLS. Furthermore the bridge is simply supported so imposed deformations are not restricted, which means that unexpected tensile stresses will not occur. So crack width verification is not necessary in this case.

See appendix E.17 for a more detailed calculation.

5.19 Deflection

It is important for the structure that the deformations caused by the working loadings during service life are within acceptable limits. When determining the deformations it is important to distinguish the deformation in a cracked and uncracked section, because this has a big influence on the deflections (in the shape of a greatly reduced stiffness). In the case of the Leiden Bridge there are no cracked sections as already was concluded in paragraph 5.18. So the structure is considered to be uncracked everywhere. The governing cross section is right in the middle of the beam, since here the highest deformations will occur, caused by the combination of the highest moments.

The occurring deflections have to satisfy a couple of limits given in NEN-EN-1992-1-1 in chapter 7:

- The camber may not exceed L/250 = -96 mm (L = 24000 mm)
- The sag may not exceed L/250 during serviceability = 96 mm
- If a chance exists of damaging adjacent parts then the sag may not exceed L/500 = 48mm

The camber is caused by prestressing. The sag should be limited to L/500, because underneath the bridge there is an unused intermediate pier.

Three load combinations will be investigated:

1. t=0; fabrication and erecting structure; self-weight + prestressing: $q_{self} - q_{pm0}$
2. t=0; after placing asphalt and such; Dead load + prestressing: $q_{self} + q_{dead} - q_{pm0}$
3. t=∞; user stage; All loads as quasi permanent combination: $q_{self} + q_{dead} + \psi_2 * q_{var} - q_{pm\infty}$

The deflection in the middle of the span is determined with: $w = \frac{5*q*L^4}{384*E_{c,eff}*Ic}$

The deflections when type I heat treatment) and no heat treatment will be investigated.
The prestress force is assumed as a line load to simplify the calculation. This will slightly reduce the upward deflection due to the prestressing. The results are seen in (Table 5-3):

Table 5-3: Results deflection

	With $E_{c,eff1}$	With $E_{c,eff2}$	Limit
Combination 1: w [mm]	-87,87	-112,97	-96,0
Combination 2: w [mm]	-55,71	-71,62	-96,0
Combination 3: w [mm]	13.03	16.75	-48,0

The results in Table 5-3 show that the occurring deflections satisfy the limits. Only the camber is too high in combination one when no heat treatment is applied ($E_{c,eff2}$). This means that in terms of deflection the prestressing force is too high. But the first situation (self-weight and prestressing force) is a situation that mostly occurs in the factory. In the factory this issue can easily be monitored and fixed. The camber limit is used when formwork is used during construction. But because prefabricated beams are used, there will be no formwork. So the - higher than the limit - deflection will not cause major issues. Eventually the beams are erected and connected and then the hardening layers are placed. Now situation 2 occurs and here the deflections are lower than the limit.

5.20 Vibration

The vibrations occurring on the structure may not cause discomfort during serviceability. This can be checked by determining the natural frequency of the structure. The natural frequency has to suffice according to the demands given by the Eurocode.
The natural frequency for the first (and governing) node is determined with:

$$n0 = \frac{C}{2\pi} * \sqrt{\frac{E_{cm} * I_c}{A_c * \rho_c * L^4}} \quad [Hz]$$

With C being the constraint factor (= 9.87 = π^2 for simply supported structures).
If all variables are filled in the formula then **n0 = 2.52Hz**

The Leiden Bridge is used both by traffic, trams and pedestrians. So the vibrations caused by each should be considered.

Pedestrians
The NEN-EN-1991-2 states for pedestrian bridges that the natural frequency should at least be 5 Hz. Furthermore it states that frequencies caused by pedestrians fall between 1 and 3 Hz.
The determined natural frequency is lower than 5 Hz and it falls in the range of the pedestrian frequencies. So there would be a chance that pedestrians could cause a frequency equal to n0, which could lead to resonance and discomfort. However, considering the high mass of the bridge, the frequency from the pedestrians will hardly have any effect on the actual bridge. So a dynamical analysis is not required to precisely determine the frequencies exerted by pedestrians. This would not be the case if considered was a pedestrian bridge. These are usually smaller in size and lighter than traffic bridges and a lot more susceptible to vibrations. This was the case with the bridge projects that were discussed in the literature study. A lot of these bridges were pedestrian bridges and almost all required dampers to limit the vibrations caused by pedestrians. But this is not the case for the Leiden Bridge so no further attention is necessary here.

Trams
For vibrations caused by trams specifically there is nothing stated in the Eurocode. However the Eurocode gives guidelines for vibrations caused by trains so these could be used to give an estimation of the vibrations caused by trams. In figure 6.9 NEN-EN-1991-2 a flowchart is given to determine if a dynamical requirement is necessary. For this design following this flowchart results in a structure that does not require a dynamic analysis.

The complete process of the flowchart is seen in appendix E.19

Attention has to be paid to the pedestrian vibrations, but because of the mass of the bridge, it is not necessary to take action against these vibrations. If one would choose to increase the natural frequency than this could be done by for example increasing the stiffness of the structure. This can be done by for example increasing the construction height, which increases I_c and thus the overall stiffness. But due to the demands given, it is would not be possible to use a thicker deck. Using a fixed beam instead of a simply supported beam would increase the natural frequency the most (the constant C goes from 9.87 to 22.4, so about a factor 2.2 higher).

5.21 Fatigue

The bridge is susceptible to cyclic loads coming from trams and traffic. In the demands for the new design it is given that there are 30 tram movements per track per hour over the bridge. That is equal to 788400 movements per year in total. Furthermore the bridge is assumed to be part of a main road with a low amount of heavy traffic. This means according to NEN-EN-1991-2 table 4.5 that there are $0.125*10^6$ vehicles per lane per year. So for a total of 100 years and 7 fictional lanes, this results in $87.5*10^6$ vehicles. So traffic is governing for the fatigue design.

In NEN-EN 1992-1 and NEN-EN 1992-2 it is described how to determine if a structure is safe concerning fatigue for both the concrete and prestressing steel. The procedures described there will be applied for Load Model 1. The fatigue resistance of both the concrete and prestressing steel will be determined separately.

5.21.1 Fatigue resistance concrete

The fatigue resistance of the concrete is checked at the mid span in both the top and bottom fibre of the cross section. To verify the fatigue resistance of concrete, cl. 6.8.7 of the Dutch National Annex of NEN-EN-1992-2 is used. This section state that the following expression must hold true:

$$N_i = 10^{\left[\frac{6}{1-0.57*k1*\left(1-\frac{f_{ck}}{250}\right)}*\frac{1-E_{cd,max,i}}{\sqrt{1-R_i}}\right]} > 10^6$$

Where:

$$R_{equ} = \frac{E_{cd,min,i}}{E_{cd,max,i}}; \quad E_{cd,min,i} = \frac{\sigma_{cd,min,i}}{f_{cd} * (0.9 + \frac{logN_i}{60})}; \quad E_{cd,max,i} = \frac{\sigma_{cd,max,i}}{f_{cd} * (0.9 + \frac{logN_i}{60})}$$

$\sigma_{cd,min,i}$ and $\sigma_{cd,max,i}$ are the lower and upper stresses of the damage equivalent stress spectrum with a number of cycles $N=10^6$. These are determined by using the following load combination:
For $\sigma_{c,max}$: $(\sum G_{k,j} + P + \psi_{1,1}Q_{k,1} + \psi_{2,j}Q_{k,j}) + Q_{fat}$
For $\sigma_{c,min}$: $(\sum G_{k,j} + P + \psi_{1,1}Q_{k,1} + \psi_{2,j}Q_{k,j})$
Q_{fat} is the fatigue load. In the governing situation traffic load model LM1 (when only vehicles are present) is the fatigue load. So the minimum and maximum stresses are determined when Q_{fat} is present and absent. For the fatigue calculation where LM1 is taken into account it is necessary according to NEN-EN 1991-2 cl. 4.6.2 to reduce the UDL with a factor 0.3 and the TS with a factor 0.7. The next and only other variable load is the pedestrian load so this one serves as $Q_{k,1}$

Furthermore, for $f_{cd,fat}$ (fatigue design strength) a different expression than the one given in the Eurocode has to be used, because the current one underestimates the fatigue design strength for UHPC too much. In the Betonkalender [1] a new expression is given for this variable:

$$f_{cd,fat} = 0.85 * \beta_{cc}(t) * \frac{f_{ck}}{\gamma_c} * (1 - \frac{f_{ck}}{40 * f_{ck0}})$$

The difference with the one in the Eurocode is the factor 40, which is originally 25. With the new expression $f_{cd,fat}$ = 55.4 N/mm². With the current expression $f_{cd,fat}$ = 26.2 N/mm², which is a large underestimation, compared with $f_{cd,fat}$ = 55.4 N/mm². The reason this is noted is because in the formula for N_i the term $1-f_{ck}/250$ is now wrong and should be $1-f_{ck}/400$ in the case of UHPC.

For the top fibre: $N_i = 9.53 * 10^9 > 10^6$
For the bottom fibre: $N_i = 9.75 * 10^{10} > 10^6$
Both the top and bottom fibre in the mid span have enough fatigue resistance.

5.21.2 Fatigue resistance prestressing steel

For the prestressing steel according to cl. 6.8.5 in NEN-EN-1992-1 it must hold true that:

$$\gamma_{F,fat} * \Delta\sigma_{S,equ}(N^*) \leq \frac{\Delta\sigma_{Risk}(N^*)}{\gamma_{s,fat}}$$

Also allowed is to use a simpler approach by verifying (according to cl. 6.8.6 in NEN-EN-1992-1) that the stress range $\Delta\sigma_s$ should be lower than value k1, which is taken as 70 N/mm^2. If this holds true, the verification stated earlier is not necessary to perform.
To determine $\Delta\sigma_s$ the maximum and minimum stress determined in paragraph 5.21.1 are used to find the stress $\Delta\sigma_{c,p}$ at the height of the prestressing. This concrete stress is then transformed in a steel stress by: $\Delta\sigma_s = \Delta\sigma_{c,p}*(E_p/E_c)$.

The absolute concrete stresses with and without the presence of LM1 are:

	Top fibre	Bottom fibre
$\sigma_{cd,max}$ (with LM1):	14,290	23,037
$\sigma_{cd,min}$ (without LM1):	5,998	14,239

This results in:
$\sigma_{c,p,max}$ = (23.037-14.29)*(H-e)/H + 14.29 = 22.08 N/mm^2
$\sigma_{c,p,min}$ = (14.239-5.998)*(H-e)/H + 5.998 = 13.335 N/mm^2

The stress difference $\Delta\sigma_{c,p}$ = 22.08-13.335 = 8.743N/mm^2
The steel stress range is:
$\Delta\sigma_s$ = 34.1 N/mm^2 which is well below 70 N/mm^2 (UC=0.487)
So the fatigue resistance of the prestesssing steel meets the requirements. Additional verifications are not necessary.

5.21.3 Conclusion fatigue

Both the concrete and the prestressing steel have enough fatigue resistance to resist the variable cyclic loads that occur on the bridge. For concrete it was necessary to apply the newly developed formula for the fatigue design strength $f_{cd,fat}$. Otherwise the concrete fatigue resistance wouldn't be enough, due to underestimation of $f_{cd,fat}$.

Appendix E.20 gives a more detailed calculation.

5.22 Conclusion Design C170/200

In this chapter a design was made for the Leiden Bridge in C170/200. The goal was to develop a design that is safe and to solve the problems that occurred in the design in C50/60 (high amount of reinforcement and trouble of fitting prestressing). Three possible modifications of the existing girder were discussed. It was chosen to reduce the width of one beam from 1.5m to 1.0m and to decrease the thicknesses of the flanges and webs. This will result in a total of 30 beams in the bridge. The beams are smaller and lighter in weight, so they are easier to transport and erect.

After the bridge was modelled in SCIA and the results were obtained, the design was first checked in the ULS to determine the moment and shear capacity. Both capacities were sufficient to resist the design bending moment and design shear force. The unity checks (M_{Rd}: UC= 0.534 and V_{Rd}: UC = 0.679) showed that there is more than enough capacity to resist the working loads. There is also enough rotational capacity to make sure the structure does not fail suddenly.
The high shear capacity in combination with the additional torsional capacity results in the exclusion of shear and torsion reinforcement. Together with the low cover, this results in sufficient space for the prestressing strands to be fitted in the cross section. All strands, both in the end span and mid span have sufficient centre-to-centre spacing to cause any issue.

Calculations in the SLS were also performed. Crack width verification was not necessary, because the maximum working moment was much lower than the cracking moment. And the entire structure was in compression as well. This was expected, as the amount of prestressing is determined with the assumption that there are no tensile stresses in the structure.
The deformations stayed between the limits. Enough fatigue resistance was determined in both the prestressing steel and the concrete. For the concrete it was necessary to use the new developed expression for $f_{cd,fat}$ in order to not underestimate the fatigue design strength.

Minor issues were found during the verification of the vibrations on the bridge. The calculated natural frequency of the bridge was in the range of the frequencies that are exerted by pedestrians (n0=2.52, pedestrian frequencies are 1 – 3 Hz). But the actual bridge will have a quite high mass, which should make sure that the vibrations exerted by pedestrians do not have a negative effect on the bridge.

Overall it can be stated that the design in C170/200 is a structurally wise safer and better design than the C50/60 design. Especially because all the problems that arose in the C50/60 design were solved in the C170/200 design. The bridge is already very slender. Normally box beams have a slenderness ratio of λ=28-32. This design however provides a ratio of λ=40. So that is a 25% more slender beam. However the UHPC design is not very optimal yet. The amount of prestressing strands is on the high side and looking at the performed calculations it is possible to reduce the amount by for example use limited prestressed instead of fully prestressed beam. Also the dimensions of the web and flanges could be adjusted to make an even more slender beam.

In the continuation of this thesis, the C170/200 design will be further optimized. Also a deeper look will be made in the construction of the bridge. But before that another calculation is going to be made. Between normal and ultra-high performance concrete there is a grey area concerning the strength. It was already concluded that high strength concrete would not lead to a safe structure. However if steel fibres would be added to the high strength mix, then there is a chance that a safe design can be developed, which will most likely be cheaper, than the UHPC design. The next chapter will look at the design of a bridge in high strength concrete with the inclusion of steel fibres.

5.23 Remark: Design philosophy

The UHPC design developed here did not make any use of any mild reinforcement. So no stirrups and no longitudinal bars were applied, because it was shown that the UHPC itself with the steel fibres is sufficient to provide the required resistance. However not using any reinforcement, not even minimum reinforcement, goes against the standard design philosophy. This could have some risks and cause doubts if such a structure is indeed safe enough. There are almost no structures that leave out minimum reinforcement, so if the UHPC design is made, further attention to certain aspects is necessary.

Some aspects have already been dealt with in this chapter, such as the influence of the steel fibres. Assumed was a strain hardening behaviour of the concrete, but if by any chance during production the concrete is poured wrongly, this could cause the fibres to be oriented in such a way that they do not cause a strain hardening behaviour anymore. This could also happen if the percentage of fibres is too low. Shown was that if strain softening occurs that there would still be enough moment and shear capacity. However there was a great influence on the shear capacity. A thicker web could be used if necessary to cover up the capacity loss if this situation of strain softening would occur.

It is also important to realise what kind of reaction the girders will have during certain calamities. Under the Leiden Bridge boats occasionally pass through. It could happen that a boat collides with the bridge. The girder that comes into collision has to be able to resist the collision, without the additional reinforcement. There could be a chance that the lower part of the bridge crumbles of if the force is too high. Too be extra safe measures could be taken. The hollow part could be thickened on the bottom side to give extra resistance, or it could be chosen to at least apply some reinforcement in the most outer box girders, to give extra resistance against collisions.

To play it safe, some reinforcement bars or stirrups could still be applied. There should be enough room to fit some extra bars in the cross section of the box girder. However the bridges in the reference projects that were discussed in the literature study all did not use mild or shear reinforcement, only if it was truly necessary and it was shown that the bridges function properly with only prestressing steel and steel fibres. So the same should hold true for this design.

However to be sure this is true, it is important to investigate the behaviour of such a girder without any mild reinforcement and comparing it to a girder that does have additional minimum reinforcement. It is important to know where and how the cracks are developed in the bridge and how the bridge will fail and how ductile the bridge actually is. During the parametric study a M-κ diagram was made, where the highest moment capacity occurred before the ultimate compressive and tensile strain were reached. So failure of the prestressing will most likely be governing. The same would probably hold true if minimum reinforcement was used.

In short designing a bridge without any reinforcement at all does go against the design philosophy, but the calculations showed that the design has a great structural performance nevertheless and if necessary, proper measurements can be taken in order to provide extra safety. However to be truly sure of the behaviour of such a bridge, experiments could be performed additionally on a girder to be sure that it is truly safe.

5.24 Summary

Amount of strands:	33ϕ15.2 strands	
Total losses in strands:	If type I heat treatment: 12.2% If no heat treatment:16%	
Slenderness ratio, λ	40	
ULS		
Bending moment capacity, M_{Rd}:	M_{Rd} = 2358.5 kNm	UC = 0.534
Rotational capacity: x_u/d	x_u/d = 0.365	UC = 0.734
Shear capacity V_{Rd}:	V_{Rd} = 1088.71 kNm	UC = 0.679
Torsional capacity T_{Rd}:	T_{Rd} = 542.6 kNm	UC = 0.584
Transverse moment capacity: $M_{Rd,joint:}$	$M_{Rd,joint}$ = 148.815 kNm	UC = 0.976
Capacity concrete at hammerhead:	$M_{Rd,head}$ = 2145.75 kNm	UC = 0.554
SLS		
Crack width verification:	M_{CR} = 1162.86	UC= 0.44
Deflection:	w2= 71mm < L/250	
	w3 = 15mm < L/500	
Vibrations:	n0 = 2.52Hz	
	$v/n0 = 7.66 < (v/n0)_{lim}$	
Fatigue:	Concrete: Top fibre:	UC = 0.440
	Bottom fibre:	UC = 0.453
	Prestressing:	UC = 0.487

Chapter 6 High strength fibre reinforced concrete

6.1 General

It was concluded that using normal strength concrete is not a good option for the Leiden Bridge. The shear capacity is low, so a lot of shear reinforcement is necessary. And torsional reinforcement is necessary as well. Fitting everything together with all prestressing strands would prove to be very difficult and uneconomical. Using High strength concrete would deliver the same issue. Even though the rotational capacity would meet the requirements now due to the higher strength, the shear capacity would still be too low and a high amount of shear reinforcement would still be necessary and thus deliver the same problems as with normal strength concrete.

UHPC however could solve all these problems. Proven was in Chapter 5 that using UHPC would deliver a safe structure that meets all requirements for ULS and SLS. However UHPC is quite expensive so it could be an option to use High strength concrete, only with fibres. This would mean that the concrete would show the same behaviour as UHPC only the compressive and tensile strength would be lower (from C170/200 to C90/105). However C90/105, with the benefit of the steel fibres, could be enough to solve the issues arising with the shear capacity and also the issues of fitting all strands and reinforcement in the concrete. If this would be true, then there would be another realistic solution for the Leiden Bridge, which is cheaper than the UHPC solution.

There are some differences though between UHPC and High strength concrete (HSC). Beside the lower strength of HSC (because of the higher wcr among other things), it has also worse durability properties than UHPC. The cement matrix is not as dense, as the matrix of UHPC, because the maximum aggregate is higher than 2 mm. Therefore HSC is more susceptible to for example carbonation or chloride penetration. HSC does have better durability properties than NSC though, moreover it is proven that HSC can have a better durability if modifications are made to the mixture, making it High Performance Concrete. The benefit for HSC is that the Eurocode methods for calculations can still be used, for example determining creep and shrinkage and such. And now with the steel fibres there a higher resistance can be achieved against the internal forces than with normal HSC. It is also cheaper to produce than UHPC. The differences between UHPC and HSC are important to consider, when eventually a design choice is made for the new bridge. But first it has to be investigated if HSC can provide a safe design.

In this chapter a design is going to be developed in C90/105 with the inclusion of steel fibres. This makes the concrete fall in the category high performance concrete. In future references this concrete will be called HPC. The design will be checked in the ULS and SLS and also will be checked if there is enough fatigue resistance. So basically the same design process as in Chapter 5.

6.2 Material properties

The material properties are based on NEN-EN-1992-1-1. Parameters linked with the steel fibres are assumed the same as with UHPC (K factors, determining tensile strains, etc.).

6.3 Cross sectional properties

The dimension and thus the cross sectional properties will be the same as for the C50/60 design. Because C90/105 has a lower strength it is wiser to keep the thicknesses of the flanges and webs the same as for the C50/60 design. Now there is a higher chance that the structure will meet the safety requirements. However the width will be 1000mm instead of 1500mm. The cross section of the HPC girder is seen in Figure 6-1.

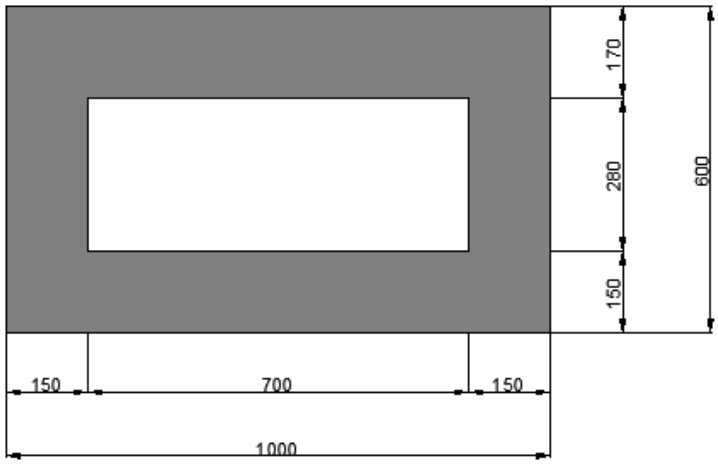

Figure 6-1: Cross section UPHC box girder

In Table 6-1 the dimensions and cross sectional properties of one girder are shown.

Table 6-1: Dimensions and cross sectional properties of box girder

L	Span	24 m
H	Height girder	0.6 m
B	Width girder	1.0 m
b_{web}	Web thickness	0.15 m
$h_{top,fl}$	Top flange thickness	0.17 m
$h_{bot,fl}$	Bottom flange thickness	0.15 m
A_c	Cross sectional area	0.404 m^2
z_t	Distance top fibre to c.a.	0.295 m
z_b	Distance bottom fibre to c.a.	0.305 m
I_c	Moment of Inertia	0.0167 m^4
$W_{c,t}$	Section Modulus top fibre	0.0566 m^3
$W_{c,b}$	Section Modulus bottom fibre	0.0548 m^3

6.4 Exposure class and concrete cover

The exposure class and concrete cover are determined according to NEN-EN-1992-1-1 cl. 4.2 and 4.4.1. For the outer perimeter of the box girder the exposure class is set to be XC4. For the inner perimeter of the box girder the exposure class is set to XC1, since the inside is not as exposed as the outside of the girder.

The nominal cover is 45mm for the outer and 30mm for the inner perimeter

6.5 Load cases and load combinations

Before the SCIA Engineer model is presented, the loads have to be determined first. There are a lot of different loads that will work on the bridge. And these loads will not occur exclusively. Therefore it is important to determine all the load cases and load combinations for the bridge. The load cases and combinations are all described extensively in appendix B.

Basically the following load cases will occur on the bridge:

Permanent loads:	
LC1: Self-weight girders (not included in SCIA)	A_c*25 kN/m
LC2: Dead load	
– Pavement	4.6 kN/m^2
– Asphalt	4.8 kN/m^2
– Concrete filling around tram rails	3.5 kN/m^2
LC3: Steel railing and natural stone elements (Edge Load)	2.0 kN/m^2
Variable loads:	
LC4&5: Traffic loads with presence of trams (UDL & tandem axle)	Conform Load Model 1
LC6&7: Traffic loads with absence of trams (UDL & tandem axle)	Conform Load Model 1
LC8: Tram-axle loads (No UDL specified for tram loads)	Conform GVB
LC9: Pedestrian loads over whole width (crowd loading)	5.0 kN/m^2
LC10: Pedestrian loads on designed locations	5.0 kN/m^2

In total there are four main load combinations:

- Combination 1: Traffic loads in the presence of tram loading, where the traffic loads are the leading variable load. (1 LM1 TS + 2 tram TS)
- Combination 2: Traffic loads in the presence of tram loading, where the tram loading is the leading variable load. (1 LM1 TS + 2 tram TS)
- Combination 3: Traffic loads in absence of tram loading. (3 LM1 TS)
- Combination 4: Crowd loading
- Combination 5: Governing transverse moment

In Table 6-2 the load combinations are presented with the load factors used in the ULS situation

Table 6-2: Load combinations with ULS load factors

	Load cases	Ψ	γ	CO1	CO2	CO3&5	CO4
LC1	Self-weight	1	1.2	1.2	1.2	1.2	1.2
LC2	Dead load (pavement, asphalt, tram rails)	1	1.2	1.2	1.2	1.2	1.2
LC3	Edge loads (railing, stone elements)	1	1.2	1.2	1.2	1.2	1.2
LC4	Traffic loads| UDL| Tram present	0.8	1.35	1.35	1.08		
LC5	Traffic loads| TS| Tram present	0.8	1.35	1.35	1.08		
LC6	Traffic load| UDL| Tram absent	0.8	1.35			1.35	
LC7	Traffic loads| TS| Tram absent	0.8	1.35			1.35	
LC8	Tram loading| TS	0.8	1.45	1.16	1.45		
LC9	Pedestrian loads| Crowd loading	0.8	1.35				1.35
LC10	Pedestrian loads| Loads on designated locations	0.8	1.35	1.08	1.08	1.08	

6.6 Results SCIA Engineer

The same results that were used in the UHPC design will be used here as well. Even though the orthotropic parameters for HPC and UHPC are not the same, this will hardly have an influence on the results. So it is assumed that the same internal forces occur in the HPC design as in the UHPC design. This is allowed, because SCIA provides higher internal forces when the stiffness is higher. The stiffness of HPC is lower so SCIA would give slightly lower values. Therefore as already said it is safe to use the results from the UHPC design.

F or bending moment resistance check:
mxD$^-$: 1712.15 kNm/m

For shear and [torsion + shear] safety check
mxy: 317.09 kNm/m (When torsion is governing)
116.75 kNm/m (When shear is governing)

vx: 235.94 kN/m (When torsion is governing)
584.56 kN/m (When shear is governing)
For transverse moment check
myD$^-$: 332.06 kNm/m
myD$^+$ 303.09 kNm/m

The presented values will be used for the safety checks. However these values are only based on the loads working on the bridge. Here no self-weight and no prestressing is included yet. These have to be added separately.

6.7 Prestress tendon profile

The beams will consist of pre-tensioned strands, as the beams are prefabricated. The tendon profile is shown in Figure 6-2. The tendon consists of straight and kinked strands. The kinked strands cause an upward force P_u at the deviation points. This point is at a distance 'a' from the support. The kinked strands are placed in the webs. The strands will be placed as high as possible to ensure a high upward force. This force slightly reduces the total shear force. Most of the strands will be placed in the bottom flange. This means that the fictitious tendon (or the gravity point) does not coincide with the neutral axis (dashed line). So these will create a moment at the heads due to eccentricity, so a capacity check at the support has to be made to make sure the structure can take the moments.

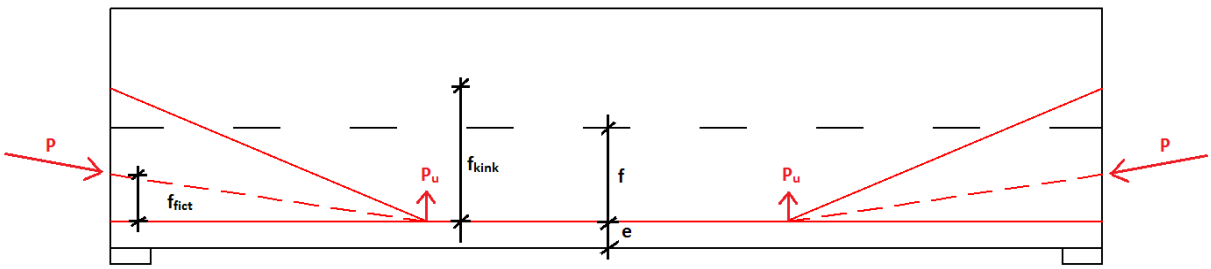

Figure 6-2: Tendon profile pre-tensioned strands

Distance strands from bottom fibre:	e = 0.076mm
Amount of kinked strands per web:	4 strands
Drape of all strands:	$f = z_b - e = 0.229m$
Distance deviation points from supports:	$a = (1/3)*L = 8m$
Drape of kinked strands:	$f_{kink} = 0.0323m$
Upward prestress force:	$P_u = P_{kink}*\sin \alpha_{kink} \approx P_{kink}* (f_{kink}/a)$ or $P*(f_{fict}/a)$
Bending moment in mid span:	$M_{p,mid} = P*f$

The prestress force is determined by taking a couple of requirements into account that concern stresses in the concrete. These requirements need to be applied in the governing cross section (cross section with highest bending moment). Here that is in the middle of the beam.

$$t = 0 \text{ at top fibre: } -\frac{P_{m0}}{A_c} + \frac{M_{p,0}}{W_{ct}} - \frac{M_g}{W_{ct}} \leq 0$$

$$t = 0 \text{ at bottom fibre: } -\frac{P_{m0}}{A_c} - \frac{M_{p,0}}{W_{cb}} + \frac{M_g}{W_{cb}} \geq -0.6 * f_{ck}$$

$$t = \infty \text{ at bottom fibre: } -\frac{P_{m\infty}}{A_c} - \frac{M_{p,\infty}}{W_{cb}} + \frac{M_{tot}}{W_{cb}} \leq 0$$

Assumed is a total loss of 16% so $P_{m\infty} = 0.84*P_{m0}$. After the prestress force is determined with the three requirements, the actual losses (direct and time dependent losses) have to be determined and checked if the assumption of a 16% loss is on the safe side.

The moment due to all static loads now becomes:
M_g = 1065.41 kNm
The moment due to the variable loads is:
M_q = 1027.95 kNm

This results in a total moment of:
M_{tot} = 2093.36 kNm

The moments and requirements result in a minimum amount of 36 strands, which have a total cross sectional area of 36*139 = 5004 mm^2. This results in a force of P_{m0} = 6980.58 kN.
The moment caused by the prestressing force is:
$M_{p\infty} = P_{m\infty}*f$ = 1343.09 kNm
The stress caused by the prestress force during t=∞ in the concrete is:
$\sigma_{cp} = 0.84*P_{mo}/A_c$ = 14.51 N/mm^2.

A more detailed calculation of the prestressing force is found in appendix F.7 and F.8

6.8 Prestressing Losses

The required amount of strands and also the resulting prestress force are determined. Now the actual losses have to be determined. The percentage of the total losses should be lower than the assumed losses of 16%, so that the determined prestress force is on the save side. If this is not the case the amount of strands has to be determined again with the correct percentage of losses.
The losses can be divided in direct and time dependent losses.

6.8.1 Direct losses

For pre-tensioned strands the elastic shortening is part of the direct losses. When the strands are released after tensioning the strands will shorten elastically. The result is that the stresses and forces in these strands decrease. Also occurring is concentrated friction at the kink points of the strands but these can be neglected when looking at the big picture.

6.8.1.1 *Losses due to elastic deformation*

The loss of force in one strand due to elastic shortening is[20]:

$$\Delta P_{el} = A_p * E_p * \frac{\Delta\sigma_c(t)}{E_{cm}(t)}$$

And $\Delta\sigma_c(t)$ being the variation of stress at the centre of gravity of the strands at time t:

$$\Delta\sigma_c(t) = \frac{P_{m0}}{A_c} * [1 + \frac{e_p^2 * A_c}{I_c}]$$

To compensate the loss in forces due to elastic shortening it is allowed to overstress the strands, provided that the stress stays under the maximum allowed stress $\sigma_{p,max}$ = 1488 N/mm^2.
The extra stress per strand needed to compensate the loss is: $\sigma_{extra} = \Delta P_{el}/A_p$ = 4.25 N/mm^2. So the total stress applied becomes $\sigma_{pm0} + \sigma_{extra}$ = 1399.25 N/mm^2 which is far below the maximum allowed stress.

6.8.2 Time dependent losses

Certain losses appear during the life span of the structure. These are shrinkage and creep of the concrete and relaxation of the strands. All these losses can be combined in one formula which is given in NEN-EN-1992-1-1 formula 5.46:

$$\Delta P_{c+s+r} = A_p \Delta\sigma_{p,c+s+r} = A_p \frac{\varepsilon_{cs} E_p + 0{,}8\Delta\sigma_{pr} + \frac{E_p}{E_{cm}} \varphi(t,t_0).\sigma_{c,QP}}{1 + \frac{E_p}{E_{cm}} \frac{A_p}{A_c}(1 + \frac{A_c}{I_c} z_{cp}^2)[1 + 0{,}8\varphi(t,t_0)]}$$

In this formula the shrinkage strain, creep coefficient and the stress loss due to relaxation can be determined separately according to NEN-EN-1992-1-1.

When all the parameters are filled in, the total stress loss due to time dependent losses becomes: $\Delta\sigma_{p,c+s+r}$ = 135.7 N/mm^2. This is **9.73%** of σ_{pm0}, which is below the assumed loss of 16% so the assumption was on the safe side.

Because the actual losses are smaller than the assumed loss, the losses will be set to 11%. Putting it to 11% results in a smaller amount of strands, while still taking unforeseen losses (such as friction at the deviators) into account. With the losses being 11% the new minimum required amount strands become 34 (instead of 36). The total area of the strands is now: A_p = 4726 mm^2 (Pm0=6592.8 kN).
The prestress force delivers a vertical force at the deviators P_u, which is equal to: $P_{u0} = P_{m0} * (f_{fict}/a)$ = 62.64 kN and $P_{u\infty}$=55.75kN.

A more detailed calculation of the losses is found in appendix F.9

[20] NEN-EN-1992-1-1 formula 5.44

6.9 Bending moment capacity

It is a requirement that the bending moment resistance is higher than the design bending moment: $M_{Rd} > M_{Ed}$.

$M_{Ed} = \gamma_g * M_g + \gamma_q * M_q - 1.0 * M_p$

It is possible that the eventual governing design bending moment is found at the construction stage (t=0) and perhaps at the support, because the prestressing causes a moment there. So the bending moment will be determined for the whole span at multiple stages: These stages and the bending moments are:

- t=0 only self weight: $M_{Ed} = M_{self} - M_p$
- t=0 permanent loads: $M_{Ed} = M_{perm} - M_p$
- t=∞ all loads + torsion: $M_{Ed} = M_{perm} + M_{var} - M_p$

In Figure 6-3 the moment lines are shown, for multiple stages. The governing M_{Ed} = 1276.1 kNm. The moment at the support is 1008.95 kNm. Technically right at the support the prestress force is also zero. The force has a certain transmission length, where after the force is fully transferred in the concrete.

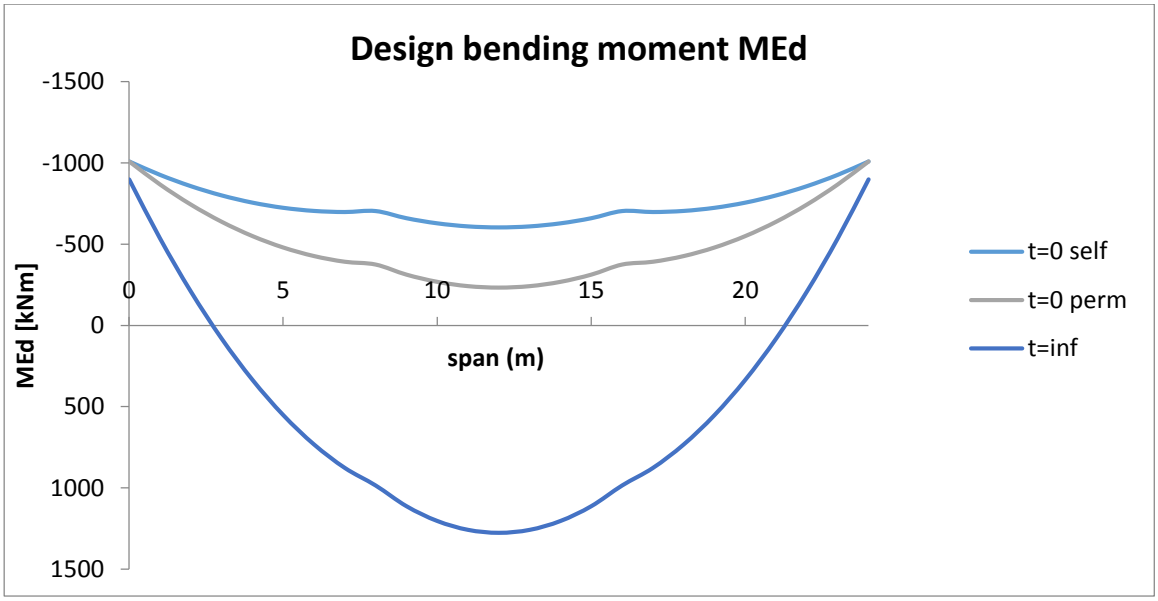

Figure 6-3: Design bending moment at multiple stages

The moment capacity should be high enough to resist the determined M_{Ed}. To determine the moment capacity the same approach is used as with the UHPC design, since both consist of steel fibres so in the HPC design the tensile capacity may be taken into account as well.
The only difference here is that $f_{ctd2} = f_{cdt1}$, because it is not known what f_{ctd2} for HPC is, so this assumption neglects the hardening part, which makes it a safe assumption as the capacity is slightly underestimated. To determine M_{Rd} one has to assume equilibrium of internal forces in the cross section and with that assumption determine M_{Rd}. The general case of internal forces is seen in Figure 6-4. For equilibrium the following statement needs to hold true: $N_c - N_t = P_{m\infty} + \Delta N_p + N_s$. The last term N_s is removed, as there is no bending reinforcement applied.

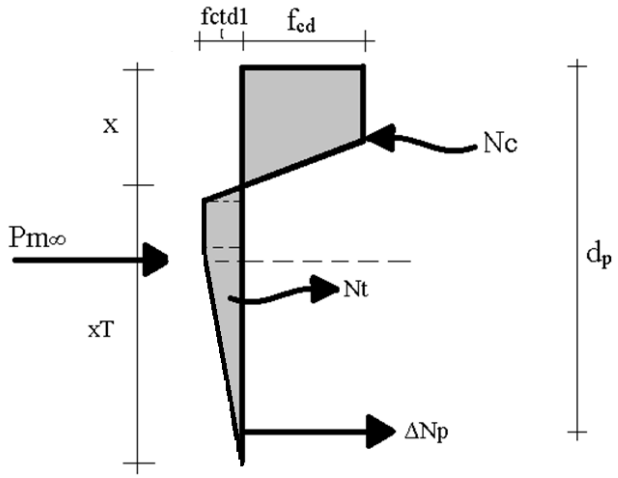

Figure 6-4: Equilibrium of internal forces

The compressive strain limits are derived from the Eurocode and the tensile strain limits are derived according to the formulas in the AFGC Recommendations:
ε_{c3} = 2.3‰
ε_{cu3} = 2.6‰
ε_{ct} =0.05303‰
$\varepsilon_{u0,3}$ = 0.80303‰
ε_{ctu} = 8.125‰

Because a box girder is used, the width is not constant over the height. It is therefore possible that the compression zone and tension zone do not have a uniform width over their height. Multiple situations can occur of how the zones are divided over the height of the section. These derivations can be found in appendix H and are the same ones as for the UHPC design.. The moment capacity, while taking the multiple situations into account, has been determined with the same maple sheet as for UHPC, which is found in appendix F.10.

The moment capacity is:
M_{Rd} = 1955.31 kNm with x = 233.67mm

Unity Check: M_{Ed}/M_{Rd} = 1276.1/1955.31 = 0.652→OK
The moment capacity is enough to resist the design bending moment.

Remark: In the case of HPC the compression height zone is higher than the top flange, whereas in the case of UHPC the whole compression zone is found in the top flange. This is logical since the compression strength of HPC is almost twice as low as the strength of UHPC, so the compression zone height increases.

In appendix F.10 a more thorough calculation is found.

6.10 Rotational capacity

The bending moment resistance suffices. But it is also important that the structure has enough rotational capacity in order to give enough warning before failure. For this the following requirement has to be met:

$x_u/d \leq 0.54$

With x = 233.73 mm: and with d=h-e = 524.2 mm

x/d = 0.446 <0.54. So the structure has enough rotational capacity.

6.11 Shear and torsion capacity

The full calculation is found in appendix F.12

6.11.1 Shear

It is a requirement that the shear resistance is higher then the design shear force:
$V_{Rd}>V_d$
The design shear force is the sum of the shear force caused by bending moments and the shear force caused by torsional moments:
$V_d = V_{Ed} + V_{Td}$
Two cases have to be investigated, of which the most governing one will be used:

Situation 1. Location of highest torsional moment in structure
Situation 2. Location of highest shear force in structure

For both locations the internal forces were calculated and the results were presented in paragraph 5.8. These were:
Mxy = TEd:

Situation 1. 317.09 kNm --> V_{Td} = 184.35 kN
Situation 2. 116.75 kNm --> V_{Td} = 67.88 kN

Vx (without self-weight and prestressing):

Situation 1. 235.94 kN
Situation 2. 584.56 kN

The shear force V_{Td} due to T_{Ed} is calculated with: $V_{Td} = h_m*T_{Ed}/(2*A_k)$.

The governing total shear force taken from SCIA is the one where the sum of V_x and V_{Td} is the largest. This is the case for situation 2, where V_{Ed} = 652.44 kN. The shear force over the length of the beam needs to be determined at multiple stages. These stages and the shear forces are:

- t=0 only self weight: $V_{Ed} = V_{self} - P_{u0}$
- t=0 permanent loads: $V_{Ed} = V_{perm}-P_{u0}$
- t=∞ all loads + torsion: $V_{Ed} = V_{perm} + V_{var} - P_{u\infty}$

For t=∞ the shear force is added with V_{Td}. Assumed is that V_{Td} is constant over the length of the beam. The shear force line is seen in Figure 6-5.

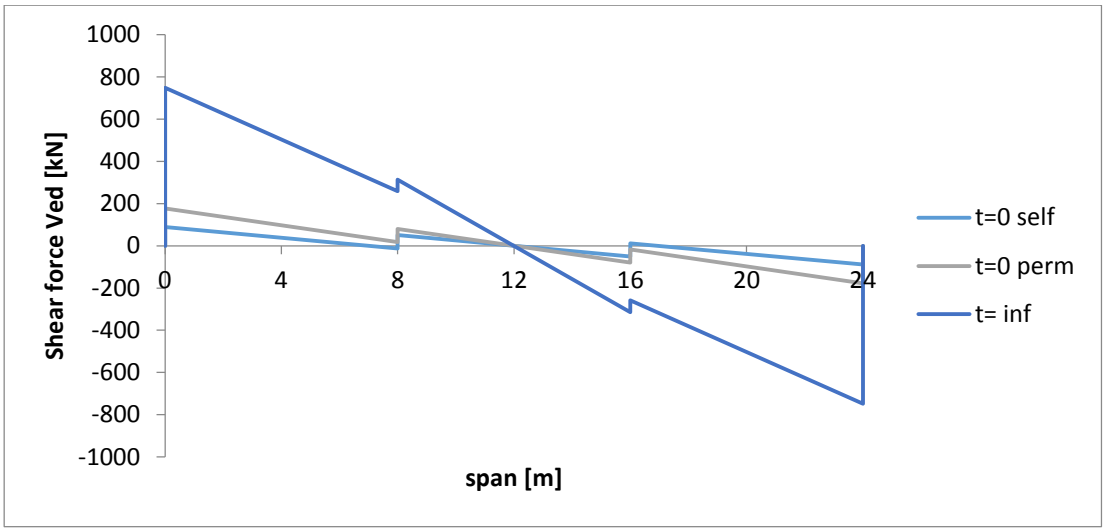

Figure 6-5: Shear force line at multiple stages

The governing shear force V_{Ed} = 748.81 kN at t=∞. The shear resistance has to be high enough to resist this force.

The shear resistance for a HPC structure is determined in more or less the same way as a UHPC structure. This is because both contain steel fibres. The shear resistance is equal to:
$V_{Rd} = V_{Rd,F} + V_{Rd,s}$

Where:
$V_{Rd,F}$ = the contribution of the steel fibre reinforced concrete to the shear capacity
$V_{Rd,s}$ = the contribution of the shear reinforcement to the shear capacity
Because of the behaviour of the steel fibres in tension, it is allowed to view it separately from the concrete, as if it is serving as reinforcement. Shear reinforcement will not be applied (unless the shear capacity is not enough to resist the design shear force), so $V_{Rd} = V_{Rd,F}$.

The Eurocode has no method to determine the shear capacity, when steel fibres are present in the concrete. Therefore the Model Code MC2010 will be used to determine the shear capacity.
According to paragraph 7.7.3.2 of MC2010 the shear resistance is determined with:

$$V_{Rd,F} = \frac{1}{\gamma_F}\left(k_v\sqrt{f_{ck}} + k_f f_{Ftuk}\cot\theta\right) z * b_w$$

If assumed is $f_{Ftuk} = f_{ctk}$ = 3.5 N/mm^2 then the shear capacity becomes:
$V_{Rd,F}$ = 695.07 kN

The minimum shear resistance is determined with (same approach as the Eurocode):
$V_{min} = (v_{min} + k1*\sigma_{cp}) * b_w*z$ = 384.36 kN
$V_{Rd,F}$ is higher so governing as well.

Unity Check: $V_{Ed}/V_{Rd,F}$ = 748.81/695.07 = 1.1 → NOT OK

The structure has not enough shear capacity. So shear reinforcement is necessary. Because steel fibres are used the Total shear resistance may be set to:
$V_{Rd} = V_{Rd,f} + V_s$. This means that the shear reinforcement needs to carry the remaining shear force. Applied is φ8-350 (A_s = 575mm^2/m), which is also assumed as minimum reinforcement.

Remark: If the shear reinforcement needs to resist V_{Ed} alone, then 3700mm^2 would be necessary (ϕ12-125). At 1.13m of the supports the shear resistance becomes high enough to resist V_{Ed}.
So only up to this point this amount of shear reinforcement is necessary. Also a hammerhead piece of 1m long is used at the supports and the hammerheads can easily resist V_{Ed}, since they are solid sections. So only a small part in the beam does not have sufficient shear capacity. The web thickness could be increased as well; If the web thickness is 170mm instead of 150mm, then UC = 0.99, which just enough capacity.

6.11.2 Torsion

There should be enough torsional resistance in the structure against working torsion moments:
$T_{Ed} \leq T_{Rd}$
If this is not the case reinforcement has to be applied. The torsion resistance can be determined with:
$T_{Rd} = f_{ctd,1} * t_{ef} * 2 * A_k$

The result is: **T_{Rd} = 261.8 kNm**

Unity Check: T_{Ed}/T_{Rd} = 317.09/261.8 = 1.211→ NOT OK

The torsional moment resistance (without taking the effect of the fibres into account) is not sufficient to resist the working torsional moments, so torsional reinforcement needs to be applied.

The required torsional reinforcement is divided over the flanges and webs and placed in two layers[21]:
Per flange: $A_s = T_{Ed}/(2 * h_m * f_{yd})$ = 828 mm^2 → 6φ10 per layer (divided over the whole flange).
Per web: $A_s = T_{Ed}/(2 * b_m * f_{yd})$ = 429 mm^2 → 3φ10 per layer (divided over the web)

To hold the torsion reinforcement in place stirrups of ϕ8-350 are placed in the cross section as well, which are also required to resist the shear force, together with the steel fibres.

6.11.3 Shear + torsion

It is also required that the combination of shear forces and torsional moments is verified. The structure should be able to resist these forces. The requirement for this states that[22]:
$T_{Ed}/T_{Rd,max} + V_{Ed}/V_{Rd,max} \leq 1.0$
The requirement means that the capacity of the concrete struts has to be sufficient to resist the loads on the structure. Here the two previous situations (shear governing or torsion governing) are going to be investigated as well.
First $T_{Rd,max}$ and $V_{Rd,max}$ have to be determined according (to NEN-EN-1992-1-1)[23]:
$T_{Rd,max} = 2 * v * \alpha_{cw} * f_{cd} * A_k * t_{ef} * \sin\theta\cos\theta$ = 1639.71 kNm
$V_{Rd,max} = \alpha_{cw} * b_w * z * v * f_{cd}/(\cot\theta + \tan\theta)$ = 2130.75 kN

Unity check:
Situation 1: $T_{Ed}/T_{Rd,max} + V_{Ed}/V_{Rd,max}$ = 317.09/1639.71 + 518.04/2130.75 = 0.349
Situation 2: $T_{Ed}/T_{Rd,max} + V_{Ed}/V_{Rd,max}$ = 116.75/1639.71 + 748.81/2130.75 = 0.390
For both situations the concrete struts suffice.

According to the Model Code $V_{Rd,max}$ is calculated as follows:
$V_{Rd,max} = k_c * f_{ck}/\gamma_c * b_w * z * \sin\theta\cos\theta$ = 1646.6 kN

[21] Determined with NEN-EN-1992-1-1 formula 6.28
[22] NEN-EN-1992-1-1 cl. 6.3.2(4)
[23] NEN-EN-1992-1-1 formula 6.9 and 6.30

This value is lower than the value determined with the Eurocode. Most likely because the Eurocode uses α_{cw} which takes the compression stress caused by the prestressing into account.

6.12 Transverse direction (moments)

Transverse moments also occur in the structure. It is necessary to validate if the box girder can resist these moments. Transverse prestressing strands, which are placed in the top flange, can benefit the transverse moment capacity. These strands are also necessary to connect all the box girders together in order for the bridge to have transverse action. Only the top flange can contribute to the transverse moment capacity, together with the joints. Assumed is that a tendon of 9φ15.7 strands with quality Y1860H are used which are placed with a centre spacing of 1000 mm. The governing section is in the joint: The joint is not made of HPC and it has no other reinforcement in the concrete, except for the transverse prestressing. It has to be verified if the joint can resist the design transverse moment. Assumed is that the joint is made of C50/60. The joint will have a thickness of 260 mm.

It is expected that the highest transverse moment is located right around the middle of the bridge. The highest moment should be found for the combination, where the loads are placed to give the highest transverse moments. In SCIA the result for the transverse moment myD^- was 322.06 kNm. However this (quite large) moment is found near the corners of the bridge. This can be explained by the fact that SCIA calculates myD^- by stating: $myD^- = my + |mxy|$. As the results showed in paragraph 5.8, mxy = 317.09 kNm. This results in a high myD^-, which occurs in the same area as the highest torsional moment mxy. But the problem is that SCIA does not link the torsional moments with the given orthotropic parameters. For a box girder the stiffness is much higher in the longitudinal direction than in the transverse direction. So this also means that mxy ≠ myx. Therefore a factor K should be applied based on the orthotropy of a box girder:

$K_x = 2*D_{xy}/(D_{xy}+D_{yx}) = 1.948$
$K_y = 2*D_{yx}/(D_{xy}+D_{yx}) = 0.052$

To calculate myD^- the following is used: $myD^- = my + K_y*mxy$. Finding m_y in the same node as where the highest mxy is and then applying the factor will lead to myD^- = 34.53 kNm. This is much lower than the given value of 322.06 kNm. If this procedure would be applied all over the structure one would find the highest myD^- in the middle of the bridge as expected. Here m_y is the largest and mxy is very low in value.
SCIA gives a value of myD^- = 113.68 kNm/m. This is the value that will be used for determining if the transverse moment capacity ($M_{Rd,y}$) is sufficient.

The moment on the box girder is the sum of the global and local transverse moments. The local transverse moment is the result of the force of a single axle load from Load Model 1.
$M_{Ed,y} = myD^-*B_{centre,spacing}$=113.68 kNm. This is the global transverse moment. The global moment in the SLS state is: M_{SLS} =85.74 kNm.

The local moment is: $M_{Ed,local}$ = 46.84 kNm and $M_{SLS,local}$ = 26.05 kNm.

Because the placement of the axle loads for the local effects usually do not coincide with the placement of the axle loads for the global effects, the local effect may be reduced. A reduction of 25% is assumed. This results in a total transverse moment of:
ULS: $M_{Ed,tot}$ = 113.68+0.75*46.84 = 148.81 kNm
SLS: $M_{SLS,tot}$ = 85.74 +0.75*34.73 = 111.79 kNm

The transverse capacity is determined where the following equilibrium needs to hold true:
$N_c = P_{m\infty}$

The moment capacity becomes: $M_{Rd,\mathbf{joint}}$ **= 161.6 kNm**

Unity Check: $M_{Ed,tot}/M_{Rd,joint}$ = 148.81/161.60 = 0.921 → OK

For joints it is also important that there are no tensile stresses at the height of the prestressing strands. At this location the joint has to remain in compression at all times. This holds true for the SLS state. The stress at the height of the strands is:
σ = -6.16 /mm^2 so there is compression.

At the location of the duct the concrete has to be thickened internally to be able to fit the anchor and for enough space for the duct itself.

The detailed calculation is found in appendix F.13

6.13 Fitting of bars and strands

The amount of strands has already been determined. The total amount is 34 strands. Four strands are placed in each web. This means there are 26 strands left to fit in the bottom flange. The area available in the bottom flange is 700mm (H-2*b_{web}). The strands will be placed in 2 layers of 13 strands. The determined cover (for inner perimeter 30 mm and outer perimeter of box girder 45mm) and the eccentricity needs to be taken into account, when fitting the concrete. In the mid span the distance of the gravity point with regards to the bottom fibre should be the same as the determined eccentricity.

In Figure 6-6 and Figure 6-7 the cross section of the end span and mid span are shown respectively. In reality there is a hammerhead at the end span, but in the figure the extra solid part is left out. In the end span the horizontal centre-to-centre spacing of the strands is sufficient according to requirements ($2\phi_{strand}$ + ϕ_{strand} in both directions). But the vertical spacing is less than the requirements (only ϕ_{strand}), but this should not cause any serious problem. In the bottom flange the distance between reinforcement bar and prestressing strand is not always large enough. There is a possibility that this will cause some issues with bond transfer. As for aggregates getting stuck, that should not be an issue as only finer aggregates are used ($D_{max} \leq$ 8mm).

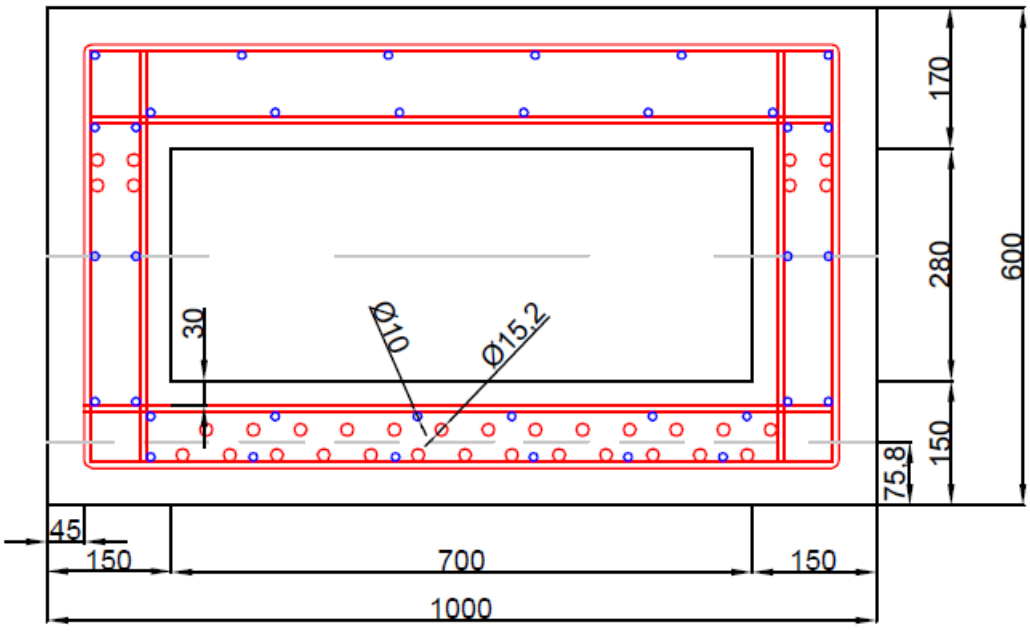

Figure 6-6: HPC cross section at end span

In the mid span the strands meet the centre-to-centre spacing requirements for the centre to centre spacing in both horizontal and vertical direction. However in the corners of the bottom flange there is quite some clustering of strands, bars and stirrups. This could cause difficulties in during placement of the strands, bars etc. There are further no serious issues.

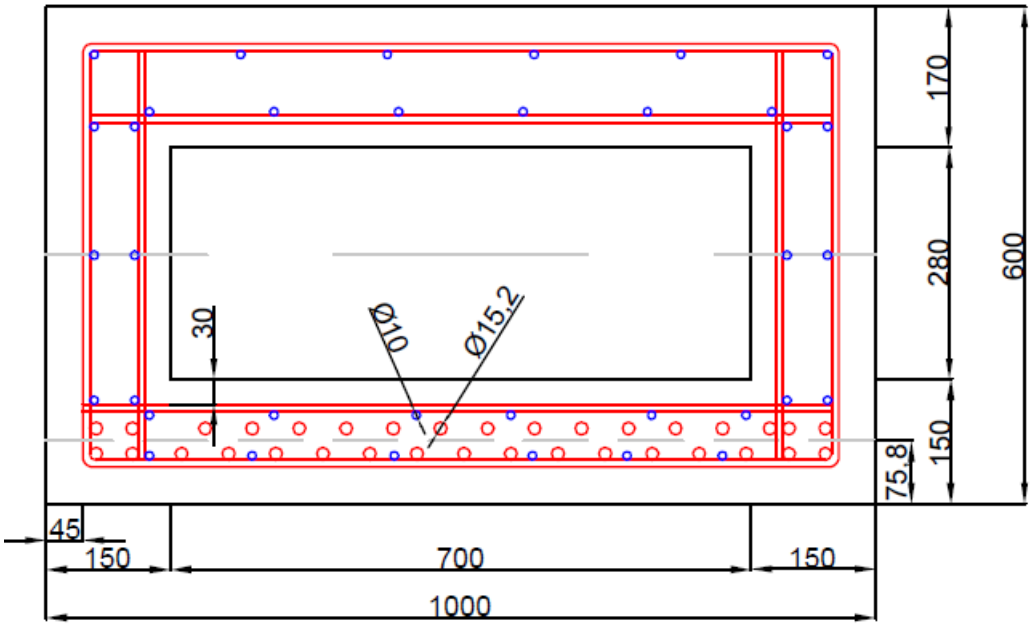

Figure 6-7: HPC cross section at mid span

It can be concluded that all the prestressing strands can fit in the cross section, but some parts will be difficult to fit all necessary steel, due to clustering of strands, bars and stirrups. Also the spacing between strands and bars and strands among each other are not always according to the requirements. Further research is advised to determine if the fitting in the manner presented will cause performance issues considering the interaction of steel and concrete and the performance of the concrete in general.

6.14 Capacity check of hammerhead

Because most of the strands are located in the bottom flange, the gravity point of strands will fall outside the neutral axis and cause an eccentric moment at the hammerheads. Since the moment due to static loading is very low close to the support it is necessary to see if there is enough capacity to resists the eccentric moment caused by the strands. The governing location is there where the strands have reached their full force and that is at the end of the transition at a distance of l_{pt} from the supports. The check should be performed at time of construction (t=0), as variable loads are not yet presented here to slightly counter balance the eccentric moment. Already was found that indeed at this stage the moment at the end support is the highest. This transmission length is calculated according to EN 1992-1-1 cl. 8.10.2.2 while taking into account the changes given in the AFGC: l_{pt} = 767.38 mm.

The design bending moment at l_{pt} is: $M_{Ed,lpt}$ = 1154.8 kNm.

At l_{pt} the situation is as in Figure 6-8 is presented. The compression zone is at the bottom side. The height of the compression zone has to be determined. Then the moment capacity can be calculated. The moment capacity $M_{Rd,head}$ should be higher than the design moment M_{Ed}.

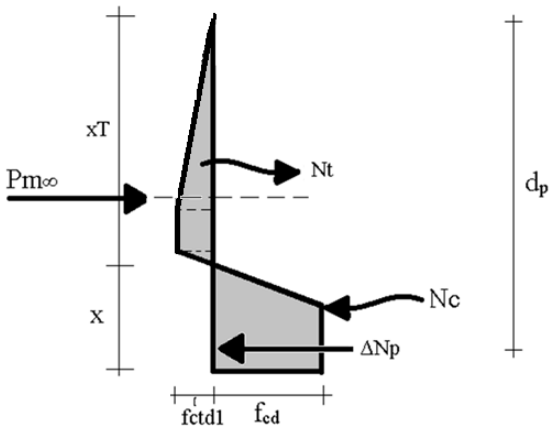

Figure 6-8: Internal forces at hammerhead

For equilibrium of the internal forces the following equation stands: $P_{m0} + N_t = N_c + \Delta N_p$. Solving this equation results in a compression zone height of x_u = 183.05 mm. Then if the moment around the point of the resultant of N_c is taken a moment capacity of **M_{Rd} = 1760.9 kNm** is found.

Unity Check: $M_{Ed,lpt}/M_{Rd}$ = 1154.8/1760.9 = 0.66 → OK

Appendix F.14 gives the detailed calculation of the capacity at the hammerhead.

6.15 Detailing

The pretress force in pre-tensioned steel is introduced by bonding. There is a certain transmission length (here l_{pt} = 532.91mm) where after the prestress force is fully transferred. Inside the transmission length the bond stresses can cause tensile stresses. In pre-tensioned steel three types of tensile stresses can occur (Figure 6-9):

- Bursting stresses
- Splitting stresses
- Spalling stresses

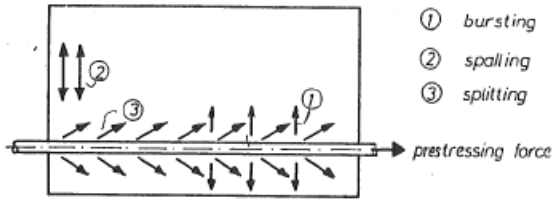

Figure 6-9: Types of tensile stresses

The bursting and splitting stresses are prevented if the cover and distance between strands is at least 2φ. That is the case here so these two types of stresses are prevented. To determine the spalling stresses a graphical method by Den Uijl [9] can be used (Figure 6-10).

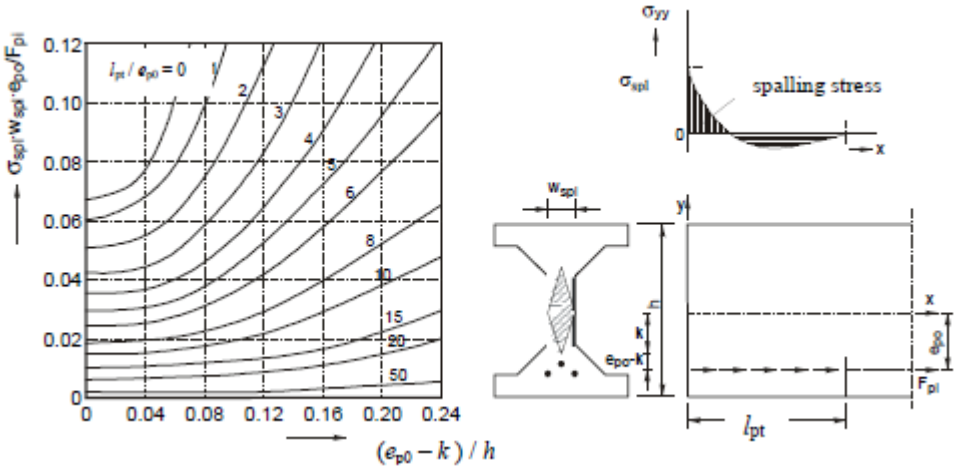

Figure 6-10: Graphical method by Den Uijl for determining the spalling stresses

A spalling stress of **σ_{spl} = 1.583 N/mm²** is found

The spalling stress is lower than the tensile strength (lower than both f_{ctd} and f_{ctk}), so no spalling reinforcement is needed in the structure.

6.16 Crack width verification

In order for a structure not to be verified for crack width, it is necessary that the maximum moments in SLS (M_{max}) do not exceed the cracking moment (M_{cr}). And it is also necessary that the tensile strength of the concrete is not exceeded anywhere in the structure. The frequent factor ψ1 has to be applied for the variable loads (is 0.8 for UDL, TS and pedestrian load).

M_{max} = 543.8 kNm

The cracking moment M_{cr} is determined with:

M_{cr} = $W_b*(f_{ctm} + P_{m\infty}/A_c)$ = **986.78 kNm**

Unity Check: M_{max}/M_{cr} = 543.8/986.78 = 0.551 → OK

The maximum moments in the SLS do not exceed the cracking moment.

Now the stresses in the structure in the SLS have to be checked. This is done with the same expressions used to determine the amount of strands:

$t = 0$ at top fibre: $\sigma_c = -\frac{P_{m0}}{A_c} + \frac{M_{p,0}}{W_{ct}} - \frac{M_g}{W_{ct}}$: σ_c = -2.99 N/mm²

$t = 0$ at bottom fibre: $\sigma_c = -\frac{P_{m0}}{A_c} - \frac{M_{p,0}}{W_{cb}} + \frac{M_g}{W_{cb}}$: σ_c = -30.08 N/mm²

$t = \infty$ at bottom fibre: $\sigma_c = -\frac{P_{m\infty}}{A_c} - \frac{M_{p,\infty}}{W_{cb}} + \frac{M_g + \psi 1 * M_q}{W_{cb}}$: σ_c = -4.59 N/mm²

The structure is in all three situations completely under compression. So crack formation is not possible. These results are expected, since the prestressing is determined with assuming a fully prestressed beam.

The cracking moment is not exceeded and no tensile stresses occur at the construction and user stage in the SLS. Furthermore the bridge is simply supported so imposed deformations are not restricted, which means that unexpected tensile stresses will not occur. So crack width verification is not necessary in this case.

Detailed calculation in appendix F.16

6.17 Deflection

It is important for the structure that the deformations caused by the working loadings during service life are within acceptable limits. When determining the deformations it is important to distinguish the deformation in a cracked and uncracked section, because this has a big influence on the deflections (in the shape of a greatly reduced stiffness). In the case of the Leiden Bridge there are no cracked sections as already was concluded in paragraph 6.16. So the structure is considered to be uncracked everywhere. The governing cross section is right in the middle of the beam, since here the highest deformations will occur, caused by the combination of the highest moments.

The occurring deflections have to satisfy a couple of limits given in NEN-EN-1992-1-1 in chapter 7:

- The camber may not exceed L/250 = -96 mm (L = 24000 mm)
- The sag may not exceed L/250 during serviceability = 96 mm
- If a chance exists of damaging adjacent parts then the sag may not exceed L/500 = 48mm

The camber is caused by prestressing. The sag should be limited to L/500, because underneath the bridge there is an unused intermediate pier.

Three load combinations will be investigated:

4. t=0; fabrication and erecting structure; self-weight + prestressing: $q_{self} - q_{pm0}$
5. t=0; after placing asphalt and such; Dead load + prestressing: $q_{self} + q_{dead} - q_{pm0}$
6. t=∞; user stage; All loads as quasi permanent combination: $q_{self} + q_{dead} + \psi_2 * q_{var} - q_{pm\infty}$

The deflection in the middle of the span is determined with: $w = \frac{5*q*L^4}{384*E_{c,eff}*Ic}$

The prestress force is assumed as a line load to simplify the calculation. This will slightly reduce the upward deflection due to the prestressing. The results are seen in (Table 6-3):

Table 6-3: Results deflection

	With $E_{c,eff2}$	Limit
Combination 1: w [mm]	-110,810	-96,0
Combination 2: w [mm]	-65,395	-96,0
Combination 3: w [mm]	19,503	-48,0

The results in Table 6-3 show that the occurring deflections satisfy the limits. Only the camber is too high. This means that in terms of deflection the prestressing force is too high. But the first situation (self-weight and prestressing force) is a situation that mostly occurs in the factory. In the factory this issue can easily be monitored and fixed. The camber limit is used when formwork is used during construction. But because prefabricated beams are used, there will be no formwork (except for small planks for the joints between the beams). So the - higher than the limit - deflection will not cause major issues. Eventually the beams are erected and connected and then the hardening layers are placed. Now combination 2 occurs and here the deflections are lower than the limit.

6.18 Vibration

The vibrations occurring on the structure may not cause discomfort during serviceability. This can be checked by determining the natural frequency of the structure. The natural frequency has to suffice according to the demands given by the Eurocode.
The natural frequency for the first (and governing) node is determined with:

$$n0 = \frac{C}{2\pi} * \sqrt{\frac{E_{cm}*I_c}{A_c*\rho_c*L^4}} \quad [Hz]$$

With C being the constraint factor (= 9.87 = π^2 for simply supported structures).
If all variables are filled in the formula then **n0 = 2.33Hz.**

The Leiden Bridge is used both by traffic, trams and pedestrians. So the vibrations caused by each should be considered.

Pedestrians
The NEN-EN-1991-2 states for pedestrian bridges that the natural frequency should at least be 5 Hz. Furthermore it states that frequencies caused by pedestrians fall between 1 and 3 Hz.
The determined natural frequency is lower than 5 Hz and it falls in the range of the pedestrian frequencies. So there would be a chance that pedestrians could cause a frequency equal to n0, which could lead to resonance and discomfort. However, considering the high mass of the bridge, the frequency from the pedestrians will hardly have any effect on the actual bridge. So a dynamical analysis is not required to precisely determine the frequencies exerted by pedestrians. This would not be the case if considered was a pedestrian bridge. These are usually smaller in size and lighter than traffic bridges and a lot more susceptible to vibrations. This was the case with the bridge projects that were discussed in the literature study. A lot of these bridges were pedestrian bridges and almost all required dampers to limit the vibrations caused by pedestrians. But this is not the case for the Leiden Bridge so no further attention is necessary here.

Trams
For vibrations caused by trams specifically there is nothing stated in the Eurocode. However the Eurocode gives guidelines for vibrations caused by trains so these could be used to give an estimation of the vibrations caused by trams. In figure 6.9 NEN-EN-1991-2 a flowchart is given to determine if a dynamical requirement is necessary. For this design following this flowchart results in a structure that does not require a dynamic analysis.

The complete process of the flowchart is seen in appendix F.18

Attention has to be paid to the pedestrian vibrations, but because of the mass of the bridge it is not necessary to take action against these vibrations. If one would choose to increase the natural frequency than this could be done by increasing the stiffness of the structure. This can be done by for example increasing the construction height, which increases I_c and thus the overall stiffness. But due to the demands given, it is would not be possible to use a thicker deck.
Using a fixed beam instead of a simply supported beam would increase the natural frequency the most (the constant C goes from 9.87 to 22.4, so about a factor 2.2 higher).

6.19 Fatigue

The bridge is susceptible to cyclic loads coming from trams and traffic. In the demands for the new design it is given that there are 30 tram movements per track per hour over the bridge. That is equal to 788400 movements per year in total. Furthermore the bridge is assumed to be part of a main road with a low amount of heavy traffic. This means according to NEN-EN-1991-2 table 4.5 that there are $0.125*10^6$ vehicles per lane per year. So for a total of 100 years and 7 fictional lanes, this results in $87.5*10^6$ vehicles. So traffic is governing for the fatigue design.

In NEN-EN 1992-1 and NEN-EN 1992-2 it is described how to determine if a structure is safe concerning fatigue for both the concrete and prestressing steel. The procedures described there will be applied for Load Model 1. The fatigue resistance of both the concrete and prestressing steel will be determined separately.

6.19.1 Fatigue resistance concrete

The fatigue resistance of the concrete is checked at the mid span in both the top and bottom fibre of the cross section. To verify the fatigue resistance of concrete, cl. 6.8.7 of the Dutch National Annex of NEN-EN-1992-2 is used. This section state that the following expression must hold true:

$$N_i = 10^{\left[\frac{6}{1-0.57*k1*\left(1-\frac{f_{ck}}{250}\right)}*\frac{1-E_{cd,max,i}}{\sqrt{1-R_i}}\right]} > 10^6$$

Where:

$$R_{equ} = \frac{E_{cd,min,i}}{E_{cd,max,i}};\quad E_{cd,min,i} = \frac{\sigma_{cd,min,i}}{f_{cd} * (0.9 + \frac{logN_i}{60})};\quad E_{cd,max,i} = \frac{\sigma_{cd,max,i}}{f_{cd} * (0.9 + \frac{logN_i}{60})}$$

$\sigma_{cd,min,i}$ and $\sigma_{cd,max,i}$ are the lower and upper stresses of the damage equivalent stress spectrum with a number of cycles $N=10^6$. These are determined by using the following load combination:
For $\sigma_{c,max}$: $(\sum G_{k,j} + P + \psi_{1,1}Q_{k,1} + \psi_{2,j}Q_{k,j}) + Q_{fat}$
For $\sigma_{c,min}$: $(\sum G_{k,j} + P + \psi_{1,1}Q_{k,1} + \psi_{2,j}Q_{k,j})$
Q_{fat} is the fatigue load. In the governing situation traffic load model LM1 (when only vehicles are present) is the fatigue load. So the minimum and maximum stresses are determined when Q_{fat} is present and absent.

For the fatigue calculation where LM1 is taken into account it is necessary according to NEN-EN 1991-2 cl. 4.6.2 to reduce the UDL with a factor 0.3 and the TS with a factor 0.7. The next and only other variable load is the pedestrian load so this one serves as $Q_{k,1}$

For the top fibre: $N_i = 4.32 * 10^9 > 10^6$
For the bottom fibre: $N_i = 3.62 * 10^9 > 10^6$
Both the top and bottom fibre in the mid span have enough fatigue resistance

6.19.2 Fatigue resistance prestressing steel

For the prestressing steel it must hold true that[24]:

$$\gamma_{F,fat} * \Delta\sigma_{S,equ}(N^*) \leq \frac{\Delta\sigma_{Risk}(N^*)}{\gamma_{s,fat}}$$

Also allowed is to use a simpler approach by verifying[25] that the stress range $\Delta\sigma_s$ should be lower than value k1, which is taken as 70 N/mm^2. If this holds true the verification stated earlier is not necessary to perform.
To determine $\Delta\sigma_s$ the maximum and minimum stress determined in paragraph 6.19.1 are used to find the stress $\Delta\sigma_{c,p}$ at the height of the prestressing. This concrete stress is then transformed in a steel stress by: $\Delta\sigma_s = \Delta\sigma_{c,p} * (E_p/E_c)$.

The steel stress range is:
$\Delta\sigma_s$ = 37.05 N/mm^2 which is well below 70 N/mm^2 (UC=0.529)
So the fatigue resistance of the prestesssing steel meets the requirements. Additional verifications are not necessary

The detailed calculation is found in appendix F.19

6.19.3 Conclusion fatigue

The concrete has enough fatigue resistance and the prestressing steel does have enough fatigue resistance to resist the variable cyclic loads that occur on the bridge.

[24] NEN-EN-1992-1 cl.6.8.5
[25] NEN-EN-1992-1 cl. 6.8.6

6.20 Conclusion HPC C90/105 design

In this chapter research has been done to determine if it is possible to achieve the same slenderness and also meeting all safety requirements if, instead of UPHC, high strength concrete with steel fibres was used. HPC is cheaper to produce than UHPC, so if a HPC design would prove to be achievable, the design could prove to be more economical than the UHPC design.

The bending moment capacity (UC = 0.652) and rotational capacity (UC=0.825) were sufficient according to the requirements. The shear capacity did not meet the safety requirements (UC=1.1), so stirrups are necessary. Sufficient is to use minimum shear reinforcement, that would otherwise be used to keep the torsion reinforcement in place. However if HSC C90/105 and HPC 90/105 are compared than the improvement in shear capacity is very large. This is mostly thanks to the contribution of the steel fibres. However this is not the case for the torsional capacity. There is not much known about how steel fibres contribute to the torsional capacity (however it is known they contribute positively) so it is assumed that only the concrete has to resist the torsional moments. The low design tensile strength cannot provide enough torsional capacity to resist the design torsional moment (UC=1.211). Therefore longitudinal reinforcement has to be applied. This also means that additional stirrups are necessary in order to hold the longitudinal bars in place. And these stirrups are needed for the shear capacity as well, as already was stated.

This extra reinforcement will make it harder to fit all bars and strands within the cross section. It is shown that everything is able to be placed in the cross section except for some local issues, which probably will not cause too many problems. Nevertheless attention has to be paid to these details. The beam is fully prestressed, which means that the beam is in compression over the whole height during service life. And with a cracking moment that is higher than the maximum moment in SLS (UC=0.551), no cracks will occur. The deflections also stay within limits. Concerning fatigue resistance, the concrete has enough resistance to resist the cyclic loading.

In short it can be said that it is possible to design the bridge in HPC with the same dimension as the UHPC or C50/60 design (with the main parameter the construction height of 600mm), as the bridge meets the safety all the safety requirements.

The UHPC design is constructive wise still better and with the UHPC design it is also easier to construct the beam, since there is no reinforcement and only prestressing strands. But the HPC design is achievable and depending on the price of HPC perhaps also cheaper to construct. The UHPC design has to be optimized further. Then after optimization it is possible to compare all the developed designs with each other and determine on multiple aspects which design is the most suitable.

6.21 Summary

Results if a thickness of 600 mm is used:

Amount of strands:	34ϕ15.2 strands	
Total losses in strands:	9.7%	
Slender ratio λ	40	
ULS		
Bending moment capacity, M_{Rd}:	M_{Rd} = 1955.31 kNm	UC = 0.652
Rotational capacity: x_u/d	x_u/d = 0.446	UC = 0.825
Shear capacity V_{Rd}:	V_{Rd} = 695.07 kNm	UC = 1.101
Shear reinforcement	A_{sw} = 575 mm^2 (min. reinf.)	
Torsional capacity T_{Rd}:	T_{Rd} =261.8 kNm	UC = 1.211
Torsion reinforcement:	A_s = 2828 mm^2	
Transverse moment capacity: $M_{Rd,y:}$	$M_{Rd,y}$ = 161.6 kNm	UC = 0.921
Capacity concrete at hammerhead:	$M_{Rd,head}$ = 1760.9 kNm	UC = 0.656
SLS		
Crack width verification:	M_{CR} = 986.78 kNm	UC= 0.551
Deflection:	w2 = 65.4mm < L/500	
	w3 = 19.5mm < L/250	
Fatigue:	Concrete: Top fibre:	UC = 0.580
	Bottom fibre:	UC = 0.859 but n_i/N_i>1
	Prestressing:	UC = 0.529

Chapter 7 Optimization C170/200 design

7.1 General

In Chapter 5 a design was developed in UHPC for the Leiden Bridge. Calculations were performed to determine the safety of the design. The design proved to be safe both in SLS, ULS and for fatigue as well. However the current UHPC design has much more capacity than is required. This means that the design is open for optimization. Optimizing the structure will lead to a more efficient design.

One of the goals of this thesis is to create a design that is as slender as possible. So the goal of the optimization process will be to create a structure that is as slender and as light as possible, while still having enough capacity, both in SLS and ULS, to resists the working loads on the bridge.
In the literature study different optimization methods were discussed with the main categories being:

- Sizing optimization
- Shape optimization
- Topology optimization

For the Leiden Bridge there is not much freedom to do extraordinary things with the design, because the requirement is that the view of the bridge remains the same as the current one.
Therefore topology optimization and shape optimization cannot be used effectively here.
So the only thing to optimize in the design is the actual box girder itself. This falls under the category of sizing optimization. There are multiple variables that could be optimized:

- *Height*: Will have the most influence on most of the aspects. The structure will become lighter. The number of strands will increase, which means an increase in compression force. The capacities in the ULS will decrease. Deflections will most likely be governing due to decrease in stiffness.
- *Width*: Smaller width could save material. But if beams are placed next to each other, more beams will be required. Or the width could be reduced, while keeping a c.t.c distance of 1000mm. However this will result in larger joints and reducing width will not have a too large influence. Especially if the web thickness remains the same.
- *Top flange*: Reducing the top flange will provide a lighter beam but the transverse capacity will decrease. Unless more strands are used in the transverse direction or the ducts are placed closer to each other.
- *Bottom flange*: Gives a lighter material, but the fitting of strands is governing here. There still needs to be enough space between all strands. This could perhaps be an option if for example limited prestressing is used.
- *Web thickness*: Smaller web thickness will reduce the shear capacity mostly. Also horizontal spacing between strands is important. In the current design there are 4 strands in each web. If for example only 2 strands are placed in a web, one below the other, the web can be reduced around 50 mm, if the capacity still remains high enough.
- *Prestressing strands*: Instead of considering a fully prestressed beam, it is possible to assume a limited prestressed beam. So tensile stresses up to the tensile strength may be allowed. This could be beneficial for UHPC as it has a high tensile strength. Also it will lead to fewer strands, which is more economical. However it is important that the capacity stays high enough and that the deflection does not surpass the given limits.
- *Location of deviators*: It is also possible to shift the location of the deviators. These deviators provide the kinks in the prestressing strand. Changing their location in the span will influence the upward force in the strands. This upward force will influence the design shear force, by reducing the total shear force. However if the deviators are too close to the support the upward force can be too high and then it will contribute negatively for the total shear force. So an optimal distance from the supports has to be found.

In this case however the upward force is very low, because only a few strands are kinked. The increasing or decreasing upward force will hardly have any effect on the design shear force.

With the results of Chapter 5 it can be determined, which variables are open to further optimize and it can also be determined what the limits are for optimization. First of all the width and top flange will remain unchanged. It is beneficial to keep the width at 1000mm, because it will keep the amount of beams the same as in the current UHPC design, while still providing more stiffness than beams which are farther apart from each other or beams with a width of 1500mm. The top flange will remain 160mm, because lowering the thickness will lower the transverse moment capacity and even though the joint was governing, the capacity of the top flange itself was also close to its limits, so it is better to keep this one at 160mm. The location of the deviators will remain the same, as changing its location will hardly effect the shear force in this case. This leaves the web, the bottom flange, the strands and the total height open for optimization.

7.2 Determining limits

7.2.1 Minimum web thickness

There exists a minimum thickness for the web, which is set by the strands in the webs (Figure 7-1). In the current UHPC design the web is 140 mm thick and there are two strands placed next to each other horizontally (in two rows which makes four per web in total). If assumed is a minimum spacing between strands of 2φ the web should be at least 2c+2φ +2φ = 131.6 mm thick.
However if instead of 4 only 2 strands are placed in each web, then the minimum thickness becomes: 2c+φ = 86 mm. So it is wise to assume only two strands per web. This means that the removed four strands will be placed in the bottom flange instead. It should be checked if these additional strands will fit together with the other present strands in the flange. For optimization the minimum web thickness will be set to 90 mm. Lower than this value is not allowed.

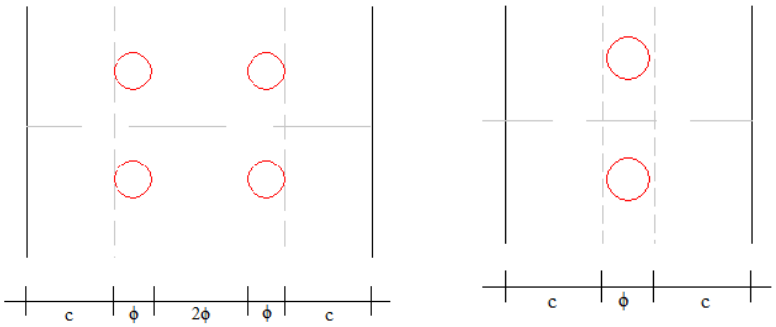

Figure 7-1: Minimum web thickness

7.2.2 Minimum bottom flange thickness

For the bottom flange there exists a same limit as for the webs: Most of the strands will be placed in the bottom flange. Two layers will be necessary in order to fit all the strands in the flange. Assuming the strands are placed in a fashion as seen in Figure 7-2, the minimum top flange thickness should be 2c+3φ = 116.4 mm. For optimization the minimum bottom flange thickness will be set to 120mm. Lower than this value is not possible, unless the strands are bundled together, for example three strands per bundle. With this the bottom flange can be reduced further by 20mm. But chosen is to keep the strands separate due to detailing reasons (spalling, bursting etc.).

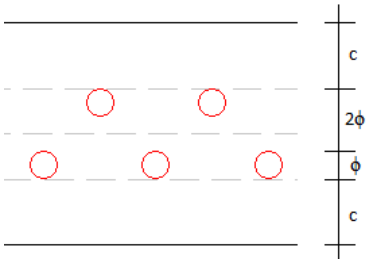

Figure 7-2: Minimum bottom flange thickness

7.2.3 Prestressing

In the current UHPC design the amount of prestressing strands were calculated under the assumption that the box beam is fully prestressed. However due to the high tensile strength of UHPC it could be interesting to assume a limited prestressed beam instead. This could reduce the amount of prestressing needed, while still making sure that the tensile strength is not exceeded. The amount of prestressing strands will be optimized by using the following stress requirements:

Limited prestressing 1 (limiting the tensile stresses up to f_{ctd1}):

- At t=0 in the top fibre: $\sigma \leq f_{ctd1}$
- At t=0 in the bottom fibre: $\sigma \geq -0.6*f_{ck}$
- At t=∞ in the bottom fibre: $\sigma \leq f_{ctd1}$

Limited prestressing 2 (limiting the tensile stresses up to f_{ctk}):

- At t=0 in the top fibre: $\sigma \leq f_{ctk}$
- At t=0 in the bottom fibre: $\sigma \geq -0.6*f_{ck}$
- At t=∞ in the bottom fibre: $\sigma \leq f_{ctk}$

Using these requirements the reduction of strands will be determined and the safety of the structure will also be determined, while using these limited prestressing requirements.

7.2.4 Height

Because the goal is to find a as slender as possible structure it would be interesting to reduce the construction height of the beam as well, since there is a lot of capacity left in the current UHPC design. There are no restrictions for the construction height, except of course that the structure still has to meet the requirements in the SLS and ULS state and for fatigue.

7.3 Optimization according to governing internal forces

The first step of the optimization process is to optimize the beam as a whole. The results of the internal forces obtained in Chapter 5 will be used here. Furthermore the same calculation procedures found in the same chapter will be used to determine the moment capacity, shear capacity and so on. This first step will be divided in multiple parts. First the prestressing is going to be altered, because changing the amount of prestressing strands will have a great influence on the structure. Afterwards the web thickness will be altered to find the smallest thickness possible. Lastly the bottom flange thickness and the construction height will be changed to even further optimize the beam. The numerical results are found in appendix G.2.

7.3.1 Results optimization of prestressing

The requirements for determining the amount of strands have been changed according to the ones given in paragraph 7.2.3 and the design has been calculated completely in the same way as in Chapter 5. The most notable change is the amount of strands. This is because it requires fewer strands to limit the stresses to a certain tensile strength than to zero. Limiting the stress to f_{ctd1} results in a decrease from 33 to 29 strands and limiting the stress to f_{ctk} reduces the amount even further to 27 strands. The decrease in strands also means a decrease in the bending moment capacity (M_{Rd}) and an increase in the design bending moment (M_{Ed}).

The shear and torsional capacity are not influenced by the reduction in strands (for the shear capacity only the contribution of the steel fibres is taken into account). However the capacities in the ULS state are all high enough for both limited prestressing 1 and 2. The cracking moment also decreases, but it nevertheless meets the requirements and the same holds true for the fatigue resistance.

However the decrease in strands has a large influence on the deflections and here it is the governing variable. The decrease in strands means a smaller hogging deformation (w2, where only permanent load is present) and a larger sagging deformation (w3, where all loads are present in the quasi permanent combination).
When the stresses are limited to f_{ctk} the deflection w3 is too high (albeit only 0.5mm higher than allowed). This would mean that further optimizing the beam would be hard, because if the height is reduced for example, then the stiffness will decrease, which means that the deformations will become higher. Looking further at the two options for limiting prestressing, the difference in strands is only two strands.

Limiting the stresses to f_{ctd1} gives more room for further optimization and there is still a notable decrease in strands compared to the initial design. Therefore for future optimization steps assumed will be a limited prestressed beam, where tensile stresses are limited to f_{ctd1}.

7.3.2 Results optimization of web thickness

With the assumption of a limited prestressed beam the next part of the optimization of the full beam is to reduce the web thickness. Reducing the web thickness will have a large influence on the shear and torsional capacity. The goal is to reduce the web thickness, until the shear and torsional capacity are just enough to resist the working torsional moment and shear force ($0.9 < UC < 1$) or until the minimum thickness of 90 mm is reached. The web thickness is changed from 140 mm to 90 mm in steps of 10mm. In Figure 7-3 the influence of the web thickness is shown for the shear, torsional and moment capacity. Most notable differences are the decrease in shear and torsional capacity. As expected the torsional and shear capacity decrease with decreasing web thickness. This can be seen with increasing the unity check.

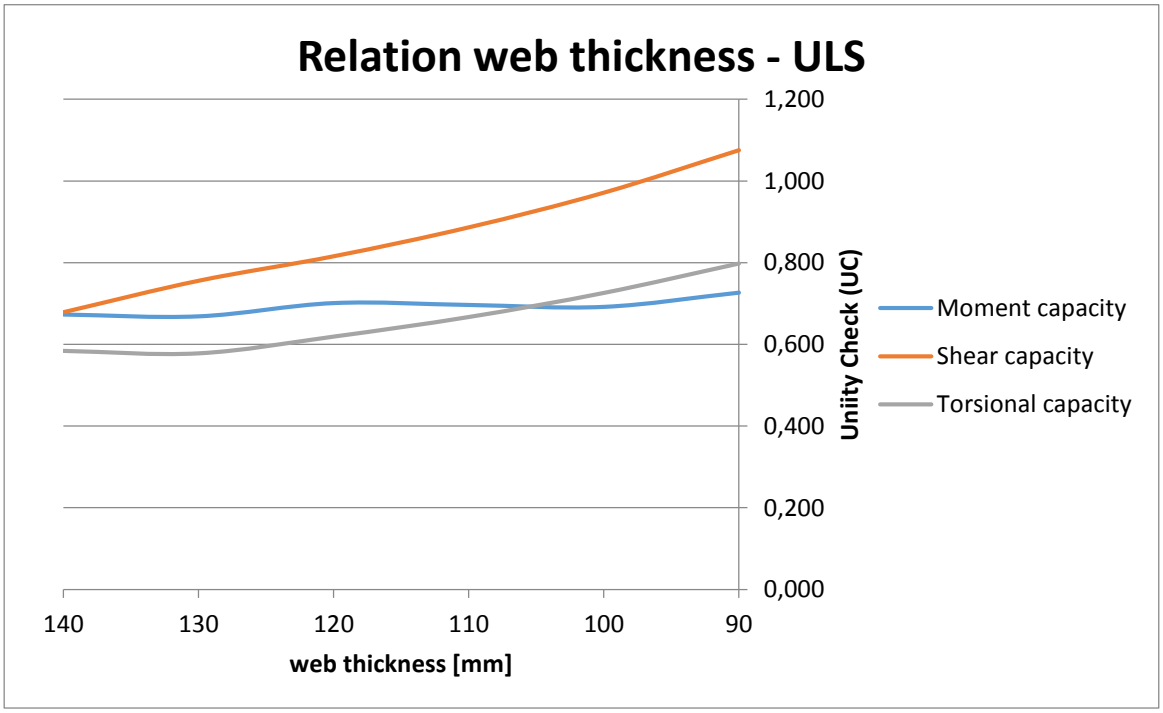

Figure 7-3: Relation web thickness and ULS

The moment capacity however shows a fluctuating unity check and not a constant increase or decrease. This 'fluctuation' occurs because the amount of strands changes as well. Decreasing the web thickness results in a lighter structure which again results in a lesser amount of strands. When the amount of strands decreases, the total prestress force decreases as well. So the moment capacity will be lower and the design bending moment will be higher. However the beam gets lighter as well so that slightly compensates the increasing bending moment. Adding all these effects will lead to the fluctuation in the unity check of the moment capacity, when the web thickness decreases.

The figure shows that with the minimum web thickness of 90 mm the structure does not have enough shear capacity. With a web thickness of 100mm the structure is safe and meets all the necessary requirements. In the other steps of the optimization process a web thickness of 100 mm will be assumed, together with the assumption of limited prestressing.

7.3.3 Results optimization bottom flange thickness

The bottom flange thickness was already near its limit in the initial UHPC design. The thickness can only be reduced 10mm. The decrease in thickness of the bottom flange also led to a decrease the eccentricity of all the strands at the bottom flange. This is done so that the strands can be fitted more effectively in the now smaller available space. Reducing the bottom flange thickness has mostly led to a weight reduction and because the eccentricity of the strands is smaller the prestress force can exert a higher moment so the design bending moment decreases. The shear capacity increases as well due to the increase of the effective height. Overall the structure still meets all safety requirements. The bottom flange thickness will therefore remain at 120 mm.

7.3.4 Results optimization construction height

The last part remaining in the optimization of the full beam, based on the governing internal forces, is optimizing the construction height. Assumed is a limited prestressed beam ($\sigma<f_{ctd1}$) with a web thickness of 100mm and a bottom flange thickness of 120mm. With these assumptions the construction height is reduced until an optimal height has been found. The construction height has been reduced in steps of 10mm from the original H=600 mm to H=500 mm. In Figure 7-4 the influence of changing the construction thickness on multiple capacities is shown.

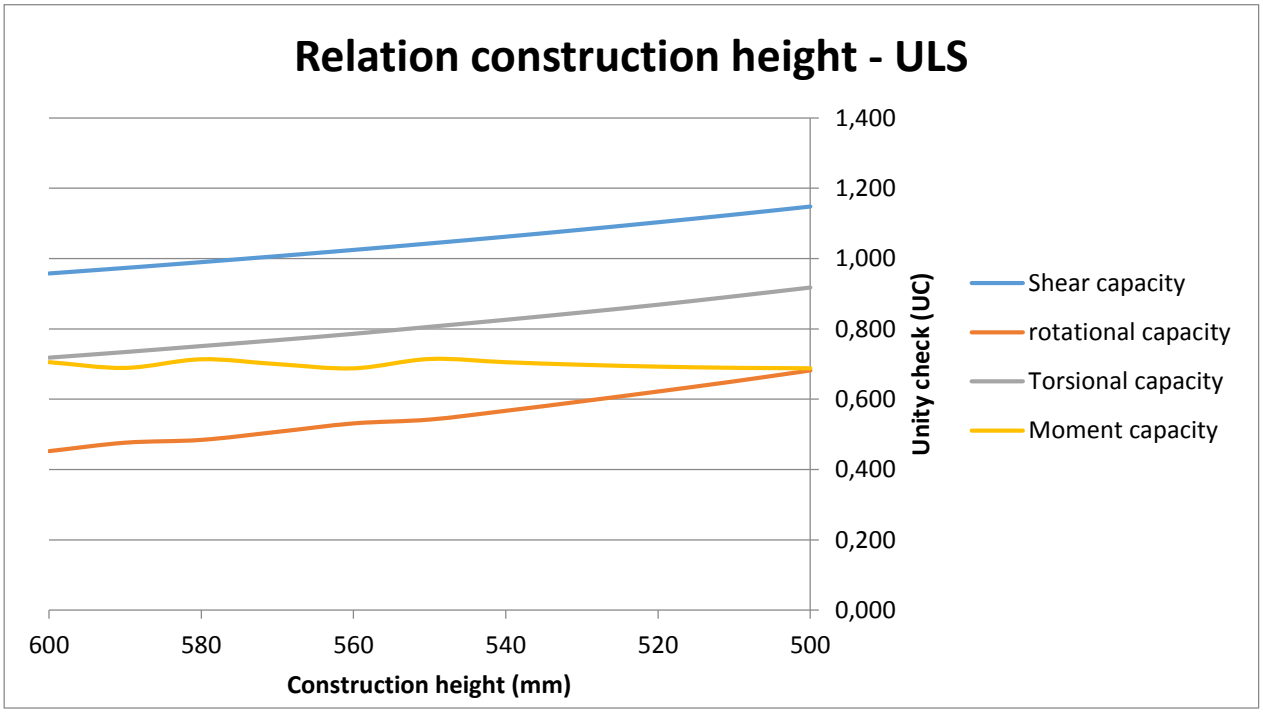

Figure 7-4: Relation between construction height and ULS

The figure clearly shows that the different capacities decrease relatively to the working design loads. This is certain for the shear, torsional and rotational capacity. A lower height means a lower effective height which results in a lower capacity.

The moment capacity however does not show a clear decline in capacity. This is the same phenomenon as explained in paragraph 7.3.2. There is a relation between the amount of strands and the moment capacity that causes the capacity to stay around the same UC. This relation is seen in Figure 7-5. The number of strands increases with decreasing construction thickness. Generally speaking a higher number of strands results in a higher moment capacity and a lower design bending moment. Meanwhile a decrease in the height results in a lower moment capacity, but also in a lower design bending moment as the weight decreases as well. When the two effects are combined one of the two will have more influence on the moment capacity. Figure 7-5 shows that when the height gets lower than H=550 mm, the increasing amount of strands has a larger effect on the moment capacity than the decreasing height. So the Unity check keeps decreasing.

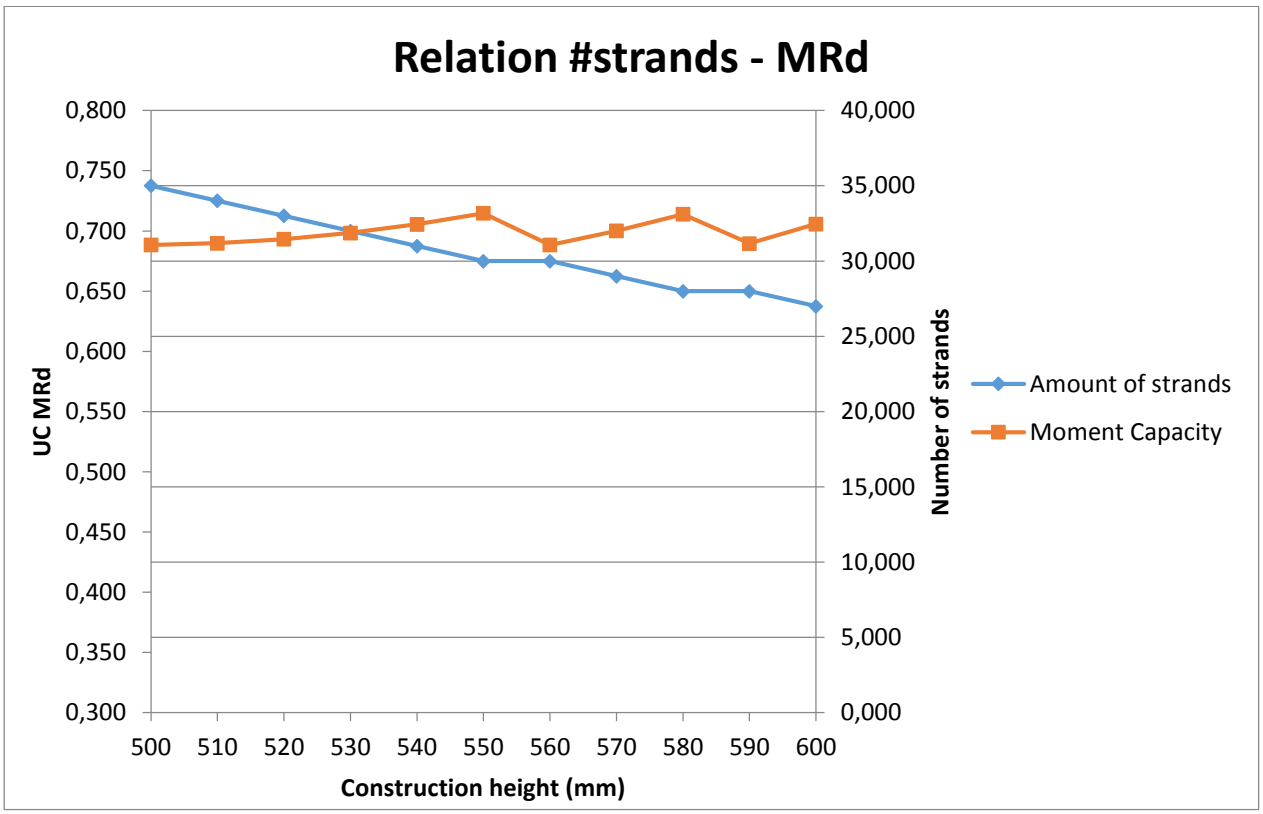

Figure 7-5: Relation between number of strands and moment capacity

Considering the Unity checks, going lower than H=580mm results in a too low shear capacity. On H=580 mm the shear capacity is on the border with UC=0.990. At H=570mm UC=1.007, which means that the shear capacity is slightly lower that the design shear force. The shear capacity is governing in the case of optimization of the construction height. The shear capacity is mostly influenced by the web thickness. So instead of having a web thickness of 100mm it could be possible to reach lower construction thicknesses with thicker webs. This can be investigated by starting at H=580mm and b_{web} = 100mm and then increasing b_{web} to 110mm and then finding a lower H. When a new H is found, b_{web} is increased again and this is done until b_{web} is again 140mm or until the height cannot be reduced any further. Also kept in mind are other variables in the ULS and SLS. This way the beam can become more slender and material can be saved as well.

In Table 7-1 the results of this process are shown. Compared are the minimum heights possible with a certain web thickness, the cross sectional area of the concrete and the amount of strands. The initial design and the design based on the results of paragraph 7.3.3 are also shown in the table.

Table 7-1: Comparison of construction thickness with different web thicknesses

	H_{min} [mm]	A_c [m2]	# strands
Initial design (b_{web}=140 mm)	600	0,377	33
Lim. Prestr. (b_{web}=100 mm)	600	0,344	27
b_{web}=100 mm	580	0,340	28
b_{web}=110 mm	530	0,335	32
b_{web}=120 mm	500	0,333	35

With a b_{web} of 110mm the thickness can be decreased further to 530mm and to 500mm if b_{web} = 120mm. This is possible because the shear capacity stays the governing variable. The problem now is that the amount of strands has increased a lot. It went from 27 to 35 strands, while the area went from 0.344 to 0.333m^2. This means that concrete is hardly saved, while a lot more prestressing is needed. Even though the structure is more slender, the structure gets more uneconomical. The increase in strands will cost more than the decrease in concrete. Furthermore it will become more difficult or even impossible to fit all the strands. Having 35 strands means that 31 strands will go in the bottom flange, because with the thinner webs there are only 2 strands per web (instead of 4 as in the initial design). This high amount of strands in the bottom flange will also cause a larger eccentricity with regards to the neutral axis, so the strands will cause a higher moment at the supports.

Based on the higher costs the extra strands will bring and the structural and constructional issues as well, it is concluded that the structure with H=580mm and b_{web}=100 is the most optimal result in this paragraph.

7.3.5 Conclusion optimization according to governing internal forces

The first step in the optimization process was to optimize the beam according to the governing internal forces. This first step was divided in multiple parts. With all the results a new optimized UHPC design is created. The dimensions of the cross section are as follows:

	Initial design	**Optimized design**
H:	600 mm	580 mm
B:	1000 mm	1000 mm
h_{top}:	160 mm	160 mm
h_{bot}:	130 mm	120 mm
b_{web}:	140 mm	100 mm
Number of strands:	33φ15.2	28φ15.2
A_c	0.377 m^2	0.340 m^2
q_{self}	9.885 kN/m	9.000 kN/m

In Figure 7-6 the cross section of the optimized girder is shown including all the strands inside the concrete. Practically it is perhaps better to keep the height at 600 mm instead of 580mm, since construction heights are usually chosen per 50mm in the prefab world. This cross section also has one strand less and is seen in Figure 7-7.

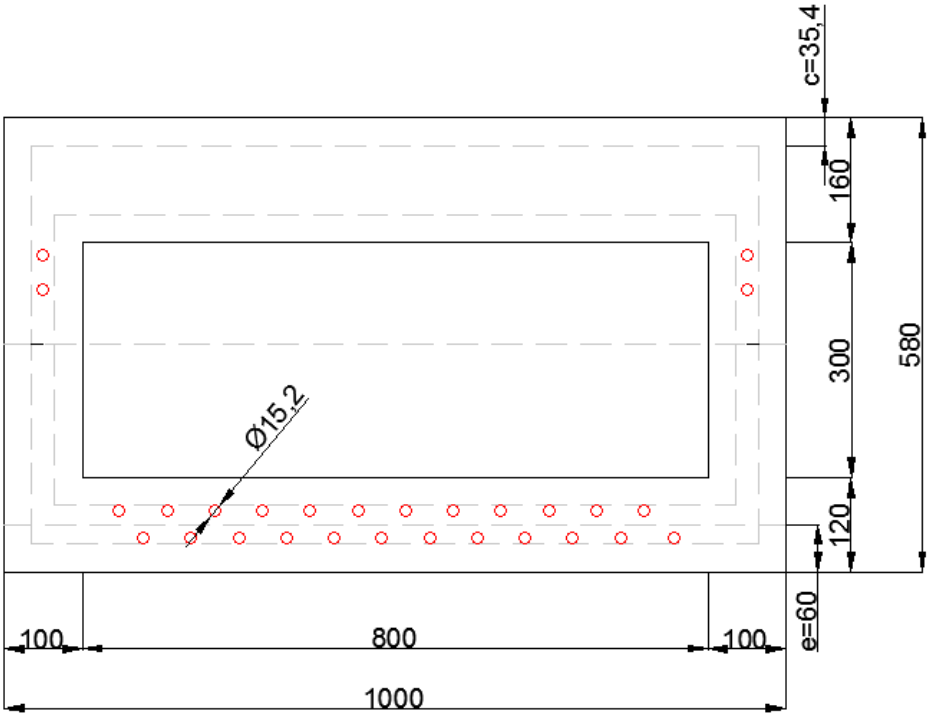

Figure 7-6: Cross section optimized UHPC box girder

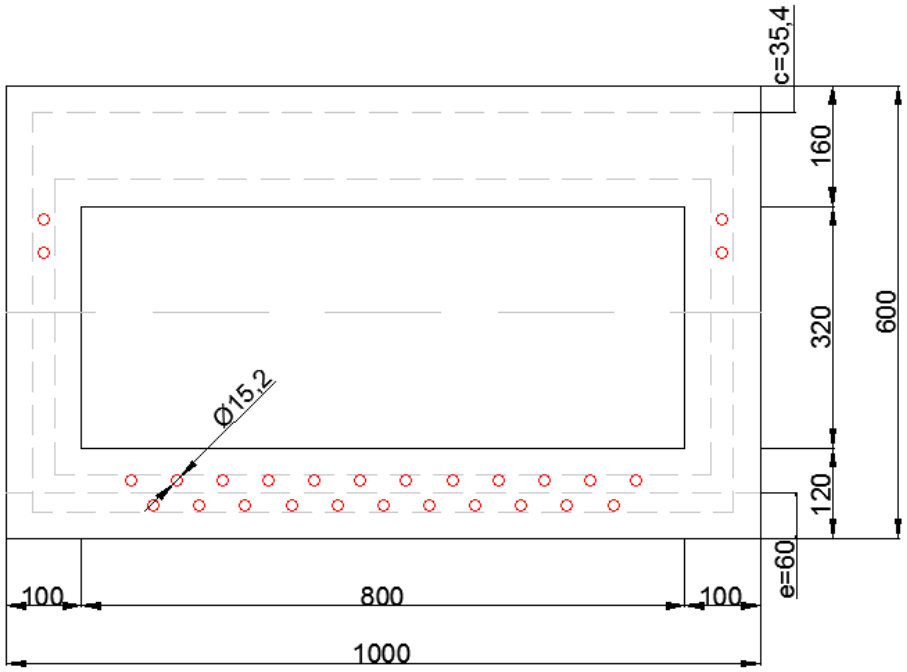

Figure 7-7:Cross section for prefab

	Prefab design
H:	600 mm
B:	1000 mm
h_{top}:	160 mm
h_{bot}:	120 mm
b_{web}:	100 mm
Number of strands:	27φ15.2
A_c	0.344 m^2
q_{self}	9.133 kN/m

7.4 Sectional optimization

7.4.1 General

In the previous paragraph the UHPC was optimized according to the governing internal forces. This resulted in a more slender and lighter box girder. However in reality the internal forces are not equal across the entire length of the beam. Assuming a single span beam, the moment is the largest in the middle of the span and the shear force is the highest at the supports. In this paragraph the design from paragraph 7.3 will be optimized further considering the fact that the internal forces are not equal over the length of the beam.

To be able to optimize the beam according to the different occurring values of the moments and shear forces, the previously developed SCIA model for the UHPC design will be used. In the model sections will be made, with each section being 1m long, and in each section the governing moment and shear force will be taken. Each section will be dimensioned according to the working moments and shear forces on that specific section. In Figure 7-8 the box beam is shown, which is divided in multiple sections. It is assumed that on each end a hammerhead will be made of 1m long each. These hammerheads will not be optimized. Their heights will be the same as the height of the adjacent sections. The numbers in the blue circles represent the locations of the sections which will be made in SCIA Engineer. The internal forces will come from these sections. As each box section is connected with two SCIA sections, the governing internal forces will be the highest found in the sections in SCIA. So for example box section 1 is connected to SCIA section 1 and 2. The highest shear force will most likely be in section 1 and the highest moment in section 2, so the box section is dimensioned according to these highest forces. Symmetry is assumed so box section 1 is the same as box section 22, section 2 the same as section 21 and so on. Therefore only 12 sections are made in SCIA.

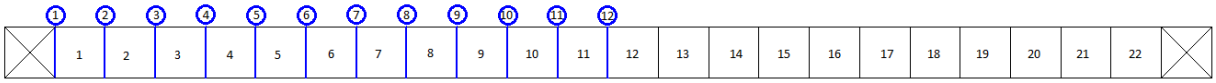

Figure 7-8: Sections for sectional optimization

7.4.2 Boundary conditions

The goal for the sectional optimization will be decreasing the construction thickness as low as possible. But it is also important that the structure is not only structurally optimal but also economically. There are multiple ways to achieve a thinner beam. The previously optimized box beam had a thickness of H=580mm with 28 strands and a web thickness of b_{web} = 100mm. This could be the starting point for the sectional optimization. But it is also possible to assume a web thickness of 90mm throughout the length of the beam. This could be possible because in reality the highest shear force is near the support but, since there is a hammerhead at the support the shear forces there are easily resisted. Further away from the support the shear force becomes lower and a web thickness of 90mm becomes possible. Also possible is to increase the amount of strands to 30. These extra two could fit in the bottom flange, when looking at Figure 7-6.

So 4 cases will be investigated and afterwards the most economical one will be chosen as the most optimal choice. The cases all have certain boundary conditions. In general the structure needs to remain safe at all times. So basically all unity checks must be lower than 1. Then the amount of strands is kept constant throughout the length. So all sections have a certain number of strands.
If during optimization more strands are required than the assumed fixed amount in a certain section, then the section cannot be further optimized. The flanges remain unaltered as they are already fully optimized. The web thickness is kept to a certain constant value as well.

The 4 cases together with their boundary conditions are:

	b_{web} =100 mm & 28 strands	b_{web} =100 mm & 30 strands	b_{web} =90 mm & 28 strands	b_{web} =90 mm & 30 strands
Web thickness	b_{web} =100mm	b_{web} =100mm	b_{web} =90mm	b_{web} =90mm
Limit number of strands	n ≤ 28	n ≤ 30	n ≤ 28	n ≤ 30
All Unity checks	UC ≤ 1	UC ≤ 1	UC ≤ 1	UC ≤ 1
h_{bot}, h_{top}	Unchanged	Unchanged	Unchanged	Unchanged

So basically the only variable that is being changed is the construction height. As already said the goal is to find the most optimal construction height per section in each case that meets the boundary conditions.

For optimization only the variables that are predicted to be governing are used. This means that the following variables are neglected during optimization, because they are assumed to be always on the safe side:

- Capacity of the hammerhead (not relevant, because sectional optimization)
- Transverse capacity (top flange not altered at all so this one always remained the same)
- Vibration (mass will never reach a point where the vibrations become truly governing)
- Fatigue (concrete across whole section strong enough to resist cyclic loading)

In reality the moments are not constant over the whole span so the moments need to be formulized in such a way that they represent the correct value of the moment at a certain section:
$M_g(x) = 0.5*q_g*x*(L-x)$
$M_{dead/var}$ = result from SCIA for a certain section
$M_p = P_u*x + P_m*(f-f_{fict})$ if $x < a$ and $M_p = P_m*f$ if $x \geq a$. f and f_{fict} are dependent on the construction height.
$V_g(x) = 0.5*q_g*(L-2x)$
$V_{dead\ or\ var}$ = result from SCIA for a certain section
$V_p = P_u$ if $x<a$ and $V_p = 0$ if $x \geq a$

7.4.3 Results sectional optimization

In Table 7-2 the results are shown of the optimization of the four cases. Shown are the smallest and largest cross section thickness per case and also the total volume of the concrete in one beam and the total mass of the strands. The smallest thickness can be found when 30 strands are used in combination with b_{web} =100mm. Also the lowest volume of the concrete is found here. The largest when 28 strands and b_{web} = 100 mm is used. The largest volume if found when 28 strands are used with b_{web} =90mm. Looking at the volume of one beam it is best to use a web thickness of 100 mm.

Table 7-2: Results of the 4 cases

	28 strands, b_{web}= 100mm	**30 strands, b_{web} = 100mm**	**28 strands, b_{web} = 90mm**	**30 strands, b_{web} = 90mm**
Smallest H [mm]	450	430	460	460
Largest H [mm]	570	550	570	550
Total volume of concrete [m3]	8,204	8,128	8,352	8,284
Total mass of strands [kg]	733,25	785,63	733,25	785,63
Price of UHPC (€1000/m3)	€ 8.204,00	€ 8.128,00	€ 8.352,00	€ 8.284,00
Price of strands (€3/kg)	€ 2.199,76	€ 2.356,88	€ 2.199,76	€ 2.356,88
Total price one beam	€ 10.403,76	€ 10.484,88	€ 10.551,76	€ 10.640,88

In Figure 7-9 and Figure 7-10 the cases are compared with one and other for a certain amount of strands. In both figures it is seen that the cases with b_{web}= 100 mm has a lower thickness in the first 5 metres from the supports. Around the mid span the thickness is pretty much the same. This is the reason why the total volume is lower when b_{web} is used. Using 30 strands allows for smaller construction thicknesses close to the mid span. Therefore the case with 30 strands in combination with b_{web} =100mm has the lowest volume.

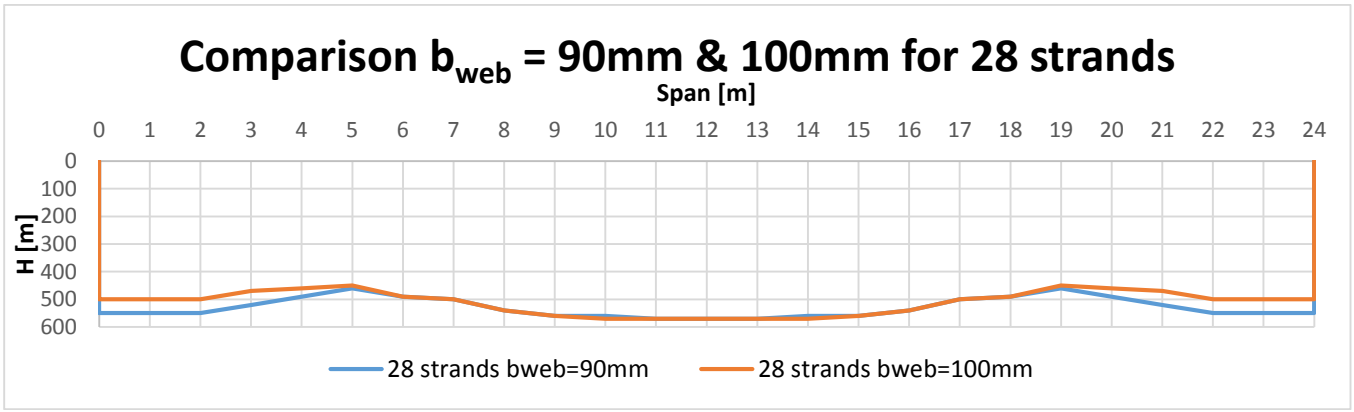

Figure 7-9: Comparison b_{web} = 90 mm and 100 mm for 28 strands

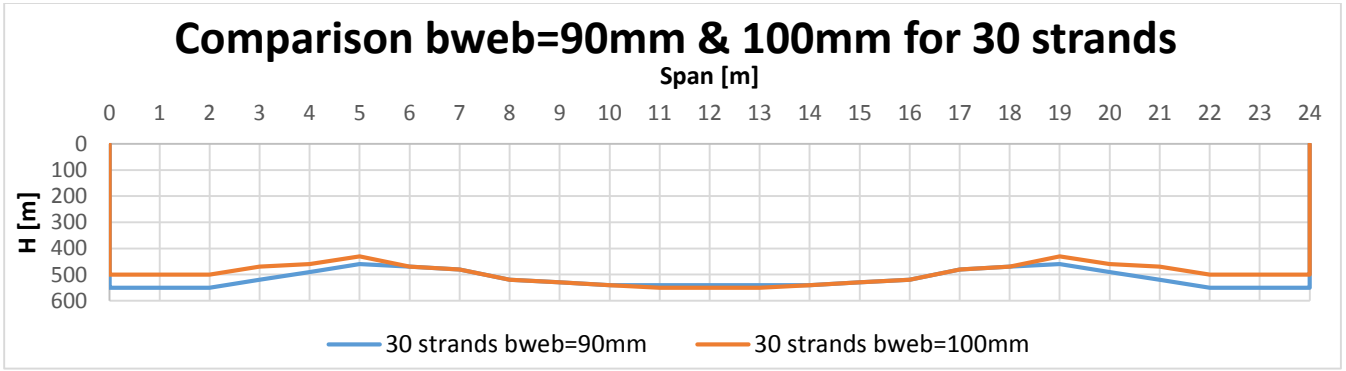

Figure 7-10: Comparison b_{web} = 90 mm and 100 mm for 30 strands

However it is not only important to have the most slender beam. The costs of one beam are also important. The total costs per case for one beam are also found in Table 7-2. Assumed is that UHPC costs 1000 euros/m^3 and prestressing strands cost 3 euros/kg. Adding the costs of steel and concrete results in the case with 28 strands in combination with b_{web} =100mm as the cheapest beam. The case with 30 strands in combination with b_{web} =100mm is the second cheapest. Purely based on costs it is better to use 28 strands instead of 30 strands. But 30 strands will result in a more slender structure and the price per beam is not much higher than when 28 strands are used.

Concluded is that, considering the slenderness and price of one beam, the case with 30 strands and b_{web} = 100mm is the most optimal one. The optimization process of this case will be elaborated further.

In appendix G.3 the first and final step of the sectional optimization are shown.

The final step of the sectional optimization showed that in the sections close to the supports the governing variables were the shear and torsional capacity. Shear forces and torsional forces are high close to the supports, so it was expected that the one or the other would be governing. In the sections close to the middle of the beam the number of strands became governing, which meant that more than 30 strands were needed. Therefore further optimization was not allowed. Indirectly this also means that the moments are governing as well, since higher moments lead to more strands. Figure 7-11 shows the varying construction height over the length of the beam for the optimal case. At the ends of the beam the height is higher than further down the length of the beam, due to the high shear forces and torsional moments. Then the height reduces and steadily increases as the moments increase towards the middle of the beam.

Figure 7-11: Construction height over length of beam

7.4.4 Deflection of optimized beam

It is important that the beam does not have high deformations. So it needs to be verified that the deflections stay within the limits. Especially now that the beam has become very slender and light it is necessary to make this verification. The beam is modelled in SCIA Engineer with on the beam the combinations and the line loads with values from paragraph 5.19. The SCIA report is found in appendix G. If again the situations, where type I or no heat treatment is used, are compared the deflections for the optimized beam become:

	$E_{c,eff1}$	$E_{c,eff2}$
w1 [mm]	-119.1	-153.1
w2 [mm]	-69.4	-89.3
w3 [mm]	30.8	39.6

The deflections all meet the requirements (w_{max}= L/500 for camber and w_{max}= L/250 for sag), except w1. But as already explained in paragraph 5.19, this is not a major issue.

7.4.5 Conclusion sectional optimization

The sectional optimization has allowed to even further optimize the UHPC box girder. The minimum thickness of the fully optimized beam is 430mm and the maximum thickness of the beam is 550 mm. This new optimized design saves even more material than the first optimized design:

	Initial design	**First optimized design**	**Sectional optimized design**
H of smallest section	600 mm	580 mm	430 mm
A_c of smallest section	0.377 m^2	0.340 m^2	0.310 m^2
Total weight of 1 beam	23.72 tons	21.6 tons	20.45 tons

However the reduction is not as large as the reduction resulted from the first optimized design compared to the initial design. That is because during the first optimization step the web thickness and bottom flange thickness were reduced as well and the sectional optimization only reduced the construction thickness. From a practical point of view this fully optimized girder is difficult to construct, because the varying heights require complex formwork. It is however possible to build this optimized girder with a constant construction thickness of 550 mm (dotted line in Figure 7-11). The bridge will be slightly heavier (21.12 tons instead of 20.45 tons), but the beam will be much easier to construct and the maximum thickness will stay the same. The cross section of this beam (with H=550mm) at the support is seen in Figure 7-12.

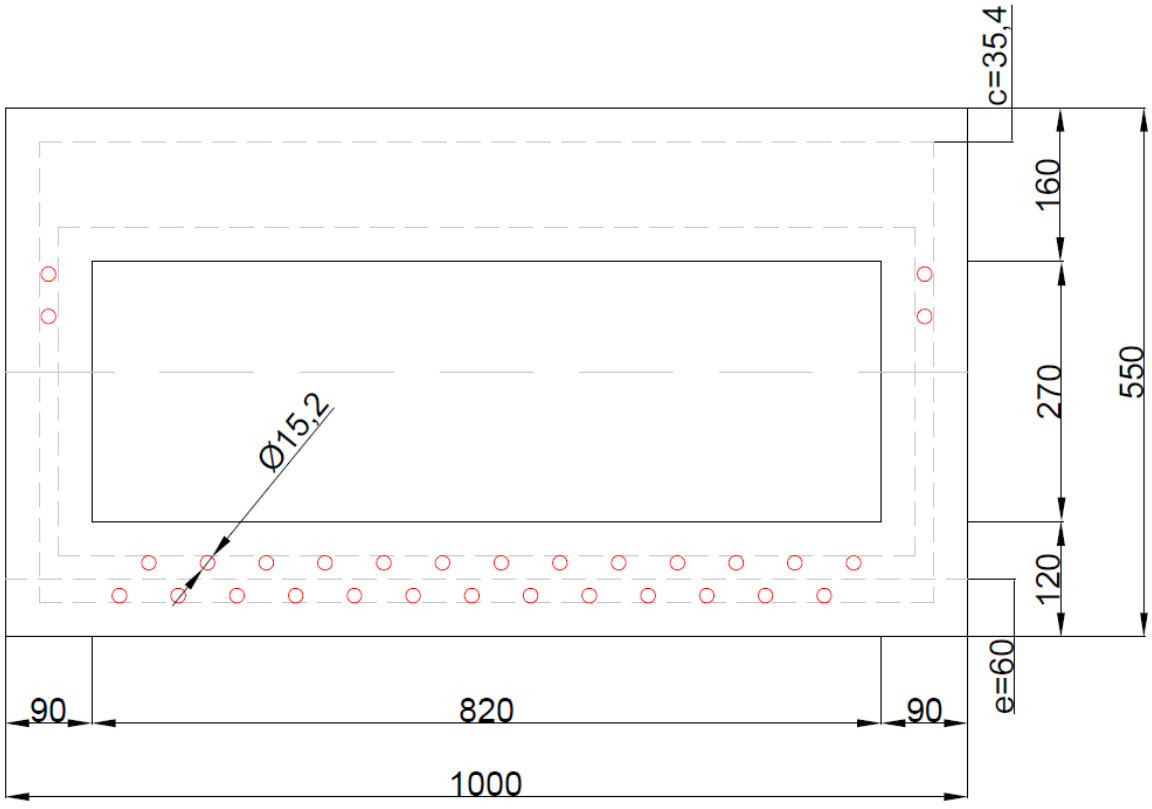

Figure 7-12: Cross section sectional optimized girder

7.5 Conclusion optimization process

In this chapter the initial UHPC design from Chapter 5 was optimized. This was necessary, as the initial design had a capacity that was higher than necessary to resist the working loads on the bridge. Optimizing the beam would mean a more efficient and lighter beam. There were multiple variables that could be optimized. Chosen was to optimize the number of strands, the construction height, the webs and the bottom flange

First the design was optimized according to the governing internal forces, so basically the forces determined for the initial UHPC design. The optimization resulted in a reduction of 40 mm for the web thickness and 20 mm for the construction height. The bottom flange was reduced 10 mm. This one was already close to its limits and governing for the thickness were the layers of strands in the flange, which needed sufficient space. The amount of strands was reduced from 33 to 28 strands. The total weight was reduced from 23.72 tons to 21.6 tons. The slenderness ratio for this optimized beam is λ=41.4 (was 40 for the initial design). However in practice beams are constructed with steps of 50mm for the construction thickness. So it is also possible to increase the height to 600mm while keeping the reduction in web and bottom flange thickness. The 20 mm difference in height will not make a whole lot of difference.

After the first optimization step a sectional optimization was applied. This was needed, because in reality the internal forces are not equal over the length of the beam. The beam was divided in multiple box sections. For each section the internal forces were determined in SCIA Engineer. Then according to these forces the box sections were optimized as much as possible (until there is just enough safety). The optimization resulted in a beam with varying height over the length of the beam. The smallest thickness was 430 mm and the largest 550 mm. This fully optimized design is theoretically the most optimal for the Leiden Bridge, concerning weight and slenderness. This design will save the most concrete. The total weight is further reduced from 21.6 tons to 20.45 tons.

However from a practical point of view, this optimized beam with varying height is very difficult to construct, especially as a prefabricated girder. Complex formwork would be necessary to construct this beam. Developing this formwork could provide high costs. Therefore this beam could be built with a constant thickness of 550mm (the maximum thickness of the beam). This would be a much more realistic solution. It is slightly heavier than the beam with varying heights, but the construction is easier and probably cheaper as well, because of the constant height.

Recommended is, if one wants to play it safe, to not choose for the fully optimized beam with varying heights but to choose the fully optimized with constant height. This design is 50mm thinner and saves material compared to the initial UHPC design.

Now that the initial design is optimized, which provided two new UHPC designs, these UHPC designs can be compared with each other on multiple aspects. These designs will also be compared with the other designs made with NSC, HSC and HPC. This comparison will be performed in the next chapter.

Chapter 8 Comparison designs

In the previous chapters multiple designs were developed and discussed, namely the NSC design (C50/60), the HPC design (C90/105 including steel fibres) and the UHPC design (C170/200). The UHPC design has also been optimized further.

All these designs including the optimized UHPC design will be compared with each other on multiple aspects. First the designs will be compared on structural performance. This will be done for the NSC, HPC and the initial UHPC design. Then all the designs will be compared with regards to the material use and costs. Finally the beams will be compared with regards to impact on the environment.

8.1 Structural performance

All the designs have been verified for multiple aspects that are required for a safe structure. Looking at the moment capacity, all have sufficient capacity to resist the design bending moment. The prestressing plays a large part in all designs for resisting the moment capacity. The prestressing also has a large influence on the rotational capacity. The NSC design did not have sufficient rotational capacity. This is due to the high number of strands in the concrete, which need to be balanced by a large compression zone. However, if the amount of strands is fictively reduced, while keeping the moment capacity high enough, the rotational capacity will suffice. The HPC and UHPC designs did not have any problems concerning the rotational capacity. This is due to a large compressive strength, which reduces the height of the compression zone and thus increases the rotational capacity.

The largest differences in the designs were for the shear capacity. The NSC design had a very low shear capacity compared to the design shear force. A lot of shear reinforcement was necessary to resist the design shear force. The HPC design already had a much better shear capacity than the NSC design, because the strength is higher and most of all because of the inclusion of steel fibres. These contribute most to the shear capacity. However HPC does not have a very high tensile strength. Therefore some shear reinforcement is necessary, which works in combination with the steel fibres to resist the design shear force. The UHPC design, because of the high compressive and tensile strength had more than enough shear capacity to resist the design shear force.

The same story applies to the torsional capacity. Both NSC and HPC had a too low torsional capacity to resist the working torsion moments. UHPC however could resist the torsion moments, because of the high tensile strength. This means that in the NSC and HPC design longitudinal reinforcement is necessary to resist the torsion moment, while UHPC does not require any longitudinal reinforcement. This allows the UHPC box girder to be made without any reinforcement.

The exclusion of reinforcement proves beneficial for fitting everything (strands, bars, stirrups) in the cross section. For the NSC-design it showed that all the reinforcement and the high amount of strands would prove difficult and nearly impossible to fit everything in the cross section. For the HPC design this issue becomes smaller, as bars with small diameters are being used. In combination with a lower amount of strands, the fitting of everything is achievable here, although the spacing of strands is at its limit. The UHPC design has no issue with fitting, because of the exclusion of reinforcement. Enough spacing between strands is available and it is possible, if necessary, to put them closer to each other (this would prove necessary during optimization). And a smaller cover also contributes positively to this.

Another important aspect is fatigue. This is due to the high slenderness of the bridge, which makes the bridge sensitive to fatigue. For the NSC design the calculations were limited to the ULS. For the other two designs however the fatigue resistance was determined. It showed that the UHPC had more than enough fatigue resistance to withstand cyclic loading on the bridge.

This is thanks to the high compressive strength, which results in a high design fatigue strength. Same goes for the HPC design.

Considering the structural performance and the results obtained for all the designs, it may be said that the UHPC design has by far the best structural performance for a certain construction thickness. The UHPC design even has room left for optimization, which has extensively been done in 0.

8.2 Material use and costs

In this paragraph all designs will be compared with each other in the use of material and material costs. The comparison of material use will be limited to the superstructure. So no substructure and also no surfacing layers will be taken into account. Purely the beam themselves. Same goes for the costs. The costs will be based on the material needed in each design. This means the amount of concrete, strands, reinforcement, etc. Other aspects such as transport or multiple stages in the lifetime of the bridge are not taken into account.

8.2.1 Material use

To determine the material use all the designs are taken into account. For the NSC-design the alternative mentioned in the summary in paragraph 3.15 (H=800) are taken into account as well. Even though these thicknesses cannot be applied it will still be interesting to bring them into comparison. The UHPC design and the optimized design are all taken into account. The theoretical and practical optimized designs are separated. This is especially important for the sectional optimized beams, because the practical one has a constant thickness over the span, while the truly optimized one varies in thickness. The results are seen in Table 8-1. The table shows the cross sectional dimensions of each design, the amount of box beams, the amount of reinforcement and the eventual amount of material needed per beam in kg or m^3.

Table 8-1: Comparison of material use in the designs

	NSC600	*NSC800*	HPC600	UHPC - initial	UHPC -1st opt	UHPC - sect opt	*UHPC pract. sect opt*
H [m]	0,6	0,8	0,6	0,6	0,58	-	0,55
B [m]	1,5	1,5	1	1	1	1	1
b_{web} [m]	0,15	0,15	0,15	0,14	0,1	0,1	0,1
h_{top} [m]	0,17	0,17	0,17	0,16	0,16	0,16	0,16
h_{bot} [m]	0,15	0,15	0,15	0,13	0,12	0,12	0,12
L [m]	24	24	24	24	24	24	24
Amount of box beams	20	20	30	30	30	30	30
A_c [m2]	0,564	0,624	0,404	0,3768	0,34	-	0,334
Amount of strands	53	38	34	33	28	30	30
A_p [mm2]	7367	5282	4726	4587	3892	4170	4170
A_{sw} [mm2/m]	6030	4110	575	-	-	-	-
A_{sl} [mm2]	3372	2828	2828	-	-	-	-
ρ_f [%]	-	-	2,15	2,15	2,15	2,15	2,15
Total concrete per beam [m3]	**13,536**	**14,976**	**10,088**	**9,4896**	**8,64**	**8,128**	**8,448**
Total prestressing [kg]	***1387,94***	***995,13***	***890,38***	***864,19***	***733,25***	***785,63***	***785,63***
Total steel fibres [kg]	-	-	***1702,60***	***1601,61***	***1458,22***	***1371,80***	***1425,81***
Total stirrups [kg]	552,12	501,76	52,65	-	-	-	-
Total bars [kg]	635,28	532,80	532,80	-	-	-	-
Total reinf (A_{sw}+A_{sl}) [kg]	***1187,41***	***1034,56***	***585,44***	-	-	-	-
Total weight steel [kg]	**2575,35**	**2029,69**	**3763,87**	**2465,80**	**2191,47**	**2157,43**	**2211,44**

To summarize the table, Figure 8-1 and Figure 8-2 show the total mass of steel per beam and total volume of concrete per beam.

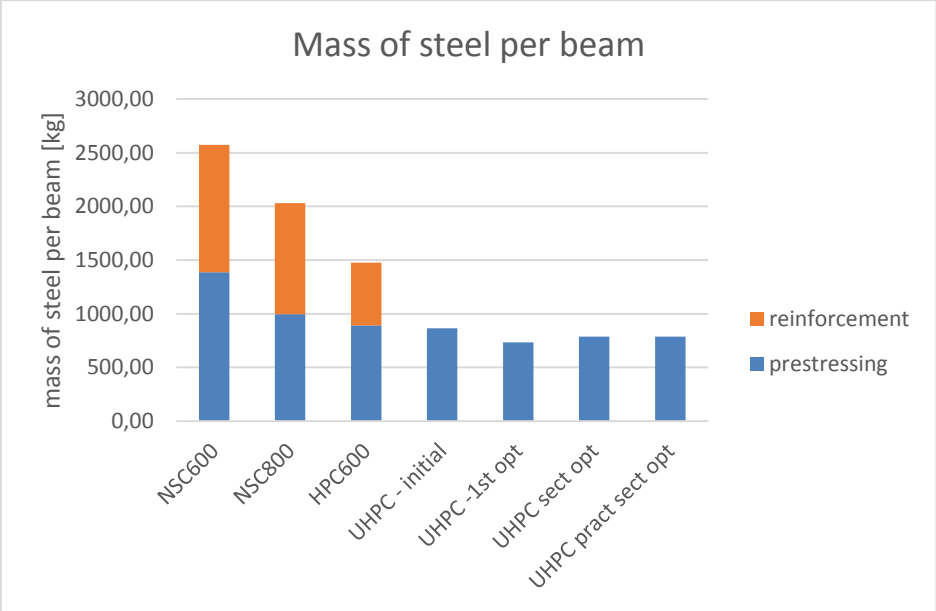

Figure 8-1: Mass of steel per beam (fibres excluded)

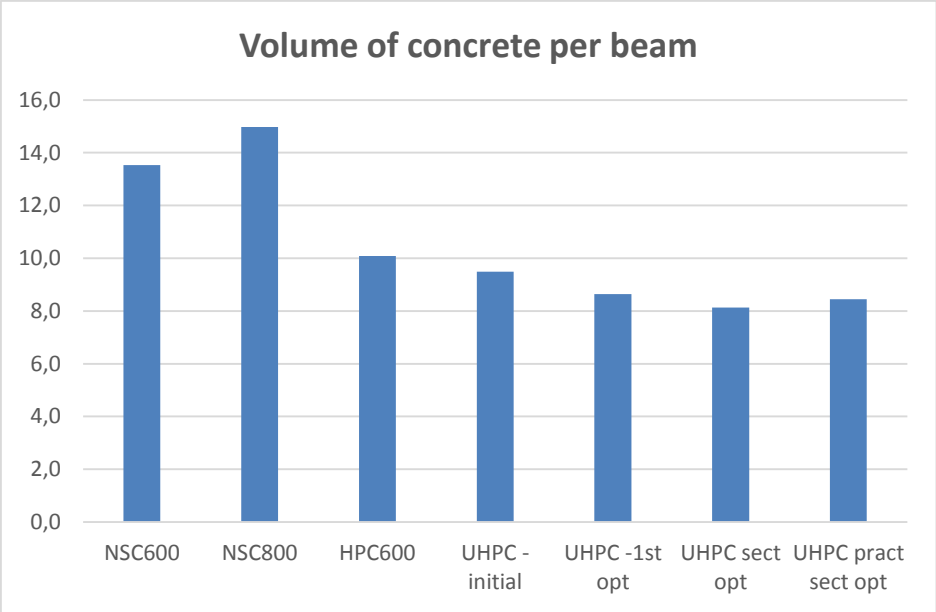

Figure 8-2: Volume of concrete per beam

The least amount of concrete per beam needed is for the sectional optimized UHPC design. This is logical as this one is the most slender and most optimized beam of all the designs. This design also has the least amount of steel (only prestressing and steel fibres). The highest amount of steel and concrete is found in the NSC design. The amount of steel reduces greatly with increasing height. The HPC design already reduces the amount of steel compared to the NSC design, because of the inclusion of steel fibres. If one looks at the use of material than it is best to use UHPC, since it saves the most material. Here recommended is the sectional optimized design, as this one saves the most material.

As comparison the material use of the current bridge can be looked at as well:

Concrete [m^3]	86,73
Steel (girders) [kg]	83700
Reinforcement [kg]	4400

This is the material use for the complete bridge. The total material used for the optimized UHPC design is (values in Table 8-1 multiplied by 30):

Concrete [m^3]	243,84
Steel (girders) [kg]	-
Reinforcement [kg]	64722,94

The amount of concrete is of course higher, because the current bridge is a composite bridge with steel girders and a concrete deck. This can be seen in the fact that the current bridge consists of a lot more steel (girders + reinforcement) than the UHPC design.

8.2.2 Costs

The amount of material needed in one beam is determined in the previous paragraph. With the amount of material the costs per beam can roughly be determined. The costs are based purely on the amount of material needed. Other factors such as transport or maintenance are not taken into account. The substructure is also not taken into account. The costs for the current bridge are left out, since the bridge was made a very long time ago and the costs of the bridge are unknown. The following prices are assumed for each material:

Reinforcement	€ 1,00/kg
Prestressing steel	€ 3,00/kg
Steel fibres	€ 1,00/kg
NSC	€ 100,00/m^3
HSC	€ 300,00/m^3
HPC	HSC + steel fibres
UHPC	€ 1.000,00/m^3

The price of UHPC is including the steel fibres. The price of HPC is assumed to be the same as the price of HSC but also including the price of steel fibres per kg.

The costs for each design per beam and also the total costs of the whole bridge are seen in Figure 8-3 shows how the costs per beam are divided and Figure 8-4 shows the total costs of the bridge for a particular design.

Table 8-2. Figure 8-3 shows how the costs per beam are divided and Figure 8-4 shows the total costs of the bridge for a particular design.

Table 8-2: Costs of designs

	NSC600	NSC800	**HPC600**	**UHPC - initial**	UHPC -1st opt	UHPC - sect opt	UHPC - pract sect opt
Concrete	€ 1.353,60	€ 1.497,60	€ 4.729,00	€ 9.489,60	€ 8.640,00	€ 8.128,00	€ 8.448,00
Prestressing	€ 4.163,83	€ 2.985,39	€ 2.671,14	€ 2.592,57	€ 2.199,76	€ 2.356,88	€ 2.356,88
Reinforcement	€ 1.187,41	€ 1.034,56	€ 585,44	-	-	-	-
Total per one beam	€ 6.704,83	€ 5.517,54	€ 7.985,58	€ 12.082,17	€ 10.839,76	€ 10.484,88	€ 10.804,88
TOTAL	**€ 134.096,69**	**€ 110.350,87**	**€ 239.567,43**	**€ 362.465,17**	**€ 325.192,75**	**€ 314.546,52**	**€ 324.146,52**

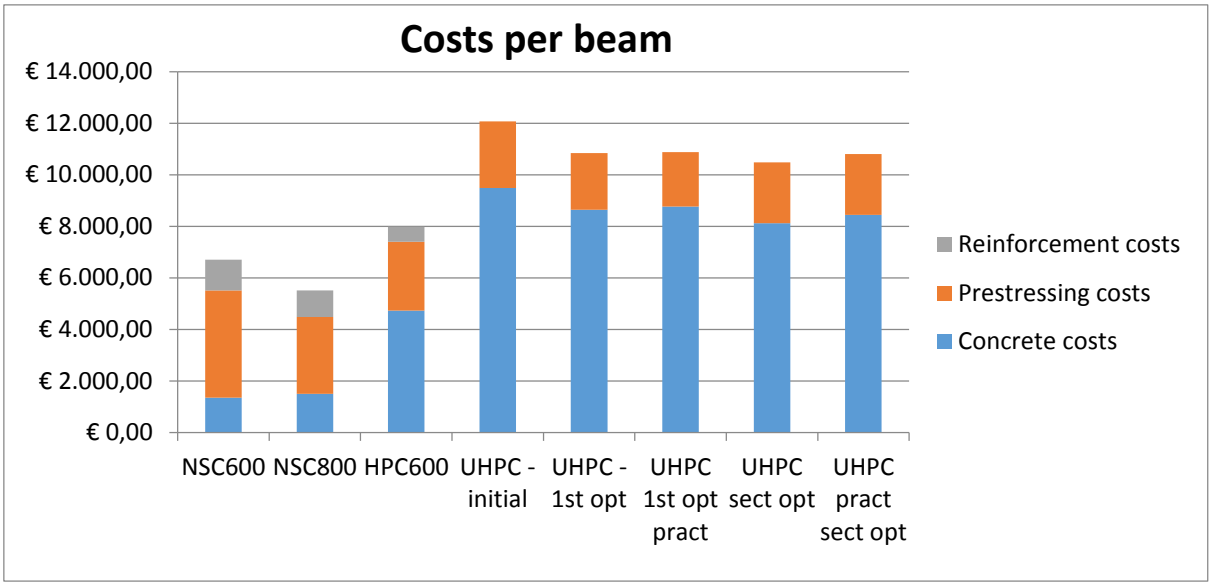

Figure 8-3: Total Costs per beam

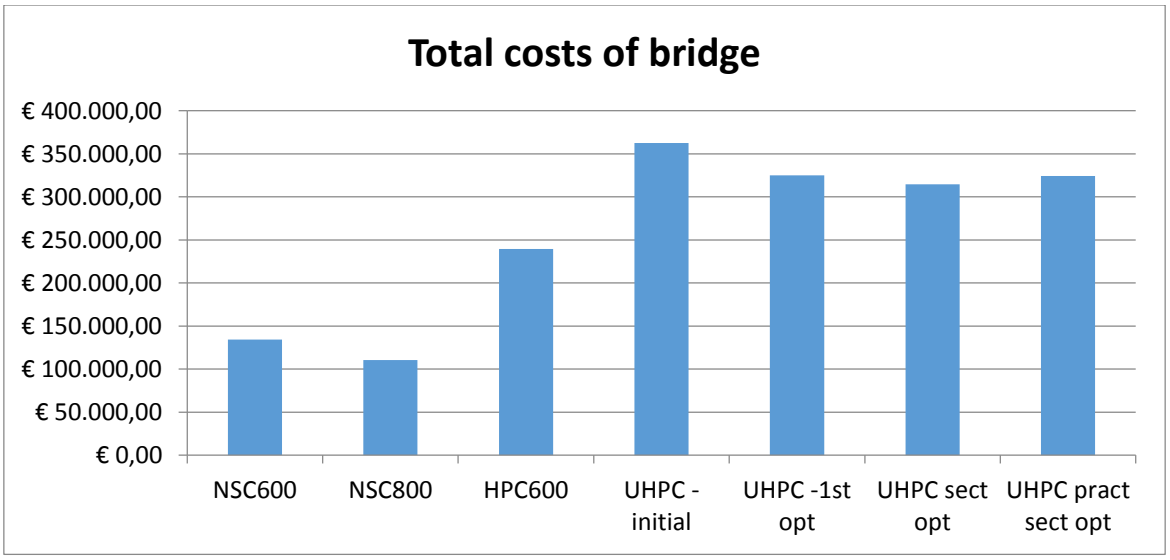

Figure 8-4: Total cost of bridge per design

The design with the lowest costs per concrete class is:

Cheapest of NSC:	NSC800:	€ 110.350,87 (NSC not achievable)
Cheapest of HPC:	HPC600:	€ 239.567,43
Cheapest of UHPC	UHPC sect opt:	€ 314.546,52
Cheapest of pract UHPC:	UHPC pract sect opt:	€ 324.146,52

Looking at the costs of all the designs, the cheapest design of all would be the NSC design with H=800mm. NSC concrete is the cheapest concrete and the thicker structure greatly reduces the amount of prestressing and reinforcement needed than if H=600 would be used. But a thickness of H=800mm cannot be used due to the restricted height. NSC with H=600mm is still pretty cheap, but this design is not achievable, as was already concluded.

The HPC design is already more expensive than the NSC design, because of the higher concrete cost. It is clear that the UHPC designs are the most expensive ones and this is because of the very high price of UHPC. The cheapest one overall is the sectional optimized beam. This one saves the most concrete and is also the most slender and lightest one. Only this design would be hard to construct

due to the varying height. The practical design costs more but it is still cheaper than the initial design. This one is still the most slender one (if one only looks at the designs with constant thickness) and it should not be a problem to construct this variant.

It has to be remarked that the price for UHPC is the commercial price of UHPC. However a study was performed, where the researches made their own UHPC mixture [5]. Here the costs price of the material was 350 dollars/yd^3 this is about 360 euros/m^3. This price is without steel fibres included. With steel fibres the total price becomes around 530 euros/m^3. Counting in production and rounding up could result in a price of €700/m^3. If a same comparison is performed as in Figure 8-4 then the total costs of the UHPC designs change as seen in Figure 8-5. If the HPC and UHPC design are compared now, the difference in price is much lower. However in short term or at least for the Leiden Bridge it would not be realistic to assume that the price could be dropped to 700 euros. For this required is that a concrete factory takes the production of UHPC In its own hands and this is something that will not happen anytime soon. However in the long term, maybe in a couple of years, it could be possible that factories in the Netherlands will start to produce their own UHPC mixture, which would definitely reduce the price of UHPC, since it does not have to be imported anymore.

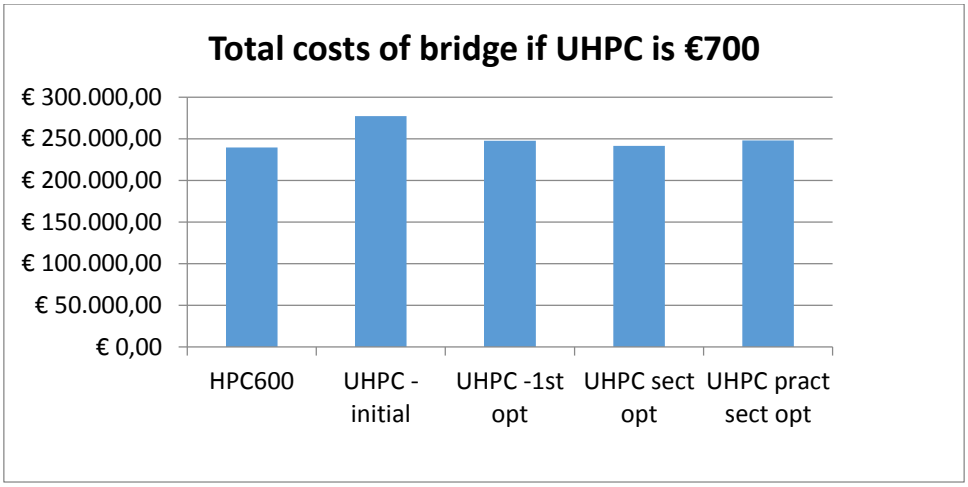

Figure 8-5: Total costs of bridge if UHPC is €700/m^3

To summarize:

HPC design:	€ 239.567,43	
Cheapest of UHPC	€ 241.394,52	UHPC sect opt
Practical UHPC	€ 247.763,87	UHPC 1st opt pract

So Looking at the costs of all designs and taking into account which design is achievable, the choice can be made between the HPC design and the (practical) sectional optimized UHPC design. The HPC design is about 100.000 euros cheaper in total than the UHPC design. The difference in price is mostly because of the high price of UHPC. But if the price would be 700 euros instead of 1000 than the difference would be around 3000 euros only. Furthermore the UHPC design is lighter than the HPC design, so this would mean that the substructure could be made smaller in dimensions, so costs would be saved here as well, which could make UHPC even the cheapest possible solution. Besides that, HPC is not as durable as UHPC. HPC does not have such a dense matrix as UHPC, so the protection against the environment will not be as great as with UHPC. This means that the UHPC design will most likely have a longer life time and a smaller maintenance need, which will save costs in the future. It has to be mentioned though that HPC still is capable to deliver a structure with a lifespan of 100 years so UHPC will not have such a benefit, since both HPC and UHPC should be able to be maintenance free for 100 years. However this is all qualitatively reasoned. A further cost analysis of the complete lifespan of the whole bridge, would be necessary to support this statement.

But that falls outside of the scope of this thesis. And as already said, in short term the price of UHPC will not be anything lower than 1000 euros/ m^3, therefore the HPC design will still be the cheapest solution for the Leiden Bridge, considering the analysis made in this paragraph.

8.3 Environmental impact

Besides the amount of material and the cost of it, it is also interesting to see what the environmental impact would be of the designs. Especially since it takes a lot of time and energy to produce UHPC. To determine the environmental impact a couple of parameters will be considered namely:

- The global warming potential (GWP)
- The equivalent embodied energy (EE)
- The CO_2 emission (also part of GWP)

The GWP is calculated as follows:
100-year GWP = $CO_2 + 298NO_x + 25CH_4$ (unit in ton of CO_2 eq.)
The environmental data is seen in
Table 8-3. The data are based on [7] and [8].

Table 8-3: Environmental data

		NSC	HPC	UHPC	Steel
Density, ρ	***kg/m³***	2500	2500	2500	7850
EE	***GJ/m³***	1,728	3,72	7,71	185,8
CO_2	***kg/m³***	297,5	553,33	1065	17123
NO_x	***kg/m³***	1,66	2,73	4,86	55,38
CH_4	***kg/m³***	0,12	0,33	0,76	30,65
GWP	***kg CO_2 eq./m³***	795,18	1374,21	2532,28	34392,49

The three parameters will be determined for the production of the designs. So they will be based on the amount of material used in each design. The designs containing the same type of concrete are first compared with one and other. The ones with the lowest values for the parameter are taken and compared with each other. The results are seen in Figure 8-6. The three main concrete classes are compared with each other and with the current bridge as well. The current bridge acts as 100% baseline. The total mass of each design is placed in the figure as well. Table 8-4 shows the designs with the lowest values for each parameter.

Table 8-4: Designs with the lowest values per parameter per concrete class

	CO2	GWP	EE	Total Mass
Lowest NSC	NSC800	NSC800	NSC800	NSC600
Lowest HPC	HPC600	HPC600	HPC600	HPC600
Lowest UHPC	UHPC sect. opt.	UHPC sect. opt.	UHPC sect. opt.	UHPC sect. opt.

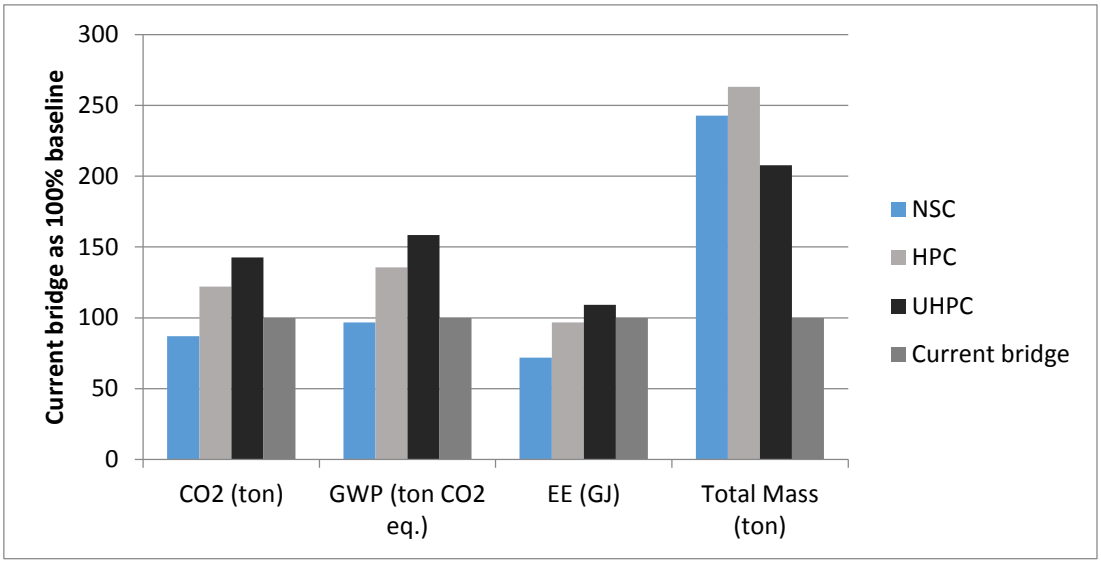

Figure 8-6: Environmental impact of different designs.

The current design has the best scores on all aspects. That is because the bridge has much less material in total than the new designs and the environmental impact is thus lower. But there is a reason the bridge has to be replaced and more important is the comparison of the concrete designs. The figure shows that on the environmental impact (GWP, CO_2 and EE) NSC scores the lowest and UHPC scores the highest, if only the new designs are considered. This is logical because it takes much more energy to produce UHPC and therefore the CO_2 becomes higher as well. This is generally true for concrete classes with increasing strength. However the UHPC design has by far the lowest mass. Also, as already said, the values are only based on the production of the beams. Other stages are not taken into account. For example transport. UHPC has the lightest structure so the emission during transport will be greatly reduced. The durability aspect is not taken into account as well. And it is generally known that UHPC has the best durability properties. So in the long term (e.g. > 100 years) UHPC will prove to be more environmental friendly as maintenance will not be necessary, while for the other design maintenance would most likely be necessary, for NSC sooner than HPC, as HPC can also reach 100 years. Still the differences in environmental impact do not differ an awful lot from each other. In the future UHPC could be produced more efficiently, which would reduce the energy required and probably also the costs as well. This would make UHPC even more competitive with other concrete types.

For the Leiden Bridge specifically however, the choice would be between HPC and UHPC. NSC with a height of 800mm cannot be achieved and NSC600 is structurally not safe even though the environmental impact is the lowest. Then without taking all life stages into account and only what has been determined here, HPC would be the design with the least environmental impact. The mass however would be much greater than is UHPC is used.

8.4 Conclusion comparison

In this chapter the concrete designs have been compared with each other on multiple aspects such as structural performance, amount of material, costs and environmental impact. Concerning structural performance the best designs were the ones made in UHPC. On all aspects the structural performance was more than good enough to resist the loads on the bride. HPC had a lesser structural performance, but it was good enough for the Leiden Bridge. As expected the worst performance is when NSC is used. Concerning material use, UHPC and more precisely the sectional optimized design has the lowest amount of material per beam. Both concrete and steel are greatly reduced when compared with the other concrete classes. However the costs for UHPC are the highest. This is because of the high UHPC price, which is 10 times higher than the price of NSC. A reduction of the

UHPC price is possible based on solely the ingredients of the mixture and the fact that UHPC could be produced in the Netherlands as well, but this will not happen anytime soon. As with the costs, the same holds true for the environmental impact, where UHPC also scores the worst of all the concrete classes. HPC scores average on all aspects. The material use, especially the amount of steel is lower than with NSC and the costs are not much higher than the costs of NSC. Also considering that HPC (and UHPC) will have 30 girders instead of 20 in total. Considering all aspects, from structural performance to environmental impact the realistic choices would either be HPC or UHPC.

Chapter 9 Construction of the new Leiden Bridge

In the previous chapters multiple designs for the new Leiden Bridge have been discussed and compared with each other. Because the Leiden Bridge is located in the centre of Amsterdam, it is important that the construction of the new bridge causes as less hindrance as possible. This is also one of the major demands given by the municipality of Amsterdam. Two possible construction processes are dealt with:

- ***Construction of the new bridge at once:*** The old bridge is completely demolished and the new bridge is built. The bridge is unavailable during construction.
- ***Phased construction of the new bridge***: The old bridge is demolished in two phases. This allows for longer use of the old bridge, while part of the new bridge is being built.

9.1 Construction of bridge as a whole

The general construction scheme of building the new bridge as a whole can be seen in Figure 9-1. The steps are:

1 Demolishing old bridge→ 2 construction new substructure→ 3.1 placement bearings→ 3.2 Transportation beams→ 3.3 Placement beams → 3.4 Placement cables →4 joints placed and beam connected with transverse post tensioning→ 5 placing surfacing layers→ 6 Finishing work → 7 Bridge open for traffic

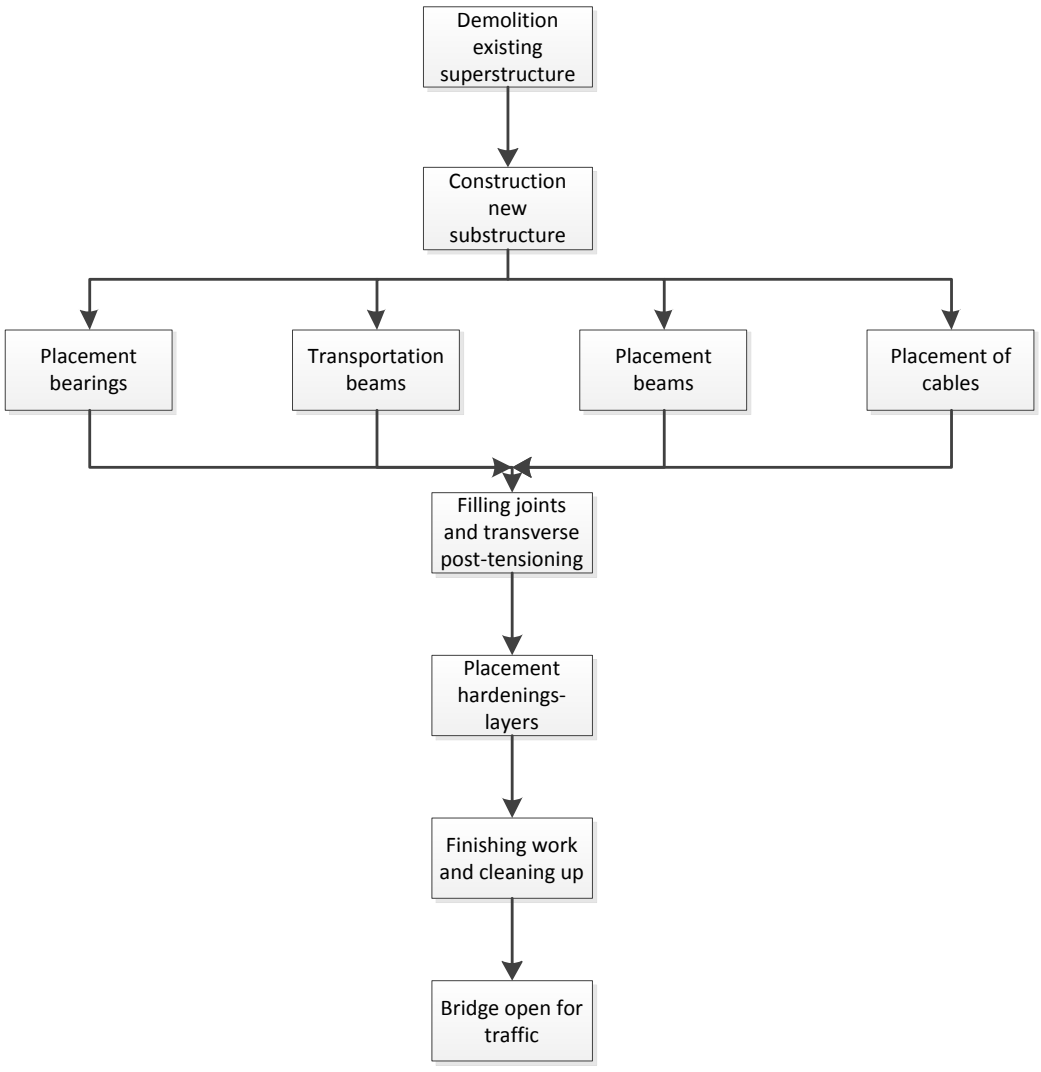

Figure 9-1: Construction scheme

9.1.1 Demolition existing superstructure

The current superstructure has to be demolished completely, before the new bridge can be built. The bridge will be closed for traffic and public transport. For cyclists and pedestrians a temporary bridge will be available. It is very important that during demolition (and during the whole construction stage) no damage is done to the old substructure, steel fences and natural stone ornaments. The fences and ornaments will have to be removed before demolishing the superstructure.

9.1.2 Construction new substructure

The current substructure will not be used at all to support the new bridge, because it is too weak to carry the working loads on the bridge. Instead of that, the new substructure will be constructed behind the current sub structure. This way the current substructure will be relieved of loading and can serve as architecture. New foundation will be made, which the superstructure will rest on. For the foundation it is beneficial that the superstructure is light as possible. Using UHPC will give a bridge with the lowest total mass. Figure 9-2 shows how the new substructure will be built behind the existing one.

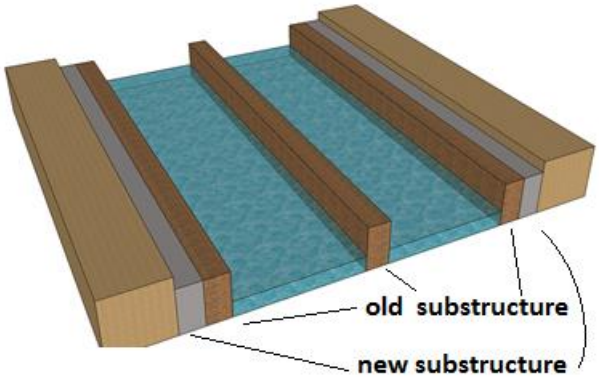

Figure 9-2: Construction new substructure

9.1.3 Placement bearings

After the substructure is finished the bearings have to be placed on which the beams will rest. There will be one bearing on each side per beam, so 30 bearings per side. The reaction forces per beam are not very high (around 740kN) so elastomeric bearings will be sufficient and the cheapest type of bearing. While bearings are being placed the beams should be transported to the construction site and placed as well. Furthermore placement of cables should also occur. So these four stages should occur parallel to each other, as also is seen back in Figure 9-1. This placement of beams and bearings is seen in Figure 9-3

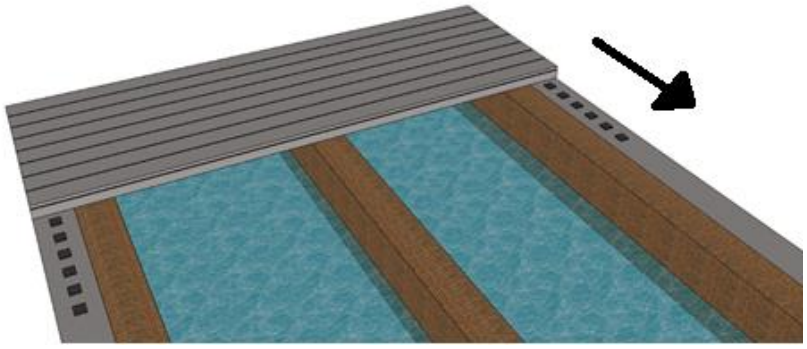

Figure 9-3: Placement of bearings and beams

9.1.4 Transportation of beams

For the transport of the beams there are two ways of transport:

- By road, so the beams are transported by trucks.
- By water, so the beams are transported by boat.

Both ways of transportation will bring challenges with them because the bridge is located in a crowded area. The general routes for the ways of transportation are seen in Figure 9-4. The red line is the route by water and the blue line is the route per road. Transport should mostly take place during the night when there is low traffic intensity.

With transportation by water there are a lot of limiting factors, with the most important one being the width of the canal to the bridge itself and the height of the bridges that have to be passed under to reach the Leiden Bridge. These bridge are all fixed bridges, with a low underpass height.
So a large ship cannot be used. This would mean that it would not be possible to transport all beams at once, meaning that the ship would have to go back and forth to the factory. Because of the limiting width of the Single Canal (canal that runs under the Leiden Bridge) it would also be difficult to turn the ship around, and the ship would most likely have to find another way to turn back to the Amstel Canal.

In this case transportation by road would be the faster and easier option to transport the beams. Usually trucks can carry less beams than ships, but the beams are small in size so it is possible that a truck can carry multiple beams at once. Furthermore the bridge is easier to reach by road than by water and the highway system is not too far away from the Leiden Bridge. Multiple trucks could be used as well to speed up the transportation process.

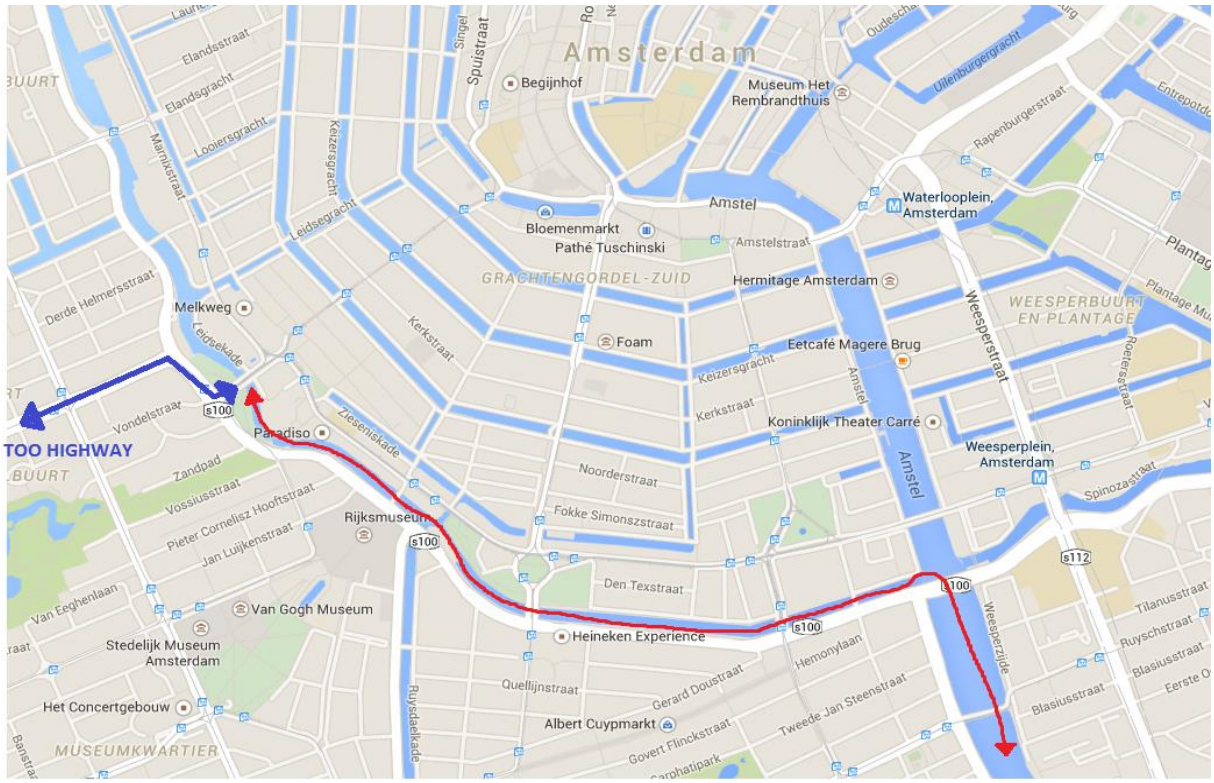

Figure 9-4: Transportation routes by road and water

9.1.5 Placement of beams

The first beams that arrive at location can be immediately placed, while the remaining beams are being brought. The beams are best lifted and placed on their location with cranes. Around the bridge there should be enough room for the cranes to manoeuvre. It could also be an option to construct a temporary moveable pontoon on the water so that the crane could be placed in the middle of the bridge span. However this would temporary block the waterway. But the placement of the beam should not take too long and if done at a time when there is hardly any waterway traffic then the hindrance would stay as less as possible. Though it would require a large arm for the crane to reach the most outer side of the bridge from one end. On land there is more room for a bigger crane and the arm would be smaller. The beam should be placed in position one by one starting from one side of the bridge (see Figure 9-3)

9.1.6 Placement of cables

It is important that space is reserved for cables (electricity, internet, etc.) in the bridge. The cables should not be exposed to the environment. Usually cables run under the ground. So the bridge should act as a connection point between the two sides of the bridge. The cables could be placed on the inside of a couple of box girders. The empty space in the box girder should be large enough to hold the cables. However the box girders have hammerheads on both sides, which are solid sections. So the girders, which will contain the cables, should have a hammerhead with a hole in them. The hole should be large enough for the cables to pass through, but it also important that the structure still has sufficient capacity in these locations in order for structural failure to be prevented. Once the cables have passed the bridge they could run further underneath the road level. The amount of cables should determine the amount of box girders used for the cables and also the size of the opening in the hammerheads. In consultation with the utility companies it should be determined what the best locations will be for the cables to pass the bridge.

Figure 9-5 shows an expression of the bridge when all the beams are in place.

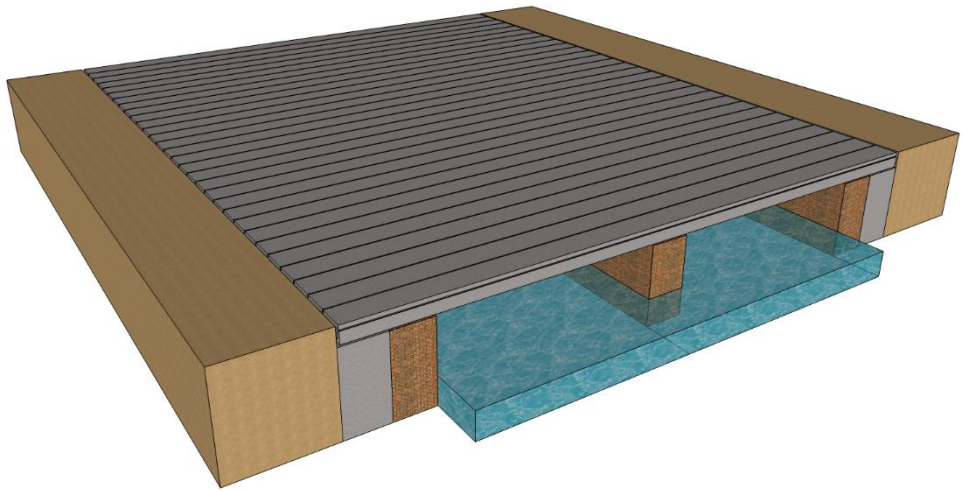

Figure 9-5: All beams in place

9.1.7 Filling of joints and transverse post tensioning

After all the beams are lifted in place the joints between the beams have to be filled. The beams also have to be transversely post tensioned, so that the top flanges act as one large deck. The joints need to harden, before the surfacing layers are placed.

9.1.8 Placement hardenings layers

After the joints are hardened long enough and after post tensioning, the hardenings layers need to be applied. The hardenings layers are asphalt, pavement and filled concrete. The filled concrete is placed, there where the tram rails will be placed. The rails are embedded in the filled concrete. The filled concrete layer should be thick enough, in order for the rails to be completely embedded. The asphalt layers are placed at the locations, where traffic will run. And pavement on the location designated for pedestrians.

9.1.9 Finishing work

After the placement of all surfacing layers, finishing work should be performed. Such as putting back the steel fencing and natural stone ornaments. Also electric poles and road lines etc. Note that the electric poles will not be located on the bridge deck, as is the case now as well. Furthermore it is important that care is taken for the stone ornaments and steel fencing, so that no damage is done to them. They play an important role in keeping the architectural view the same, as is now the case.

After all the work is completed, the site should be cleaned up and the bridge can be opened for use again. A final expression of the bridge is seen in Figure 9-6.

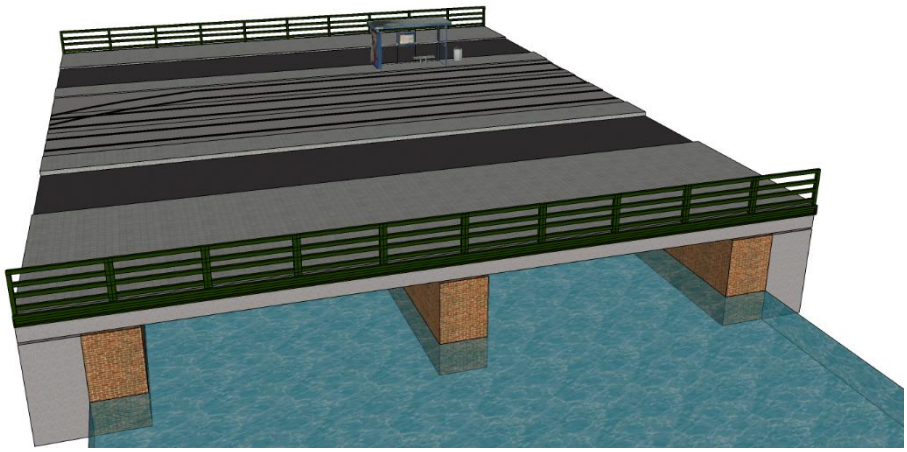

Figure 9-6: Final expression of Leiden Bridge

9.2 Phased construction of new bridge

A second option is to build the new bridge in phases. This will allow for the current bridge to be used longer, while the new bridge can already be built partially. This is most beneficial for the trams, as it is preferred that the tram traffic is hindered as less as possible.

The general construction scheme of building the new bridge in phases can be seen in Figure 9-7. The steps are:

1 Demolition half of existing superstructure→ 2 construction first part new substructure→ 3.1 placement bearings→ 3.2 Transportation beams→ 3.3 Placement beams → 3.4 Placement cables → 4 joints placed and first beams connected with transverse post tensioning→ 5 optional relocation of tram tracks to finished first part→ 6 Closing and demolition of second part of current bridge → 7 Construction remaining substructure, transportation and placement of beams, bearings and cables → 8 Closing of whole bridge and removing tracks → 9 Coupling of first and second group of beams → 10 Placement of pavement and rails→ 11 finishing work → 12 reopen bridge

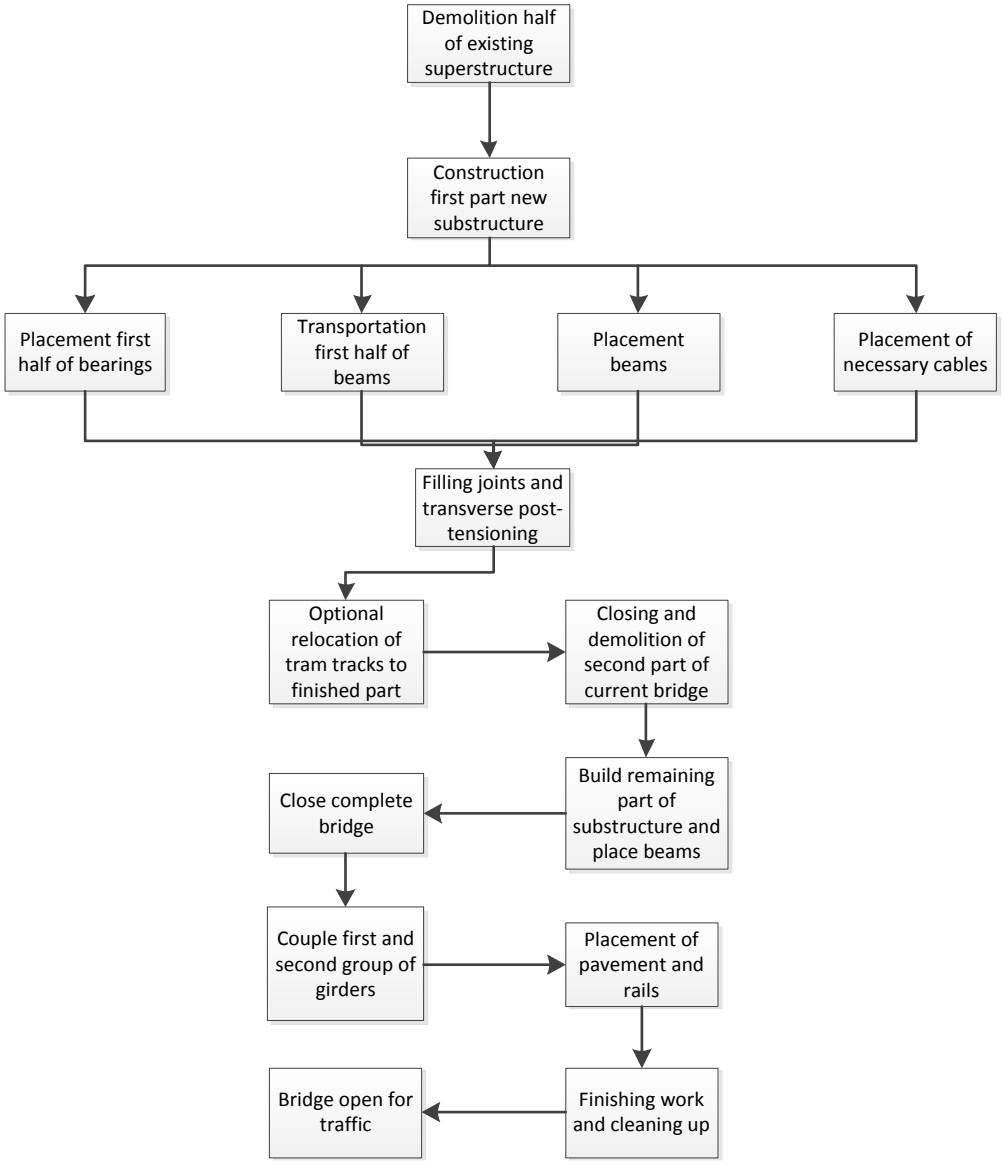

Figure 9-7: Construction scheme of phased construction

9.2.1 Demolition half of existing superstructure

In order for the bridge to still be in use partially, around half of the existing superstructure is demolished. It can be chosen to at least keep one or two track tracks available so the trams can keep crossing the bridge, so slightly more or less than the half of the bridge is demolished. Of course the bridge is now weakened, so the trams and remaining traffic are allowed to cross the bridge with minimum speed. As with the other construction method, care must be taken to not damage the natural stone ornaments and steel fencing. For pedestrians a temporary bridge will be available.

9.2.2 Construction first part of new bridge

One part of the bridge is demolished, so the first part of the new substructure can be built already. The substructure is built behind the old one, so that the existing substructure is relieved of its bearing function, as already explained in paragraph 9.1.2. In Figure 9-8 the new substructure is seen next to the still open existing part. Of course also necessary is to apply safety measures around the construction site (fencing and such), which are not seen in the figure.

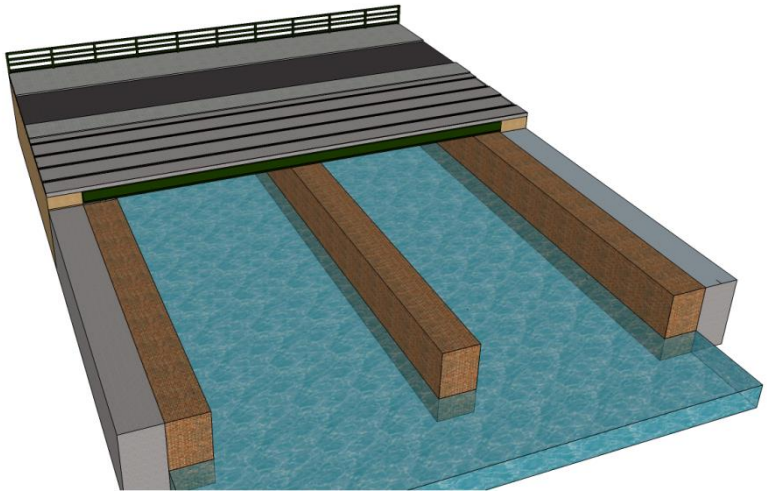

Figure 9-8: New substructure next to existing part

After the first part of the substructure is built, the first half bearings can be placed. Meanwhile the first group of beams are transported and then placed into position. The transportation and placement should occur mostly at night, because then the bridge is hardly used. During the day there would be a lot of hindrance, because a part of the bridge is still in use. The transportation methods are explained in 9.1.4 and they can be applied here as well. So transportation by truck is the easier and faster option. Same goes for the placement method. Now it is also a possibility to position the crane on the still available old bridge, so placement becomes easier. The necessary cables can also be positioned in the selected beams. In the hammerheads a hole has to be made, as explained in 9.1.6. The placement of the beams and the direction of placement are seen in Figure 9-9.

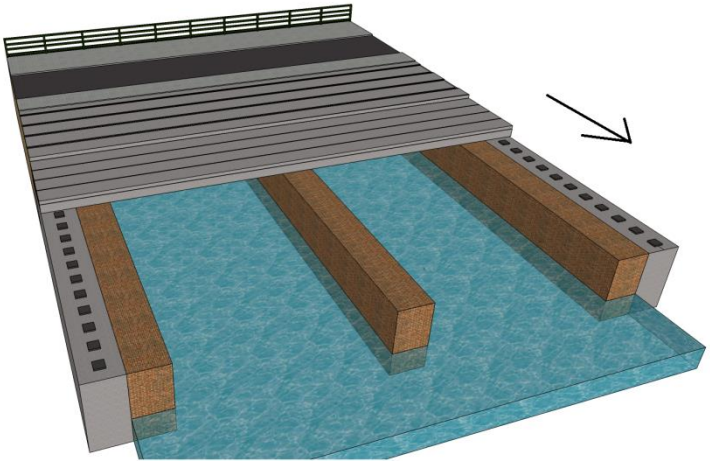

Figure 9-9: Placement of beams (phased)

After the placement of the first group of beams the joints have to be filled. The group is also post tensioned already. This is done so that this part can be used temporarily, while the other part of the bridge is being built.

9.2.3 Relocation of tram tracks

The first part of the bridge is in place. This means that the last part needs to be constructed. This part is still in use by traffic and it will have to be closed. Instead of rerouting the trams or temporary cancelling them, it could be an option to temporarily relocate the available tram tracks to the part that is finished. This part is transverse post tensioned, so the available beams already act as a whole structure. This way the tram can still cross the bridge (at slow pace).
The problem here would be that the tracks around the bridge have to be modified to allow for the tram tracks to be relocated to the side. So this results in extra activities and also extra costs. It is important to weigh the advantages and disadvantages of the relocation of the tram tracks to those of rerouting the trams, namely in costs. Also it is important to verify that the existing part is able to temporary resist the crossing trams.

9.2.4 Construction remaining part of the new bridge

The second part of the bridge is closed for all traffic. If chosen is for relocation of the tram tracks, then the trams can use the new section of the bridge. The remaining old part is demolished and the last part of the substructure is built. It is important to monitor the hardening of the concrete in the substructure, especially at the interface of the already poured part and the fresh part of the substructure, as the first half is already hardened and in use. The interface should be monitored, so that unsuspecting cracks are prevented. When the substructure is built and hardened, the remaining bearings and beams are placed.

When this is done the whole bridge should be completely closed, including the new part. The (if available) relocated tram tracks should be removed. The remaining joints have to be filled and the two groups of beams have to be coupled to each other in order to have the whole bridge acting as one structure. This coupling is done according to Figure 9-10. Anchors are placed at the last beam of the first group. Then the post tensioning for the second group is attached to the anchor as seen in the figure. After tensioning the open part is filled with concrete. This will result in a joint that is larger than the other smaller joints. The gap here between beams will also be larger. Attention has to be paid to this detail and the required space has to be made available in order to be able to fulfill this process.

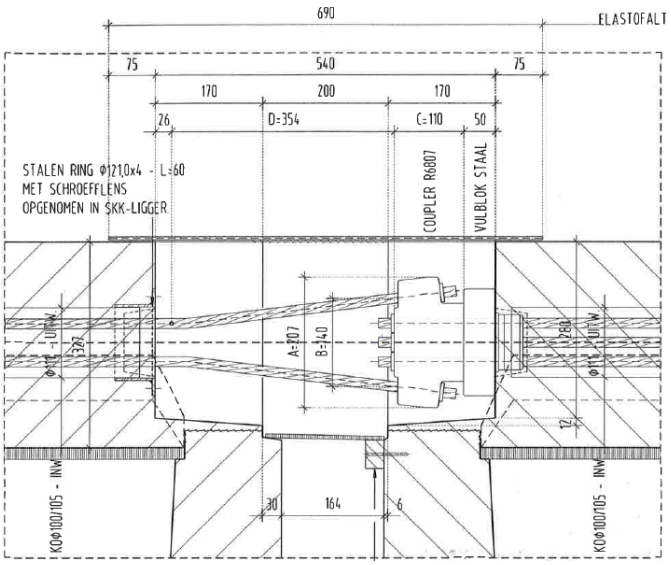

Figure 9-10: Coupler for post tensioning

9.2.5 Remaining work

After post tensioning the pavement and trams tracks are placed. Remaining finishing work is done such as the installation of the stone ornaments, steel fencing, electric wires etc. After all the remaining work is completed the bridge can be opened for all traffic.

9.3 Alternative for phased construction

Paragraph 9.2 described a way to apply a phased construction method to build the new Leiden Bridge. Since it is very important that the construction time remains as short as possible it is interesting to find an alternative way for the phased construction method that specifically looks at reducing the time the trams remain out of order. The alternative discussed in this paragraph basically modifies the construction sequence. First the part of the bridge, where the tram tracks are located, is demolished and the new part is built. Meanwhile the remaining part of the bridge can still be used by vehicles. The new part is built by using a complete prefabricated section. After the section is constructed, it is then transported to its position. This results in a new section, which can be used instantly by the trams, while the rest of the remaining bridge is demolished and built around the new section in about the same way as in the earlier methods. While the remaining part is being built the bridge is only open for the trams. Eventually, all the beam groups are connected in the same way as described in paragraph 9.2.4. While the beams are being coupled, the bridge should be closed completely.

9.3.1 Section

The section is made for the location on the bridge where the trams will be driving over. At least two trams should be able to cross the bridge. Considering the fact that the track gauge is 1.435m wide and that there needs to be a minimum distance between two trams and also near the sides, the section should be around 6 meters wide (see Figure 9-11). The section is made out of multiple beams. If each beam is 1 meter wide, then 6 beams are necessary. In order to speed up construction the tram tracks should already be anchored on the beams beforehand. It is important to first couple the beams and monitor the deflections in the beam to make sure there are no height deviations between adjacent tracks, when they are being installed.

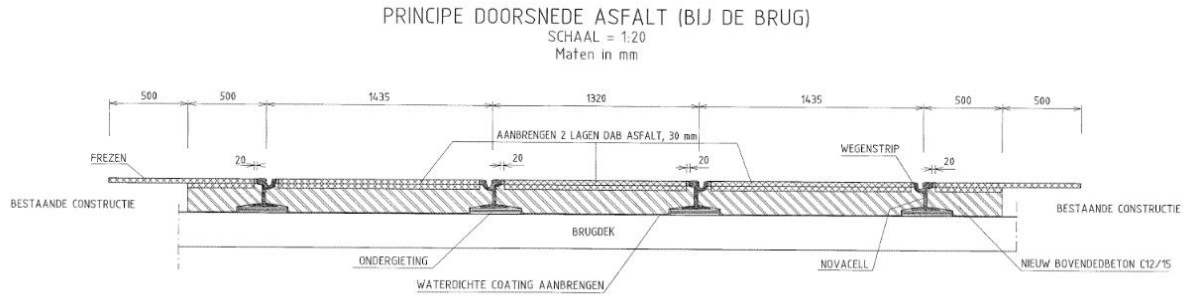

Figure 9-11: cross section of two adjacent tram tracks

Also possible is to use wider box girders, for example girders with a width of 1.5m or even 2m. This will allow mounting a pair of tram tracks on one girder, so the height deviations become lower. However using wider sections also means higher forces per beam. Especially the shear force becomes governing as the web thickness hardly increases while the beam width increases much more, so one beam takes up a higher force.

To resist the higher shear forces more stirrups will be required or a much thicker web is required. Here UHPC would have a benefit, as it can better resist high shear forces with a smaller web thickness than a weaker type of concrete and this will result in a lighter section, which benefits the transport and placement of the section. For example if a width of 2m is taken, a quick calculation shows that a HPC girder with H=0.6m needs a web thickness of 340mm to resist the shear forces without stirrups, while a UHPC girder with H=0.55mm needs a web thickness of 200 mm to resist the shear forces. So the UHPC girder will be much lighter, which is beneficial, when lifting the section. And looking at the costs the UHPC section would then be around 18000 euros more expensive, but the section will be around 30 tons lighter as well. Which means less weight needs to be lifted by a crane. Multiple variants of the section depending on the girder width are seen in Figure 9-12. It is also optional to incorporate the substructure to the section (also seen in the figure) to reduce construction time. Of course if this is done measurements have to be made to be able to connect the section with the foundation.

Figure 9-12: Section variants, from right to left: B=1000, 1500 and 2000mm

9.3.2 Transport

The section is transported in its whole to the Leiden Bridge and then lifted and placed in position. The transport of this section is an important issue. The section is 5m wide, so it is not simple to transport such a big section. It is very difficult to mount such a section on a truck and also to manoeuvre the truck with such a big section, especially when it is entering the city centre. The section is also wider than a driving lane so this gives problems on the road as well.
A better option in this case is to transport the section by boat. As already discussed earlier it is important to take into account the canals that lead to the Leiden Bridge and if the bridges on this route and also the width of the canal are high and wide enough respectively for the ship to pass with the section on it. The used ship has to have a low height and it has to be easy manoeuvrable, since the canal is not straight at all locations. Also some narrow points in the canal are present as well so it is important to investigate if the ship, which should be at least 6m wide to carry the section, can pass these narrow points. The narrowest point of the canal is around 7m so there is just enough room for the ship to pass very slowly, depending on the width of the ship.

So in short transport by boat is the better alternative for such a bridge section, only it is important to take into account the canal route and to take into account if it is possible to actually transport the bridge section all the way to the Leiden Bridge, without too many issues.

9.3.3 Lifting and placing

When the section is delivered at the bridge, it has to be lifted in its place. It must be realised that such a section is quite heavy. For example the UHPC girder is around 21.5 tons, 6 girders make around 130 tons. This is a large weight for a simple crane to hoist and place. So necessary are larger cranes, which have a high capacity. Using wider girders, for example girders of 2m wide (around 80 tons in total), will slightly reduce the weight, but the weight is still too large for a simple crane to carry. Large cranes are very heavy in general. So it is important to investigate if the surrounding soil, especially close to the abutments, is strong enough to resist such heavy cranes. The old abutments do not have enough capacity as it is, so if a large crane is stationed nearby, this could lead to failure in the form of failing abutments together with the surrounding soil falling as well. Therefore the cranes need to be located further away from the bridge and this will result in a large required boom length of the crane (the length the crane needs to extend). A larger boom length or in other words a larger arm decreases the load capacity of the crane. Two cranes will be necessary, one for each side in order to lift the section out of the ship into its place. This will halve the total mass per crane. So the arm of the crane can be longer before the load capacity becomes too low.

Assumed is the section will be located next to the bridge on a pontoon. Furthermore two cranes are at each side located in the middle of the street. They cannot be right at the abutments, but further away in order to avoid failure. Each crane has to lift at least around 75 tons. And the arm length of the crane will certainly lie around 20 to 30 meters in order to reach the section and be able to lift it and put it in place. Considering the available cranes[26] a large mobile crane with a ballast of 204 tons on each side of the bridge will be necessary in order to lift the section. Besides that a lot of space needs to be made around the bridge in order for the cranes to be installed. And considering the high ballast, the soil around the bridge should be investigated as well, as already mentioned earlier. And then it is still the question if the largest crane available for these purposes can lift 75 tons. If the radius of the crane is between 20 and 30m the load capacity is between 60 and 100 tons, depending on the boom length and the angle of the crane's arm as well. So it is clearly important that the crane is as close as possible to the bridge and therefore further research is necessary.

[26] http://www.mammoet.com/Global/Homepage/Equipment/Cranes/MobileCranes/Datasheet%20LTM-1750-9.1.pdf
Last seen 27 – 01 – 2015, last modified 2006.

Another point is the remaining part of the bridge. The superstructure can be built fast, by lifting the section in place, but before that is possible the substructure and foundation need to be built first. It is an option to incorporate the substructure in the superstructure (as seen in Figure 9-12). This would become an integral bridge. This would save quite some construction time. Only beforehand the foundation needs to be placed, in form of poles. Piling the foundation should not take too long. Same goes for placing the section. So this part of the bridge should be completed in matter of weeks.
And the construction method will be faster than the phased construction method discussed in paragraph 9.2.

The alternative discussed in this paragraph will result in the shortest time the trams have to remain out of order. Of course the mentioned issues, such as transport issues and issues regarding large cranes and soil strength are important to investigate, as already stated multiple times, to see if it is actually achievable considering the surroundings of the Leiden Bridge. And besides that it is also important to see which girders are the most suitable to realise such a section in terms of the width. In the end it is quite possible that the other methods will be more realistic even though the construction time would probably be longer. The input of the public transport company is also important for this matter, since they can tell, what construction time and method is allowable.

9.4 Comparison of the two construction methods

The phased construction allows for longer use of the old bridge, while the new one is being built. This is most beneficial for keeping the trams crossing the bridge. More so if a complete section is built beforehand for the part of the bridge where the tram tracks are located. This section can be placed quickly so that the tram can keep on using the bridge. The phased construction method however is more complex and probably more expensive than the construction of the bridge at once. Also expensive detailing is necessary for the post tensioning.

The construction of the bridge at once, is an easier construction method and it does not require complex detailing. However, problems could arise with the substructure. Building the substructure will cost a lot of time depending on the design of the substructure. And closing the bridge too long will not be accepted by the Amsterdam Public Transport Company (GVB). So a phased construction, which is more expensive, would probably be accepted sooner, as the tram can use the bridge for a longer time and maybe even during construction of the second part if the tram tracks are relocated or if a prefabricated section is used. For this it is important to make a cost analysis on rerouting or cancelling the tramlines or relocating the tram tracks or even building a complete section with its mentioned arising issues in combination with the available construction methods.

9.5 Attention points during construction and service of bridge

9.5.1 Fast construction and rerouting traffic

Multiple times it is already stated that the Leiden Bridge is located in a crowded area. The bridge is used a lot by public transport, traffic and pedestrians. So it is very important that the construction of the new bridge is as fast as possible. The construction should preferably also take place during a time when there is not much traffic around the bridge, which is most likely at nights and during the weekends for example. Transportation and placing of the girders or placing sections will have to take place during the night. It is most likely possible to transport all the necessary beams and place them in one night, if multiple beams can be fitted on one truck and if multiple trucks are being used. Then the other construction stages could take place during the day and night if multiple work shifts are used. Parallel construction will be important in order to reduce the construction time. According to the construction demands, the bridge may be closed for a maximum of four weeks straight for trams, so the whole bridge should be ready for use in this period. Given that prefabricated beams are used, this should be possible to achieve.

Building the substructure however will probably cost a lot of time, as already is mentioned when comparing the construction methods, and it will probably result in a construction that lasts longer than four weeks. So therefore the phased construction would be more beneficial than constructing the whole bridge in one go, especially if a section of the bridge is prefabricated, since this will result in the bridge to be open faster for at least the trams.

During construction a temporary bridge for pedestrians and cyclists will become available. However for traffic and public transport that is not the case. Traffic has to be rerouted to other crossing points of the canal, which will cause a temporary increase in intensity at those locations.
Same goes for public transport, which also needs to be rerouted to other crossing points, if chosen not to relocate the tracks and/or use the phased construction method.
In Figure 9-13 an alternate route is seen for the public transport. The red line is the current route that crosses the Leiden Bridge (red circle) and the green line is the alternative route. The green line goes through streets, which contain tram tracks, so the tram lines that cross the Leiden Bridge, could be rerouted using this route. This will however result in a longer travelling time.

It will be important to check if the other bridges (Green circles) can handle the extra cyclic loading. And besides that, the increased intensity at the new route should also be taken into account. If too many tram lines are operable in one route, then there is a high chance in traffic congestions. Otherwise the tram lines could be split up, where a part of a certain tram line only operates south of the bridge and the other part north of the bridge. This way the tram lines are still in use, except it cannot cross the bridge, so people who have to cross the bridge will either have to walk to the other side and continue with the same tram line, or use another tram to cross at another location or maybe even use another type of public transport (subway or bus).

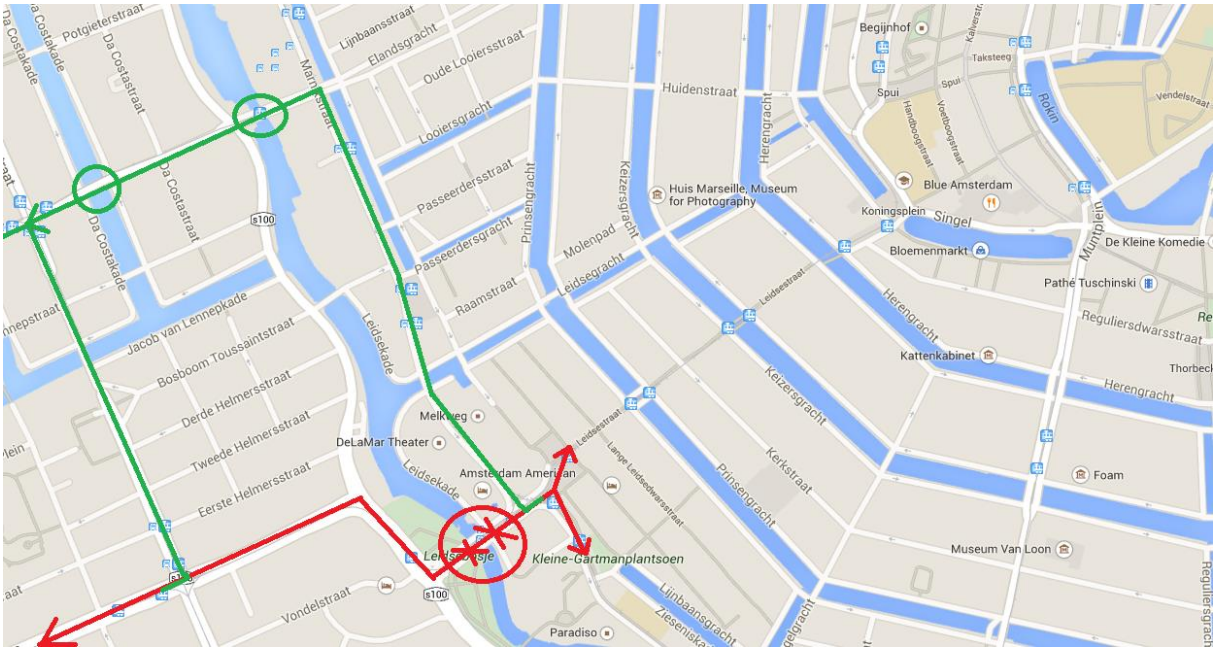

Figure 9-13: Alternative route for public transport

9.5.2 Maintenance Bearings and reaching them;

In the design the beam is modelled as simply supported. So bearings will be used. For the Leiden Bridge, the new substructure will be built behind the current one. Bearings do not have a large lifespan as for example UHPC or normal strength concrete for that matter. So maintenance will be necessary for the bearings.

However looking at the future situation, it will be difficult to reach the bearing, because the current substructure will not be removed and the gap between the super and substructure will be too small to reach the bearings. Therefore the bridge would probably have to be jacked or lifted up completely in order to reach the bearing and to inspect or replace them.
This would require large jacking equipment or a large crane, since the bridge is very wide and the beams cannot be disconnected anymore from each other.

A possibility would be to not use bearings and instead place the superstructure directly on the substructure. This would create a certain degree of fixation and the beam would not be a true simply supported bridge. However the supports would not be completely fixed but more or less flexible so the moments would not be very high. And the exclusion of bearings would lead to a more durable bridge structure overall as bearings are usually the weakest link when talking about durability.
If chosen for this alternative, then it has to be made sure that the change in the mechanical scheme does not result in a structure that does not have enough structural safety anymore. New calculations would then be necessary.

9.6 Conclusion construction of new Leiden Bridge

In this chapter the construction of the new Leiden Bridge was discussed. Two options were given to construct the bridge, namely constructing the whole bridge in one go and construction in phases. The process of both construction methods are discussed in whole. Important aspects to consider during construction are making sure that the tram can use the bridge as long as possible and a fast transportation and placement of beams. Phased construction will result in a longer use of the existing bridge for the trams, because at first only the half of the bridge is demolished and replaced with the new beam. However this construction method is more complex than the construction method where the bridge is built at once. Furthermore a choice has to be made with rerouting the tram or to relocate the tram tracks on the bridge and place them on the first built part of the new bridge. This choice has to be discussed with GVB. And lastly the fact that a prefabricated section can be used will bring multiple issues, such as transporting and lifting a large segment. Further research is necessary to see if this alternative is achievable. Attention should be paid to the possibility of using heavy crane and if these can be installed near the bridge, without causing any type of failure of the substructure or the ground. In the end the construction of the new bridge is a difficult subject and to eventually make a choice in which construction method should be used, the discussed methods should be further investigated. Still by using a design with prefabricated beams and by using a single span instead of the original two spans, time is already saved in not having to reinforce the intermediate pier and by not having to cast the concrete in-situ.

Chapter 10 Conclusion

In this report a study was performed on the possible application of Ultra High Performance concrete in the Leiden Bridge. The current Leiden Bridge has deteriorated quite a lot and it needs to be replaced by a new bridge. For the new bridge it was important that the construction height and the architectural view remained the same and also that the construction of the bridge caused as less hindrance as possible. After analysing the current structure, the maximum construction height was set to 600 mm, with an option to increase the thickness to 650mm if proven necessary.

In the study three designs, with each a different type of concrete were developed and checked on its structural safety. The main boundaries were an initial construction height of 600 mm with a single span of 24m. Concluded was that the most suitable type of bridge would be a prefabricated bridge consisting of box girders.

10.1.1 Structural performance

10.1.1.1 NSC C50/60 design

It is not possible to achieve a safe structure with this concrete type with H=600mm. A high amount of strands and reinforcement is necessary. Both will lead to issues in fitting everything in the cross section, which will make the production of the girders complex and uneconomical. Using a thicker deck of H = 800mm would deliver sufficient structural safety, but this is higher than the maximum allowed construction thickness, so not possible in this case.

10.1.1.2 UHPC C170/200 design

It is more than possible to design a bridge in UHPC with H=600 mm. Achieved is a design, where the reinforcement is completely left out, so the structure relies completely on the steel fibres and the prestressing steel. However this does go against the design philosophy so it is important to realise if the bridge can still be structurally safe, if certain negative situations occur and also to understand the structural behaviour of such a structure. Still the calculations showed that the design has more structural capacity than is necessary to resist the loads on the bridge, so achieving this design is possible. Further optimization is possible for the bridge, to make better use of the material.

10.1.1.3 HPC C90/105 design

Using a thickness of H=600 mm will not be possible, because the fatigue resistance is not sufficient. However increasing the thickness to H=650 mm, results in an overall safe structure, which actually could be used for the new bridge. The reason that the design is achievable is because of the inclusion of steel fibres. If plain high strength concrete is used, then the same issues as with the C50/60 design will arise. The HPC design cannot be made without stirrups and reinforcement bars, because additional reinforcement is needed to resist the shear forces and torsional moments.

10.1.1.4 Optimized UHPC design

The optimization of the initial UHPC design results in an improved design which is more slender and lighter, while still being structurally safe. The optimization results in a beam, which varies in height over the length. This shows that it is possible to produce beams that are both safe and aesthetic. However such a beam is hard to produce in general, especially if box girders are used. Therefore an option is to keep the height constant over the length of the beam. The construction thickness is reduced to a maximum thickness of 550mm instead of 600mm, as result of the optimization. The web thickness is reduced to 100 mm instead of 140 mm.

10.1.2 Material use and costs

All the three designs were compared with each other on the amount of material needed, on the material costs and on the environmental impact of each design However only two designs are actually possible to use for the new bridge namely the HPC and UHPC design.

As far as material use goes, the UHPC design used the least amount of concrete and steel compared with HPC. This means that this design will provide the lightest bridge structure. Unfortunately the costs for producing UHPC are about 3 times higher than for producing high performance concrete.

The environmental impact in terms of the GWP and embodied energy is also higher, because producing UHPC requires a lot of energy. However a couple of things have to be remarked. First of all the comparisons were only based on material use, so it was expected that UHPC would provide the highest costs and the worst environmental impact, but also the lightest structure. So in accordance to other researches performed, the same conclusions are found here. For the cost of UHPC the current commercial price is used. If the production of UHPC would be brought to the Netherlands, the cost could be reduced (reduction of around €300/m^3), which would result in the UHPC design being cheaper than the HPC design. But this is something that is not easy to achieve in the short term, so for the Leiden Bridge the commercial price will have to be paid most likely. UHPC is proven to have much better durability properties than NSC and HPC, because of its very dense matrix. So a maintenance free life span of at least 100 years is almost certain. However the same holds true for HPC. Maintenance would most likely be required for both concrete types in a life span of 100 years. If the whole life cycle is considered, then there is a chance that a UHPC design would be more profitable and durable than a HPC design, but only if one looks beyond 100 years, as UHPC still has better durability properties than HPC. Besides that, the UHPC design is also more slender and structurally safer than if HPC is used.

10.1.3 Construction of the new bridge

The report looked at two possible ways of constructing the new bridge. Considering the fact that the bridge is located in a crowded area and also the fact that it is desired to cause as less hindrance as possible (especially for public transport), it is recommended to use a form of phased construction, where it is possible for the tram to (partially) still use the bridge, while the new one is being built. The construction is faster when a complete bridge section for the trams is prefabricated. But the issues arising with this method (transport, heavy cranes, soil strength), etc. need to be investigated further in order to find out if the method is achievable. Same goes for the other construction methods as well. However, since only a single span is used instead of two spans like in the current bridge, time is already saved in not having to reinforce the intermediate pier. Furthermore time is also saved by using prefabricated beams. Of course as time is very limited, the most optimal construction method has to be found, by investigating the discussed construction methods further and choosing the most optimal one.

10.1.4 Design choice for the Leiden Bridge

Now that conclusions are made with regards to the three designs, a design choice has to be made for the bridge. Which of the designs is the most realistic one to apply for the new Leiden Bridge?

Based on structural performance the UHPC design is hands down the best choice. The structural performance is much better compared to NSC or HPC and the most slender bridge can be achieved with UHPC, which was also one of the goals of this study. But proven is that HPC has enough safety so all the extra capacity is not necessary.

However there are more aspects than the structural performance itself. One has to realise that 30 prefabricated box girders will be necessary in total. Known is that it takes a lot of energy and precise work to produce UHPC girders.

If something goes slightly wrong, then the concrete loses its guaranteed performance. High strength concrete is already used in a larger scale, also for prefabricated beams, so the production is easier. Only now steel fibres are included and the method of pouring is important in order for the steel fibres to contribute properly to the structural performance. Therefore precise work will still be necessary, also for the HPC design, even though the mixture itself is easier to create.

For the Leiden Bridge it would be the better option to choose the HPC design. This design is cheaper and somewhat easier to produce as far as the girders go. And it will be able to withstand the loads for years to come. Same goes for the durability, as the HPC design still can result in a structure that is maintenance free for 100 years. At this point choosing UHPC for the Leiden Bridge would not bring benefits except for more slender beams. However these slender beams will hardly be visible, since the current (and future) architecture on the bridge hides the beams.

10.1.5 Purpose of (Ultra) High Perfomance Concrete

Still, even though the Leiden Bridge should be made in HPC, one must not ignore UHPC. This report has shown that UHPC delivers an innovative bridge structure that has a great structural performance; that is very durable, maintenance free (which is very important in the always crowded Amsterdam) and also more slender than can ever be achieved with normal or high strength concrete. If one looks at the Leiden Bridge, the UHPC design and also the HPC design make sure that a single span with a limited construction height is possible to achieve, so the intermediate pier does not have to be strengthened. This is most beneficial since this saves costs and also reduces construction time. Considering that Amsterdam has tons of old bridges, which need to be replaced in a short amount of time and where a high durability and a maintenance free service life is required, using UHPC and HPC is most beneficial and eventually a much better alternative that ordinary concrete, which can never achieve the same things as UHPC and HPC, as shown in the report.

Looking specifically at UHPC, UHPC has a much higher strength than HPC. This becomes beneficial when large spans are required. Where HPC would be limited by its lower strength, UHPC could achieve much longer spans that were ever possible. There is also the fact that bridges in UHPC can be made very slender and will be beneficial for saving material and also for aesthetical purposes. For example, when a bridge over a wide, crowded highway or waterway needs to be realised, UHPC would result in for example a single span bridge, which does not require intermediate piers, so that already saves material, construction time and also traffic would hardly be hindered by the construction, and it is already shown that it is important to cause as less hindrance as possible. For such purposes UHPC would most likely prove to be the most economical solution. Especially if eventually UHPC would be produced in factories in the Netherlands, which would greatly reduce the price of UHPC.

If one is willing to invest in UHPC and to consider it as a serious solution for a certain structure, especially, when long spans are necessary, then this could be a step in a wider application of UHPC in traffic bridges and structurally wise things could be achieved, which were never possible before UHPC.

Chapter 11 Recommendations

The recommendations are split in recommendations for UHPC in general and recommendations specifically for the Leiden Bridge.

11.1.1.1 UHPC in general

- In the NEN-EN 1992-1-1 a table can be found where all concrete classes are listed with their mechanical properties, such as compressive and tensile strength, stiffness etc. It would be beneficial for the design of UHPC structures, if such a table is developed for UHPC or fibre reinforced concrete in general as well. This table should give the different properties for different strength classes with most importantly a value for the residual tensile stress, because this one still needs to be determined with experiments.
- Developing a uniform UHPC mixture and developing guidelines for this mixture. This would also benefit the previous point, because a uniform mixture will lead to easier determination of mechanical properties.
- Further research in the effect of steel fibres for the torsional resistance and trying to develop new formulas to determine the torsional resistance with taking into account the effect of the steel fibres.
- In the UHPC design chosen was to not use any reinforcement at all, only prestressing. This goes against the current design philosophy in the Netherlands. Experiments should be performed which show the effects of using beams with no reinforcement at all, while having only steel fibres and prestressing, compared to having beams that incorporate minimum reinforcement. Important is to view if the ductility of the bridge still sufficient enough in accidental situations.
- Research in finding a more optimal method to produce UHPC mixtures. Also a method that would allow mass production of UHPC girders. This method should also result in a decrease in productions costs and energy needed for production.
- In combination with the previous bullet, research in pouring methods, which result in the most optimal steel fibre orientation in UHPC structures. This is important because the orientation of steel fibres has a great influence on the structural performance.
- Research in production methods in order to achieve (box) girders with varying thickness over the length without much difficulty. Preferably methods that can be applied in prefabricated girders as well.
- Broader use of optimization methods to produce more optimal and more aesthetic structures.

11.1.1.2 Specifically for the Leiden Bridge

There are some subjects discussed in the report, which could not be dealt with in detail, due to the subjects falling outside of the scope of the thesis. The recommendations are based on a couple of those subjects.

- A further study on the construction methods discussed in this thesis. One should look at how long the construction of the new bridge would take for each method. Also the solutions for keeping the tram operable, during construction should be compared, with each other in more detail (in cooperation with GVB), to find the most economical solution. And most importantly, if a prefabricated bridge section is used, it has to be investigated if it is actually achievable. The study should result in the most economical and achievable construction method.
- A design that looks at an integral bridge made of UHPC, which can be constructed fast. This could prove beneficial for other old bridges which also have massive walls acting as superstructure. Bearings would not be necessary as well, so less maintenance will be required.
- A life cycle analysis, where the three designs discussed in this thesis are compared with each other. This analysis could back up the positive aspects of UHPC, by actually proving that UHPC is more durable and more profitable in the long term (> 100 years).
- Perform an experiment on one girder (HPC and or UHPC), to investigate its behaviour under different types of loading. This would give a better understanding of the behaviour of the beams and also serve as a verification of the calculations made here in this study.
- Design a bridge with an unfamiliar type of girder such as the PI – girder. It is possible that this type of girder can result in an even more slender bridge that can perhaps save some more material. This could be done for other bridges, which require replacement in the (not so distant) future.

Reference list

[1] **Fehling,** E., Schmidt, M., Walraven, J.C., Leutbecher, T. & Fröhlich, S. (2014) "*Betonkalender – Ultra-High Performance Concrete UHPC*", Ernst & Sohn, Germany.

[2] **Griede**, M. (2013) *"Programma van Eisen Brug 174 Versie 1.6",* Dienst Infrastructuur Verkeer en Vervoer, Gemeente Amsterdam.

[3] **Kelpsa.** S**.** et al (2014) *"Analysis of Crack Width Calculation of Steel Fibre and Ordinary Reinforced Concrete Flexural Members",* Kaunas University of Technology, Kaunas, Lithuania.

[4] **Ketel,** M., Willemse, R., Van Rijen, P., & Koolen, E. (2011) "*Rekenmodel VVUHSB, Toepassing van vezelversterkt ultra-hogesterktebeton in bouwkundige constructies (1)"*, Cement Online.

[5] **Tadros, M.K.,** Morcous, G. (2008) Application of Ultra-High Performance Concrete to Bridge Girders, University of Nebraska-Lincoln

[6] **Van den Broek**, B. (2012) *"Constructieve beoordeling van brug 174 – De Leidsebrug",* Ingenieursbureau Gemeente Amsterdam.

[7] **Voo,** Y. L., and Foster S. J. (2010) '*Characteristics of ultra-high performance 'ductile' concrete and its impact on sustainable construction'*, The IES Journal Part A: Civil & Structural Engineering, 3/3, 2010, p 168 – 187.

[8] **Voo,** Y.L., Augustin, P.C., Thambroe, T.A.J. (2012) '*Design and Construction of a 50m Single Span Ultra-high Performance Ductile Concrete Composite Road Bridge*' International Journal of Sustainable Construction Engineering & Technology Vol. 3 Issue 1.

[9] **Walraven, J.C**., Braam, C.R. (2012) *"Reader prestressed concrete"*, Delft University of Technology.

List of figures

List of tables

Appendix

A. Literature study
B. Load cases and combinations
C. Theory regarding UHPC
D. Bridge design in NSC C50/60, calculations
E. Bridge design in UHPC C170/200, calculations
F. Bridge design in HPC C90/105, calculations
G. Results optimization process
H. Derivation of x_u for multiple situations
I. Drawings

Appendix A Literature study

Delft University of Technology Gemeente Amsterdam Ingenieursbureau

Application of Ultra High Performance Concrete in the new Leiden Bridge

Graduation committee:

- Prof.dr.ir. D.A Hordijk, Delft University of Technology
- Dr.ir. C. van der Veen, Delft University of Technology
- Ir. A.D. Reitsema, Delft University of Technology
- Dr.ir. M.A.N. Hendriks, Delft University of Technology
- Ir. A. Quansah, Ingenieursbureau Amsterdam

Antonio Paškvalin

Preface

This document contains the literature study done for the master thesis 'Application of Ultra High Performance Concrete in the new Leiden Bridge'. Discussed are the findings during the study and also incorporated are subjects relevant for the thesis.

This literature study is divided in a couple of chapters. The first chapter discusses the Leiden Bridge. Aspects such as the bridge's characteristics and the demands and constraints of the renovation of the bridge will be dealt with. The second chapter deals with Ultra High Performance Concrete (UHPC) in general. A couple of things concerning UHPC are discussed such as material and durability properties, but also the economic aspects and aesthetics. The third chapter deals with several reference projects. Here structural as well as architectural applications are presented. The fourth chapter deals with bridges in general. Here one can think of the bridge types, methods of construction etc. The fifth chapter discusses a couple of researches done in the past. These researches are dealing with material properties, application of UHPC in bridges and the sustainability of UHPC. The sixth chapter deals with structural optimization and the methods available for it.
The seventh chapter contains an example calculation of a simple structure where ordinary concrete and UHPC are compared with respect to moment and shear capacity and the way of calculating them.
The eighth chapter is a conclusion of the whole literature study and also considerations are made here, which are going to be used during the thesis.

TABLE OF CONTENTS

A1. Leiden Bridge

References: [10], [22]

A1.1 General

The Leiden Bridge is a traffic bridge located in the centre of Amsterdam. The bridge crosses the Singelcanal and it connects Leiden Square with Stadhouderskade. In Figure 1 a map is shown, which indicates where the bridge is located. The bridge is located in a popular and crowded area, where the traffic flow is very intense. Leiden Bridge serves as a main route and connection for traffic, especially for pedestrians, cyclists and trams in that area. Moreover a tram and bus station is located on the bridge, which serves as a station for multiple different lines, so public transportation frequently stops on and passes the bridge.

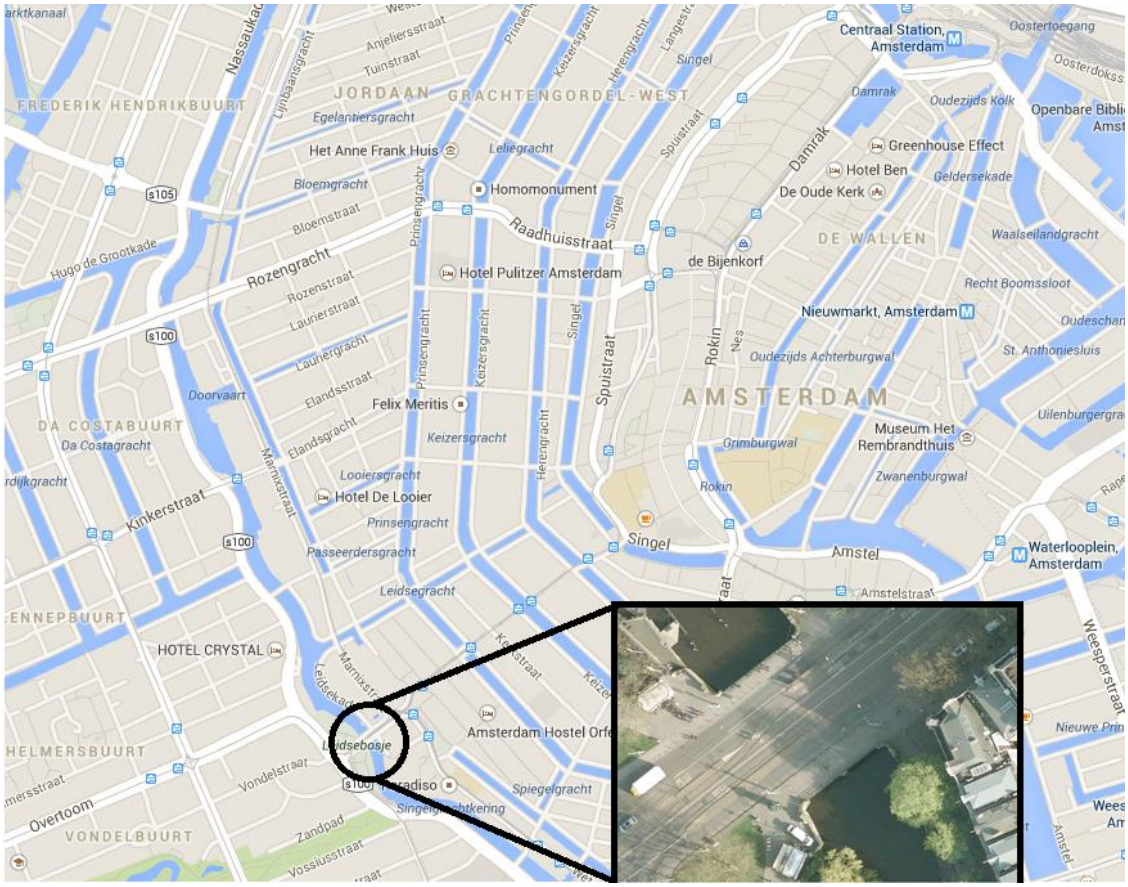

Figure 1: Location of Leiden Bridge in Amsterdam

A1.2 History

Back in the day the Leiden Bridge was actually an old stone arch bridge. The bridge has been renovated a lot over the years, but the first recorded renovation occurred in 1877. Around that time the old stone bridge was replaced by the current design. In 1903 the bridge was strengthened and in 1925 the bridge was widened from 20 to 30 meters (5m on both sides), which is now the current width of the bridge.

A1.3 Specification bridge structure

A1.3.1 General dimensions and bridge function

The total length of the bridge is 21m and the bridge has one intermediate support so the bridge consists of two spans. Under the bridge are two passageways with a width of 9m each. The total width of the bridge is 30m.

As already mentioned earlier the bridge serves as a traffic bridge that is used by cars, public transportation, pedestrians and cyclists. The bridge is arranged in such a way, that each mode of transportation has its own lane. The road layout of the bridge is seen in Figure 2. The layout is such that the heaviest loads are on the inside (tram, bus) and the lightest loads on the outside (pedestrians, cyclists). This layout will also be used for the new design.

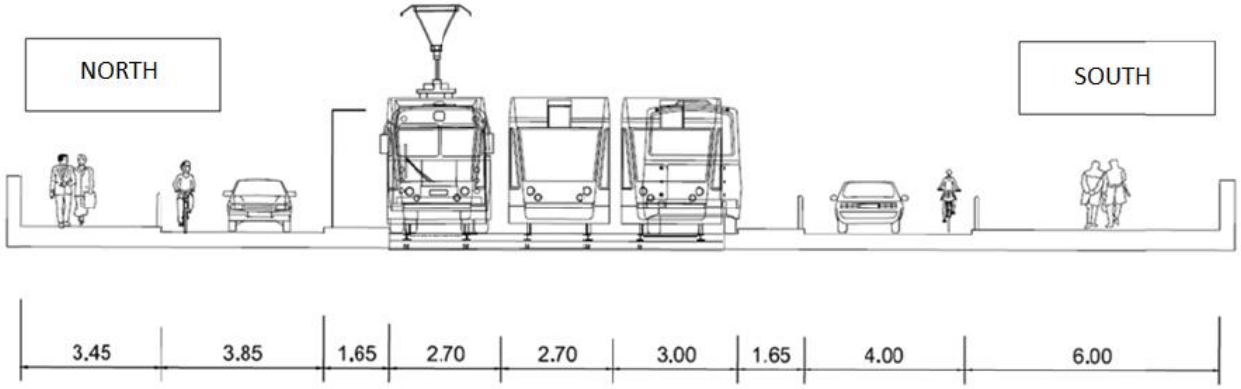

Figure 2: Road layout Leiden Bridge

A1.3.2 Superstructure

The superstructure of the Leiden Bridge is a composite structure that consists of steel girders with a concrete cast in situ deck. The structure, because it was widened in the past, consists of an old midsection part and the widened parts. The steel girders are stiffened with steel diagonals in the mid-section, which serve as diaphragms. The steel profiles for the girders are INP 425 in the mid-section and INP360 and HEB300 in the widened parts. All steel profiles have a steel quality of S235. The concrete deck consists of concrete with strength class C30/37 and thickness of 140mm. The concrete is reinforced with steel bars with quality FeB220. The reinforcement net consists of **ϕ**8-110 mm in both directions with a concrete cover of 30mm.

In Figure 3 the cross section of the bridge in transverse direction is seen. One can see that the section of the wider parts differs from the midsection, as described.

Figure 3: Cross section Leiden Bridge

A1.3.3 Substructure

The substructure consists of two abutments and one intermediate pier. The substructure at the old midsection differs from the substructure at the widened section.

Midsection

At the abutments and the pier of the mid-section the steel girders are supported by natural stone elements. The abutments and pier are made out of masonry bricks. The abutments have a thickness of 1.75m and the pier a thickness of 1.5m. The substructure lies on a 80mm thick wooden floor, which is supported by wooden piles.

Widened section
The substructure is almost the same as in the midsection. At the abutments and the pier of the mid-section the steel girders are supported by natural stone elements. The abutments and pier are made out of masonry bricks. At the widened section however the abutments have a thickness of 1.21m instead of 1.75m. The pier thickness stayed the same with 1.5m. The substructure lies on a 300mm thick unreinforced concrete floor, which is supported by wooden piles.

A1.4 Recent inspection and recalculation results

Leiden Bridge is a very old bridge so it was important to perform inspections on the bridge to see if the bridge could still function properly. The most recent inspection showed that there are some issues with the bridge. It was clear that the bridge was too heavy loaded; a lot of cracks were found in the walls. The steel girders were in good state generally speaking, but at the supports the steel thickness has been halved due to severe corrosion. Also the masonry works on the abutments and on the pier were in bad condition. Furthermore leakages were also discovered in the structure.
The bridge has been recalculated as well. The recalculation was based on NEN 8700 and the Eurocode. The structure had to be reviewed to see if the rejection level given in NEN 8700 is satisfied. In the recalculation assumed was the consequence class 2 (CC2), where the minimum requirement is a rest life span of one year and a reference period of 15 years.
The results of the recalculation showed that the steel girders in the midsection do not suffice on moment capacity in the ULS. Same goes for the concrete deck for the moment capacity in transverse direction. Also the abutments and the pier do not suffice structurally. In a lot of the piles the capacity has been exceeded. With these findings it was concluded that the current structure of the Leiden Bridge did not suffice according to the rejection level stated in NEN 8700.
Based on the inspection and recalculation results it is wise to strengthen or replace the Leiden Bridge. The latter case will be studied further in this research.

A1.5 Product design specification

For the renovation of the Leiden Bridge there are a lot of factors that need to be taken account when designing the new bridge.
A product design specification has been formulated by the municipality of Amsterdam [10]. Here all the demands and constraints by different stakeholders are described. The relevant demands and constraints are going to be summed up in the following.

Functional demands:

- The bridge must keep the status of National monument after renovation.
- Preservation of monumental parts goes before repair and repair goes before replacement of monumental parts.
- The intermediate pier may not be removed, as it is a monumental part.
- As result of maintenance the unavailability of the bridge is allowed to be 4 hours/year at maximum.
- The boat passage width of the bridge is 2x9.0m of which 2x4.5 navigable.
- The minimal life span for new constructions per part are:
    - Concrete structures: 100 years
    - Foundation structures: 100 years
    - Steel work: 100 years
    - Preservation: 10 years
    - Natural stone: 100 years
    - Bearings: 25 years
    - Joints: 25 years
    - Asphalt: 10 years
- Sections of the bridge which are kept after the renovation need to have the following rest life span:
    - Existing structures with function:
        - Intermediate pier: 25 years
        - Fly walls: 25 years
    - Existing structures without function:
        - Intermediate pier: 50 years
        - Abutments: 50 years
        - Fly walls: 25 years

Design demands:

- The full bridge deck width, including the cycle and pedestrian lanes, must be dimensioned on traffic loads according to the Eurocode.
- The architectural view of the bridge (side view, railing and vertical alignment of the edge of the bridge may not be altered.
- The reference period of the structure is 100 years.
- The traffic intensity over the structure is 7000 trucks per direction per year.
- The traffic intensity over the structure is 30 tram movements per hour per direction.
- The railings must be earthed in the bridge.

Demands for execution

- During construction the bridge may not be fully closed for waterway traffic
- Slow traffic will be replaced to a temporary bridge.
- The bridge will be closed for vehicular traffic during construction.
- The tram exploitation can be closed for a maximum of 4 weeks straight in order to replace the bridge deck under the tram rails.

These were the relevant demands concerning the bridge design. To summarize these demands, the most important demands that absolutely need to be taken into account are:

- The architectural view needs to remain unaltered. For the bridge design this will mean that the construction height will stay the same as the current height. And it will mean that the intermediate pier must remain in its place. (However it doesn't have to be used structurally wise).
- There has to be as less traffic disruption as possible. Especially for the public transport, because restricting its access for a long time can bring high costs.

A2. Ultra High Performance Concrete

References: [9], [15], [i1]

A2.1 General

Concrete has been one of the most used building materials, since Portland cement developed in the late 19th century, a type of cement which is still used widespread to this day. Moreover since the last century, researchers were constantly trying to make concrete as strong as possible, by optimizing the mixture of concrete. First signs of higher strength concrete emerged in the 1950's. Since then high strength concrete has gone through a lot of research and nowadays it is applied more and more. In the 1990's the first steps of creating concrete with even higher strength were made. This type of concrete would be known as Ultra High Performance Concrete (UHPC).

UHPC is founded on four principles that can be summarized as follows:

1. Optimized granular packing which improves homogeneity and causes ultra-dense matrix.
2. Extremely low water cement ratio which reduces the amount of pores and capillaries, pore sizes, concrete cancer issues e.g. carbonation, improves permeability, and results in remarkable durability and strength.
3. Inclusion of very high strength micro-fibres which enhance tensile strength and ductility, improve impact and abrasive resistance, and bridge micro-crack more effectively.
4. Steam cured for long period of time which accelerates all early and drying shrinkage, improves overall material properties, which cause volumetrically stability, minimal creep, and negligible shrinkage.

A2.2 Mixture Composition

Ultra High Performance Concrete has a mixture composition which differs from that of ordinary concrete (OC) and high strength concrete (HSC). The mixture of UHPC has the following characteristics (which are actually based on the four principles):

- UHPC contains only fine materials and no coarse aggregates.
- UHPC contains steel fibres, to increase the tensile strength and the ductility.
- The water cement ratio is less than 0.20.
- UHPC is much more durable than OC and HSC. This because of much less and irregular pores, which leads to a higher resistance from external threats, such as chloride attack or ASR. Also because of the higher durability less maintenance is required for structures made of UHPC.

In short the mixture of UHPC is composed of the following main items:

- Portland cement
- Silica fume
- Fine washed and sieved sand
- Super plasticizers
- Quartz Powder
- Water
- Steel fibres (around 2% by volume. PVA fibres also possible)

In Table 1 a comparison is made between the mixture compositions of ordinary concrete and UHPC.

Table 1: Mixture compositions OC and UHPC

	OC	UHPC
	kg/m^3	
Cement	360	710
Silica fume	0	230
Sand (0-2 mm)	790	1020
Aggregates (2-16 mm)	1110	0
Quartz powder	0	210
Water	145	140
Steel fibres	0	40 - 160
Super-plasticizers	0,5	13

Looking at the mixtures notable differences compared to ordinary concrete are visible:

A2.2.1 Cement and aggregates (coarse and fine)

As already stated earlier on UHPC doesn't use any coarser aggregates. Ordinary concrete on the other hand uses a lot of aggregates between 2 and 16 mm. Furthermore UHPC has silica fume and quartz powder in its mixture, which are ultra-fine materials. Also much more cement is used in UHPC. Because of the low water content not all cement will hydrate, so some cement will stay un-hydrated and act as filler. A combination of fine sand, cement and silica fume gives UHPC a very dense matrix and thus is much stronger than ordinary concrete.

A2.2.2 Super-Plasticizers

Another difference is the high amount of super-plasticizers in UHPC. UHPC has a very low water cement ratio, as already mentioned, compared to ordinary concrete. UHPC has a water cement ratio which is always less than 0.2, while ordinary concrete has a ratio around 0.4. Because of the low wcr in UHPC super plasticizers must be added in order to improve the workability of UHPC.

A2.2.3 Steel fibres

The inclusion of steel fibres in UHPC is also a major difference compared to ordinary concrete. Using steel fibres increases the tensile strength and it also improves the ductility of UHPC. The steel fibres will be dealt with more detailed later on in paragraph 2.3.3.

A2.3 Mechanical properties and behaviour

Because UHPC has a different mixture composition than ordinary concrete, the mechanical properties will also be different. So it is important to learn the mechanical properties of UHPC and how these properties differ from the properties of ordinary concrete.

A2.3.1 Stress-strain relation

In Figure 4 the stress-strain relations of ordinary concrete, HSC and UHPC are put together in one diagram, so that they could be compared with each other. When making a design with standard concrete, it is neglected that the concrete can take tensile forces, after cracking even though there are uncracked areas left. This also goes for a design in HSC. As for the compressive strength, the ultimate strain for the ordinary concrete up to C50/60 is 3.5‰.

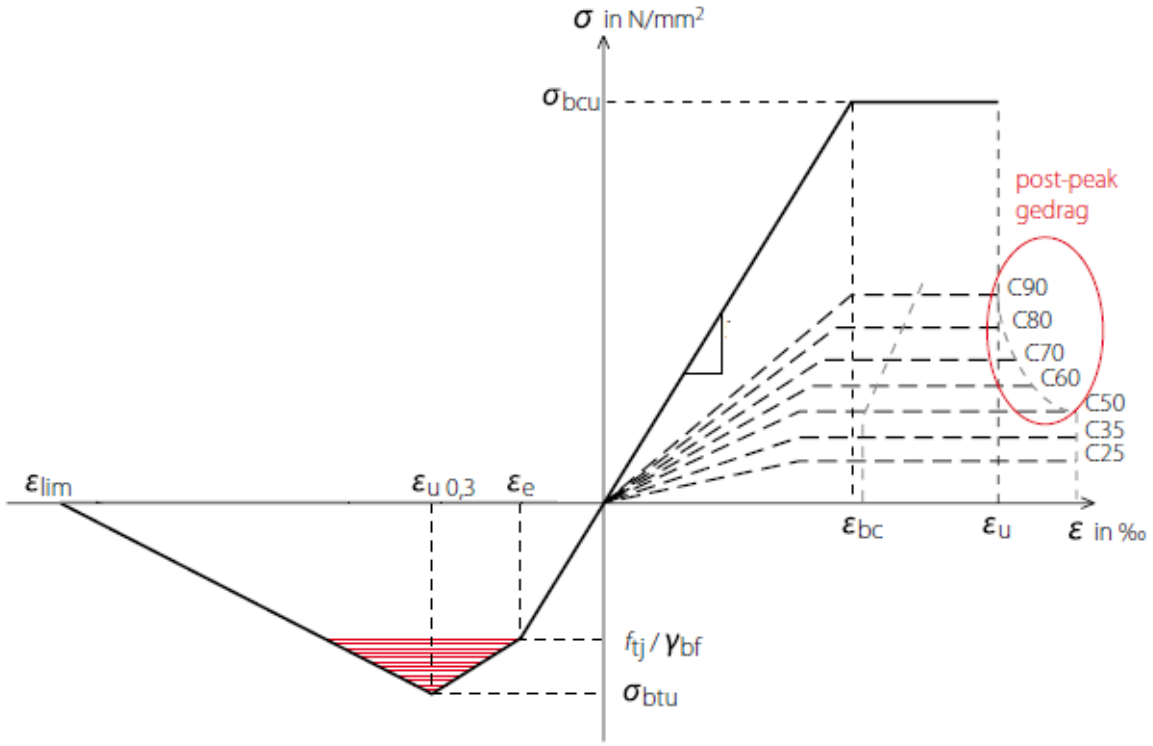

Figure 4: σ-ε diagrams of OC, HPC and UHPC

When the strength gets higher, so when HSC is being used, the ultimate strain decreases. This happens because concrete gets more brittle when its strength increases. So for UHPC it means that the ultimate strain will be around 2.6-2.7‰. The difference with UHPC compared to OC and HSC is that the tensile strength is taken into account for UHPC. This thanks to the steel fibres in the concrete. In the figure, the strain hardening behaviour is clearly seen. At ε_e the tensile strength of the concrete is reached, so the fibres take over and the hardening commences. Eventually the maximum strain will be reached at ε_{lim}. For design purposes this value is kept at 2.5‰, but the strain can reach 5‰. Also when designing, the red hatched area in the figure is usually neglected.
This tensile behaviour also has an advantage that no mild reinforcement or shear reinforcement is necessary as UHPC has enough capacity to withstand shear and cracks, thanks to the steel fibres.

A2.3.2 Compressive strength and Modulus of Elasticity

As already mentioned UHPC is much stronger than OC and HPC. If the concrete types are divided by their compressive strength and elasticity modulus one could say:

- Ordinary concrete: f_c = 20-60 MPa & E_c = 20-35 GPa
- High strength concrete: f_c =60-110 MPa & E_c = 35-40 GPa
- Ultra high performance concrete: f_c =150-200 MPa & E_c = 50-53 GPa

The high compressive strength in UHPC is caused by the very dense packing, caused by use of fine materials and silica fume and also by the low achieved water cement ratio of under 0.2. Although because of this low water cement ratio the workability reduces. Therefore super-plasticizers are also used in UHPC to enhance the workability. Some super plasticizers have a positive influence on the early strength development. It is clear that in terms of compressive strength UHPC has a much higher value than ordinary concrete. It has to be stated though that the modulus of elasticity doesn't increase in the same rate as the compressive strength does. So in terms of stiffness the benefit of using UHPC won't be as high as for strength benefits.

A2.3.3 Tensile strength (and Micro Steel fibres)

UHPC has a tensile strength that is higher than that of ordinary concrete. But it is a combination of a high tensile strength and high ductility that gives UHPC a significantly better tensile behaviour that ordinary concrete. What gives UHPC such a good tensile behaviour are the steel fibres in the concrete.

As mentioned before, because of the higher strength UHPC, on its own, shows a very brittle behaviour. This is something that wants to be avoided, because brittle materials won't give a warning when on the verge of failing. Therefore micro steel fibres are added in the UHPC mixture. These steel fibres greatly increase the tensile and flexural strength of UHPC. Also the ductility is increased, which gives better post cracking properties to the concrete. The tensile strength of UHPC is stated by AFGC (2013) to be around 8-9 MPa. Ordinary concrete on the other hand has a strength around 2-4 MPa. This improvement is higher, if a mix of long (30-60mm) and short (6-30mm) steel fibres are used: The short fibres are activated by microcracking and they will increase the tensile and flexural strength, while the long fibres are activated by macrocracking and they will lead to better ductility. In Figure 5 the behaviour of the fibres can be seen.

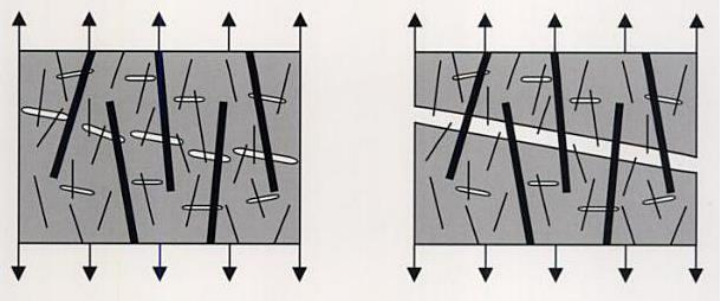

Figure 5: Short fibres for microcracks (left) Long fibres for macrocracks (right).

Steel fibres are not only used in UHPC. It is also used with normal concrete, with the name conventional Steel Fibre Reinforced Concrete (SFRC). Only these steel fibres have different properties: Their tensile strength is up to 1000 MPa so fibre fracture could already occur during cracking. But the steel fibres used for UHPC are much stronger with strengths above 2000 MPa. So fibre fracture will almost never take place, which ensure the high ductility of UHPC during cracking.

Because of the strong steel fibres, the tensile behaviour of UHPC is strain hardening. This means that the composite material continues to resist higher residual tensile strength after the concrete matrix has cracked. In other words, the post cracking strength of UHPC is greater than the matrix cracking strength.

Besides steel fibres, Polyvinylalcholic (PVA) fibres can also be used. This type of fibres has an extra benefit for fire resistance. When fire occurs in UHPC, the steam in the concrete can't escape anywhere because UHPC is very dense. When using PVA fibres the fibres will melt due to the high temperature, so that the steam can travel through the created voids. This will prevent spalling of the concrete.

There are certain aspects that need attention when using steel fibres. The orientation of the steel fibres is important. The orientation has a great influence on the structural behaviour of UHPC. When wrongly oriented the tensile properties won't benefit much from the steel fibres. So during casting of the concrete a casting method has to be used, where the fibres are directed in the most optimal direction.

Also steel fibres will reduce the workability, especially when the steel fibres are long, as they cluster together. Using more short fibres and finer aggregates will improve the workability.

A2.3.4 Shrinkage

Considering time-dependent losses, UHPC behaves differently compared to OC. Looking at shrinkage, the differences occur in drying and autogenous shrinkage. Because UHPC has a much lower water cement ratio than ordinary concrete, the autogenous shrinkage will be much higher than in ordinary concrete. Also the addition of silica fume causes a high autogenous shrinkage. This type of shrinkage will only occur in the early stages. However UHPC has hardly any drying shrinkage because there is hardly any water in UHPC due to the low wcr, especially if steam curing is applied as well. On the other hand OC almost always has drying shrinkage, because of the higher wcr. So in short, Ordinary concrete has low autogenous shrinkage (< 100 μs) and high long term shrinkage (1000-2000 μs) and UHPC has a high autogenous shrinkage (600-800 μs) and low long term shrinkage (<100 μs). When making a design in UHPC, attention has to be paid to the fact that early cracks could arise if the high early shrinkage causes tensile stresses higher than the tensile strength of early age concrete.

A2.3.5 Creep

The creep behaviour of UHPC also differs from the behaviour of ordinary concrete. Research has shown that large compressive stresses on low strength levels UHPC can cause significant short-term creep. Earlier was mentioned that steam curing is also applied when producing UHPC. Curing of the concrete can significantly improve the creep (and also shrinkage) behaviour, especially in the long term.
Curing of the concrete, will speed up the creep and shrinkage process so that after curing and in the long term there's hardly any creep and shrinkage left. For example, by ductal it was stated that the creep coefficient was reduced from 0.8 to 0.3. And ordinary concrete has creep coefficient that range from 2 to 5. Still the conclusions of performed researches differ from each other. So when designing it is best to stick with values given by recommendations.

A2.3.6 Dynamic behaviour

Because of the very high strength of UHPC structures can become very light and slender. The problem that could arise is a higher susceptibility to non-static loadings. Lighter and thinner structures are more sensitive to cyclic loading, so the governing issue could shift from static loads to fatigue loading. The problem is that the current design rules for fatigue don't apply yet to UHPC. Research for this subject is being performed.

Also chances are that the Eigen frequencies will not suffice according to the design recommendations. So when designing a structure in UHPC it is important that these issues are taken into account.

A2.4 Durability

Earlier was mentioned that UHPC has a very dense microstructure, because of the use of fine materials and silica fume and no coarse aggregates. This dense structure has a lot of benefits for the durability of UHPC. Also the steel fibres in UHPC will cause a better distribution of cracks, so instead of a couple of big cracks, there will be several smaller cracks. These small cracks have a very small crack width; UHPC will have less chance to get severely contaminated by an aggressive environment than ordinary concrete.

Corrosion of the steel fibres will only happen at the outer surfaces of structural elements. Because UHPC is very impermeable compared to ordinary concrete rusting will not permeate beyond 2 mm from the outer surface. This also means that chloride is not able to penetrate any further as well as oxygen and moisture. The rusted steel fibres on the outside will not have structural consequences. They will increase a bit in volume because of the rusting, but the volume increase will not cause internal stresses that could lead to spalling of the concrete.

UHPC also has a much better resistance against alkali-silica reactions and an enhanced abrasion resistance. The dense structure will also provide a higher resistance against impact loads.
Because of the better durability less maintenance will be necessary for structures in UHPC. So UHPC structures have a longer life span than structures made out of ordinary concrete.
In Table 2 an overview is seen where UHPC is compared with ordinary concrete in terms of durability. It is obvious that UHPC performs much better than normal concrete.

Table 2: Comparison durability properties OC and UHPC

		OC	UHPC
Rapid chloride permeability	[coulomb]	2000 - 4000	< 200
Chloride diffusion coefficient	[mm^2/s]	4 - 8 x 10^{-6}	0.05 - 0.1 x 10^{-6}
Carbonation depth	[mm]	5 - 15	<0.1
Abrasion resistance	[mm]	0.8-1.0	<0.03

A2.5 Costs and sustainability

One of the disadvantages of UHPC is its costs. Ordinary concrete roughly costs around 100 €/m^3. UHPC costs between 1000 and 1700 €/m^3. Producing UHPC requires more energy than producing ordinary concrete. This leads to longer mixture times and will decrease the producing capacity in a concrete factory. Also UHPC uses more cement and silica fume, which both are quite expensive. In the beginning stages of UHPC the material wasn't used optimally so a design solution in UHPC wouldn't necessarily be cheaper than a solution with standard concrete.

But in terms of sustainability, because UHPC is a very strong material, it is theoretically possible to make very slender structures. This leads to less cement and concrete use. Since producing concrete is one of the bigger polluters in terms of CO_2, needing less concrete will lead to decreases in energy use and CO_2 emissions.

The last few years a lot of research on UHPC girders has been done to make a girder that uses the UHPC properties to its fullest. But costs are not only saved with using less concrete, UHPC does not require any mild or shear reinforcement: Not needing additional steel reinforcement reduces costs and it also leads to considerable savings in human labour and construction time. And this of course means less immediate project costs.

Because UHPC structures are lighter, transportation and installation are more convenient than with normal concrete structures. Using modular elements will also benefit transport and construction time.
Further advantages of UHPC arise in span lengths. If for example a highway needs to be crossed by a bridge, using UHPC will lead to longer spans compared to using ordinary concrete, so a bridge could be made without needing an intermediate support. This would lead to considerable savings, because in this way it would not be necessary to close down a busy highway road, which nowadays is crucial to maintain a steady traffic flow without interruptions.
Specifically for the Netherlands, using UHPC also means that for a certain span a minimal height for a girder is necessary. Since the Netherlands are a flat country, using a girder with lower height would save costs for approach bridges. Usually these are one of the more expensive parts in a bridge project.
And finally, because UHPC is very durable less maintenance is needed for structures. So looking at life cycle costs, money can be saved here as well. So for the longer term using UHPC could save more money than using ordinary concrete.

A2.6 Summary

In conclusion the advantages and disadvantages are summed up for quick reference. And in Figure 6 a comparison in properties between different concrete types is seen.

Advantages

- High strength properties
- Great ductility
- Outstanding durability and sustainability
- No need for mild and shear reinforcement
- Very slender structures possible.

Disadvantages

- UHPC is more expensive that ordinary concrete (Slender materials so less concrete necessary)
- Longer production times due to longer mixing (optimize mixture packing)
- Steel fibres decrease workability (use more short fibres and finer materials)
- Hard to control orientation of steel fibres (Use horizontal casting)
- Worse fire resistance than ordinary concrete (use PVA fibres)
- High early shrinkage and creep (can be controlled and reduced by using steam based curing)
- Possibility of insufficient resistance against dynamic loads due to higher slenderness.

In short UHPC has a lot of advantages compared to ordinary concrete. Even though UHPC has its disadvantages, a lot of these can be solved by using proper measurements.

Characteristics		Unit	Codes / Standards	NSC	HPC	UHPdC
Specific Density, □		kg/m^3	[1]	2300	2400	2350 – 2450
Cylinder Compressive Strength, f_{cy}		MPa	[2]	20 – 50	50 – 100	120 – 160
Cube Compressive Strength, f_{cc}		MPa	[3]	20 – 50	50 – 100	130 – 170
Creep Coefficient at 28 days, □$_{cc}$			[4]	2 – 5	1 – 2	0.2 – 0.5
Post Cured Shrinkage		□□	[4]	1000 – 2000	500 – 1000	< 100
Modulus of Elasticity, E_o		GPa	[5]	20 – 35	35 – 40	40 – 50
Poisson's Ratio, □				0.2	0.2	0.18 – 0.2
Split Cyl. Cracking Strength, f_t		MPa	[6] or [7]	2 – 4	4 – 6	5 – 10
Split Cyl. Ultimate Strength, f_{tp}		MPa		2 – 4	4 – 6	10 – 18
Flexural 1st Cracking Strength, $f_{cr,4P}$		MPa	[8] (Four-Point Test on Un-notched Specimen)	2.5 – 4	4 – 8	8 – 9.3
Modulus of Rupture, $f_{cf,4P}$		MPa		2.5 – 4	4 – 8	18 – 35
Bending Fracture Energy, $G_{f(□=0.46mm}$		N/mm		< 0.1	< 0.2	1 – 2.5
Bending Fracture Energy, $G_{f(□=5.0mm}$		N/mm		< 0.1	< 0.2	10 – 20
Bending Fracture Energy, $G_{f(□=10mm}$		N/mm		< 0.1	< 0.2	15 – 30
Toughness Indexes	I_5			1	1	4 – 6
	I_{10}			1	1	10 – 15
	I_{20}			1	1	20 – 35
Rapid Chloride Permeability		coulomb	[9]	2000 – 4000	500 – 1000	< 200
Chloride Diffusion Coefficient, D		mm^2/s	[10]	4 – 8x10^{-6}	1 – 4x10^{-6}	0.05 – 0.1x10^{-6}
Carbonation Depth		mm	[11]	5 – 15	1 – 2	< 0.1
Abrasion Resistance		mm	[12]	0.8 – 1.0	0.5 – 0.8	< 0.03
Water Absorption		%	[13]	> 3	1.5 – 3.0	< 0.2

Figure 6: Characteristics of ordinary concrete, high strength concrete and UHPC

A3. Reference projects

References: [1], [3], [4], [7], [8], [12], [14], [17], [19], [20], [23], [26], [27], [28], [29]

Over the past years, UHPC has already been applied worldwide. In the following examples of completed projects in UHPC are going to be dealt with. Because the thesis is about designing a bridge in UHPC the emphasis of the reference projects will be on bridges, so mostly old bridge projects will be discussed. But since UHPC can also be used to improve structures aesthetically wise, there will also be a part with more architectural examples without too much going into detail.

A3.1 Aesthetics

Before moving on with the reference projects it is important to mention aesthetics. As already discussed, UHPC has very good mechanical properties and it also has great durability and sustainability (in the long term). But these are not the only important things when designing a certain structure. Aesthetics, or in other words, the way a structure looks is of course also important to take into consideration. A structure can be very strong and durable, but usually the way a structure looks will be decisive, when choosing a certain design.

Using UHPC will have benefits in terms of aesthetics. Because of elimination of coarse aggregates and a very good granular packing distribution, a very smooth finished surface can be achieved compared to ordinary concrete. Also painting or coating is not needed, as the natural face concrete finish will maintain its properties over time.
Moreover because UHPC is very strong, very slender structures are possible to make and structures can take on more challenging and exciting forms than when using ordinary concrete.
There already exist a couple of projects in which the properties of UHPC are used to make extraordinary shapes in structures. A couple of projects that are using UHPC in an architectural way are dealt with in 3.2.

A3.2 Architectural reference projects

A3.2.1 LRT Station Canopy (2003), Calgary, Canada

Figure 7: LRT Station Canopy

In Calgary, Canada a roof canopy was constructed out of UHPC for a light rail transit (LRT) station in Calgary. The canopy was made out of 24 thin shelled precast segments which were only 20 mm thick. For the structure no mild reinforcement has been applied. This project was one of the earlier projects that applied UHPC in a structure. Furthermore this project was the first one to use UHPC for architectural, thin shelled, curved canopies.
This project showed that building with UHPC, next its superior material and durability properties, can also achieve beautiful complex shapes such as these canopies. Besides it also showed that with UHPC even complex shapes can be prefabricated instead of only cast in-situ as it's the case when using ordinary concrete.

A3.2.2 Millau tollgate (2004), Millau, France

Figure 8: Millau Tollgate

The Millau tollgate is part of the famous Millau viaduct in France. This tollgate is one of the many examples of how UHPC can be used architecturally.
The roof of the tollgate (the part of the tollgate which is made out of UHPC) is a shell structure with a helicoidal shape. The roof consists of 53 segments, making the roof 98m long and 28m wide. What is special with this shell structure is that there is no conventional reinforcement or any prestressing tendons. The only reinforcement available are the longitudinal prestress ties that connect all the segments and also of course the steel fibres. Because of the elimination of reinforcement bars such a complex shape that is applied for the design is made possible.

A3.2.3 Le Stade Jean Bouin (2012), Paris, France

Figure 9: Stade Jean Bouin

The architectural (and of course also structural) use of UHPC on a large scale for a large project has been done in France, for the rebuilding of the Stade Jean Bouin in Paris. The rebuilding of the stadium allowed a capacity increase from 5000 to 20000 spectators. The rebuilding presents a lattice roof and façade of more than 20000 m^2 together, which is made out of UHPC.
The envelope is made out of 3600 precast, self-supporting Ductal triangle elements, each around 8-9m long and 2.5 wide. The thickness of a triangle is 45 mm thick.
There were a lot of technical challenges faced during this project. First of all in the roof elements protective light diffusing glass had to be placed. For this the behaviour of a combination of glass and UHPC had to be studied carefully, in order to make it a watertight structure. Also sound insulation was important in order to create the best atmosphere as possible in the stadium.
But all these challenges were overcome and the completion of this project showed the superiority of UHPC over ordinary concrete structurally and architecturally wise. And it was also the first time UHPC was used in this way and such a large scale.

A3.3 Structural reference projects

A3.3.1 Sherbrooke Footbridge (1997), Sherbrooke, Quebec, Canada

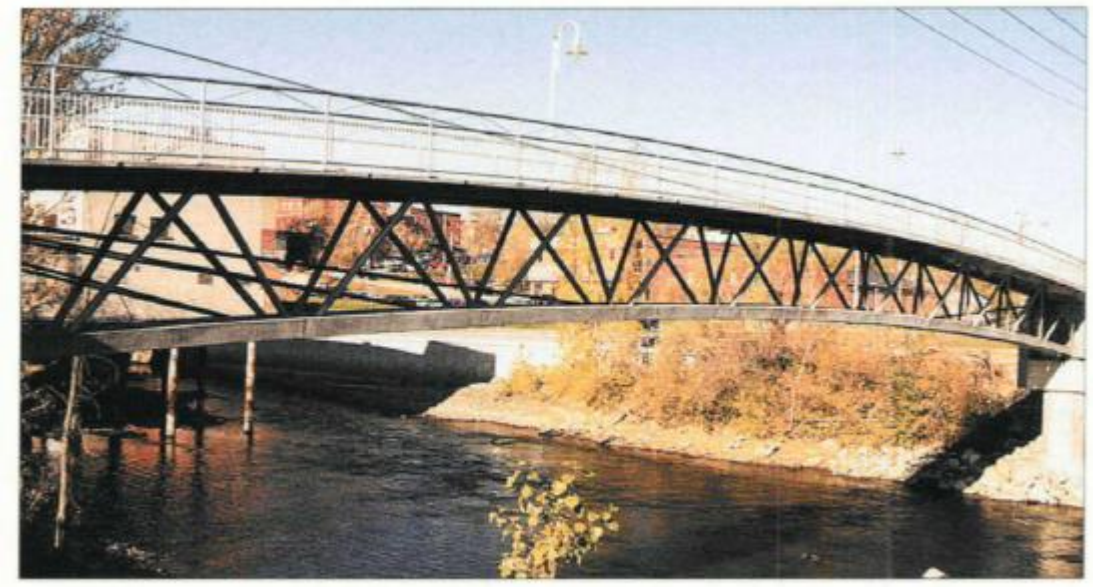

Figure 10: Sherbrooke Footbridge

The Sherbrooke Footbridge was the first bridge built in UHPC or more specifically in Reactive Powder Concrete (RPC). It was built in Canada in 1997. The bridge functions as a pedestrian and a bicycle bridge over the Magog River in Sherbrooke. The aim of this project was to explore the first full applications of RPC in transportation structures.
The bridge's superstructure consists of an open-web space truss that spans 60 m. The web members are made with RPC confined in thin-wall steel tubes. Confining the concrete in these tubes allowed the use of confined properties of RPC, including ultimate compressive strengths of up to 350 MPa. The RPC mix was designed with a water cement ratio of 0.21. The concrete was produced using locally available materials in a conventional precasting plant with no experience of producing RPC. Furthermore the concrete was steam cured for two days. The composition of the concrete is seen in Figure 11.

Material	Quantity
Cement	705 kg/m^3
Silica Fume	230 kg/m^3
Crush quartz	210 kg/m^3
Sand	1010 kg/m^3
Superplasticizer	37.5 l/m^3
Steel fibers	190 kg/m^3
Water	195 l/m^3
Water/binder ratio:	0.21

Figure 11: Composition RPC

The truss is post-tensioned and consists of six match-cast segments. No passive reinforcement was used. The cross section of the truss is seen in Figure 12.
The cross section is composed of two 380x320 mm bottom chords and a 30mm upper slab with 70mm deep transverse stiffening ribs embedded in two 300x200 mm longitudinal ribs. The total height of the truss is 3.0 m and the overall width is 3.3 m.

With these measurements the segments were easily transportable by normal trucks. The truss diagonals were joined to the top and bottom chords through two greased and sheathed anchored monostrands. The top slab is transversally prestressed. Longitudinal prestressing is composed of 2x2 cables running along the bottom beams, 2 cables along the top beam and 2x3 deviated external cables. All cables are anchored in the end diaphragm. For the design no tension was allowed in the diagonals and the lower beams.

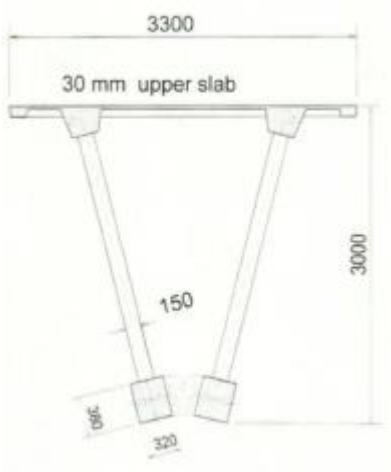

Figure 12: cross section Sherbrooke Footbridge.

The bridge was also monitored for a short and long term. The purpose was to obtain field data and to gain a better understanding of the behaviour of the structure under actual service conditions and loads. The total costs for the bridge including two approach bridges of 30m were 790.000 Canadian dollars. The costs were slightly higher than a traditional concrete construction. But the project showed good potential of using RPC. Also the elimination of passive reinforcement will allow for much more freedom in structural shape and form.

A3.3.2 Seonyu Footbridge (2001), Seoul, South Korea

Figure 13: Seonyu footbridge

Another bridge which was one of the first projects to use UHPC was the Seonyu Footbridge.
This bridge connects the city of Seoul to Sunyudo Island in the Han River. The bridge was a part of a long-term project called 'New Seoul, Our Han River'. This project consisted of setting up easily accessible parks near the river, re-establishing the ecosystem of the river and organizing a variety of cultural events. A park was planned to be made on Sunyudo Island and in order to encourage more visits to the island the Seonyu footbridge was built for pedestrians, in order to improve the accessibility of the island from Seoul.

The total length of the bridge is 430m. It is composed of a 120m arch spanning the Han River and steel footbridge at each end. The arch remains one of the largest bridges made out of UHPC. The arch has a pi-shaped cross section, consisting of a transversally ribbed upper slab and two girders. The width of the arch is 4.3 m and its depth is 1.3m. For the cross section a UPHC mixture with steel fibres made by Ductal was used. The mean compressive strength was 200 MPa. The mixture was prepared in France and shipped to South Korea. Because of the steel fibres no passive reinforcement was necessary in the design. In Figure 14 the cross section of the arch is shown.

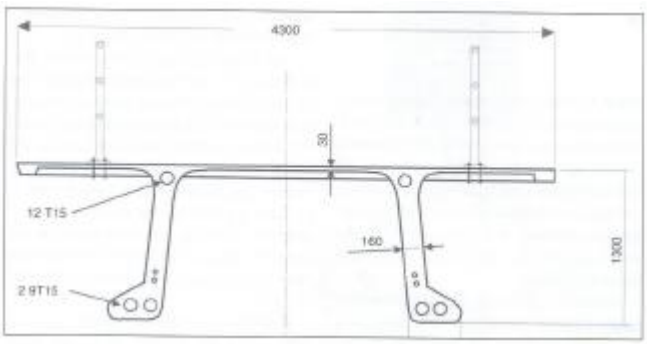

Figure 14: Cross section Seonyu Footbridge

As already mentioned, the cross section consists of a 30 mm thin, ribbed slab. The slab is supported by 160mm thick webs. The transverse ribs were prestressed by one or two 0.5 inch monostrands. In longitudinal direction the structure is prestressed with 3 cables in each web.
The cables had 9-12 strands each. Also two 0.5 inch monostrands were placed in each web. These were added for temporary handling of the elements.

The whole arch consists of six segments which were 20-22m long. The slope of the curved segments is 8%. For the segments a special steel mould of 50t was designed. The segments were erected by using temporary supports in the river. During erection, first three segments, which consisted of the half of the arch, were positioned on the temporary supports using a crane. When the second half of the arch was positioned, the continuity prestressing was installed and the gap between the two halves of the arch was closed with cast in place material, to establish the continuity of the structure. The erection of the bridge is seen in Figure 15. The bridge was completed in 2002.

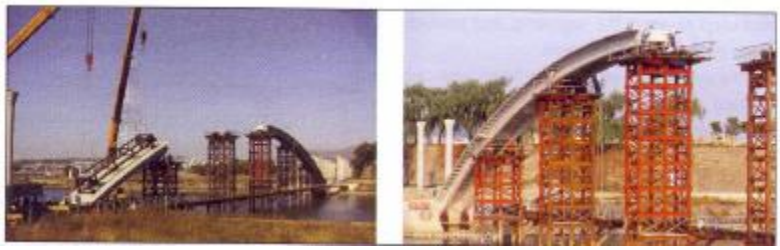

Figure 15: Erection of the bridge

A special study of vibrations was made for this bridge. It turned out that the calculated natural frequencies were within the range of values that could make people crossing the bridge uncomfortable. Therefore tuned mass dampers were designed and installed to damp the vibrations, so that the comfort criteria were met.

A3.3.3 Mars Hill Bridge (2006), Wapello County, Iowa

Figure 16: Mars Hill Bridge

During this time there were already existing pedestrian bridges made out of UHPC. One of the first traffic bridges built in UHPC (at least in the USA) was the Mars Hill Bridge in Wapello County, Iowa in the United States. The bridge is a single span that consists of three beams of 33.5m each. The beams were pre-tensioned with 49 0.6 inch strands. The spacing of the beams was 2,92m. Furthermore no mild reinforcement was used, except to provide composite action with the cast in-place deck. The beams were connected to the deck with U-bars. This allowed the best shear transfer between the beam and deck and its detailing wasn't complicated.
The beams were casted at the factory and transported to the site. There a crane was placed at each end of the crossing and the beams were hoisted in place. This process is seen in Figure 17.

Figure 17: Hoisting of beams

Because this was the first highway bridge in UHPC in The United States, there were no reference projects available to use as aid in developing the Mars Hill Bridge. So before the bridge was actually built, tests were performed by Bierwagen et al. [4] Small-scale specimens tested and also full-scale girders were tested for their behaviour and structural capacities. The girders' cross section was modified to make the area smaller as seen in Figure 18. This is done to reduce the used material, since UHPC has much higher strength than normal concrete. Additional in this project was the testing of the actual bridge after completion (which was in the fall of 2005). This test comprised of monitoring and evaluating the behaviour of the bridge for 2 years.

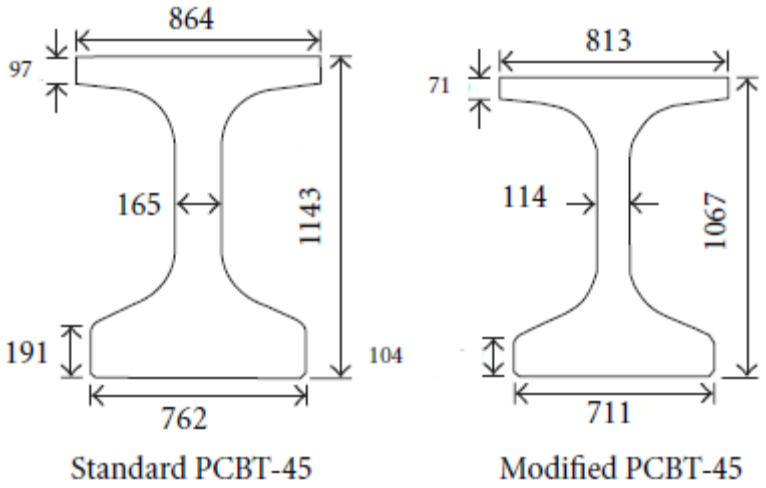

Figure 18: Comparison original girder and modified girder used in bridge

In support of this research a master thesis has been performed in 2006, where analytical models were developed, based on the Modified Compression Field Theory (MCFT), to develop an understanding on the flexural and shear behaviour of the girders.
The researchers concluded that the constructed bridge was within the service limit under live load. Furthermore, the stresses were below the expected live load stresses and no cracks were observed in the UHPC girders or concrete deck.
As for the analytical model, the MCTF method was able to accurately determine the ultimate shear capacity of the UHPC beams. The model correlated well with the large scale test results as well as for shear, as for flexure.
Also in this project the girders were not yet fully optimized to take the most out of the properties UHPC.

A3.3.4 The Jakway Park Bridge (2008, Iowa, USA) and Development of Pi-girders

The Jakway Park Bridge was, next to the Mars Hill Bridge, one of the first highway bridges made of UHPC constructed in Iowa and in North America. It was however the first one to use the newly developed 'Pi-girder'. This new type of girder is developed in an attempt to optimize the use of the UHPC in girders.
The project served to replace an existing bridge in Buchanan County, Iowa. The total span of the bridge is 115 ft. 4 in. (35.15m). The centre span is the UHPC component, which is 51 ft. 4 in. long (15.65m). The span consists of three simply supported Pi girders. The girders are pre-tensioned longitudinally and tied together transversally with mild reinforcing steel and steel diaphragms. The end spans are cast-in-place concrete slabs. The bridge was completed in the fall of 2008. In Figure 19 an impression of the Jakway Park Bridge is seen.

Figure 19: Completed Jakway Park bridge (left) and Erection of the bridge (right).

Looking at the history of the Pi-girder, the girder used in this project is actually the 2nd-generation of Pi-girders, which were made to overcome the shortcomings of the first generation. The research process of the Pi-girder from first to second generation and also the experiments performed for and on the Jakway Park Bridge are documented in a paper made in 2011 [20]. The findings of this paper will be presented in the following.
Before the construction of the Jakway Park Bridge, tests on the 1st generation Pi girders showed shortcomings in structural performances. The first generation was designed at MIT in 2003. This section was optimized to exploit the high tensile, shear and compressive properties of UHPC while minimizing the cross sectional area. It was designed to span 21.3m - 36.6m and it contained no mild reinforcement. The cross section of the Pi girder is seen in Figure 20.

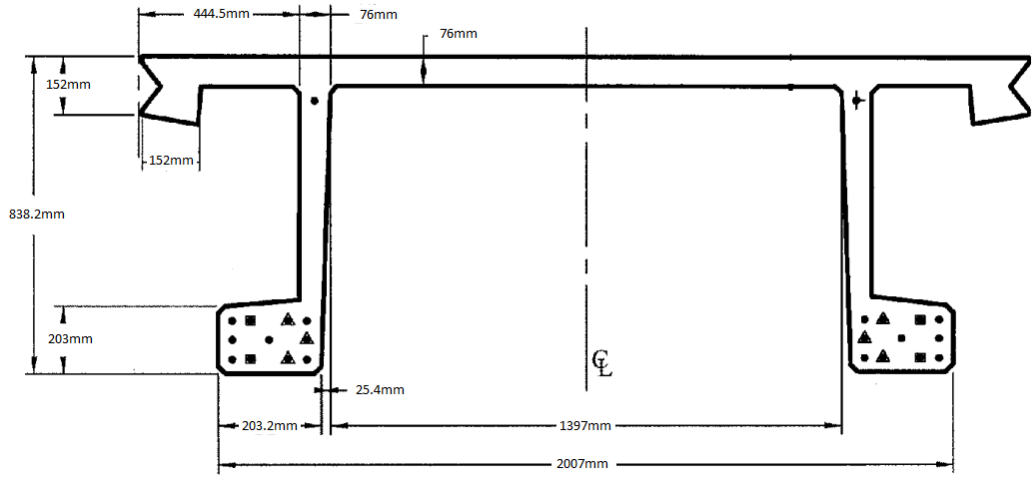

Figure 20: 1st generation Pi –girder

Tests were performed on this girder. The tests showed that the global shear and flexural strength were sufficient, but there were issues. The main issues were the insufficient transverse flexural response and the low transverse live load distribution.
Before the bridge could be made, the Pi-girder had to be modified to resolve the issues found for the first Pi girders. The modifications were kept as simple as possible to keep the cost of modifying the beam forms within budget limits. The modifications that were made were eventually too expensive. So decided was to make further revisions and to create new forms, which would become the 2nd generation Pi girders. Model analyses were made with a finite element program. These analyses led to the eventual 2nd generation Pi section in 2008. The main changes compared to the first generation were:
The fillets at the web-deck interface were thickened to decrease the stress concentrations at the interface and to improve material flow during placement. The web thickness was also increased for the latter. The thickness of the deck was also increased and the web spacing was reduced. This to enhance the transverse strength and stiffness of the deck. These improvements were also intended to improve the lateral live load distribution.
In Figure 21 the cross section of the improved Pi girder is seen.

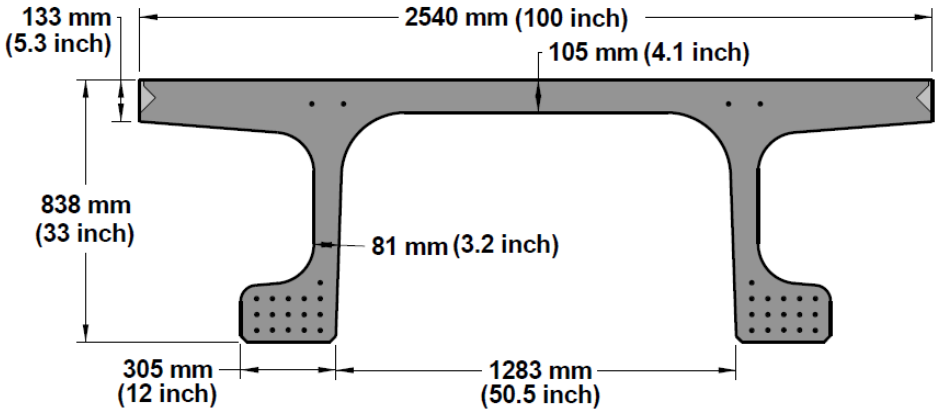

Figure 21: 2nd generation Pi-girder

These new Pi-sections were then used for the construction of the Jakway Bridge.
After the completion of the bridge, the bridge underwent field testing to observe and quantify the response of the bridge under service level loads and to quantify the conservatism present in the design in terms of load distribution factors.

Two tests were performed, which were a year apart (2008 and 2009), so as to quantify changes in bridge behaviour. The tests consisted of monitoring the strains and deflections under liver loads. The bridge was tested on both static and dynamic loads (the latter only in 2009). For the live load a fully loaded truck according to the AASHTO codes, was used. The truck had to be driven over the bridge along 7 specified load paths. The truck had to pass each load path twice. In total 28 passes were made in one test. 14 were with the steel diaphragm bolts tight and 14 with the bolts loose.

In general, from the results can be concluded that the bridge performs well and within the general design parameters. The strain results suggested that no cracking will occur in the bulbs, the webs or in the deck under service level loads. This goes for both longitudinal and transverse cracking.
The behaviour of the bridge in the first test was between that of a partially restrained bridge and a simply supported bridge, leaning more to that of a partially restrained bridge, due to the continuity of the end spans and Pi-girder span. This is caused by the concrete diaphragms at the pier. Furthermore, it could be stated that the overall behaviour of the bridge was affected little by loosening the bolts on the centre diaphragm. So the steel diaphragms didn't have a huge effect on the distribution.

Comparing the 2008 and 2009 static load tests, it was observed that the second test exhibited a general increase in the strains. According to the paper it has to do with a reduction of continuity between end spans and pi-girder span. This decrease again is caused by freeze thaw cycles over the course of the winter, thus breaking down any bond remaining between the spans. This causes the girder to act more like a simply supported beam, therefore generally increasing strains due to positive moments. However the decrease in continuity only had an effect in the longitudinal direction. In the transverse direction there weren't any large changes.
The results also concluded that the design approach was appropriately conservative in terms of live load distribution factors, in consideration of the relatively new geometry and materials (in the design a factor of 1.0 is used; the codes give a factor around 0.9; the experiment give factors around 0.7). Also from the dynamic load test it was found that the dynamic amplification factor was conservative for the bridge (found 1.15, used in design 1.33).

At the end the research it was recommended to investigate potential use of partial prestressing in the UHPC Pi-girder, to save costs. Also life cycle costs of the Pi-girder compared to traditional prestressed beams should be quantified.

A3.3.5 Gärtnerplatzbrücke Pedestrian Bridge (2007), Kassel, Germany

Figure 22: The 'Gärtnerplatzbrücke' pedestrian bridge

In 2007 in Kassel, Germany the Gärtnerplatz Pedestrian Bridge was constructed, made out of a hybrid UHPC-Steel truss structure and of UHPC plates for the bridge deck was constructed [5]. It was one of the first larger bridge projects using UHPC in Germany. This bridge was a replacement for an old pedestrian bridge made of timber, which crossed the river Fulda.
A requirement was that the new bridge had to be a durable and a lightweight structure. If innovative materials were used the costs shouldn't exceed the costs of a conventional solution.

The bridge is 132m long consisting of six spans, with the largest span being 36m. The bridge consists of a light 3D steel truss being combined with two upper chords and a 80mm thin bridge deck. The deck is 5m wide. The chords and the deck are made of UHPC. The cross section of the bridge is seen in Figure 23. The upper chords consist of spaghetti-like filigree prefabricated and prestressed elements with a length of 12 to 36m and a cross section of 300x400 mm. They were fitted to the steel framework and the pre-mounted elements were placed on the pillars. The deck was glued to the chords with an epoxy resin only. For the transfer of shear forces from the truss diagonals to the chords prestressed bolted friction connections were used.

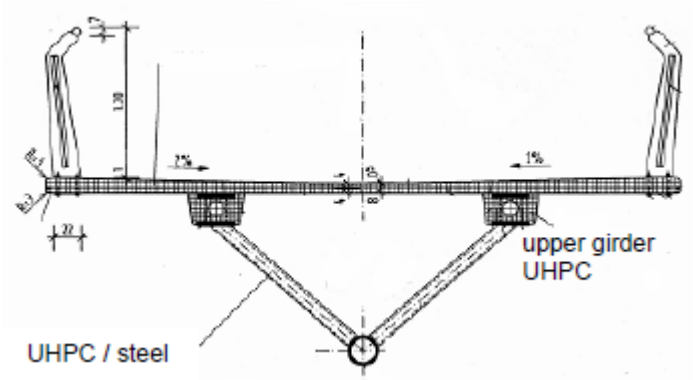

Figure 23: Cross section Gärtnerplatz bridge

An interesting subject for this bridge is the research that has been done for the sustainability for the bridge [23]. In this research a comparison has been made between the actual bridge, with the steel truss and UHPC deck (version 1), a bridge if made completely out of UHPC, so deck and girder (version 2) and a bridge if made out of ordinary prestressed concrete (version 3). For the comparison one looked at the material content of the versions and the amount of energy they needed and the amount of produced Greenhouse effect. If one would only look at the material itself, one would see that UHPC has a much higher energy demand and thus a higher greenhouse effect than ordinary concrete.
But in this case one had to look at the total mass of concrete, steel etc. being used in the bridge versions. The actual bridge is much lighter (350 American tons) than if the bridge were made out of normal concrete (850 American tons). Making the girder out of UHPC would lead to a further reduction of 15 tons.
In Figure 24 the material amount and energy demand of the three alternatives is shown. From the figure it is obvious that version 2 has by far the lowest energy demand. Furthermore version 2 has a lower contribution to the Greenhouse effect, compared to the other two versions. So from ecological point of view the actual design is not the most optimal one, especially due to the high energy demand of the steel truss.

Material	**UHPC + Steel** (Version 1) (truss structure of steel)		**UHPC+UHPC** (Version 2) (truss made of UHPC)		**Ordinary concrete** (Version 3) (presstressed massive)	
	Raw material	Energy	Raw material	Energy	Raw material	Energy t
	to	MJ	to	MJ	to	MJ
Cement	87	31.000	98	35.199	120	43.080
Silica fume	16	-	18	-	-	-
Aggregates	151	2.200	170	2.518	620	9.176
Water	19	-	21	-	60	-
Steel fibres	7.2	171.000	10	242.800	-	-
Reinforcing steel (incl. foundation, abutment, pillars)	22	541.000	22	541.000	70	1.720.000
Prestressing steel	8	223.000	12	327.000	10	278.000
Steel truss incl. connectors	51 62	1.441.000	-	-	-	-
Sum	-	2.409.200	-	1.148.517	-	2.050.256

Figure 24: Demand of raw materials and energy of 3 alternative bridge designs

Not only is a bridge completely made out of UHPC ecological more optimal, but the durability of UHPC is also much better than that of steel or ordinary concrete. So costs will also be saved for maintenance purposes.
From this research it can be concluded, that a structure made of UHPC, which are designed to really exploit the properties of UHPC, are of superior sustainability to common concrete or steel structures.

A3.3.6 La Passerelle des Anges Footbridge (2008), Gorge de l'Herault, France

Figure 25: La Passerelle des Anges Footbridge

The Passerelle des Anges Footbridge (also called Pont du Diable) is the first pedestrian bridge built in France and in Europe. It was built in 2008. The bridge is built in the Gorge de l'Heraut, a highly cultural region and a popular tourist area. The bridge, located at a UNESCO heritage site, had to cross a gap of almost 70 m. Because of its location and in order to minimize the impact on the environment, the bridge consists of only one span. Moreover the use of UHPC with post-tensioned prestressing along two beams that form the handrails, allows a minimum visual impact through a very small static height. In Figure 26 the cross section of the bridge is shown.

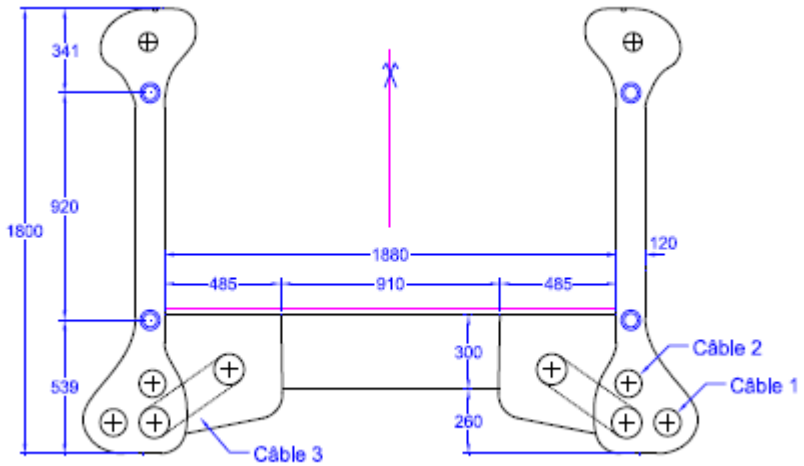

Figure 26: Cross section La Passerelle des Anges Footbridge

The span of the bridge is 67.5m and the span is composed of 15 prefabricated segments of 4.6m in length. The cross section is composed by two bone-shaped webs with a depth of 1.80 and a web thickness of 120 mm. these two beams are used as parapets.
The beams are connected with transversal ribs. Each segment has three ribs. Furthermore a 30 mm thick deck is fixed to the segment. The cross section is 1.88m wide. The structure is prestressed using eight cables, four in each beam.

Because the bridge consists of a single span, a very accurate analysis was made for the dynamic behaviour of the bridge. Even though the natural frequencies were according to the codes, the bridge was sensitive to wind loading with turbulent flows. In order to improve the dynamic behaviour dampers were installed on the bridge.
The segments were moulded and steam cured at the factory. For moulding a steel mould for casting upside down was used to cast al 15 segments. The mould was modular, which resulted in a high repetition factor. After demoulding, the segments were transported two by two per truck. Along the footbridge a layer type scaffolding was installed. Because of the surroundings and al the loose segments, placing the bridge in one go wasn't possible. The segments were positioned on the scaffolding and afterwards the cables were installed and prestressed. The scaffolding is seen in Figure 27. Attention had to be paid, when placing the scaffolding, because the height under the bridge was variable (with the deepest point being 10m). And also attention had to be paid on the vegetation on the bottom. Finally the dampers were installed.

Figure 27: Placing of scaffolding

By building this bridge it was shown, that UHPC could be used for large spans while keeping the depth of the bridge low. The slenderness accomplished for this bridge was 38, which is very slender. However the bridge had some dynamic behaviour issues. But these were easily solved using dampers.

A3.3.7 Hoekerbridge (2012), Rotterdam, the Netherlands

Figure 28: Hoekerbridge

In 2012 a pedestrian bridge has been made out of UHPC in Rotterdam, the Netherlands, which has the thinnest deck at the moment in The Netherlands. The deck is only 60 mm thick and it has a span of 19m. The bridge was part of a project of the municipality of Rotterdam to replace old pedestrian bridges across the city. It was important that the future bridge had a high durability and low maintenance need. The engineering department of the municipality Rotterdam came to the conclusion that the future bridge should be made out of UHPC or out of composite material. Furthermore it was important to design a modular bridge which could be economically built and set an example for future modular bridges in the Netherlands.
Because of lack of experience in the field of UHPC construction in the Netherlands, this project served as a pilot-project to convince that bridges made of UHPC is a feasible solution and to make an important step in UHPC construction in the Netherlands.
The municipality worked together with FDN engineering to make the bridge a reality.

Eventually a modular design was made for the bridge, with a span of 18.9m and a width of 3.4m. The bridge consisted of railing and plate elements. Making a modular design will allow bridge construction with low costs. The handrail elements were prestressed to each other. The plate elements were put on the railing elements and fastened special patented bolts. The bridge deck contained reinforcement bars as well as steel fibres. The handrails had no reinforcement bars. Furthermore a pair of prestressing tendons has been placed in the handrails. In Figure 29 the cross section of the bridge is shown.

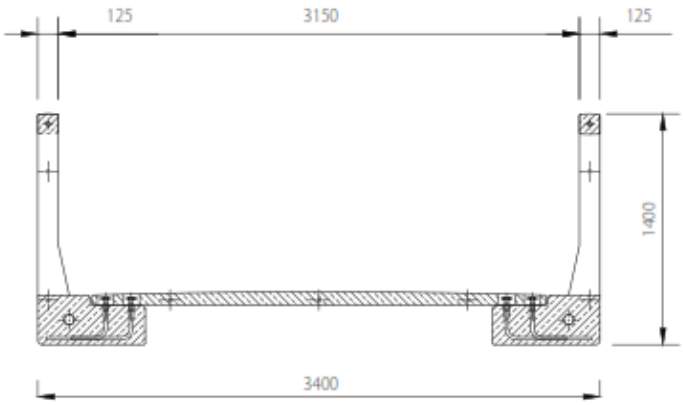

Figure 29: Cross section of Hoeker Bridge

Besides the check of the design calculations, additional testing was also required. The bridge had to be tested on the load based on the Eurocode recommendations on pedestrian loads. The test result should correspond with the calculated values. The bridge was also checked for cracks during the testing. The test showed that that the deflection were similar to the calculated values. Also no cracks were visible during testing. So all in all, the design met the requirements.
This project showed that a mould system can successfully be used to construct the bridge. The current mould system enables to build a bridge with lengths up to 30m en widths of 5m. This system also has an advantage that it can fit into a 20-foot container. This makes transportation easy and inexpensive.

A3.4 Conclusion Reference projects

The previous discussed reference projects have proven that over the past years UHPC has been applied successfully to bridge structures. Not only does UHPC result in a structurally good structure it also results in a structure which is aesthetically very pleasing. This can be for example seen in The Stade Jean Bouin (2012), which consists of a complete façade made out of UHPC that is structurally sufficient and also architecturally of high quality, which makes the structure stand out even more.

From the discussed structural reference projects a lot can be learned and used in the main thesis. First the Sherbrooke footbridge (1997), which was the first bridge projects that used UHPC, showed that UHPC can be combined with steel in a positive way by confining UHPC in steel tubes. Then for the Seonyu Footbridge (2001) and a couple of years later for the Jakway Park Bridge (2008) a special UHPC girder was used, which was the Pi-girder. This girder was a modified double Tee girder, which was improved even further to optimize the use of UHPC, by the time the Jakway Park Bridge was built. These improvements were based on researches performed in the United States specifically for the purposes of the Jakway Bridge. For the design of the Leiden Bridge this type of girders could be taken into consideration even though they are not produced in the Netherlands.

Then there is the Mars Hill Bridge (2006) the first highway bridge in the US. For this bridge existing girder types were modified by reducing the thickness of the flanges and web to use the UHPC more efficiently. But stated was eventually that the girders were not optimized enough. So this could mean that girders can be made even more slender than in the case of the Mars Hill Bridge.But going too slender and crossing a large gap can result in issues with the dynamic behaviour, which was the case with La Passerelle des Anges footbridge (2008) (and also with the Seonyu Footbridge). This bridge was very long and a high slenderness ratio was achieved, but dampers had to be installed on the bridge to improve the dynamic behaviour.

In cost related terms, building the Gartnerplatz Bridge (2008) showed that using UHPC instead of conventional concrete reduces material use and thus reduces the amount of energy needed and the material costs.

Looking closer at home the Hoeker Bridge (2012) showed that a very slender bridge can be made in the Netherlands by using modular segments made out of UHPC. So for the Leiden Bridge this could be an option as well as it reduces construction time.

All in all UHPC is a material that can successfully be used for bridge construction. Even though nowadays there are many more examples of structures in UHPC, the examples discussed here were one of the first ones in their specific country or even in the world that showed that UHPC is a very good material structurally and architecturally wise.

A3.5 Summary reference projects

- Through the years UHPC has successfully been applied in to structures both structurally and architectural wise.
- In a couple of projects the newly developed Pi-girder has been used, which optimally used the UHPC material properties.
- UHPC will provide the lightest structures compared to conventional concrete and steel.
- The high slenderness that can be achieved with UHPC will lead to dynamic behaviour issues, which need to be resolved, with dampers.
- Modular UHPC segments can be used in structures for a faster execution.
- The older bridge projects haven't used fully optimized UHPC girders, but existing girders that were slightly modified.

A4. Bridges

References: [13], [16], [30], [i2]

A4.1 General

When constructing and designing a bridge there are a lot of choices to be made. These choices need to take into account the important issues in bridge construction, namely:

- Speed of construction
- Minimum costs
- Minimum disturbance of traffic and people

These choices are mainly the type of bridge and the method of construction. But also the structural system and type of bearing. In the following paragraphs the bridge types and structural systems will be dealt with starting with bridge types. The method of construction will not be discussed as extensively.

A4.2 Bridge types

A lot of different bridge types exist. A couple of common used concrete bridge types are going to be dealt with. Bridges can be built either cast in-situ or they can be prefabricated. Usually this depends on the type of bridge used.

A4.2.1 Solid deck bridges

The solid deck bridge is one of the most basic types of bridges. This type of bridge can either be made with reinforced concrete or with prestressed concrete. Using prestressed concrete will require material with higher strength so they will be more expensive than using reinforced concrete. But prestressed slabs can take more load and they have higher spans. Furthermore a solid deck can be cast in situ or prefabricated.

For smaller spans up to 8-13m a massive slab system can be used. Using a reinforced slab for these spans is the most economical solution, because even though they use more concrete and reinforcement than girder type bridges, the design details and execution of the slab are easier and less expensive. In Figure 30 the massive slab system is shown.

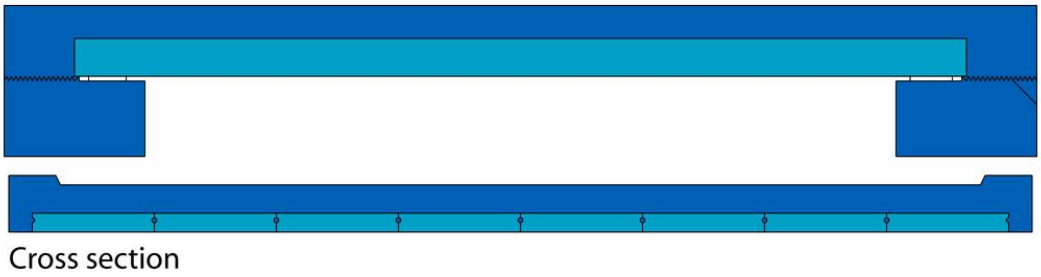

Figure 30: Deck with massive plates and topping

For larger spans between 6 and 20 m the deck is composed of I-shaped or inverted T profiles, placed side by side and connected with a cast in-situ topping and infill concrete. These profiles are usually prefabricated. A cross section of this type of solid deck bridge is seen in Figure 31.

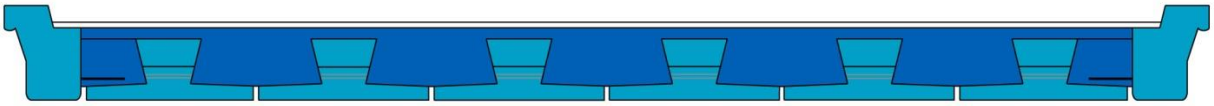

Figure 31: Deck with infilled beams

Main advantages of the solid deck bridge are massive production and limited labour input. But with this type of bridge large spans are not possible and as already mentioned a lot of material and reinforcement is necessary.
A precast solid bridge deck has a slenderness ratio of λ=20-25. If the slab is cast in-situ, it has a slenderness ratio of λ=30.

An alternative for a solid deck bridge that still looks a bit like a solid deck is a voided slab bridge. In this case voids are used of a diameter of 0.5-1.25m. These voids reduce the amount of material needed for the slab. Less material means a lighter construction, so with a voided slab a larger span can be built. An example of a cross section of a voided slab is seen in Figure 32.
Voided slabs are usually cast in-situ. They have slenderness ratio of around λ=40 and spans of l=30-55m can be achieved.

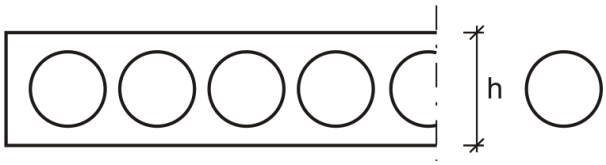

Figure 32: cross section voided slab

A4.2.2 Girder bridges

Girder bridges constitute the main solution for prefabricated bridges built from the sixties on. The bridge deck consists of several I-shaped or inverted T beams positioned at a certain distance from each other. The beams are placed on abutments and/or piers. Furthermore the beams are connected by a crossbeam at the supports. Sometimes intermediate crossbeams are also used for better transversal response. On top of the girders a cast in-situ deck slab is placed. The deck and girders are connected with each other with protruding bars coming out of the girders.
The girder bridges are prestressed most of the time with pre-tensioned strands. Edge beams are also used on the sides to give the whole bridge a closed appearance.
A girder bridge can achieve spans of 15-60m and it has a slenderness ratio of λ=20-28.
This system allows for bridges with a closed underdeck. In the Netherlands it is a requirement to have a closed underdeck. One of the reasons is to have a better resistance against collisions.
In Figure 33 an example of a girder bridge system with inverted T beams is shown.
It is seen that the gap between the beams is filled with concrete. Also between the edge beam and inverted T-beam a thick layer of concrete is poured. Now that al the beams are connected there is a good resistance against collisions.

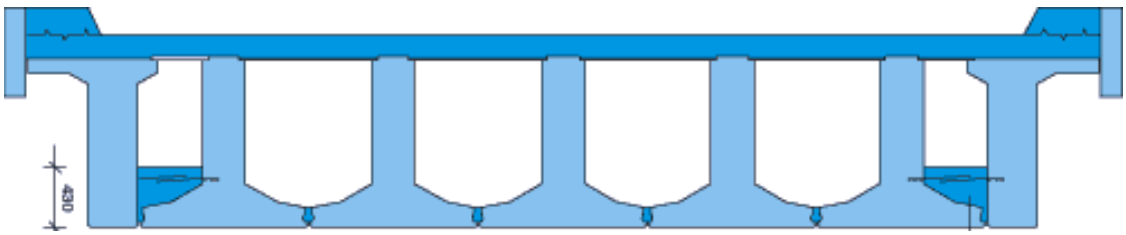

Figure 33: Cross section of a beam bridge with inverted T-beams

This bridge type uses less material than a solid deck, which means that it's lighter than a solid deck. This leads to higher spans. Also girders are fast and cheap to produce and economical for shorter spans.
But for too long spans the girder bridge becomes too expensive, because an intermediate pier will become necessary. It is however not always possible to build an intermediate pier, for example at a river crossing.

A4.2.3 Box-beam bridges

An alternative for the (I-shaped or inverted T) girder bridges is the box beam bridge. This type of bridge consists of box shaped prestressed beams placed next to each other. An example is seen in Figure 34. Comparing figures 33 and 34 it is seen, that because of the box shape of the box-beam, a structural topping is not necessary as with the girder bridges. Only thing necessary for the box beam is filling the longitudinal joints between the beams and also transversal post-tensioning. So this means that a box-beam bridge has a lower height than a girder bridge and a box-beam bridge is prestressed in two directions.

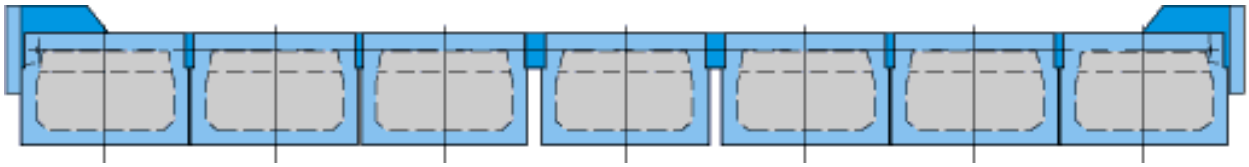

Figure 34: Cross section of box-beam bridge

This type of bridge has a slenderness ratio of λ=28-32 and it has spans of l=15-60m.
Further advantages of a box beam next to the higher slenderness ratio and transversal post-tensioning is a high torsional resistance. Because of the good torsional properties it is also possible to make curved box beams if necessary. Also special edge beams are not necessary because the box-beams already result in a closed structure. Furthermore the box beams don't need complicated formwork and they can be built fast.

A4.2.4 (Mono-) Box bridges

Instead of having multiple smaller box beams next to each other, a bridge can also be made of a single box girder. The development of this type of bridge was necessary in order to achieve longer spans. The box bridge typically has a large rectangular or trapezoidal cross section. The box girder usually also includes a cantilevering deck. In Figure 35 examples of box girder cross sections are seen. As seen in the figure, internal webs can be used in the box girders if for example the road is very wide. These types of bridges are post-tensioned most of the time and use mild reinforcement. The box girder can be prestressed either internally in the webs or externally.

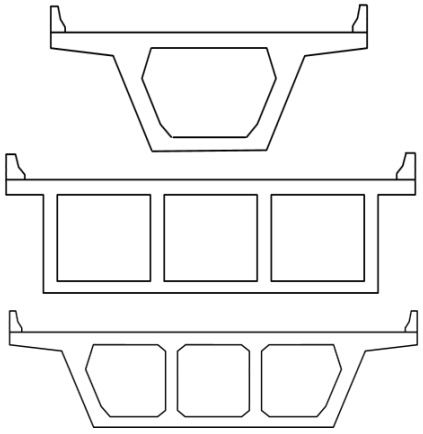

Figure 35: Examples of cross sections for box girders

The box girder bridge has the same advantages as a box-beam bridge (good torsional stiffness etc.) It can be used in combination with many construction methods such as span by span method, cantilevering method and incremental launching method. These construction methods will be dealt with later on.
The box girder can be cast in-situ or prefabricated in multiple segments which are later connected with post tensioning. The box girder can reach spans from l=30-200m and have slenderness ratios of λ=18-25, both depending on the construction method used.

A4.2.5 Arch bridge

The arch bridge is one the oldest bridge types used. Back in the Roman Ages arch bridges were used for aqueducts for example. When limiting arch bridges to the ones made in concrete there are two types of arch bridges:

- The suspended deck arch bridge (Arch supports the deck by means of suspension cables)
- The supported deck arch bridge (Arch supports the deck by means of vertical columns)

Figure 36: Left: Suspended deck arch bridge; right: Supported deck arch bridge

These two types are seen in Figure 36. In theory the perfect arch is one in which only a compressive force acts at the centre of each element of the arch. Practically this is impossible to achieve if a bridge is subjected to multiple loadings. These loadings can produce bending moment stresses, but these are small compared with the axial compressive stresses. Arch bridges are mostly used for longer spans, which also often have to cross deep valleys or spots with a large height under the bridge. An arch bridge can be used for spans ranging from 40 up to 550m. Arch bridges have a rise to span ratio of 1:4.5 to 1:6.

Arch bridges (at least the supported deck type) aren't very common in the Netherlands. Although aesthetically pleasing, arch bridges are more expensive to build than the more common bridge types. These bridges are economical for spans around 275m, but for longer spans, especially over water, it is better to use cable stayed bridges.

A4.2.6 Cable stayed bridge

With these types of bridges very large spans form 110m up to around 1000m can be achieved. A cable stayed bridge consists of a high pylon which supports the deck by its cables. There are three main cable systems (seen in Figure 37):

- Fan cable system

The cables are laid within a tower top saddle, so they all pass the pylon at one point. Because of this all stays are located at their maximum eccentricity from the deck and apply minimum moment to the pylon. This type is good for moderate spans up to 200m.
For larger spans the amount and size of the cables will increase, which will cause difficulty when passing the pylon at the one point. Moreover maintenance and cable replacement will become more difficult then.

- Modified fan cable system

This system is generally the same as the previous cable system only with the modified fan system the stays are individually anchored near the top of the pylon. Now all the cables won't go through only one point.

- Harp cable system

For this system all the stays are anchored at equal spacing over the height of the pylon and are placed parallel to each other. This arrangement provides a visual emphasis on the flow of forces from the back span to the main span and it's also aesthetically pleasing. However, the arrangement is not as structurally efficient as the fan layout; also the harp system has a higher horizontal load which leads to a lower rotation capacity.

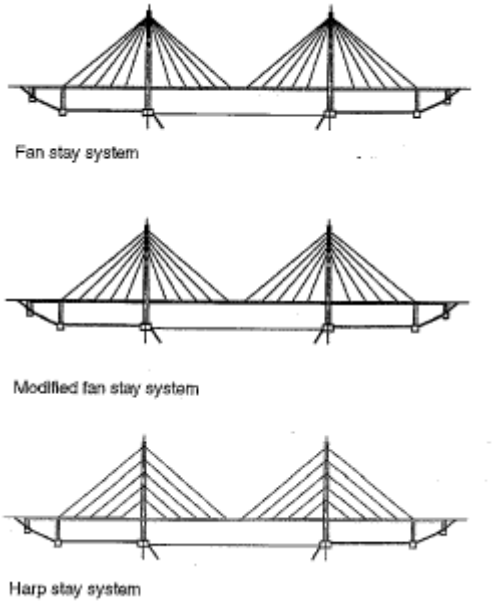

Figure 37: Stay cable systems

Cable stayed bridges do not require anchorage blocks like in suspension bridges, which makes them cheaper than suspension bridges. Also this type of bridge is possible to use in countries with soft soils, because anchorage blocks (which require a hard rocky soil) aren't needed. This type of bridge is economical when applied to large spans up to 1000m. It is economical because of the lightness of the deck which is supported by the cables. The disadvantage however of such a light and flexible deck is that it is not very capable of spreading the live load over a larger span compared with a stiffer bridge deck.

A4.2.7 Suspension bridge

A suspension bridge is a type of bridge in which the deck is hung below suspension cables on hangers. The bridge consists of large main cables which support the stiffening girders (acting as a deck). These cables are supported by the main towers. The cables transfer loads to the towers and the towers transfer the loads to the foundations.

The main cables are anchored in massive concrete blocks, which act as end supports. In Figure 38 the principle of a suspension bridge is shown.

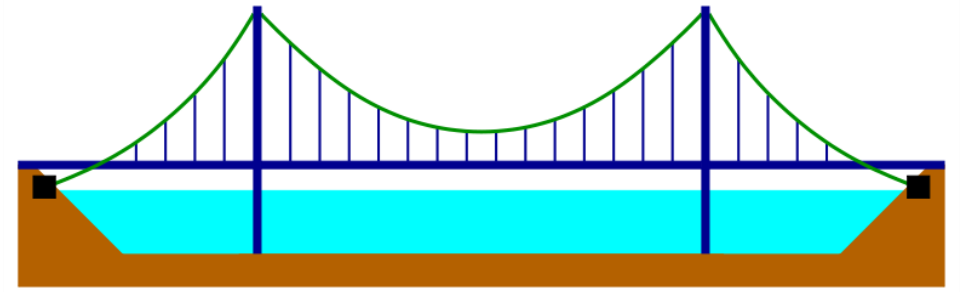

Figure 38: System of a suspension bridge

The main forces in this type of bridge are tension forces in the cables and compressive forces in the towers. The deck can be made quite slender, but it has a low stiffness compared to other types of bridges. This makes it difficult to carry large live loads. Furthermore, because of high horizontal forces at the anchorage blocks a very strong soil is required to build the anchorage blocks on. Having a soft soil would require large and expensive foundation, which would undo other cost benefits of this bridge type. Because for a suspension bridge long main span are achievable and less material may be required than with other bridge types. This reduces the construction costs and allows very large spans.
Instead of anchoring the cables to blocks, nowadays the cables are anchored in the bridge deck. However this would require a thicker deck.
The span range of a suspension bridge is 500-2000m. Going lower than 500m will take away the benefits of a suspension bridge and only leave high construction costs.

A4.2.8 Span length overview

As a summary the spans ranges for the discussed bridges are shown in Figure 39 and Figure 40.

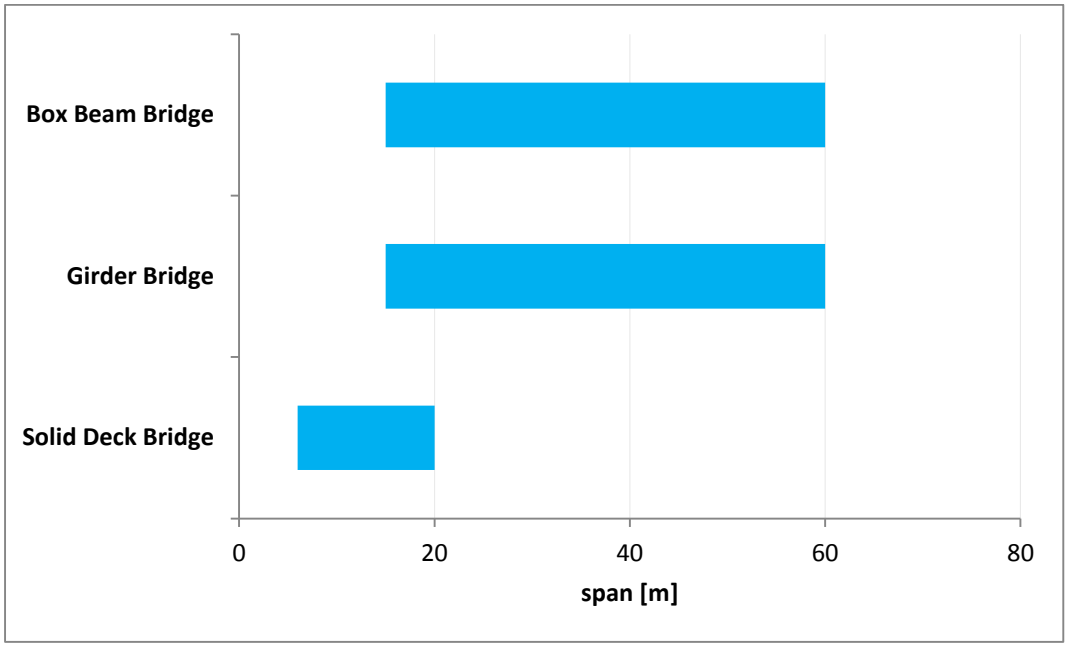

Figure 39: span ranges short-to-medium length bridges

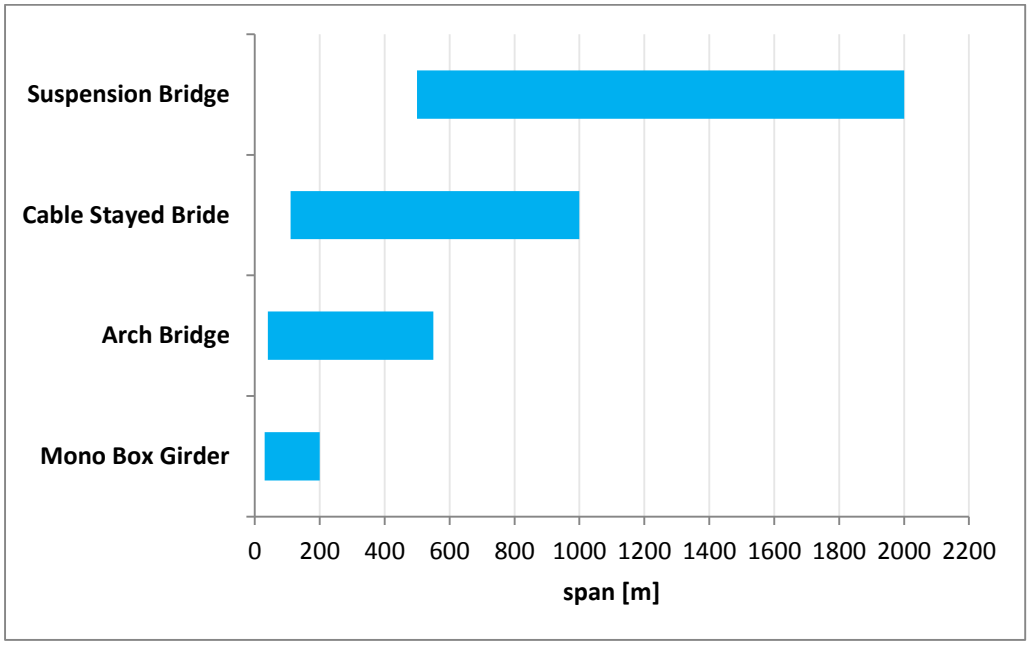

Figure 40: span ranges medium-to-large length bridges

A4.3 Structural systems

When designing a bridge different structural systems can be used. Three structural systems are going to be discussed namely:

- Simply supported
- Simply supported with continuous slab (or partial continuity)
- Full continuity

Also integral bridges will be discussed.

NB. The details discussed her are mainly applicable for precast bridges, but in some cases it could also be applicable for cast in situ beams.

A4.3.1 Simply supported

Back in the day a lot of bridges were designed as simply supported structures. This system is simple to calculate with, since it assumes that the moments are zero at the supports. With this system the beams are normally positioned on individual bearings (one at each beam end). If an intermediate support is available the gap between beams is closed with transversal expansion joints. They are also placed between end spans and abutments. These joints allow for thermal movement of the deck. Also deformations caused by creep and shrinkage are taken up.

As said, a lot of bridges are built this way and still behave well. But this system has a couple of disadvantages: Bearings are required at each beam end, so at an intermediate support you'll get a double row of bearings, for each beam one bearing. These bearings are expensive and not very durable. Also the expansion joints can cause issues. They are susceptible to de-icing salts and they are a discomfort for traffic. So when detailing the supports it is important to take into account possible inspection and replacement of bearings and joints and to take into account installation of drainage channels for water removal. Also possible is to eliminate transversal joints by using a different structural system.

A4.3.2 Simply supported with continuous slab

In this structural system only continuity of the deck slab is provided. The beams are designed as simply supported. This means that no distribution of vertical load effects between the intermediate bridge decks can occur.

Two methods are used to provide partial continuity in beam and slab decks. Both solutions are quite simple methods to provide partial continuity with a minimum of extra design and construction effort.

In the first method the continuity is only restricted to the slab, which deflects to accommodate the rotations of the simply supported deck beams. In Figure 41 this solution can be seen.

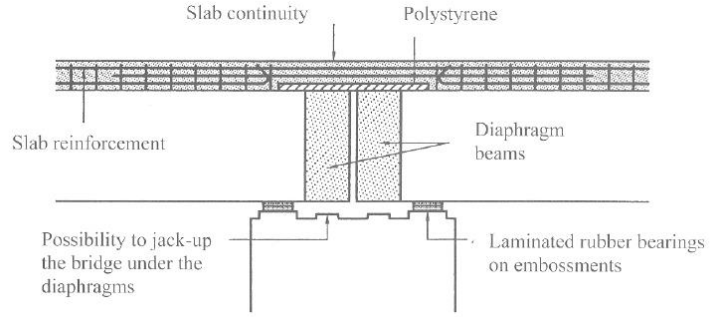

Figure 41: Partial continuity - Detail type 1: continuous separate slabs

Typical features of this method are:

- Separate bearings and diaphragms are provided for each span
- The deck slab is separated from the support beams over a short length to provide rotational flexibility
- There is no continuity reinforcement between ends of beams and there is moment continuity between spans for live load only.

In the second method, the bridge decks are designed and constructed in the conventional manner for simply supported bridges, with slab trimmer diaphragms at the beam ends. An example of this method is seen in Figure 42. Typical features of this method are:

- Separate bearings and diaphragms are provided for each span (just like in the 1st method)
- Tie reinforcement at mid depth of the slab, which is debonded over a short length at each side of the joint is used to permit deck rotation. There is no moment continuity between spans.
- Slabs between spans are separated using compressible assembly joint filling, but deck water proofing and deck surfacing are continuous and special seals are provided over the joint for double protection.

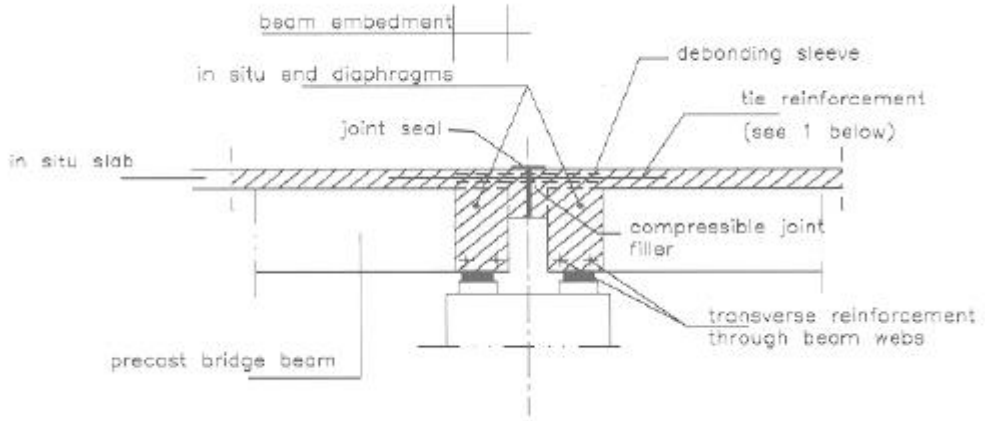

Figure 42: Partial continuity - Detail type 2: Tied deck slab

When using this structural system, the expansion joints present in the simply supported system are eliminated, while still maintaining a high rotational capacity at intermediate supports.
But also here bearings are necessary for each beam end.

A4.3.3 Fully continuous

Fully continuous systems in multi-span bridges are realised by integration of the bridge beams into a reinforced concrete crosshead on top of the piers. This is done in two steps:
First the beams are simply supported and the concrete slab is cast together with the cross head. Second the concrete hardens and the structure becomes continuous, but only for the additional dead load and the variable loading. Also for this system a couple of solutions exist. The first one consists of a wide in-situ integral crosshead as seen in Figure 43:

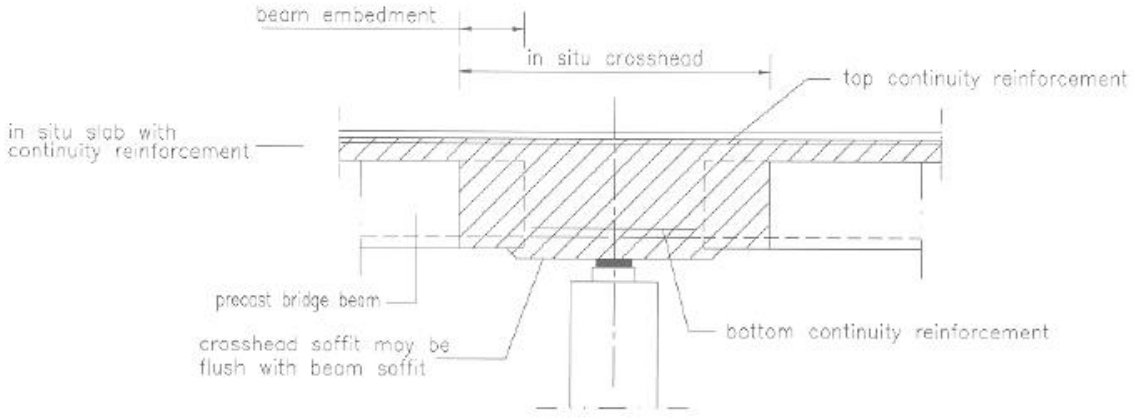

Figure 43: Full continuity - Detail type 1: wide in-situ integral crosshead

Features of this solution are:

- The beams are erected on temporary supports generally off pier foundations
- Continuity reinforcement is provided in the slab and at the top and bottom of the bridge beams. The lapping of the reinforcement is normally not difficult.
- The crosshead is supported on a single row of bearings.

The second solution is a narrow in-situ integral crosshead. Here the beams are provisionally supported on top of the piers. The integral crosshead is then cast between and around the beam over a width of about 1m at both sides. This solution is seen in Figure 44. Features for this solution are:

- Temporary supports are not required.
- Beams are placed on two rows of temporary bearings which are later replaced with one permanent bearing. Also possible is to use one wide bearing where both beams can rest on.
- Continuity reinforcement is provided in the slab and at the bottom of the bridge beams.
- The gap between the beams is narrower than at the first solution. This makes it more difficult to realize an adequate lapping of the bottom reinforcement.

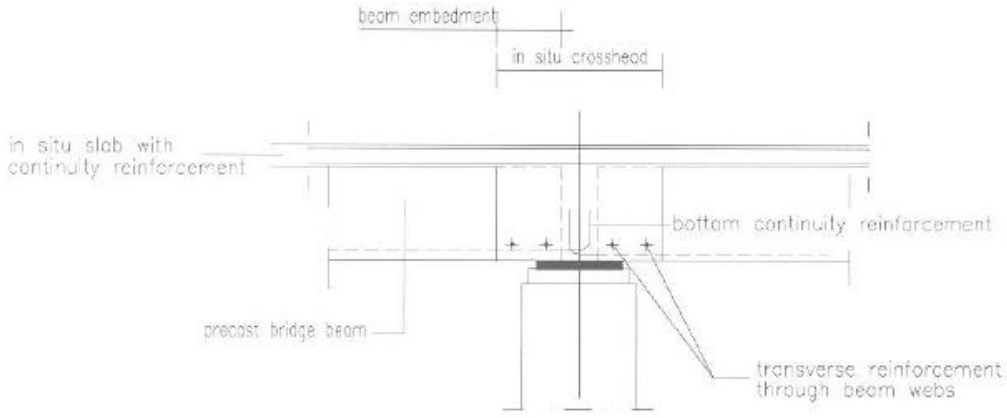

Figure 44: Full continuity - Detail type 2: narrow in-situ integral crosshead

Although more complex to design and more expensive to construct than any of the other systems, these solution offers advantages such as, that only one row of bearings is needed instead of two, which saves costs in the bearing department.

And because only one row is necessary the pier can also become more slender. Type 2 is easier to construct than type 1, but for type two it becomes harder to obtain an adequate connection between the bottom flanges.
Besides the two solutions it is also possible to obtain full continuity by post-tensioning systems.

A4.3.4 Integral bridges

Although not specifically a structural system, integral bridges are worth mentioning because their design approach differs from standard bridge systems.
An integral bridge is a specific type of bridge, where the superstructure is monolithically connected to the abutments. This means that the bridge is designed without expansion joints, neither between adjacent intermediate spans nor between end spans and abutments.
Also possible is, just like continuous bridges at intermediate supports can be constructed with bearing pads, to provide such pads at abutments without expansion joints. This type is referred to semi-integral bridges. This type is particularly suited for bridges with prestressed beams, since the bearings eliminate the problems associated with moment continuity and rotation due to creep and thermal effects. A layout example of an integral bridge can be seen in Figure 45.

Figure 45: example integral bridge

The benefit of using an integral bridge is a complete elimination of expansion joints. Since these joints are always an issue, because of their short life span, eliminating them means a reduction of maintenance. This leads to lower maintenance costs and also less nuisance for traffic. Also the field moment is decreased so a lower height of the superstructure is possible. Besides, eliminating expansion joints also benefits for the traffic users, by providing a much smoother ride.
However there are some disadvantages. There is a large influence caused by temperature loads, time dependent effects and settlements. These can cause movements in the bridge. These movements are normally allowed, when bearings and joint are used. But since the abutments are monolithically connected with the superstructure, they must be designed to allow these movements to occur and at the same time be able to resist traffic loads.

A couple of types of abutments exist for the integral bridge (Figure 46a –Figure 46d):

- **A Full height frame abutment (a)**: These are suitable for short single span bridges. Here the horizontal movements will only be small, so the earth pressures should not be very high.
- **Embedded wall abutments (b)**: These don't go over the full height and they are supported by piles. There are also suitable for short spans
- **A pilled abutment with reinforced soil (c):** For this type the piles are surrounded by soft material in tubes to limit the resistance to horizontal movement and rotation of the abutment.
- **Spread footings (d)**: These can also be used on reinforced soil. Spread footings are considered suitable, where the foundations are very stiff and where settlements are very low.

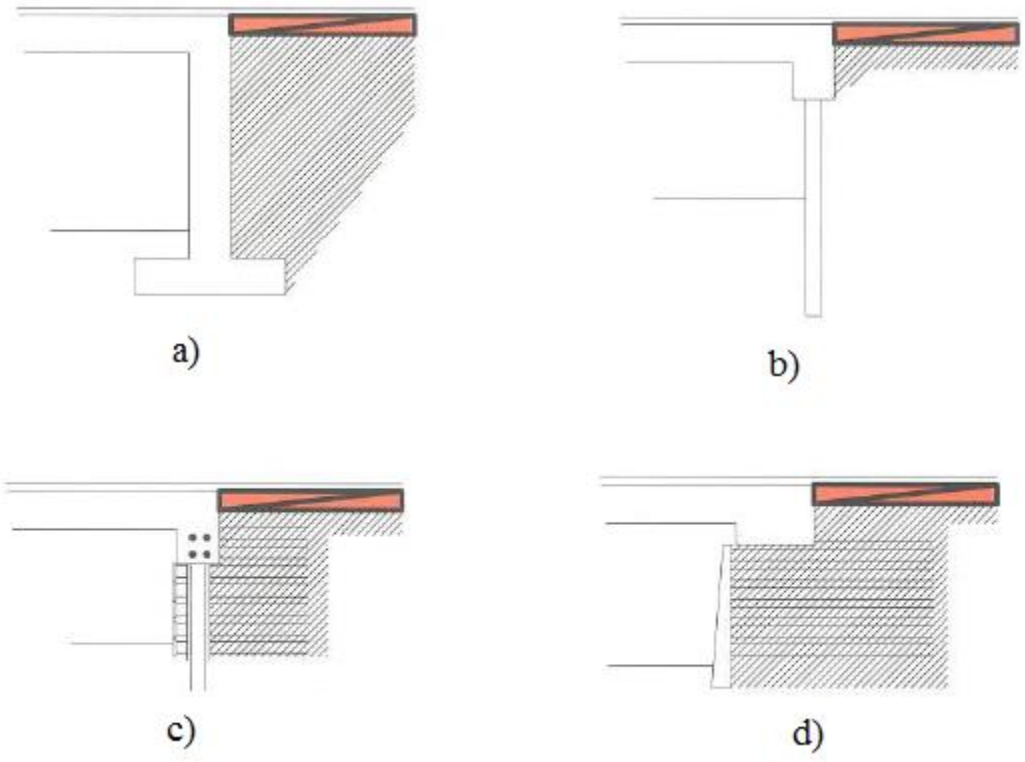

Figure 46: a) Full height frame b) Embedded wall abutment c) Pilled with reinforced soil d) spread footing

A4.4 Construction methods

When building bridges a lot of different construction methods can be used. When choosing a certain construction method certain factors have to be taken into account. These factors are for example the required span length, existing constraints at the site, construction schedule, size of the project, etc.

In general there are three main methods of construction:

- In-situ casting in formwork in position of the works
- Precasting off the works and subsequent transportation and erection
- Combination of in-situ and precasting

Also there are four main forms of erection:

- On centering (stationary or travelling falsework)
- Cantilevering (Cantilever method)
- Horizontal incremental jacking (Incremental launching method)
- Vertical hoisting, lifting or jacking (Used with prefabricated elements)

Before actually choosing a construction method, one must also make a decision between using prefabricated or in-situ concrete.

In situ concrete can be used if complex shapes are required which are difficult to pre-build in a factory. But casting in-situ requires good environmental conditions since these can influence the quality of the concrete.

The problem with the environment can be overcome by used prefabricated segments. These are constructed at the factory, where environmental conditions can be influenced. Because of the prefabrication it will save a lot of construction time on site comparing it to in situ casting. Not only is prefabrication time saving, it doesn't require scaffolding, because precast segment are usually put in place with cranes.
Now to determine the choice between in situ and precast concrete, one must also look at the method of erection.

A4.5 Conclusion bridges

In the previous paragraphs various bridge types, structural systems and construction methods used in bridge construction have been described. While taking the factors and constraints of the project into account, appropriate choices concerning these matters have to be taken into account. When choosing a bridge type attention has to be paid to the length of the gap that needs to be crossed. This will determine which bridge type is the most suitable. Also very important is the environment which the bridge will be built in. The latter is also important when choosing an appropriate construction method. The surroundings will determine the transportation possibilities of material, the amount of space available for a construction site and it will also influence the construction schedule for example when dealing with a very busy area, that can't be disturbed for too long.

These factors also decide if a bridge should be made with cast in-situ or precast concrete.
Besides these factors one must also look at the function of the bridge. Will it serve as a pedestrian bridge or a traffic bridge and what kind of loads can be expected on the bridge. These factors also play a role in determining a bridge type and also for a certain bearing type since each type of bearing has its own maximum load capacity.

A5. Research on UHPC

References: [2], [6], [9], [11], [18], [24], [25]

In this chapter summaries of a couple of researches are given that could be relevant for the thesis. The researches presented here are used to illustrate the benefits of UHPC over other concrete types, with respect to material properties and also sustainability. And some of them look specifically at the application for bridges, for example suitable girder types.

A5.1 Characterization of the behaviour of ultra-high performance concrete (Graybeal)

In 2005 a research has been done by B. Graybeal [9] to provide insight into the potential structural behaviour of UHPC in highway bridge girders. This was done by characterizing the material behaviour through small-scale specimen testing and by characterizing structural material behaviour through full-scale girder testing. During the period of this research UHPC was mainly used for pedestrian bridges. So this research was one of the steps to an application of UHPC on a larger scale in highway bridges. As mentioned, the research was divided into two main parts: The first part is a small scale experimental phase, where over 1000 specimens where tested for their structural and durable properties. Besides that, different types of curing treatment were used, to see their influence on the material properties of UHPC. The second part is a large scale experiment, where tests were made on large prestressed I-girders. There was also an analytical phase, where the results of the experiment were combined, analysed and elaborated upon. In this phase predictor equations for basic UHPC properties were also developed, including design philosophies for flexure and shear design.

In general the results of the research showed significantly enhanced material properties (structural, durability) compared with normal and high performance concrete. It can serve as a viable substitute for ordinary concrete and HPC in prestressed I-girders.
The shear and flexural capacities also showed positive results. This increased capacity is primarily the result of the sustained post cracking tensile capacity of UHPC. This again is due to the steel fibres in the concrete. These steel fibres also made possible that the use of mild and shear reinforcement was unnecessary.

Overall UHPC is a great alternative structurally wise. However the cross sections of the tested girders weren't as optimized as is possible, when using UHPC. The I-girders weren't much more slender compared to I-girders made in ordinary concrete. One of the recommendations for future research was to develop optimized bridge girders that take advantage of the material properties of UHPC. These bridge girders should use the tensile and compressive capacities of UHPC, while also enhancing the design life of the bridge as a whole by eliminating many of the less durable components of a normal bridge.

A5.2 Optimal Design of UHPC Highway Bridges Based on Crack Criteria (Sorelli)

In 2007 a research was completed at MIT, where a design approach based on the crack opening criteria was proposed, to be able to optimize the cross-section of highway bridges of medium span between 23 and 36m [24]. The design approach accounted for the UHPC ultimate admissible crack opening within the context of the Load Resistance Factor Design (LRFD) design method. The LRFD design method is based on the AASHTO design specifications.
In the research three bridge sections were considered in the optimization problem: A Double-tee section, a girder section and a box section (Figure 47). Also five different span lengths were accounted for (24.38; 27.43; 30.48; 33.52; 36.57 m). Besides this additional design constraints were assumed in the optimum design.

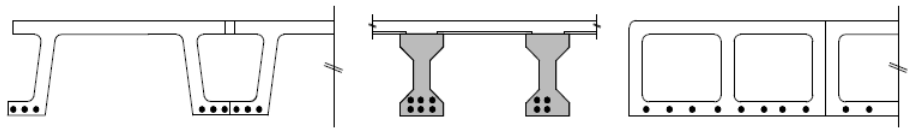

Figure 47: The three bridge sections used in study

The optimized solutions that came out of the research are plotted in Figure 48. From the results could be concluded that the optimized box sections allow the highest span-to-depth ratios (between 25 and 30), while the girder sections save significant UHPC material volume per span length and prestressing cables. Using a 3D model allowed further optimization of the sections.

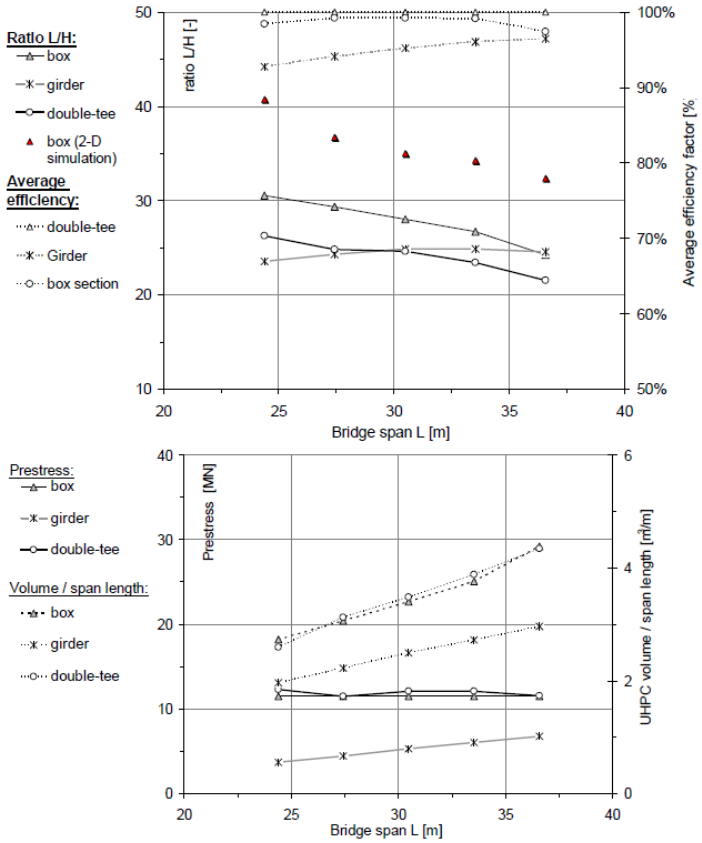

Figure 48: 1D design bridge optimal solutions plotted in terms of (top) span-depth ratio vs. bridge span, and (bottom) prestressing force and UHPC volume vs. bridge span.

A5.3 Innovative Design of Precast/Prestressed Girder Bridge Superstructures using Ultra High Performance Concrete (Almansour)

Another research has been done in Canada, which served as an aid to the development of innovative solutions for the Canadian infrastructure [2]. The objective of this research was to evaluate the structural efficiency of CPCI (Canadian precast prestressed Concrete Institute) UHPC I-girder bridges to that of HPC I-girder bridges. One had to look at the span length capability, the maximum feasible girder spacing and minimum girder size that will yield the minimum number of girders and minimum weight of the entire superstructure. Furthermore a cast in place slab would be placed on the girders. The bridges were designed according to the Canadian codes with additional existing requirements for UHPC design. The bridges were modelled using a finite element method, which was used to get information about the appropriate span length, girder size, spacing etc.

The results of the research showed that using UHPC girders instead of HPC girders enabled a significant increase in the bridge span. Besides that, UHPC yields a considerable reduction in girder size and the number of required girders. This means a concrete volume reduction of 49% to 65%. Also reducing the girder spacing showed high increase of the span length of the UHPC-bridge, while the HPC-bridge showed less improvement. In Figure 49 a comparison is made between spans when using HPC or UHPC girders. Clearly it is seen, that using UHPC girders will increase the span significantly and reduce the amount of girders needed of the width.

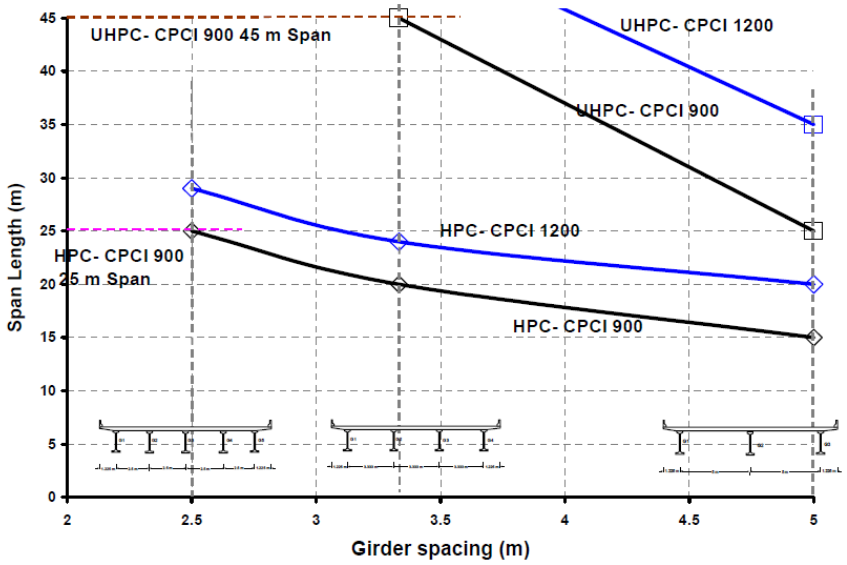

Figure 49: Comparison of the Slab-on-Girders Bridge span length for different girder spacing

Finally the research suggested optimizing the existing CPCI-girders to create an optimal practical UHPC girder section for future use. The development of an optimum practical UHPC girder section and hence structurally efficient and cost effective bridge superstructure would lead to a longer life bridges.

A5.4 Case Studies Using Ultrahigh-Performance Concrete for Prestressed Girder Bridge Design (Taylor)

In the United States a case study has been performed on the application of UHPC in prestressed concrete girder bridges in New Mexico [25]. For this study two existing bridges made out of high performance concrete were redesigned using UHPC. The two bridges were the I-25/Doña Ana Interchange Bridge (length of 34.29m) and the Sunland river Crossing Bridge (37.16m each span). Here a comparison was made between HPC and UHPC, with the main considerations being the required number of girders, girder size, number of prestressing strands, deck thickness and shear detailing. Furthermore the goal of the study was to incorporate UHPC in standard AASHTO girder sections with little to no geometric modification to the standard girder sections (which were standard bulb tee girders).
The sections used were the standard BT-63 and BT-54 girders as shown in Figure 50.

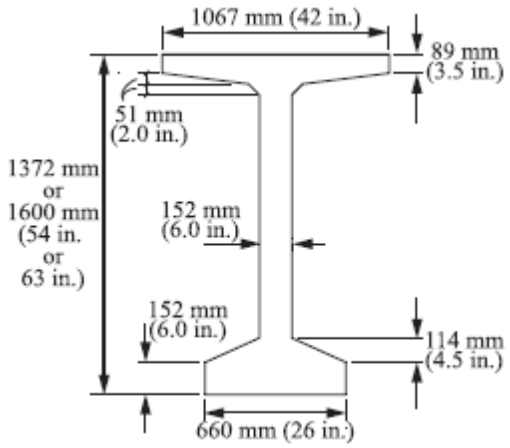

Figure 50: Typical dimensions of BT-63 and BT-54 girders

Because of the high cost associated with UHPC the design goal of this study was to reduce the amount of concrete used for girders. Only minor modifications were made on the girders (such as slightly increasing the web thickness), so that precasters don't have to make large modifications on formwork. Also two different sizes of prestressing strands were used (15 and 18 mm-diameter).
The results of the study show that the use of UHPC leads in a decrease in the amount of girder concrete needed compared with HPC (reduction up to 43%). However this decrease of concrete lead to an increase in amount of strands (46% increase), because there are less and/or smaller girders used. The deck thickness increased as well (46% increase), because of the greater spacing now between girders. Using 18mm strands instead of 15mm can further reduce the amount of girder concrete used. At some locations of the bridges the shear capacity did not suffice so shear reinforcement had to be applied at the critical locations, but the amount required was far less than with High performance concrete.
So in short in can be stated that UHPC has the potential to allow the maximum girder spacing and fewest girder lines to be used and that it has a much better performance that high performance concrete.

A5.5 Use of UHPC in Bridge Structures: Material Modelling and Design (Gunes)

A research has been performed in 2011 at MIT [11], where a model was used to study the material behaviour of UHPC. In the beginning there were mostly empirical approaches based on large-scale testing of structures. But an appropriate model was needed to simulate the material behaviour of UHPC. This could also aid in optimization of the material. The model had to take in to account the pre and post-cracking behaviour of UHPC. The model used in this research was a rheological model proposed by Chuang and Ulm in their research [6]. The model is seen in Figure 51. Chuang and Ulm developed a two-phase damage-plasticity model, based on the action of the composite phases, which accurately predicts the non-linear overall stress-strain relationship in tension.

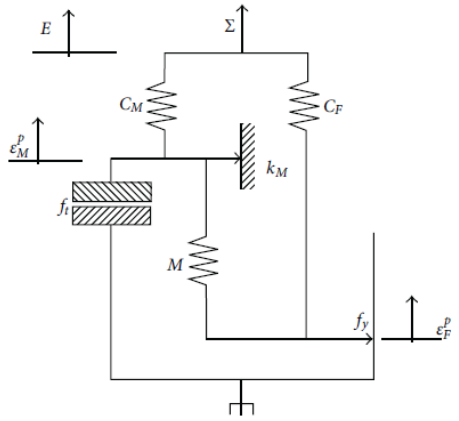

Figure 51: The two-phase rheological model of UHPC

The developed model was then used to determine section capacities of PCBT-45 VODT Bulb-T bridge girders. The calculations had to be based on the critical crack opening criterion given by the French Recommendations (AFGC). The design consisted of a UHPC prestressed girder and a lightweight concrete slab. Calculations showed that that the UHPC version of the girder compared to a standard Bulb T-section of normal concrete, is more than sufficient for the span the section is meant for.
The UHPC section could be used for a longer span or a smaller section can be used, because the compressive stress in the top flange was only 1/3 of the compressive strength.
The research also stated that a couple of optimizations are still possible: The web can be reduced. The total dead load can be reduced, by for example making the top deck out of UHPC, which would subsequently lead to a smaller beam height.
At the end the research stated that there is still a need for development of optimized member design to make better use of the material.

A5.6 Life cycle cost analysis of a UHPC-Bridge on Example of two Bridge Refurbishment Designs (Piotrowski)

At the University of Kassel a life cycle cost analysis study has been performed on two alternative designs for the Eder-Bridge in Felsberg [18]. This bridge was due for replacement and an opportunity was seen to compare the life cycle costs between a design in ordinary prestressed concrete and a design in both UHPC and normal concrete units.
Within the scope of this work, first an economic efficiency analysis was carried out including the cost of construction. For the analysis only the superstructure was considered. This study made use of UHPC costs that were taken from the few available literature sources on structural engineering.

The result of the economic efficiency analysis shows that the design with UHPC, was 23% more expensive that the design with traditional concrete (costs of normal concrete: €149.359,00; costs of UHPC: €183.225,20). For this analysis however not all stages in the life cycle were considered. Apart from historical costs (investment and construction costs), consequential expenditures (user costs) are also a part of the life cycle. These expenditures are all costs that occur during the bridge age throughout its life cycle. So another analysis considering all these costs was performed next.
The analysis compares the sums of the final values of given designs including both construction and user costs. Two methods to express the time value of money were used: the net present value method and the annuity method.
The most important factors for the life cycle costs calculation of a bridge besides the construction costs are the lifetime of a bridge, the annual maintenance and operational costs and the inflation adjusted interest rate needed in order to discount the future payments.
The results of the analysis were put against the lifetime of the bridge. These are seen in Figure 52. The percentages stand for the percentage of maintenance expenditures per year.

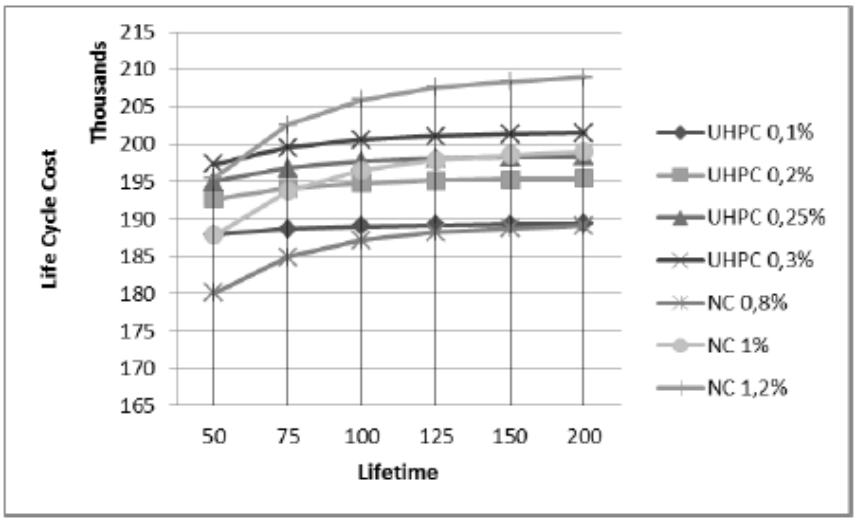

Figure 52: Capitalized life cycle costs

The figure shows that the life cycle costs of the design with normal concrete are lower than the design with UHPC considering a short lifetime of 50 years. But when looking at 100 years or more, UHPC becomes cheaper.
This is because UHPC has lower maintenance costs and a longer lifetime. A comparison of maintenance costs can be seen in Figure 53. It is clearly visible that UHPC has much lower maintenance costs.

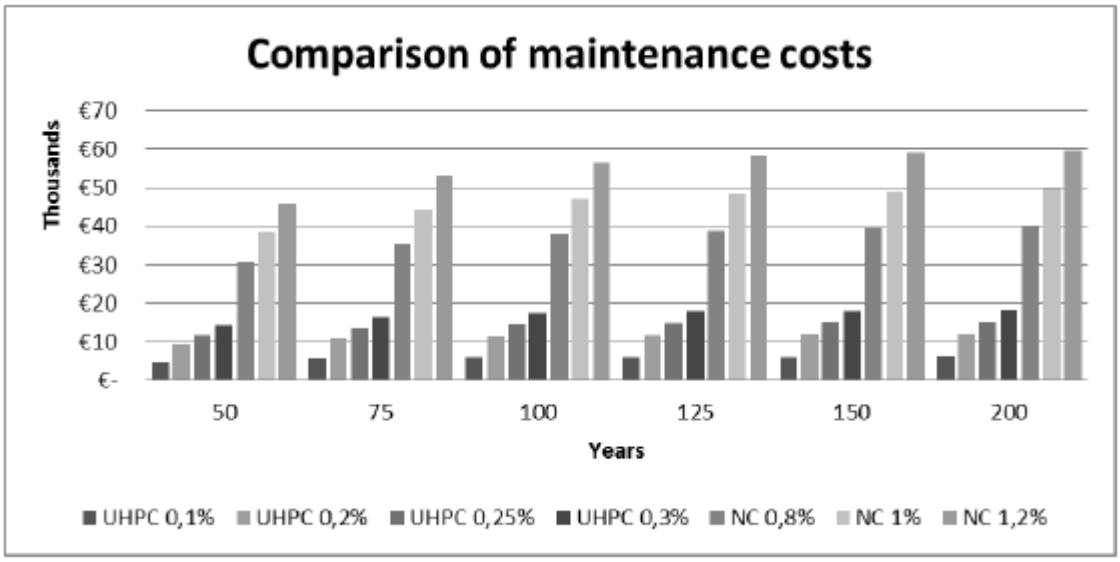

Figure 53: Comparison of maintenance costs

Furthermore it is assumed that over 100 years the bridge in normal concrete would have been renovated or replaced, while the UHPC bridge would still be functioning properly.
Looking at the future further optimization of the UHPC manufacturing process, precast production as well as in-situ, UHPC may increase saving potential, so that the construction costs will decrease and the advantage of the user costs will be fully used.

A5.7 Conclusion research on UHPC

Discussed in this chapter were a couple of researches dealing with UHPC and their application in bridge structures. In general it can be stated that UHPC is a serious competitor for ordinary and high strength concrete. *Graybeal(2005)* showed that UHPC has a much higher shear and moment capacity than ordinary and high strength concrete (especially the shear capacity) and that UHPC can be a viable substitute for ordinary and high strength concrete.
Then the research performed by *Almansour (2008)* and the research performed later by *Taylor (2013)* showed that using UHPC instead of high strength concrete results in a reduction of used concrete material (by reducing the required amount of girders) and also that UHPC can span a much higher length than High strength concrete.
The study by Sorelli (2007) showed that for bridge spans between 25 and 30 meters the box section will allow the highest span to depth ratio and that girder section will result in a significant reduction of the material volume.
The study by Piotrowski *(2012)* showed that even though the material costs of UHPC and also the production are more expensive, for the long term the total LCA costs for UHPC will be lower than that of ordinary concrete, because of the very long lifetime and the lower maintenance need.

What is noticeable though is that in most of the discussed researches the final remark was that the UHPC sections used for the researches weren't optimized to the fullest. For example when looking at the used girders in the studies, most of the time only a slight modification was made on existing girders when UHPC was used. So the girders didn't use the UHPC properties to the fullest. Since it is important to efficiently use UHPC, it will be a challenge during the design of the Leiden Bridge to develop a bridge that uses as less material as possible in order to use UHPC to its fullest potential.

A5.8 Summary research on UHPC

- In general UHPC has better material properties (structural, durability) than Normal strength and high strength concrete.
- Girders are not optimized enough.
- Box sections provide highest span-to-depth ratio and girder sections save most material volume per span length.
- Using UHPC in bridge structures will require a lesser amount of girders compared to HSC and smaller sections as well. Both will lead to a concrete volume reduction. Using less and smaller girders can result in an increase in prestressing cables per girder.
- Besides volume reduction, using UHPC over HSC results in a high increase in span length.
- UHPC has higher material and production costs than normal concrete. However when the complete life cycle is considered, UHPC becomes cheaper (after 100+ years), due to the longer life span and less maintenance needs.
- Researchers concluded that further optimization is required for the use of UHPC in structures. Options for optimization can be:
    - Optimizing cross section (construction height, web and flange thickness)
    - Optimising amount of girders
    - Optimizing concrete composition and production process

A6. Optimization

References: [5], [21], [i3]

A6.1 General

When looking at the design process, there are a couple of main steps that are usually followed:

- Defining the function
- Conceptual design
- Optimization
- Details

Here optimization is the third step, but what does it stand for. Optimization basically means making things the best way possible. So structural optimization deals with making a combination of materials sustain loads in the best way.

When looking at the way to make something the 'best' as possible, a couple of ways are possible. For a bridge for example, the costs have to be as low as possible. This can be achieved indirectly by making the structure as light as possible (by minimizing weight).

But these methods of making something better aren't without constrains. For example if there are no limitations for material use, a structure could be made very stiff without any limits. But then there would not be an optimal solution. So usually constraints are defined to be able to find a well-defined and realistic solution. Quantities that are usually constrained in structural optimization problems are stresses, displacements and/or geometry. These constraints can for example be defined in certain design recommendations.

A6.2 Method of optimization

When performing an optimization a couple of methods can be used. The traditional, and still dominant, way of optimizing is the Iterative-intuitive Method. It can be described as follows:

1. A specific design is suggested
2. Requirements based on the function are investigated
3. If they are not satisfied (e.g. stresses are too high), a new design must be suggested.
4. The suggested new design is brought back to second step.

In this way an iterative process is formed where (mostly intuitive) a series of designs are created which will hopefully converge to an acceptable final design. This process is also seen in Figure 54. For mechanical structures this method is nowadays almost exclusively formed by means of computer based methods (FEM).

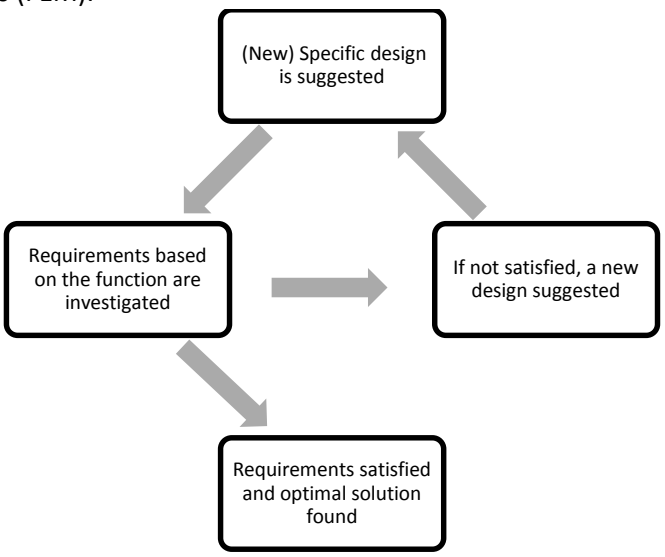

Figure 54: Iterative-intuitive Method

Another method is the Mathematical Design Optimization Method. With this method a mathematical optimization problem is formulated, where requirements due to the function act as constraints and where the concepts 'as good as possible' are given precise mathematical form. So this method makes the design process much more automatic than the iterative-intuitive method.
A basic requirement is that the factor needs to be measurable in mathematical form.

In a general mathematical form of a structural optimization problem the things always present are:

- **An objective function (*f*):** this is a function used to classify designs. Usually f is chosen such that a small value is better than larger one.
- **A design variable (*x*):** a function or vector that describes the design, and which can be changed during optimization (for example thickness of a web or deck).
- **A state variable (*y*):** a function or vector, for a given design x, that represents the response of the structure (stress, displacement, etc.).

As for the constraints, there exist three types of constraints:

- Behavioural constraints: Constraints on the state variable y
- Design constraints: Constraints on design variable x.
- Equilibrium constraints

So a general optimization problem now takes the form:

$$(SO)\quad \begin{cases} \text{minimize } f(x,y) \text{ with respect to } x \text{ and } y \\ \text{subject to} \begin{cases} \text{behavioral constraints on } y \\ \text{design constraints on } x \\ \text{equilibrium constraint.} \end{cases} \end{cases}$$

A6.3 Types of structural optimization

Structural optimization can be done in three different ways (Figure 55):

- Sizing optimization
- Shape optimization
- Topology optimization

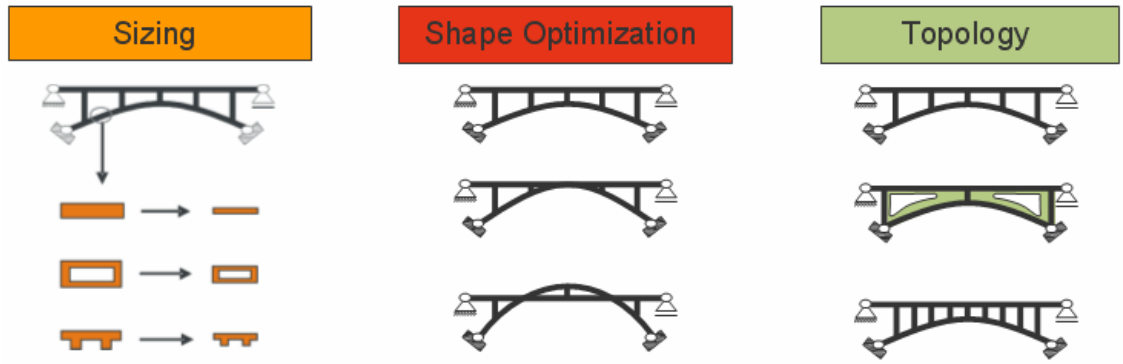

Figure 55: Types of optimization

Sizing optimization

Sizing optimization deals with optimization of a structural thickness, such as the cross section of a bridge. Starting with a certain cross section size, the goal is to reduce the area of the section while still being able to fulfil the requirements. Reducing the area can be done by for example lowering the thickness of the webs and/or flanges. When performing the sizing optimization the geometry of the structure and the topology stay constant. This allows for simple and efficient formulations. The

result is a cross section with a minimal area that leads to a more slender and lighter structure, which can reduce costs.

Shape optimization
Shape optimization deals with, as the name states, with the actual shape of a structure. Usually the variables altered are for example node coordinates. Here the whole geometry of the structure is optimized. When the geometry is altered, the loading distribution is also going to be completely different. Shape optimization will not change the topology (connectivity) of the structure. So no extra connections are created, nor 'voids' in the structure. This type of optimization will be complex and time consuming, because of formulation of shape derivatives and also because of the changing load distributions.

Topology optimization
Topology optimization is the most general form of structural optimization. Here neither the geometry, nor the topology of the structure is predefined. Basic parameters are the design space and the boundary conditions of the structure. When using topology optimization the most efficient material distribution in the design space has to be computed. A good example of topology optimization is seen in Figure 56. Here 50% of the material is saved by optimizing the top box structure and turning it into the bottom structure. There are several methods to perform this optimizing with the most common one being SIMP (Solid Isotropic microstructures with Penalization), which establishes a relation between material properties like Young's modulus and material density.

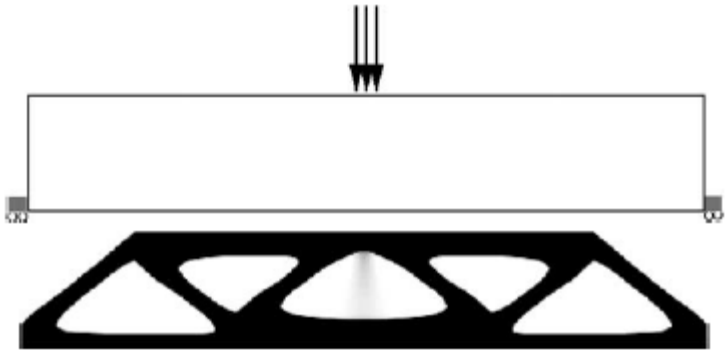

Figure 56: Topology Optimization

A6.4 Topology Optimization methods

Before actually naming the methods it is important to look at the types of topologies available. The main types of topologies available are:

- *Isotropic-Solid/Empty (ISE):* Here a set of elements is used which can be either empty or filled entirely with one or more isotropic materials.
- *Anisotropic-Solid/Empty (ASE)*: Here a set of elements is used which can be either empty or filled entirely with one or more anisotropic materials. This type can be used for optimization with continuous variables.
- *Isotropic-Solid/Empty/Porous (ISEP)*: Here homogenized anisotropic properties of originally nonhomogeneous elements are used. The elements contain an optimal microstructure consisting of void and one or more isotropic materials. So before the homogenization takes place the topology is called ISEP. After homogenization the topology is ASE.

Of these types the ISE and IS types are most commonly used in practice. For these types certain methods exist to use. These are:

A6.4.1 The SIMP method

Already briefly mentioned earlier, SIMP stands for Solid Isotropic Microstructures with Penalization. These microstructures are used for intermediate densities. For a structure that consists of a set of elements it is only possible for the elements to have a thickness of zero or a prescribed thickness and nothing in between. By altering the penalty parameter ρ and the constraints, different solid-void designs will be made until an optimal solution is found.

The advantages of the SIMP method are:

- Computational efficiency, in the sense that not a lot of CPU power is needed.
- Good robustness, which means that it is suitable for (almost) any design condition.
- Penalization can be adjusted freely
- Conceptual simplicity, so no higher mathematics required
- Convexity can be preserved for the early iterations with ρ=1
- No homogenization is necessary

There are also some disadvantages namely:

- The solution is dependent on the degree of penalization
- There is a possibility of the solution not converging to the most optimal one
- The method is mesh dependent, which can cause local minima and thus could result in a checkerboard pattern if a fine mesh is used. This can be solved by using filtering.

A6.4.2 The ESO method

ESO, which stands for evolutionary structural optimization, optimizes a structure by slowly removing material which has the lowest sensitivity value (for example the lowest strain energy). This method shares some similarities to the SIMP method, but it differs in terms of volume. SIMP finds an optimal solution by changing the volume given a-priori while ESO reduces the (not a-priori given) volume to find an optimal solution.

The advantages of the ESO method are:

- It is a fairly simple and effective method for optimization
- No homogenization is necessary

The disadvantages are:

- High solution time, long iterations are needed.
- The robustness is not so great.
- The method is mesh dependent just like the SIMP method

A6.4.3 The OMP method

Another method that can be used is the OMP method. OMP stands for Optimal Microstructures with Penalization. Here first the solution is optimized using for each finite element an optimal microstructure, derived accurately for the particular type of design constrains and objective function. This basically means that first homogenization is necessary. For this method a number of free parameters is required: For a 2D problem three free parameters and for a 3D problem five. This is more than with the SIMP method which requires only one free parameter.

The advantage of this method is:

- Additional information can be gathered about the optimal ISEP topology

But there are more disadvantages for this method compared to the SIMP method:

- There is a greater computational effort that SIMP
- The method is highly non-robust
- Advanced mathematics are required for deriving optimal microstructures
- Essentially non-convex
- OMP requires homogenization
- The solution is dependent on the degree of penalization

A6.4.4 The NOM Method

NOM, which stands for Non-Optimal Microstructures are used without penalty. This because the microstructure is non-optimal, which assure a certain degree of 'fixed' penalization, but this is often not adequate for an ISE or IS topology.

The advantage for the NOM method is:

- Potentially smaller number of variables per element than OMP

The disadvantages are:

- Even though there are less variables it is still more variables per element than SIMP
- The penalization is fixed and often insufficient for reaching correct ISE/IS topology
- Essentially non-convex
- NOM also requires homogenization like OMP

A6.4.5 Conclusion topology optimization methods

Comparing the discussed methods with each other it becomes clear, that the SIMP method is the most straight forward one to use for topology optimization. For the purposes of this master thesis it suffices to use this method, which is actually also the most frequently one used in practice. However when using this method it will be important to choose the correct penalty parameter and also to keep an eye out for the checkerboard pattern, when using a fine mesh.

A7. Calculation example; comparing C50/60 with C170/200

A7.1 General

In the following a case example is going to be performed for a simply supported rectangular beam. This case will be used to show the differences between ordinary concrete and UHPC in terms of strength. For the comparison only the moment and shear capacity will be taken into account. For the sake of simplicity of the example, the calculations for crack width and deflection won't be made here. However, these will have to be done during the actual research.
For the calculations these guidelines and recommendations are used:

- Eurocode 2: Design of concrete structures – Part 1-1: General rules and rules for buildings.
- AFGC 2013.
- Cementonline articles: "Rekenmodel VVUHSB"(2011)" and "*Dwarskracht- en kolomberekening VVUHSB"(2011).*

A7.2 Specifications

The structure consists of a rectangular beam, which is simply supported. The span is 10m. The cross section is 1(L) x 0.5(W)m. The beam is reinforced with steel bars on the bottom with an area of 1000 mm^2. The structure is seen in Figure 57.

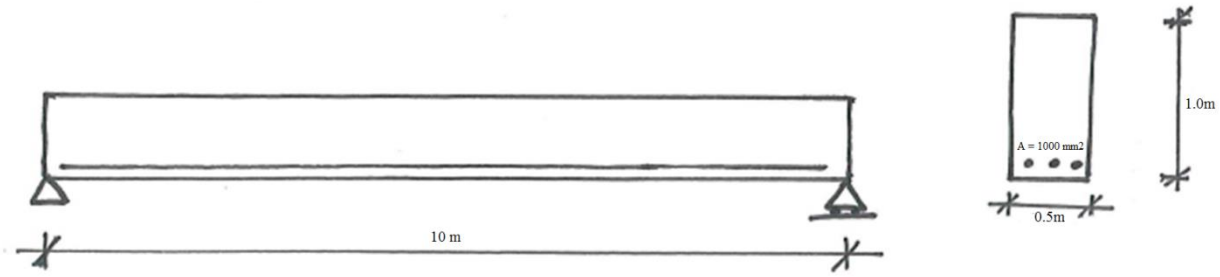

Figure 57: Rectangular beam

Besides the self-weight of the beam, there is also a variable load of 10 kN/m, working over the whole span. For the comparison ordinary concrete C50/60 and UHPC C170/200 is going to be used. The material properties are given in Table 3. In the same table the cross section properties and also the loads are given. The design values are determined as follows:

$A = b*h$
$I = (1/12)*b*h^3$
$W = (1/6)*b*h^2$
$E_{cracked} = (1/3) * E_{cm}$

C50/60:	C170/200:	B500:
$f_{cd} = f_{ck}/ \gamma_c$	$f_{cd} = \alpha_{cc} * f_{ck}/ \gamma_c$	$f_{yd} = f_{yk} / \gamma_s$
$f_{ctd} = f_{ctk}/ \gamma_c$	$f_{ctd} = f_{ctk}/ \gamma_c$	

Table 3: Material characteristics and loads

	C50/60	C170/200
ρ_c [kg/m^3]	2500	2500
f_{ck} [N/mm^2]	50	170
f_{cd} [N/mm^2]	33,33	96,33
f_{ctk} [N/mm^2]	2,9	9
f_{ctd} [N/mm^2]	1,93	6
E_{cm} [N/mm^2]	37000	50000
$E_{cracked}$ [N/mm^2]	12333.3	16666.7
A [m^2]	0,5	
I [m^4]	0,041667	
W [m^3]	0,083333	

	B500
f_{yk} [N/mm^2]	500
f_{yd} [N/mm^2]	435
E_s [N/mm^2]	210000
A_s [mm^2]	1000

Q_g [kN/m]	12,5
Q_q [kN/m]	20
Q_d [kN/m]	45
γ_c	1,5
γ_s	1,15
γ_g	1,2
γ_q	1,5
K_{global}	1,25
K_{local}	1,5
α_{cc}	0.85

A7.3 Design internal forces

First the design bending moment and shear force are calculated:
$M_{Ed} = 1/8 * Q_d * L^2 = 562.5$ kNm.
$V_{Ed} = ½ * Q_d * L = 225$ kN.

For this structure to suffice structurally the rule is that the bending moment capacity is higher than the design bending moment and that the shear strength capacity is higher than the design shear force. In other words:
$M_{Rd} \geq M_{Ed}$ & $V_{Rd} \geq V_{Ed}$

A7.4 Bending moment capacity

For both types of concrete the bending moment capacity has to be calculated. First the moment capacity of C50/60 will be determined and afterwards the moment capacity of C170/200.

A7.4.1 M_{Rd}: C50/60

The moment capacity can be decided by stating that the internal forces in the governing cross section (which is in the middle of the beam at the highest moment) have to be in equilibrium.
The internal forces are seen in Figure 58.

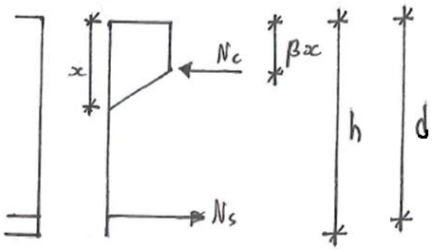

Figure 58: Internal forces C50/60

So to satisfy the equilibrium: $N_c = N_s$. N_c is the internal force from the concrete in the compression zone and N_s is the internal force coming from the reinforcement in the bottom.

$N_c = \alpha * f_{cd} * b * x$
$N_s = A_s * f_{yd}$

The only unknown here is the height of the compression zone x. With α=0.75:

$$x = \frac{A_s * f_{yd}}{\alpha * f_{cd} * b} = 34.8 \text{ mm}$$

Now that x is known the moment capacity can be calculated:
$M_{Rd} = N_s * (d - \beta x)$; with β=0.39 and d=0.9h:
M_{Rd} = 385.6 kNm.

Unity check: M_{Ed}/M_{Rd} = 562.5/385.6 = 1.46. Clearly the cross section is not safe. By applying more reinforcement this problem could be solved. Using 1500mm^2 reinforcement instead 1000mm^2 gives a moment capacity of 574 kNm which is just enough to resist the design bending moment.

A7.4.2 M_{Rd}: C170/200

Also here the moment capacity can be decided by assuming equilibrium of internal forces in the cross section. Because UHPC is much stronger than ordinary concrete and because it contains steel fibres, the concrete is much more ductile than ordinary concrete and it has a higher tensile strength too. So when calculating the moment capacity, the tensile capacity of the concrete needs to be taken into account as well (for ordinary concrete this part is always neglected). So for UHPC a different approach is used to determine M_{Rd}. In Figure 59 the internal forces are shown.
The shapes of the forces can be derived using the stress-strain diagram of UHPC. In the French recommendations the diagram can be found. For calculation purposes a slightly simplified version is used as seen in figure 67b.

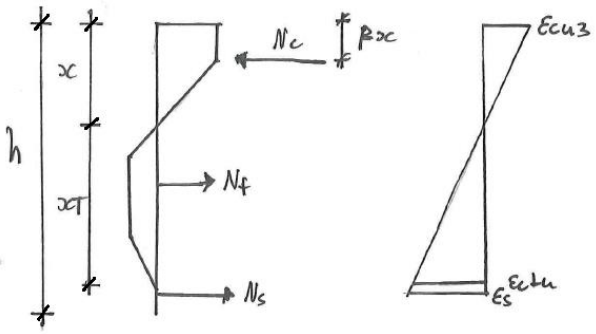

Figure 59a: internal forces UHPC

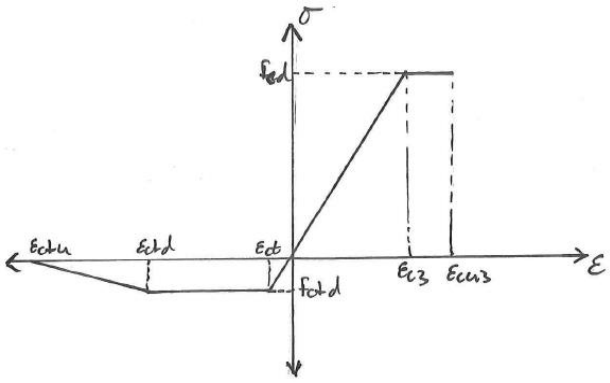

Figure 67b: simplified σ-ε diagram

The approach of calculating M_{Rd} is derived from a combination of AFGC 2013 and the articles in Cementonline about the design model for UHPFRC.
As stated earlier there has to be equilibrium of internal forces:
$N_c = N_f + N_s$, with N_s being the contribution of concrete of the tensile part. Before continuing with the calculation it is necessary to determine the strains given in the diagram in figure 67b.
ε_{c3} = 2.3‰
ε_{cu3} = 2.6‰
$\varepsilon_{ct} = f_{ctd}/E_{cm}$.
$\varepsilon_{ctd} = w_{1\%}/l_c + \varepsilon_{ct}$
$\varepsilon_{ctu} = l_f/(4*l_c)$

$w_{1\%}$ = 0.01h (h is the height of cross section)
l_c (characteristic length) = 2/3*h
l_f (length steel fibre) = 60 mm

Calculating these strains gives:
ε_{ct} = 0.12‰
ε_{ctd} = 15.12‰
ε_{ctu} = 22.5‰

Also α and β need to be calculated because they're not the same as with ordinary concrete (where α=0.75 and β=0.39). α and β can be calculated with ε_{c3} and ε_{cu3}.

$$\alpha := \frac{\left(0.5\cdot\varepsilon c3 + \left(\varepsilon cu3 - \varepsilon c3\right)\right)}{\varepsilon cu3}$$

$$\beta := \frac{1}{\varepsilon cu3}\left(\frac{1}{0.5\cdot\varepsilon c3 + \left(\varepsilon cu3 - \varepsilon c3\right)}\left(0.5\cdot\varepsilon c3\cdot\left(\frac{1}{3}\cdot\varepsilon c3 + \left(\varepsilon cu3 - \varepsilon c3\right)\right) + 0.5\cdot\left(\varepsilon cu3 - \varepsilon c3\right)\cdot\left(\varepsilon cu3 - \varepsilon c3\right)\right)\right)$$

Using these formulae gives: α=0.56 and β=0.34.
Now to solve the equilibrium equation N_f has to be determined. In Figure 59, the height of the tension zone is given with x_T. This value has to be written in terms of x (height compression zone), so that there's only one unknown in the equation. This can be done using the strain diagram also seen in Figure 59: $x_T = \varepsilon_{ctu} * x / \varepsilon_{cu3}$.
Because N_f hasn't got a constant shape, it needs to be split in three components: N_{f1}, N_{f2} and N_{f3}.

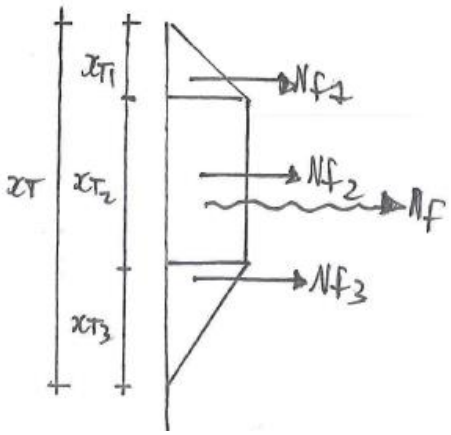

Figure 60: Components of N_f

All these components and also their lengths (Figure 60) have to be expressed in terms where x is the only unknown:

$$xT1 := \frac{xT\cdot\varepsilon ct}{\varepsilon ctu}$$

$$xT2 := \frac{xT\cdot\left(\varepsilon ctd - \varepsilon ct\right)}{\varepsilon ctu}$$

$$xT3 := \frac{xT\cdot\left(\varepsilon ctu - \varepsilon ctd\right)}{\varepsilon ctu}$$

$$Nf1 := \frac{0.5\cdot fctd\cdot b\cdot x\cdot\varepsilon ct}{\varepsilon cu3}$$

$$Nf2 := fctd\cdot b\cdot\frac{x\cdot\left(\varepsilon ctd - \varepsilon ct\right)}{\varepsilon cu3}$$

$$Nf3 := 0.5\cdot fctd\cdot b\cdot\frac{x\cdot\left(\varepsilon ctu - \varepsilon ctd\right)}{\varepsilon cu3}$$

Combining the x_T components gives the already calculated x_T value of $\varepsilon_{ctu}*x/\ \varepsilon_{cu3}$.
And for N_f one gets by combining the three components a total of:
$N_f = 0.5 * (1/\ \varepsilon_{cu3})* x * f_{ctd} * b * (\varepsilon_{ctu} + \varepsilon_{ctd} - \varepsilon_{ctu})$.

N and N_s are determined the same way as with C50/60:
$N_c = \alpha*f_{cd}*b*x$
$N_s = A_s*f_{yd}$

Filling everything in the equation gives for x:

$$x = \frac{A_s * f_{yd}}{b * (\alpha * f_{cd} - \frac{1}{\varepsilon_{cu3}} * f_{ctd} * (\varepsilon_{ctu} + \varepsilon_{ctd} - \varepsilon_{ct})} = 83.21\ mm$$

x_T = 720.11 mm

Now that everything is determined, the bending moment capacity can be calculated:
$M_{Rd} = N*x*(1-\beta) + N_f*a + N_s*(0.9h-x)$.
a is the distance of the N_f resultant to the neutral axis:

$$a := \frac{\left(\frac{Nf1 \cdot 2}{3} \cdot xT1 + Nf2 \cdot (0.5 \cdot xT2 + xT1) + Nf3 \cdot \left(\frac{1}{3} \cdot xT3 + xT2 + xT1\right)\right)}{Nf}$$

Solving this equation gives a=305.83 mm
Filling everything in in the equation for M_{Rd} gives a moment capacity of:
M_{Rd} = 1029.16 kNm

Unity check: M_{Ed}/M_{Rd} = 562.5/1029.16 = 0.55. The structure is safe enough.

A7.4.3 Comparison M_{Rd}

When comparing the moment capacities of C50/60 and C170/200 it is obvious that UHPC outperforms ordinary concrete. The structure in ordinary concrete wasn't safe enough to resist the bending moment with its initial reinforcement, while the structure in UHPC can easily take the design moment.

A7.5 Shear capacity

For both types of concrete the shear capacity has to be calculated. First the shear capacity of C50/60 will be determined and afterwards the shear capacity of C170/200.

A7.5.1 V_{Rd} C50/60

In Eurocode 2 a formula is given in §6.2.2 to determine the shear capacity of a concrete structure. This shear capacity has to be larger than the design shear force. So: $V_{Rd} \geq V_{Ed}$.
The Eurocode states that:

$V_{Rd,c} = [C_{Rd,ck}*(100*\rho_l*f_{ck})^{1/3} + k1*\sigma_{cp}]* b_w*d$

with a minimum of
$V_{Rd,c} = (v_{min} + k1*\sigma_{cp})* b_w*d$ and $v_{min} = 0.035*k^{1.5}*f_{ck}^{0.5}$

Since there is no prestressing, the term $k1*\sigma_{cp}$ is left out.
$C_{Rd,ck} = 0.18/ \gamma_c = 0.12$
$\rho_l = A_s/(b_w*d) = 0.0022$
$d=0.9h = 900$ mm
$k=1+(200/d)^{0.5} = 1.471$

Filling this in the formulae gives:
$V_{Rd,c} = 177.3$kN and $V_{min} = 198.8$kN. So this means $V_{Rd,c} = 198.8$kN
The design shear force was determined earlier and is 225kN.

Unity check: $V_{Ed}/V_{Rd,c} = 1.13$. Clearly the structure does not suffice. So shear reinforcement needs to be applied. This will not be done here in the example.

A7.5.2 V_{Rd} C170/200

When determining the shear capacity for UHPC one must also now take into account the fact that there are steel fibres in the concrete. Determining the shear capacity is done according to AFGC 2013. These recommendations state that the shear capacity is:
$V_{Rd} = V_{Rd,c} + V_{Rd,f} + V_{Rd,s}$ with:

$V_{Rd,c}$ = the contribution of the concrete
$V_{Rd,f}$ = the contribution of the steel fibres
$V_{Rd,s}$ = the contribution of shear reinforcement (which is not used in this example so it's left out)

For a reinforced section $V_{Rd,c}$ is:
$V_{Rd,c} = (0.21/\gamma_{cf}\gamma_e)*k*f_{ck}^{0.5}*b_w*d$
with
$\gamma_{cf}\gamma_e = 1.5$
$k=1+3*\sigma_{cp}/f_{ck}$ (since there is no prestressing k=1)

So $V_{Rd,c} = 821.4$kN

Now the steel fibres term $V_{Rd,f}$ has to be determined. AFGC states that:
$V_{Rd,f} = A_{fv} * \sigma_{Rd,f}/\tan\theta$
With
A_{fv} (area of fibre effect) = b_w*d
θ (angle between principal compression stress and beam axis) = 30
$\sigma_{Rd,f}$ (residual tensile strength) = $\frac{1}{K*\gamma_{cf}} * \frac{1}{w_{lim}} * \int_0^{w_{lim}} \sigma_f(w)dw$

with $K=K_{global}1.25$ and γ_{cf}.

The integral basically stands for the area under the tension part of the stress strain diagram in figure 67b. The area taken into consideration is from the part where the first crack occurs (ε_{ct}) until there where w=0.3mm ($\varepsilon_{ct,0.3}$). So $\sigma_{Rd,f}$ becomes:

$$\sigma_{Rd,f} = \frac{1}{K * \gamma_{cf}} * \frac{1}{\epsilon_{ct,0.3} - \varepsilon_{ct}} * [f_{ctk} * (\varepsilon_{ct,0.3} - \varepsilon_{ct})]$$

When everything is filled in the formula: $\sigma_{Rd,f}$ = 3.79 N/mm^2.
Now that all the variables are determined, $V_{Rd,f}$ can be calculated:
$V_{Rd,f}$ = 2658,2 kN.

Combining the shear capacity terms gives:
V_{Rd} = 3479.7 kN

Unity check: $V_{Ed}/V_{Rd,c}$ = 0.07. It is quite obvious that the structure is more than safe.

A7.5.3 Comparison V_{Rd}

It definitely shows that UHPC is much stronger, concerning shear, than ordinary concrete. Actually for this case even without steel fibres the UHPC variant suffices for shear capacity.

A7.6 Influence variables

All in all this example shows that structurally UHPC is much stronger than ordinary concrete.
But for research purposes it is also interesting to find out what the influences of certain variables are in the determination of the moment and shear capacity for UHPC. Examining these influences now can be useful, for the main research in the thesis for example in the optimization faze. While making calculations for this example, it was noticed that a couple of parameters had a large influence on the final result of the moment and shear capacities. These were:
The height (h), the width (b), the amount of reinforcement (A_s) and the length of the steel fibres (l_f).
So these are the parameters which are going to be changed to see their influences.
While changing parameters it is important to make sure that the height of the tension and compression zone stay within the limits of the height of the cross section. So: $x + x_T \leq 0.9h$

The starting values for the iteration are:
h: 1.0 m
b: 0.5 m
l_f: 60 mm
A_s: 1000mm^2

A7.6.1 Influence on Moment capacity

In Table 4 the iteration process that is made for the moment capacity is seen. The process starts by changing one variable, while keeping the others constant. Then slowly other variables are changed as well.

Table 4: Iteration process

	start	1	2	3	4	5	6	7	8	9	10	11	12	13
H	1	0,9	0,9	0,9	1,1	1,1	1	1	1	1	1	1	1	1
B	0,5	0,5	0,5	0,5	0,5	0,5	0,4	0,4	0,6	0,6	0,5	0,5	0,5	0,5
Lf	60	60	50	50	60	60	60	50	60	60	50	50	60	60
As	1000	1000	1000	1200	1000	1600	1000	1450	1000	1300	1000	1800	900	1200
x+xT (mm)	803,32	1210	633	760	602	963	1004	876	669	870	483	870	723	884
MRd (kNm)	1029	-	766	1020	809	1658	-	1243	923	1407	649	1538	869	1202

Influence of changing the height

First the height has been manipulated. Lowering the height by 100mm results in a too high tension and compression zone, because a lower height causes a higher ε_{ctu}, which leads to a higher tension zone. But lowering the length of the steel fibres to 50mm leads to a lower height of the zones, but also a lower M_{Rd}. Lowering the l_f allows using more steel bars.

On the other hand, increasing the height to 1.1m leads to a smaller tension and compression zone. And since the cross section is higher the zone limits increase as well. Adding extra reinforcement as well (up to 1600mm^2) increases the moment capacity from 1029 to 1658 kNm.

Influence of changing the width

Lowering the width down to 0.4m instead of 0.5m, will result in a higher compression zone. Together with the tension zone height (which also increases) it surpasses the allowed limit of 0.9h. As with the height manipulation, decreasing the length of steel fibres to 50mm, will lead to a lower compression and tension zone height. Even though this also lowers the moment capacity, adding extra reinforcement can further increase the moment capacity (with a maximum of 1450 mm^2 the resulting M_{Rd} = 1243 kNm)

Increasing the width, leads to a lower compression zone, so a lower tension zone as well. Because the moment capacity decreases as well, extra reinforcement can be placed to make it as high as possible.

Influence of changing length of steel fibres

As already noticed while changing the height and width, if the length of the fibres is changed (in the earlier case lowering the length, because steel fibres are in practice 60mm long at most), it will lead to a smaller tension and compression zone. This is because the steel fibres have a direct influence on the limit tensile strain ε_{ctu}. Smaller fibre length, leads to a lower ε_{ctu}, and this eventually leads to a lower tensile zone height.

In this case only lowering l_f lowers the total zone height of tension and compression by almost 300mm. This also leads to a lower moment capacity. But adding reinforcement (up to 1800mm^2) can drastically increase the eventual moment capacity (=1538 kNm).

Influence of changing amount of reinforcement

Changing the amount of reinforcement has also already been done. As seen earlier, increasing A_s (while making sure that the compression and tension zone don't surpass 0.9h) together with changing others variables leads to a higher moment capacity. However it doesn't only increase the moment capacity but also the compression zone (more steel means more tension, so more compression is needed to balance the forces. So in contrast, decreasing A_s means a lower compression zone and a lower moment capacity. Furthermore it was noticed that increasing the height and/or decreasing the length of steel fibres results in a higher maximum allowed A_s.

A7.6.2 Influence on shear capacity

In contrast to the moment capacity, the shear capacity isn't highly influenced by the four parameters. Of course, lowering and raising the height and width have an influence, for example if you lower the height (and/or width) the total area of the cross section decreases, which leads to a lower shear capacity of the concrete and steel fibre part. And the opposite occurs if you raise the height (and/or width). But the amount of steel reinforcement has no influence on the shear capacity; because the formulas used for determine the shear capacity don't take the reinforcement bars into account. Also the length of the steel fibres doesn't have an influence on the shear capacity. If one looks at the formula for the shear capacity of the steel fibre part, it is seen that the residual tensile strength only takes into account the area under the diagram until the strain at w=0.3mm is reached. Since l_f only influences the limit strain and not the one at w=0.3mm, the residual tensile strength won't change with changing l_f.

So in short the shear capacity is only influenced by manipulation of the height and width of the cross section.

A7.7 Conclusion calculation example

This calculation example made a comparison between ordinary concrete and UHPC in terms of moment and shear capacity. The results have shown that UHPC indeed has a higher moment capacity than ordinary concrete and an even more impressive shear capacity compared with normal concrete.

As for the influence of the variables, looking at the moment capacity the length of the steel fibres has the biggest influence on the final value of the capacity. Manipulating l_f leads to the biggest changes for the limit strains, compression and tension zone heights and finally the moment capacity. When optimising the structure for the moment capacity, one must realise what is more important: saving money on concrete or reinforcement. And this goes down to the costs of each material. Because UHPC is an expensive material compared to reinforcement or steel fibres, it is best to reduce the amount of UHPC needed. And in order to keep the moment capacity high, an optimal balance between the amount of steel fibres (and the length of them) and the reinforcement has to be found. And since the shear capacity is also influenced by the cross sectional area, it has to be taken into account that lowering the amount of UHPC used also lowers the shear capacity.

A8. Conclusion, considerations and continuation

A8.1 Conclusion and considerations

For the master thesis an extensive literature study has been performed to get a better understanding on the phenomenon Ultra High Performance Concrete (UHPC).

For the literature study first information has been sought on what UHPC is, so what is the mixture composition, what are the properties of UHPC, how does UHPC differ from ordinary and high strength concrete etc. UHPC stands out form other concrete types by having a very high compressive strength up to 200 MPa and by having an exceptional tensile behaviour over other concrete types. Also the durability of UHPC is very good. It is important to realize though that UHPC is quite more expensive than ordinary concrete. Its materials cost more and the production costs more as well. So even though for the total life span UHPC can cheaper, it is still very important to save as much material as possible.

General information about bridges (types, construction methods, structural systems etc.) has been gathered as well to have something to reference to and use when making choices for the Leiden Bridge design.

Information was also gathered on reference projects of UHPC in structures, especially in bridge structures and also about performed studies on UHPC, where the emphasis lied on bridge application. These reference projects and researches showed that UHPC can be applied successfully in bridge structures and using UHPC instead of ordinary or high strength concrete can save a lot of concrete material needed.
From the reference projects and discussed studies there are a couple of points that should be taken into account when performing the main thesis research namely:

- In earlier projects the girders used in the bridges were not always as optimized as possible. In order to use the UHPC as efficient as possible, it will be important to further optimize and slim down the girders in the design.
- UHPC can result in slender structures this could result in a shift where fatigue and dynamic loading become governing for the design. So attention should be paid to the dynamic behaviour.
- For bridges between 25 and 30 meters girder sections will save the most material and box section provide the highest slenderness. So when choosing an appropriate bridge type, this statement could be taken into account.

Some information was gathered about structural optimization. It is likely that a form of optimization is going to be used during the thesis, so it is important to have a basic understanding about optimization methods and the tools available for it. In this thesis sizing optimization could be very relevant for making a slender cross section. Also topology optimization could prove its use when trying to reduce material in girders. And it also can be used to make the bridge aesthetically more pleasing, as topology optimization creates unusual shapes. For this the SIMP method or even the ESO method would be the most straight forward ones to use. So it will be important to use a FEM program that supports these topology optimization tools.

Lastly a calculation was made to compare the structural behaviour of ordinary concrete and UHPC. Here only moment and shear capacity were taken into account. It became clear that the calculation method for UHPC differs from the method for normal concrete. This is mainly due to the fact that the tensile capacity is taken into account for UHPC. And also the fact that UHPC contains steel fibres, which benefit a lot for the shear capacity.

The calculations showed that UHPC has a much better moment and especially shear capacity. For future calculations during the main thesis, this calculation example can be used as reference and also further expanded to also incorporate prestressing. Furthermore it will be very important to pay close attention to the heights of the tension and compression zones. Found out was that these are greatly influenced by certain factors, especially the length of the steel fibres.

All the considerations made and lessons learned during the literature study should aid in making a feasible design for the new Leiden Bridge. This design must satisfy the most important demands given which are:

- The architectural view needs to remain unaltered. For the bridge design this will mean that the construction height will stay the same as the current height. And it will mean that the intermediate pier must remain in its place. (However it doesn't have to be used structurally wise).
- There has to be as less traffic disruption as possible. Especially for the public transport. Restricting its access for a long time can bring high costs.

A8.2 Continuation

With the literature study completed the actual main thesis can commence, were the first objective is to analyse the current bridge and make choices concerning the bridge type and construction method. Then a design will be made in ordinary concrete followed by a design in UHPC. The design in UHPC will be optimized further to make better use of the material. Lastly all the designs will be compared to one and other and conclusions will be drawn from this. This method of approach is discussed more detailed in the proposal which is a separate document.

A9. Summary literature study

All mentioned points in the summaries in the different chapters are collected here for future quick reference. The points mentioned in this chapter are considered the most useful findings of the literature study for the main research.

- Advantages UHPC
    - High strength properties
    - Great ductility
    - Outstanding durability and sustainability
    - No need for mild and shear reinforcement
    - Very slender structures possible.

- Disadvantages UHPC
    - UHPC is more expensive that ordinary concrete (Slender materials so less concrete necessary)
    - Longer production times due to longer mixing (optimize mixture packing)
    - Steel fibres decrease workability (use more short fibres and finer materials)
    - Hard to control orientation of steel fibres (Use horizontal casting)
    - Worse fire resistance than ordinary concrete (use PVA fibres)
    - High early shrinkage and creep (can be controlled and reduced by using steam based curing)
    - Possibility of insufficient resistance against dynamic loads due to higher slenderness.

Concerning application of UHPC
- Through the years UHPC has successfully been applied in structures both structurally and architecturally wise.
- In a couple of projects the newly developed Pi-girder has been used, which optimally used the UHPC material properties.
- UHPC will provide the lightest structures compared to conventional concrete and steel
- The high slenderness that can be achieved with UHPC will lead to dynamic behaviour issues, which need to be resolved, with dampers.
- Modular UHPC segments can be used in structures for a faster execution.
- The older bridge projects haven't used fully optimized UHPC girders, but existing girders that were slightly modified.

Concerning researches on UHPC
- In general UHPC has better material properties (structural, durability) than normal strength and high strength concrete.
- Box sections provide highest span-to-depth ratio and girder sections save most material volume per span length.
- Using UHPC in bridge structures will require a lesser amount of girders compared to HSC and smaller sections as well. Both will lead to a concrete volume reduction. Using less and smaller girders can result in an increase in prestressing cables per girder.
- Besides volume reduction, using UHPC over HSC results in a high increase in span length.
- UHPC has higher material and production costs than normal concrete. However when the complete life cycle is considered, UHPC becomes cheaper (after 100+ years), due to the longer life span and less maintenance needs.

- Researchers concluded that further optimization is required for the use of UHPC in structures. Options for optimization can be:
    - Optimizing cross section (construction height, web/flange thickness)
    - Optimising amount of girders
    - Optimizing concrete composition and production process

Concerning design in UHPC

- The steel fibres provide a high ductility. This allows for the use of the tensile capacity of UHPC.
- The consideration of the high tensile capacity leads to a better bending moment and shear resistance.
- The length and amount of the steel fibres will have an positive influence on crack propagation and distribution, by resulting in well distributed micro cracks.

A10. Reference list

Literature

[1] **Aitcin**, P., Adeline, R., *"The Sherbrooke Reactive Powder Concrete Footbridge"*, Structural Engineering International 2/98, pp140-144

[2] **Almansour**, H., Lounis, Z. (2008), "Innovative Design of Precast/Prestressed Girder Bridge Superstructures using Ultra High Performance Concrete", Canada.

[3] **Behloul**, M., Lee, K.C., *"Ductal Seonyu Footbridge"*, Structural Concrete No 4 2003, pp195-201.

[4] **Bierwagen**, D., Abu-Hawash, A. (2005), *"Ultra High Performance Concrete Highway Bridge"*, Iowa State University, USA.

[5] **Christensen**, P.W., Klarbring, A. (2009), *"An Introduction to Structrural Optimization",* Springer Science+ Bussiness Media B.V.

[6] **Chuang**, E. Y., Ulm, F. J. (2002), *"Two-phase composite model for high performance cementitious composites",* Journal of Engineering Mechanics, vol. 128, no. 12, pp. 1314–1323.

[7] **Degen**, B.E. (2006), "Shear Design and Behavior of Ultra-high Performance Concrete", Iowa State University, USA.

[8] **Fehling**, E. et al. (2008), *"The 'Gärtnerplatzbrucke', Design of first hybrid UHPC-steel Bridge across the River Fulda in Kassel Germany",* Proc. Second International Symposium on Ultra High, Performance Concrete, pp 581-588, Kassel, Germany.

[9] **Graybeal**, B.A. (2005), "Characterization of the behavior of ultra-high performance concrete", University of Maryland, College Park, USA.

[10] **Griede**, M. (2013) *"Programma van Eisen Brug 174 Versie 1.6",* Dienst Infrastructuur Verkeer en Vervoer, Gemeente Amsterdam.

[11] **Gunes**, O. et al. (2012*), "Use of UHPC in Bridge Structures: Material Modelling and Design."* Advances in Materials Science and Engineering 2012, pp 1–12.

[12] **Iowa State University** (2009), *"Design and Evaluation of a Single-Span Bridge Using UHPC",* USA.

[13] **Kenter**, R.J.A (2010) "Master Thesis: The elevated metro structure in concrete, UHPC and composite", TU Delft.

[14] **Mazzacane**, P., Riccioti, R., Teply, F., *"La Passerelle des Anges",* UHPFRC 2009 November 17th & 18th, Marseille, France.

[15] [**Nematollahi**, B., Saifulnaz, R. M. R.., Saleh Jaafar, M., Voo, Y. L. (2012), *'A review on ultra-high performance 'ductile' concrete (UHPdC) technology',* International journal of civil and structural engineering, Volume 2, no 3, 2012, pp 1003-1018.

[16] **Paskvalin**, A (2013), "Case assignments 1-4 for CIE5127 Concrete Bridges", TU Delft.

[17] **Perry**, V.H., Zakariasen, D**. "**First Use of UHPFRC in Thin Precast Concrete Roof Shell for Canadian LRT Station", PCI Journal, Sept-Oct 2005, pp50-67.

[18] **Piotrowski**, S., Schmidt, M. (2012) *"Life cycle cost analysis of a UHPC-Bridge on Example of two Bridge Refurbishment Designs",* Proceedings of Hipermat 2012 3rd international Symposium on UHPC and Nanotechnology for High Performance Construction Materials, pp 957-964.

[19] **Ricciotti**, R. *"Stade Jean Bouin, a successful expansion"*, Ductal Solutions, September 2012.

[20] **Rouse**, J., Wipf, T.J., Phares, B., Fanous, F. and Berg, O. (2011), "Design, Construction, and Field Testing of an Ultra-High Performance Concrete Pi-Girder Bridge", Iowa State University, USA.

[21] **Rozvany**, G.I.N., (2001) "Aims, scope, methods, history and unified terminology of computer-aided topology optimization in structural mechanics", Struct Multidisc Optim 21, pp90-108.

[22] **Van der Broek**, B. (2012) *'Constructieve beoordeling van brug 174 – De Leidsebrug',* Ingenieursbureau Gemeente Amsterdam.

[23] **Schmidt**, M., Jerebic, D (2008), *"UHPC: Basis for Sustainable Structures – the Gaertnerplatz Bridge in Kassel",* Proc. Second International Symposium on Ultra High, Performance Concrete, pp 619-625, Kassel, Germany.

[24] **Sorelli** et al. (2007), "Optimal Design of UHPC Highway Bridges Based on Crack Criteria", CONSEC'07, Tours, France.

[25] **Taylor**, C., Weldon, B., Jáuregui, D., Newtson, C. (2013). *"Case Studies Using Ultrahigh-Performance Concrete for Prestressed Girder Bridge Design.",* Pract. Period. Struct. Des. Constr., 18(4), 261–267

[26] **Toutlemonde**, F., Resplendino, J. (2011) "*Designing and Building with UHPFRC"*, ISTE Ltd and John Wiley & Sons Inc., UK and USA.

[27] *"FDN SUSTAINABLE UHPFRC BRIDGES - FiB 2014 FDN Modular UHPFRC bridges",* FDN Engineering, Amsterdam, The Netherlands.

[28] "FHWA, Iowa optimize pi girder", Aspire, winter 2010, pp 24-29.

[29] Symposium UHSB 2014, 27-02-2014, Delft, the Netherlands.

[30] Reader Concrete Bridges CIE5127

Internet pages

[i1] www.ushb.nl, last modified 2012, last seen 15-4-2014.

[i2] http://www.steelconstruction.info/Bridge_articulation_and_bearing_specification last seen 30-04-2014

[i3] http://carat.st.bv.tum.de/caratuserswiki/index.php/Users:Structural_Optimization/General_Formulation, last modified 30-08-2010, last seen 19-05-2014

A11. List of Figures

A12. List of Tables

B. Elaboration load cases and load combinations

There are multiple load cases and load combinations present on the bridge. These loads will not occur exclusively. Therefore it is important to determine the correct load cases and combinations. These will be used to develop a model in SCIA Engineer to then determine the forces on the bridge.

B1 General load cases

Basically the following load cases will occur on the bridge. These are valid for all designs:

Permanent loads:
- LC1: Self-weight girders
- LC2: Dead load
  - Pavement
  - Asphalt
  - Concrete filling around tram rails
- LC3: Steel railing and natural stone elements (Edge load)

Variable loads:
- LC4&5: Traffic loads with presence of trams (UDL & tandem axle)
- LC6&7: Traffic loads with absence of trams (UDL & tandem axle)
- LC8: Tram-axle loads (No UDL specified for tram loads)
- LC9: Pedestrian loads over whole width (crowd loading)
- LC10: Pedestrian loads on designed locations.
- (LC11: Wind loading)
- (LC12: Temperature loading)

The static loads are quite straight forward to determine. The variable loads however need to be expanded further based on the design codes. Already a division is made for traffic loads. These can occur in presence or absence of tram loading. For example when trams are not present, vehicles (also including transportation buses) can drive over the tram lanes. When trams are present, vehicles only drive on their designated lanes. Furthermore the tandem axles for the traffic loads can appear at multiple different locations over the bridge lengths. All of these have to be checked and then determined which position is the governing one for bending moments and shear forces. The road layout is changeable so for the traffic (and also tram) loads it is important to take into account the layout which has the most negative impact on the structure. For the Leiden Bridge this is the case when the traffic lanes are the closest to the edge of the bridge. So at least for these variable loads this situation has to be taken into account.

Pedestrian loads are also divided over the width of the bridge. Usually pedestrians only walk on the pavement, but on rare occasions (such as festivities) it can be possible that the bridge is fully crowded. This last situation has to be taken into account as well. For the pedestrian loads the planned pavement lay-out will be used to determine the loads.
Even though wind and temperature loading are mentioned, these will not be taken into account for this design. That's because the Leiden Bridge is situated low to the ground and because the bridge is very wide so the wind loads won't have a governing effect as with for example high viaducts. If the bridge is simply supported the bridge has no restriction to expand and contract so temperature will not have large effects on the bridge. But if the bridge is designed with fixed supports (for example integral bridges), then the temperature will have a large effect.

B2 Static loads

LC1 - Self-weight

The self-weight of one girder is calculated by taking the area of the cross section and multiplying it with the volumetric weight of concrete (25kN/m^3).

LC2 - Dead load

With dead load meant is all the surfacing layers placed on top of the bridge. This includes pavement, asphalt and infill concrete. These layers can be seen in Figure B-1 along with the heights of each layer. For asphalt and pavement a weight of 23 kN/m^3 is assumed and for the infill concrete 24 kN/m^3. The thickness of the layers is based on the current thicknesses.

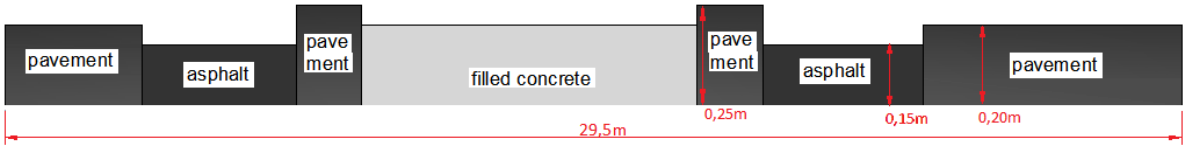

Figure B-1: Thickening layers

LC3 - Edge load

The steel fences and natural stone elements on the edges of the bridge represent the edge load. This load is taken 2.0 kN/m.

B3 Variable loads

For the variable loads the calculation methods are given in various Eurocode documents. These documents explain how to calculate a certain variable load. Their calculation method will be elaborated further in the following.

LC4-7 - Traffic loading

NEN-EN-1991-2 + C1 chapter 4 gives four load models concerning traffic loading:

- LM1: General (normal) loading due to lorries or lorries plus cars
- LM2: A single axle for local effects
- LM3: Special vehicles for the transportation of exceptional loads
- LM4: Crowd loading

For structural calculations Load Model 1 is the most governing model. Especially since for the Leiden Bridge it is unlikely that special vehicles will cross the bridge. Load model 1 consists of a uniform distributed load (α_{qi}*q_i) plus a tandem axle loading (α_{Qi}*Q_i). To determine these values the bridge deck has to be divided into theoretical lanes first. Each lane is 3m wide. The division goes as follows:
1 lane if w ≤ 5.4m
2 lanes if 5.4m < w ≤ 9m
3 lanes if w > 9m
w is the total width of the bridge deck. This total width only takes the parts between the safety rails into account. Which means for the Leiden Bridge the total width goes from fence to fence. In Figure B-2 the lane division is showed.

This division is also used to determine how big a certain load is in each lane. The rule is that lane 1 is the most unfavourable lane. Then as the lane number increases the loads decrease. Also shown in Figure B-2 is the tandem axle distribution for LM1. Each square (400x400mm) represents a wheel on which a force of 0.5* α_{Q1}*Q_i works.

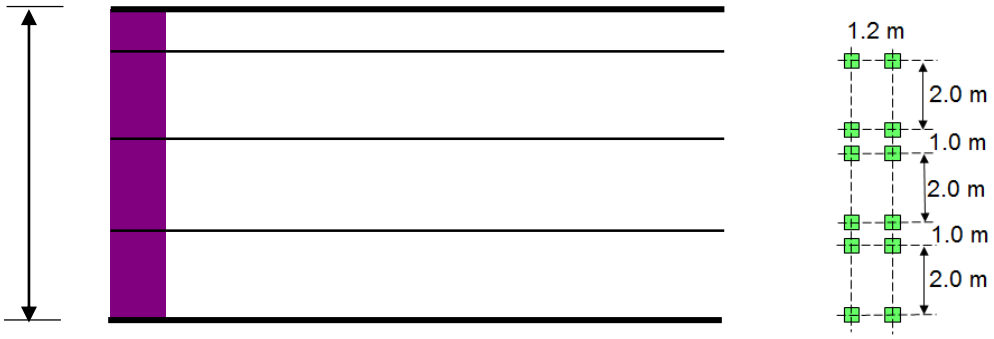

Figure B-2: Division of lanes for traffic loading and axle distribution LM1

The values for the UDL and axle loading for LM1 are given in Table B-1. The alpha values are load factors which are influenced by the traffic intensity. For general uses the factors are:
$\alpha_{Qi} = 1.0$
$\alpha_{q1} = 1.15$ all α_{qi} past this one are 1.4

Table B-1: Values UDL and axle loading

Location	Total axle load: $2*Q_i$ [kN]	UDL: q_i [kN/m^2]
Lane 1	$2*\alpha_{Q1}*300$	$\alpha_{q1}*9.0$
Lane 2	$2*\alpha_{Q2}*200$	$\alpha_{q2}*2.5$
Lane 3	$2*\alpha_{Q3}*100$	$\alpha_{q3}*2.5$
Other lanes	0	$\alpha_{qi}*2.5$
Remaining area	0	$\alpha_{qr}*2.5$

LC8 - Tram loading

No specific design rules exist for loads exerted by light rail, such as metro's and trams. But for the Leiden Bridge a tram load model is given by the GVB, the public transport company of Amsterdam, to use in calculations. This model is seen in Figure B-3. The width between two axles is 1435mm, which is the standard track gauge in the Netherlands. There are no additional load factors specified for tram loading.

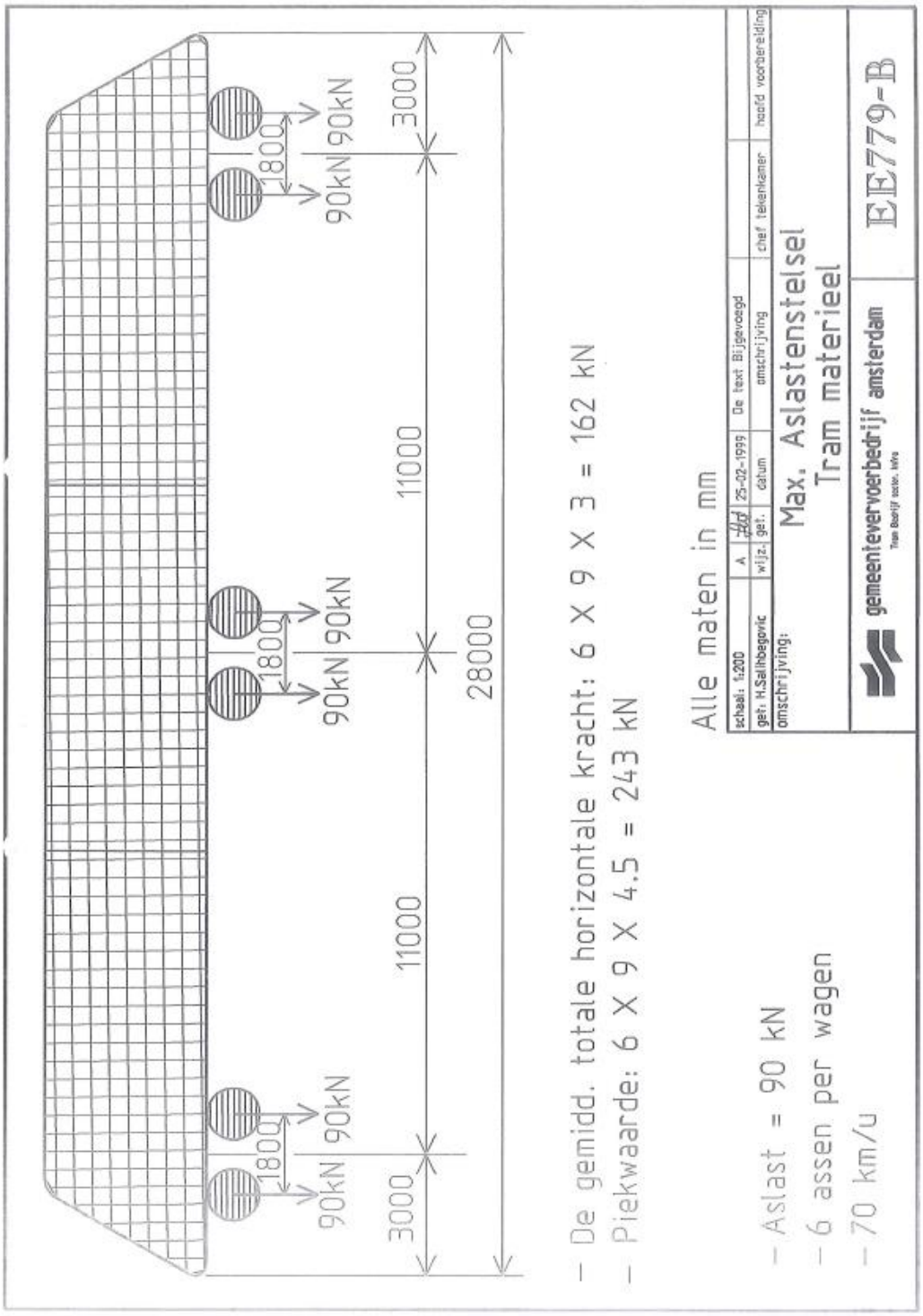

Figure B-3: Tram loading model (in Dutch)

LC9-10 - Pedestrian loading

For pedestrian loading design rules can be found in NEN-EN-1991-2+C1 chapter 5. When looking at loads caused by pedestrians the loads are categorized as:

- Group 1: Uniform distributed load, q_{fk}
- Group 2: Special vehicle loads, Q_{serv} (maintenance, emergency, etc.)

Because the bridge suffers from traffic loading only the uniform distributed load will be taken into account (since the special vehicle loads will use the same bridge locations as other vehicles). In this way the pedestrian loading is equal to Traffic Load model 4 (Crowd loading).
The value given for q_{fk} is 5.0 kN/m^2.

LC11 - Wind Loading

Wind loads can be calculated according to NEN-EN 1991-1-4. Concerning bridges the wind creates a force equal to:
$F_w = q_b(z)*A_{ref}$

With $q_b(z)$ being the basic velocity pressure and A_{ref} the reference area of the structure.
When calculating the wind action on the bridge the wind directions and notations as in Figure B-4 are applied. A_{ref} becomes d*L. For the Leiden Bridge, d consists of the girder height plus the height of the pavement. L is equal to the length of the bridge.
The velocity pressure can be determined with the Dutch National Annex of NEN-EN 1991-1-4. Amsterdam is located in wind area II. The height of the bridge above ground is assumed 2 meters. With these values $q_b(z)$= 0.58 kN/m^2.

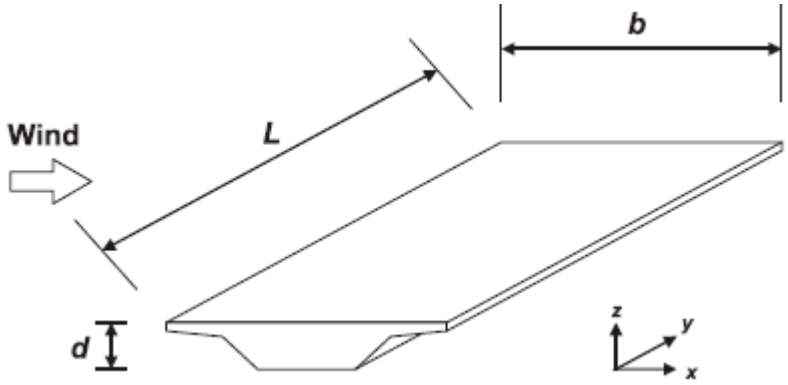

Figure B-4: Wind directions on bridge

The wind loading in the case of the Leiden Bridge is negligible compared to other variable load cases. First of all the wind force is not high and second the width of the bridge is very high which results in a high b/d ratio. Furthermore the bridge is located pretty low to the ground level. All of these make sure that the wind force hardly has an effect on the bridge.

LC12 - Temperature Loading

Temperature loading causes a temperature profile over the height of the bridge. This profile is influenced by the thickness of the bridge and also by the thickness of the surfacing layer. A temperature profile consists of a mean temperature component, a linear temperature component and an Eigen temperature component. These components for a certain case can be determined using values and procedures given in NEN-EN-1991-1-5.
The minimum and maximum temperatures are given in the Dutch NA as:
T_{min} = -25°
T_{max} = 30°

The resulting mean temperature components are (concerning a type 3 bridge):
$T_{e,min} = T_{min} + 8 = -17°$
$T_{e,max} = T_{max} + 2 = 32°$
For the reference temperature T_0 assumed is 10°. With this the mean components for heating and cooling can be determined:
$\Delta T_{N,con} = - (T_0 - T_{e,min}) = -27°$
$\Delta T_{N,exp} = T_{e,max} - T_0 = 22°$

Then for the linear temperature component ($\Delta T_{M,heat}$ and $\Delta T_{M,cool}$) two approaches are given by NEN-EN-1991-5. Here the second approach will be applied. In Figure B-5 the temperatures profiles for the linear temperature component are shown for both heating (expansion) and cooling (contraction). The ΔT_i components are determined with table B.3 in NEN-EN-1991-1-5. For this the thickness of the bridge and the thickness of the surfacing layer are necessary. The linear profile has to be divided in its own mean and linear component so that it can easily be added with ΔT_N.

Eurocode states that when both ΔT_N and ΔT_M are present, reduction factors ω_N =0.35 and ω_M = 0.75 may be applied. So this means that now the temperature component will be the governing of: $\Delta T_M + \omega_N * \Delta T_N$ or $\omega_M * \Delta T_M + \Delta T_N$

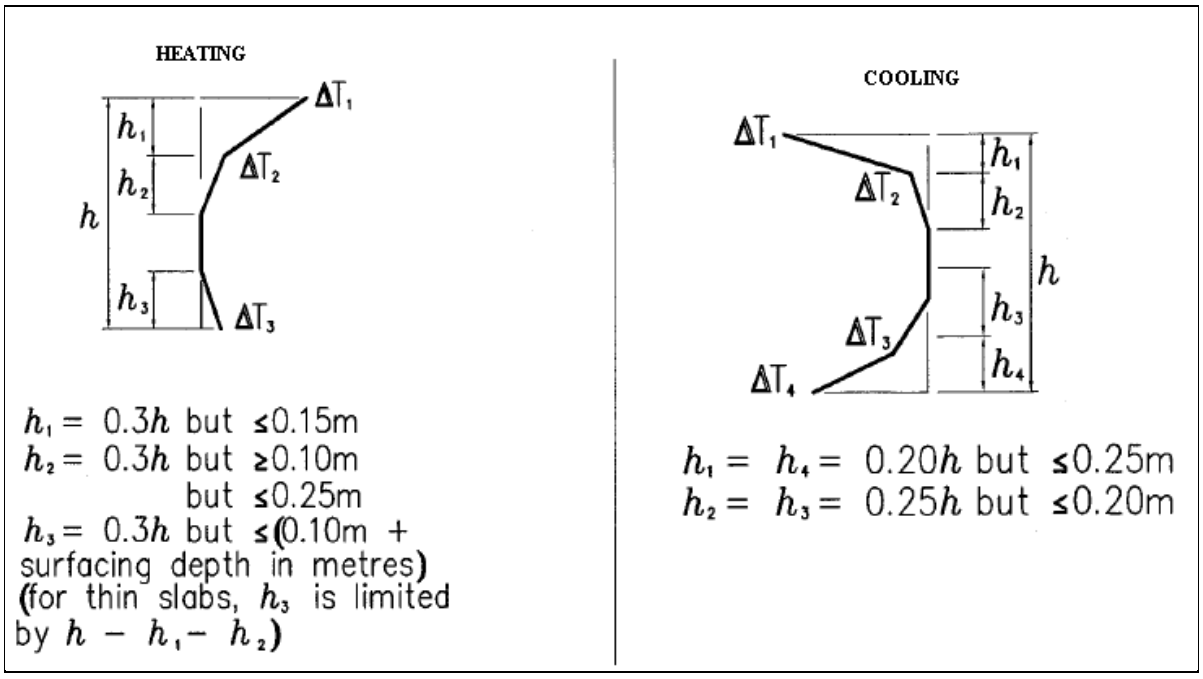

Figure B-5: Temperature profiles for linear components

B4 Application load cases in the design

LC1: Self-weight: A_c*25.0 kN/m (not used in SCIA calculation)
LC2: Dead load:
- Pavement: 4.6 kN/m^2
- Filled concrete: 4.8 kN/m^2
- Asphalt: 3.5 kN/m^2

LC3: Edge load: 2.0 kN/m
LC9-10: Pedestrian load: 5.0 kN/m^2

LC4-8 Traffic and tram load:
The total width of the Leiden Bridge (w) is calculated from fence to fence. Assumed is that the fencing system (so the railings plus kerbs) take 0,5m per side. This means that the width between the kerbs will be 29 m (as the actual width of the bridge is 30m). The number of lanes will be 29/3 = 9.67 lanes. This gives 9 lanes of 3m each plus 2m of remaining area.

There are two different combination of vehicles and trams, namely one in presence and one in absence of tram loading. So the combination without tram loading will contain 3 lanes of traffic loading tandem systems and the one with tram loading will have 1 lane with traffic loading tandem systems and 2 lanes with tram tandem systems. As for the UDL of the traffic loads, in the situation where trams are present, the UDL is not located at the positions of the tram loading. The tandem systems will be placed all on one side of the bridge, exactly against the kerb. This will present the governing situation in both load combinations. In Figure B-6 the general division of the traffic and tram loads for both combinations are shown.

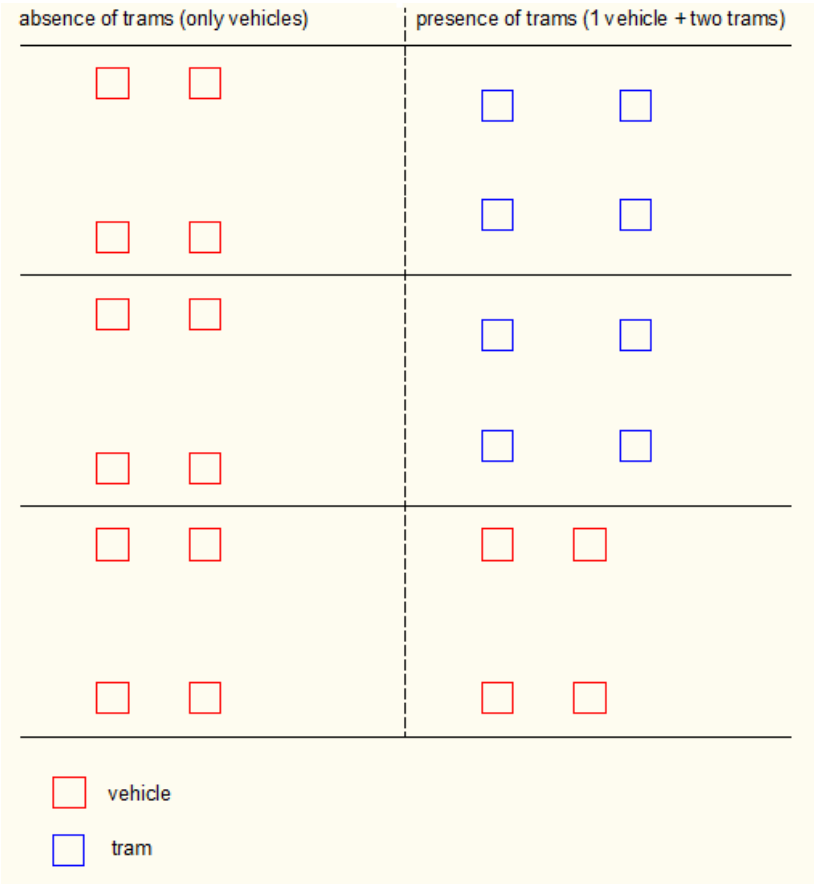

Figure B-6: Division of loads per load case

For the tandem systems it is important to calculate the effective width of each point load. This is necessary, because of the spreading of the load (in both length and width of the bridge) on the top flange of the girder. When the loads are entered in SCIA, the program will automatically spread the load to the neutral line of the structure. Only SCIA cannot take the spreading until the top flange into account. Therefore the load spreading until the centre of the top flange is determined by hand. In Figure B-7 the spreading of the forces and thus the effective width in both longitudinal and transverse direction is determined for both the traffic and tram TS. The loads including the calculated spreading will be entered in SCIA Engineer as block loads. These block loads have the size of the determined effective width as seen in Figure B-7

In theory, the same effective width and thus the same determined block load can be used in SCIA for all the designs, even though the top flanges do not necessarily have the same thickness. This is because the value of the point loads remains the same so it does not matter per se what the area of the spreading is as long as the area times the block load results in Q_i. This has been verified in SCIA Engineer. The difference in moments was around 1 kNm and the difference in shear force was around 1 kN which are both negligible differences. So for the all the designs the spreading and loads are based on Figure B-7.

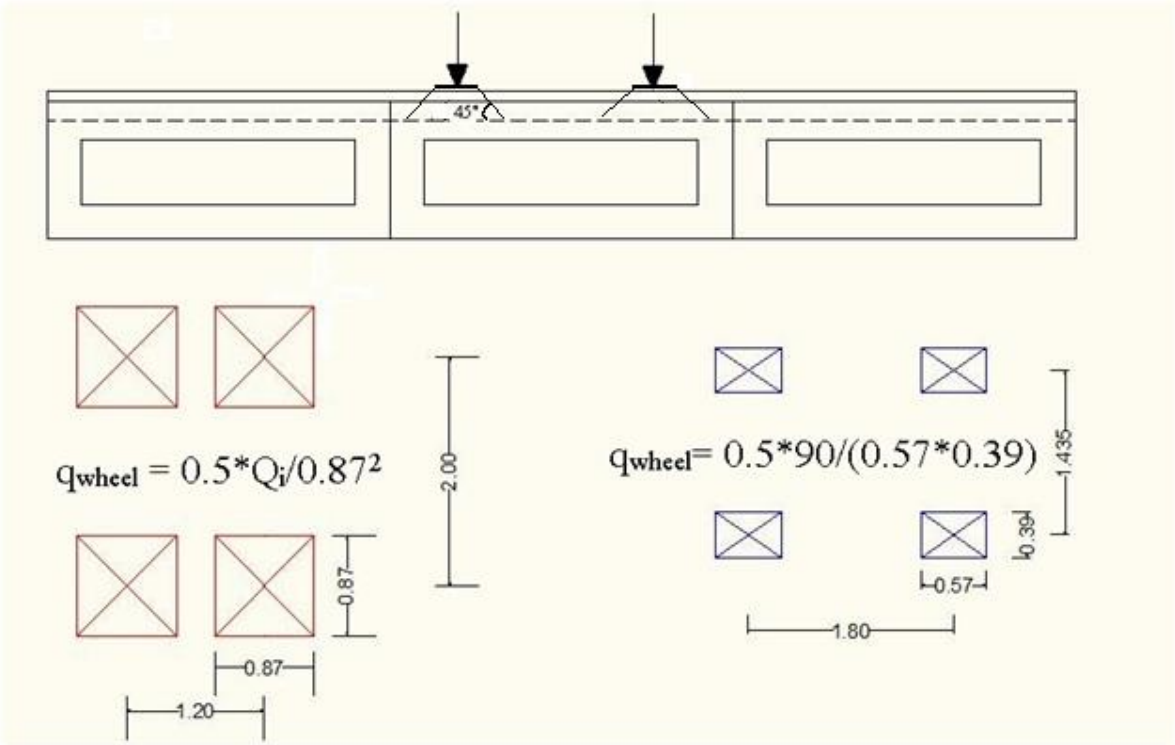

Figure B-7: Spreading of the load

The value 90 in Figure B-7 is the axle load in kN given by GVB, the Public transportation company in Amsterdam. Q_i is 300kN, 200kN and 100kN for respectively lane 1, lane 2 and lane 3.

B5 Load combinations

Already stated is that the presented load cases will not occur exclusively. So load combinations have to be made that cause the most unfavourable load situations. The bridge must also be calculated in SLS and ULS state. In general there are four combinations possible. These are given in NEN-EN-1990:

Characteristic combination (used for ULS calculations):

$$\sum \gamma_{G,j} G_{k,j} + \gamma_P P + \gamma_{Q,} Q_{k,1} + \sum \gamma_{Q,j} \psi_{0,j} Q_{k,j}$$

Characteristic combination for fatigue (given in NEN-EN-1992-1-1)

$$\sum G_{k,j} + P + \psi_{1,1} Q_{k,1} + \sum \psi_{2,j} Q_{k,j} + Q_{fat}$$

Frequent combination (used for SLS, namely crack width verification):

$$\sum G_{k,j} + P + \psi_{1,1} Q_{k,1} + \sum \psi_{1,j} Q_{k,j}$$

Quasi-permanent combination (used for SLS, namely the deflection check):

$$\sum G_{k,j} + P + \sum \psi_{2,j} Q_{k,j}$$

NEN-EN-1990 gives the load factors and the instantaneous factors for static and variable loads. These are:

	Ψ0	Ψ1	Ψ2	γ
Permanent loads (G)	-	-	-	1.2
Prestressing (P)	-	-	-	1.0
Traffic loads: LM1 - TS	0.8	0.8	0.4	1.35
Traffic loads: LM1- UDL	0.8	0.8	0.4	1.35
Tram loading: TS	0.8	0.8	0.4	1.45
Pedestrian loads	0.8	0.8	0.4	1.35

Tram loading has a factor of 1.45, because tram loading falls under the category ‘other variable loads’ in NEN-EN 1990

In total there are five main load combinations that will be investigated:

- Combination 1: Traffic loads in the presence of tram loading, where the traffic loads are the leading variable load. (1 LM1 TS + 2 tram TS)
- Combination 2: Traffic loads in the presence of tram loading, where the tram loading is the leading variable load. (1 LM1 TS + 2 tram TS)
- Combination 3: Traffic loads in absence of tram loading. (3 LM1 TS)
- Combination 4: Crowd loading
- Combination 5: Governing transverse moment (Only in HPC and UHPC design)

For the permanent loads only the unfavourable, linear situation is taken into account. Combination 5 is used to find the governing transverse moment in the structure. In order to find this moment, the traffic loads in absence of the trams are placed in the middle of the transverse direction. This will lead to the highest moment in the transverse direction as the highest loads are now right in the middle.

In Table B-2 the load combinations are presented with the load factors used in the ULS situation. Combination 5 has the same load factors as load combination 3, because the same traffic loads are used. These factors given will be entered in SCIA Engineer to find the governing internal forces in ULS.

NB. When in absence of trams the standard Load Model 1 (LM1) for traffic loads is used (So Tandem Systems (TS) in 3 lanes). However when trams are present two tandem systems are replaced with two tram tandem systems.

Table B-2: Load combinations with ULS load factors

	Load cases	Ψ0	γ	CO1	CO2	CO3&5	CO4
LC1	Self-weight	1	1.2	1.2	1.2	1.2	1.2
LC2	Dead load (pavement, asphalt, tram rails)	1	1.2	1.2	1.2	1.2	1.2
LC3	Edge loads (railing, stone elements)	1	1.2	1.2	1.2	1.2	1.2
LC4	Traffic loads| UDL| Tram present	0.8	1.35	1.35	1.08		
LC5	Traffic loads| TS| Tram present	0.8	1.35	1.35	1.08		
LC6	Traffic load| UDL| Tram absent	0.8	1.35			1.35	
LC7	Traffic loads| TS| Tram absent	0.8	1.35			1.35	
LC8	Tram loading| TS	0.8	1.45	1.16	1.45		
LC9	Pedestrian loads| Crowd loading	0.8	1.35				1.35
LC10	Pedestrian loads| Loads on designated locations	0.8	1.35	1.08	1.08	1.08	

C. Theory regarding UHPC

This appendix contains some extra information about certain aspects of UHPC that were not dealt with quite in detail in the literature study. The appendix deals with Shrinkage and creep for UHPC and some methods to determine them and also with crack width verification for UHPC, where multiple ways of verification are compared to each other.

C.1 Shrinkage and creep for UHPC

The shrinkage strain and creep-coefficient are not allowed to be determined conform the Eurocode, because UHPC behaves differently than ordinary concrete. Therefore the AFGC recommendations give recommended values for shrinkage and creep to use in preliminary studies. There is not yet one uniform method to determine the shrinkage and creep. Instead the AFGC describes a couple sets of formulas which were derived in different researches named in the recommendations and these formulas are based on the fact if the concrete was heat treated or not.
These methods will be discussed in this section to see if the methods could possibly be used in this case. However to actually determine the losses, the recommended values are used and not the values derived with the given methods.

C.1.1 Shrinkage

The main difference between UHPC and NSC lies in the fact that UHPC has a much higher autogenous shrinkage than NSC because of the very low water-cement ratio. But UHPC hardly has any drying shrinkage compared to NSC. In order for the shrinkage to occur only at the early stages of the concrete, heat treatment is applied. The AFGC describes two types of heat treatment:

- Type 1: This type of heat treatment is applied in the first few hours and corresponds to the 'heat curing' described in EN 1992-1-1, which redirects to EN 12390. Its aim is to anticipate the moment at which the UHPC starts to set and accelerate the initial hardening. The treatment is carried out at a moderate temperature.
- Type 2: The second type of treatment is applied when the concrete is hardened. Its aim is to develop new hydrates in order to further increase the mechanical strength of the cement matrix and reduce the delayed deformations. This treatment is carried out at a high temperature level of around 90°. This treatment especially enhances the strength and durability properties of UHPC and results in basically no shrinkage after treatment. Also the creep is reduced immensely. The AFGC states that the creep coefficient goes from 0.8 (without treatment) to 0.2 (type 2 treatment).

The formulas given in Annex 7 of AFGC2013 are based on experiments carried out using no heat treatment and using type 1 and 2 heat treatment (performed by Loukili[1] and CERIB[2]).
When the type 2 treatment is used, it is stated that there is no autogenous or drying shrinkage after heat treatment. So no shrinkage has to be taken into account in this case. When no treatment is applied the autogenous shrinkage is determined with (based on Loukili):

$$\varepsilon_{ac}(t) = 525 * \exp[\frac{-2.5}{\sqrt{t-0.5}}]$$

[1] **Loukili**, A. (1996) "*Etude du retrait et du fluage de bétons à ultra-hautes performances*", l'École Centrale de Nantes, France.
[2] Centre d'Etudes et de Recherches de l'Industrie du Béton

For drying shrinkage no formula is given in case of not using any heat treatment. Stated is that UHPC acts like HPC when no heat treatment is applied. For long term drying shrinkage a value of 150 microstrain is advised.

When type 1 heat treatment (based on the work of CERIB) is applied, the long term autogenous and drying shrinkage are reduced, but not enough to neglect them in the long term.

The equations for shrinkage that were developed by CERIB, are adaption of the equations in NEN-EN-1992-2 Annex B. For autogenous shrinkage:

$$\varepsilon_{ca}(t) = \beta_{ca1} * (f_{ck} - 20) * \left[\beta_{ca2} - \beta_{ca3} * e^{-\frac{t}{\beta_{ca4}}}\right] * 10^{-6}$$

And for drying shrinkage:

$$\varepsilon_{cd}(t) = \frac{K * \left[72 * e^{-0.046 * f_{ck}} + 75 - RH\right] * (t - t_s) * 10^{-6}}{(t - t_s) + \beta_{cd} * h_0^2}$$

Then the total shrinkage becomes:

$\varepsilon_{cs} = \varepsilon_{cd} + \varepsilon_{ca}$

Most of the unknown parameters are constants and given by AFGC:

β_{ca1}:	Coefficient of adjustment	0.902
β_{ca2}:	Coefficient of adjustment	2.80
β_{ca3}:	Coefficient of adjustment	2.729
β_{ca4}:	Coefficient of adjustment	103.655
β_{cd}:	Coefficient of adjustment	0.007
h0:	$2*A_c/u_c$ (from box girder)	235.5 mm
t_s:	Age at beginning of drying process	28 days
RH:	Relative humidity	50 -80%
K:	Coefficient of adjustment	4.484

The values β_{ca1} to β_{ca4} are so chosen that they result in a minimal sum of the squares of the differences between the estimation of the model and the experimental results from the beginning of the measurement until 28 days.

When the relative humidity is above 80% the drying shrinkage is set to zero. However changing the RH in the formula has a large influence on the drying shrinkage. For example, if RH=50% on t=20850 days (57 years) the shrinkage is 110 microstrain, but at RH=70% the shrinkage is 22 microstrain. Exceeding RH=75% results in a negative number so actually if RH>75% the drying shrinkage can be set to zero already instead of above 80% like stated (or assume that the concrete swells). So it is not certain how reliable the formula is for humidity other than 50% as used in the experiment. Furthermore the humidity in the Netherlands hardly ever gets lower than around 70%. For the sake of comparison assumed will be RH=70%.

Because time t is variable, the strain caused by the shrinkage can be plotted against the time. This is done in Figure C-1. Compared are the shrinkage when no treatment is used (Loukili) and the shrinkage when type 1 heat treatment is used (CERIB). The influence of the heat treatment is clearly seen, as the total strain is around 250 microstrain lower for type I treatment than for no treatment. It is also seen that most of the shrinkage occurs in the early stages. But for both situations the shrinkage is still very high compared with NSC.

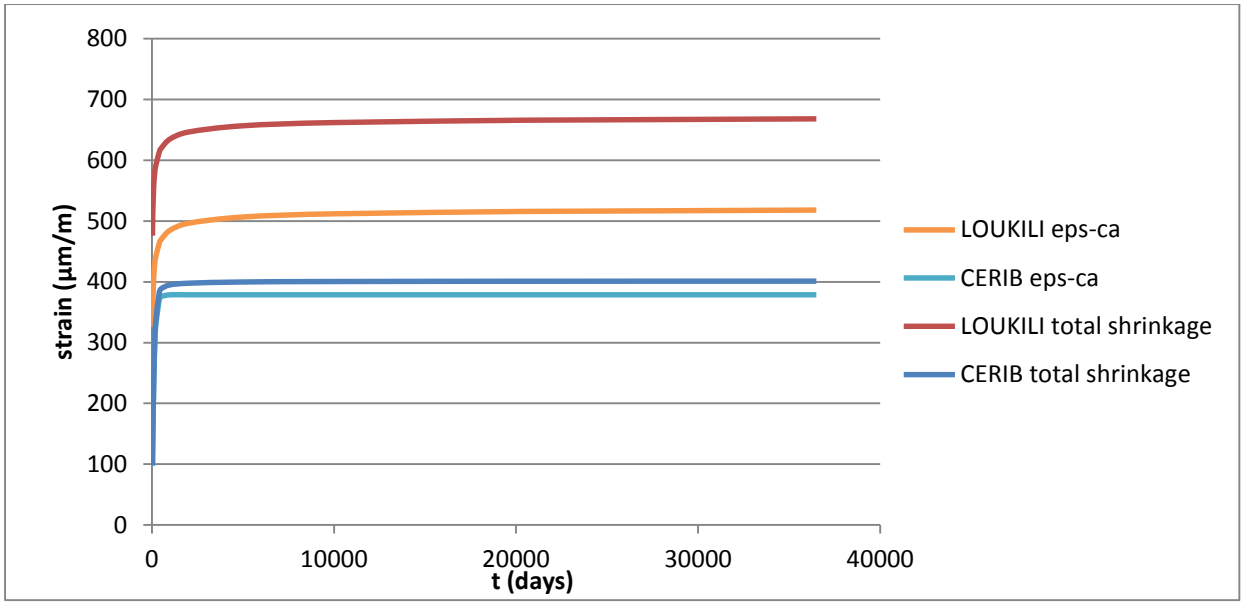

Figure C-1: Strain-time relationship for shrinkage

It can be said though that the methods show expected values, namely using heat treatment reduces the shrinkage. However the methods come from two different researches, which were not performed in a same time span (90's versus 00's). And the methods are based on solely the experiments performed in these researches. So the reliability and a link between the methods cannot be verified. And the composition of the mixture could also have an influence on the results.

C.1.2 Creep

As with shrinkage the creep has to be determined in accordance with the AFGC as well. And also here a couple of formulas based on different researches are given to estimate the creep loss. These will be discussed in this section. Different creep formulas are given for each type of treatment and for when no treatment is used:

- If no treatment is used only a formula for basic creep is given by AFGC (based on Loukili's research):

$$\varepsilon_c = \mathrm{k(t0)} * \mathrm{f(t-t0)} + \mathrm{h(t0)}$$

With:

$$\mathrm{k(t0)} = 19 * \exp * \sqrt{\frac{0.1}{\mathrm{t0} - 2.65}}$$

$$\mathrm{f(t-t0)} = \frac{\sqrt{\frac{\mathrm{t-t0}}{3\mathrm{t0}-5}}}{\sqrt{\frac{\mathrm{t-t0}}{3\mathrm{t0}-5}} + 1}$$

$$\mathrm{h(t0)} = 18 * \exp \sqrt{\frac{0.2}{\mathrm{t0}+1.2}}$$

Nothing more is stated further about the procedure for when no treatment is used so this situation will not be discussed further.

- For type I treatment (formula is made by CERIB) the total strain is given as:

$$\varepsilon_c(t,t0) = \frac{\sigma(t0)}{E_c} * [\varphi_b(t,t0) + \varphi_d(t,t0)]$$

With

$\varphi_b(t,t0) = \beta_{bc1} * \varphi_{b0} * \frac{\sqrt{t-t0}}{\sqrt{t-t0}+\beta_{bc}}$ and $\varphi_d(t,t0) = \varphi_{d0} * [\varepsilon_{cd}(t) - \varepsilon_{cd}(t0)]$

Furthermore $\beta_{bc} = \beta_{bc2} * e^{2.8*\frac{fcm(t0)}{f_{ck}}}$ And $\varphi_{b0} = \frac{3.6}{f_{cm}(t0)^{0.37}}$

t0 = 28 days so $f_{cm}(t0) = f_{cm} = 178 N/mm^2$.

The term $\phi_d(t,t0)$ is linked with the drying shrinkage. It is stated in the AFGC that this term is zero if RH>80%. But as already concluded at the shrinkage section, if RH=70% the drying shrinkage is very low. If the strain due to drying shrinkage is filled in the formula for $\phi_d(t,t0)$, one would get a negligible low value for it. So only the term $\phi_b(t,t0)$ is needed in this case. The values for the remaining parameters are:

β_{bc1}:	Coefficient of adjustment	2.49
β_{bc2}:	Coefficient of adjustment	0.71
β_{bc}:	-	13.32
φ_{b0}:	-	0.529

When everything is filled and when t=36500 days: $\phi_b(t,t0) = 1.23$

- For type II treatment the total strain is given as (Loukili):

$$\varepsilon_c(t) = \frac{\sigma_c}{E_c} * [1 + K_{fl} * f(t-t0)]$$

With K_{fl} =0.3 and $f(t-t0) = \frac{(t-t0)^{0.6}}{(t-t0)^{0.6}+10}$, t0 is the age of concrete at the beginning of loading. Assumed is t0 = 28 days. If t=36500 days is filled: $[1+K_{fl}*f(t-t0)] = 1.29$

If one looks at the factors next to the term $[\sigma_c/E_c]$ in the formulas for type 1 and 2 heat treatment then it can be seen that the factor for type 1 treatment is slightly smaller than for type 2. But according to the AFGC the creep coefficient of type 2 heat treatment is supposed to be lower than for type 1. This can be seen when the development of the coefficient is put in a graph (see Figure C-2). But it can be observed that the factor becomes steady after a while for type 2 while for type 1 there is still an increasing line even after 100 years.

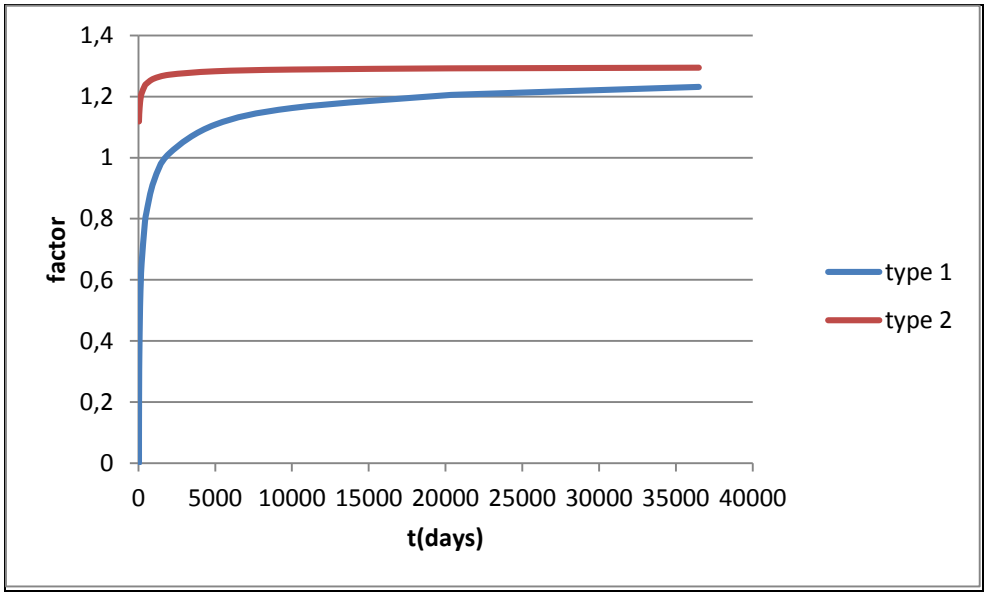

Figure C-2: Difference in creep factors type 1 and 2 heat treatments

C.1.3 Conclusion methods presented for shrinkage and creep

What can be said when looking at the results from the methods discussed? First of all it has to be remarked that there is no link between the researches performed. One research only focused on the type 1 heat treatment and here the formulas are adapted from the Eurocode and the other research only focused on the type 2 heat treatment and compared it with a case without treatment. These formulas derived are not based on the Eurocode. So this will give results that are neither quite reliable nor comparable, as for example with the creep, where the factors for type 1 and 2 were almost the same. Also a lot of parameters in all the formulas were predefined based on the experiment itself without giving a background or the method of calculation for these parameters. These parameters could prove to be case specific, as in only applicable in the research performed. And the composition of the mixtures used in the experiments are most likely not the same. The mixture usually also have an influence on shrinkage and creep.

Based on all the discussed methods and their results it is best to leave the discussion as it is and use shrinkage and creep values as recommended by the AFGC, since these give a safe value in case of a preliminary design and also because the methods are not generally accepted yet to use in calculations. Perhaps in the future it would be possible to use these formulas when more research is done. But again for now it is best to stay on the safe side and use the given values in AFGC.

C.2 Crack width verification UHPC

C.2.1 Crack width determination methods for UHPC

The inclusion of steel fibres in UHPC will result in a crack behaviour that is different than the crack behaviour of ordinary concrete. A lot of research has been done on the effect of the steel fibres on the crack behaviour, also in how to incorporate the effect of the steel fibres in the existing Eurocode formulas for determining the crack width. Literature has given different methods to determine the crack width. These will be discussed in the following, starting with the standard method from the Eurocode. The new methods for UHPC will be compared with the Eurocode and also with the AFGC, since this is the main guideline for UHPC design.

C.2.1.1 NEN-EN-1992-1-1

For determining the crack width NEN-EN-1992-1-1 paragraph 7.3.4(1) states that:
$w_k = s_{r,max}*(\varepsilon_{sm} - \varepsilon_{cm}) \leq w_{max}$

Where:
w_k is the crack opening
$s_{r,max,f}$ is the maximum crack spacing
$\varepsilon_{sm,f}$ is the mean strain of reinforcement
$\varepsilon_{cm,f}$ is the mean strain of concrete between cracks

$\varepsilon_{sm} - \varepsilon_{cm}$ can be calculated with the following expression (EN 1992 paragraph 7.3.4(2)), which is derived from the theory:

$$\varepsilon_{sm} - \varepsilon_{cm} = \frac{\sigma_s - k_t * \frac{f_{ct,eff}}{\rho_{eff}}(1 + \alpha_e * \rho_{eff})}{E_s} \geq 0.6\frac{\sigma_s}{E_s}$$

For the maximum crack spacing the following formula is given (EN 1992 formula 7.11):
$s_{r,max} = k3*c+k1*k2*k4* \phi/\rho_{eff}$

The term for $s_{r,max}$ is based on $s_{r,max} = 2*l_t$.
l_t is the transfer length which is:
$l_t = 0.25*(f_{ctm}/\tau_{bm})* (\phi/\rho_{eff})$.
So $s_{r,max}$ would be:
$s_{r,max} = 0.5*(f_{ctm}/\tau_{bm})* (\phi/\rho_{eff})$. (Usually assumed also is that $\tau_{bm} = 2f_{ctm}$)

If assumed that the mean bond stress is directly proportional to the concrete tensile strength, the term $[2*l_t]$ can be transformed in the expression from the Eurocode. Only in the Eurocode the reinforcement bar type and also the strain distribution are taken into account as they have an influence on the tensile and bond strength:
$0.5*(f_{ctm}/\tau_{bm}) \approx 0.25$ and k1*k2*k4 (for bending and high bond bars) = 0.5*0.8*0.425 = 0.17.
So the expression from Eurocode gives a lower value than 0.25, but the value is dependent on the type of bar used and also the type of loading, so the value can also be higher than 0.25. Nevertheless the terms are comparable. Furthermore the term k3*c is added as a minimum value for crack spacing, because it is stated that this will give better results (especially for high reinforcement ratios)

The maximum crack width w_{max} is given in paragraph 7.3.1, Table 7.1N in NEN-EN 1992-1-1. With the earlier described formulas the crack width can be determined. However in these formulas the effect of the steel fibres is not taken into account. Therefore the AFGC Recommendations give an alternate set of formulas for determining the crack width.

C.2.1.2 AFGC Recommendations

The expressions in the AFGC are relatable to the expressions in the Eurocode. For determining the crack width the expression used is (AFGC2013 paragraph 2.5 section 7.3.4(1):

$w_s = s_{r,max,f} * (\varepsilon_{sm,f} - \varepsilon_{cm,f})$

Where

w_s is the crack opening

$s_{r,max,f}$ is the maximum crack spacing

$\varepsilon_{sm,f}$ is the mean strain of reinforcement combined with fibres

$\varepsilon_{cm,f}$ is the mean strain of concrete between cracks

$w_t = w_s(h-x-x')/(d-x-x')$

w_t is the crack width under highest tension

h is the total height of cross section

x is the compressed height

x' is the uncracked height under tension

$w_t \leq w_{max}$

$\varepsilon_{sm} - \varepsilon_{cm}$ can be calculated with (AFGC2013 paragraph 2.5 section 7.3.4(2):

$$\varepsilon_{sm,f} - \varepsilon_{cm,f} = \frac{\sigma_s}{E_s} - \frac{f_{ctfm}}{E_{cm}} - \frac{k_t(f_{ctm,el} - f_{ctfm})(\frac{1}{\rho_{eff}} + \frac{E_s}{E_{cm}})}{E_s}$$

If prestressed tendons are used then $\sigma_s = \Delta\sigma_p$

$\rho_{eff} = A_s/A_{c,eff}$ or $A_p/A_{c,eff}$ or $(A_s + \xi_1^2 A_p)/A_{c,eff}$

k_t = {0.6 for short term loading;0.4 for long term loading}

For the crack spacing the following expressions are used AFGC2013 paragraph 2.5 section 7.3.4(3):

$s_{r,min,f} = l_0 + l_t$ (minimum crack spacing)

$s_{r,ave,f} = 1.5 * s_{r,min,f}$ (average crack spacing)

The maximum crack spacing follows from the average and minimum crack spacing:

$s_{r,max,f} = 1.7 * s_{r,ave,f} = 2.55 * (l_0 + l_t)$

Where:

$l_0 = 1.33 * c/\delta$

$$l_t = \frac{0.3 * k2 * \left(1 - \frac{f_{ctfm}}{f_{ctm,el}}\right) * \eta}{\delta} * \frac{\phi}{\rho_{eff}} \geq \frac{l_f}{2}$$

$\delta = 1 + 0.5(f_{ctfm}/f_{ctfm,el})$

c is the cover

ϕ is the diameter of the bar/strand

η is the bond factor

δ is a parameter that reflects how the fibres improve the contribution of the cover zone and the bond strength of the reinforcement

k2 =1 for pure tension and 0.5 for bending

This results in:

$$s_{r,max,f} = 1.33 * \frac{c}{\delta} + \frac{0.3 * k2 * \left(1 - \frac{f_{ctfm}}{f_{ctm,el}}\right) * \eta}{\delta} * \frac{\phi}{\rho_{eff}}$$

All these expressions from the AFGC are derived from the expression in Eurocode 2. If in the expression for $\varepsilon_{sm} - \varepsilon_{cm}$ from AFGC $f_{ctf,m}$ is taken zero (so this means that there are no steel fibres), then the expression changes into:

$$\varepsilon_{sm} - \varepsilon_{cm} = \frac{\sigma_s}{E_s} - \frac{k_t * f_{ctfm,el}(\frac{1}{\rho_{eff}} + \frac{E_s}{E_{cm}})}{E_s}$$

And knowing that $E_s/E_{cm} = \alpha_e$, the formula becomes the same one as given in the Eurocode.
Same goes for the expression for the maximum crack spacing. Assuming that 1.33 is an assigned value for k3 and 0.3 an assigned value for k4 (in EC2 k3=3.4 and k4=0.425) and if η=k1, this will result in:

$$s_{r,max,f} = k3 * \frac{c}{\delta} + \frac{k4 * k2 * \left(1 - \frac{f_{ctfm}}{f_{ctm,el}}\right) * k1}{\delta} * \frac{\phi}{\rho_{eff}}$$

Then if $f_{ctfm} = 0$ (results in δ=1) the formula is exactly the same as the one from Eurocode.

C.2.1.3 Betonkalender[3]

The Betonkalender which is a kind of 'state of the art' booklet for UHPC that gives information about UHPC, including dealing with crack width, gives a set of expressions to determine the crack width.

$w_k = s_{r,max} * (\varepsilon_{sm} - \varepsilon_{cm})$

$$\varepsilon_{sm} - \varepsilon_{cm} = \varepsilon_s^f - \varepsilon_{cs}^* - \frac{\alpha_b * f_{ctfm}(1 + \alpha_e * \rho_{eff}) - \sigma_{cf}}{\rho_{eff} * E_s} \geq (1 - \alpha_b)(\varepsilon_s^f - \varepsilon_{cs}^*)$$

Where
ε^f_s is the steel strain at crack taking into account the fibres (cross section in equilibrium)
α_b is the shape coefficient (0.6 for short term loading and 0.4 for long term loading)
f_{ctfm} is the mean value of cracking stress in fibre reinforced UHPC (concrete matrix + fibre effect)
ρ_{eff} is the effective reinforcement ratio
σ_{cf} is the tensile stress transferred by fibres at crack
ε_{cs}^* is the post-cracking shrinkage strain in concrete. It may be taken as ε_{cs} to be on the safe side.
$\alpha_e = E_s/E_c$

The left hand expression is found by assuming a stabilized cracking stage and the right hand expression is found by assuming a crack formation stage.

$$s_{r,max} = \frac{(f_{ctfm} - \sigma_{cf}) * d_s}{2 * \tau_{sm} * \rho_{eff}} \leq \frac{(\varepsilon_s^f - \varepsilon_{cs}^*) * E_s * d_s}{2 * \tau_{sm}}$$

Where
D_s is the diameter of the steel bars
τ_{sm} is the average bond stress of bar within $s_{r,max}$

The left hand is the stabilized cracking stage and right hand side the crack formation stage.

What Betonkalender states is that first of all the force in the reinforcement has to be calculated by taking into account the steel fibres.

[3] **Fehling,** E., Schmidt, M., Walraven, J.C., Leutbecher, T. & Fröhlich, S. (2014) "*Betonkalender – Ultra-High Performance Concrete UHPC*", Ernst & Sohn, Germany.

This will result in a lower steel force than in ordinary concrete, since the steel fibres relieve some load on the reinforcement. In order for a new crack to be created, only the cracking stress of f_{ctfm} reduced by σ_{cf} has to be transferred by the contribution of the reinforcement.
Furthermore the Betonkalender method uses the influence of shrinkage in the expressions. This is done because UHPC is known to have a high autogenous shrinkage, which influence cannot be neglected easily. As can be seen in the expressions the shrinkage will have an influence, except for the maximum crack spacing in the stabilized crack stage. In non-prestressed members the shrinkage will cause the concrete to already be in tension, which will reduce the cracking load level.

Comparison with AFGC
The expressions in the Betonkalender are not written in the form of the AFGC (or the Eurocode), as they are derived directly from the theory ($s_{r,max} = 2*l_t$). But it is possible to link both formulas by taking certain assumptions. The reduction of f_{ctfm} with σ_{cf} is the same as applying the term (1-$f_{ctfm}/f_{ctm,el}$) in the AFGC expression, both result in the same factor if the expression from AFGC would be rewritten in the style of the expression of the Betonkalender. Neglecting 1.33*c/δ and δ gives:

$$s_{r,max,f} = k4 * k2 * \left(1 - \frac{f_{ctfm}}{f_{ctm,el}}\right) * k1 * \frac{\phi}{\rho_{eff}} \approx \frac{f_{ctm,el}}{2 * \tau_{sm}} * \frac{\phi}{\rho_{eff}} * \left(1 - \frac{f_{ctfm}}{f_{ctm,el}}\right)$$

f_{ctfm} in AFGC is defined as the mean post cracking stress, which is σ_{cf} in Betonkalender.
$f_{tm,el}$ in AFGC is the same term as f_{ctfm} in Betonkalender.
With these changes the term from AFGC can be changed in the term from Betonkalender:

$$f_{ctm,el}\left(1 - \frac{f_{ctfm}}{f_{ctm,el}}\right) = f_{ctm,el} - f_{ctfm}\ (\text{AFGC}) = f_{ctfm} - \sigma_{cf}\ (\text{Betonkalender})$$

As confusing as this may look, this just shows that apart from slight changes and factors, the influence of the steel fibres is used in the same manner, which is the most important thing here.
And now that there is a link with the AFGC expression, this automatically means that the Betonkalender method could be linked with the Eurocode (since AFGC method is based on the Eurocode).

The expression for $\varepsilon_{sm} - \varepsilon_{cm}$ is basically the same for both methods, except for the fact that Betonkalender takes the shrinkage into account and AFGC does not. If the remainder of the expression of the AFGC method is rewritten one will find that:

$$\frac{f_{ctfm}}{E_{cm}} - \frac{k_t(f_{ctm,el} - f_{ctfm})(\frac{1}{\rho_{eff}} + \frac{E_s}{E_{cm}})}{E_s} = \frac{\alpha_b * f_{ctfm}(1 + \alpha_e * \rho_{eff}) - \sigma_{cf}}{\rho_{eff} * E_s}$$

So again the expressions are the same if shrinkage would be neglected.

C.2.1.4 RILEM TC 162-TDF 2003 and modified EC2

A research[4] based on analysis of crack width calculation for steel fibre reinforced concrete has been looking into the formulas that are used for calculating the crack width when concrete is reinforced with steel fibres. A comparison is made with the Eurocode and a modification in the Eurocode expression is made as well. Even though the research doesn't deal with UHPC specifically, the research can be applied to UHPC as well, because the tensile behaviour of UPHC and SFRC is basically the same.
First the crack width calculation method given by RILEM (International Union of Laboratories and Experts in Construction Materials, Systems and Structures) was discussed:

The crack width for a reinforced member is determined by:
$W_k = \beta * s_{rm} * \varepsilon_{sm}$

Where
β is a coefficient relating the average crack width with the design value
s_{rm} is the average final crack spacing
ε_{sm} is the mean strain in the tension reinforcement

The mean strain is defined as:

$$\varepsilon_{sm} = \frac{\sigma_s}{E_s} * [1 - \beta 1 * \beta 2 * \left(\frac{\sigma_{sr}}{\sigma_s}\right)^2]$$

β1 takes into account the bond properties of the bars
β2 takes into account the duration of the (repeated) loading
The crack spacing is defined as:

$$s_{rm} = \left(50 + 0.25 * k_1 * k_2 * \frac{\phi_b}{\rho_r}\right) * \left(\frac{50}{L/\phi}\right)$$

An extra term placed in this formula is 50/(L/φ) ≤ 1. This is a proposed coefficient by RILEM, which considers the influence of the steel fibre on the average crack spacing. This coefficient only considers the influence of the length and diameter of the steel fibre, but not the fibre content.
The rest of the expression is basically the same as the one in the Eurocode:
$s_{r,max} = k3*c+k1*k2*k4 * \phi/\rho_{eff}$
k3*c = 50 and k4=0.25. The remaining terms are determined the same way.

The expressions given by RILEM are then used in the research to modify the expressions from the Eurocode (which are given in the beginning of this paragraph). In the expression for $s_{r,max}$ the extra term 50/(L/φ) is added:
$s_{r,max} = k3*c+k1*k2*k4 * (\phi/\rho_{eff})*(50/[L/\varphi])$

But as already said, this term doesn't consider the fibre content, but the crack spacing is influenced by the fibre content. Therefore a different term is added in the formula (k5):

$s_{r,max} = 3.4*c+0.425*k1*k2*k5* \phi/\rho_{eff}$

With the new term k5 = $(1-(\sigma_{fb}/f_{ctm}))$. This term reduces the crack spacing depending on the residual tensile stress σ_{fb}. This term is practically the same term as is the AFGC $(1-f_{ctfm}/f_{ctm,el})$

[4] **Kelpsa. S.** et al (2014) *"Analysis of Crack Width Calculation of Steel Fibre and Ordinary Reinforced Concrete Flexural Members",* Kaunas University of Technology, Kaunas, Lithuania.

In short there are 3 different expressions given in the research for the maximum crack spacing:

RILEM: $s_{rm} = \left(50 + 0.25 * k_1 * k_2 * \frac{\phi_b}{\rho_r}\right) * \left(\frac{50}{L/\phi}\right)$

EC2 supplemented: $s_{r,max}$ = k3*c+k1*k2*k4 * (ϕ/ρ_{eff})*(50/[L/φ])

EC2 corrected: $s_{r,max}$ = 3.4*c+0.425*k1*k2*(1-(σ_{fb}/f_{ctm})) * ϕ/ρ_{eff}

From the three expressions the corrected EC2 looks the most like the one in AFGC, except for a couple of constants, which are different in AFGC (3.4 is 1.33 and 0.425 is 0.3)

C.2.2 Discussion crack width methods

Looking back at paragraph C.2.1 there are a lot of similarities between the discussed methods. It is safe to say that the methods are mostly the same, except for some different constants. But these constants will provide different results for the crack width. It could be possible that there will be large deviations between the results of the different methods.

The methods are derived for reinforced concrete members. But it is also possible to take into account prestressing by adding the necessary terms, as is usually done with normal concrete structures. The biggest issue however would be determining σ_{cf} (or f_{ctfm}) or in other words the tensile stress transferred by fibres at cracking. The expression for this is:

$$\sigma_{cf} = \sigma_{cf0k} * \left(2 * \sqrt{\frac{w_k}{w_0}} - \frac{w_k}{w_0}\right) \quad for\ fibre\ activaiton\ phase$$

$$\sigma_{cf} = \sigma_{cf0k} \quad for\ pull\ out\ phase\ when\ (w_k > w_0)$$

Where $\sigma_{cf0k} = \sigma_{cf0k}^{test}$ / K (characteristic value of fibre efficiency)

As the expression for σ_{cf0k} shows, for now it is only possible to determine this value by performing tests, because each mixture (with also a different fibre content) will result in certain fibre efficiency. This luxury is not always available when designing a structure. This is also the case for this thesis. Tests on multiple specimens would have to be performed to determine the correct σ_{cf}. Afterwards the determined σ_{cf} would have to be used in calculations while using the same UHPC mixture in order to get reliable results for the crack width.

The AFGC, which is the leading guideline in this research, recommends different values for f_{ctfm} depending on the type of strain behaviour. For example the AFGC states that when the concrete shows low strain hardening behaviour:

$f_{ctfm} = f_{ctfk}$ = 9 N/mm^2 and $f_{ctm,el} = f_{ctk,el}$ = 9 N/mm^2. If these value would be filled in the expression for $s_{r,max}$ this would lead to δ=0 which leads to $s_{r,max}$ = 0 mm.

This would mean that the minimum value of $l_f/2$ (=6.5mm for the Leiden Bridge) would have to be used, which is a very low value. For the crack width this would mean that:

$$w_k = 6.5 * \left(\frac{\sigma_s}{E_s} - \frac{f_{ctfm}}{E_{cm}}\right)$$

This would most likely result in a very low value for w_k, which would certainly be lower than the maximum allowed crack width. Such a low crack width would prove that the steel fibres lead to a lot of distributed micro cracks, which is what the fibres are supposed to do.

The fibre efficiency uncertainty aside, if the new methods are compared with the Eurocode method, the new term (1-(σ_{fb}/f_{ctm})) will definitely lead to a lower maximum crack spacing, where a higher fibre efficiency would result in a lower maximum spacing and thus a lower crack width.

D. Bridge design in C50/60, calculations

D.1 General

In the following the calculations are presented for the C50/60 design. These calculations serve the purpose to back up the results given in the main part of the report.
First the dimensions and properties of the concrete and of the box beam girder will be determined. Afterwards the load cases and load combinations will be determined. Then the calculation model of the bridge will be presented. With the loads and the model the internal forces will be determined. This will be done with SCIA Engineer. After the results from SCIA are obtained the structure will be checked in the Ultimate Limit State (ULS) if it can resist the loads working on the bridge. For the calculation in C50/60 the safety check will only be limited to the ULS.

D.2 Determining h_{min}

Three possible bridge types were considered the most realistic for the new Leiden Bridge. Since prefab girders will be used, it is helpful to consult various girder producers to obtain the available girder sizes. First the minimum height needed for the span has to be calculated with a rule of thumb. In Table D-1 the minimum construction height for each type of girder is determined. Also the minimum height for a two span bridge is shown.

Table D-1: Minimum heights for the new design

	Slenderness ratio (λ)	h_{min} for l=12m [m]	h_{min} for l=24m [m]
Solid deck bridge	20 - 25	480 - 600	960 - 1200
inverted T/I - girder	20 - 28	429 - 600	858 - 1200
Box beam girder	28 - 32	375 - 429	750 - 858

From the results it becomes clear that building the bridge with only one span with C50/60 would not meet the height requirements. When the most slender bridge type is used (box beam) the minimum height will be around 750mm. So actually for a bridge in normal strength concrete C50/60 the best bet would be to build the bridge in two spans, concerning the construction height. However if two spans are considered only a solid deck bridge would be appropriate, since box and inverted T girders are not produced for such short spans. If one would ignore the limited construction height a box beam bridge would be the best option for a C50/60 one span bridge. Using this girder will give the most slender bridge and an additional deck will not be necessary.

Looking at the determined limits of h_{min} and the available girder heights produced by manufacturers, a box beam girder with h=800mm should be used for the C50/60 design.
It is however much wiser to investigate if the bridge could be made in C50/60 concrete, while also using a girder with a height of 600mm. To achieve the goal of the research, this height has to be used for the UHPC design so, it will be much better to also design the bridge in C50/60 with a girder of 600mm thick. This will result in a better comparison later with the UHPC design. So for the design a height of 600 mm will be used.

D.3 Material Properties

The concrete and steel material properties are shown in Table D-2. These values will be used in future calculations. The values are based on NEN-EN-1992-1-1.

Table D-2: Concrete and steel material properties

Concrete C50/60		
ρ_c		2500 kg/m^3
f_{ck}		50 N/mm^2
f_{cm}	$f_{ck}+8$	58 N/mm^2
f_{ctm}	$0,3*f_{ck}^{(2/3)}$	4.1 N/mm^2
$f_{ctk0,05}$	$0,7*f_{ctm}$	2.9 N/mm^2
γ_c		1.5
f_{cd}	f_{ck}/γ_c	33.33 N/mm^2
f_{ctd}	$f_{ctk0,05}/\gamma_c$	1.933 N/mm^2
E_{cm}	$22(f_{cm}/10)^{0,3}$	37000 N/mm^2
ε_{c3}		1.75 ‰
ε_{cu3}		3.5 ‰

Reinforcing steel B500		
ρ_s		7850 kg/m^3
f_{yk}		500 N/mm^2
γ_s		1.15
f_{yd}	f_{yk}/γ_s	435 N/mm^2
E_s		210000 N/mm^2

Prestressing steel Y1860		
ρ_p		7850 kg/m^3
f_{pk}		1860 N/mm^2
$f_{p0.1k}$	$0,9*f_{pk}$	1674 N/mm^2
γ_s		1.1
f_{pd}	$f_{pk0.1}/\gamma_s$	1522 N/mm^2
σ_{pm0}	$0,75*f_{pk}$	1395 N/mm^2
E_p		195000 N/mm^2
φ strand		15.2 mm
A_p (one strand)		139 mm^2

Additional assumptions	
Environmental class	XD1
Concrete cover	45 mm
φ shear reinforcement	12 mm
φ longitudinal reinforcement	12 mm
Maximum aggregate size d_g	32mm

D.4 Bridge dimensions and cross sectional properties

Box beam girders are used for the bridge design. Manufacturers do not produce box girders of 600 mm so a modified box girder of h=600 mm will be used instead, of which the properties will be determined with hand calculations. This basically means that the same dimensions will be used except for the total height of the beam. The cross section of one box beam girder is seen Figure D-1. The web and flange thicknesses are based on values given by Spanbeton BV. Same goes for the width.

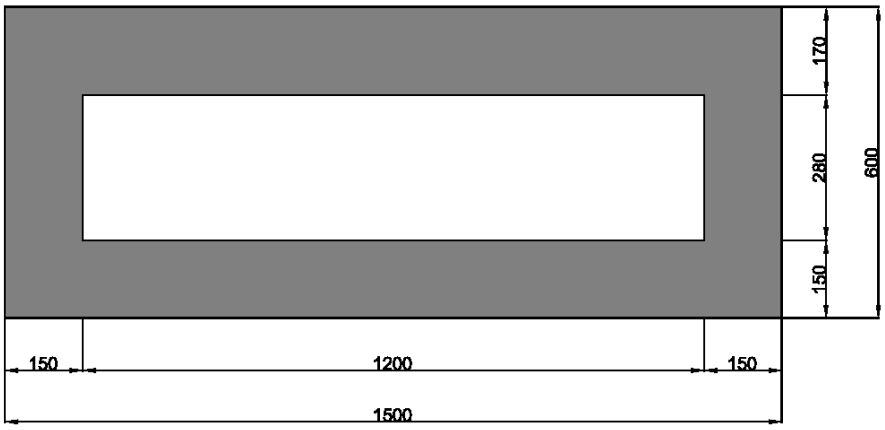

Figure D-1: Cross section of one box beam girder [m]

In Table D-3 the dimensions and cross sectional properties of one girder are shown.

Table D-3: Dimensions and cross sectional properties of box girder

L	Span	24 m
H	Height girder	0.6 m
B	Width girder	1.5 m
b_{web}	Web thickness	0.15 m
$h_{top,fl}$	Top flange thickness	0.17 m
$h_{bot,fl}$	Bottom flange thickness	0.15 m
A_c	Cross sectional area	0.564 m^2
z_t	Distance top fibre to c.a.	0.294 m
z_b	Distance bottom fibre to c.a.	0.306 m
I_c	Moment of Inertia	0.025 m^4
$W_{c,t}$	Section Modulus top fibre	0.084 m^3
$W_{c,b}$	Section Modulus bottom fibre	0.081 m^3

The values in the table are calculated as follows:

$A_c = B*H - (H - h_{top,fl} – h_{bot,fl}) *(B-2* b_{web})$

$z_t = \{B*H*0.5H – (H- h_{top,fl} – h_{bot,fl}) * (B-2* b_{web}) * 0.5*(H- h_{top,fl} – h_{bot,fl})+h_{top,fl})\}/ A_c$

$z_b = H - z_t$

$I_c = 2 * [(1/12)*b_{web}*H^3+b_{web}*H*(0,5*H-zt)^2] + [(1/12)*(B-2*b_{web})*h_{top,fl}^3+ (B -2*b_{web}) *h_{top,fl}* (z_t - 0,5*h_{top,fl})^2] + [(1/12)*(B-2*_{bweb})*h_{bot,fl}^3 + (B-2*b_{web})*h_{bot,fl}*(z_b-0,5*h_{bot,fl})]$

$W_{c,t} = I_c/z_t$

$W_{c,b} = I_c/z$

D.5 Load cases and combinations

Before the SCIA Engineer model is presented, the loads have to be determined first. There are a lot of different loads that will work on the bridge. And these loads will not occur exclusively. Therefore it is important to determine all the load cases and load combinations for the bridge. The load cases and combinations are described more in detail in appendix B.

Basically the following load cases will occur on the bridge:

Permanent loads:	
LC1: Self-weight girders (not included in SCIA)	A_c*25 kN/m
LC2: Dead load	
– Pavement	4.6 kN/m^2
– Asphalt	4.8 kN/m^2
– Concrete filling around tram rails	3.5 kN/m^2
LC3: Steel railing and natural stone elements (Edge Load)	2.0 kN/m^2
Variable loads:	
LC4&5: Traffic loads with presence of trams (UDL & tandem axle)	Conform Load Model 1
LC6&7: Traffic loads with absence of trams (UDL & tandem axle)	Conform Load Model 1
LC8: Tram-axle loads (No UDL specified for tram loads)	Conform GVB
LC9: Pedestrian loads over whole width (crowd loading)	5.0 kN/m^2
LC10: Pedestrian loads on designed locations.	5.0 kN/m^2

In total there are four main load combinations:

- Combination 1: Traffic loads in the presence of tram loading, where the traffic loads are the leading variable load. (1 LM1 TS + 2 tram TS)
- Combination 2: Traffic loads in the presence of tram loading, where the tram loading is the leading variable load. (1 LM1 TS + 2 tram TS)
- Combination 3: Traffic loads in absence of tram loading. (3 LM1 TS)
- Combination 4: Crowd loading

D.6 Calculation model

The bridge is modelled in SCIA Engineer as a 2D orthotropic plate. This way the transverse action of all girders combined can be modelled in a good way. With this model the internal forces caused by the loads on the bridge will be determined. The self-weight will be left out, because the 2D model will be inputted as a plate. So the self-weight calculated will not be correct. Using the correct orthotropic parameters will still give the correct internal forces. Furthermore in SCIA, results in 2D are usually given per meter width. So the governing internal forces can easily be transformed to give results for one girder. Then adding the self-weight of one girder, which can easily be determined by hand, will result in the total internal forces in one girder. With these internal forces a safety check can be performed for one girder. The aforementioned orthotropic parameters are calculated with a Mathcad sheet that is presented at the end of this paragraph.

The bridge is modelled as a simply supported bridge. In reality the amount of supports on each side will be the same as the amount of girders. Each girder is 1.5m wide. The bridge is 30m wide, so this results in a total of 20 girders. So in the model 20 internal nodes are placed on each side, which represent the location of the supports. The locations of the support in the model are determined by taking the centre location of each girder (right in the middle). In Figure D-2 the SCIA model is shown.

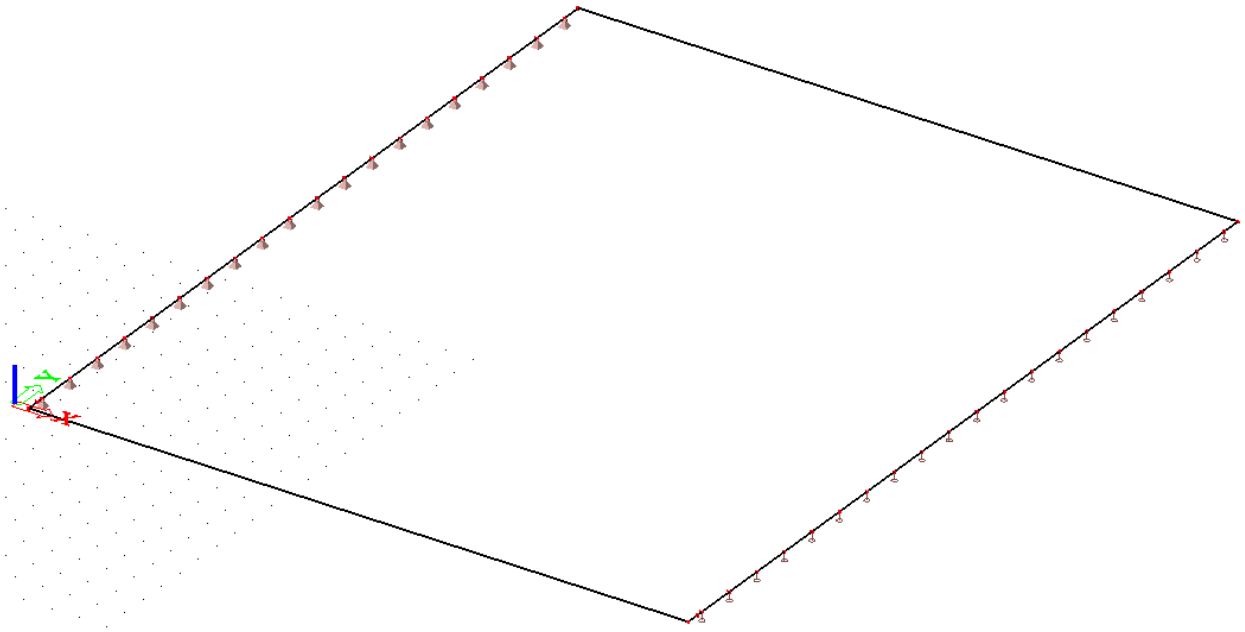

Figure D-2: SCIA 2D model of C50/60

Because vehicles and trams constantly cross the bridge, these are defined as variable loads. In the model the traffic and tram loads are defined as mobile loads. Because they are defined as mobile loads the program can determine at which position of the load, across the length of the bridge, is the governing one for the bending moments, Shear force etc. These mobile loads will be combined with the other, static loads to determine the maximum internal forces on the bridge.
A full report on the model (such as coordinates, loads, etc.) and also the results from the model can be found in the engineering report at the end of this appendix.

MATHCAD FILE: Calculation orthotropic parameters for C50/60 Box girder

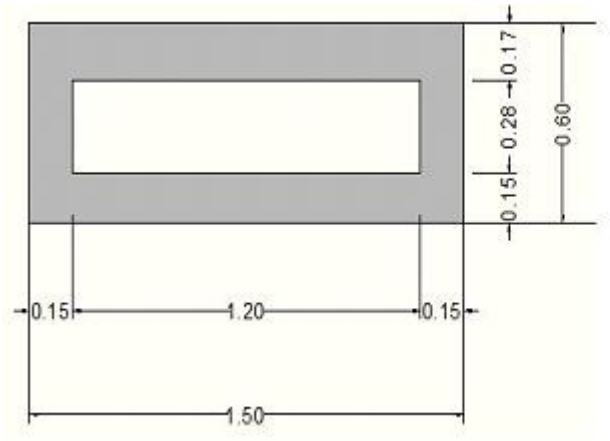

Dimensions and cross sectional properties

$H := 0.6$

$B := 1.5$

$b\_web := 0.15$

$h\_topfl := 0.17$

$h\_botfl := 0.15$

$Ec := 37300$

$\nu := 0.15$

$Gc := \frac{Ec}{2(1+\nu)} = 1.622 \times 10^{4}$

$Hvoid := H - h\_topfl - h\_botfl = 0.28$

$Bvoid := B - 2 \cdot b\_web = 1.2$

$Ac := \begin{pmatrix} H \cdot B \\ -Hvoid \cdot Bvoid \end{pmatrix} = \begin{pmatrix} 0.9 \\ -0.336 \end{pmatrix}$ $\quad z := \begin{pmatrix} 0.5 \cdot H \\ h\_topfl + 0.5 \cdot Hvoid \end{pmatrix} = \begin{pmatrix} 0.3 \\ 0.31 \end{pmatrix}$

$Sc := \overrightarrow{(Ac \cdot z)} = \begin{pmatrix} 0.27 \\ -0.104 \end{pmatrix}$

$ztop := \frac{\sum Sc}{\sum Ac} = 0.294$ $\quad zbot := H - ztop = 0.306$

$Asteiner := \overrightarrow{\left[Ac \cdot (ztop - z)^2\right]} = \begin{pmatrix} 3.194 \times 10^{-5} \\ -8.556 \times 10^{-5} \end{pmatrix}$ $\quad Ieigen := \left(\frac{1}{12}\right) \cdot \begin{pmatrix} B \cdot H^3 \\ -Bvoid \cdot Hvoid^3 \end{pmatrix}$

$I := \sum (Asteiner + Ieigen) = 0.025$

Flexural stiffness

$$D11 := (Ec)\cdot\frac{I}{B} = 615.479 \qquad \textbf{in MNm}$$

$i := 1..3$

$b_i :=$

$0.5\cdot B - 0.5\cdot b\_web$
$H - h\_topfl - h\_botfl$
$0.5\cdot B - 0.5\cdot b\_web$

$t_i :=$

h_topfl
b_web
h_botfl

$$\lambda_i := 12\cdot\frac{b_i}{\left[Ec\left(\left(t_i\right)\right)^3\right]}$$

$\lambda_1 = 0.044$

$$e := \left[\frac{\lambda_2\cdot\left(\lambda_2 + 4\cdot\lambda_3\right)}{\lambda_2\cdot\left(4\cdot\lambda_1 + \lambda_2\right) + \lambda_3\cdot\left(12\cdot\lambda_1 + 4\cdot\lambda_2\right)}\right] = 0.163$$

$$hf := \left[h\_topfl^3\cdot\left(\frac{1}{e}\right)\right]^{\frac{1}{3}} = 0.311$$

$$D22 := 1\cdot Ec\cdot\frac{hf^3}{12} = 93.517 \qquad \textbf{in MNm}$$

Torsional stiffness

$$Am := (B - b\_web)\cdot(H - 0.5\cdot h\_topfl - 0.5\cdot h\_botfl) = 0.594$$

$$Sum1 := 2\cdot\frac{b_1}{t_1} + \frac{(2\cdot b)_2}{t_2} + 2\cdot\frac{b_3}{t_3} = 20.675$$

$$Sum2 := \left(\frac{1}{3}\right)\cdot\left[2\cdot b_1\cdot\left[\left(t_1\right)^3 + \left(t_3\right)^3\right] + 2\cdot b_2\cdot\left(t_2\right)^3\right] = 4.36\times 10^{-3}$$

$$It := 4\cdot\frac{Am^2}{Sum1} + Sum2 = 0.073$$

$$Dxy := Gc\cdot\frac{1It}{1B} = 785.187$$

$$Dyx := Gc\cdot\frac{\left(h\_topfl^3 + h\_botfl^3\right)}{6} = 22.402$$

$$D33 := \frac{(Dxy + Dyx)}{2} = 403.794 \qquad \textbf{in MNm}$$

Shear stiffness

$$D44 := 2Gc \cdot b\_web \cdot \frac{(H - 0.5 \cdot h\_topfl - 0.5 \cdot h\_botfl)}{B} = 1.427 \times 10^3 \quad \textbf{in MN/m}$$

$$D55 := Gc \cdot \frac{hf}{1.5} = 3.363 \times 10^3 \quad \textbf{in MN/m}$$

$$D12 := \nu \cdot \sqrt{(D11 \cdot D22)} = 35.987 \quad \textbf{in MNm}$$

Orthotropic parameters box beam girder

$D11 = 615.479$	MNm	$D44 = 1.427 \times 10^3$	$\frac{MN}{m}$
$D22 = 93.517$	MNm	$D55 = 3.363 \times 10^3$	$\frac{MN}{m}$
$D33 = 403.794$	MNm	$D12 = 35.987$	MNm

To be filled in SCIA Engineer

D.7 Results SCIA Engineer

Presented here are the internal forces necessary to perform the safety checks in ULS. The results are all from the ULS. The results for vx are taken from a section made near the supports. A section there is used, because of very high peak values occurring right at the internal nodes which represent the supports. These are likely caused by singularities in the calculations. Therefore a section is placed just outside the peak area to give more realistic results for the shear force.

For bending moment resistance check:
mxD^-: 1602.82 kNm/m

For shear and [torsion + shear] safety check
mxy: 344.75 kNm/m (When torsion is governing)
172.3 kNm/m (When shear is governing)

vx: 220.76 kN/m (When torsion is governing)
645.0 kN/m (When shear is governing)

The values given by SCIA are per meters width. These values have to be recalculated to represent the forces on one girder. The width of one girder is 1.5m:

For bending moment resistance check:
mxD^-: 2404.24 kNm

For torsion + shear safety check
mxy: 517.13 kNm (When torsion is governing)
258.39 kNm (When shear is governing)

vx: 331.14 kN (When torsion is governing)
967.5 kN (When shear is governing)

These last presented values will be used for the safety checks. However these values are only based on the loads working on the bridge. Here nor self-weight nor prestressing is included. These have to be added separately. This will be done in the following, where also the amount of prestressing will be determined.

D.8 Tendon profile and prestress force

The beams will consist of pre-tensioned strands, as the beams are prefabricated. The tendon profile is shown in Figure D-3. The tendon consists of straight and kinked strands. The kinked strands cause an upward force P_u at the deviation points. This point is at a distance 'a' from the support. The kinked strands are placed in the webs. In each web *6* strands are placed so in total there are *12* kinked profiles. The strands will be placed as high as possible to ensure a high upward force. This force slightly reduces the total shear force.

Assumed is that the kinked strands will be placed so that the gravity point of these strands is:
$z_b - h_{top} - 4*\varphi_{strand}$ = 63 mm above the centroid axis. Most of the strands will be placed in the bottom flange. This means that the fictitious tendon (or the gravity point) does not coincide with the neutral axis (dashed line). So these will create a moment at the heads due to eccentricity, so a capacity check at the support has to be made to make sure the structure can take the moments.

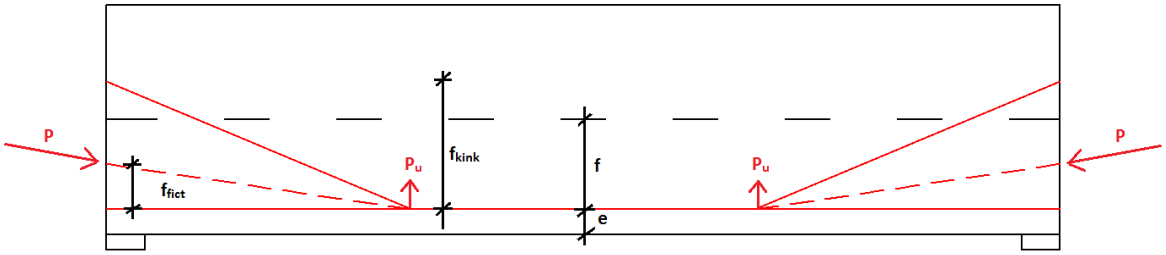

Figure D-3: Tendon profile pre-tensioned strands

The strands have a certain eccentricity in the mid span with reference to the bottom fibre. The minimum eccentricity (e) for the fictitious tendon with reference to the bottom fibre can be determined by taking the cover, the reinforcement and strand spacing into account.
e = 0.093m (c_{nom} + φ_{shear} + 0.5*φ_{strand} + d_g).
This results in a drape of: f = z_b - e = 0.213m.
The kinks are at a distance of a = (1/3)L= 8m from the support.
The upward force is calculated according to the drape of the kinked strands f_{kink} = f+0.063=0.276m.
The drape of the fictitious tendon can be determined once the total amount of strands is determined. Then it will be known how much strands will go in the bottom flange.
The rest of the values in the figure are:
P_u =P_{kink}*sin α_{kink} ≈ P_{kink}* (f_{kink}/a) or P*(f_{fict}/a)
$M_{p,mid}$ = P*f

The prestress force is determined by taking a couple of requirements into account that concern stresses in the concrete. These requirements need to be applied in the governing cross section (cross section with highest bending moment). Here that is in the middle of the beam. These requirements are:

$$t = 0 \text{ at top fibre: } -\frac{P_{m0}}{A_c} + \frac{M_{p,0}}{W_{ct}} - \frac{M_g}{W_{ct}} \leq 0$$

$$t = 0 \text{ at bottom fibre: } -\frac{P_{m0}}{A_c} - \frac{M_{p,0}}{W_{cb}} + \frac{M_g}{W_{cb}} \geq -0.6 * f_{ck}$$

$$t = \infty \text{ at bottom fibre: } -\frac{P_{m\infty}}{A_c} - \frac{M_{p,\infty}}{W_{cb}} + \frac{M_{tot}}{W_{cb}} \leq 0$$

The first requirement states that at the construction of the bridge, when only dead loads are present, no tensile stresses are allowed which could be caused by the prestressing.
The second requirement states that the compression stresses can't be too high at the bottom of the beam during construction.
The third requirement states that during the use of the bridge, where all the loads are present, no tensile stresses are allowed at the bottom of the beam. Here $P_{m\infty}$ is used instead of P_{m0}. The difference is that immediate and time dependent losses are taken into account here. Assumed is a total loss of 20% so $P_{m\infty}$ = 0.8*P_{m0}.

To determine the total moments and the moments caused by the dead load. The result of mxD- in SCIA has to be split apart. This means finding out what load cases contribute to the governing moment. This has been done by finding the node in SCIA, where the highest moment is located and writing down the results that SCIA gives in that node. The results are presented in Table D-4. The results are both in SLS and ULS. Also given are the resulting loads in kN/m.

Table D-4: Bending moments

mxD-		SLS			ULS	
	kNm/m	kNm (*1 beam*)	q [kN/m]	γ	kNm (*1 beam*)	q [kN/m]
dead load	297,110	445,665	6,190	1,2	534,798	7,428
edge load	13,610	20,415	0,284	1,2	24,498	0,340
AT| UDL	291,950	437,925	6,082	1,35	591,199	8,211
AT| TS	483,220	724,830	10,067	1,35	978,521	13,591
Pedestrian loads	169,890	254,835	3,539	1,08	275,222	3,823
TOTAL	**1255,780**	**1883,670**	**26,162**		**2404,237**	**33,392**

In addition to these moments the moment due to self-weight needs to be determined as well:
$q_{self} = A_c * \gamma_c = 0.564*25 = 14.1$ kN/m in SLS *1.2 = 16.96 kN/m in ULS
$M_{self} = (1/8)*q_{self}*L^2 = 1015.1$ kNm

The moment due to static loads now becomes:
$q_{perm} = q_{dead} + q_{edge} + q_{self} = 20.57$ kN/m in SLS and 24.69 kN/m in ULS
$M_g = 1481.3$kNm
The moment due to the variable loads is:
$q_{var} = 19.69$ kN/m in SLS and 25.62 kN/m in ULS
$M_q = 1417.6$ kNm
This results in a total moment (SLS) of:
$M_{tot} = 2898.9$ kNm

Now that the moments have been determined, the prestressing force can be calculated:

t=0: σ < 0	P_{m0} <	23105.26 kN
t=0: σ >-0,6*f_{ck}	P_{m0} <	10953.71 kN
t=∞: σ < 0	P_{m0} >	10156.0 kN

The minimum prestressing force has to be 10156.0 kN. This results in (σ_{pm0} = 1395MPa; $A_{p,strand}$ = 139mm^2): 10156.0/(1395*139) = 53 strands. These strands have a cross sectional area of $A_p = 7367$mm^2 in total, which results in a force of $P_{m0} = 10276.97$ kN.
The moment caused by the prestressing force is:
$M_{p\infty} = P_{m\infty} * f = 1754.13$kNm
The stress caused by the prestress force during t=∞ in the concrete is:
$\sigma_{cp} = 0.8*P_{m0}/A_c = 14.58$ N/mm^2.

The prestress force delivers a vertical force at the deviators P_u, which is equal to: $P_{u0} = P_{m0}*(f_{fict}/a)$. The fictitious drape f_{fict} can be determined by finding the gravity point of all strands. There are 53 strands in total. With 12 strands in the webs the amount of strands in the bottom flange are 41.
$f_{fict} = f_{kink} - (41A_p*f_{kink}/53A_p) = 0.0626$m. This results in a $P_{u0} = 80.38$kN and $P_u = 64.30$kN.

As can be expected the fictitious drape is low because the gravity point is very close to the bottom flange, due to the high amount of strands there. The gravity point is at a distance of $f-f_{fict} = 0.151$m from the neutral axis. This basically means the moment due to prestressing isn't zero anywhere.

D.9 Bending moment resistance

It is a requirement that the bending moment resistance is higher than the design bending moment: $M_{Rd} > M_{Ed}$.

$M_{Ed} = \gamma_g * M_g\ M_g + \gamma_q * M_q - 1.0 * M_p$
Where:
$M_g(x) = 0.5 * q_g * x * (L-x)$
$M_q(x) = 0.5 * q_q * x * (L-x)$
$M_p(x) = P_u * a + P_m * (f - f_{fict})$ $0 \leq x < a$
$P_m * f$ $x \geq a$

It is possible that the eventual governing design bending moment is found at the construction stage (t=0) and perhaps at the support, because the prestressing causes a moment there.. So the bending moment will be determined for the whole span at multiple stages: These stages and the bending moments are:

- t=0 only self weight: $M_{Ed} = M_{self} - M_p$
- t=0 permanent loads: $M_{Ed} = M_{perm} - M_p$
- t=∞ all loads + torsion: $M_{Ed} = M_{perm} + M_{var} - M_p$

The parameters are:

Load of self-weight (ULS):	q_{self} =	16.92 kN/m
Permanent load (ULS):	q_{perm} =	24.69 kN/m
Variable load (ULS):	q_{var} =	25.624 kN/m
Prestress force at t=0:	P_{m0} =	10276.97 kN
Prestress force at t=∞:	$P_{m\infty}$ =	8221.57 kN
Drape:	f =	0.213 m
Eccentricity of strands with regards to neutral axis:	$f-f_{fict}$ =	0.151m

In Figure D-4 the moment lines are shown, for multiple stages. The governing M_{Ed} = 1868.343 kNm. The moment at the support is 1549.62 kNm. Technically right at the support the prestress force is also zero. The force has a certain transmission length, where after the force is fully transferred in the concrete.

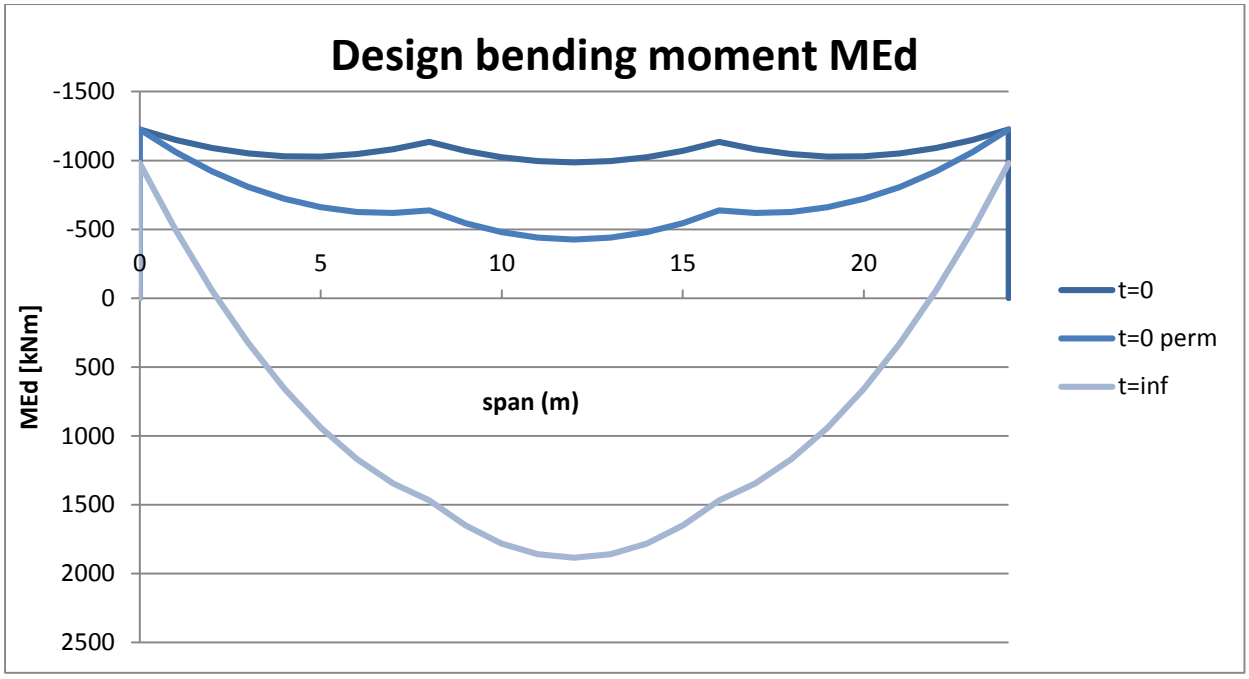

Figure D-4: Design bending moment at multiple stages

The design bending moment needs to be lower than the moment capacity. To determine M_{Rd} one has to assume equilibrium of internal forces in the cross section and with that assumption determine M_{Rd} (see Figure D-5): $N_c = P_{m\infty} + \Delta N_p + N_s$. The last term N_s is removed, as there is no bending reinforcement applied. Writing out the equilibrium results in:
$\alpha * x_u * B * f_{cd} = A_p * \sigma_{pm\infty} + A_p * (\sigma_{pu} - \sigma_{pm\infty})$.

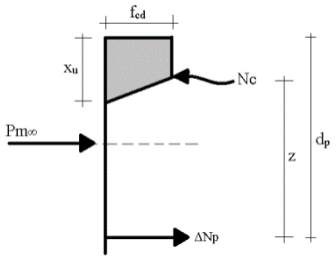

Figure D-5: Equilibrium of internal forces

Here the only unknown is the height of the compression zone x_u:
$x_u = (A_p * \sigma_{pu}) / (\alpha * x_u * B * f_{cd})$

$A_p = 7367\ mm^2$
$\sigma_{pu} = 0.95 * f_{pk} / \gamma_p = 1606.36 N/mm^2$
$\sigma_{pm\infty} = 0.8 * \sigma_{pm0} = 1116\ N/mm^2$
f_{cd} $33.33 N/mm^2$
$\alpha = 0.75$
B=1500 mm

Result: $x_u = 311.86$ mm

The compression zone is larger than the height of the top flange. When this situation occurs it is conventional to use the rectangular stress strain relationship as seen in Figure D-6.
The new parameters:
$\eta = 1.0 - (f_{ck} - 50) / 200 = 1.0$
$\lambda = 0.8 - (f_{ck} - 50) / 400 = 0.8$

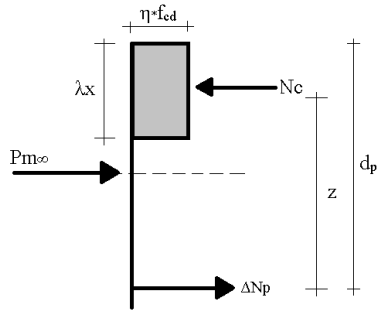

Figure D-6: Rectangular stress strain relationship

With this new equilibrium the compression zone needs to be recalculated. With the new x the bending moment resistance will be calculated. It has to be noted that a part of the compression zone is located in the webs. So the effective width needs to be changed accordingly. The new equilibrium is: $N_{c,flange} + N_{c,web} = P_{m\infty} + \Delta N_p \rightarrow h_{top,fl} * B * f_{cd} + (\lambda x - h_{top,fl}) * 2 b_{web} * f_{cd} = A_p * \sigma_{pm\infty} + A_p * (\sigma_{pu} - \sigma_{pm\infty})$.
This equilibrium, with again the only unknown being x, results in:
$\lambda x = h_{top,fl} + \{[A_p * \sigma_{pu} - h_{top,fl} * B * f_{cd}] / [2 b_{web} * f_{cd}]\} = 489.479$ mm

If the point of rotation is taken at the top fibre:
$M_{Rd} = P_{m\infty}*z_t + \Delta N_p*d_p - N_{c,flange}* h_{top,fl} - N_{c,web} * (\lambda x - 0.5(\lambda x - h_{top,fl})) = 2403.85$ kNm.

Unity Check: $M_{Ed}/M_{rd} = 1868/2404 = 0.778$ --> OK.

D.10 Rotational capacity

The bending moment resistance suffices. But it is also important that the structure has enough rotational capacity in order to give enough warning before failure. For this the following requirement has to be met (NEN-EN-1992-1-1 Dutch NB cl.5.5):

$x_u/d \leq 500/(500+f)$ with $f= [(f_{pk}/\gamma_p - \sigma_{pm\infty})*A_p + f_{yd}*A_s]/(A_p + A_s) = (1860/1.1-1116)*7367/7367 = 567.1$
The requirement becomes: $x_u/d \leq 0.471$.
Filling in x_u and with d=h-e = 507.4 mm x_u/d becomes 0.96 which is much higher than the required value.

Possible is to fictively reduce the amount of prestressing until M_{Rd} is just above M_{Ed} and then calculate the rotational capacity. For this the same process as above is used for determining the moment capacity, only with constantly a different A_p. After a few iterations the prestressing has to be fictively reduced to $A_p = 5700$ mm^2. Here xu/d = 0.46, which is just below the max requirement. UC: $M_{Ed}/M_{Rd} = 0.778$.

D.11 Shear and Torsion resistance

D.11.1 Shear

It is a requirement that the shear resistance is higher then the design shear force:
$V_{Rd}>V_d$
The design shear force is the sum of the shear force caused by bending moments and the shear force caused by torsional moments:
$V_d = V_{Ed} + V_{Td}$
Two cases have to be investigated, of which the most governing one will be used:

1. Location of highest torsional moment in structure
2. Location of highest shear force in structure

For both locations the internal forces were calculated and the results were presented in paragraph D.7. These were:
Mxy = TEd:
Situation 1. 517.13 kNm --> $V_{Td} = 191.53$ kN
Situation 2. 258.39 kNm --> $V_{Td} = 95.7$ kN
Vx (without self-weight and prestressing):
Situation 1. 331.14 kN
Situation 2. 967.51 kN

The shear force V_{Td} due to T_{Ed} is calculated with: $V_{Td} = h_m*T_{Ed}/(2*A_k)$.
A_k is the area inside the hart lines (b_m*h_m) as seen in Figure D-7. Also seen in Figure D-7 is the sum of the shear forces. The governing total shear force is the the one where the sum of V_{Ed} and V_{Td} is the largest (left web).

$h_m = H-0.5*(h_{top,fl} + h_{bot,fl}) = 0.6-0.5*(0.17+0.15) = 0.44$ m
$b_m = B-2*0.5*b_{web} = 1.5-2*0.5*0.15=1.35$ m
$A_k = b_m*h_m = 0.594$ m^2

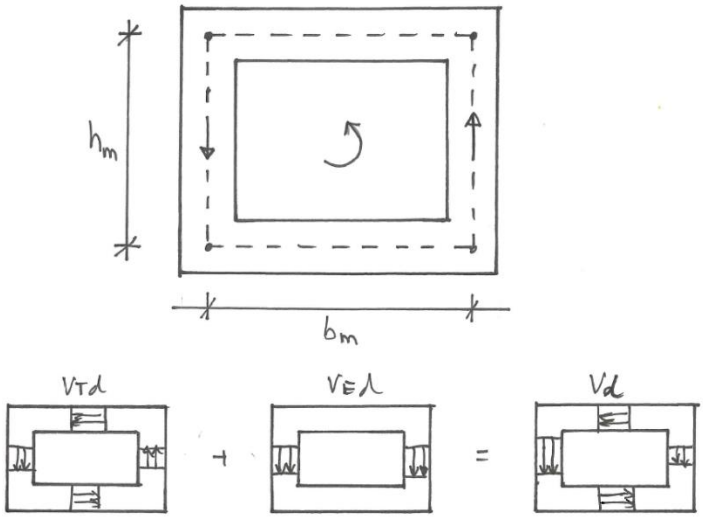

Figure D-7: Shear + torsion

The governing total shear force taken from SCIA is the one where the sum of V_x and V_{Td} is the largest:

Situation 1. V_{Ed} =449.92 kN

Situation 2. V_{Ed} = 1063.21 kN

So the governing situation for the shear resistance check wil be the location were the shear force is governing (situation 2). Furthermore the self-weight and prestressing also have to be taken into account with the result of V_{Ed} from SCIA. It is also possible that the eventual governing design shear force is found at the construction stage (t=0). So the shear force over the length of the beam needs to be determined at multiple stages. These stages and the shear forces are:

- t=0 only self weight: $V_{Ed} = V_{self} - P_{u0}$
- t=0 permanent loads: $V_{Ed} = V_{perm} - P_{u0}$
- t=∞ all loads + torsion: $V_{Ed} = V_{perm} + V_{var} - P_{u\infty}$

The upward force of the prestressing reduces the total shear force. But it only works between the support and the deviation point. The shear force is determined at the supports and just on each side of the deviation point. In general the shear force at these locations is determined as follows:

$V_{sup} = 0.5*q*L - P_u$

$V_{dev1} = 0.5*q*L - 0.5*q*a - P_u$

$V_{dev2} = 0.5*q*L - 0.5*q*a$

For t=∞ the shear force is added with V_{Td}. Assumed is that V_{Td} is constant over the length of the beam.

The parameters are:

Load of self-weight (ULS):	q_{self} =	16.92 kN/m
Permanent load (ULS):	q_{perm} =	30.659 kN/m
Variable load (ULS):	q_{var} =	66.89 kN/m
Upward Prestress force at t=0:	P_{u0} =	80.38 kN
Upward Prestress force at t=∞:	$P_{u\infty}$ =	64.31 kN
Distance deviators to support:	a =	8m

The result are seen in Table D-5 with the shear force lines in Figure D-8.

Table D-5: Results shear forces over length of beam

V [kN] at:	t=0 self	t=0 perm	t=inf
V_{sup}	122,659	260,044	1201,943
V_{dev1}	-12,701	33,094	421,578
V_{dev2}	67,680	113,475	485,882

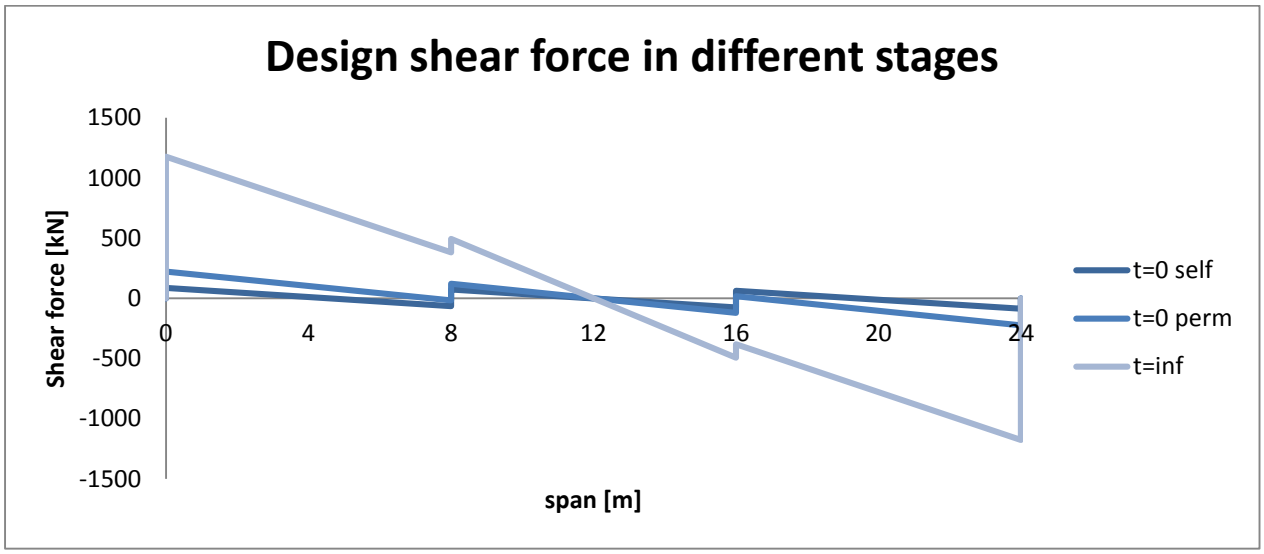

Figure D-8: Shear force line at multiple stages

The governing shear force V_{Ed} = 1201.94 kN at t=∞. The shear resistance has to be high enough to resist this force.

For determining the shear resistance two areas in the beam have to be considered: the cracked and uncracked area. The cracked area can be calculated by stating:
$M_{cr} = V_{Ed}*x-0,5q*x^2 - P_u$ with $M_{cr} = (f_{ctd} + \sigma_{cp})*W_c$.

Where
V_{Ed} = 1201.943 kN
q = 97.55 kN/m
P_u = 64.31 kN
f_{ctd} = 1.933 N/mm^2
σ_{cp} = 14.58 N/mm^2
$W_c = 0.081*10^9$ m^3
$M_{cr} = (1.933+14.58)*10^3*0.081$= 1335.7 kNm
The cracked area starts from a distance of x=1.07m of the support

In the cracked area if no shear reinforcement is applied the design shear force has to be smaller than the shear resistance of the concrete ($V_{Rd,c}$). According to NEN-EN 1992-1-1 cl 6.2.2(1):
$V_{Rd,c} = (v_{min} + k_1*\sigma_{cp})*b*d$
$V_{Rd,c} = (0.035*k^{1.5}*f_{ck}^{0.5} + k_1*P_{m\infty}/A_c)*2b_{web}*(h-e)$.

$k=1+(200/d)^{0.5} \leq 2.0$ with d=h-e = 600-92.6 = 507.4 mm --> k=1.628
k1=0.15
$V_{Rd,c}$ = 411.1 kN

For the uncracked area it is a requirement that the principal tensile stress is smaller than the design value of the concrete tensile strenght (f_{ctd}). This requirement leads to (NEN-EN 1992-1-1 cl 6.2.2(2)):
$V_{Rd,c} = [I/(d*S)]*[(f_{ctd})^2 + \alpha_l * fctd * \sigma_{cp}]^{0.5}$

S is the area of the first moment above and around the centroid axis: $S = 4.27*10^7$ mm^3.
The first crack that causes failure is at a distance of l_x = 400 mm from the end (100mm +H/2 see Figure D-9).

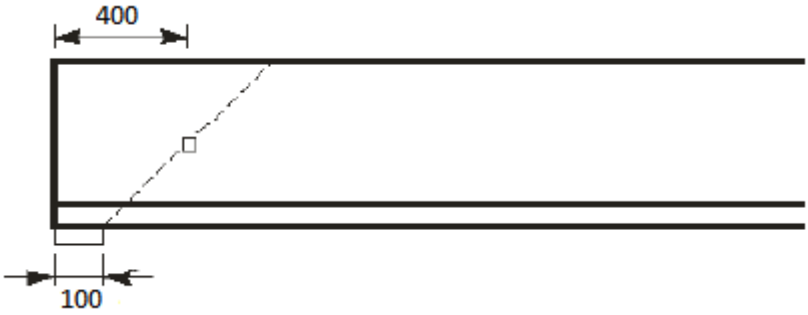

Figure D-9: Location of first crack

Because the strands are bonded by anchorage, there is a certain transmission length where the strands become fully prestressed. This transmission length is calculated according to EN 1992-1-1 cl. 8.10.2.2):
$f_{ctd}(t) = 0.7*f_{ctm}/1.5 = 1.913$ N/mm^2
$f_{bpt} = f_{ctd}(t)* \eta_{p1}* \eta_p = 1.913*2.7*1 = 5.166$ N/mm^2
$l_{pt} = \alpha 1* \alpha 1*\phi_{strand}*\sigma_{pm0}/f_{bpt} = 779.86$ mm
$l_{pt1} = 0.8*l_{pt} = 623.9$ mm
$l_{pt2} = 1.2*l_{pt} = 935.83$ mm

For ULS l_{pt2} is used. So before the prestress force is fully transferred, there is a reduced shear resistance (taken into account by $\alpha_l = l_x/l_{pt} = 0.43$). This results in:
$V_{Rd,c} = [0.025*10^{12}/\{507.4*4.27*10^7\})]*[(1.933)^2+0.43*1.933*14.58]^{0.5} = 691.54$ kN.

Then when the prestressing is fully transferred the shear resistance becomes ($\alpha_l = 1$):
$V_{Rd,c} = [0.025*10^{12}/\{507.4*4.27*10^7\})]*[(1.933)^2+1.0*1.933*14.58]^{0.5} = 983.43$ kN.

This is the resistance until the first crack appears at x=1.07m from the support. The governing shear resistance is the one in the cracked area. This resistance has to be checked if it can resist the shear force at location l_x. $V_{Ed}(l_x) = 1162.92$ kN
UC= $V_{Ed}/V_{Rd,c}$ = 1162.92/411.1 = 2.83 NOT OK!

It is obvious that the shear resistance does not suffice at all. So shear reinforcement has to be applied. The area of the shear reinforcement is calculated with the following formula (NEN-EN-1992-1-1 formula 6.8):
$A_{sw}/s_w = V_{Ed}/(z*f_{ywd}*\cot\theta)$.
A_{sw} is the area of one stirrup = $0.25*\pi*12^2 = 452.39$ mm^2
s_w is the distance between the stirrups.
$f_{ywd} = 435$ N/mm^2
z=0.9*d = 456.7mm
The only unknown is s_w. with everything filled in the formula: $s_w = 75$ mm. So φ12-75 which is equal to $A_s = 6030$ mm^2.
The stirrups have to be placed until 8.6m from the supports. At that location $V_{Rd,c} = V_{Ed}$.

D.11.2 Shear + torsion

It is also required that the combination of shear forces and torsional moments is verified. The structure should be able to resist these forces. The requirement for this states (NEN-EN-1992-1-1 cl. 6.3.2(4)):

$T_{Ed}/T_{Rd,max} + V_{Ed}/V_{Rd,max} \leq 1.0$

The requirement means that the capacity of the concrete struts has to be sufficient to resist the loads on the structure. Here the two previous situations are going to be investigated as well.

First $T_{Rd,max}$ and $V_{Rd,max}$ have to be determined:

NEN-EN-1992-1-1 formula 6.30: $T_{Rd,max} = 2*\nu*\alpha_{cw}*f_{cd}*A_k*t_{ef}*\sin\theta\cos\theta$

NEN-EN-1992-1-1 formula 6.9: $V_{Rd,max} = \alpha_{cw}*b_w*z*\nu*f_{cd}/(\cot\theta+\tan\theta)$

$\nu = 0.6 - f_{ck}/250 = 0.48$

α_{cw}:

$(1 + \sigma_{cp}/f_{cd})$ for $0 < \sigma_{cp} \leq 0.25\ f_{cd}$

1.25 for $0.25\ f_{cd} < \sigma_{cp} \leq 0.5\ f_{cd}$

$2.5\ (1 - \sigma_{cp}/f_{cd})$ for $0.5\ f_{cd} < \sigma_{cp} < 1.0\ f_{cd}$

For this case σ_{cp} 14.58 N/mm^2 = $0.43 f_{cd}$ so $\alpha_{cw} = 1.25$

$\theta = 45°$

t_{ef} =A/u which is the effective wall thickness (in hollow sections upper limit is the real thickness) --> with A the total area of the cross section including hollow part and u=4.2 as the circumference of area inside the centrelines.

t_{ef} = 0.214 m.

The smallest real thickness is 0.15m so this will be taken for t_{ef}.

$b_w = 2b_{web} = 300$ mm

$z = 0.9d = 457$mm

Filling everything in the equations gives:

$T_{Rd,mac}$ = 1782 kNm

$V_{Rd,max}$ = 1370kNm

Unity check:

Situation 1: 517.125/1782 + 236.3/1370 = 0.633

Situation 2: 469.87/1782 + 1106.24/1370 = 0.952

For both situations the concrete struts suffice.

The required torsional reinforcement can be determined with (NEN-EN-1992-1-1 formula 6.28):

$$\frac{\sum A_{sl}*f_{yd}}{u_k} = \frac{T_{Ed}}{2A_k}*\cot\theta$$

The only unknown in the equation is A_{sl}. When everything is filled in the equation:

A_{sl} = 3580 mm^2. This has to be divided over the webs and flanges. Furthermore the reinforcement is divided in two layers in te webs and flanges.

The amount of reinforcement per flange: $A_s = T_{Ed}/(2*h_m*f_{yd})$ = 1350 mm^2 → 9φ10 per layer (divided over the whole flange).

The amount of reinforcement per web: $A_s = T_{Ed}/(2*b_m*f_{yd})$ = 440 mm^2 → 3φ10 per layer (divided over the web, which is $H - h_{top} - h_{bot}$).

D.12 Capacity check at point of full transfer of prestress force

When looking at the support, most of the prestressing strands are concentrated in the bottom flange, while a couple are located in the webs (6 per web). So the gravity point of all strands will not coincide with the neutral axis of the box girder. This means that the strands will cause a moment here. At time of construction (t=0) this moment could possibly cause failure as there are no variable loads present. Because of the required transfer length of the prestress forces there are no moments caused by the strands directly at the supports, since the force is not fully transferred yet. But at the end of the transfer length, the moment capacity will have to be checked, because here the prestress force is fully transferred and a moment is caused by the eccentricity of the strands. This check will be performed here. The transfer length is l_{pt} = 779.86 mm. So the cross section at a distance of 779.86 mm from the support will be checked.
The moment at l_{pt} due to the prestressing is: $Pm0*(f-f_{fict}) + P_{u0}*l_{pt}$ = 1612.31 kNm. In the UGT this has to be multiplied with factor γ_p = 1.2 (because moment is unfavourable in this situation). So:
$M_{p,lpt}$ = 1934.77 kNm.

The moment by the self-weight of the beam at l_{pt} is $0.5*q_g*l_{pt}*(L-l_{pt})$ = 153.2 kNm (factor 1.2 included). Adding the moments leads to:
$M_{Ed} = M_{p,lpt} – M_g$ = 1781.57 kNm.

At l_{pt} the situation is as in Figure D-10 is presented. The compression zone is at the bottom side. The torsion reinforcement ($A_{s,top} = A_{s,bot}$ = 1350mm^2) is also taken into account, as it benefits the moment capacity. The gravity point of the bars in each flange is at a distance of h_s=62mm from the edge. The height of the compression zone has to be determined. Then the moment capacity can be calculated. The moment capacity will show if the longitudinal reinforcement applied is enough to assist in resisting the moment caused by the prestressing strands. If this is not the case additional reinforcement will have to be applied.

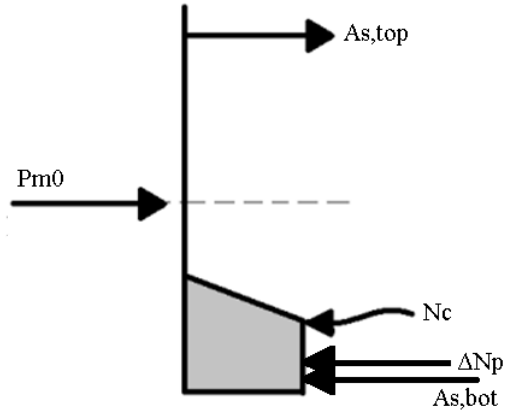

Figure D-10: Cross section at l_{pt}

For equilibrium of the internal forces the following equation stands: $P_{m0} + A_s,bot = N_c + \Delta N_p + A_{s,bot}$, which results in:
$P_{m0} – A_p*(\sigma_{pu} - \sigma_{pm0}) = \alpha*B*x_u*f_{cd}$
Solving this equation results in a compression zone height of:
x_u = 10277-7367*(1606.36-1395)/(0.75*1500*33.33) = 232.53mm.

Then if the moment around the point of the resultant of N_c is taken, a moment capacity of:
$M_{Rd} = P_{m0}*(z_b-\beta*x_u) + A_p*(\sigma_{pu} - \sigma_{pm0})*(\beta*x_u-e) + A_s*f_{yd}*[(H-h_s- \beta*x_u)+(\beta*x_u-h_s)]$ = 2488.9 kNm is found. This is higher than $M_{p,lpt}$ (UC=0.72) so the structure is safe. No extra longitudinal reinforcement is required.

D.13 Summary

Also added are results if H=800mm would be used. The same procedure as above is followed to determine the required parameters.

H=600mm

Amount of strands:	53ϕ15.2 strands	
Total losses in strands:	20%	
Slenderness ratio, λ	40	
ULS		
Bending moment capacity, M_{Rd}:	M_{Rd} = 2403.85 kNm	UC = 0.778
Rotational capacity: x_u/d	x_u/d = 0.965	UC = 2.049
Shear capacity V_{Rd}:	$V_{Rd,c}$ = 411.08 kN	UC = 2.829
Shear reinforcement	A_{sw} = 6030 mm^2	
Torsion reinforcement:	A_s = 3772 mm^2	
Capacity concrete at hammerhead:	$M_{Rd,head}$ = 2488.9 kNm	UC = 0.716

H=800mm

Amount of strands:	38ϕ15.2 strands	
Total losses in strands:	20%	
Slenderness ratio, λ	30	
ULS		
Bending moment capacity, M_{Rd}:	M_{Rd} = 3296.2 kNm	UC = 0.572
Rotational capacity: x_u/d	x_u/d = 0.207	UC = 0.433
Shear capacity V_{Rd}:	$V_{Rd,c}$ = 400.28 kN	UC = 2.82
Shear reinforcement	A_{sw} = 4110 mm^2	
Torsion reinforcement:	A_s = 2828 mm^2	
Capacity concrete at hammerhead:	$M_{Rd,head}$ = 2785.81 kNm	UC = 0.514

Note: Using H= 800 mm still does not result in a high shear capacity, but the amount of strands and reinforcement is greatly reduced and the design would therefore be more economical and easier to construct (concerning fitting everything).

SCIA ENGINEER REPORT C50/60

1. Project

Licence name	IBA
Project	Leidse Brug
Part	C50/60
Description	-
Author	A. Paskvalin
Date	08.09.2014
Structure	General XYZ
No. of nodes :	48
No. of beams :	0
No. of slabs :	1
No. of solids :	0
No. of used profiles :	0
No. of load cases :	84
No. of used materials :	1
Acceleration of gravity [m/s^2]	10,000
National code	EC - EN

2. Table of contents

3. Materials

Concrete EC2

Name	Type	Unit mass [kg/m^3]	E mod [MPa]	Poisson - nu	Thermal exp [m/mK]	Characteristic compressive cylinder strength fck(28) [MPa]
C50/60	Concrete	2500,0	1,2433e+04	0.0001	0,00	50,00

4. Calculation Model

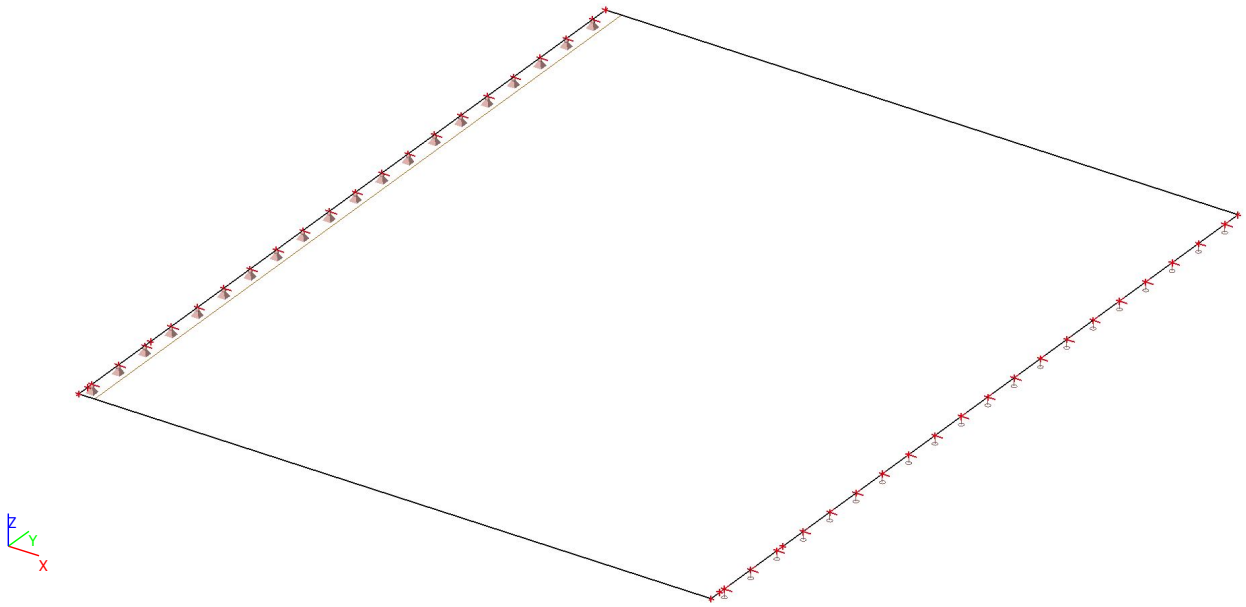

5. Orthotropy

OT1	
Type of orthotropy	Standard
Thickness of Plate/Wall [mm]	170
Material	C50/60
D11 [MNm]	6,1550e+02
D22 [MNm]	9,3500e+01
D12 [MNm]	3,6600e+01
D33 [MNm]	4,0379e+02
D44 [MN/m]	1,4270e+03
D55 [MN/m]	3,3630e+03
d11 [MN/m]	2,1137e+03
d22 [MN/m]	2,1137e+03
d12 [MN/m]	2,1137e-01
d33 [MN/m]	1,0567e+03
K xy [MN/m]	1,0000e+00
K yx [MN/m]	1,0000e+00

6. Nodes

Name	Coord X [m]	Coord Y [m]	Coord Z [m]
K5	0,500	0,750	0,000
K6	0,500	2,250	0,000
K7	0,500	3,750	0,000
K8	0,500	5,250	0,000
K9	0,500	6,750	0,000
K10	0,500	8,250	0,000
K11	0,500	9,750	0,000
K12	0,500	11,250	0,000
K13	0,500	12,750	0,000
K14	0,500	14,250	0,000
K15	0,500	15,750	0,000
K16	0,500	17,250	0,000
K17	0,500	18,750	0,000
K18	0,500	20,250	0,000
K19	0,500	21,750	0,000
K20	0,500	23,250	0,000

Name	Coord X [m]	Coord Y [m]	Coord Z [m]
K21	0,500	24,750	0,000
K22	0,500	26,250	0,000
K23	0,500	27,750	0,000
K24	0,500	29,250	0,000
K25	24,500	0,750	0,000
K26	24,500	2,250	0,000
K27	24,500	3,750	0,000
K28	24,500	5,250	0,000
K29	24,500	6,750	0,000
K30	24,500	8,250	0,000
K31	24,500	9,750	0,000
K32	24,500	11,250	0,000
K33	24,500	12,750	0,000
K34	24,500	14,250	0,000
K35	24,500	15,750	0,000
K36	24,500	17,250	0,000

Name	Coord X [m]	Coord Y [m]	Coord Z [m]
K37	24,500	18,750	0,000
K38	24,500	20,250	0,000
K39	24,500	21,750	0,000
K40	24,500	23,250	0,000
K41	24,500	24,750	0,000
K42	24,500	26,250	0,000
K43	24,500	27,750	0,000
K44	24,500	29,250	0,000
K45	0,500	0,500	0,000
K46	24,500	0,500	0,000
K47	0,500	0,000	0,000
K48	24,500	0,000	0,000
K49	24,500	30,000	0,000
K50	0,500	30,000	0,000
K51	0,500	4,088	0,000
K52	24,500	4,088	0,000

7. 2D members

Name	Layer	Type	Analysis model	Material	Thickness type	Th. [mm]
E1	Laag1	plate (90)	Standard	C50/60		170

8. Nodal supports

Name	Node	System	Type	X	Y	Z	Rx	Ry	Rz
Sn1	K5	GCS	Standard	Rigid	Rigid	Rigid	Free	Free	Free
Sn2	K6	GCS	Standard	Rigid	Rigid	Rigid	Free	Free	Free

Name	Node	System	Type	X	Y	Z	Rx	Ry	Rz
Sn3	K7	GCS	Standard	Rigid	Rigid	Rigid	Free	Free	Free
Sn4	K8	GCS	Standard	Rigid	Rigid	Rigid	Free	Free	Free
Sn5	K9	GCS	Standard	Rigid	Rigid	Rigid	Free	Free	Free
Sn6	K10	GCS	Standard	Rigid	Rigid	Rigid	Free	Free	Free
Sn7	K11	GCS	Standard	Rigid	Rigid	Rigid	Free	Free	Free
Sn8	K12	GCS	Standard	Rigid	Rigid	Rigid	Free	Free	Free
Sn9	K13	GCS	Standard	Rigid	Rigid	Rigid	Free	Free	Free
Sn10	K14	GCS	Standard	Rigid	Rigid	Rigid	Free	Free	Free
Sn11	K15	GCS	Standard	Rigid	Rigid	Rigid	Free	Free	Free
Sn12	K16	GCS	Standard	Rigid	Rigid	Rigid	Free	Free	Free
Sn13	K17	GCS	Standard	Rigid	Rigid	Rigid	Free	Free	Free
Sn14	K18	GCS	Standard	Rigid	Rigid	Rigid	Free	Free	Free
Sn15	K19	GCS	Standard	Rigid	Rigid	Rigid	Free	Free	Free
Sn16	K20	GCS	Standard	Rigid	Rigid	Rigid	Free	Free	Free
Sn17	K21	GCS	Standard	Rigid	Rigid	Rigid	Free	Free	Free
Sn18	K22	GCS	Standard	Rigid	Rigid	Rigid	Free	Free	Free
Sn19	K23	GCS	Standard	Rigid	Rigid	Rigid	Free	Free	Free
Sn20	K24	GCS	Standard	Rigid	Rigid	Rigid	Free	Free	Free
Sn21	K25	GCS	Standard	Free	Rigid	Rigid	Free	Free	Free
Sn22	K26	GCS	Standard	Free	Rigid	Rigid	Free	Free	Free
Sn23	K27	GCS	Standard	Free	Rigid	Rigid	Free	Free	Free
Sn24	K28	GCS	Standard	Free	Rigid	Rigid	Free	Free	Free
Sn25	K29	GCS	Standard	Free	Rigid	Rigid	Free	Free	Free
Sn26	K30	GCS	Standard	Free	Rigid	Rigid	Free	Free	Free
Sn27	K31	GCS	Standard	Free	Rigid	Rigid	Free	Free	Free
Sn28	K32	GCS	Standard	Free	Rigid	Rigid	Free	Free	Free
Sn29	K33	GCS	Standard	Free	Rigid	Rigid	Free	Free	Free
Sn30	K34	GCS	Standard	Free	Rigid	Rigid	Free	Free	Free
Sn31	K35	GCS	Standard	Free	Rigid	Rigid	Free	Free	Free
Sn32	K36	GCS	Standard	Free	Rigid	Rigid	Free	Free	Free
Sn33	K37	GCS	Standard	Free	Rigid	Rigid	Free	Free	Free
Sn34	K38	GCS	Standard	Free	Rigid	Rigid	Free	Free	Free
Sn35	K39	GCS	Standard	Free	Rigid	Rigid	Free	Free	Free
Sn36	K40	GCS	Standard	Free	Rigid	Rigid	Free	Free	Free
Sn37	K41	GCS	Standard	Free	Rigid	Rigid	Free	Free	Free
Sn38	K42	GCS	Standard	Free	Rigid	Rigid	Free	Free	Free
Sn39	K43	GCS	Standard	Free	Rigid	Rigid	Free	Free	Free
Sn40	K44	GCS	Standard	Free	Rigid	Rigid	Free	Free	Free

9. Load cases

Name	Description	Action type	LoadGroup	Duration	Master load case
	Spec	Load type			
BG2	Dead load	Permanent	LG1		
		Standard			
BG3	Edge load	Permanent	LG1		
		Standard			
BG4	Traffic load| P.T| UDL	Variable	LG2	Short	None
	Standard	Static			
BG6	Traffic load| A.T| UDL	Variable	LG2	Short	None
	Standard	Static			
BG9	Pedestrian load| crowd	Variable	LG2	Short	None
	Standard	Static			
BG10	Pedestrian load| des loc	Variable	LG2	Short	None
	Standard	Static			
BG7	AT| TS (3x)	Variable	LG3	Short	None
	Standard	Static			
BG5	PT| car TS (1x)	Variable	LG3	Short	None
	Standard	Static			
BG8	PT| tram TS (2x)	Variable	LG3	Short	None
	Standard	Static			
LC4	TR1/BM10,000 m	Variable	LG3	Short	None
	Standard	Static			
LC5	TR1/BM11,000 m	Variable	LG3	Short	None
	Standard	Static			
LC6	TR1/BM12,000 m	Variable	LG3	Short	None
	Standard	Static			
LC7	TR1/BM13,000 m	Variable	LG3	Short	None
	Standard	Static			
LC8	TR1/BM14,000 m	Variable	LG3	Short	None
	Standard	Static			
LC9	TR1/BM15,000 m	Variable	LG3	Short	None
	Standard	Static			
LC10	TR1/BM16,000 m	Variable	LG3	Short	None
	Standard	Static			

Name	Description	Action type	LoadGroup	Duration	Master load case
	Spec	Load type			
LC11	TR1/BM17,000 m Standard	Variable Static	LG3	Short	None
LC12	TR1/BM18,000 m Standard	Variable Static	LG3	Short	None
LC13	TR1/BM19,000 m Standard	Variable Static	LG3	Short	None
LC14	TR1/BM110,000 m Standard	Variable Static	LG3	Short	None
LC15	TR1/BM111,000 m Standard	Variable Static	LG3	Short	None
LC16	TR1/BM112,000 m Standard	Variable Static	LG3	Short	None
LC17	TR1/BM113,000 m Standard	Variable Static	LG3	Short	None
LC18	TR1/BM114,000 m Standard	Variable Static	LG3	Short	None
LC19	TR1/BM115,000 m Standard	Variable Static	LG3	Short	None
LC20	TR1/BM116,000 m Standard	Variable Static	LG3	Short	None
LC21	TR1/BM117,000 m Standard	Variable Static	LG3	Short	None
LC22	TR1/BM118,000 m Standard	Variable Static	LG3	Short	None
LC23	TR1/BM119,000 m Standard	Variable Static	LG3	Short	None
LC24	TR1/BM120,000 m Standard	Variable Static	LG3	Short	None
LC25	TR1/BM121,000 m Standard	Variable Static	LG3	Short	None
LC26	TR1/BM122,000 m Standard	Variable Static	LG3	Short	None
LC27	TR1/BM123,000 m Standard	Variable Static	LG3	Short	None
LC28	TR1/BM124,000 m Standard	Variable Static	LG3	Short	None
LC29	TR2/BM20,000 m Standard	Variable Static	LG3	Short	None
LC30	TR2/BM21,000 m Standard	Variable Static	LG3	Short	None
LC31	TR2/BM22,000 m Standard	Variable Static	LG3	Short	None
LC32	TR2/BM23,000 m Standard	Variable Static	LG3	Short	None
LC33	TR2/BM24,000 m Standard	Variable Static	LG3	Short	None
LC34	TR2/BM25,000 m Standard	Variable Static	LG3	Short	None
LC35	TR2/BM26,000 m Standard	Variable Static	LG3	Short	None
LC36	TR2/BM27,000 m Standard	Variable Static	LG3	Short	None
LC37	TR2/BM28,000 m Standard	Variable Static	LG3	Short	None
LC38	TR2/BM29,000 m Standard	Variable Static	LG3	Short	None
LC39	TR2/BM210,000 m Standard	Variable Static	LG3	Short	None
LC40	TR2/BM211,000 m Standard	Variable Static	LG3	Short	None
LC41	TR2/BM212,000 m Standard	Variable Static	LG3	Short	None
LC42	TR2/BM213,000 m Standard	Variable Static	LG3	Short	None
LC43	TR2/BM214,000 m Standard	Variable Static	LG3	Short	None
LC44	TR2/BM215,000 m Standard	Variable Static	LG3	Short	None
LC45	TR2/BM216,000 m Standard	Variable Static	LG3	Short	None
LC46	TR2/BM217,000 m Standard	Variable Static	LG3	Short	None
LC47	TR2/BM218,000 m Standard	Variable Static	LG3	Short	None
LC48	TR2/BM219,000 m	Variable	LG3	Short	None

Name	Description	Action type	LoadGroup	Duration	Master load case
	Spec	Load type			
	Standard	Static			
LC49	TR2/BM220,000 m	Variable	LG3	Short	None
	Standard	Static			
LC50	TR2/BM221,000 m	Variable	LG3	Short	None
	Standard	Static			
LC51	TR2/BM222,000 m	Variable	LG3	Short	None
	Standard	Static			
LC52	TR2/BM223,000 m	Variable	LG3	Short	None
	Standard	Static			
LC53	TR2/BM224,000 m	Variable	LG3	Short	None
	Standard	Static			
LC54	TR3/BM30,000 m	Variable	LG3	Short	None
	Standard	Static			
LC55	TR3/BM31,000 m	Variable	LG3	Short	None
	Standard	Static			
LC56	TR3/BM32,000 m	Variable	LG3	Short	None
	Standard	Static			
LC57	TR3/BM33,000 m	Variable	LG3	Short	None
	Standard	Static			
LC58	TR3/BM34,000 m	Variable	LG3	Short	None
	Standard	Static			
LC59	TR3/BM35,000 m	Variable	LG3	Short	None
	Standard	Static			
LC60	TR3/BM36,000 m	Variable	LG3	Short	None
	Standard	Static			
LC61	TR3/BM37,000 m	Variable	LG3	Short	None
	Standard	Static			
LC62	TR3/BM38,000 m	Variable	LG3	Short	None
	Standard	Static			
LC63	TR3/BM39,000 m	Variable	LG3	Short	None
	Standard	Static			
LC64	TR3/BM310,000 m	Variable	LG3	Short	None
	Standard	Static			
LC65	TR3/BM311,000 m	Variable	LG3	Short	None
	Standard	Static			
LC66	TR3/BM312,000 m	Variable	LG3	Short	None
	Standard	Static			
LC67	TR3/BM313,000 m	Variable	LG3	Short	None
	Standard	Static			
LC68	TR3/BM314,000 m	Variable	LG3	Short	None
	Standard	Static			
LC69	TR3/BM315,000 m	Variable	LG3	Short	None
	Standard	Static			
LC70	TR3/BM316,000 m	Variable	LG3	Short	None
	Standard	Static			
LC71	TR3/BM317,000 m	Variable	LG3	Short	None
	Standard	Static			
LC72	TR3/BM318,000 m	Variable	LG3	Short	None
	Standard	Static			
LC73	TR3/BM319,000 m	Variable	LG3	Short	None
	Standard	Static			
LC74	TR3/BM320,000 m	Variable	LG3	Short	None
	Standard	Static			
LC75	TR3/BM321,000 m	Variable	LG3	Short	None
	Standard	Static			
LC76	TR3/BM322,000 m	Variable	LG3	Short	None
	Standard	Static			
LC77	TR3/BM323,000 m	Variable	LG3	Short	None
	Standard	Static			
LC78	TR3/BM324,000 m	Variable	LG3	Short	None
	Standard	Static			

10. LC2 - Dead load

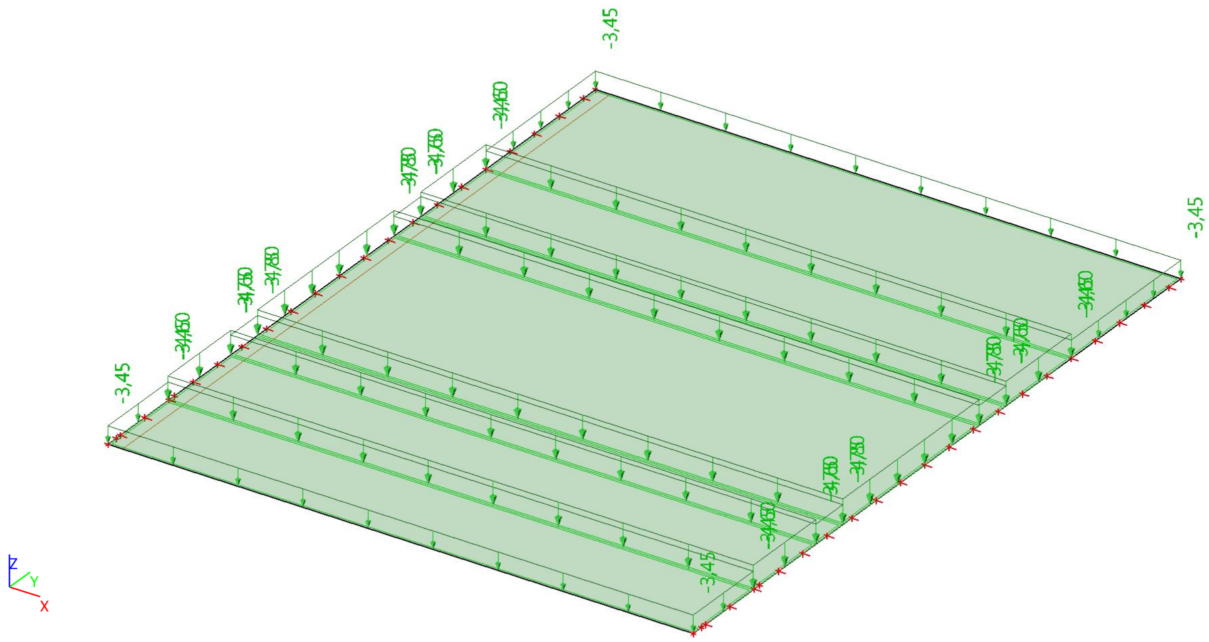

11. LC3- Edge load

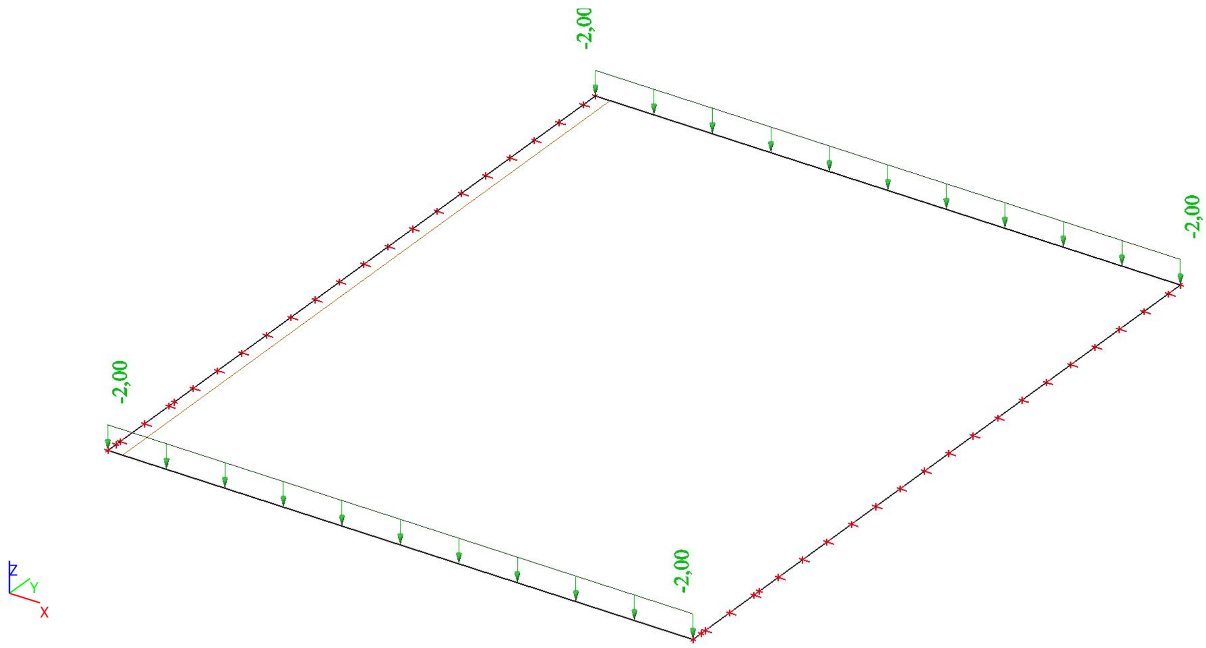

12. LC4 - Traffic load| P.T| UDL

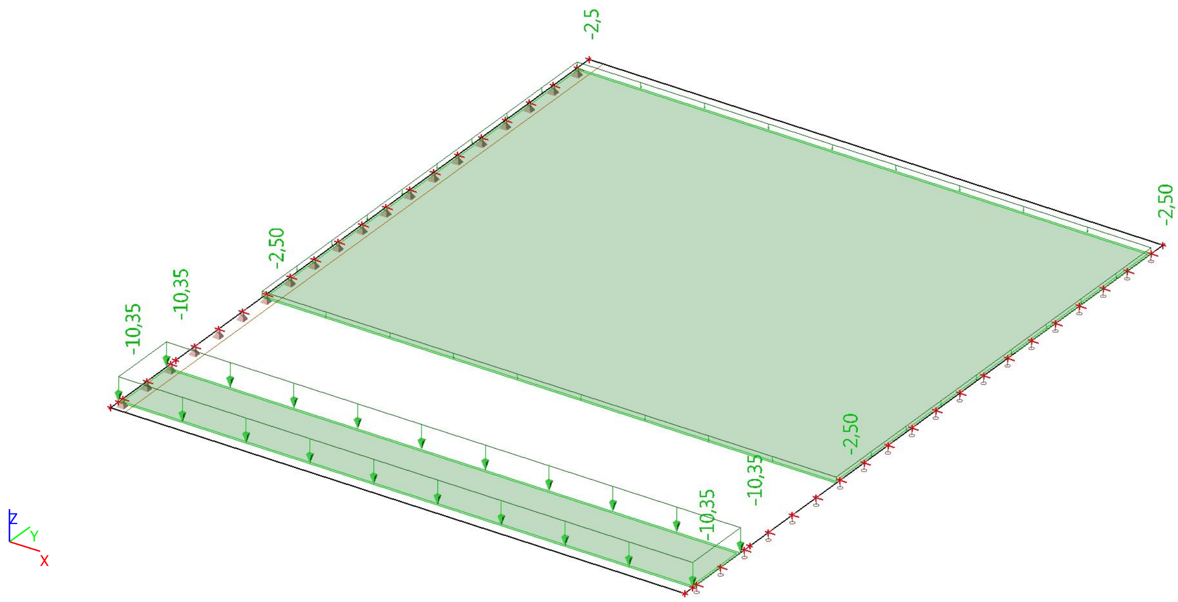

13. LC5- Tandem system| PT

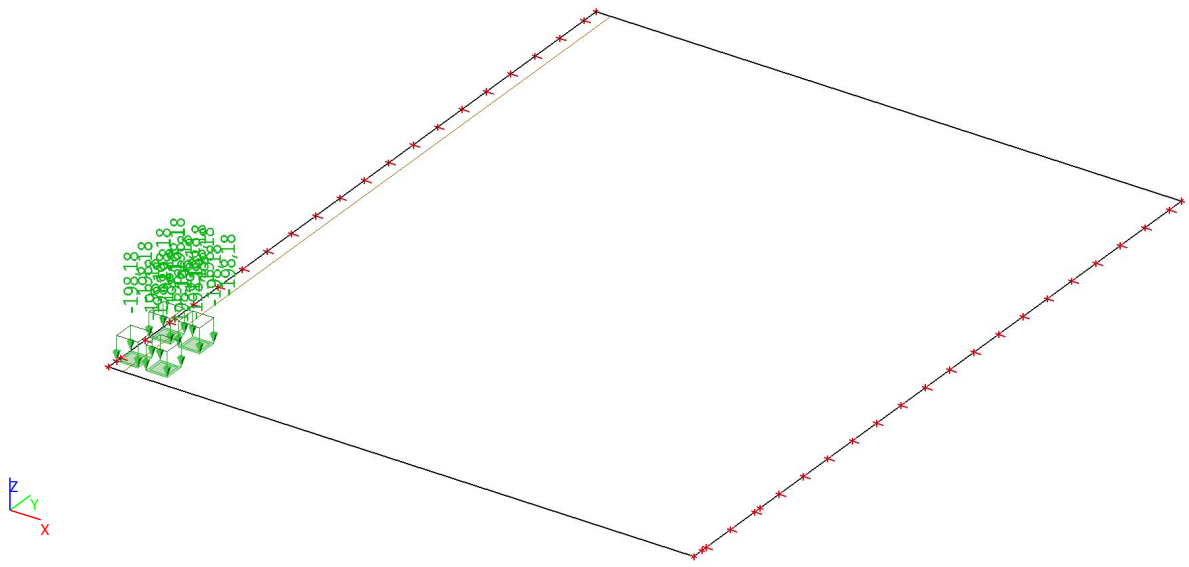

14. LC6 - Traffic load| A.T| UDL

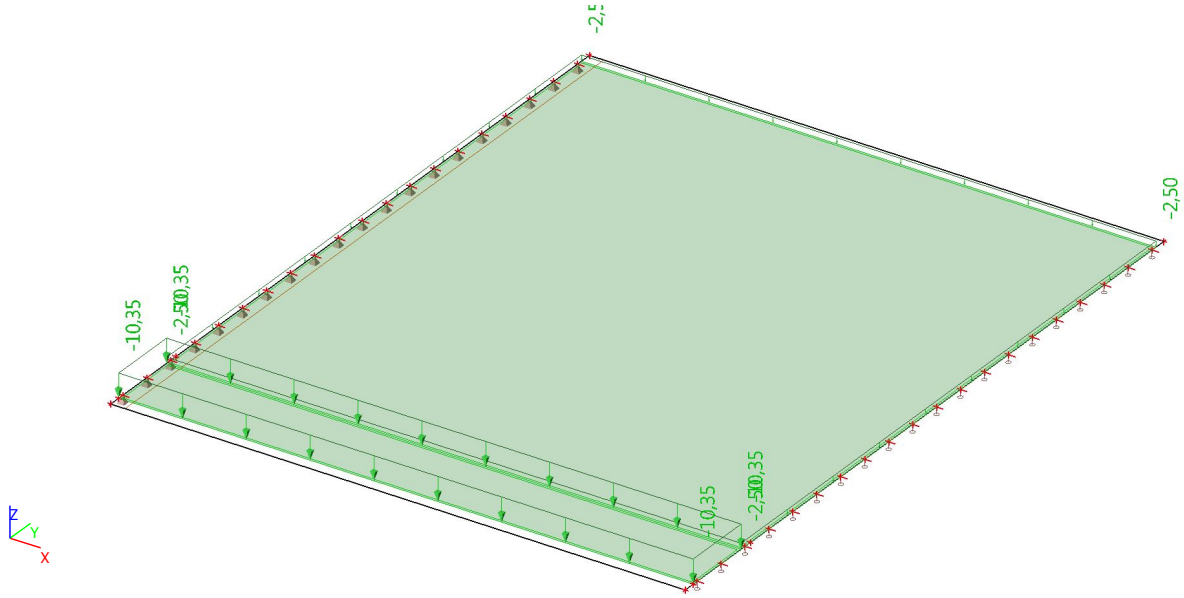

15. LC7 - Tandem systems | AT

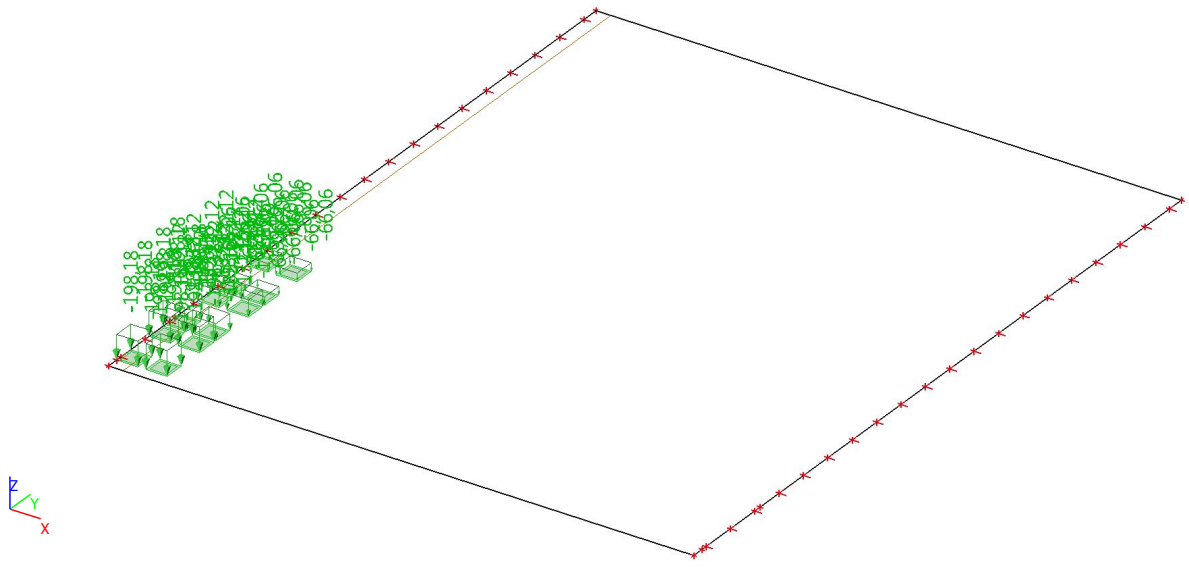

16. LC8 - Tram loading

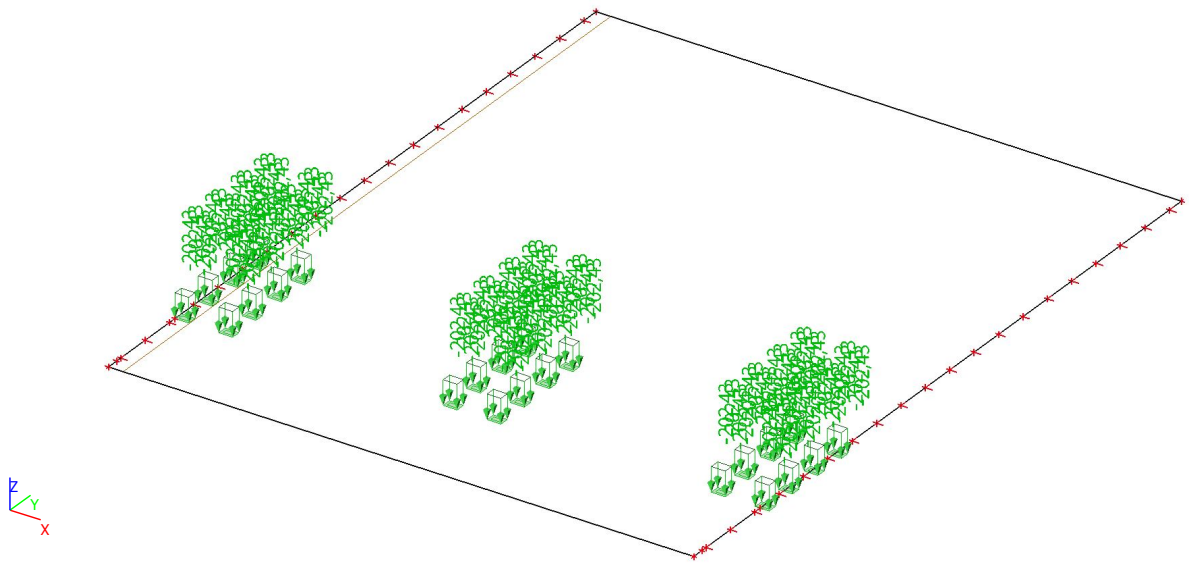

17. LC9 - Pedestrian load| crowd

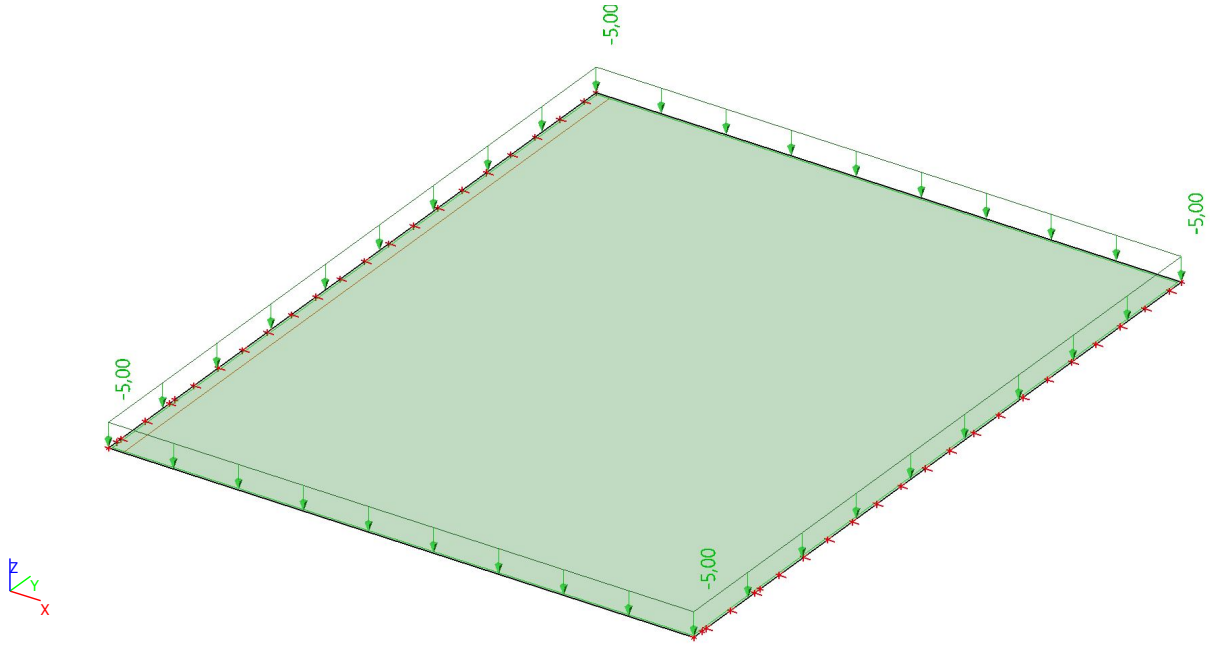

18. LC10 - Pedestrian load| des loc

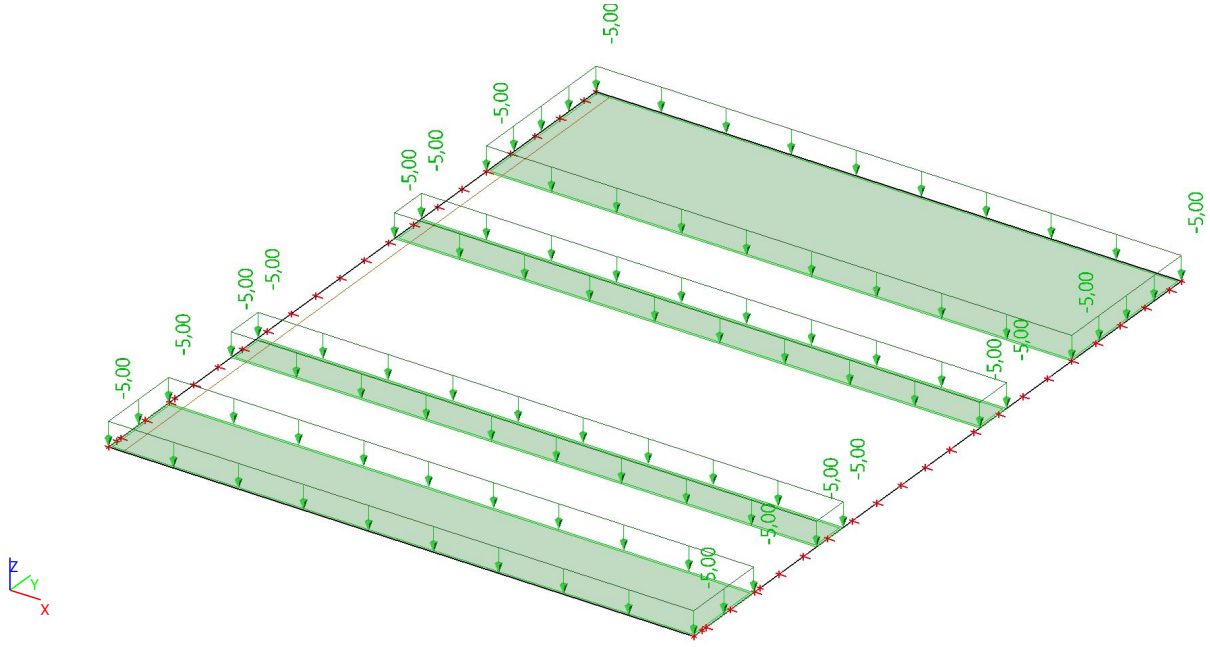

19. Traffic lane

Name	Used nodes	Node	Use for calculation
TR1	2	Head	✓
		End	
TR2	2	Head	✓
		End	
TR3	2	Head	✓
		End	

20. Lane loads manager

Name	Traffic Loads	Traffic lane	Load group	Load case name	Step [m]
LL1	BM1	TR1	LG3	TR1/BM1	1,000
LL2	BM2	TR2	LG3	TR2/BM2	1,000
LL3	BM3	TR3	LG3	TR3/BM3	1,000

21. Load pattern

Name	Type	Description	Force [kN/m²]	Position x1 [m]	Position y1 [m]	Position y2 [m]
				Repeat x (n)	Delta x [m]	Delta y [m]
				Position x2 [m]		
				Repeat y (n)		
BM1	Rectangle	3 vehicles	-198,18	0,000	0,000	0,870
	Rectangle		-132,12	0,000	3,000	3,870
	Rectangle		-66,06	0,000	6,000	6,870
				2	1,200	2,000
				2	1,200	2,000
				2	1,200	2,000
				0,870		
				0,870		
				0,870		
				2		
				2		
				2		
BM2	Rectangle	1 vehicle + 2 trams| vehicle	-198,18	0,000	0,000	0,870
				2	1,200	2,000
				0,870		
				2		
BM3	Rectangle	1 vehicle + 2 trams| tram	-202,43	0,000	0,000	0,390
	Rectangle		-202,43	0,000	3,000	3,390
	Rectangle		-202,43	11,000	0,000	0,390
	Rectangle		-202,43	22,000	0,000	0,390
	Rectangle		-202,43	11,000	3,000	3,390
	Rectangle		-202,43	22,000	3,000	3,390
				2	1,800	1,435
				2	1,800	1,435

Name	Type	Description	Force [kN/m²]	Position x1 [m]	Position y1 [m]	Position y2 [m]
				Repeat x (n)	Delta x [m]	Delta y [m]
				Position x2 [m]		
				Repeat y (n)		
				2	1,800	1,435
				2	1,800	1,435
				2	1,800	1,435
				2	1,800	1,435
				0,570		
				0,570		
				11,570		
				22,570		
				11,570		
				22,570		
				2		
				2		
				2		
				2		
				2		
				2		

22. Load groups

Name	Load	Relation	Type
LG1	Permanent		
LG2	Variable	Standard	Cat G : Vehicle >30kN
LG3	Variable	Exclusive	Cat G : Vehicle >30kN

23. Combinations

Name	Description	Type	Load cases	Coeff. [-]
CO1.1|UGT	PT,ugt, auto gov	Envelope - ultimate	BG2 - Dead load	1,20
			BG3 - Edge load	1,20
			BG4 - Traffic load| P.T| UDL	1,35
			BG10 - Pedestrian load| des loc	1,08
			LC29 - TR2/BM20,000 m	1,35
			LC30 - TR2/BM21,000 m	1,35
			LC31 - TR2/BM22,000 m	1,35
			LC32 - TR2/BM23,000 m	1,35
			LC33 - TR2/BM24,000 m	1,35
			LC34 - TR2/BM25,000 m	1,35
			LC35 - TR2/BM26,000 m	1,35
			LC36 - TR2/BM27,000 m	1,35
			LC37 - TR2/BM28,000 m	1,35
			LC38 - TR2/BM29,000 m	1,35
			LC39 - TR2/BM210,000 m	1,35
			LC40 - TR2/BM211,000 m	1,35
			LC41 - TR2/BM212,000 m	1,35
			LC42 - TR2/BM213,000 m	1,35
			LC43 - TR2/BM214,000 m	1,35
			LC44 - TR2/BM215,000 m	1,35
			LC45 - TR2/BM216,000 m	1,35
			LC46 - TR2/BM217,000 m	1,35
			LC47 - TR2/BM218,000 m	1,35
			LC48 - TR2/BM219,000 m	1,35
			LC49 - TR2/BM220,000 m	1,35
			LC50 - TR2/BM221,000 m	1,35
			LC51 - TR2/BM222,000 m	1,35
			LC52 - TR2/BM223,000 m	1,35
			LC53 - TR2/BM224,000 m	1,35
			LC54 - TR3/BM30,000 m	1,08
			LC55 - TR3/BM31,000 m	1,08
			LC56 - TR3/BM32,000 m	1,08
			LC57 - TR3/BM33,000 m	1,08
			LC58 - TR3/BM34,000 m	1,08
			LC59 - TR3/BM35,000 m	1,08
			LC60 - TR3/BM36,000 m	1,08
			LC61 - TR3/BM37,000 m	1,08
			LC62 - TR3/BM38,000 m	1,08
			LC63 - TR3/BM39,000 m	1,08
			LC64 - TR3/BM310,000 m	1,08
			LC65 - TR3/BM311,000 m	1,08
			LC66 - TR3/BM312,000 m	1,08
			LC67 - TR3/BM313,000 m	1,08

Name	Description	Type	Load cases	Coeff. [-]
			LC68 - TR3/BM314,000 m	1,08
			LC69 - TR3/BM315,000 m	1,08
			LC70 - TR3/BM316,000 m	1,08
			LC71 - TR3/BM317,000 m	1,08
			LC72 - TR3/BM318,000 m	1,08
			LC73 - TR3/BM319,000 m	1,08
			LC74 - TR3/BM320,000 m	1,08
			LC75 - TR3/BM321,000 m	1,08
			LC76 - TR3/BM322,000 m	1,08
			LC77 - TR3/BM323,000 m	1,08
			LC78 - TR3/BM324,000 m	1,08
CO2.1|UGT	PT,ugt, tram gov	Envelope - ultimate	BG2 - Dead load	1,20
			BG3 - Edge load	1,20
			BG4 - Traffic load| P.T| UDL	1,08
			BG10 - Pedestrian load| des loc	1,08
			LC29 - TR2/BM20,000 m	1,08
			LC30 - TR2/BM21,000 m	1,08
			LC31 - TR2/BM22,000 m	1,08
			LC32 - TR2/BM23,000 m	1,08
			LC33 - TR2/BM24,000 m	1,08
			LC34 - TR2/BM25,000 m	1,08
			LC35 - TR2/BM26,000 m	1,08
			LC36 - TR2/BM27,000 m	1,08
			LC37 - TR2/BM28,000 m	1,08
			LC38 - TR2/BM29,000 m	1,08
			LC39 - TR2/BM210,000 m	1,08
			LC40 - TR2/BM211,000 m	1,08
			LC41 - TR2/BM212,000 m	1,08
			LC42 - TR2/BM213,000 m	1,08
			LC43 - TR2/BM214,000 m	1,08
			LC44 - TR2/BM215,000 m	1,08
			LC45 - TR2/BM216,000 m	1,08
			LC46 - TR2/BM217,000 m	1,08
			LC47 - TR2/BM218,000 m	1,08
			LC48 - TR2/BM219,000 m	1,08
			LC49 - TR2/BM220,000 m	1,08
			LC50 - TR2/BM221,000 m	1,08
			LC51 - TR2/BM222,000 m	1,08
			LC52 - TR2/BM223,000 m	1,08
			LC53 - TR2/BM224,000 m	1,08
			LC54 - TR3/BM30,000 m	1,35
			LC55 - TR3/BM31,000 m	1,35
			LC56 - TR3/BM32,000 m	1,35
			LC57 - TR3/BM33,000 m	1,35
			LC58 - TR3/BM34,000 m	1,35
			LC59 - TR3/BM35,000 m	1,35
			LC60 - TR3/BM36,000 m	1,35
			LC61 - TR3/BM37,000 m	1,35
			LC62 - TR3/BM38,000 m	1,35
			LC63 - TR3/BM39,000 m	1,35
			LC64 - TR3/BM310,000 m	1,35
			LC65 - TR3/BM311,000 m	1,35
			LC66 - TR3/BM312,000 m	1,35
			LC67 - TR3/BM313,000 m	1,35
			LC68 - TR3/BM314,000 m	1,35
			LC69 - TR3/BM315,000 m	1,35
			LC70 - TR3/BM316,000 m	1,35
			LC71 - TR3/BM317,000 m	1,35
			LC72 - TR3/BM318,000 m	1,35
			LC73 - TR3/BM319,000 m	1,35
			LC74 - TR3/BM320,000 m	1,35
			LC75 - TR3/BM321,000 m	1,35
			LC76 - TR3/BM322,000 m	1,35
			LC77 - TR3/BM323,000 m	1,35
			LC78 - TR3/BM324,000 m	1,35
CO3.1|UGT	AT,ugt	Envelope - ultimate	BG2 - Dead load	1,20
			BG3 - Edge load	1,20
			BG6 - Traffic load| A.T| UDL	1,35
			BG10 - Pedestrian load| des loc	1,08
			LC4 - TR1/BM10,000 m	1,35
			LC5 - TR1/BM11,000 m	1,35
			LC6 - TR1/BM12,000 m	1,35
			LC7 - TR1/BM13,000 m	1,35
			LC8 - TR1/BM14,000 m	1,35
			LC9 - TR1/BM15,000 m	1,35
			LC10 - TR1/BM16,000 m	1,35

Name	Description	Type	Load cases	Coeff. [-]
			LC11 - TR1/BM17,000 m	1,35
			LC12 - TR1/BM18,000 m	1,35
			LC13 - TR1/BM19,000 m	1,35
			LC14 - TR1/BM110,000 m	1,35
			LC15 - TR1/BM111,000 m	1,35
			LC16 - TR1/BM112,000 m	1,35
			LC17 - TR1/BM113,000 m	1,35
			LC18 - TR1/BM114,000 m	1,35
			LC19 - TR1/BM115,000 m	1,35
			LC20 - TR1/BM116,000 m	1,35
			LC21 - TR1/BM117,000 m	1,35
			LC22 - TR1/BM118,000 m	1,35
			LC23 - TR1/BM119,000 m	1,35
			LC24 - TR1/BM120,000 m	1,35
			LC25 - TR1/BM121,000 m	1,35
			LC26 - TR1/BM122,000 m	1,35
			LC27 - TR1/BM123,000 m	1,35
			LC28 - TR1/BM124,000 m	1,35
CO4|UGT	Crowd	Linear - ultimate	BG2 - Dead load	1,20
			BG3 - Edge load	1,20
			BG9 - Pedestrian load| crowd	1,35
CO1.1|BGT	PT,bgt, auto gov	Envelope - serviceability	BG2 - Dead load	1,00
			BG3 - Edge load	1,00
			BG4 - Traffic load| P.T| UDL	1,00
			BG10 - Pedestrian load| des loc	0,80
			LC29 - TR2/BM20,000 m	1,00
			LC30 - TR2/BM21,000 m	1,00
			LC31 - TR2/BM22,000 m	1,00
			LC32 - TR2/BM23,000 m	1,00
			LC33 - TR2/BM24,000 m	1,00
			LC34 - TR2/BM25,000 m	1,00
			LC35 - TR2/BM26,000 m	1,00
			LC36 - TR2/BM27,000 m	1,00
			LC37 - TR2/BM28,000 m	1,00
			LC38 - TR2/BM29,000 m	1,00
			LC39 - TR2/BM210,000 m	1,00
			LC40 - TR2/BM211,000 m	1,00
			LC41 - TR2/BM212,000 m	1,00
			LC42 - TR2/BM213,000 m	1,00
			LC43 - TR2/BM214,000 m	1,00
			LC44 - TR2/BM215,000 m	1,00
			LC45 - TR2/BM216,000 m	1,00
			LC46 - TR2/BM217,000 m	1,00
			LC47 - TR2/BM218,000 m	1,00
			LC48 - TR2/BM219,000 m	1,00
			LC49 - TR2/BM220,000 m	1,00
			LC50 - TR2/BM221,000 m	1,00
			LC51 - TR2/BM222,000 m	1,00
			LC52 - TR2/BM223,000 m	1,00
			LC53 - TR2/BM224,000 m	1,00
			LC54 - TR3/BM30,000 m	0,80
			LC55 - TR3/BM31,000 m	0,80
			LC56 - TR3/BM32,000 m	0,80
			LC57 - TR3/BM33,000 m	0,80
			LC58 - TR3/BM34,000 m	0,80
			LC59 - TR3/BM35,000 m	0,80
			LC60 - TR3/BM36,000 m	0,80
			LC61 - TR3/BM37,000 m	0,80
			LC62 - TR3/BM38,000 m	0,80
			LC63 - TR3/BM39,000 m	0,80
			LC64 - TR3/BM310,000 m	0,80
			LC65 - TR3/BM311,000 m	0,80
			LC66 - TR3/BM312,000 m	0,80
			LC67 - TR3/BM313,000 m	0,80
			LC68 - TR3/BM314,000 m	0,80
			LC69 - TR3/BM315,000 m	0,80
			LC70 - TR3/BM316,000 m	0,80
			LC71 - TR3/BM317,000 m	0,80
			LC72 - TR3/BM318,000 m	0,80
			LC73 - TR3/BM319,000 m	0,80
			LC74 - TR3/BM320,000 m	0,80
			LC75 - TR3/BM321,000 m	0,80
			LC76 - TR3/BM322,000 m	0,80
			LC77 - TR3/BM323,000 m	0,80
			LC78 - TR3/BM324,000 m	0,80
CO2.1|BGT	PT,bgt, tram gov	Envelope - serviceability	BG2 - Dead load	1,00

Name	Description	Type	Load cases	Coeff. [-]
			BG3 - Edge load	1,00
			BG4 - Traffic load| P.T| UDL	0,80
			BG10 - Pedestrian load| des loc	0,80
			LC29 - TR2/BM20,000 m	0,80
			LC30 - TR2/BM21,000 m	0,80
			LC31 - TR2/BM22,000 m	0,80
			LC32 - TR2/BM23,000 m	0,80
			LC33 - TR2/BM24,000 m	0,80
			LC34 - TR2/BM25,000 m	0,80
			LC35 - TR2/BM26,000 m	0,80
			LC36 - TR2/BM27,000 m	0,80
			LC37 - TR2/BM28,000 m	0,80
			LC38 - TR2/BM29,000 m	0,80
			LC39 - TR2/BM210,000 m	0,80
			LC40 - TR2/BM211,000 m	0,80
			LC41 - TR2/BM212,000 m	0,80
			LC42 - TR2/BM213,000 m	0,80
			LC43 - TR2/BM214,000 m	0,80
			LC44 - TR2/BM215,000 m	0,80
			LC45 - TR2/BM216,000 m	0,80
			LC46 - TR2/BM217,000 m	0,80
			LC47 - TR2/BM218,000 m	0,80
			LC48 - TR2/BM219,000 m	0,80
			LC49 - TR2/BM220,000 m	0,80
			LC50 - TR2/BM221,000 m	0,80
			LC51 - TR2/BM222,000 m	0,80
			LC52 - TR2/BM223,000 m	0,80
			LC53 - TR2/BM224,000 m	0,80
			LC54 - TR3/BM30,000 m	1,00
			LC55 - TR3/BM31,000 m	1,00
			LC56 - TR3/BM32,000 m	1,00
			LC57 - TR3/BM33,000 m	1,00
			LC58 - TR3/BM34,000 m	1,00
			LC59 - TR3/BM35,000 m	1,00
			LC60 - TR3/BM36,000 m	1,00
			LC61 - TR3/BM37,000 m	1,00
			LC62 - TR3/BM38,000 m	1,00
			LC63 - TR3/BM39,000 m	1,00
			LC64 - TR3/BM310,000 m	1,00
			LC65 - TR3/BM311,000 m	1,00
			LC66 - TR3/BM312,000 m	1,00
			LC67 - TR3/BM313,000 m	1,00
			LC68 - TR3/BM314,000 m	1,00
			LC69 - TR3/BM315,000 m	1,00
			LC70 - TR3/BM316,000 m	1,00
			LC71 - TR3/BM317,000 m	1,00
			LC72 - TR3/BM318,000 m	1,00
			LC73 - TR3/BM319,000 m	1,00
			LC74 - TR3/BM320,000 m	1,00
			LC75 - TR3/BM321,000 m	1,00
			LC76 - TR3/BM322,000 m	1,00
			LC77 - TR3/BM323,000 m	1,00
			LC78 - TR3/BM324,000 m	1,00
CO3.1|BGT	AT,bgt,mid	Envelope - serviceability	BG2 - Dead load	1,00
			BG3 - Edge load	1,00
			BG6 - Traffic load| A.T| UDL	1,00
			BG10 - Pedestrian load| des loc	0,80
			LC4 - TR1/BM10,000 m	1,00
			LC5 - TR1/BM11,000 m	1,00
			LC6 - TR1/BM12,000 m	1,00
			LC7 - TR1/BM13,000 m	1,00
			LC8 - TR1/BM14,000 m	1,00
			LC9 - TR1/BM15,000 m	1,00
			LC10 - TR1/BM16,000 m	1,00
			LC11 - TR1/BM17,000 m	1,00
			LC12 - TR1/BM18,000 m	1,00
			LC13 - TR1/BM19,000 m	1,00
			LC14 - TR1/BM110,000 m	1,00
			LC15 - TR1/BM111,000 m	1,00
			LC16 - TR1/BM112,000 m	1,00
			LC17 - TR1/BM113,000 m	1,00
			LC18 - TR1/BM114,000 m	1,00
			LC19 - TR1/BM115,000 m	1,00
			LC20 - TR1/BM116,000 m	1,00
			LC21 - TR1/BM117,000 m	1,00
			LC22 - TR1/BM118,000 m	1,00

Name	Description	Type	Load cases	Coeff. [-]
			LC23 - TR1/BM119,000 m	1,00
			LC24 - TR1/BM120,000 m	1,00
			LC25 - TR1/BM121,000 m	1,00
			LC26 - TR1/BM122,000 m	1,00
			LC27 - TR1/BM123,000 m	1,00
			LC28 - TR1/BM124,000 m	1,00
CO4|BGT	Crowd	Linear - serviceability	BG2 - Dead load	1,00
			BG3 - Edge load	1,00
			BG9 - Pedestrian load| crowd	1,00

24. Result classes

Name	Description	List
RC1	omhullende ugt	CO1.1|UGT - Envelope - ultimate
		CO2.1|UGT - Envelope - ultimate
		CO3.1|UGT - Envelope - ultimate
		CO4|UGT - Linear - ultimate
RC2	omhullende bgt	CO1.1|BGT - Envelope - serviceability
		CO2.1|BGT - Envelope - serviceability
		CO3.1|BGT - Envelope - serviceability
		CO4|BGT - Linear - serviceability

25. Line force on 2D member edge

Name	2D member	Type	Dir	Value - P_1 [kN/m]	Pos x_1	Loc	Edge
	Load case	System	Distribution	Value - P_2 [kN/m]	Pos x_2	Coor	Orig
LFS1	E1	Force	Z	-2,00	0.000	Length	1
	BG3 - Edge load	LCS	Uniform		1.000	Rela	From start
LFS2	E1	Force	Z	-2,00	0.000	Length	3
	BG3 - Edge load	LCS	Uniform		1.000	Rela	From start

26. 2D member - Internal forces

Linear calculation, Extreme : Global
Selection : All
Class : RC1
Elementary design magnitudes. In nodes, avg. on macro.

Member	elem	Case	mxD+ [kNm/m]	myD+ [kNm/m]	mxD- [kNm/m]	myD- [kNm/m]	nxD [kN/m]	nyD [kN/m]
E1	1	RC1	**-2,73**	0,00	0,47	3,18	**0,00**	**0,00**
E1	642	RC1	**190,43**	308,52	446,28	321,42	0,00	0,00
E1	840	RC1	0,00	**-115,12**	373,68	14,08	0,00	0,00
E1	161	RC1	102,56	**557,23**	29,50	**0,00**	0,00	0,00
E1	320	RC1	22,23	90,50	**-89,45**	0,00	0,00	0,00
E1	285	RC1	0,00	-3,45	**1602,82**	97,21	0,00	0,00
E1	2	RC1	0,00	6,20	48,81	0,00	0,00	0,00
E1	1606	RC1	0,00	293,30	709,60	**363,05**	0,00	0,00
E1	1	RC1	-0,26	0,00	4,85	17,25	0,00	0,00

27. 2D member - Internal forces

Linear calculation, Extreme : Global
Selection : All
Class : RC1
Basic magnitudes. In nodes, avg. on macro.

Member	elem	Case	mxy [kNm/m]
E1	1915	RC1	**-344,72**
E1	1845	RC1	**344,75**

28. 2D element - Internal forces; mxD-

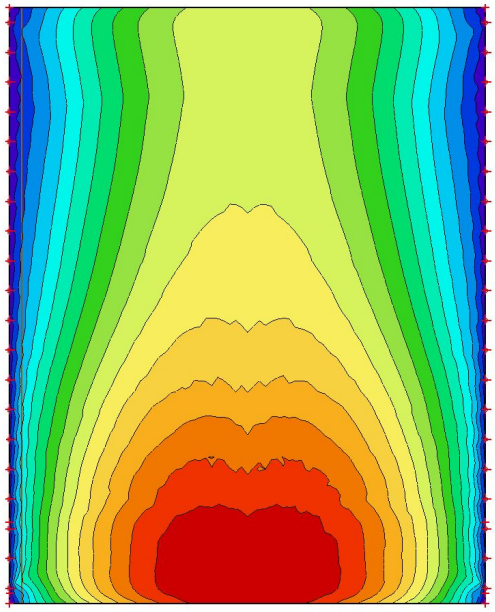

29. 2D element - Internal forces; myD-

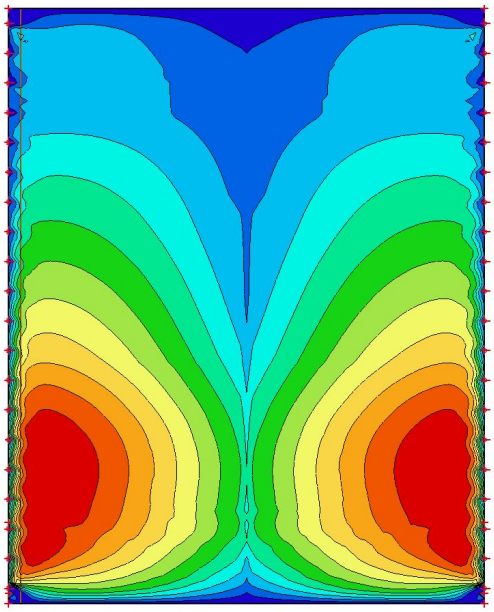

30. 2D element - Internal forces; mxy

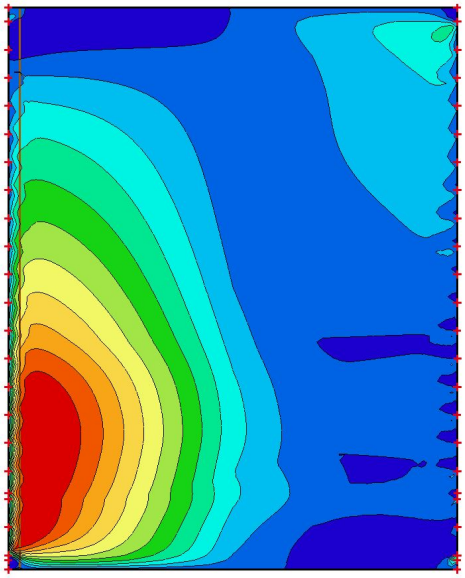

31. Section on plate

Name	Draw	Direction of cut
section for vx and vy	Z direction	0.000000 / 0.000000 / 1.000000

32. 2D member - Internal forces

Linear calculation, Extreme : Global
Selection : section for vx and vy0,E1
Class : RC1
Basic magnitudes. In nodes, avg. on macro.

Section	elem	Case	vx [kN/m]	vy [kN/m]
section for vx and vy	7202	RC1	**37,28**	-34,55
section for vx and vy	162	RC1	**644,77**	68,77
section for vx and vy	7522	RC1	41,48	**-41,39**
section for vx and vy	1842	RC1	254,03	**158,78**

33. 2D element - Internal forces; vx

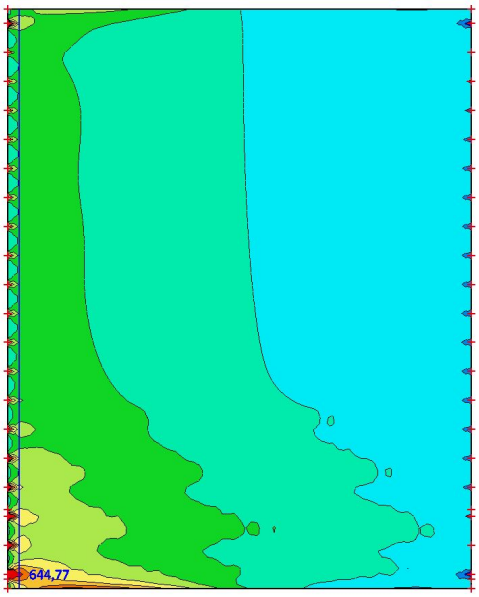

34. 2D element - Internal forces; vy

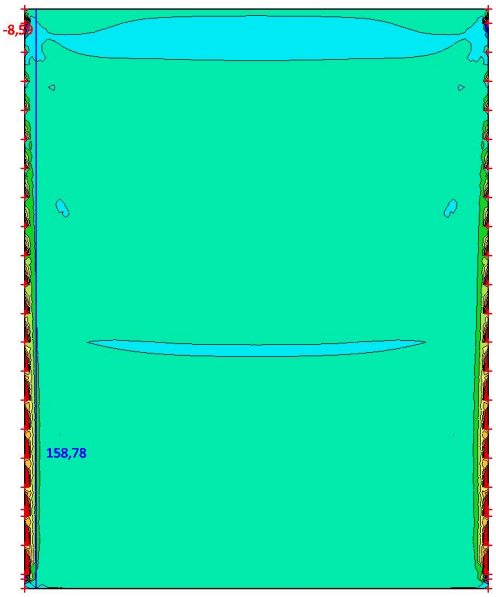

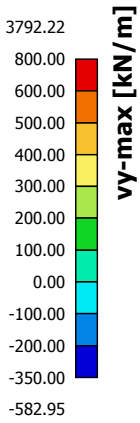

E. Bridge design in UHPC C170/200, calculations

E.1 General

In the following the calculations are presented for the UHPC C170/200 design. These calculations serve the purpose to back up the results given in the main part of the report. This calculation will be more profound than the calculation of the C50/60 design. First the cross-sectional and material properties are specified. Then the loads are going to be defined. Afterwards a SCIA model presented. With this model the forces caused by the loads will be determined. Then with these results a design calculation will be performed in both ULS (moment and shear capacity) and SLS (crack width, deflection and fatigue).

E.2 Material properties

The concrete and steel material properties are shown in Table E-1. The concrete values are based on the recommended values in the AFGC Recommendations 2013 and also on an article in Cement magazine, which deals with UHPC calculations[1]. There are multiple UHPC mixtures available, which result in different material properties. This article is based on a UHPC mixture produced by Ductal and it used the AFGC to give specific values for certain parameters in order to give designers the ability to perform calculations for a UHPC design. The assumptions made in the article and also the mixture will be used in this thesis as well. The steel properties are based on NEN-EN-1992-1-1.

Table E-1: Concrete and steel material properties

Concrete C170/200		
ρ_c		2500 kg/m3
f_{ck}		170 N/mm^2
f_{cm}	$f_{ck}+8$	178 N/mm^2
$\sigma_{w=0.3}$		12 N/mm^2
f_{ctk}		8 N/mm^2
γ_c		1.5
α_{cc}		0.85
K_{glob}		1.25
K_{loc}		1.75
f_{cd}	$\alpha_{cc}*f_{ck}/\gamma_c$	113.33 N/mm^2
$f_{ctd,1}$	f_{ctk}/γ_c	5.33 N/mm^2
$f_{ctd,2}$	$\sigma_{w=0.3} / (\gamma_c*K_{glob})$	6.4 N/mm^2
E_{cm}		50000 N/mm^2
ε_{c3}		2.3 ‰
ε_{cu3}		2.6 ‰

Reinforcing steel B500		
ρ_s		7850 kg/m3
f_{yk}		500 N/mm^2
γ_s		1.15
f_{yd}	f_{yk}/γ_s	435 N/mm^2
E_s		210000 N/mm^2

Prestressing steel Y1860		
f_{pk}		1860 N/mm^2
$f_{p0.1k}$	$0,9*f_{pk}$	1674 N/mm^2
γ_s		1.1
f_{pd}	$f_{pk0.1}/\gamma_s$	1522 N/mm^2
σ_{pm0}	$0.75*f_{pk}$	1395 N/mm^2
E_p		195000 N/mm^2
A_p [ϕ_{strand}] (main direction)		139 mm^2 [15.2mm]
A_p [ϕ_{strand}] (transverse dir.)		150 mm^2 [15.7mm]

[1] **Ketel,** M., Willemse, R., Van Rijen, P., & Koolen, E. (2011) "Rekenmodel VVUHSB, Toepassing van vezelversterkt ultra-hogesterktebeton in bouwkundige constructies (1)", Cement Online.

E.3 Cross sectional properties

The main dimensions are a height of 600 mm and a width of 1000 mm. The flanges and webs are slightly reduced in size compared to the design in C50/60. The cross section of the UPHC box girder can be seen in Figure E-1.

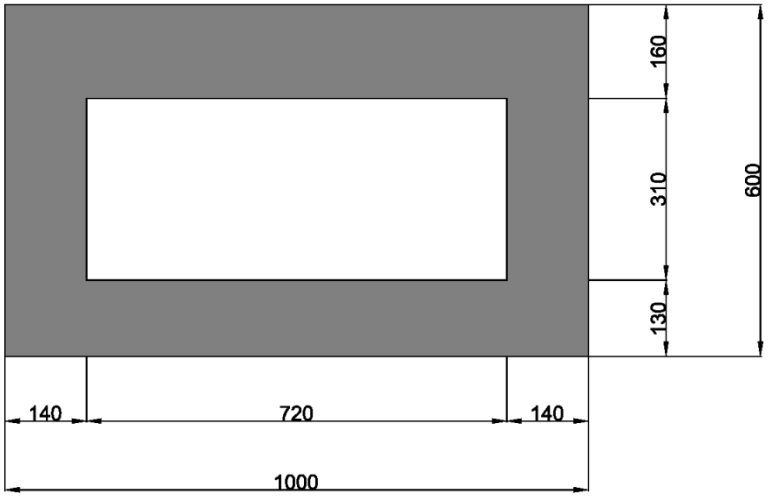

Figure E-1: Cross section UPHC box girder

In Table E-2 the dimensions and cross sectional properties of one girder are shown.

Table E-2: Dimensions and cross sectional properties of box girder

L	Span	24 m
H	Height girder	0.6 m
B	Width girder	1.0 m
b_{web}	Web thickness	0.14 m
$h_{top,fl}$	Top flange thickness	0.16 m
$h_{bot,fl}$	Bottom flange thickness	0.13 m
A_c	Cross sectional area	0.377 m^2
z_t	Distance top fibre to c.a.	0.291 m
z_b	Distance bottom fibre to c.a.	0.309 m
I_c	Moment of Inertia	0.0161 m^4
$W_{c,t}$	Section Modulus top fibre	0.0554 m^3
$W_{c,b}$	Section Modulus bottom fibre	0.0522 m^3

The values in the table are calculated as follows:

$A_c = B*H - (H - h_{top,fl} – h_{bot,fl}) *(B-2* b_{web})$

$z_t = \{B*H*0.5H – (H- h_{top,fl} – h_{bot,fl}) * (B-2* b_{web}) * 0.5*(H- h_{top,fl} – h_{bot,fl})+h_{top,fl})\}/ A_c$

$z_b = H - z_t$

$I_c = 2 * [(1/12)*b_{web}*H^3+b_{web}*H*(0,5*H-zt)^2] + [(1/12)*(B-2*b_{web})*h_{top,fl}^3+ (B -2*b_{web}) *h_{top,fl}* (z_t - 0,5*h_{top,fl})^2] + [(1/12)*(B-2*_{bweb})*h_{bot,fl}^3 + (B-2*b_{web})*h_{bot,fl}*(z_b-0,5*h_{bot,fl})]$

$W_{c,t} = I_c/z_t$

$W_{c,b} = I_c/z$

E.4 Exposure class and concrete cover

The exposure class for superstructures in bridges is set to be XC4 in paragraph 2.3 section 4.2 of AFGC2013. For the inside of the box girder the exposure class can be set to XC1, since the inside is not as exposed as the outside of the girder.

The cover can also be determined conform the AFGC2013 paragraph 2.3 section 4.4. Here basically the same method is used as in NEN-EN-1992-1-1, only with a couple of modifications. The most notable one is the reduction of all values given for the minimum cover. The values are divided by √5, which takes into account the diffusion coefficient of UHPC. This is due to the fact that UHPC has a much better durability than ordinary concrete, due to the very dense matrix. So the cover does not have to be as high as for ordinary concrete.
The nominal cover is $c_{nom} = c_{min} + \Delta c_{dev}$ (with Δc_{dev} = 5 mm)
The minimum cover is determined with:
$c_{min} = \max \{c_{min,b}; c_{min,dur} + c_{dur,\gamma} - \Delta c_{dur,st} - \Delta c_{dur,add}; 10\ mm\}$

- $c_{min,b}$ = the minimum cover due to bond requirement. For pretensioned member: $c_{min,b} = \max(2*\varphi_{strand} ; d_{g,max})$. Since the maximum aggregate is very small the governing value is $2*\varphi_{strand}$ = 30.4 mm
- $c_{min,dur}$ is the minimum cover due to environmental conditions. So it has to be based on exposure class XC4. In the case for prestressing steel and with structural class S4, $c_{min,dur}$ = 20mm (for XC1 $c_{min,dur}$= 15mm). Reinforcement is not considered as it is the goal to use no passive or shear reinforcement in the structure.
- $c_{min,p}$ = is the minimum cover due to the concrete placement conditions, which is $\max(1.5l_f; 1.5D_{max} ; \varphi_{strand})$. $c_{min,p}$ = 19.5 mm
- $\Delta c_{dur,\gamma} = \Delta c_{dur,st} = \Delta c_{dur,add}$ = 0mm

Based on the determined values, the governing minimum cover is the one due to bond requirement. So c_{nom} = 30.4+5 mm = **35.4mm** for both the inner and outer perimeter of the box girder.

E.5 Load cases and load combinations

Before the SCIA Engineer model is presented, the loads have to be determined first. There are a lot of different loads that will work on the bridge. And these loads will not occur exclusively. Therefore it is important to determine all the load cases and load combinations for the bridge. The load cases and combinations are described more in detail in appendix B

Basically the following load cases will occur on the bridge:

Permanent loads:	
LC1: Self-weight girders (not included in SCIA)	A_c*25 kN/m
LC2: Dead load	
– Pavement	4.6 kN/m^2
– Asphalt	4.8 kN/m^2
– Concrete filling around tram rails	3.5 kN/m^2
LC3: Steel railing and natural stone elements (Edge Load)	2.0 kN/m^2
Variable loads:	
LC4&5: Traffic loads with presence of trams (UDL & tandem axle)	Conform Load Model 1
LC6&7: Traffic loads with absence of trams (UDL & tandem axle)	Conform Load Model 1
LC8: Tram-axle loads (No UDL specified for tram loads)	Conform GVB
LC9: Pedestrian loads over whole width (crowd loading)	5.0 kN/m^2
LC10: Pedestrian loads on designed locations.	5.0 kN/m^2

In total there are five main load combinations:

- Combination 1: Traffic loads in the presence of tram loading, where the traffic loads are the leading variable load. (1 LM1 TS + 2 tram TS)
- Combination 2: Traffic loads in the presence of tram loading, where the tram loading is the leading variable load. (1 LM1 TS + 2 tram TS)
- Combination 3: Traffic loads in absence of tram loading. (3 LM1 TS)
- Combination 4: Crowd loading
- Combination 5: Governing transverse moment

E.6 SCIA calculation model

As with the earlier C50/60 design, the UHPC bridge is modelled in SCIA Engineer as a 2D orthotropic plate. This way the transverse action of all girders combined can be modelled in a good way. With this model the internal forces caused by the loads on the bridge will be determined. The self-weight will be left out, because the 2D model will be inputted as a plate. So the self-weight calculated will not be correct. Using the correct orthotropic parameters will still give the correct internal forces, caused by loads other than the self-weight. Furthermore in SCIA, results in 2D are usually given per meter width. So the governing internal forces can easily be transformed to give results for one girder. But in this case the girder has a width of 1 meter so the results from SCIA are directly the correct moments for one box beam. When the self-weight is added of one girder, which can easily be determined by hand, the total internal forces in one girder can be determined. With these internal forces a safety check can be performed for one girder. The aforementioned orthotropic parameters are calculated with a Mathcad sheet that is presented at the end of this paragraph.

The bridge is modelled as a simply supported bridge. In reality the amount of supports on each side will be the same as the amount of girders. Each girder is 1.0m wide. The bridge is 30m wide, so this results in a total of 30 girders. So in the model 30 internal nodes are placed on each side, which represent the location of the supports. The locations of the support in the model are determined by taking the centre location of each girder (right in the middle). All supports are fixed in the vertical Z direction. On X=0 one support, which is located in the middle of the transverse (Y) span, is also fixed in X and Y direction, while the support parallel to this one is fixed in Y direction. This provides stability in the structure and it will not cause strange results, which could occur if on one side of the span all support nodes are made fixed in all directions. But in this case only vertical loads are applied so the additional fixations in X and Y direction on one side would not influence the results. In Figure E-2 the SCIA model is shown.

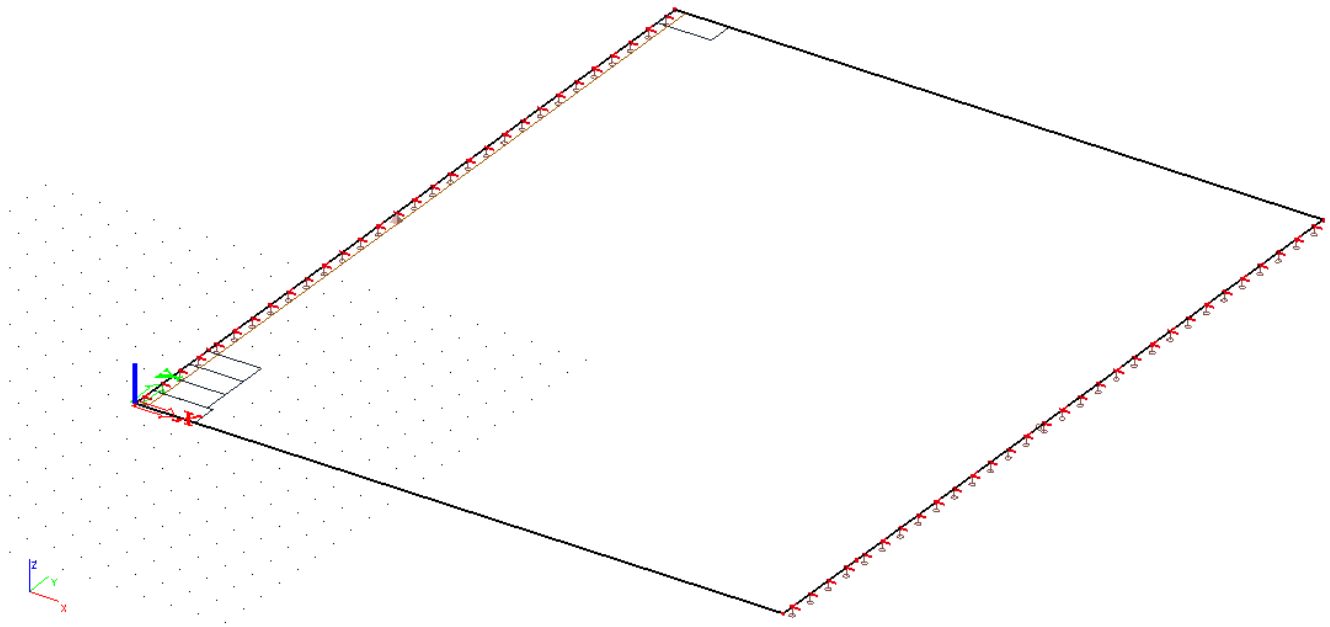

Figure E-2: SCIA 2D model of C170/200

Because vehicles and trams constantly cross the bridge, these are defined as variable loads. In the model the traffic and tram loads are defined as mobile loads. Because they are defined as mobile loads the program can determine at which position of the load, across the length of the bridge, is the governing one for the bending moments, Shear force etc. These mobile loads will be combined with the other, static loads to determine the maximum internal forces on the bridge.
Furthermore, a section is placed close to the support and an averaging strip is placed at the location where the highest shear forces could be present. This is necessary, because the support nodes will result in very high unrealistic values for the shear force. The strip will average the peak points out over a certain length (which is taken 4d according to RBK 1.1) to give more realistic values. Then a section is placed at a distance d from the support edge, in order to not take a certain value right at the edge, the combination of a section and an averaging strip will provide a shear force value that is realistic and can be used for further calculations.

A full report on the model (such as coordinates, loads, etc.) and also the results from the model can be found in the last paragraph of this appendix.

MATHCAD FILE: Calculation orthotropic parameters for UHPC Box girder

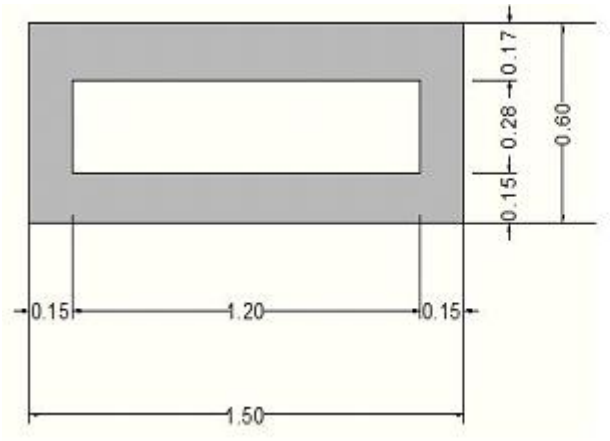

Dimensions and cross sectional properties

$H := 0.6$ $\quad Ec := 50000$

$\nu := 0.15$

$B := 1.0$

$b\_web := 0.14$ $\quad Gc := \frac{Ec}{2(1+\nu)} = 2.174 \times 10^{4}$

$h\_topfl := 0.16$

$h\_botfl := 0.13$

$Hvoid := H - h\_topfl - h\_botfl = 0.31$

$Bvoid := B - 2 \cdot b\_web = 0.72$

$$Ac := \begin{pmatrix} H \cdot B \\ -Hvoid \cdot Bvoid \end{pmatrix} = \begin{pmatrix} 0.6 \\ -0.223 \end{pmatrix} \qquad z := \begin{pmatrix} 0.5 \cdot H \\ h\_topfl + 0.5 \cdot Hvoid \end{pmatrix} = \begin{pmatrix} 0.3 \\ 0.315 \end{pmatrix}$$

$$Sc := \overrightarrow{(Ac \cdot z)} = \begin{pmatrix} 0.18 \\ -0.07 \end{pmatrix}$$

$$ztop := \frac{\sum Sc}{\sum Ac} = 0.291 \qquad zbot := H - ztop = 0.309$$

$$Asteiner := \overrightarrow{\left[Ac \cdot (ztop - z)^2\right]} = \begin{pmatrix} 4.737 \times 10^{-5} \\ -1.273 \times 10^{-4} \end{pmatrix} \qquad Ieigen := \left(\frac{1}{12}\right) \cdot \begin{pmatrix} B \cdot H^3 \\ -Bvoid \cdot Hvoid^3 \end{pmatrix}$$

$$I := \sum (Asteiner + Ieigen) = 0.016$$

Flexural stiffness

$D11 := (Ec)\cdot\frac{I}{B} = 806.629$ **in MNm**

$i := 1..3$

$b_i :=$

$0.5\cdot B - 0.5\cdot b\_web$
$H - h\_topfl - h\_botfl$
$0.5\cdot B - 0.5\cdot b\_web$

$t_i :=$

h_topfl
b_web
h_botfl

$$\lambda_i := 12\cdot\frac{b_i}{\left[Ec\left(\left(t_i\right)\right)^3\right]}$$

$\lambda_1 = 0.025$

$$e := \left[\frac{\lambda_2\cdot\left(\lambda_2 + 4\cdot\lambda_3\right)}{\lambda_2\cdot\left(4\cdot\lambda_1 + \lambda_2\right) + \lambda_3\cdot\left(12\cdot\lambda_1 + 4\cdot\lambda_2\right)}\right] = 0.256$$

$$hf := \left[h\_topfl^3\cdot\left(\frac{1}{e}\right)\right]^{\frac{1}{3}} = 0.252$$

$D22 := 1\cdot Ec\cdot\frac{hf^3}{12} = 66.644$ **in MNm**

Torsional stiffness

$Am := (B - b\_web)\cdot(H - 0.5\cdot h\_topfl - 0.5\cdot h\_botfl) = 0.391$

$$Sum1 := 2\cdot\frac{b_1}{t_1} + \frac{(2\cdot b)_2}{t_2} + 2\cdot\frac{b_3}{t_3} = 16.419$$

$$Sum2 := \left(\frac{1}{3}\right)\cdot\left[2\cdot b_1\cdot\left[\left(t_1\right)^3 + \left(t_3\right)^3\right] + 2\cdot b_2\cdot\left(t_2\right)^3\right] = 2.371\times 10^{-3}$$

$$It := 4\cdot\frac{Am^2}{Sum1} + Sum2 = 0.04$$

$$Dxy := Gc\cdot\frac{1It}{1B} = 862.462$$

$$Dyx := Gc\cdot\frac{\left(h\_topfl^3 + h\_botfl^3\right)}{6} = 22.801$$

$D33 := \frac{(Dxy + Dyx)}{2} = 442.631$ **in MNm**

Shear stiffness

$$D44 := 2Gc \cdot b\_web \cdot \frac{(H - 0.5 \cdot h\_topfl - 0.5 \cdot h\_botfl)}{B} = 2.77 \times 10^{3} \quad \textbf{in MN/m}$$

$$D55 := Gc \cdot \frac{hf}{1.5} = 3.652 \times 10^{3} \quad \textbf{in MN/m}$$

$$D12 := \nu \cdot \sqrt{(D11 \cdot D22)} = 34.778 \quad \textbf{in MNm}$$

Orthotropic parameters box beam girder

$D11 = 806.629$	MNm	$D44 = 2.77 \times 10^{3}$	$\frac{MN}{m}$
$D22 = 66.644$	MNm	$D55 = 3.652 \times 10^{3}$	$\frac{MN}{m}$
$D33 = 442.631$	MNm	$D12 = 34.778$	MNm

To be filled in SCIA Engineer

Correction factors for result mxy in SCIA. Necessary to determine the percentage of mxy carried in each direction.

$$k1 := \frac{Dxy}{D33} = 1.948$$

$$k2 := \frac{Dyx}{D33} = 0.052$$

E.7 Results SCIA Engineer

Presented here are the internal forces necessary to perform the safety checks in ULS. The results are all from the ULS:

For bending moment resistance check:
mxD^-: 1712.15 kNm/m

For shear and [torsion + shear] safety check
mxy: 317.09 kNm/m (When torsion is governing)
116.75 kNm/m (When shear is governing)

vx: 235.94 kN/m (When torsion is governing)
584.56 kN/m (When shear is governing)
For transverse moment check
myD^-: 332.06 kNm/m
myD^+ 303.09 kNm/m

The presented values will be used for the safety checks. However these values are only based on the loads working on the bridge. Here no self-weight and no prestressing is included yet. These have to be added separately. This will be done in the following, where also the amount of prestressing will be determined.

E.8 Prestress tendon profile

The beams will consist of pre-tensioned strands, as the beams are prefabricated. The tendon profile is shown in Figure E-3. The tendon consists of straight and kinked strands. The kinked strands cause an upward force P_u at the deviation points. This point is at a distance 'a' from the support. The kinked strands are placed in the webs. In each web *4* strands are placed so in total there are *8* kinked profiles. The strands will be placed as high as possible to ensure a high upward force. This force slightly reduces the total shear force.

Assumed is that the kinked strands will be placed so that the gravity point of these strands is $z_b - h_{top} - 2*\varphi_{strand}$ = 100 mm above the centroid axis. Most of the strands will be placed in the bottom flange. This means that the fictitious tendon (or the gravity point) does not coincide with the neutral axis (dashed line). So these will create a moment at the heads due to eccentricity, so a capacity check at the support has to be made to make sure the structure can take the moments.

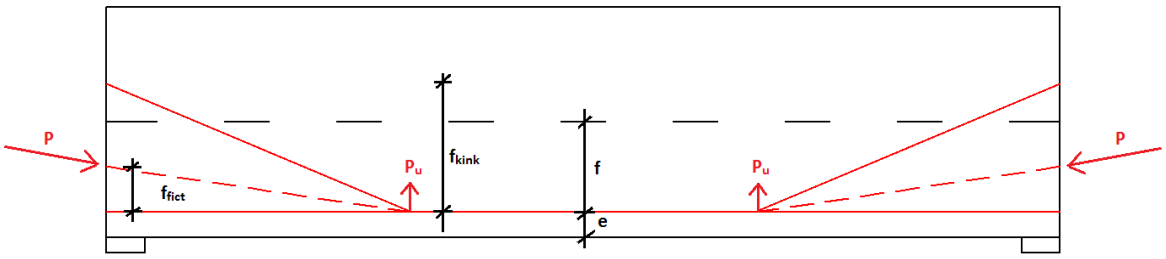

Figure E-3: Tendon profile pre-tensioned strands

The strands have a certain eccentricity in the mid span with reference to the bottom fibre. The minimum eccentricity (e) for the fictitious tendon with reference to the bottom fibre can be determined by taking the cover and strand spacing into account.

The nominal cover is 35.4mm. One strand has a diameter of 15.2mm and the gap between two strands vertically has to be $2*\varphi_{strand}$ which is 30.4 mm (here the maximum aggregate is not governing as only fine material is used.
So the eccentricity is: $e=c_{nom} + 2\varphi_{strand} = 65.8$ mm.
This results in a drape of: $f = z_b - e = 0.243$m.
The kinks are at a distance of a = 8m from the support.
The upward force is calculated according to the drape of the kinked strands $f_{kink} = f+0.1=0.343$m. The drape of the fictitious tendon can be determined once the total amount of strands is determined. Then it will be known how much strands will go in the bottom flange.
The rest of the values in the figure are:
$P_u = P_{kink}*\sin \alpha_{kink} \approx P_{kink}* (f_{kink}/a)$ or $P*(f_{fict}/a)$
$M_{p,mid} = P*f$

The prestress force is determined by taking a couple of requirements into account that concern stresses in the concrete. These requirements need to be applied in the governing cross section (cross section with highest bending moment). Here that is in the middle of the beam:

$$t = 0 \text{ at top fibre: } -\frac{P_{m0}}{A_c} + \frac{M_{p,0}}{W_{ct}} - \frac{M_g}{W_{ct}} \leq 0$$

$$t = 0 \text{ at bottom fibre: } -\frac{P_{m0}}{A_c} - \frac{M_{p,0}}{W_{cb}} + \frac{M_g}{W_{cb}} \geq -0.6 * f_{ck}$$

$$t = \infty \text{ at bottom fibre: } -\frac{P_{m\infty}}{A_c} - \frac{M_{p,\infty}}{W_{cb}} + \frac{M_{tot}}{W_{cb}} \leq 0$$

The first requirement states that at the construction of the bridge, when only dead loads are present, no tensile stresses are allowed which could be caused by the prestressing. The second requirement states that the compression stresses can't be too high at the bottom of the beam during construction. The third requirement states that during the use of the bridge, where all the loads are present, no tensile stresses are allowed at the bottom of the beam. Here $P_{m\infty}$ is used instead of P_{m0}. The difference is that immediate and time dependent losses are taken into account here.

Assumed is a total loss of 20% so $P_{m\infty} = 0.8*P_{m0}$. After the prestress force is determined with the three requirements, the actual losses (direct and time dependent losses) have to be determined and checked if the assumption of a 20% loss is on the safe side.

E.9 Required amount of prestressing strands

The required amount of prestressing strands in one beam is determined using the three requirements presented in paragraph E.8. To use these requirements the bending moments working on the beam need to be determined. To determine the total moments and the moments caused by the dead load. The result of mxD- in SCIA (paragraph E.7) has to be split apart. This means finding out what load cases contribute to the governing moment. This has been done by finding the node in SCIA, where the highest moment is located and writing down the results that SCIA gives in that node.

The results are presented in Table E-3. The results are both in SLS and ULS. Also given are the resulting loads in kN/m.

Table E-3: Bending moments in one beam

mxD-	SLS			ULS	
	kNm (*1 beam*)	q [kN/m]	γ	kNm (*1 beam*)	q [kN/m]
dead load	294,83	4,095	1,2	353,796	4,914
edge load	13,98	0,194	1,2	16,776	0,233
AT| UDL	351,05	4,876	1,35	473,9175	6,582
AT| TS	505,96	7,027	1,35	683,046	9,487
Pedestrian loads	170,94	2,374	1,08	184,6152	2,564
TOTAL	**1336,76**	**18,566**		**1712,1507**	**23,780**

In addition to these moments the moment due to self-weight needs to be determined as well. Assumed is that on each side a hammerhead of 1m long is located:
$q_{self} = (L-2)*A_c*\gamma_{conc} + 2*(H*B)*\gamma_{conc} = 9.885$ kN/m in SLS*1.2 = 11.86 kN/m in ULS
$M_{self} = (1/8)*q_{self}*L^2 = 711.72$ kNm
The moment due to all static loads now becomes:
$q_{perm} = q_{dead} + q_{edge} + q_{self} = 14.174$ kN/m in SLS and 17.01 kN/m in ULS
$M_g = 1020.53$ kNm
The moment due to the variable loads is:
$q_{var} = 14.28$ kN/m in SLS and 18.63 kN/m in ULS
$M_q = 1027.95$ kNm
This results in a total moment (SLS) of:
$M_{tot} = 2048.48$ kNm

Now that the moments have been determined, the prestressing force can be calculated:

t=0: $\sigma < 0$	$P_{m0} <$	10628.99 kN
t=0: $\sigma > -0,6*f_{ck}$	$P_{m0} <$	16630.59 kN
t=∞: $\sigma < 0$	$P_{m0} >$	6708.49 kN

The minimum prestressing force has to be 6708.49 kN. This results in (σ_{pm0} = 1395MPa; $A_{p,strand}$ = 139mm^2): 6708.49/(1395*139) = 35 strands. These 35 strands have a cross sectional area of $A_p = 4865$ mm^2 in total, which results in a force of $P_{m0} = 6786.675$ kN.
The moment caused by the prestressing force is:
$M_p = P_{m0}*(f/a)*a = 1319.79$ kNm (resulting $q_p = 18.33$ kN/m)
The stress caused by the prestress force during t=∞ in the concrete is:
$\sigma_{cp} = 0.8*P_{mo}/A_c = 14.41$ N/mm^2.

E.10 Prestressing Losses

The required amount of strands and also the resulting prestress force are determined. Now the actual losses have to be determined. The percentage of the total losses should be lower than the assumed losses of 20%, so that the determined prestress force is on the save side. If this is not the case the amount of strands has to be determined again with the correct percentage of losses.
The losses can be divided in direct and time dependent losses.

E.10.1 Direct losses

For pre-tensioned strands the elastic shortening is part of the direct losses. When the strands are released after tensioning the strands will shorten elastically. The result is that the stresses and forces in these strands decrease. Also occurring is concentrated friction at the kink points of the strands but these can be neglected when looking at the big picture.

E.10.1.1 Losses due to elastic deformation

The loss of force in one strand due to elastic shortening is (NEN-EN-1992-1-1 formula 5.44):

$$\Delta P_{el} = A_p * E_p * \frac{\Delta\sigma_c(t)}{E_{cm}(t)}$$

And $\Delta\sigma_c(t)$ being the variation of stress at the centre of gravity of the strands at time t:

$$\Delta\sigma_c(t) = \frac{P_{m0}}{A_c} * [1 + \frac{e_p^2 * A_c}{I_c}]$$

Here e_p is the distance of the neutral axis to the considered strand. In this case the governing strands are those in the bottom flange, because these provide the highest eccentricity.
For these strands e_p = f (drape) =243.1 mm.
The elastic deformation occurs after releasing the strands so at t=0.
For one strand: A_p = 139 mm^2 and $P_{m0} = A_p * \sigma pm0$ = 193.91kN.
$\Delta\sigma_c$ = 1.22N/mm^2. The loss of force in one strand now becomes: ΔP_{el} = 0.66 kN.
The loss in force becomes 35*0.66 = 23.9 kN.

To compensate the loss in forces due to elastic shortening it is allowed to overstress the strands, provided that the stress stays under the maximum allowed stress $\sigma_{p,max}$ = min{k1*f_{pk};k2*$f_{p0,1k}$) = min{0.8*1860; 0.9*1674} = 1488 N/mm^2.

The extra stress per strand needed to compensate the loss is: $\sigma_{extra} = \Delta P_{el}/A_p$ = 4.78 N/mm^2. So the total stress applied becomes $\sigma_{pm0} + \sigma_{extra}$ = 1399.78 N/mm^2 which is far below the maximum allowed stress.

E.10.2 Time dependent losses

Certain losses appear during the life span of the structure. These are shrinkage and creep of the concrete and relaxation of the strands. All these losses can be combined in one formula which is given in NEN-EN-1992-1-1 formula 5.46:

$$\Delta P_{c+s+r} = A_p \Delta\sigma_{p,c+s+r} = A_p \frac{\varepsilon_{cs} E_p + 0{,}8\Delta\sigma_{pr} + \frac{E_p}{E_{cm}} \varphi(t,t_0).\sigma_{c,QP}}{1 + \frac{E_p}{E_{cm}} \frac{A_p}{A_c}(1 + \frac{A_c}{I_c} z_{cp}^2)[1 + 0{,}8\,\varphi(t,t_0)]}$$

E.10.2.1 Shrinkage and creep

The shrinkage strain and creep-coefficient are not allowed to be determined conform the Eurocode, because UHPC behaves differently than ordinary concrete. There is not yet one uniform method to determine the shrinkage and creep. In appendix C already a couple of methods were discussed, which can be used to determine the shrinkage and creep. But these are not methods that can be used generally, as was concluded. Therefore the AFGC recommendations give recommended values for shrinkage and creep to use in calculations. The values that are recommended are (AFGC2013 paragraph 1.9):

	Shrinkage strain	**Creep coefficient**
Without heat treatment:	Total shrinkage of $\varepsilon_{cs} = \varepsilon_{cd} + \varepsilon_{ca} = 550 + 150 = 700*10^{-6}$	$\Phi(t,t0) = 0.8$
Type 1 heat treatment:	Total shrinkage of $\varepsilon_{cs} = 550*10^{-6}$	$\Phi(t,t0) = 0.4$
Type 2 heat treatment:	Only autogenous shrinkage of $\varepsilon_{ca} = 550*10^{-6}$ during treatment. Afterwards no shrinkage	$\Phi(t,t0) = 0.2$

Assumed is that at least type1 heat treatment is going to be used, as some sort of heat treatment should actually be a part of producing UHPC. So this means that:
Shrinkage: $\varepsilon_{cs} = 550*10^{-6}$
Creep: $\Phi(t,t0) = 0.4$

E.10.2.2 Losses due to relaxation

The relaxation in the prestress steel can be determined with the following equation, which is given in NEN-EN-1992-1-1 formula 3.30:

$$\text{class 2: } \frac{\Delta\sigma_{pr}}{\sigma_{pi}} = 0.66 * \rho_{1000} * e^{(9.1*\mu)} * \left(\frac{t}{1000}\right)^{(0.75*(1-\mu)} * 10^{-5}$$

With:

Absolute value of initial prestress:	$\sigma_{pi} = P_{m0}/A_p = 1395$ N/mm^2
Value of relaxation loss at 1000 hours after tensioning: ρ_{1000}:	2.5%
Time after tensioning:	t=500.000 hours
μ:	σ_{pi}/f_{pk} =0.75

Filling everything in the equation gives: $\Delta\sigma_{pr} = 67.95$N/mm^2. Shrinkage and creep reduce the relaxation. Therefore, when combining the three, the relaxation loss can be reduced with a factor 0.8. The loss in force due to relaxation becomes: $P_{pr} = 0.8* \Delta\sigma_{pr}*A_p = 264.45$ kN

E.10.2.3 Total time dependent losses

The formula for the total time dependent losses was:

$$\Delta P_{c+s+r} = A_p \Delta\sigma_{p,c+s+r} = A_p \frac{\varepsilon_{cs}E_p + 0{,}8\Delta\sigma_{pr} + \frac{E_p}{E_{cm}}\varphi(t,t_0).\sigma_{c,QP}}{1+\frac{E_p}{E_{cm}}\frac{A_p}{A_c}(1+\frac{A_c}{I_c}z_{cp}^2)[1+0{,}8\,\varphi(t,t_0)]}$$

All values are determined except for $\sigma_{c,QP}$. This is the compressive stress in the concrete caused by the dead load, prestressing and quasi permanent actions:

$$\sigma_c = -\frac{P_{m0}}{A_c} - \frac{P_{m0} * f^2}{I_c} + \frac{M_g}{W_b} + \frac{\psi * M_q}{W_b}$$

The quasi permanent factor ψ_2 for LM1 and pedestrian loads is 0.4. This results in a compressive stress of:

$$\sigma_c = -\frac{6787}{0.3768} - \frac{6787 * 0.2431^2}{0.0161} + \frac{1020}{0.052} + \frac{0.4 * 712}{0.052} = -23.05 \text{N/mm}^2$$

The losses have to be added up so the absolute value is taken:
$|\sigma_{c,QP}|$ = 23.05 N/mm^2.
When all the parameters are filled in the main formula for the time dependent losses, the total stress loss due to time dependent losses becomes:

$\Delta\sigma_{p,c+s+r}$ = 170.58 N/mm^2.

This is 12.23% of σ_{pm0}, which is below the assumed loss of 20% so the assumption was on the safe side.

*Remark: When no heat treatment is used shrinkage becomes 700*10^{-6} and the creep factor 0.8. If this would be filled in the formula for the losses, then the total losses would be around 16%, which is still lower than the assumed 20%.*

E.10.2.4 New amount of required prestress strands

Because the actual losses are smaller than the assumed loss, the losses will be set to 16%. Putting it to 16% results in a smaller amount of strands, while still taking unforeseen losses (such as friction at the deviators) into account and also the fact that no heat treatment could be applied. With the losses being 16% the new minimum prestress force becomes: Pm0 = 6389 kN.
The minimum required strands become 33 (instead of 35).
The total area of the strands is now: A_p = 4587 mm^2 (Pm0=6398.87 kN).

The prestress force delivers a vertical force at the deviators P_u, which is equal to: $P_{u0} = P_{m0}*(f_{fict}/a)$.
The fictitious drape f_{fict} can be determined by finding the gravity point of all strands:
There are 33 strands in total. With 8 strands in the webs the amount of strands in the bottom flange are 25. $F_{fict} = f_{kink} - (25A_p*f_{kink}/33A_p)$ = 0.0832 m.
This results in a P_{u0} = 66.53kN and P_u = 55.88kN.

As can be expected the fictitious drape is very low because the gravity point is very close to the bottom flange, due to the high amount of strands there. The gravity point is at a distance of f-f_{fict} = 0.16m from the neutral axis. This basically means the moment due to prestressing isn't zero anywhere.

E.11 Bending moment capacity

E.11.1 Hand calculation

It is a requirement that the bending moment resistance is higher than the design bending moment: $M_{Rd} > M_{Ed}$.

$M_{Ed} = \gamma_g * M_g\ M_g + \gamma_q * M_q - 1.0 * M_p$
Where:
$M_g(x) = 0.5 * q_g * x * (L-x)$
$M_q(x) = 0.5 * q_q * x * (L-x)$
$M_p(x) = P_u * a + P_m * (f - f_{fict})$ $0 \leq x < a$
$P_m * f$ $x \geq a$

It is possible that the eventual governing design bending moment is found at the construction stage (t=0) and perhaps at the support, because the prestressing causes a moment there. So the bending moment will be determined for the whole span at multiple stages: These stages and the bending moments are:

- t=0 only self weight: $M_{Ed} = M_{self} - M_p$
- t=0 permanent loads: $M_{Ed} = M_{perm} - M_p$
- t=∞ all loads + torsion: $M_{Ed} = M_{perm} + M_{var} - M_p$

The parameters are:

Load of self-weight (ULS):	q_{self} = 11.86 kN/m
Permanent load (ULS):	q_{perm} = 17.01 kN/m
Variable load (ULS):	q_{var} = 18.63kN/m
Prestress force at t=0:	P_{m0} = 6398.87 kN
Prestress force at t=∞:	$P_{m\infty}$ = 5375.05 kN
Drape:	f = 0.243 m
Eccentricity of strands with regards to neutral axis:	$f - f_{fict}$ = 0.160m

In Figure E-4 the moment lines are shown, for multiple stages. The governing M_{Ed} = 1259.62 kNm. The moment at the support is 1023.26 kNm. Technically right at the support the prestress force is also zero. The force has a certain transmission length, where after the force is fully transferred in the concrete.

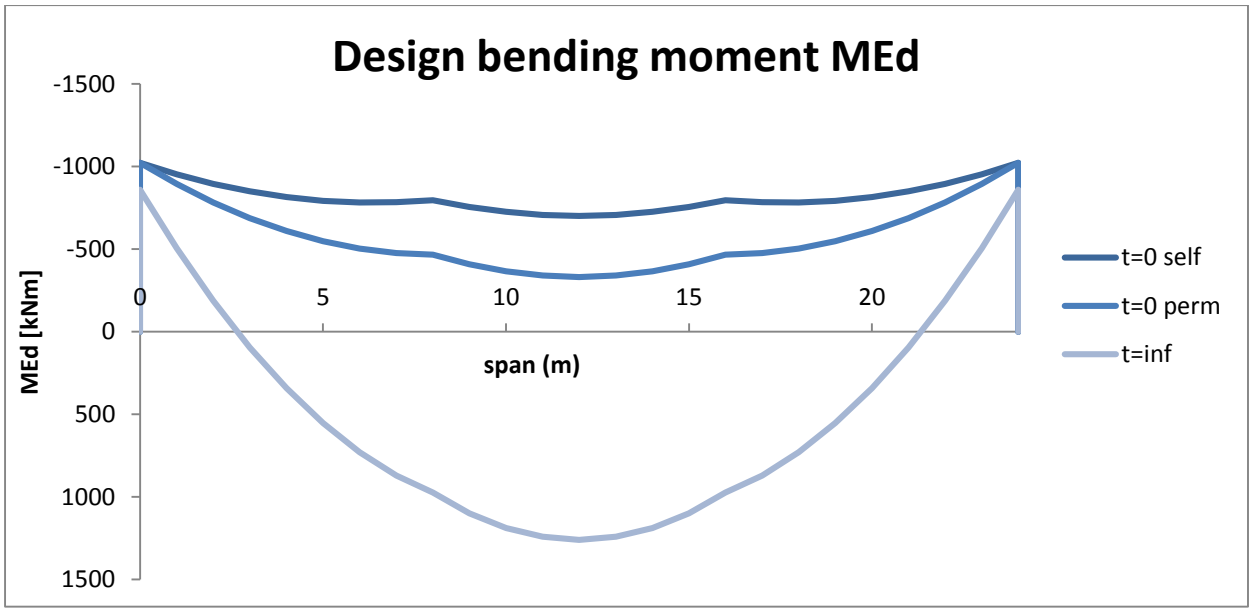

Figure E-4: Design bending moment at multiple stages

The moment capacity should be high enough to resist the determined $M_{Ed.}$ When the moment capacity of a UHPC structure needs to be determined, a slight different approach has to be taken than when ordinary concrete is used. The main difference is the inclusion of the tensile capacity of UHPC. This gives an additional internal tensile force in the structure. To determine M_{Rd} one has to assume equilibrium of internal forces in the cross section and with that assumption determine M_{Rd}. The general case of internal forces is seen in Figure E-5.

For equilibrium the following statement needs to hold true: $N_c - N_t = P_{m\infty} + \Delta N_p + N_s$. The last term N_s is removed, as there is no bending reinforcement applied.

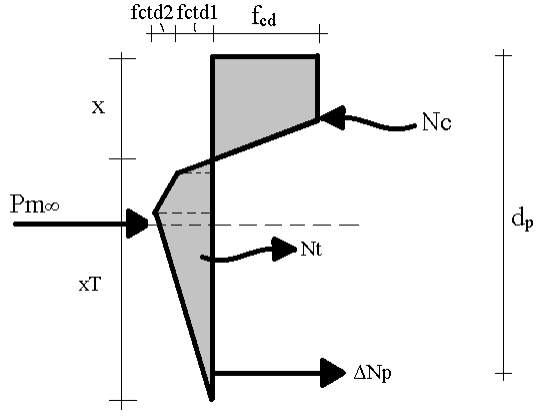

Figure E-5: Equilibrium of internal forces

Here unknowns are the height of the compressive (x) and tension (xT) zone. Because of the strain being assumed linear over the whole height, xT can be rewritten in terms of x. For a certain x there is equilibrium of forces. These forces can all be written in terms of x, making x the only unknown. However a box girder is used, which means that the width is not constant over the height. This will lead to multiple situations that can occur and thus to different derivations (of internal forces) and results for the compressive zone height. These situations have to be determined and the forces have to be derived according to the occurring situation. The stress-strain relationship assumed and used in aid for the derivations is seen in Figure E-6. The stress strain diagram is based on the derived diagram in Cement article, Rekenmodel VVUHSB[1]. The diagram in the article is again derived from the one in the AFGC Recommendations. Same goes for the values for the strain limits:

ε_{c3} = 2.3‰
ε_{cu3} = 2.6‰
$\varepsilon_{ct} = f_{ctd,1}/E_c$ =0.10667 ‰
$\varepsilon_{u0,3} = \varepsilon_{ct}$ + w0.3(=0.3mm)/ l_c(=2H/3) = 0.85667‰
$\varepsilon_{ctu} = l_f$ (=13mm)/4l_c = 8.125‰

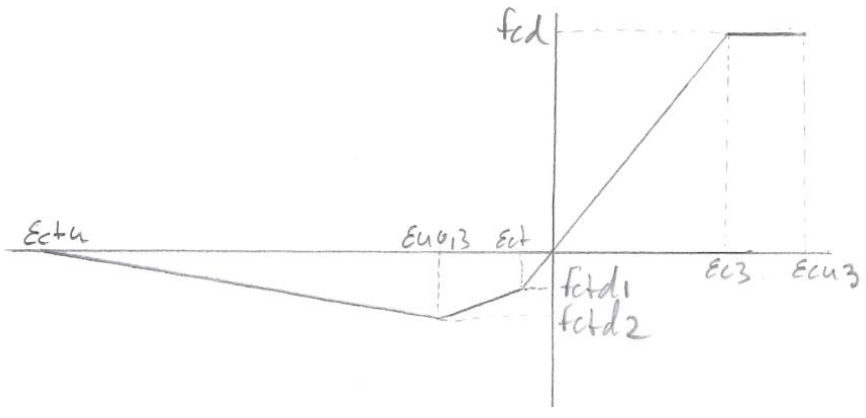

Figure E-6: Stress diagram UHPC

The occurring situations are split for the compressive and tension zone. The situations for the compressive zone are:

Situation 1.1 $x \leq h_{top,fl}$

Situation 1.2 $x \geq h_{top,fl}$ and the height of the plastic area (named y) $\leq h_{top,fl}$

Situation 1.3 $x \geq h_{top,fl}$ and $y \geq h_{top,fl}$

The situations for the tension zone are:

Situation 2.1 The tension zone is located completely outside the top flange. This situation can only occur if $x_u \geq h_{top,fl}$, so with either situation 1.2 or 1.3.

Situation 2.2 Only the elastic part of the tension zone is partially located in the top flange. This situation can only occur when $x_u \leq h_{top,fl}$ (same goes for 2.3 and 2.4). However in most cases the elastic tensile part will fall completely in the top flange, when situation 1.1 occurs, as it is a very small area. Therefore situation 2.2 can often be neglected.

Situation 2.3 The whole elastic part of the tension zone and a part of the area between ε_{ct} and $\varepsilon_{u0.3}$ are located in the top flange. If x_u is around the height of the top flange, situation 2.3 will most likely occur.

Situation 2.4 The area between ε=0 and $\varepsilon_{u0.3}$ is located in the top flange as well as a part of the area between ε_{ctu} and $\varepsilon_{u0.3}$.This situation will occur is x_u is much smaller than the height of the top flange.

For the determination of the bending moment resistance, the combination of situation 1.1 and 2.3 will be assumed first. So the height of the compressive zone is expected to be smaller than the height of the top flange, in such a way that the elastic part and a part of the area between ε_{ct} and $\varepsilon_{u0.3}$ are located in the top flange. If this proves not to be the case then the x_u will be calculated again using a different combination (1.2 with 2.4 or 1.3 with 2.4).
These derivations can be found in appendix H. The maple sheet used to determine the correct moment capacity is presented in the following:

MAPLE SHEET: DETERMINATION OF Xu and MRd FOR C170/200

Dimension

$restart;$
$H := 600 :$
$B := 1000 :$
$htop := 160 :$
$hbot := 130 :$
$bweb := 2 \cdot 140 :$
$Ac := H \cdot B - (H - htop - hbot) \cdot (B - bweb) :$
$ztop := \frac{1}{Ac}(H \cdot B \cdot 0.5 \cdot H - ((H - htop - hbot) \cdot (B - bweb) \cdot (htop + 0.5 \cdot (H - htop - hbot)))) :$

Concrete strength

$fck := 170 : \alpha c := 0.85 : fcd := \frac{\alpha c \cdot fck}{1.5} :$
$fctk := 8 :$
$\sigma 03 := 12 :$
$fctd1 := \frac{fctk}{1.5} : fctd2 := \frac{\sigma 03}{1.25 \cdot 1.5} :$
$E := 50000 :$

Concrete strains

$\varepsilon c3 := 2.3 \cdot 10^{-3} : \varepsilon cu3 := 2.6 \cdot 10^{-3} :$
$lf := 13 : \varepsilon ct := \frac{fctd1}{E} : \varepsilon u03 := \frac{0.3}{\frac{2}{3} \cdot H} + \varepsilon ct : \varepsilon ctu := \frac{lf}{\frac{4 \cdot 2}{3} \cdot H} :$

Prestressing

$n := 33 :$
$Ap := n \cdot 139 :$
$\sigma pt := 1171.8 : fpd := 1522 :$
$Ep := 195000 :$
$\varepsilon pd := \frac{1522}{Ep} :$
$e := 65.8 :$
$dp := H - e :$

Internal compressive force

$x1 := \frac{x \cdot (\varepsilon cu3 - \varepsilon c3)}{\varepsilon cu3} : x2 := x - x1 :$
$Nx1 := B \cdot fcd \cdot x1 : Nx2 := \frac{B \cdot (fcd)}{2} \cdot x2 :$
$Ncc := Nx1 + Nx2;$

$53724.35898\, x$

Internal tensile force

$$xT := H - x :$$

$$xT1 := \frac{xT \cdot \varepsilon ct}{\varepsilon ctu} : xT2 := htop - x - xT1 : xT3 := \frac{xT \cdot (\varepsilon u03 - \varepsilon ct)}{\varepsilon ctu} - xT2 : xT4 := \frac{xT \cdot (\varepsilon ctu - \varepsilon u03)}{\varepsilon ctu} - hbot : xT5 := hbot :$$

$$Nt1 := 0.5 \cdot B \cdot fctd1 \cdot xT1 :$$

$$\sigma t1 := \frac{(fctd2 - fctd1)}{xT2 + xT3} \cdot xT2 + fctd1 : Nt2 := \frac{B \cdot xT2 \cdot (\sigma t1 + fctd1)}{2} :$$

$$Nt3 := \frac{bweb \cdot xT3 \cdot (\sigma t1 + fctd1)}{2} :$$

$$\sigma t2 := \frac{(fctd2 \cdot hbot)}{xT4 + xT5} : Nt4 := \frac{bweb \cdot xT4 \cdot (fctd2 + \sigma t2)}{2} :$$

$$Nt5 := 0.5 \cdot B \cdot xT5 \cdot \sigma t2 :$$

$$Nt := Nt1 + Nt2 + Nt3 + Nt4 + Nt5;$$

$$21005.12821 - 35.00854702\,x + 500\,(152.1230769 - 0.9868717949\,x)\left(\frac{1.066666666\,(152.1230769 - 0.9868717949\,x)}{55.38461539 - 0.0923076923\,x} + 10.66666667\right) + 140\,(-96.73846151 + 0.8945641026\,x)\left(\frac{1.066666666\,(152.1230769 - 0.9868717949\,x)}{55.38461539 - 0.0923076923\,x} + 10.66666667\right) + 140\,(406.7384615 - 0.8945641025\,x)\left(6.400000000 + \frac{832.0000000}{536.7384615 - 0.8945641025\,x}\right) + \frac{5.408000000\,10^{7}}{536.7384615 - 0.8945641025\,x}$$

Prestress force

$$\varepsilon p := \frac{\sigma pt}{Ep} + \varepsilon cu3 \cdot \left(\frac{dp}{x} - 1\right) : \sigma pu := fpd + \left(\frac{(\varepsilon p - \varepsilon pd)}{(35 \cdot 10^{-3} - \varepsilon pd)}\right) \cdot (1691 - fpd) :$$

$$dNp := Ap \cdot (\sigma pu - \sigma pt) : P := Ap \cdot \sigma pt;$$

$$5.3750466\,10^{6}$$

Solve compressive zone x

$eq1 := Ncc = Nt + P + dNp$

$$53724.35898\,x = 6.877111939\,10^{6} - 35.00854702\,x + 500\,(152.1230769 - 0.9868717949\,x)\left(\frac{1.066666666\,(152.1230769 - 0.9868717949\,x)}{55.38461539 - 0.0923076923\,x} + 10.66666667\right) + 140\,(-96.73846151 + 0.8945641026\,x)\left(\frac{1.066666666\,(152.1230769 - 0.9868717949\,x)}{55.38461539 - 0.0923076923\,x} + 10.66666667\right) + 140\,(406.7384615 - 0.8945641025\,x)\left(6.400000000 + \frac{832.0000000}{536.7384615 - 0.8945641025\,x}\right) + \frac{5.408000000\,10^{7}}{536.7384615 - 0.8945641025\,x} + \frac{3.959183771\,10^{7}}{x}$$

$z := solve(eq1, x)$

143.5931702, 570.5563302, 600.0000000, -4.625362435

$xin := z[1]$

143.5931702

Check if determined x is completely located in top flange

If a value is shown, proceed with determination of MRd. Otherwise determine x again.

if xin $<$ htop **then** xu $:=$ xin **else** $print(FIND\ NEW\ X)$ **end if**

143.5931702

Determination of x when $\mathbf{xin \geq htop}$

$$y := \frac{xin \cdot (\varepsilon cu3 - \varepsilon c3)}{\varepsilon cu3}$$

16.56844272

Maple function '*procedure*' is used to instantly determine the correct x for a given situation

SITUATION 1: y≤htop

$$
\begin{aligned}
it1 :=& \mathbf{proc}(B, bweb, htop, \varepsilon c3, \varepsilon cu3, fcd, Ap, \sigma pt, fpd, e, dp, Ep, \varepsilon pd, \\
& fctk, \sigma u03, fctd1, fctd2, lf, \varepsilon ct, \varepsilon u03, \varepsilon ctu, hbot)\mathbf{local}\ N1c\ , x11, \\
& x12, x13, N11, N12, N13, eq1, \sigma c, \varepsilon p, \sigma pu, dNp1, P1, xT10, xT11, \\
& xT12, xT13, xT14, Nt11, Nt12, Nt13, \sigma t2, Nt14, NT1, x; x11 \\
& := \frac{x\cdot(\varepsilon cu3 - \varepsilon c3)}{\varepsilon cu3}; x12 := htop - x11; x13 := x - htop; \sigma c \\
& := \frac{fcd\cdot(x13)}{x - x11}; N11 := B\cdot fcd\cdot x11; N12 := \frac{B\cdot(fcd + \sigma c)}{2}\cdot x12; \\
& N13 := bweb\cdot 0.5\cdot\sigma c\cdot x13; N1c := N11 + N12 + N13; xT10 := H \\
& - x; xT11 := \frac{xT10\cdot\varepsilon ct}{\varepsilon ctu}; xT12 := \frac{xT10\cdot(\varepsilon u03 - \varepsilon ct)}{\varepsilon ctu}; xT13 \\
& := \frac{xT10\cdot(\varepsilon ctu - \varepsilon u03)}{\varepsilon ctu} - hbot; xT14 := hbot; Nt11 := 0.5 \\
& \cdot bweb\cdot fctd1\cdot xT11; Nt12 := \frac{bweb\cdot xT12\cdot(fctd2 + fctd1)}{2}; \sigma t2 \\
& := \frac{(fctd2\cdot hbot)}{xT13 + xT14}; Nt13 := \frac{bweb\cdot xT13\cdot(\sigma t2 + fctd2)}{2}; Nt14 \\
& := 0.5\cdot B\cdot xT14\cdot\sigma t2; NT1 := Nt11 + Nt12 + Nt13 + Nt14; \varepsilon p \\
& := \frac{\sigma pt}{Ep} + \varepsilon cu3\cdot\left(\frac{dp}{x} - 1\right) : \sigma pu := fpd \\
& + \left(\frac{(\varepsilon p - \varepsilon pd)}{(35\cdot 10^{-3} - \varepsilon pd)}\right)\cdot(1691 - fpd) : dNp1 := Ap\cdot(\sigma pu \\
& - \sigma pt) : P1 := Ap\cdot\sigma pt : eq1 := N1c = P1 + dNp1 + NT1; x \\
& := solve(eq1, x); eval(x); \mathbf{end\ proc}\ ;
\end{aligned}
$$

```
proc(B, bweb, htop, εc3, εcu3, fcd, Ap, σpt, fpd, e, dp, Ep, εpd, fctk,
    σu03, fctd1, fctd2, lf, εct, εu03, εctu, hbot)
    local N1c, x11, x12, x13, N11, N12, N13, eq1, σc, εp, σpu, dNp1,
    P1, xT10, xT11, xT12, xT13, xT14, Nt11, Nt12, Nt13, σt2, Nt14,
    NT1, x;
    x11 := x*(εcu3 − εc3)/εcu3;
    x12 := htop − x11;
    x13 := x − htop;
    σc := fcd*x13/(x − x11);
    N11 := B*fcd*x11;
    N12 := 1/2*B*(fcd + σc)*x12;
    N13 := bweb*0.5*σc*x13;
    N1c := N11 + N12 + N13;
    xT10 := H − x;
    xT11 := xT10*εct/εctu;
    xT12 := xT10*(εu03 − εct)/εctu;
    xT13 := xT10*(εctu − εu03)/εctu − hbot;
    xT14 := hbot;
    Nt11 := 0.5*bweb*fctd1*xT11;
    Nt12 := 1/2*bweb*xT12*(fctd2 + fctd1);
    σt2 := fctd2*hbot/(xT13 + xT14);
    Nt13 := 1/2*bweb*xT13*(σt2 + fctd2);
    Nt14 := 0.5*B*xT14*σt2;
    NT1 := Nt11 + Nt12 + Nt13 + Nt14;
    εp := σpt/Ep + εcu3*(dp/x − 1);
    σpu := fpd + (εp − εpd)*(1691 − fpd)/(7/200 − εpd);
    dNp1 := Ap*(σpu − σpt);
    P1 := Ap*σpt;
    eq1 := N1c = P1 + dNp1 + NT1;
    x := solve(eq1, x);
    eval(x)
end proc
```

```
x := it1(B, bweb, htop, εc3, εcu3, fcd, Ap, σpt, fpd, e, dp, Ep, εpd,
    fctk, σu03, fctd1, fctd2, lf, εct, εu03, εctu, hbot)[1]
```

143.9847866

SITUATION 2: y≥ htop

$$
\begin{aligned}
it2 :=& \textbf{proc}(B, bweb, htop, \varepsilon c3, \varepsilon cu3, fcd, Ap, \sigma pt, fpd, e, dp, Ep, \varepsilon pd, \\
& fctk, \sigma u03, fctd1, fctd2, lf, \varepsilon ct, \varepsilon u03, \varepsilon ctu, hbot) \textbf{ local } x21, x22, \\
& x23, N21, N22, N23, eq2, N2c, \varepsilon p, \sigma pu, dNp2, P2, xT20, xT21, \\
& xT22, xT23, xT24, Nt21, Nt22, Nt23, \sigma t12, Nt24, NT2, z; x21 \\
& := htop; x22 := \frac{z\cdot(\varepsilon cu3 - \varepsilon c3)}{\varepsilon cu3} - htop; x23 := z \\
& - \frac{z\cdot(\varepsilon cu3 - \varepsilon c3)}{\varepsilon cu3}; N21 := B\cdot fcd\cdot x21; N22 := bweb\cdot fcd\cdot x22; \\
& N23 := bweb\cdot 0.5\cdot fcd\cdot x23; N2c := N21 + N22 + N23; xT20 := H \\
& - x; xT21 := \frac{xT20\cdot\varepsilon ct}{\varepsilon ctu}; xT22 := \frac{xT20\cdot(\varepsilon u03 - \varepsilon ct)}{\varepsilon ctu}; xT23 \\
& := \frac{xT20\cdot(\varepsilon ctu - \varepsilon u03)}{\varepsilon ctu} - hbot; xT24 := hbot; Nt21 := 0.5 \\
& \cdot bweb\cdot fctd1\cdot xT21; Nt22 := \frac{bweb\cdot xT22\cdot(fctd2 + fctd1)}{2}; \sigma t12 \\
& := \frac{(fctd2\cdot hbot)}{xT23 + xT24}; Nt23 := \frac{bweb\cdot xT23\cdot(\sigma t12 + fctd2)}{2}; Nt24 \\
& := 0.5\cdot B\cdot xT24\cdot\sigma t12; NT2 := Nt21 + Nt22 + Nt23 + Nt24; \varepsilon p \\
& := \frac{\sigma pt}{Ep} + \varepsilon cu3\cdot\left(\frac{dp}{z} - 1\right) : \sigma pu := fpd \\
& + \left(\frac{(\varepsilon p - \varepsilon pd)}{(35\cdot 10^{-3} - \varepsilon pd)}\right)\cdot(1691 - fpd) : dNp2 := Ap\cdot(\sigma pu \\
& - \sigma pt) : P2 := Ap\cdot\sigma pt : eq2 := N2c = P2 + dNp2 + NT2; z \\
& := solve(eq2, z); eval(z); \textbf{ end proc };
\end{aligned}
$$

```
proc(B, bweb, htop, εc3, εcu3, fcd, Ap, σpt, fpd, e, dp, Ep, εpd, fctk,
    σu03, fctd1, fctd2, lf, εct, εu03, εctu, hbot)
    local x21, x22, x23, N21, N22, N23, eq2, N2c, εp, σpu, dNp2, P2,
    xT20, xT21, xT22, xT23, xT24, Nt21, Nt22, Nt23, σt12, Nt24,
    NT2, z;
    x21 := htop;
    x22 := z*(εcu3 − εc3)/εcu3 − htop;
    x23 := z − z*(εcu3 − εc3)/εcu3;
    N21 := B*fcd*x21;
    N22 := bweb*fcd*x22;
    N23 := bweb*0.5*fcd*x23;
    N2c := N21 + N22 + N23;
    xT20 := H − x;
    xT21 := xT20*εct/εctu;
    xT22 := xT20*(εu03 − εct)/εctu;
    xT23 := xT20*(εctu − εu03)/εctu − hbot;
    xT24 := hbot;
    Nt21 := 0.5*bweb*fctd1*xT21;
    Nt22 := 1/2*bweb*xT22*(fctd2 + fctd1);
    σt12 := fctd2*hbot/(xT23 + xT24);
    Nt23 := 1/2*bweb*xT23*(σt12 + fctd2);
    Nt24 := 0.5*B*xT24*σt12;
    NT2 := Nt21 + Nt22 + Nt23 + Nt24;
    εp := σpt/Ep + εcu3*(dp/z − 1);
    σpu := fpd + (εp − εpd)*(1691 − fpd)/(7/200 − εpd);
    dNp2 := Ap*(σpu − σpt);
    P2 := Ap*σpt;
    eq2 := N2c = P2 + dNp2 + NT2;
    z := solve(eq2, z);
    eval(z)
end proc
```

```
z := it2(B, bweb, htop, εc3, εcu3, fcd, Ap, σpt, fpd, e, dp, Ep, εpd,
    fctk, σu03, fctd1, fctd2, lf, εct, εu03, εctu, hbot)
```

10.25386057, −256.6781966

The following statement determines which situation is at hand, based on y. Then it determines the right value for xu. If the first determined x was correct, than this value will be shown, otherwise it will be the result of situation 1 or 2.

if x ≤ htop **then** x := xin **elif** $x \geq htop$ **and** $y \leq htop$ **then** $x := it1(B, bweb, htop, \varepsilon c3, \varepsilon cu3, fcd, Ap, \sigma pt, fpd, e, dp, Ep, \varepsilon pd, fctk, \sigma u03, fctd1, fctd2, lf, \varepsilon ct, \varepsilon u03, \varepsilon ctu, hbot)[1]$ **elif** $x \geq htop$ **and** $y \geq htop$ **then** $x := it2(B, bweb, htop, \varepsilon c3, \varepsilon cu3, fcd, Ap, \sigma pt, fpd, e, dp, Ep, \varepsilon pd, fctk, \sigma u03, fctd1, fctd2, lf, \varepsilon ct, \varepsilon u03, \varepsilon ctu, hbot)[1]$ **end if**

143.5931702

$xu := x$

143.5931702

Determining Bending Moment resistance

There are three situations, which influence the determination of MRd. Situation A is used, when the first determined x is the correct one. Situation B is used, when the first determined x is higher than the top flange and y ≤ htop . Situation C is used when the first determined x is higher than the top flange and y ≥ htop.

SITUATION A: MRD when xu ≤ htop. **IGNORE SUBSECTION IF xu > htop!!**

Re-determination compressive and tensile forces and prestress force, due to change in variables during previous calculations:

$$x1 := \frac{x \cdot (\varepsilon cu3 - \varepsilon c3)}{\varepsilon cu3} : x2 := x - x1 :$$

$$Nx1 := B \cdot fcd \cdot x1 : Nx2 := \frac{B \cdot (fcd)}{2} \cdot x2 : Ncc := Nx1 + Nx2;$$

$7.714451025\ 10^{6}$

$$xT := H - x : xT1 := \frac{xT \cdot \varepsilon ct}{\varepsilon ctu}; xT2 := htop - x - xT1; xT3 := \frac{xT \cdot (\varepsilon u03 - \varepsilon ct)}{\varepsilon ctu} - xT2; xT4 := \frac{xT \cdot (\varepsilon ctu - \varepsilon u03)}{\varepsilon ctu} - hbot : xT5 := hbot :$$

5.991802485

10.41502732

31.71483390

$Nt1 := 0.5 \cdot B \cdot fctd1 \cdot xT1;$

15978.13996

$$\sigma t1 := \frac{(fctd2 - fctd1)}{xT2 + xT3} \cdot xT2 + fctd1; Nt2 := \frac{B \cdot xT2 \cdot (\sigma t1 + fctd1)}{2};$$

$$Nt3 := \frac{bweb \cdot xT3 \cdot (\sigma t1 + fctd2)}{2} :$$

$$Nt3 := \frac{bweb \cdot xT3 \cdot (\sigma t1 + fctd2)}{2} :$$

5.597026642

56919.99890

$$\sigma t2 := \frac{(fctd2 \cdot hbot)}{xT4 + xT5} : Nt4 := \frac{bweb \cdot xT4 \cdot (fctd2 + \sigma t2)}{2} : \; Nt5 := 0.5 \cdot B \cdot xT5 \cdot \sigma t2 :$$

$$Nt := Nt1 + Nt2 + Nt3 + Nt4 + Nt5;$$

$5.873580041\ 10^{5}$

$$\varepsilon p := \frac{\sigma pt}{Ep} + \varepsilon cu3 \cdot \left(\frac{dp}{x} - 1\right) : \sigma pu := fpd + \left(\frac{(\varepsilon p - \varepsilon pd)}{(35 \cdot 10^{-3} - \varepsilon pd)}\right) \cdot (1691 - fpd) :$$

$$dNp := Ap \cdot (\sigma pu - \sigma pt); P := Ap \cdot \sigma pt;$$

$1.756782501\ 10^{6}$

$5.3750466\ 10^{6}$

Check if equilibrium between internal forces (difference in [N])

$$\frac{Ncc - (dNp + P + Nt)}{1000};$$

-4.7360801

Determination of distance of all forces to the rotation point. Rotation point on utmost top fibre:

$$armc1 := 0.5 \cdot x1 : armc2 := x1 + \frac{x2}{3} :$$

$$armt1 := x + \frac{2}{3} xT1 : armt2 := x + xT1 + \frac{xT2}{3} \cdot \frac{(2 \cdot \sigma t1 + fctd1)}{\sigma t1 + fctd1} :$$

$$armt3 := x + xT1 + xT2 + \frac{xT3}{3} \cdot \frac{(\sigma t1 + 2 \cdot fctd2)}{\sigma t1 + fctd2} : armt4 := x + xT1 + xT2 + xT3 + \frac{1 \cdot xT4}{3} \cdot \frac{(2 \cdot \sigma t2 + fctd2)}{\sigma t2 + fctd2} : armt5 := H - \frac{2 \cdot xT5}{3} :$$

Bending moment resistance

$$MRd1 := \frac{1}{1000000}(((Nt1 \cdot armt1 + Nt2 \cdot armt2 + Nt3 \cdot armt3 + Nt4 \cdot armt4 + Nt5 \cdot armt5) + (dNp \cdot dp) + P \cdot \text{ztop}) - (Nx1 \cdot armc1 + Nx2 \cdot armc2));$$

2319.007246

SITUATION B: MRd when xu determined with iteration 1for y≤htop and x≥htop. **IGNORE SUBSECTION IF x ≤ htop OR y≥ htop!!**

SITUATION C: MRd when xu determined with iteration 2 for y≥htop and x≥htop. **IGNORE SUBSECTION IF x ≤ htop OR y ≤ htop!!**

FINAL RESULTS

Height of compressive zone

$xu;$

143.5931702

Height of tension zone

$xT;$

456.4068298

Bending moment resistance

$$\textbf{if } x < htop \textbf{ then } MRd := MRd1 \textbf{ elif } x \geq htop \textbf{ and } y \leq htop \textbf{ then } MRd := MRd2 \textbf{ else } MRd := MRd3 \textbf{ end if}:$$

$MRd;$

2319.007246

Rotational capacity check

$$f := \frac{\left(\frac{1860}{1.1} - \sigma pt\right) \cdot Ap}{Ap}:$$

$$g := 1 - \frac{f}{500 + f}: \frac{xu}{dp};$$

0.2688003935

$$\textbf{if} \frac{xu}{dp} \leq \mathrm{g} \textbf{ then } print(rotational\ capacity\ OK) \textbf{ else } print\ (rotaional\ capacity\ NOT\ OK)\ \textbf{end if}$$

rotational capacity OK

$$UC := \frac{xu}{dp \cdot g};$$

0.5478738492

kappa:= $\frac{\varepsilon cu3}{xu} \cdot 1000$

0.01810671076

END MAPLE SHEET

With the maple sheet found is the moment capacity is:
M_{Rd} = 2319 kNm with a compression zone height of x = 143.59mm
Unity Check: M_{Ed}/M_{Rd} = 1259.62/2319 = 0.543→ OK.

The moment capacity is more than enough to resist the working moments on the structure.

E.11.2 Parametric study Moment capacity

For determining the moment capacity it was assumed that the ultimate tensile strain limit (ε_{ctu}) is reached. In reality this is often not the case. It is also possible that during a stage of loading, where the ultimate compressive strain limit (ε_{cu3}) is not yet reached, that the total tensile capacity is higher than when ε_{cu3} reached. This could possibly result in a higher moment capacity. So it is necessary to perform a parametric study, where at different stages of loading (so basically at different values of the compressive strain ε_c) the moment capacity is determined. For this a Maple sheet is developed. The sheet is based on the following procedure:

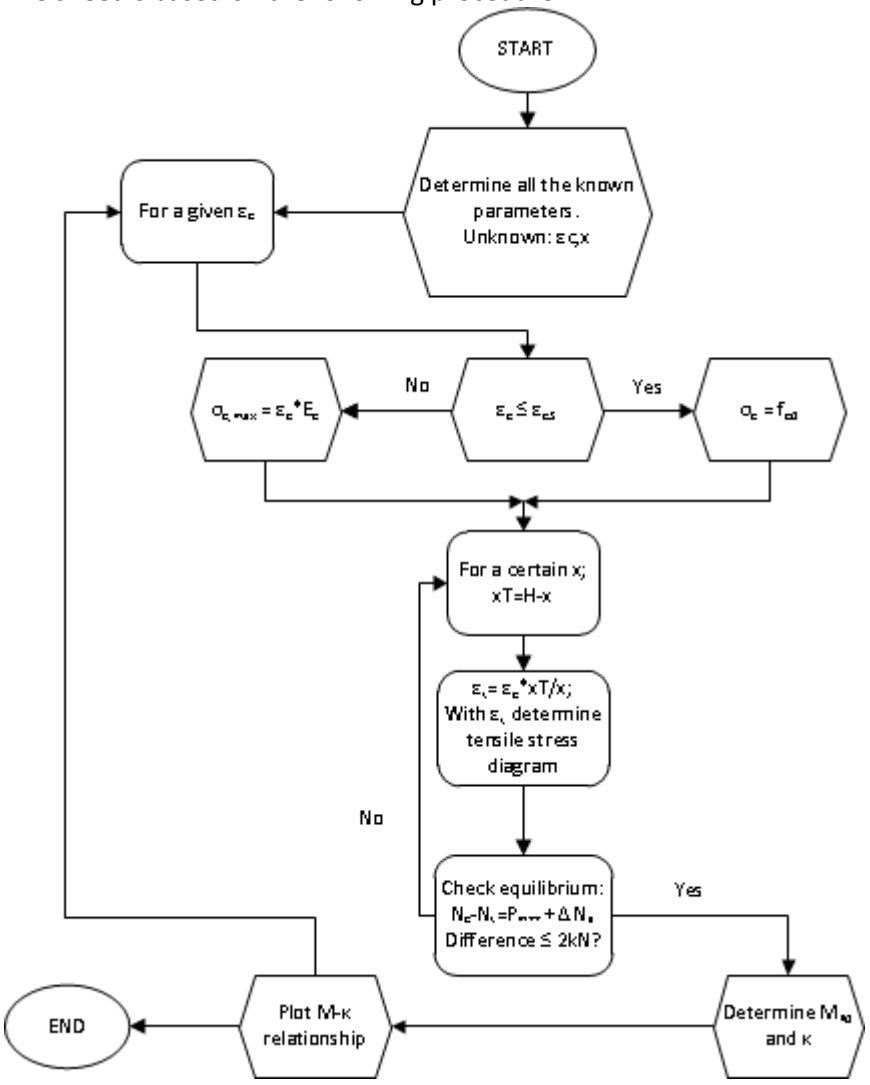

So a certain value for ε_c is assigned. With this value a check needs to be made if the strain limit ε_{c3} is reached. On basis of this check the maximum compressive stress for the given ε_c can be determined. Then with trial and error the correct x needs to be determined. Assigning a value for x will subsequently determine the tension zone height xT and thus the tensile strain ε_t in the bottom fibre. This tensile strain will determine the tensile stress diagram.

That is done by checking if $\varepsilon_t \leq \varepsilon_{ct}$ or $\varepsilon_{ct} \leq \varepsilon_t \leq \varepsilon_{u0,3}$ or $\varepsilon_{u0,3} \leq \varepsilon_t \leq \varepsilon_{ctu}$. With the tensile strain in one of these three areas, the stress diagram changes accordingly. The internal forces are determined and checked if they are in equilibrium. In this case that will be where the difference between the compression and tension forces is equal or lower than 2 kN. This will still give an accurate x value, while keeping the calculation time low. The maple sheet is presented in the following:

MAPLE SHEET: Parametric study; Iteration of xu to find M-κ diagram

In this the influence of the compressive strain εc on the moment capacity will be investigated. If εc is changed the moment capacity and the curvature will change as well. Eventually a M-κ diagram can be plotted. This way the maximum moment capacity of the structure can be found. When a certain εc is inputted, the compressive zone needs to be changed by trial and error until there is equilibrium of the internal forces. Then the moment capacity can be determined.

Dimension

$$restart; with(plots) : Digits := 5 :$$
$$H := 600 :$$
$$B := 1000 :$$
$$htop := 160 :$$
$$hbot := 130 :$$
$$bweb := 2 \cdot 140 :$$
$$Ac := H \cdot B - (H - htop - hbot) \cdot (B - bweb) :$$
$$ztop := \frac{1}{Ac}(H \cdot B \cdot 0.5 \cdot H - ((H - htop - hbot) \cdot (B - bweb) \cdot (htop + 0.5 \cdot (H - htop - hbot)))) :$$

Concrete strength

$$fck := 170 : \alpha c := 0.85 : fcd := \frac{\alpha c \cdot fck}{1.5} :$$
$$fctk := 8 :$$
$$\sigma 03 := 12 :$$
$$fctd1 := \frac{fctk}{1.5} : fctd2 := \frac{\sigma 03}{1.25 \cdot 1.5} :$$
$$E := 50000 :$$

Concrete strains

$$\varepsilon c3 := 2.3 \cdot 10^{-3} : \varepsilon cu3 := 2.6 \cdot 10^{-3} :$$
$$lf := 13 :$$
$$\varepsilon ct := \frac{fctd1}{E}; \varepsilon u03 := \frac{0.3}{\frac{2}{3} \cdot H} + \varepsilon ct; \varepsilon ctu := \frac{lf}{\frac{4 \cdot 2}{3} \cdot H}; kap1 := \frac{(fctd2 - fctd1)}{\varepsilon u03 - \varepsilon ct} : kap2 := \frac{fctd2}{\varepsilon ctu - \varepsilon u03} :$$

0.00010667

0.00085667

$$\frac{13}{1600}$$

Prestressing

$$Ap := 4587 :$$
$$\sigma pt := 1185 : fpd := 1522 :$$
$$Ep := 195000 :$$
$$\varepsilon pd := \frac{1522}{Ep} :$$
$$e := 65.8 :$$
$$dp := H - e :$$

Main iteration

εc (compressive strain in top fibre) and x (height compressive zone) are both unknowns. Interested is to find the moment capacity (MRd) belonging to a certain εc (in combination with a x). A certain x value is correct, when the difference in internal forces is ±2kN at most. This x is used to determine the moment capacity and the curvature as well. Eventually a M-κ diagram can be determined, after the iterations are completed.

εc is limited from 0.9 to 2.6 promille. 2.6 is the ultimate compressive strain. After 0.9 the iteration cannot find equilibrium. This is due to the present compressive force created by the prestressing. So in reality there is already a compressive strain available in the structure. x is limited from 145 to dp. Hand calculation showed that x will not be lower than around 145 mm and going lower than 145mm results in a tensile strain that surpasses the ultimate tensile strain limit (which can be increased by taking longer steel fibres if necessary. This particular mixture has fibres with lf=13mm as already defined earlier).

for εc **from** $0.9\cdot10^{-3}$ **by** 0.0001 **to** $2.6\cdot10^{-3}$ **do for** x **from** 140 **by** 0.01 **to** dp **do**

if $\varepsilon c \le \varepsilon c3$ **and** $x \le htop$ **then** $x1 := x; x2 := 0; fcc1 := \dfrac{\varepsilon c\cdot fcd}{\varepsilon c3}; Nx1 := 0.5\cdot B\cdot fcc1\cdot x1; Nx2 := 0\ ; Nx3 := 0$

elif $\varepsilon c \le \varepsilon c3$ **and** $x > htop$ **then** $x1 := htop\ ; x2 := x - x1; fcc1 := \dfrac{\varepsilon c\cdot fcd}{\varepsilon c3}; fcc2 := \dfrac{fcc1\cdot x2}{x}; Nx1 := 0.5\cdot(fcc1 + fcc2)\cdot B\cdot x1; Nx2 := 0.5\cdot fcc2\cdot bweb\cdot x2; Nx3 := 0$

elif $\varepsilon c > \varepsilon c3$ **and** $x \le htop$ **then** $x1 := \dfrac{x\cdot(\varepsilon c - \varepsilon c3)}{\varepsilon c}; x2 := x - x1; Nx1 := fcd\cdot B\cdot x1; Nx2 := 0.5\cdot fcd\cdot B\cdot x2; Nx3 := 0$

elif $\varepsilon c > \varepsilon c3$ **and** $x > htop$ **then** $x1 := \dfrac{x\cdot(\varepsilon c - \varepsilon c3)}{\varepsilon c}; x2 := htop - x1; x3 := x - htop; Nx1 := fcd\cdot x1\cdot B; fcc1 := \dfrac{fcd\cdot x3}{x2 + x3}; Nx2 := 0.5\cdot B\cdot(fcd + fcc1)\cdot x2; Nx3 := 0.5\cdot fcc1\cdot bweb\cdot x3$ **end if**;

$Ncc := Nx1 + Nx2; xT := H - x; \varepsilon t := \dfrac{\varepsilon c\cdot xT}{x};$

if $\varepsilon t \le \varepsilon ct$ **and** $x \ge htop$ **then** $xT1 := xT$; $xT2 := hbot$; $fc1 := \frac{E \cdot \varepsilon t \cdot xT1}{xT}$; $Nt1 := 0.5 \cdot bweb \cdot fc1 \cdot xT1$; $Nt2 := 0.5 \cdot (fc1 + E \cdot \varepsilon t) \cdot B \cdot xT2$; $Nt3 := 0$; $Nt4 := 0$; $Nt5 := 0$

elif $\varepsilon t > \varepsilon ct$ **and** $\varepsilon t \le \varepsilon u03$ **and** $x \ge htop$ **then** $xT1 := \frac{xT \cdot \varepsilon ct}{\varepsilon u03}$; $xT2 := xT - xT1 - hbot$; $xT3 := hbot$; $Nt1 := 0.5 \cdot fctd1 \cdot bweb \cdot xT1$; $fc2 := fctd1 + kap1 \cdot (\varepsilon t - \varepsilon ct)$; $fc1 := \frac{(fc2 - fctd1)}{xT2 + xT3} \cdot xT2 + fctd1$; $Nt2 := 0.5 \cdot (fc1 + fctd1) \cdot bweb \cdot xT2$; $Nt3 := 0.5 \cdot (fc2 + fc1) \cdot B \cdot xT3$; $Nt4 := 0$; $Nt5 := 0$

elif $\varepsilon t > \varepsilon u03$ **and** $\varepsilon t \le \varepsilon ctu$ **and** $x \ge htop$ **then** $xT1 := \frac{xT \cdot \varepsilon ct}{\varepsilon t}$; $xT2 := \frac{xT \cdot (\varepsilon u03 - \varepsilon ct)}{\varepsilon t}$; $xT3 := \frac{xT \cdot (\varepsilon t - \varepsilon u03)}{\varepsilon t} - hbot$; $xT4 := hbot$; $Nt1 := 0.5 \cdot bweb \cdot fctd1 \cdot xT1$; $Nt2 := \frac{bweb \cdot (fctd1 + fctd2) \cdot xT2}{2}$; $fc2 := fctd2 - kap2 \cdot (\varepsilon t - \varepsilon u03)$; $fc1 := \frac{(fc2 - fctd2)}{xT3 + xT4} \cdot xT3 + fctd2$; $Nt3 := 0.5 \cdot (fc1 + fctd2) \cdot bweb \cdot xT3$; $Nt4 := 0.5 \cdot (fc1 + fc2) \cdot B \cdot xT4$; $Nt5 := 0$

elif $\varepsilon t > \varepsilon u03$ **and** $\varepsilon t \le \varepsilon ctu$ **and** $x < htop$ **then** $xT1 := \frac{xT \cdot \varepsilon ct}{\varepsilon t}$; $xT2 := htop - x - xT1$; $xT3 := \frac{xT \cdot (\varepsilon u03 - \varepsilon ct)}{\varepsilon t} - xT2$; $xT4 := \frac{xT \cdot (\varepsilon t - \varepsilon u03)}{\varepsilon t} - hbot$; $xT5 := hbot$; $Nt1 := 0.5 \cdot B \cdot fctd1 \cdot xT1$; $fc1 := \frac{(fctd2 - fctd1)}{xT2 + xT3} \cdot xT2 + fctd1$; $Nt2 := \frac{B \cdot xT2 \cdot (fc1 + fctd1)}{2}$; $Nt3 := \frac{bweb \cdot xT3 \cdot (fc1 + fctd2)}{2}$; $fc2 := \frac{(fctd2 \cdot hbot)}{xT4 + xT5}$: $Nt4 := \frac{bweb \cdot xT4 \cdot (fctd2 + fc2)}{2}$; $Nt5 := 0.5 \cdot B \cdot xT5 \cdot fc2$ **end if**;

$Nt := Nt1 + Nt2 + Nt3 + Nt4 + Nt5$; $\varepsilon p := \frac{\sigma pt}{Ep} + \varepsilon c \cdot \left(\frac{dp}{x} - 1 \right)$;

if $\varepsilon p \le \varepsilon pd$ **then** $\sigma pu := Ep \cdot \varepsilon p$ **else** $\sigma pu := fpd + \left(\frac{(\varepsilon p - \varepsilon pd)}{(35 \cdot 10^{-3} - \varepsilon pd)} \right) \cdot (1691 - fpd)$ **end if**;

$dNp := Ap \cdot (\sigma pu - \sigma pt)$; $P := Ap \cdot \sigma pt$;

$dif[\varepsilon c] := Ncc - Nt - P - dNp$; **if** $dif[\varepsilon c] \ge -2000$ **and** $dif[\varepsilon c] \le 2000$ **then break end if end do**;

if $\varepsilon c \le \varepsilon c3$ **and** $x \le htop$ **then** $armc1 := \left(\frac{1}{3}\right)\cdot x$; $armc2 := 0$; $armc3 := 0$

elif $\varepsilon c \le \varepsilon c3$ **and** $x > htop$ **then** $armc1 := \frac{x1}{3}\cdot\frac{(fcc1 + 2\cdot fcc2)}{fcc1 + fcc2}$;
$armc2 := x1 + \frac{x2}{3}$; $armc3 := 0$

elif $\varepsilon c > \varepsilon c3$ **and** $x \le htop$ **then** $armc1 := 0.5\cdot x1$; $armc2 := x1 + \frac{x2}{3}$;
$armc3 := 0$

elif $\varepsilon c > \varepsilon c3$ **and** $x > htop$ **then** $armc1 := 0.5\cdot x1$; $armc2 := x1 + \frac{x2}{3}$
$\cdot\frac{(fcd + 2\cdot fcc1)}{fcc1 + fcd}$; $armc3 := x1 + x2 + \frac{x3}{3}$ **end if**;

if $\varepsilon t \le \varepsilon ct$ **and** $x \ge htop$ **then** $armt1 := x + \frac{2\cdot xT1}{3}$; $armt2 := x + xT1$
$+ \frac{xT2}{3}\cdot\frac{(2\cdot E\cdot\varepsilon t + fc1)}{E\cdot\varepsilon t + fc1}$; $armt3 := 0$; $armt4 := 0$

elif $\varepsilon t > \varepsilon ct$ **and** $\varepsilon t \le \varepsilon u03$ **and** $x \ge htop$ **then** $armt1 := x + \frac{2\cdot xT1}{3}$;
$armt2 := x + xT1 + \frac{xT2}{3}\cdot\frac{(2\cdot fc1 + fctd1)}{fc1 + fctd1}$; $armt3 := x + xT1$
$+ xT2 + \frac{xT3}{3}\cdot\frac{(2\cdot fc2 + fc1)}{fc2 + fc1}$

elif $\varepsilon t > \varepsilon u03$ **and** $\varepsilon t \le \varepsilon ctu$ **and** $x \ge htop$ **then** $armt1 := x + \frac{2}{3}\cdot xT1$;
$armt2 := x + xT1 + \frac{xT2}{3}\cdot\frac{(2\cdot fctd2 + fctd1)}{fctd2 + fctd1}$; $armt3 := x + xT1$
$+ xT2 + \frac{xT3}{3}\cdot\frac{(2\cdot fc1 + fctd2)}{fc1 + fctd2}$; $armt4 := x + xT1 + xT2$
$+ xT3 + \frac{xT4}{3}\cdot\frac{(2\cdot fc2 + fc1)}{fc1 + fc2}$

elif $\varepsilon t > \varepsilon u03$ **and** $\varepsilon t \le \varepsilon ctu$ **and** $x < htop$ **then** $armt1 := x + \frac{xT1\cdot 2}{3}$;
$armt2 := x + xT1 + \frac{xT2}{3}\cdot\frac{(2\cdot fc1 + fctd1)}{fc1 + fctd1}$; $armt3 := x + xT1$
$+ xT2 + \frac{xT3}{3}\cdot\frac{(fc1 + 2\cdot fctd2)}{fc1 + fctd2}$; $armt4 := x + xT1 + xT2$
$+ xT3 + \frac{xT4}{3}\cdot\frac{(2\cdot fc2 + fctd2)}{fc1 + fctd2}$; $armt5 := H - \frac{2\cdot xT5}{3}$ **end if**;

$MRd[\varepsilon c] := \frac{1}{1000000}(((Nt1\cdot armt1 + Nt2\cdot armt2 + Nt3\cdot armt3$
$+ Nt4\cdot armt4 + Nt5\cdot armt5) + (dNp\cdot dp) + P\cdot \text{ztop}) - (Nx1$
$\cdot armc1 + Nx2\cdot armc2 + Nx3\cdot armc3))$;

$\text{kappa}[\varepsilon c] := \frac{\varepsilon c}{x}\cdot 1000$;

$pltMkap[\varepsilon c] := plot(Vector([\text{kappa}[\varepsilon c]]), Vector([MRd[\varepsilon c]]), style = point)$:

$pltdifeps[\varepsilon c] := plot\left(Vector([\varepsilon c]), Vector\left(\left[\frac{dif[\varepsilon c]}{1000}\right]\right), style = point\right)$;

$pltepsx[\varepsilon c] := plot(Vector([\varepsilon c]), Vector([x]), style = point)$;

if $dif[\varepsilon c] \geq -2000$ **and** $dif[\varepsilon c] \leq 2000$ **then** $print(x, \text{"at εc="}, \varepsilon c, \text{"MRd="}, MRd[\varepsilon c], \text{"with κ="}, \text{kappa}[\varepsilon c])$ **end if end do**:

484.67, "at εc=", 0.00090000, "MRd=", 1301.5, "with κ=", 0.0018569

427.52, "at εc=", 0.0010000, "MRd=", 1464.2, "with κ=", 0.0023391

384.34, "at εc=", 0.0011000, "MRd=", 1615.2, "with κ=", 0.0028620

351.17, "at εc=", 0.0012000, "MRd=", 1759.7, "with κ=", 0.0034171

325.61, "at εc=", 0.0013000, "MRd=", 1900.0, "with κ=", 0.0039925

302.47, "at εc=", 0.0014000, "MRd=", 2024.7, "with κ=", 0.0046286

283.52, "at εc=", 0.0015000, "MRd=", 2146.7, "with κ=", 0.0052906

267.82, "at εc=", 0.0016000, "MRd=", 2266.9, "with κ=", 0.0059742

248.93, "at εc=", 0.0017000, "MRd=", 2337.3, "with κ=", 0.0068292

227.82, "at εc=", 0.0018000, "MRd=", 2351.1, "with κ=", 0.0079010

210.12, "at εc=", 0.0019000, "MRd=", 2357.8, "with κ=", 0.0090425

195.21, "at εc=", 0.0020000, "MRd=", 2358.5, "with κ=", 0.010245

182.64, "at εc=", 0.0021000, "MRd=", 2355.4, "with κ=", 0.011498

171.92, "at εc=", 0.0022000, "MRd=", 2349.1, "with κ=", 0.012797

158.09, "at εc=", 0.0023000, "MRd=", 2242.1, "with κ=", 0.014549

152.51, "at εc=", 0.0024000, "MRd=", 2261.8, "with κ=", 0.015737

147.75, "at εc=", 0.0025000, "MRd=", 2278.7, "with κ=", 0.016920

143.36, "at εc=", 0.0026000, "MRd=", 2295.3, "with κ=", 0.018136

Plots

M-κ diagram

$V := plot(Vector([0]), Vector([0]), style = point) : W := plot(Vector([0]), Vector([2500])) : Z := plot(Vector([0.018]), Vector([0])) : display(V, W, Z, entries(pltMkap), title = \text{"M−κ diagram"}, labels = [\text{"curvature (κ) [1/m]"}, \text{"Moment capacity (MRd) [kNm]"}], labeldirections = [\text{"horizontal"}, \text{"vertical"}], axes = boxed)$

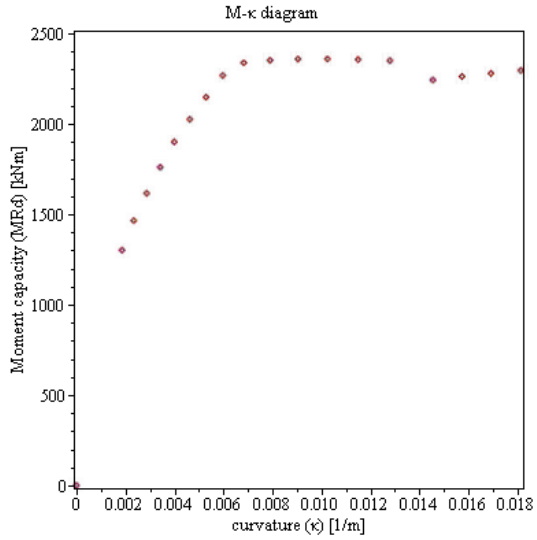

Difference internal forces

$A := plot(Vector([0]), Vector([0])) : B := plot(Vector([0.0027]), Vector([-2.01])) : display(A, B, entries(pltdifeps), title = "Difference internal compressive and tensile forces", labels = ["compressive strain (εc)", "Difference in kN"], labeldirections = ["horizontal", "vertical"], axes = boxed)$

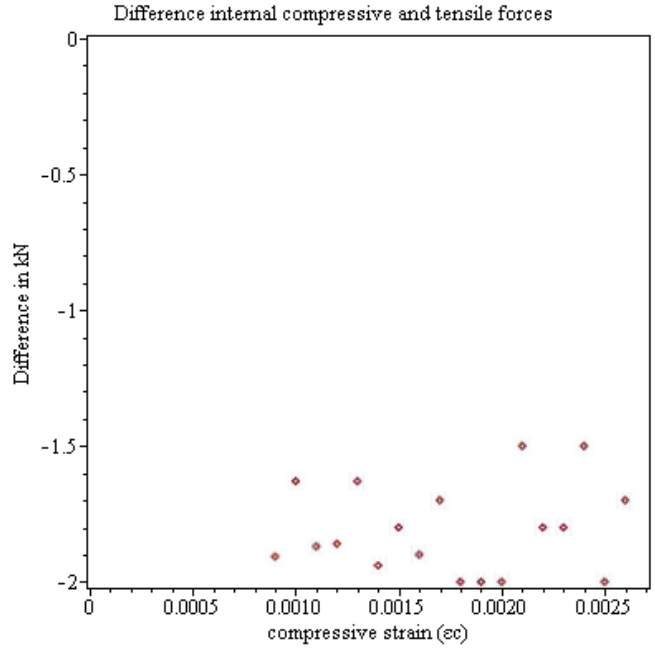

Relation x-εc

$C := plot(Vector([0.0005]), Vector([0.5])) : CC := plot(Vector([0.0028]), Vector([550])) : display(C, CC, entries(pltepsx), title = "x-ε relation", labels = ["compressive strain (εc)", "height compression zone (x)"], labeldirections = ["horizontal", "vertical"], axes = boxed);$

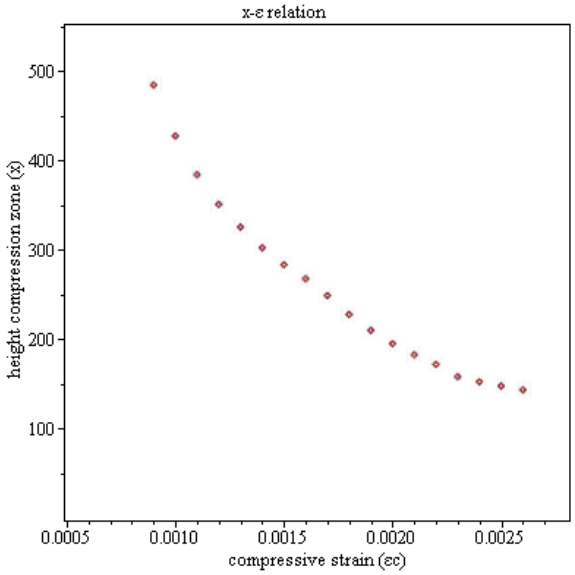

Rotational capacity check

$$f := \frac{\left(\frac{1860}{1.1} - \sigma pt\right) \cdot Ap}{Ap};$$

505.91

$$g := 1 - \frac{f}{500 + f};\ x := 195.21 : \frac{x}{dp};$$

0.49706

0.36542

if $\frac{x}{dp} \le$ g **then** *print*(*rotational capacity OK*)
else *print* (*rotaional capacity NOT OK*) **end if**

rotational capacity OK

END MAPLE SHEET

Results from the maple sheet show that the highest moment capacity is found at:
ε_c = 2.0‰.
Here a moment capacity of M_{Rd} = 2358.5 kNm is found, with a curvature of κ = 0.0102 m^{-1}.
The corresponding compressive zone height is x = 195.21 mm.

The value for M_{Rd} determined in the parametric study is around 39 kNm higher than the value calculated earlier, where assumed was that $\varepsilon_c = \varepsilon_{c3}$ and $\varepsilon_t = \varepsilon_{ctu}$. In the parametric study the moment capacity for $\varepsilon_c = \varepsilon_{cu3}$ = 2.6‰ was M_{Rd} = 2295.3 kNm. The difference between this value and the earlier determined value is around 1.0% so the procedure of the parametric study is pretty accurate.
The new unity check: UC = 1259.62 / 2358.5 = 0.534.

The structure would already be one the safe side even without the new determined M_{Rd}. Now the structure is even safer concerning the moment capacity (not much safer though as the increase in moment is only 39 kNm).

It is possible that strain softening occurs instead of strain hardening. This can occur for example if during pouring the positioning of the steel fibres is very negatively impacting the tensile behaviour. Or if the percentage of steel fibres is too low which also causes strain softening. The stress diagram changes, which results in no strength increase between ε_{ct} and $\varepsilon_{u0,3}$ (Figure E-7).

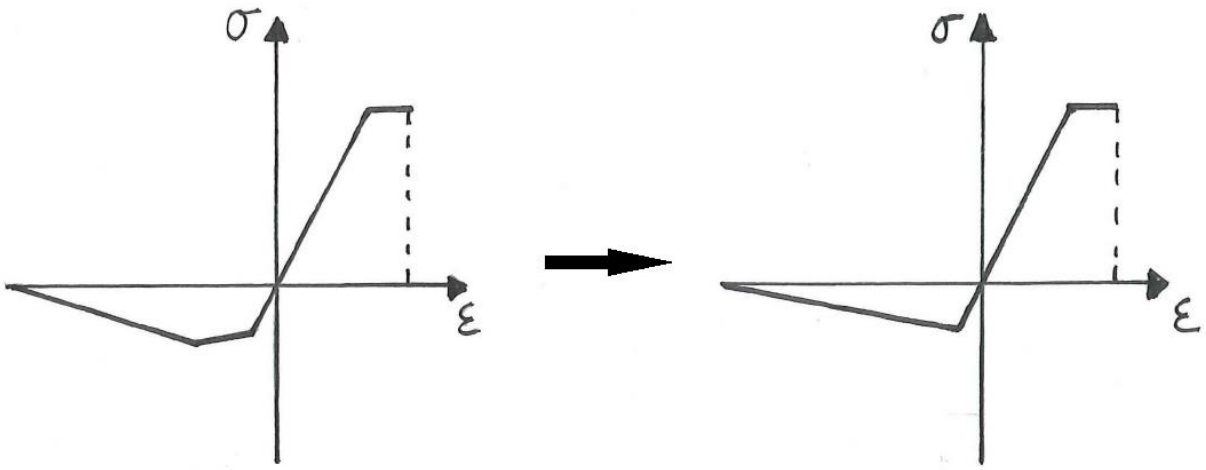

Figure E-7: From strain hardening to strain softening

The tensile capacity decreases, which subsequently leads to a decrease in moment capacity. The moment capacity if strain softening occurs is determined in the following, which is the second part of the same maple sheet that is used to make the calculation in paragraph E.11.1:

MAPLE SHEET: Case of strain softening

There is a possibility than the concrete shows strain softening behaviour instead of the assumed strain hardening behaviour. This would lead to a reduction of the moment capacity. This reduction will be determined in the following.

Internal compressive force

$$xs1 := \frac{xs\cdot(\varepsilon cu3 - \varepsilon c3)}{\varepsilon cu3} : xs2 := xs - xs1 :$$

$$Nxs1 := B\cdot fcd\cdot xs1 : Nxs2 := \frac{B\cdot(fcd)}{2}\cdot xs2 :$$

$$Nsc := Nxs1 + Nxs2 :$$

Internal tensile force

$$xsT := H - xs :$$

$$xsT1 := \frac{xsT\cdot\varepsilon ct}{\varepsilon ctu} : xsT2 := htop - xs - xsT1 : xsT3 := \frac{xsT\cdot(\varepsilon ctu - \varepsilon ct)}{\varepsilon ctu} - xsT2 - hbot : xsT4 := hbot :$$

$$Nst1 := 0.5\cdot B\cdot fctd1\cdot xsT1 :$$

$$\sigma st1 := \frac{(fctd1)}{\frac{xsT\cdot(\varepsilon ctu - \varepsilon ct)}{\varepsilon ctu}}\cdot(xsT3 + xsT4) : Nst2 := \frac{B\cdot xsT2\cdot(\sigma st1 + fctd1)}{2} :$$

$$\sigma st2 := \frac{(fctd1)\cdot xsT4}{\frac{xsT\cdot(\varepsilon ctu - \varepsilon ct)}{\varepsilon ctu}} : Nst3 := \frac{bweb\cdot xsT4\cdot(\sigma st2 + \sigma st1)}{2} :$$

$$Nst4 := 0.5\cdot B\cdot xsT4\cdot\sigma st2 :$$

$$Nst := Nst1 + Nst2 + Nst3 + Nst4 :$$

Prestress force

$$\varepsilon p := \frac{\sigma pt}{Ep} + \varepsilon cu3\cdot\left(\frac{dp}{xs} - 1\right) : \sigma pu := fpd + \left(\frac{(\varepsilon p - \varepsilon pd)}{(35\cdot 10^{-3} - \varepsilon pd)}\right)\cdot(1691 - fpd) :$$

$$dNp := Ap\cdot(\sigma pu - \sigma pt) : P := Ap\cdot\sigma pt :$$

Solve compressive zone xs

$$eq1 := Nsc = Nst + P + dNp$$

$$53724.35898\,xs = 6.877111939\,10^{6} - 35.00854702\,xs + 500\,(152.1230769 - 0.9868717949\,xs)\left(\frac{2377.884016}{600 - xs} + 5.333333334\right) + \frac{1.017302016\,10^{8}}{600 - xs} + \frac{3.959183771\,10^{7}}{xs}$$

$$xs := solve(eq1, xs)$$

138.8093265, 616.0715370, -4.926030834

$xs := xs[1];$

138.8093265

Check if determined x is completely located in top flange

if xs < htop **then** xs := xs **else** *print*(*FIND NEW X*) **end if**

138.8093265

Determination of x when $xs \geq htop$

$$ys := \frac{xs \cdot (\varepsilon cu3 - \varepsilon c3)}{\varepsilon cu3} :$$

Check if equilibrium between internal forces (difference in [N])

$$\frac{Nsc - (dNp + P + Nst)}{1000};$$

0.000003

Determination of distance of all forces to the rotation point. Rotation point on utmost top fibre.

$$armcs1 := 0.5 \cdot xs1 : armcs2 := xs1 + \frac{xs2}{3} :$$

$$armts1 := xs + \frac{2}{3} xsT1 : armts2 := xs + xsT1 + \frac{xsT2}{3} \cdot \frac{(2 \cdot \sigma st1 + fctd1)}{\sigma st1 + fctd1} : armts3 := xs + xsT1 + xsT2 + \frac{xsT3}{3} \cdot \frac{(\sigma st1 + 2 \cdot \sigma st2)}{\sigma st1 + \sigma st2} : armts4 := H - \frac{2 \cdot xsT4}{3} :$$

Bending moment resistance

$$MRds := \frac{1}{1000000}(((Nst1 \cdot armts1 + Nst2 \cdot armts2 + Nst3 \cdot armts3 + Nst4 \cdot armts4) + (dNp \cdot dp) + P \cdot \text{ztop}) - (Nxs1 \cdot armcs1 + Nxs2 \cdot armcs2));$$

2259.240748

Reduction of MRd (in kNm)

$red := MRd - MRds;$

59.766498

END MAPLE SHEET

The maple sheet shows that for this design in case of softening the moment capacity becomes M_{Rd} = 2259 kNm. In the original case M_{Rd} = 2319 kNm. The reduction in capacity is around 60 kNm. This is not a dramatic decrease in moment capacity. This is most likely due to the fact that the prestressing provides the largest contribution in moment capacity, so a decrease in tensile capacity will not have a large influence in this case. And the moment capacity in softening is still much higher than the design bending moment M_{Ed}.

E.12 Rotational capacity

The bending moment resistance suffices. But it is also important that the structure has enough rotational capacity in order to give enough warning before failure. For this the following requirement has to be met (NEN-EN-1992-1-1 Dutch NB cl.5.5):
$x_u / d \leq 500/(500+f)$ with $f= [(f_{pk}/\gamma_p - \sigma_{pm\infty})*A_p + f_{yd}*A_s]/(A_p + A_s)$ =
(1860/1.1-1172)*4587/4587 = 505.91.

The requirement becomes: $x_u/d \leq 0.497$.
Filling in x_u = 195.21 and with d=h-e = 534.2 mm x/d becomes 0.365 < 0.497. So the structure has enough rotational capacity.

E.13 Shear and torsion capacity

E.13.1 Shear

It is a requirement that the shear resistance is higher then the design shear force:
$V_{Rd}>V_d$
The design shear force is the sum of the shear force caused by bending moments and the shear force caused by torsional moments:
$V_d = V_{Ed} + V_{Td}$
Two cases have to be investigated, of which the most governing one will be used:

Situation 1. Location of highest torsional moment in structure
Situation 2. Location of highest shear force in structure

For both locations the internal forces were calculated and the results were presented in paragraph E.7. These were:
Mxy = T_{Ed}:

Situation 1. 317.09 kNm --> V_{Td} = 184.35 kN
Situation 2. 116.75 kNm --> V_{Td} = 67.88 kN

Vx (without self-weight and prestressing):

Situation 1. 235.94 kN
Situation 2. 584.56 kN

The shear force V_{Td} due to T_{Ed} is calculated with: $V_{Td} = h_m*T_{Ed}/(2*A_k)$:
$h_m = H-0.5*(h_{top,fl} + h_{bot,fl})$ = 0.6-0.5*(0.16+0.13) = 0.455 m
$b_m = B-2*0.5*b_{web}$ = 1.0-2*0.5*0.14=0.86 m
$A_k = b_m*h_m$ = 0.391 m^2

The governing total shear force taken from SCIA is the one where the sum of V_x and V_{Td} is the largest:

Situation 1. V_{Ed} =420.29 kN
Situation 2. V_{Ed} = 652.44 kN

So the governing situation for the shear resistance check wil be the location were the shear force is governing (situation 2). Furthermore the self-weight and prestressing also have to be taken into account with the result of V_{Ed} from SCIA. It is also possible that the eventual governing design shear force is found at the construction stage (t=0). So the shear force over the length of the beam needs to be determined at multiple stages. These stage and the shear forces are:

- t=0 only self weight: $V_{Ed} = V_{self} - P_{u0}$
- t=0 permanent loads: $V_{Ed} = V_{perm}-P_{u0}$
- t=∞ all loads + torsion: $V_{Ed} = V_{perm} + V_{var} - P_{u\infty}$

The upward force of the prestressing reduces the total shear force. But it only works between the support and the deviation point. The shear force is determined at the supports and just on each side of the deviation point.

In general the shear force at these locations is determined as follows:
$V_{sup} = 0.5*q*L - P_u$
$V_{dev1} = 0.5*q*L - 0.5*q*a - P_u$
$V_{dev2} = 0.5*q*L - 0.5*q*a$
For t=∞ the shear force is added with V_{Td}. Assumed is that V_{Td} is constant over the length of the beam. The result are seen in Table E-4 with the shear force lines in Figure E-8.

The parameters are:

Load of self-weight (ULS):	q_{self} =	11.86 kN/m
Permanent load (ULS):	q_{perm} =	20.72 kN/m
Variable load (ULS):	q_{var} =	39.86 kN/m
Upward Prestress force at t=0:	P_{u0} =	66.53 kN
Upward Prestress force at t=∞:	$P_{u\infty}$ =	55.88 kN
Distance deviators to support:	a =	8m

Table E-4: Results shear forces over length of beam

V [kN] at:	t=0 self	t=0 perm	t=inf
V_{sup}	75,818	164,358	738,901
V_{dev1}	-19,078	10,435	254,298
V_{dev2}	47,448	76,961	310,180

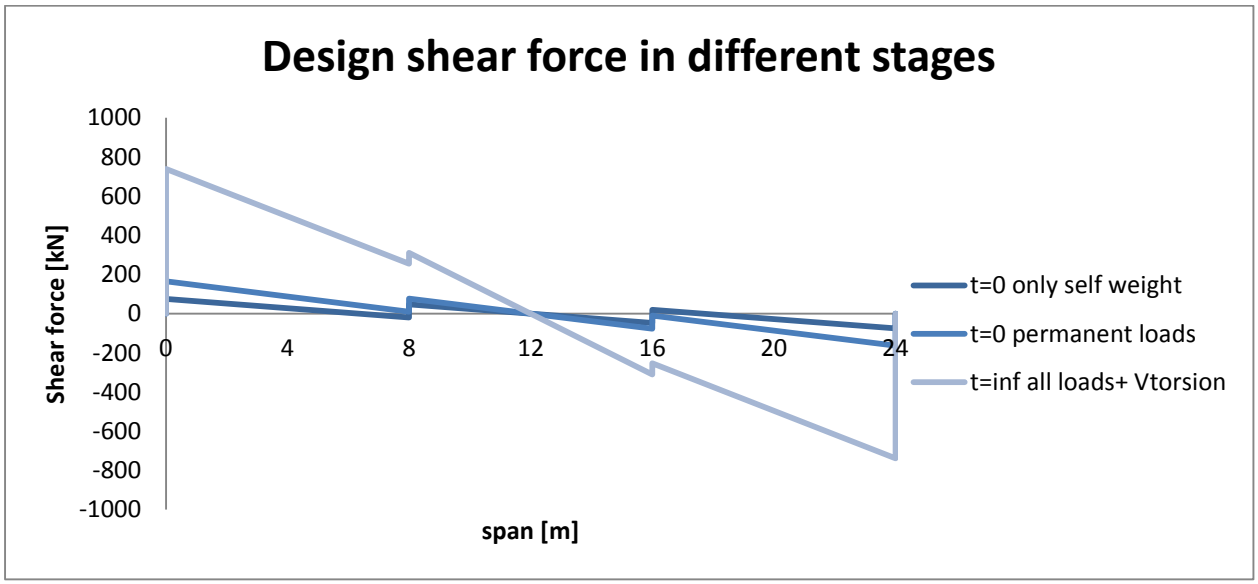

Figure E-8: Shear force line at multiple stages

The governing shear force V_{Ed} = 738.9 kN at t=∞. The shear resistance has to be high enough to resist this force.

The shear resistance for a UHPC structure is determined in a different way than the resistance for a NSC structure. This is mainly due to the inclusion of steel fibres in UHPC. AFGC gives a procedure to determine the shear resistance. It states that the shear resistance is equal to the smaller values of the two parameters V_{Rd} (tensile resistance of ties in concrete) and $V_{Rd,max}$ (resistance of compressive struts).
$V_{Rd} = V_{Rd,c} + V_{Rd,f} + V_{Rd,s}$
Where:
$V_{Rd,c}$ = the contribution of the concrete to the shear capacity
$V_{Rd,f}$ = the contribution of the steel fibres to the shear capacity

$V_{Rd,s}$ = the contribution of the shear reinforcement to the shear capacity
Because of the behaviour of the steel fibres in tension, it is allowed to view it seperately from the concrete, as if it is serving as reinforcement. Shear reinforcement will not be applied (unless the shear capacity is not enough to resist the design shear force), so $V_{Rd} = V_{Rd,c} + V_{Rd,f}$.

For a prestressed section the shear resistance $V_{Rd,c}$ is (AFGC2013 paragrapgh 2.4 section 6.2(1)):
$V_{Rd,c} = 0.24*(1/\gamma_{cf}\gamma_E)*k*f_{ck}^{1/2} * b_w*z$.

$\gamma_{cf}\gamma_E$ = 1.5
b_w = $2*b_{web}$ = 280 mm
z =0.9d = 480.78 mm
k =$3*\sigma_{cp}/f_{ck}$ =1.262 with $\sigma_{cp} = P_{m\infty}/A_c$

The result is $V_{Rd,c}$ = 351.53 kN

The contribution of the steel fibres can be determined with (AFGC2013 paragrapgh 2.4 section 6.2(2)): $V_{Rd,f} = A_{fv}*\sigma_{Rd,f}/\tan\theta$

Where
A_{fv} is the area of fibre effect = b_w*z
θ = 30° (minimum value recommended; lower value results in higher $V_{Rd,f}$, but lower $V_{Rd,max}$)
$\sigma_{Rd,f} = \frac{1}{K*\gamma_{cf}} * \frac{1}{w_{lim}} * \int_0^{w_{lim}} \sigma_f(w)dw$ with w_{lim} = 0.3mm
$\sigma_{Rd,f}$ is the residual tensile strength of the fibre reinforced cross-section. This strength is dependent on the mixture used. Assuming the mixture used here along with the assumed stress-strain diagram, the integral can be translated as being the area between ε_{ct} and $\varepsilon_{u0,3}$ in the diagram. So:

$$\sigma_{Rd,f} = \frac{1}{K * \gamma_{cf}} * \frac{1}{\varepsilon_{u0,3} - \varepsilon_{ct}} * [0.5 * (f_{ctd2} + f_{ctd1}) * (\varepsilon_{u0,3} - \varepsilon_{ct})]$$

K=1.25
γ_{cf} = 1.5

The strain values were already determined in paragraph E.11.1 (ε_{ct} = 0.10667 ‰ and $\varepsilon_{u0,3}$ = 0.85667‰). With everything filled in the formula:
$\sigma_{Rd,f} = \frac{1}{1.25*1.5} * \frac{1}{0.8567-0.1067} * [0.5 * (6.4 + 5.3) * (0.8667 - 0.1067)]$ = 4.67N/mm^2.

This results in:
$V_{Rd,f}$ = 1088.71 kN, which is much higher than $V_{Rd,c}$.

Now with both terms determined the shear capacity can be determined:
V_{Rd} = 1440.24 kN

Unity Check: V_{Ed}/V_{Rd} = 738.9/1440.24 = 0.513 → OK

However V_{Ed} is larger than the concrete contribution $V_{Rd,c}$. Theoretically this part may not be taken into account because the concrete capacity is exceeded. So only the contribution of steel fibres may be taken into account (this assumption will hold true during other design stages as well). Now for the unity check:

Unity Check = 738.9/1088.71 = 0.679→ OK
The shear capacity is more than enough to resist the design shear force, also if only $V_{Rd,f}$ is taken into account.

However it is possible that the concrete shows strain softening behaviour instead of strain hardening (Figure E-7). So it is necessary to verify if there is still enough shear capacity with a strain softening behaviour. It is assumed that the stress decreases linearly when ε_{ct} is reached. So σ(w=0.3) cannot be taken as 12 N/mm^2, as in the case of strain hardening. The new value is σ(w=0.3) = 7.25N/mm^2 (found by interpolation). If then the residual stress is calculated again and afterwards $V_{Rd,f}$, the new shear capacity (without the concrete part) becomes:
V_{Rd} = 830.24 kN and UC = 0.89.

The change from strain hardening to softening has a large influence on the shear capacity, more than for the moment capacity. The reduction is around 250 kN, which is quite a lot. But in spite of the large decrease, there is still enough capacity to resist the design shear force, as the unity check shows.

E.13.2 Torsion

There should be enough torsional resistance in the structure against working torsion moments:
$T_{Ed} \leq T_{Rd}$
If this is not the case reinforcement has to be applied. The torsion resistance can be determined with:
$T_{Rd} = f_{ctd,1} * t_{ef} * 2 * A_k$

Where
t_{ef} =A/u which is the effective wall thickness (in hollow sections upper limit is the real thickness) --> with A the total area of the cross section including hollow part and u as the circumference of area inside the centrelines:
t_{ef} = 0.6/3.2=0.1875 m.
The smallest real thickness is 0.13m so this will be taken for t_{ef}.

The result is: T_{Rd} = 5.33*0.13*2*0.391 = 542.6 kNm
Unity Check: T_{Ed}/T_{Rd} = 317.09/542.6 = 0.584 --> OK
The torsional moment resistance (without taking the effect of the fibres into account) is sufficient to resist the working torsional moments, so no torsional reinforcement needs to be applied.

E.13.3 Shear + torsion

It is also required that the combination of shear forces and torsional moments is verified. The structure should be able to resist these forces. The requirement for this states:
$T_{Ed}/T_{Rd,max} + V_{Ed}/V_{Rd,max} \leq 1.0$
The requirement means that the capacity of the concrete struts has to be sufficient to resist the loads on the structure. Here the two previous situations (shear governing or torsion governing) are going to be investigated as well.

First $T_{Rd,max}$ and $V_{Rd,max}$ have to be determined:
AFGC2013 paragrapgh 2.4 section 6.3.2(4): $T_{Rd,max} = 2*1.14*(\alpha_{cc}/\gamma_c)* f_{ck}^{2/3} *2A_k*t_{ef}*\sin\theta\cos\theta$
AFGC2013 paragrapgh 2.4 section 6.2(4): $V_{Rd,max} = 2*1.14*(\alpha_{cc}/\gamma_c)*b_w*z*f_{ck}^{2/3}/(\cot\theta+\tan\theta)$

θ=30°
t_{ef} =0.13m
$b_w = 2b_{web}$ = 0.28m
z = 0.9d = 0.481m
u_k= 3.2m

α_{cc} = 0.85
γ_c = 1.5
f_{ck} = 170 N/mm^2
A_k = 0.391

Filling everything in the equations gives:
$T_{Rd,mac}$ = 1747 kNm
$V_{Rd,max}$ = 2311 kNm

Unity check:
Situation 1: 317.09/1747 + 322.41/2311 = 0.321 →OK
Situation 2: 116.75/1747 + 671.02/2311 = 0.357 →OK
For both situations the concrete struts suffice.

E.13.4 Shear resistance according to Model Code

In the recent version of the fib Model Code for Concrete Structures (MC2010) the determination of the shear resistance (both V_{Rd} and $V_{Rd,max}$) is done in a different way than how it is described in the Eurocode. Also described is the determination of the shear resistance, when steel fibres are included in the concrete. It is wise to compare the results from the Model Code with the results from AFGC. Usually the Model Code is considered more reliable than a certain guideline such as the AFGC.

According to paragraph 7.7.3.2 of MC2010 the shear resistance is determined with:

$$V_{Rd,F} = \frac{1}{\gamma_F}\left(k_v\sqrt{f_{ck}} + k_f f_{Ftuk}\cot\theta\right) z * b_w$$

Where

$$k_v = \frac{0.4}{1 + 1500\varepsilon_x} * \frac{1300}{1000 + k_{dg} * z}$$

k_{dg} = 32/(16+d_g). If d_g <16mm (which is the case here) then k_{dg} = 1
The term k_v*√f_{ck} represents the contribution of the concrete and the term k_f*f_{Ftuk}*cotθ represents the contribution of the steel fibres.
k_f=0.8

f_{Ftuk} is the ultimate residual tensile strength(formula 5.6-6 in MC2010):
f_{Ftuk} = 0.45f_{R1} – (w_u/$CMOD_3$)(0.45f_{R1}-0.5f_{R3}+0.2f_{R1})
where f_{R1} and f_{R3} are determined with experiments. Since it is not possible to perform experiments it is safe to assumed that f_{Ftuk} = f_{ctk} if the concrete shows strain hardening behaviour.
The term for the steel fibres is pretty much the same as in AFGC (=$\sigma_{Rd,f}$/tanθ). Only the residual stresses are defined differently. The factor k_f=0.8 is already incorporated in $\sigma_{Rd,f}$ as 1/K = 1/1.25=0.8. Moreover if for $\sigma_{Rd,f}$ is assumed f_{ctk} than the result for the steel fibre contribution would be the same for AFGC and MC2010. The main difference lies in the concrete part.

*Note: In paragraph E.13.1 $\sigma_{Rd,f}$ is determined the way it is because f_{ctk} and σ(w=0.3) are both known values. However the terms necessary for determining f_{Ftuk} are not known and not possible to determine for this thesis. Therefore in the Model Code formula f_{Ftuk} = f_{ctk}. If in paragraph E.13.1 $\sigma_{Rd,f}$ would be set to [1/(K*γf)]*fctk then obivously $V_{Rd,f}$ would be lower and the results of both methods for the steel fibre part would be the same.*

ε_x is defined as (see also Figure E-9):

$$\varepsilon_x = \frac{\left(\frac{M_d}{z} + V_{Ed} + N_{Ed} * \frac{(z_p - e_p)}{z}\right)}{2 * \left(\frac{z_s}{z} E_s A_s + \frac{z_p}{z} E_p A_p\right)}$$

No steel reinforcement is used so A_s = 0 and z=z_p = 0.9*d
M_d = M_{Ed} + M_{Pd} = 1259.6 + $P_{m\infty}$*Δe = 1254 + 5375.05*(z_b – 0.5z+e_p) = 1274.1kNm
N_{Ed} = - $P_{m\infty}$ = - 5375.05 kN
V_{Ed} = 631.46 kN

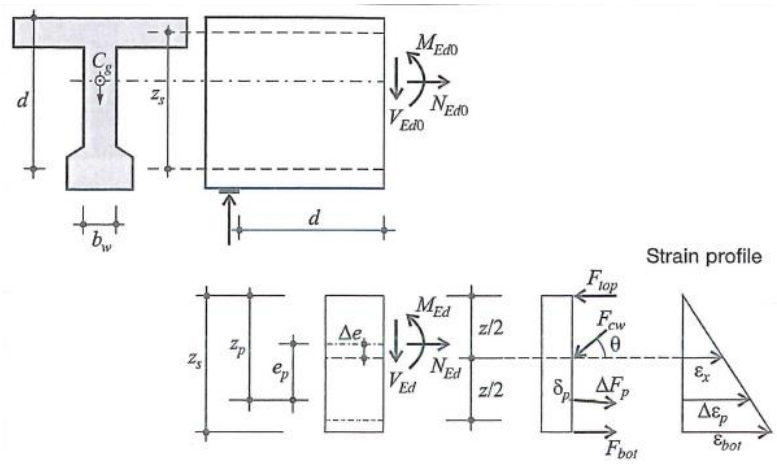

Figure E-9: Situation for determining ε_x

Filling all the unknown results in:
$\varepsilon_x = 0.349*10^{-3}$.
This results in $k_v = 0.231$
$\theta_{min} = 29° + 7000\varepsilon_x = 31.44$ => assumed is 32°
If assumed is $f_{Ftuk} = f_{ctk} = 8N/mm^2$ then the shear capacity becomes:

$V_{Rd,F} = 1188.93$ kN.

The total shear resistance according to AFGC was: $V_{Rd} = 1440.24$ kN (where $\theta=\theta_{min}=30°$)
The total value according to AFGC is higher because of the higher concrete part. If in MC2010 the fibre part would be left out then only the concrete part would remain then: $V_{Rd,c} = 269.74$ kN.
And AFGC: $V_{Rd,c} = 351.53$ kN. So around 70 kN higher. This is most likely due to the 'k' factor in AFGC which directly takes the compression force of prestressing into account.
However in paragraph E.13.1 it is assumed eventually that when $V_{Ed} > V_{Rd,c}$ then $V_{Rd} = V_{Rd,f} + V_{Rd,s}$ instead of $V_{Rd,c} + V_{Rd,f} + V_{Rd,s}$ (if additional shear reinforcemeent would be used).
In the Model Code however is stated that (if shear reinforcement would be used) $V_{Rd} = V_{Rd,F} + V_{Rd,s}$.
This means that:
MC2010 => $V_{Rd} = 1188.93$kN
AFGC => $V_{Rd} = 1088.71$ kN
So considering the assumptions made the model code would in this case provide a higher shear resistance than the AFGC. So the result from AFGC is on the safe side.

$V_{Rd,max}$ is calculated in a different way as well in MC2010. The maximum shear resistance is determined with (MC2010 formula 7.3-26):

$$V_{Rd,max} = k_c \frac{f_{ck}}{\gamma_c} b_w z * \sin\theta\cos\theta$$

Where
k_c is the strength reduction factor and defined as: $k_c = k_\varepsilon * \eta_{fc}$
η_{fc} $= (30/f_{ck})^{1/3} = 0.561$
k_ε $= 1/(1.2+55\varepsilon_1) = 0.622$ where $\varepsilon_1 = \varepsilon_x + (\varepsilon_x+0.002)\cot^2\theta = 0.0074$
So $k_c = 0.349$
With $\theta=32°$ and $\gamma_f = 1.5$

$V_{Rd,max} = 2393.496$ kN.
This value is close to the $V_{Rd,max}$ calculated according to AFGC (=2311 kN). The one from AFGC is slightly lower, because θ is taken 30 instead of 32. So AFGC gives a reliable result (if assumed is that the Model Code gives the most reliable result).

E.14 Transverse direction (moments)

E.14.1 Design transverse moment

Transverse moments also occur in the structure. It is necessary to validate if the box girder can resist these moments. Transverse prestressing strands, which are placed in the top flange, can benefit the transverse moment capacity. These strands are also necessary to connect all the box girders together in order for the bridge to have transverse action. Only the top flange can contribute to the transverse moment capacity, together with the joints.

Assumed is that a tendon of 7φ15.7 strands with quality Y1860H are used which are placed with a centre spacing of 1000 mm.

The governing section is in the joint: The joint is not made of UHPC and it has no other reinforcement in the concrete, except for the transverse prestressing. It has to be verified if the joint can resist the design transverse moment. Assumed is that the joint is made of C90/105. For box girders made out of normal or high strength concrete, a strength of C35/45 is used usually, but here it is chosen to make the joint out of high strength concrete, because the bridge itself is made out of UHPC. This way the difference in strength between box girder and joint will not be too high. The joint will have a thickness of 250 mm.

Expected is for the highest transverse moment to be located right around the middle of the bridge. The highest moment should be found for the combination, where the loads are placed to give the highest transverse moments. In SCIA the result for the transverse moment myD^- was 322.06 kNm. However this (quite large) moment is found near the corners of the bridge. This can be explained by the fact that SCIA calculates myD^- by stating: $myD^- = my + |mxy|$. As the results showed in paragraph E.7, mxy = 317.09 kNm. This results in a high myD^-, which occurs in the same area as the highest torsional moment mxy. But the problem is that SCIA does not link the torsional moments with the given orthotropic parameters. For a box girder the stiffness is much higher in the longitudinal direction than in the transverse direction. So this also means that mxy ≠ myx. Therefore a factor K should be applied based on the orthotropy of a box girder:

$K_x = 2*D_{xy}/(D_{xy}+D_{yx})$
$K_y = 2*D_{yx}/(D_{xy}+D_{yx})$
This has been done in the Mathcad sheet for determining the orthotropic parameters (paragraph E.6). The resulting factors are:
$K_x = 1.948$
$K_y = 0.052$

To calculate myD^- the following is used: $myD^- = my + K_y*mxy$. Finding m_y in the same node as where the highest mxy is and then applying the factor will lead to myD^- = 34.53 kNm. This is much lower than the given value of 322.06 kNm. If this procedure would be applied all over the structure one would find the highest myD^- in the middle of the bridge as expected. Here m_y is the largest and mxy is very low in value.
SCIA gives a value of myD^- = 113.68 kNm/m. This is the value that will be used for determining if the transverse moment capacity ($M_{Rd,y}$) is sufficient. The moment on the box girder becomes:
$M_{Ed,y} = myD^-*B_{centre,spacing}$=113.68 kNm. This is the global transverse moment. The global moment in the SLS state is: M_{SLS} =85.74 kNm.

Also necessary is to take into account the local transverse moment. For this Load Model 1 is turned into a single axle load where each wheel is 300 kN. To determine the local effect the transverse direction can be schematized as a continuous beam on multiple supports.

The schematization is seen in Figure E-10. The point loads are spread until the heart lines of the top flange and transformed into line loads. Each line load has a value of q_{wheel} = 300/ (2*0.080+2*0.150+0.4) = 348.84 kN/m.
In combination with the dead load (assumed 4.8kN/m) a governing moment is found: $M_{Ed,local}$ = 46.84 kNm and $M_{SLS,local}$ = 26.05 kNm.

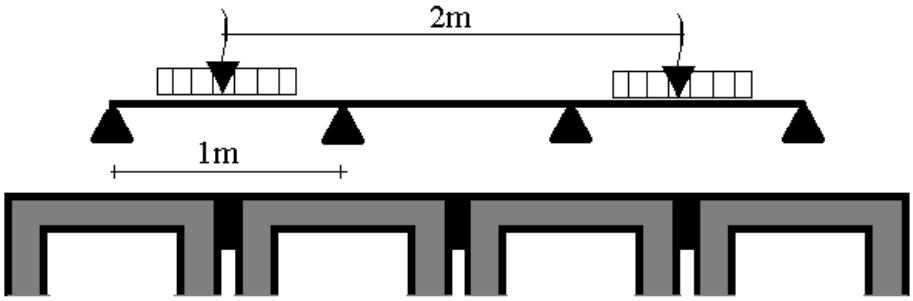

Figure E-10: Schematization for local effects

Because the placement of the axle loads for the local effects usually do not coincide with the placement of the axle loads for the global effects, the local effect may be reduced. A reduction of 25% is assumed. This results in a total transverse moment of:
ULS: $M_{Ed,tot}$ = 113.68 + 0.75*46.84 = 148.81 kNm
SLS: $M_{SLS,tot}$ = 85.74 + 0.75*34.73 = 111.79 kNm

The transverse capacity is determined where the following equilibrium needs to hold true:
$N_c = P_{m\infty}$

Where
$N_c = \alpha * B * f_{cd} * x$
$P_{m\infty} = A_p * \sigma_{pm0} * 0.85$
With f_{cd} = 60 MPa and α=0.5577 the compression height is: x= 37.21 mm

The moment capacity becomes: $M_{Rd,joint}$ = 140 kNm. UC=1.06
There is not enough enough capacity. Increasing the thickness of the joint to 270mm results in a moment capacity of $M_{Rd,joint}$ = 152.45 kNm and UC=0.976. Now there is enough capacity.

For joints it is also important that there are no tensile stresses at the height of the prestressing strands. At this location the joint has to remain in compression at all times. This holds true for the SLS state. The stresses in the joints are ($-P_{m\infty}/A_{c,joint} \pm M_{SLS,local}/W_{c,b,joint}$)
At top fibre: -13.81 N/mm^2
At bottom fibre: +4.59 N/mm^2
At height of strands: -4.61 N/mm^2
The stress at the height of the strands is negative so there is compression.
So there is just enough capacity to resist the transverse moments. At the location of the duct the concrete has to be thickened internally to be able to fit the anchor and for enough space for the duct itself.

E.15 Capacity check of hammerhead

Because most of the strands are located in the bottom flange, the gravity point of strands will fall outside the neutral axis and cause an eccentric moment at the hammerheads. Since the moment due to static loading is very low close to the support it is necessary to see if there is enough capacity to resists the eccentric moment caused by the strands. The governing location is there where the strands have reached their full force and that is at the end of the transition at a distance of l_{pt} from the supports. The check should be performed at time of construction (t=0), as variable loads are not yet presented here to slightly counter balance the eccentric moment. Already was found that indeed at this stage the moment at the end support is the highest.
This transmission length is calculated according to EN 1992-1-1 cl. 8.10.2.2 while taking into account the changes given in AFGC2013 paragraph 2.6 section 8.10.2:

f_{ctd} = 5.33 N/mm^2
f_{bpt} = f_{ctd}* η* η1*κ= 5.33*1.35*1*1.5 =7.56 N/mm^2
l_{pt} = α1* α1*ϕ_{strand}*σ_{pm0}/f_{bpt} = 532.91 mm
l_{pt1} = 0.4*l_{pt} = 213.16 mm
l_{pt2} = 1.2*l_{pt} = 639.5 mm

So for this calculation l_{pt} = 639.5 mm.

At l_{pt} the situation is as in Figure E-11 is presented. The compression zone is at the bottom side. The height of the compression zone has to be determined. Then the moment capacity can be calculated. For equilibrium of the internal forces the following equation stands: $P_{m0} + N_t = N_c + \Delta N_p$. The moment capacity $M_{Rd,head}$ should be higher than the design moment M_{Ed}.

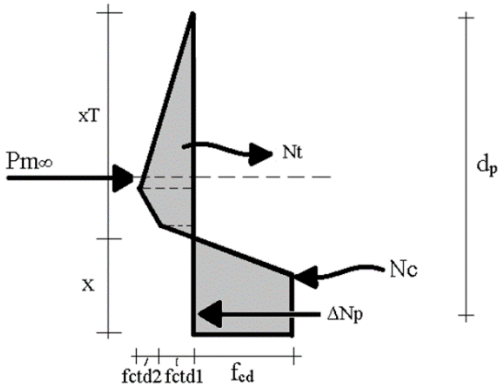

Figure E-11: Internal forces at hammerhead

The whole calculation including determining the design bending moment is done with a maple sheet that is shown in the following:

MAPLE SHEET: Capacity check hammerhead at lpt UHPC

$$restart:\ H := 600 : B := 1000 : L := 24000;$$

24000

$$htop := 160 :$$
$$hbot := 130 :$$
$$bweb := 2\cdot 140 :$$
$$Ac := H\cdot B - (H - htop - hbot)\cdot(B - bweb);\ qg := \frac{(H\cdot B\cdot 25\cdot 2000 + Ac\cdot 25\cdot(L - 2000))}{24\cdot 1000000000};$$
$$zb := H - \frac{1}{Ac}(H\cdot B\cdot 0.5\cdot H - ((H - htop - hbot)\cdot(B - bweb)\cdot(htop + 0.5\cdot(H - htop - hbot))));$$

376800

$$\frac{1977}{200}$$

308.8853503

$$E := 50000;\ \varepsilon c3 := 2.3\cdot 10^{-3} :\ \varepsilon cu3 := 2.6\cdot 10^{-3} :$$
$$lf := 13 :\ \varepsilon ct := \frac{fctd1}{E} :\ \varepsilon u03 := \frac{0.3}{\frac{2}{3}\cdot H} + \varepsilon ct :\ \varepsilon ctu := \frac{lf}{\frac{4\cdot 2}{3}\cdot H};$$

$$\frac{13}{1600}$$

$$fcd := 96.3333 :\ fctd1 := 5.33333 :\ fctd2 := 6.4 :$$

Data from excel:

$$lpt := 639.486 :$$
$$nstrands := 33 :$$
$$Apstr := 139 :$$
$$Ap := Apstr\cdot nstrands :$$
$$\sigma pm0 := 1395 :$$
$$Pm0 := Ap\cdot\sigma pm0 :$$

$$a := 8000 :\ e := 65.8 :\ n1 := 4 :\ n2 := 4 :\ f := zb - e;$$
$$\mathrm{Mg} := 1.2\cdot 0.5\cdot \mathrm{qg}\cdot lpt\cdot(L - lpt);$$

$8.860155816\ 10^{7}$

$$Pkink := (n1 + n2)\cdot Apstr\cdot\sigma pm0;$$

1551240

$$gravkink := (H - zb) - htop - 15.2\cdot 2;$$

100.7146497

$$fkink := f + gravkink;$$

343.8000000

$$ffict := \frac{(n1 + n2)\cdot fkink}{nstrands};$$

83.34545455

$$Pufict := \frac{Pm0 \cdot ffict}{a};$$

66664.53900

$$Mp := Pufict \cdot lpt + Pm0 \cdot (f - ffict);$$

$1.064785067\ 10^{9}$

$$Mpugt := 1.2 \cdot Mp;$$

$1.277742080\ 10^{9}$

$$MEd := \frac{(Mpugt - Mg)}{1000000};$$

1189.140522

Determination x

$$\alpha := \frac{((\varepsilon cu3 - \varepsilon c3) + 0.5 \cdot \varepsilon c3)}{\varepsilon cu3};$$

0.5576923077

$$\beta := \frac{1}{\varepsilon cu3}\left(\frac{1}{(\varepsilon cu3 - \varepsilon c3) + 0.5 \cdot \varepsilon c3}\left(\left(0.5 \cdot (\varepsilon cu3 - \varepsilon c3)^{2} + 0.5 \cdot \varepsilon c3 \cdot \left(\frac{\varepsilon c3}{3} + (\varepsilon cu3 - \varepsilon c3)\right)\right)\right)\right);$$

0.3373121133

$$Nc := \alpha \cdot B \cdot x \cdot fcd;$$

$53724.34039\ x$

$$xT := H - x :$$

$$xT1 := \frac{\varepsilon ct \cdot xT}{\varepsilon ctu} : Nt1 := 0.5 \cdot xT1 \cdot B \cdot fctd1 :$$

$$xT2 := \frac{(\varepsilon u03 - \varepsilon ct) \cdot xT}{\varepsilon ctu} : Nt2 := 0.5 \cdot B \cdot xT2 \cdot (fctd1 + fctd2) :$$

$$xT3 := \frac{(\varepsilon ctu - \varepsilon u03) \cdot xT}{\varepsilon ctu} : Nt3 := 0.5 \cdot B \cdot xT3 \cdot fctd2 :$$

$$Nt := Nt1 + Nt2 + Nt3;$$

$$\sigma pu := 1606.36363 : \Delta Np := Ap \cdot (\sigma pu - \sigma pm0);$$

$9.695249708\ 10^{5}$

$$eq := Nc + \Delta Np = Nt + Pm0$$

$53724.34039\ x + 9.695249708\ 10^{5} = 8.462356180\ 10^{6} - 3439.151964\ x$

$$x := solve(eq, x);$$

131.0772121

$$armt1 := x(1 - \beta) + \frac{2 \cdot xT1}{3} : armt2 := xT1 + x(1 - \beta) + \frac{xT2}{3} \cdot \frac{(2 \cdot fctd1 + fctd2)}{fctd1 + fctd2} : armt3 := xT1 + xT2 + x(1 - \beta) + \frac{xT3}{3} :$$

$$MRd := \frac{1}{10^6}\left(Nt1\cdot armt1 + Nt2\cdot armt2 + Nt3\cdot armt3 + Pm0\cdot\left(zb - \beta \cdot x\right) + \Delta Np\cdot\left(\beta\cdot x - e\right)\right);$$

2145.079029

$MEd;$

1189.140522

$$UC := \frac{MEd}{MRd};$$

0.5543574413

END MAPLE SHEET

The maple sheet result in a design bending moment of:
M_{Ed} = 1189.14 kNm
The moment capacity is:
M_{Rd} = 2145.08 kNm

Unity Check: M_{Ed}/M_{Rd} = 1189/2145 = 0.554→ OK

E.16 Detailing

The pretress force in pre-tensioned steel is introduced by bonding. There is a certain transmission length (here l_{pt} = 532.91mm) where after the prestress force is fully transferred. Inside the transmission length the bond stresses can cause tensile stresses. In pre-tensioned steel three types of tensile stresses can occur (Figure E-12):

- Bursting stresses
- Splitting stresses
- Spalling stresses

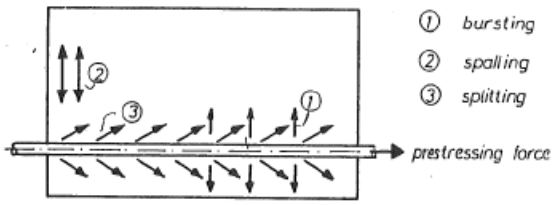

Figure E-12: Types of tensile stresses

The bursting and splitting stresses are prevented if the cover and distance between strands is at least 2φ. That is the case here so these two types of stresses are prevented. To determine the spalling stresses a graphical method by Den Uijl[2] can be used (Figure E-13).

[2] **Walraven, J.C.**, Braam, C.R. (2012) *"Reader prestressed concrete"*, Delft University of Technology

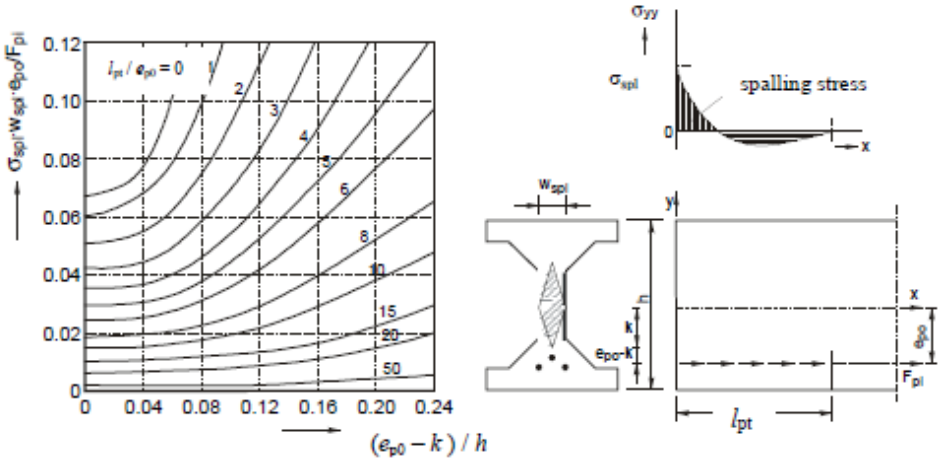

Figure E-13: Graphical method by Den Uijl for determining the spalling stresses

Starting from (e_{p0} - k) / h and l_{pt} / e_{p0} the value for $\sigma_{spl} \cdot w_{spl} \cdot e_{p0} / F_{pi}$ can be read from the diagram. After substitution of the known values for w_{spl}, e_{p0} and F_{pi}, the spalling stress σ_{spl} is obtained.
The values are:
L_{pt} = 532.1 mm. This means that the transfer of forces is completely in the hammerhead, which is a solid section.

e_{p0} =	f - f_{fict} = 160 mm
k =	W_b/A_c = 138.6 mm
h =	600mm
$(e_{p0}-k)/h$ =	0.0355
L_{pt}/e_{p0} =	3.33

With these values it can be read that $\sigma_{spl} \cdot w_{spl} \cdot e_{p0} / F_{pi}$ = 0.042
W_{spl} = B = 1000mm (hammerhead)
F_{pi} = P_{m0} = 6398.87 kN
Filling everything in leads to:
σ_{spl} = 1.68 N/mm^2
The spalling stress is lower than the tensile strength (lower than both f_{ctd} and f_{ctk}), so no spalling reinforcement is needed in the structure.

E.17 Crack width verification

In order for a structure not to be verified for crack width, it is necessary that the maximum moments in SLS (M_{max}) do not exceed the cracking moment (M_{cr}). And it is also necessary that the tensile strength of the concrete is not exceeded anywhere in the structure. The maximum moment M_{max} can be determined by using Table E-3 and by using the value determined for the moment due to the prestressing force M_p. Only the frequent factor ψ1 has to be applied for the variable loads (is 0.8 for UDL, TS and pedestrian load). M_{max} becomes:
$M_{max} = M_g + M_q – M_p$ = 1020.5+0.8*1027.9-1306.6 = 536.3 kNm

The cracking moment M_{cr} is determined with:
$M_{cr} = W_b*(f_{ctm} + P_{m\infty}/A_c)$. For f_{ctm} is taken f_{ctk} instead. With $P_{m\infty}/A_c$ = 14.26 N/mm^2:
M_{cr} = 0.052*(8.0+14.26)*10^3 = 1162.86 kNm.

Unity Check: M_{max}/M_{cr} = 536.3/1162.9 = 0.447→OK

The maximum moments in the SLS do not exceed the cracking moment.

Now the stresses in the structure in the SLS have to be checked. This is done with the same expressions used to determine the amount of strands:

t = 0 at top fibre: $\sigma_c = -\frac{P_{m0}}{A_c} + \frac{M_{p,0}}{W_{ct}} - \frac{M_g}{W_{ct}}$: σ_c = -1.76 N/mm^2

t = 0 at bottom fibre: $\sigma_c = -\frac{P_{m0}}{A_c} - \frac{M_{p,0}}{W_{cb}} + \frac{M_g}{W_{cb}}$: σ_c = -33.14 N/mm^2

t = ∞ at bottom fibre: $\sigma_c = -\frac{P_{m\infty}}{A_c} - \frac{M_{p,\infty}}{W_{cb}} + \frac{M_g + \psi 1 * M_q}{W_{cb}}$: σ_c = -4.0 N/mm^2

The structure is in all three situations completely under compression. So crack formation is not possible. These results are expected, since the prestressing is determined with assuming a fully prestressed beam.

The cracking moment is not exceeded and no tensile stresses occur at the construction and user stage in the SLS. Furthermore the bridge is simply supported so imposed deformations are not restricted, which means that unexpected tensile stresses will not occur. So crack width verification is not necessary in this case.

E.18 Deflection

It is important for the structure that the deformations caused by the working loadings during service life are within acceptable limits. When determining the deformations it is important to distinguish the deformation in a cracked and uncracked section, because this has a big influence on the deflections (in the shape of a greatly reduced stiffness). In the case of the Leiden Bridge there are no cracked sections as already was concluded in paragraph E.17. So the structure is considered to be uncracked everywhere. The governing cross section is right in the middle of the beam, since here the highest deformations will occur, caused by the combination of the highest moments.

The occurring deflections have to satisfy a couple of limits given in NEN-EN-1992-1-1 in chapter 7:

- The camber may not exceed L/250 = -96 mm (L = 24000 mm)
- The sag may not exceed L/250 during serviceability = 96 mm
- If a chance exists of damaging adjacent parts then the sag may not exceed L/500 = 48mm

The camber is caused by prestressing. The sag should be limited to L/500, because underneath the bridge there is an unused intermediate pier.
Three load combinations will be investigated:

1. t=0; fabrication and erecting structure; self-weight + prestressing: $q_{self} - q_{pm0}$
2. t=0; after placing asphalt and such; Dead load + prestressing: $q_{self} + q_{dead} - q_{pm0}$
3. t=∞; user stage; All loads as quasi permanent combination: $q_{self} + q_{dead} + \psi_2 * q_{var} - q_{pm\infty}$

The Eurocode states that for traffic loads the following quasi-permanent factors ψ_2 have to be used:

- UDL: ψ_2 =0.4
- Tandem system: ψ_2=0.4
- Pedestrians: ψ_2=0.4

The deflection in the middle of the span is determined with: $w = \frac{5 * q * L^4}{384 * E_{c,eff} * Ic}$

$E_{c,eff} = E_{cm}/(1+\phi(\infty,t0))$ with $\phi(\infty,t0)$ being the creep coefficient.
The deflections when $\phi(\infty,t0)$= 0.4 (type I heat treatment) and $\phi(\infty,t0)$ = 0.8 (no heat treatment) will be investigated. This gives $E_{c,eff}$ = 35714.29N/mm^2 and $E_{c,eff}$ = 27777.78 N/mm^2 respectively.
The case when no heat treatment is used is the governing one. The values of the loads are:

q_{self} = 9.89 kN/m
q_{dead} = 4.29 kN/m
q_{pm0} = 21.6 kN/m
$q_{pm\infty}$ = 18.15 kN/m
$\psi * q_{var}$ = 5.71 kN/m

The prestress force is assumed as a line load to simplify the calculation. This will slightly reduce the upward deflection due to the prestressing. Using these values in the three combinations and then filling q in the formula for w will results in (Table E-5):

Table E-5: Results deflection

	With $E_{c,eff1}$	With $E_{c,eff2}$	Limit
Combination 1: w [mm]	-87,87	-112,97	-96,0
Combination 2: w [mm]	-55,71	-71,62	-96,0
Combination 3: w [mm]	13.03	16.75	-48,0

The results in Table E-5 show that the occurring deflections satisfy the limits. Only the camber is too high in combination 1 when no heat treatment is applied ($E_{c,eff2}$). This means that in terms of deflection the prestressing force is too high. But the first situation (self-weight and prestressing force) is a situation that mostly occurs in the factory. In the factory this issue can easily be monitored and fixed. The camber limit is used when formwork is used during construction. But because prefabricated beams are used, there will be no formwork. So the - higher than the limit - deflection will not cause major issues. Eventually the beams are erected and connected and then the hardening layers are placed. Now combination 2 occurs and here the deflections are lower than the limit.

E.19 Vibration

The vibrations occurring on the structure may not cause discomfort during serviceability. This can be checked by determining the natural frequency of the structure. The natural frequency has to suffice according to the demands given by the Eurocode.
The natural frequency for the first (and governing) node is determined with:

$$n0 = \frac{C}{2\pi} * \sqrt{\frac{E_{cm} * I_c}{A_c * \rho_c * L^4}} \quad [Hz]$$

With C being the constraint factor (= 9.87 = π^2 for simply supported structures).
If all variables are filled in the formula then n0 = 2.52Hz

The Leiden Bridge is used both by traffic, trams and pedestrians. So the vibrations caused by each should be considered.

Pedestrians
The NEN-EN-1991-2 states for pedestrian bridges that the natural frequency should at least be 5 Hz. Furthermore it states that frequencies caused by pedestrians fall between 1 and 3 Hz.
The determined natural frequency is lower than 5 Hz and it falls in the range of the pedestrian frequencies. So there would be a chance that pedestrians could cause a frequency equal to n0, which could lead to resonance and discomfort. However the natural frequency is actually determined for a single beam. Combining all the beams together will result in a higher mass, which means that the frequency from the pedestrians will hardly have any effect on the actual bridge. So a dynamical analysis is not required to precisely determine the frequencies exerted by pedestrians. This would not be the case if considered was a pedestrian bridge. These are usually smaller in size and lighter than traffic bridges and a lot more susceptible to vibrations. This was the case with the bridge projects that were discussed in the literature study. A lot of these bridges were pedestrian bridges and almost all required dampers to limit the vibrations caused by pedestrians. But this is not the case for the Leiden Bridge so no further attention is necessary here.

Trams
For vibrations caused by trams specifically there is nothing stated in the Eurocode. However the Eurocode gives guidelines for vibrations caused by trains so these could be used to give an estimation of the vibrations caused by trams. In figure 6.9 NEN-EN-1992-2 a flowchart is given to determine if a dynamical requirement is necessary:

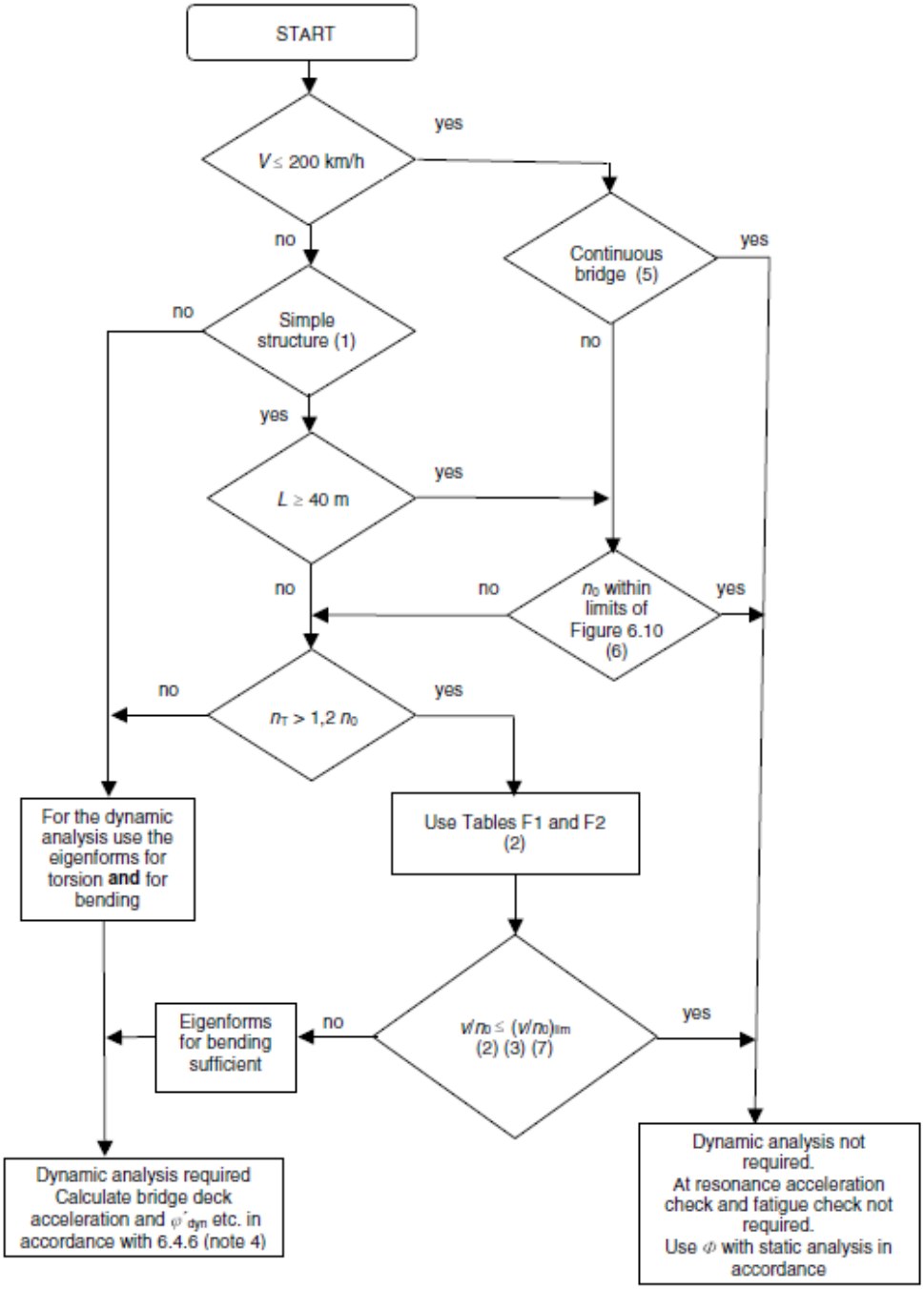

Figure 6.9 - Flow chart for determining whether a dynamic analysis is required

GVB (Amsterdam Public Transport) state that the tram has a maximum speed of 70km/h. The bridge is not continuous. Figure 6.10 in the NEN-EN-1992-2 gives the upper and lower limits of the natural frequency with the length L=24m:

$n_{0,min} = 94.76*L^{-0.748} = 8.8$ Hz

$n_{0,max} = 23.58*L^{-0.592} = 3.6$ Hz

The upper limit of n_0 is governed by dynamic enhancements due to track irregularities and is given by :

$n_0 = 94{,}76L^{-0{,}748}$ (6.1)

The lower limit of n_0 is governed by dynamic impact criteria and is given by :

$n_0 = 80/L$
for $4\text{m} \le L \le 20\text{m}$
$n_0 = 23{,}58L^{-0{,}592}$
for $20\text{m} < L \le 100\text{m}$ (6.2)

where:

n_0 is the first natural frequency of the bridge taking account of mass due to permanent actions,
L is the span length for simply supported bridges or L_e for other bridge types.

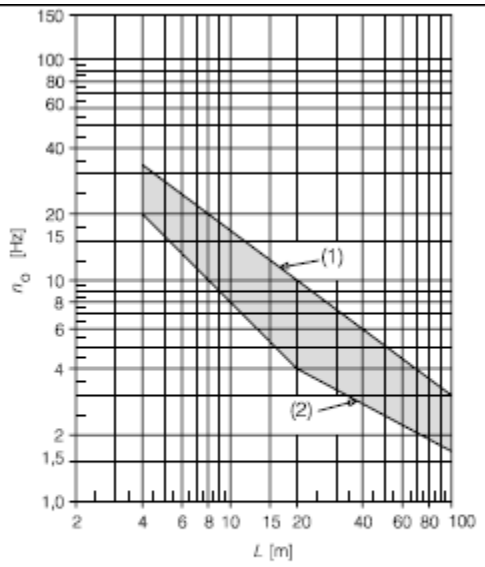

Key
(1) Upper limit of natural frequency
(2) Lower limit of natural frequency

Figure 6.10 - Limits of bridge natural frequency n_0 [Hz] as a function of L [m]

The natural frequency of the bridge (2.52 Hz) falls outside these limits, being lower than the minimum required frequency.

The natural torsional frequency n_T for a simply supported beam is determined with:

$$nT = \frac{\pi}{2\pi} * \sqrt{\frac{G*I_t}{I_p*\rho_c*L^2}}\ \text{Hz}$$

Where
G = E/(2(1+v) = 21740 MPa
I_t = torsional constant = 0.043m^4
I_p = Polar area of moment = I_z +I_y = 0.56 m^4

Filling the variables in the expression gives: nT = 53.7 Hz. This is higher than 1.2*n0.

Final step in the flow chart is to determine if v/n0 < $(v/n0)_{lim}$. In NEN-EN-1991-2 table F.1 the limits are given for v/n0, with v being the speed of the train (in this case tram). Assumed is that the acceleration of the tram is lower than 3.5m/s^2. The speed of the tram is 70/3.6 = 19.44 m/s. The bridge has a length of 24m. The mass of the total bridge is 30*A_c *ρ_c = 28.26*10^3 kg/m. This results in a $(v/n0)_{lim}$ of 13.96 m. The occurring v/n0 is 19.44/2.52 = 7.7, which is below the limit.

Table F.1 - Maximum value of $(v/n_0)_{lim}$ for a simply supported beam or slab and a maximum permitted acceleration of a_{max}< 3.50m/s^2.

Mass m 10^3 kg/m		≥5,0 <7,0	≥7,0 <9,0	≥9,0 <10,0	≥10,0 <13,0	≥13,0 <15,0	≥15,0 <18,0	≥18,0 <20,0	≥20,0 <25,0	≥25,0 <30,0	≥30,0 <40,0	≥40,0 <50,0	≥50,0 -
Span $L\in$ m [a]	ζ %	v/n_0 m	v/n_0 m	v/n_0 m	v/n_0 m	v/n_0 m	v/n_0 m	v/n_0 m	v/n_0 m	v/n_0 m	v/n_0 m	v/n_0 m	v/n_0 m
[5,00,7,50)	2	1,71	1,78	1,88	1,88	1,93	1,93	2,13	2,13	3,08	3,08	3,54	3,59
	4	1,71	1,83	1,93	1,93	2,13	2,24	3,03	3,08	3,38	3,54	4,31	4,31
[7,50,10,0)	2	1,94	2,08	2,64	2,64	2,77	2,77	3,06	5,00	5,14	5,20	5,35	5,42
	4	2,15	2,64	2,77	2,98	4,93	5,00	5,14	5,21	5,35	5,62	6,39	6,53
[10,0,12,5)	1	2,40	2,50	2,50	2,50	2,71	6,15	6,25	6,36	6,36	6,45	6,45	6,57
	2	2,50	2,71	2,71	5,83	6,15	6,25	6,36	6,36	6,45	6,45	7,19	7,29
[12,5,15,0)	1	2,50	2,50	3,58	3,58	5,24	5,24	5,36	5,36	7,86	9,14	9,14	9,14
	2	3,45	5,12	5,24	5,24	5,36	5,36	7,86	8,22	9,53	9,76	10,36	10,48
[15,0,17,5)	1	3,00	5,33	5,33	5,33	6,33	6,33	6,50	6,50	6,50	7,80	7,80	7,80
	2	5,33	5,33	6,33	6,33	6,50	6,50	10,17	10,33	10,33	10,50	10,67	12,40
[17,5,20,0)	1	3,50	6,33	6,33	6,33	6,50	6,50	7,17	7,17	10,67	12,80	12,80	12,80
[20,0,25,0)	1	5,21	5,21	5,42	7,08	7,50	7,50	13,54	13,54	13,96	14,17	14,38	14,38
[25,0,30,0)	1	6,25	6,46	6,46	10,21	10,21	10,21	10,63	10,63	12,75	12,75	12,75	12,75
[30,0,40,0)	1				10,56	18,33	18,33	18,61	18,61	18,89	19,17	19,17	19,17
≥40,0	1				14,73	15,00	15,56	15,56	15,83	18,33	18,33	18,33	18,33

[a] $L \in [a,b)$ means $a \le L < b$

NOTE 1 Table F.1 includes a safety factor of 1.2 on $(v/n_0)_{lim}$ for acceleration, deflection and strength criteria and a safety factor of 1,0 on the $(v/n_0)_{lim}$ for fatigue.

NOTE 2 Table F.1 includes an allowance of $(1+\varphi''/2)$ for track irregularities.

According to the flowchart there is no dynamical analysis needed concerning the vibrations caused by the tram.

E.20 Fatigue

The bridge is susceptible to cyclic loads coming from trams and traffic. In the demands for the new design it is given that there are 30 tram movements per track per hour over the bridge. That is equal to 788400 movements per year in total. Furthermore the bridge is assumed to be part of a main road with a low amount of heavy traffic. This means according to NEN-EN-1991-2 table 4.5 that there are $0.125*10^6$ vehicles per lane per year. So for a total of 100 years and 7 fictional lanes, this results in $87.5*10^6$ vehicles. So traffic is governing for the fatigue design.

In NEN-EN 1992-1 and NEN-EN 1992-2 it is described how to determine if a structure is safe concerning fatigue for both the concrete and prestressing steel. The procedures described there will be applied for Load Model 1. The fatigue resistance of both the concrete and prestressing steel will be determined separately.

E.20.1 Fatigue resistance concrete

The fatigue resistance of the concrete is checked at the mid span in both the top and bottom fibre of the cross section. To verify the fatigue resistance of concrete, cl. 6.8.7 of the Dutch National Annex of NEN-EN-1992-2 is used. This section state that the following expression must hold true:

$$N_i = 10^{\left[\frac{6}{1-0.57*k1*\left(1-\frac{f_{ck}}{250}\right)}*\frac{1-E_{cd,max,i}}{\sqrt{1-R_i}}\right]} > 10^6$$

Where:

$$R_{equ} = \frac{E_{cd,min,i}}{E_{cd,max,i}};\quad E_{cd,min,i} = \frac{\sigma_{cd,min,i}}{f_{cd} * (0.9 + \frac{logN_i}{60})};\quad E_{cd,max,i} = \frac{\sigma_{cd,max,i}}{f_{cd} * (0.9 + \frac{logN_i}{60})}$$

$\sigma_{cd,min,i}$ and $\sigma_{cd,max,i}$ are the lower and upper stresses of the damage equivalent stress spectrum with a number of cycles $N=10^6$. These are determined by using the following load combination:
For $\sigma_{c,max}$: $(\sum G_{k,j} + P + \psi_{1,1}Q_{k,1} + \psi_{2,j}Q_{k,j}) + Q_{fat}$
For $\sigma_{c,min}$: $(\sum G_{k,j} + P + \psi_{1,1}Q_{k,1} + \psi_{2,j}Q_{k,j})$
Q_{fat} is the fatigue load. In the governing situation traffic load model LM1 (when only vehicles are present) is the fatigue load. So the minimum and maximum stresses are determined when Q_{fat} is present and absent. For the fatigue calculation where LM1 is taken into account it is necessary according to NEN-EN 1991-2 cl. 4.6.2 to reduce the UDL with a factor 0.3 and the TS with a factor 0.7. The next and only other variable load is the pedestrian load so this one serves as $Q_{k,1}$

So the maximum minimum and permanent stresses are determined by:

$$t = \infty \text{ at top fibre: } \sigma_{c,max,equ} = -\frac{P_{m\infty}}{A_c} + \frac{M_{p,\infty}}{W_{ct}} - \frac{(M_{perm} + \psi_1 M_{peds} + M_{LM1,red})}{W_{ct}}$$

$$t = \infty \text{ at top fibre : } \sigma_{c,min,equ} = -\frac{P_{m\infty}}{A_c} + \frac{M_{p,\infty}}{W_{ct}} - \frac{(M_{perm} + \psi_1 M_{peds})}{W_{ct}}$$

$$t = \infty \text{ at bottom fibre: } \sigma_{c,max,equ} = -\frac{P_{m\infty}}{A_c} - \frac{M_{p,\infty}}{W_{cb}} + \frac{(M_{perm} + \psi_1 M_{peds} + M_{LM1,red})}{W_{cb}}$$

$$t = \infty \text{ at bottom fibre: } \sigma_{c,min,equ} = -\frac{P_{m\infty}}{A_c} - \frac{M_{p,\infty}}{W_{cb}} + \frac{(M_{perm} + \psi_1 M_{peds})}{W_{cb}}$$

The resulting stresses are (in N/mm^2):

	Top fibre	Bottom fibre
$\sigma_{cd,max,equ}$:	-14,290	-23,037
$\sigma_{cd,min,equ}$:	-5,998	-14,239

The absolute values of the stresses will be used in further calculations.
For $f_{cd,fat}$ (fatigue design strength) a different expression than the one given in the Eurocode has to be used, because the current one underestimates the fatigue design strength for UHPC too much. In the Betonkalender[3] a new expression is given for this variable:

$$f_{cd,fat} = 0.85 * \beta_{cc}(t) * \frac{f_{ck}}{\gamma_c} * (1 - \frac{f_{ck}}{40 * f_{ck0}})$$

With f_{ck0} 10 MPa and $\beta_{cc}(t) = \exp\left\{s\left[1 - \left(\frac{28}{t}\right)^{0.5}\right]\right\} = 1 \text{ for } t = 28$

The difference with the one in the Eurocode is the factor 40, which is originally 25. With the new expression $f_{cd,fat}$ = 55.4 N/mm^2. With the current expression $f_{cd,fat}$ would be 26.2 N/mm^2, which is a large underestimation, compared with $f_{cd,fat}$ = 55.4 N/mm^2. The reason this is noted is because in the formula for N_i the term 1-f_{ck}/250 is now wrong and should be 1-f_{ck}/400 in the case of UHPC.

	Top fibre	Bottom fibre
$\sigma_{cd,maxi}$	14,290	23,037
$\sigma_{cd,min,i}$	5,998	14,239
$E_{cd,max,i}$	0.149	0,239
$E_{cd,min,i}$	0,063	0,148
$R_{c,i}$	0,422	0,618

For the top fibre: $N_i = 9.53 * 10^9 > 10^6$
For the bottom fibre: $N_i = 9.75 * 10^{10} > 10^6$
Both the top and bottom fibre in the mid span have enough fatigue resistance.

[3] Fehling, E., Schmidt, M., Walraven, J.C., Leutbecher, T. & Fröhlich, S. (2014) "Betonkalender – Ultra-High Performance Concrete UHPC", Ernst & Sohn, Germany

E.20.2 Fatigue resistance prestressing steel

For the prestressing steel according to cl. 6.8.5 in NEN-EN-1992-1 it must hold true that:

$$\gamma_{F,fat} * \Delta\sigma_{S,equ}(N^*) \leq \frac{\Delta\sigma_{Risk}(N^*)}{\gamma_{s,fat}}$$

Where
$\Delta\sigma_{Risk}(N^*)$ is the stress range at N* cycles from the appropriate S-N curves given in figure 6.30 in NEN-EN-1992-1-1:

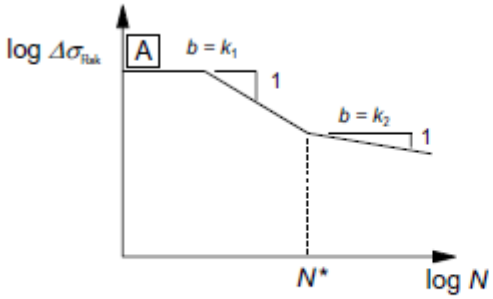

Figure 6.30: Shape of the characteristic fatigue strength curve (S-N-curves for reinforcing and prestressing steel)

For pre-tensioned steel:

$N^*=10^6$
k1=5
k2=9
$\Delta\sigma_{Risk}(N^*)$ = 185 MPa
$\Delta\sigma_{S,equ}(N^*)$ is the damage equivalent stress range for the steel considering N*.

Also allowed is to use a simpler approach by verifying (according to cl. 6.8.6 in NEN-EN-1992-1) that the stress range $\Delta\sigma_s$ should be lower than value k1, which is taken as 70 N/mm^2. If this holds true the verification stated earlier is not necessary to perform.
To determine $\Delta\sigma_s$ the maximum and minimum stress determined in paragraph E.20.1 are used to find the stress $\Delta\sigma_{c,p}$ at the height of the prestressing. This concrete stress is then transformed in a steel stress by: $\Delta\sigma_s = \Delta\sigma_{c,p}*(E_p/E_c)$.

The absolute concrete stresses with and without the presence of LM1 are:

	Top fibre	Bottom fibre
$\sigma_{cd,max}$ (with LM1):	14,290	23,037
$\sigma_{cd,min}$ (without LM1):	5,998	14,239

This results in:
$\sigma_{c,p,max}$ = (23.037-14.29)*(H-e)/H + 14.29 = 22.08 N/mm^2
$\sigma_{c,p,min}$ = (14.239-5.998)*(H-e)/H + 5.998 = 13.335 N/mm^2

The stress difference $\Delta\sigma_{c,p}$ = 22.08-13.335 = 8.743N/mm^2
This results in a steel stress range of:
$\Delta\sigma_s$ = 8.743*195000/50000 = 34.1 N/mm^2 which is well below 70 N/mm^2 (UC=0.487)
So the fatigue resistance of the prestesssing steel meets the requirements. Additional verifications are not necessary.

E.20.3 Conclusion fatigue

Both the concrete and the prestressing steel have enough fatigue resistance to resist the variable cyclic loads that occur on the bridge. For concrete it was necessary to apply the newly developed formula for the fatigue design strength $f_{cd,fat}$. Otherwise the concrete fatigue resistance wouldn't be enough, due to underestimation of $f_{cd,fat}$.

E.21 Summary

Amount of strands:	33ϕ15.2 strands	
Total losses in strands:	If type I heat treatment: 12.2% If no heat treatment:16%	
Slenderness ratio, λ	40	
ULS		
Bending moment capacity, M_{Rd}:	M_{Rd} = 2358.5 kNm	UC = 0.534
Rotational capacity: x_u/d	x_u/d = 0.365	UC = 0.734
Shear capacity V_{Rd}:	V_{Rd} = 1088.71 kNm	UC = 0.679
Torsional capacity T_{Rd}:	T_{Rd} = 542.6 kNm	UC = 0.584
Transverse moment capacity: $M_{Rd,joint:}$	$M_{Rd,joint}$ = 148.815 kNm	UC = 0.976
Capacity concrete at hammerhead:	$M_{Rd,head}$ = 2145.75 kNm	UC = 0.555
SLS		
Crack width verification:	M_{CR} = 1162.86	UC= 0.44
Deflection:	w2= 71mm < L/250	
	w3 = 15mm < L/500	
Vibrations:	n0 = 2.52Hz < 5 Hz (should be higher)	
	$v/n0 = 7.66 < (v/n0)_{lim}$	
Fatigue:	Concrete: Top fibre:	UC = 0.440
	Bottom fibre:	UC = 0.453
	Prestressing:	UC = 0.487

SCIA ENGINEERING REPORT C170/200

1. Project

Licence name	IBA
Project	Leidsebrug
Part	C170/200
Description	-
Author	Antonio Paskvalin
Date	16. 09. 2014
Structure	General XYZ
No. of nodes :	68
No. of beams :	0
No. of slabs :	1
No. of solids :	0
No. of used profiles :	0
No. of load cases :	207
No. of used materials :	2
Acceleration of gravity [m/s^2]	9,810
National code	EC - EN

2. Table of contents

3. Materials

Concrete EC2

Name	Type	Unit mass [kg/m^3]	E mod [MPa]	Poisson - nu	Thermal exp [m/mK]	Characteristic compressive cylinder strength fck(28) [MPa]
C90/105	Concrete	2500,0	4,3600e+04	0.2	0,00	90,00
C170/200	Concrete	2500,0	5,0000e+04	0.15	0,00	170,00

4. Orthotropy

OT1	
Type of orthotropy	Standard

Thickness of Plate/Wall [mm]	160
Material	C170/200
D11 [MNm]	8,0660e+02
D22 [MNm]	6,6640e+01
D12 [MNm]	3,4780e+01
D33 [MNm]	4,4260e+02
D44 [MN/m]	2,2700e+03
D55 [MN/m]	3,6520e+03
d11 [MN/m]	8,1841e+03
d22 [MN/m]	8,1841e+03
d12 [MN/m]	1,2276e+03
d33 [MN/m]	3,4783e+03
K xy [MN/m]	1,0000e+00
K yx [MN/m]	1,0000e+00

5. Nodes

Name	Coord X [m]	Coord Y [m]	Coord Z [m]
K1	0,000	0,000	0,000
K2	24,000	0,000	0,000
K67	0,000	4,093	0,000
K68	24,000	4,093	0,000
K43	0,000	0,500	0,000
K45	0,000	2,500	0,000
K46	0,000	3,500	0,000
K47	0,000	4,500	0,000
K48	0,000	5,500	0,000
K49	0,000	6,500	0,000
K50	0,000	7,500	0,000
K51	0,000	8,500	0,000
K52	0,000	9,500	0,000
K53	0,000	10,500	0,000
K54	0,000	11,500	0,000
K55	0,000	12,500	0,000
K56	0,000	13,500	0,000
K57	0,000	14,500	0,000
K58	0,000	15,500	0,000
K59	0,000	16,500	0,000
K60	0,000	17,500	0,000
K61	0,000	18,500	0,000
K69	0,000	19,500	0,000

Name	Coord X [m]	Coord Y [m]	Coord Z [m]
K70	24,000	0,500	0,000
K71	24,000	1,500	0,000
K72	24,000	2,500	0,000
K73	24,000	3,500	0,000
K74	24,000	4,500	0,000
K75	24,000	5,500	0,000
K76	24,000	6,500	0,000
K77	24,000	7,500	0,000
K78	24,000	8,500	0,000
K79	24,000	9,500	0,000
K80	24,000	10,500	0,000
K81	24,000	11,500	0,000
K82	24,000	12,500	0,000
K83	24,000	13,500	0,000
K84	24,000	14,500	0,000
K85	24,000	15,500	0,000
K86	24,000	16,500	0,000
K87	24,000	17,500	0,000
K88	24,000	18,500	0,000
K89	24,000	19,500	0,000
K44	0,000	1,500	0,000
K90	24,000	30,000	0,000
K91	0,000	30,000	0,000

Name	Coord X [m]	Coord Y [m]	Coord Z [m]
K92	0,000	20,500	0,000
K93	0,000	21,500	0,000
K94	0,000	22,500	0,000
K95	0,000	23,500	0,000
K96	0,000	24,500	0,000
K97	0,000	25,500	0,000
K98	0,000	26,500	0,000
K99	0,000	27,500	0,000
K100	0,000	28,500	0,000
K101	0,000	29,500	0,000
K102	24,000	20,500	0,000
K103	24,000	21,500	0,000
K104	24,000	22,500	0,000
K105	24,000	23,500	0,000
K106	24,000	24,500	0,000
K107	24,000	25,500	0,000
K108	24,000	26,500	0,000
K109	24,000	27,500	0,000
K110	24,000	28,500	0,000
K111	24,000	29,500	0,000
K112	0,000	10,570	0,000
K113	24,000	10,570	0,000

6. 2D members

Name	Layer	Type	Analysis model	Material	Thickness type	Th. [mm]
E1	Laag1	plate (90)	Standard	C170/200		160

7. Nodal supports

Name	Node	System	Type	X	Y	Z	Rx	Ry	Rz
Sn22	K43	GCS	Standard	Free	Free	Rigid	Free	Free	Free
Sn23	K45	GCS	Standard	Free	Free	Rigid	Free	Free	Free
Sn24	K46	GCS	Standard	Free	Free	Rigid	Free	Free	Free
Sn25	K47	GCS	Standard	Free	Free	Rigid	Free	Free	Free
Sn26	K48	GCS	Standard	Free	Free	Rigid	Free	Free	Free
Sn27	K49	GCS	Standard	Free	Free	Rigid	Free	Free	Free
Sn28	K50	GCS	Standard	Free	Free	Rigid	Free	Free	Free
Sn29	K51	GCS	Standard	Free	Free	Rigid	Free	Free	Free
Sn30	K52	GCS	Standard	Free	Free	Rigid	Free	Free	Free
Sn31	K53	GCS	Standard	Free	Free	Rigid	Free	Free	Free
Sn32	K54	GCS	Standard	Free	Free	Rigid	Free	Free	Free
Sn33	K55	GCS	Standard	Free	Free	Rigid	Free	Free	Free
Sn34	K56	GCS	Standard	Free	Free	Rigid	Free	Free	Free
Sn35	K57	GCS	Standard	Rigid	Rigid	Rigid	Free	Free	Free
Sn36	K58	GCS	Standard	Free	Free	Rigid	Free	Free	Free
Sn37	K59	GCS	Standard	Free	Free	Rigid	Free	Free	Free
Sn38	K60	GCS	Standard	Free	Free	Rigid	Free	Free	Free
Sn39	K61	GCS	Standard	Free	Free	Rigid	Free	Free	Free
Sn40	K69	GCS	Standard	Free	Free	Rigid	Free	Free	Free
Sn41	K70	GCS	Standard	Free	Free	Rigid	Free	Free	Free
Sn42	K71	GCS	Standard	Free	Free	Rigid	Free	Free	Free
Sn43	K72	GCS	Standard	Free	Free	Rigid	Free	Free	Free
Sn44	K73	GCS	Standard	Free	Free	Rigid	Free	Free	Free
Sn45	K74	GCS	Standard	Free	Free	Rigid	Free	Free	Free
Sn46	K75	GCS	Standard	Free	Free	Rigid	Free	Free	Free
Sn47	K76	GCS	Standard	Free	Free	Rigid	Free	Free	Free

Name	Node	System	Type	X	Y	Z	Rx	Ry	Rz
Sn48	K77	GCS	Standard	Free	Free	Rigid	Free	Free	Free
Sn49	K78	GCS	Standard	Free	Free	Rigid	Free	Free	Free
Sn50	K79	GCS	Standard	Free	Free	Rigid	Free	Free	Free
Sn51	K80	GCS	Standard	Free	Free	Rigid	Free	Free	Free
Sn52	K81	GCS	Standard	Free	Free	Rigid	Free	Free	Free
Sn53	K82	GCS	Standard	Free	Free	Rigid	Free	Free	Free
Sn54	K83	GCS	Standard	Free	Free	Rigid	Free	Free	Free
Sn55	K84	GCS	Standard	Free	Rigid	Rigid	Free	Free	Free
Sn56	K85	GCS	Standard	Free	Free	Rigid	Free	Free	Free
Sn57	K86	GCS	Standard	Free	Free	Rigid	Free	Free	Free
Sn58	K87	GCS	Standard	Free	Free	Rigid	Free	Free	Free
Sn59	K88	GCS	Standard	Free	Free	Rigid	Free	Free	Free
Sn60	K89	GCS	Standard	Free	Free	Rigid	Free	Free	Free
Sn61	K44	GCS	Standard	Free	Free	Rigid	Free	Free	Free
Sn62	K102	GCS	Standard	Free	Free	Rigid	Free	Free	Free
Sn63	K103	GCS	Standard	Free	Free	Rigid	Free	Free	Free
Sn64	K104	GCS	Standard	Free	Free	Rigid	Free	Free	Free
Sn65	K105	GCS	Standard	Free	Free	Rigid	Free	Free	Free
Sn66	K106	GCS	Standard	Free	Free	Rigid	Free	Free	Free
Sn67	K107	GCS	Standard	Free	Free	Rigid	Free	Free	Free
Sn68	K108	GCS	Standard	Free	Free	Rigid	Free	Free	Free
Sn69	K109	GCS	Standard	Free	Free	Rigid	Free	Free	Free
Sn70	K110	GCS	Standard	Free	Free	Rigid	Free	Free	Free
Sn71	K111	GCS	Standard	Free	Free	Rigid	Free	Free	Free
Sn72	K92	GCS	Standard	Free	Free	Rigid	Free	Free	Free
Sn73	K93	GCS	Standard	Free	Free	Rigid	Free	Free	Free
Sn74	K94	GCS	Standard	Free	Free	Rigid	Free	Free	Free
Sn75	K95	GCS	Standard	Free	Free	Rigid	Free	Free	Free
Sn76	K96	GCS	Standard	Free	Free	Rigid	Free	Free	Free
Sn77	K97	GCS	Standard	Free	Free	Rigid	Free	Free	Free
Sn78	K98	GCS	Standard	Free	Free	Rigid	Free	Free	Free
Sn79	K99	GCS	Standard	Free	Free	Rigid	Free	Free	Free
Sn80	K100	GCS	Standard	Free	Free	Rigid	Free	Free	Free
Sn81	K101	GCS	Standard	Free	Free	Rigid	Free	Free	Free

8. Load cases

Name	Description	Action type	LoadGroup	Duration	Master load case
	Spec	Load type			
LC2	Dead Load	Permanent	LG1		
	Standard	Standard			
LC3	Edge Load	Permanent	LG1		
	Standard	Standard			
LC4	Traffic load| P.T| UDL	Variable	LG2	Short	None
	Standard	Static			
LC5	Traffic load| P.T| TS	Variable	LG3	Short	None
	Standard	Static			
LC6	Traffic load| A.T| UDL	Variable	LG2	Short	None
	Standard	Static			
LC7	Traffic load| A.T| TS	Variable	LG3	Short	None
	Standard	Static			
LC8	Tram Load	Variable	LG3	Short	None
	Standard	Static			
LC9	Pedestrian Loading on des. loc.	Variable	LG2	Short	None
	Standard	Static			
LC10	Crowd Loading	Variable	LG2	Short	None
	Standard	Static			
LC11	TR1/LP20,000 m	Variable	LG3	Short	None
	Standard	Static			
LC12	TR1/LP20,500 m	Variable	LG3	Short	None
	Standard	Static			
LC13	TR1/LP21,000 m	Variable	LG3	Short	None
	Standard	Static			
LC14	TR1/LP21,500 m	Variable	LG3	Short	None
	Standard	Static			
LC15	TR1/LP22,000 m	Variable	LG3	Short	None
	Standard	Static			
LC16	TR1/LP22,500 m	Variable	LG3	Short	None
	Standard	Static			
LC17	TR1/LP23,000 m	Variable	LG3	Short	None
	Standard	Static			
LC18	TR1/LP23,500 m	Variable	LG3	Short	None
	Standard	Static			
LC19	TR1/LP24,000 m	Variable	LG3	Short	None
	Standard	Static			

Name	Description	Action type	LoadGroup	Duration	Master load case
	Spec	Load type			
LC20	TR1/LP24,500 m Standard	Variable Static	LG3	Short	None
LC21	TR1/LP25,000 m Standard	Variable Static	LG3	Short	None
LC22	TR1/LP25,500 m Standard	Variable Static	LG3	Short	None
LC23	TR1/LP26,000 m Standard	Variable Static	LG3	Short	None
LC24	TR1/LP26,500 m Standard	Variable Static	LG3	Short	None
LC25	TR1/LP27,000 m Standard	Variable Static	LG3	Short	None
LC26	TR1/LP27,500 m Standard	Variable Static	LG3	Short	None
LC27	TR1/LP28,000 m Standard	Variable Static	LG3	Short	None
LC28	TR1/LP28,500 m Standard	Variable Static	LG3	Short	None
LC29	TR1/LP29,000 m Standard	Variable Static	LG3	Short	None
LC30	TR1/LP29,500 m Standard	Variable Static	LG3	Short	None
LC31	TR1/LP210,000 m Standard	Variable Static	LG3	Short	None
LC32	TR1/LP210,500 m Standard	Variable Static	LG3	Short	None
LC33	TR1/LP211,000 m Standard	Variable Static	LG3	Short	None
LC34	TR1/LP211,500 m Standard	Variable Static	LG3	Short	None
LC35	TR1/LP212,000 m Standard	Variable Static	LG3	Short	None
LC36	TR1/LP212,500 m Standard	Variable Static	LG3	Short	None
LC37	TR1/LP213,000 m Standard	Variable Static	LG3	Short	None
LC38	TR1/LP213,500 m Standard	Variable Static	LG3	Short	None
LC39	TR1/LP214,000 m Standard	Variable Static	LG3	Short	None
LC40	TR1/LP214,500 m Standard	Variable Static	LG3	Short	None
LC41	TR1/LP215,000 m Standard	Variable Static	LG3	Short	None
LC42	TR1/LP215,500 m Standard	Variable Static	LG3	Short	None
LC43	TR1/LP216,000 m Standard	Variable Static	LG3	Short	None
LC44	TR1/LP216,500 m Standard	Variable Static	LG3	Short	None
LC45	TR1/LP217,000 m Standard	Variable Static	LG3	Short	None
LC46	TR1/LP217,500 m Standard	Variable Static	LG3	Short	None
LC47	TR1/LP218,000 m Standard	Variable Static	LG3	Short	None
LC48	TR1/LP218,500 m Standard	Variable Static	LG3	Short	None
LC49	TR1/LP219,000 m Standard	Variable Static	LG3	Short	None
LC50	TR1/LP219,500 m Standard	Variable Static	LG3	Short	None
LC51	TR1/LP220,000 m Standard	Variable Static	LG3	Short	None
LC52	TR1/LP220,500 m Standard	Variable Static	LG3	Short	None
LC53	TR1/LP221,000 m Standard	Variable Static	LG3	Short	None
LC54	TR1/LP221,500 m Standard	Variable Static	LG3	Short	None
LC55	TR1/LP222,000 m Standard	Variable Static	LG3	Short	None
LC56	TR1/LP222,500 m Standard	Variable Static	LG3	Short	None
LC57	TR1/LP223,000 m	Variable	LG3	Short	None

Name	Description	Action type	LoadGroup	Duration	Master load case
	Spec	Load type			
	Standard	Static			
LC58	TR1/LP223,500 m	Variable	LG3	Short	None
	Standard	Static			
LC59	TR1/LP224,000 m	Variable	LG3	Short	None
	Standard	Static			
LC60	TR1/LP10,000 m	Variable	LG3	Short	None
	Standard	Static			
LC61	TR1/LP10,500 m	Variable	LG3	Short	None
	Standard	Static			
LC62	TR1/LP11,000 m	Variable	LG3	Short	None
	Standard	Static			
LC63	TR1/LP11,500 m	Variable	LG3	Short	None
	Standard	Static			
LC64	TR1/LP12,000 m	Variable	LG3	Short	None
	Standard	Static			
LC65	TR1/LP12,500 m	Variable	LG3	Short	None
	Standard	Static			
LC66	TR1/LP13,000 m	Variable	LG3	Short	None
	Standard	Static			
LC67	TR1/LP13,500 m	Variable	LG3	Short	None
	Standard	Static			
LC68	TR1/LP14,000 m	Variable	LG3	Short	None
	Standard	Static			
LC69	TR1/LP14,500 m	Variable	LG3	Short	None
	Standard	Static			
LC70	TR1/LP15,000 m	Variable	LG3	Short	None
	Standard	Static			
LC71	TR1/LP15,500 m	Variable	LG3	Short	None
	Standard	Static			
LC72	TR1/LP16,000 m	Variable	LG3	Short	None
	Standard	Static			
LC73	TR1/LP16,500 m	Variable	LG3	Short	None
	Standard	Static			
LC74	TR1/LP17,000 m	Variable	LG3	Short	None
	Standard	Static			
LC75	TR1/LP17,500 m	Variable	LG3	Short	None
	Standard	Static			
LC76	TR1/LP18,000 m	Variable	LG3	Short	None
	Standard	Static			
LC77	TR1/LP18,500 m	Variable	LG3	Short	None
	Standard	Static			
LC78	TR1/LP19,000 m	Variable	LG3	Short	None
	Standard	Static			
LC79	TR1/LP19,500 m	Variable	LG3	Short	None
	Standard	Static			
LC80	TR1/LP110,000 m	Variable	LG3	Short	None
	Standard	Static			
LC81	TR1/LP110,500 m	Variable	LG3	Short	None
	Standard	Static			
LC82	TR1/LP111,000 m	Variable	LG3	Short	None
	Standard	Static			
LC83	TR1/LP111,500 m	Variable	LG3	Short	None
	Standard	Static			
LC84	TR1/LP112,000 m	Variable	LG3	Short	None
	Standard	Static			
LC85	TR1/LP112,500 m	Variable	LG3	Short	None
	Standard	Static			
LC86	TR1/LP113,000 m	Variable	LG3	Short	None
	Standard	Static			
LC87	TR1/LP113,500 m	Variable	LG3	Short	None
	Standard	Static			
LC88	TR1/LP114,000 m	Variable	LG3	Short	None
	Standard	Static			
LC89	TR1/LP114,500 m	Variable	LG3	Short	None
	Standard	Static			
LC90	TR1/LP115,000 m	Variable	LG3	Short	None
	Standard	Static			
LC91	TR1/LP115,500 m	Variable	LG3	Short	None
	Standard	Static			
LC92	TR1/LP116,000 m	Variable	LG3	Short	None
	Standard	Static			
LC93	TR1/LP116,500 m	Variable	LG3	Short	None
	Standard	Static			
LC94	TR1/LP117,000 m	Variable	LG3	Short	None
	Standard	Static			

Name	Description	Action type	LoadGroup	Duration	Master load case
	Spec	Load type			
LC95	TR1/LP117,500 m Standard	Variable Static	LG3	Short	None
LC96	TR1/LP118,000 m Standard	Variable Static	LG3	Short	None
LC97	TR1/LP118,500 m Standard	Variable Static	LG3	Short	None
LC98	TR1/LP119,000 m Standard	Variable Static	LG3	Short	None
LC99	TR1/LP119,500 m Standard	Variable Static	LG3	Short	None
LC100	TR1/LP120,000 m Standard	Variable Static	LG3	Short	None
LC101	TR1/LP120,500 m Standard	Variable Static	LG3	Short	None
LC102	TR1/LP121,000 m Standard	Variable Static	LG3	Short	None
LC103	TR1/LP121,500 m Standard	Variable Static	LG3	Short	None
LC104	TR1/LP122,000 m Standard	Variable Static	LG3	Short	None
LC105	TR1/LP122,500 m Standard	Variable Static	LG3	Short	None
LC106	TR1/LP123,000 m Standard	Variable Static	LG3	Short	None
LC107	TR1/LP123,500 m Standard	Variable Static	LG3	Short	None
LC108	TR1/LP124,000 m Standard	Variable Static	LG3	Short	None
LC109	TR2/LP30,000 m Standard	Variable Static	LG3	Short	None
LC110	TR2/LP30,500 m Standard	Variable Static	LG3	Short	None
LC111	TR2/LP31,000 m Standard	Variable Static	LG3	Short	None
LC112	TR2/LP31,500 m Standard	Variable Static	LG3	Short	None
LC113	TR2/LP32,000 m Standard	Variable Static	LG3	Short	None
LC114	TR2/LP32,500 m Standard	Variable Static	LG3	Short	None
LC115	TR2/LP33,000 m Standard	Variable Static	LG3	Short	None
LC116	TR2/LP33,500 m Standard	Variable Static	LG3	Short	None
LC117	TR2/LP34,000 m Standard	Variable Static	LG3	Short	None
LC118	TR2/LP34,500 m Standard	Variable Static	LG3	Short	None
LC119	TR2/LP35,000 m Standard	Variable Static	LG3	Short	None
LC120	TR2/LP35,500 m Standard	Variable Static	LG3	Short	None
LC121	TR2/LP36,000 m Standard	Variable Static	LG3	Short	None
LC122	TR2/LP36,500 m Standard	Variable Static	LG3	Short	None
LC123	TR2/LP37,000 m Standard	Variable Static	LG3	Short	None
LC124	TR2/LP37,500 m Standard	Variable Static	LG3	Short	None
LC125	TR2/LP38,000 m Standard	Variable Static	LG3	Short	None
LC126	TR2/LP38,500 m Standard	Variable Static	LG3	Short	None
LC127	TR2/LP39,000 m Standard	Variable Static	LG3	Short	None
LC128	TR2/LP39,500 m Standard	Variable Static	LG3	Short	None
LC129	TR2/LP310,000 m Standard	Variable Static	LG3	Short	None
LC130	TR2/LP310,500 m Standard	Variable Static	LG3	Short	None
LC131	TR2/LP311,000 m Standard	Variable Static	LG3	Short	None
LC132	TR2/LP311,500 m	Variable	LG3	Short	None

Name	Description	Action type	LoadGroup	Duration	Master load case
	Spec	Load type			
	Standard	Static			
LC133	TR2/LP312,000 m	Variable	LG3	Short	None
	Standard	Static			
LC134	TR2/LP312,500 m	Variable	LG3	Short	None
	Standard	Static			
LC135	TR2/LP313,000 m	Variable	LG3	Short	None
	Standard	Static			
LC136	TR2/LP313,500 m	Variable	LG3	Short	None
	Standard	Static			
LC137	TR2/LP314,000 m	Variable	LG3	Short	None
	Standard	Static			
LC138	TR2/LP314,500 m	Variable	LG3	Short	None
	Standard	Static			
LC139	TR2/LP315,000 m	Variable	LG3	Short	None
	Standard	Static			
LC140	TR2/LP315,500 m	Variable	LG3	Short	None
	Standard	Static			
LC141	TR2/LP316,000 m	Variable	LG3	Short	None
	Standard	Static			
LC142	TR2/LP316,500 m	Variable	LG3	Short	None
	Standard	Static			
LC143	TR2/LP317,000 m	Variable	LG3	Short	None
	Standard	Static			
LC144	TR2/LP317,500 m	Variable	LG3	Short	None
	Standard	Static			
LC145	TR2/LP318,000 m	Variable	LG3	Short	None
	Standard	Static			
LC146	TR2/LP318,500 m	Variable	LG3	Short	None
	Standard	Static			
LC147	TR2/LP319,000 m	Variable	LG3	Short	None
	Standard	Static			
LC148	TR2/LP319,500 m	Variable	LG3	Short	None
	Standard	Static			
LC149	TR2/LP320,000 m	Variable	LG3	Short	None
	Standard	Static			
LC150	TR2/LP320,500 m	Variable	LG3	Short	None
	Standard	Static			
LC151	TR2/LP321,000 m	Variable	LG3	Short	None
	Standard	Static			
LC152	TR2/LP321,500 m	Variable	LG3	Short	None
	Standard	Static			
LC153	TR2/LP322,000 m	Variable	LG3	Short	None
	Standard	Static			
LC154	TR2/LP322,500 m	Variable	LG3	Short	None
	Standard	Static			
LC155	TR2/LP323,000 m	Variable	LG3	Short	None
	Standard	Static			
LC156	TR2/LP323,500 m	Variable	LG3	Short	None
	Standard	Static			
LC157	TR2/LP324,000 m	Variable	LG3	Short	None
	Standard	Static			
LC158	UDL for max my	Variable	LG2	Short	None
	Standard	Static			
LC159	TS (AT) for max my	Variable	LG3	Short	None
	Standard	Static			
LC160	TR3/LP10,000 m	Variable	LG3	Short	None
	Standard	Static			
LC161	TR3/LP10,500 m	Variable	LG3	Short	None
	Standard	Static			
LC162	TR3/LP11,000 m	Variable	LG3	Short	None
	Standard	Static			
LC163	TR3/LP11,500 m	Variable	LG3	Short	None
	Standard	Static			
LC164	TR3/LP12,000 m	Variable	LG3	Short	None
	Standard	Static			
LC165	TR3/LP12,500 m	Variable	LG3	Short	None
	Standard	Static			
LC166	TR3/LP13,000 m	Variable	LG3	Short	None
	Standard	Static			
LC167	TR3/LP13,500 m	Variable	LG3	Short	None
	Standard	Static			
LC168	TR3/LP14,000 m	Variable	LG3	Short	None
	Standard	Static			
LC169	TR3/LP14,500 m	Variable	LG3	Short	None
	Standard	Static			

Name	Description	Action type	LoadGroup	Duration	Master load case
	Spec	Load type			
LC170	TR3/LP15,000 m Standard	Variable Static	LG3	Short	None
LC171	TR3/LP15,500 m Standard	Variable Static	LG3	Short	None
LC172	TR3/LP16,000 m Standard	Variable Static	LG3	Short	None
LC173	TR3/LP16,500 m Standard	Variable Static	LG3	Short	None
LC174	TR3/LP17,000 m Standard	Variable Static	LG3	Short	None
LC175	TR3/LP17,500 m Standard	Variable Static	LG3	Short	None
LC176	TR3/LP18,000 m Standard	Variable Static	LG3	Short	None
LC177	TR3/LP18,500 m Standard	Variable Static	LG3	Short	None
LC178	TR3/LP19,000 m Standard	Variable Static	LG3	Short	None
LC179	TR3/LP19,500 m Standard	Variable Static	LG3	Short	None
LC180	TR3/LP110,000 m Standard	Variable Static	LG3	Short	None
LC181	TR3/LP110,500 m Standard	Variable Static	LG3	Short	None
LC182	TR3/LP111,000 m Standard	Variable Static	LG3	Short	None
LC183	TR3/LP111,500 m Standard	Variable Static	LG3	Short	None
LC184	TR3/LP112,000 m Standard	Variable Static	LG3	Short	None
LC185	TR3/LP112,500 m Standard	Variable Static	LG3	Short	None
LC186	TR3/LP113,000 m Standard	Variable Static	LG3	Short	None
LC187	TR3/LP113,500 m Standard	Variable Static	LG3	Short	None
LC188	TR3/LP114,000 m Standard	Variable Static	LG3	Short	None
LC189	TR3/LP114,500 m Standard	Variable Static	LG3	Short	None
LC190	TR3/LP115,000 m Standard	Variable Static	LG3	Short	None
LC191	TR3/LP115,500 m Standard	Variable Static	LG3	Short	None
LC192	TR3/LP116,000 m Standard	Variable Static	LG3	Short	None
LC193	TR3/LP116,500 m Standard	Variable Static	LG3	Short	None
LC194	TR3/LP117,000 m Standard	Variable Static	LG3	Short	None
LC195	TR3/LP117,500 m Standard	Variable Static	LG3	Short	None
LC196	TR3/LP118,000 m Standard	Variable Static	LG3	Short	None
LC197	TR3/LP118,500 m Standard	Variable Static	LG3	Short	None
LC198	TR3/LP119,000 m Standard	Variable Static	LG3	Short	None
LC199	TR3/LP119,500 m Standard	Variable Static	LG3	Short	None
LC200	TR3/LP120,000 m Standard	Variable Static	LG3	Short	None
LC201	TR3/LP120,500 m Standard	Variable Static	LG3	Short	None
LC202	TR3/LP121,000 m Standard	Variable Static	LG3	Short	None
LC203	TR3/LP121,500 m Standard	Variable Static	LG3	Short	None
LC204	TR3/LP122,000 m Standard	Variable Static	LG3	Short	None
LC205	TR3/LP122,500 m Standard	Variable Static	LG3	Short	None
LC206	TR3/LP123,000 m Standard	Variable Static	LG3	Short	None
LC207	TR3/LP123,500 m	Variable	LG3	Short	None

Name	Description	Action type	LoadGroup	Duration	Master load case
	Spec	Load type			
	Standard	Static			
LC208	TR3/LP124,000 m	Variable	LG3	Short	None
	Standard	Static			

9. LC2 / Tot. value

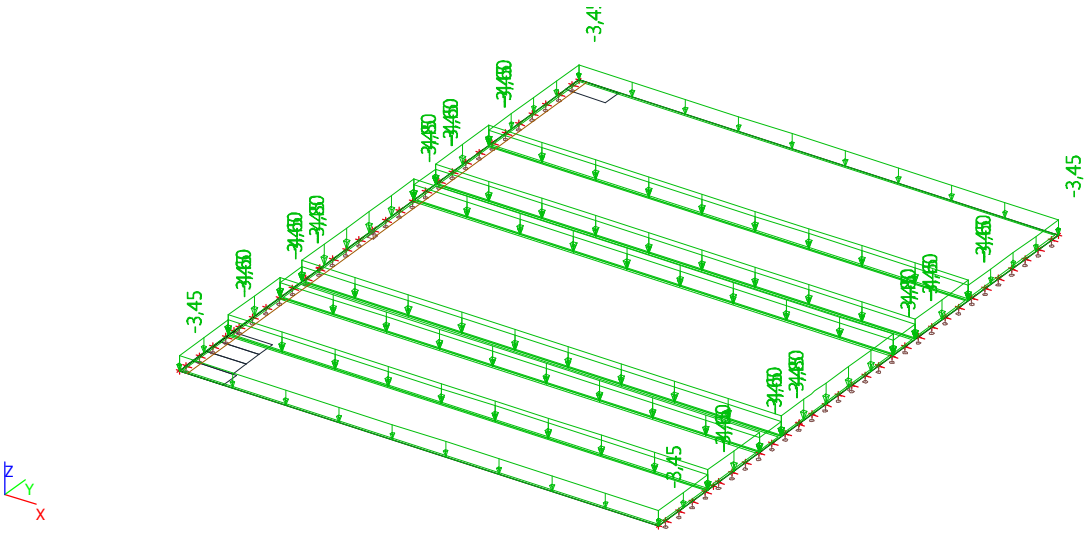

10. LC3 - Edge Load

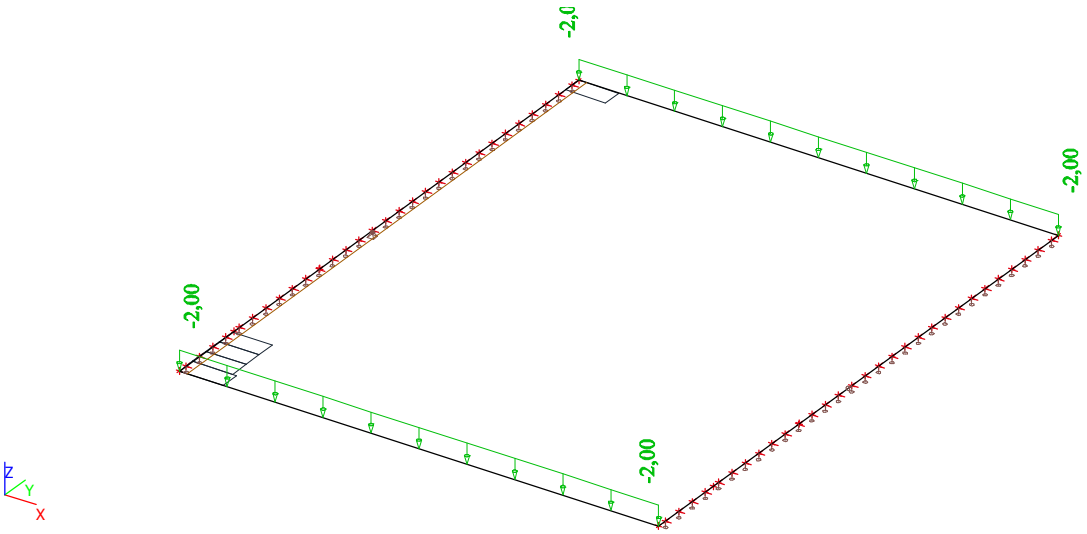

11. LC4 - Traffic load| P.T| UDL

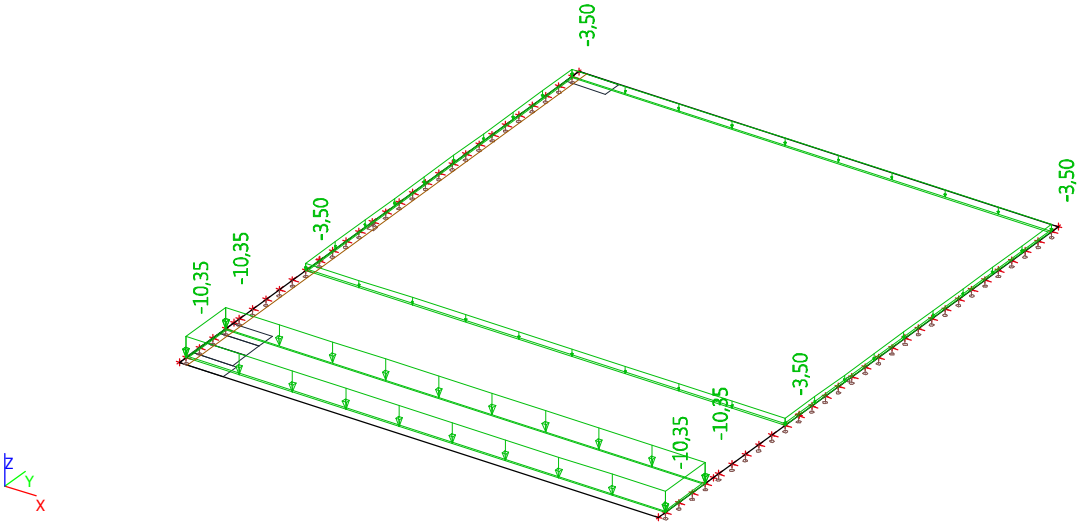

12. LC5 - Traffic load| P.T| TS

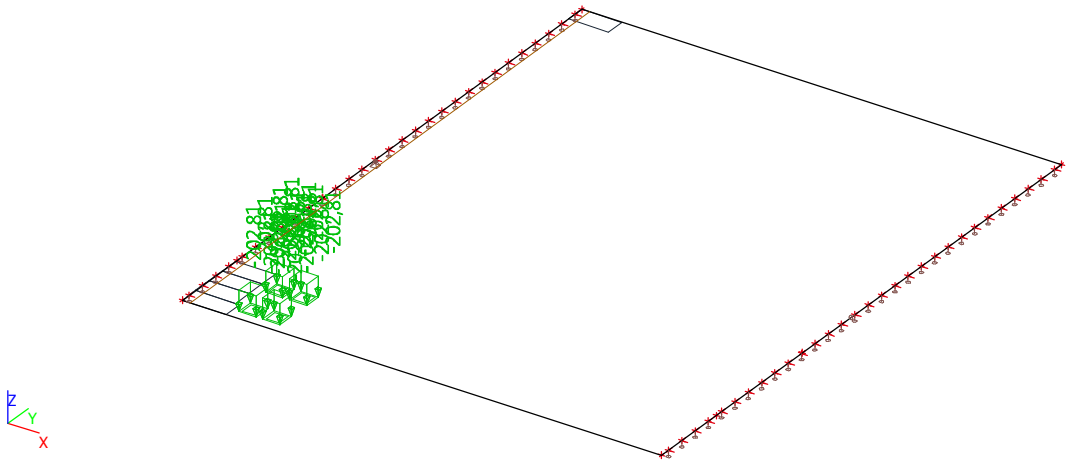

13. LC6 - Traffic load| A.T| UDL

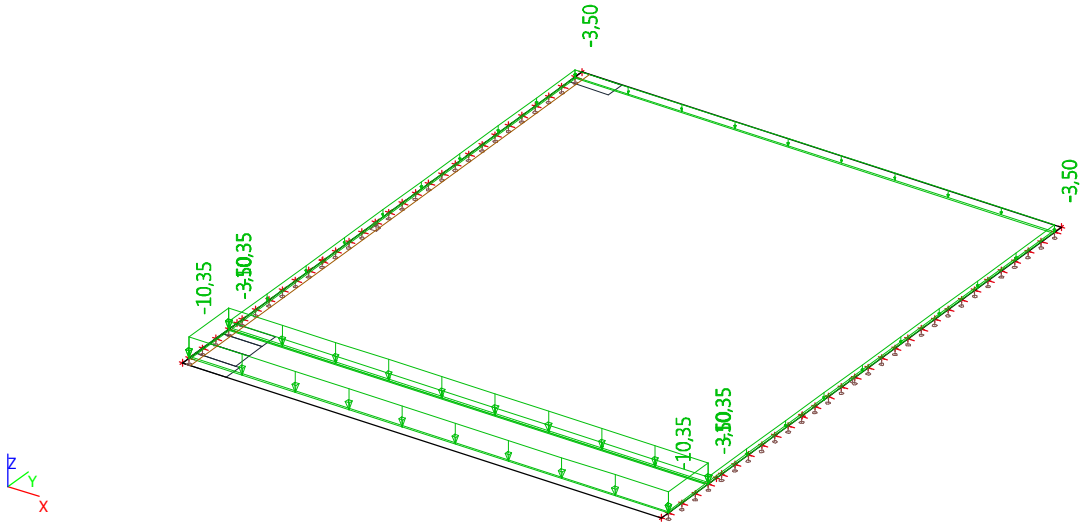

14. LC7 - Traffic load| A.T| TS

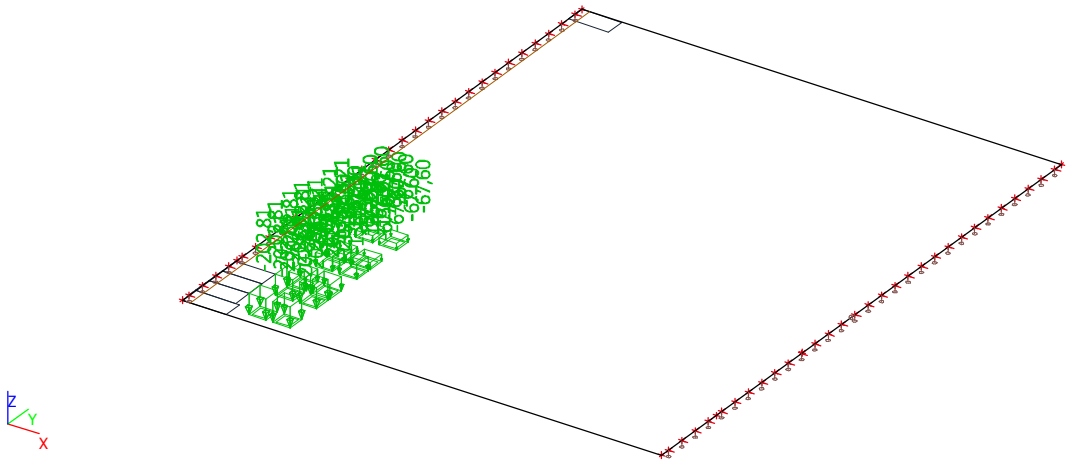

15. LC9 - Pedestrian Loading on des. loc.

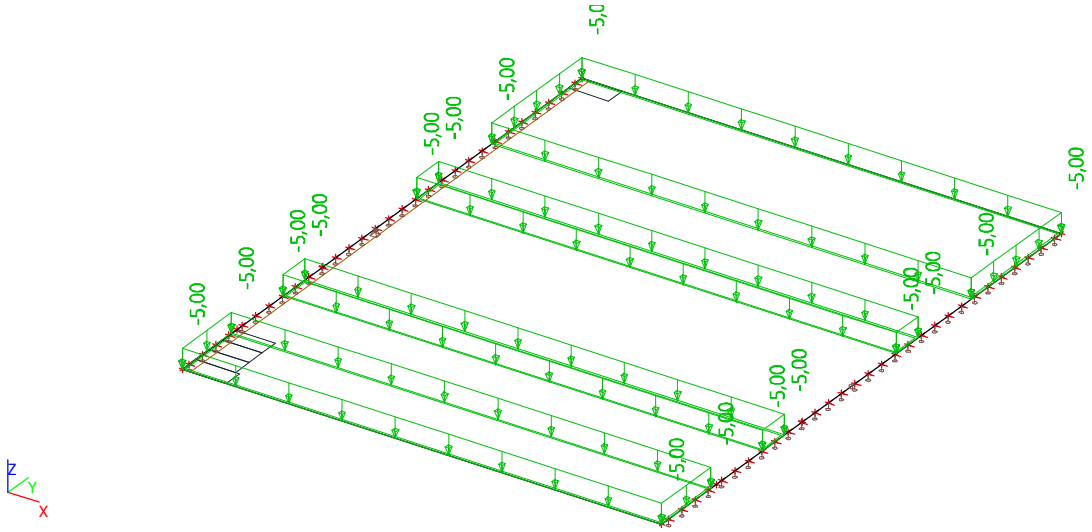

16. LC11 - UDL for max My

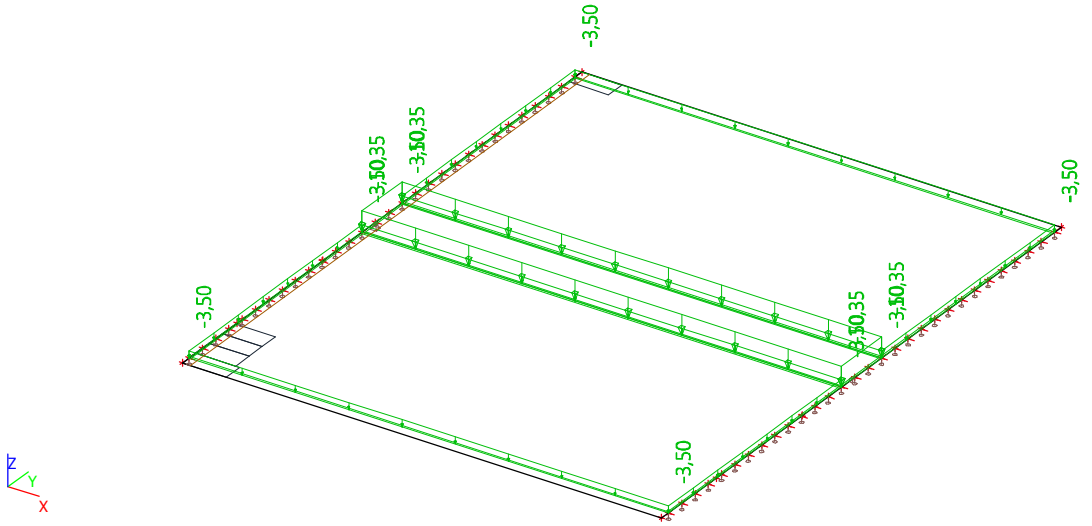

17. LC10 - Crowd Loading

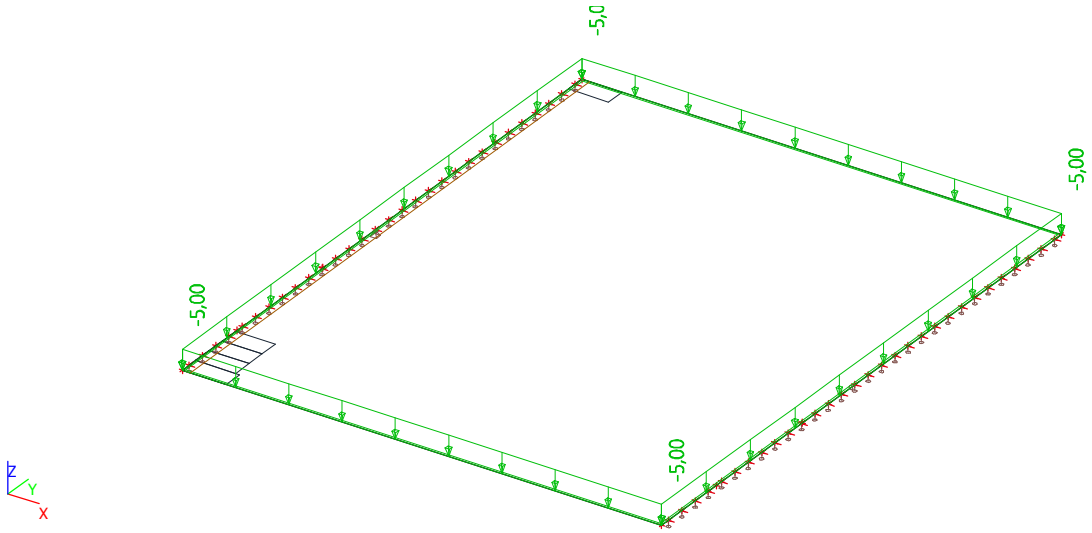

18. LC12 - T.S. for max my

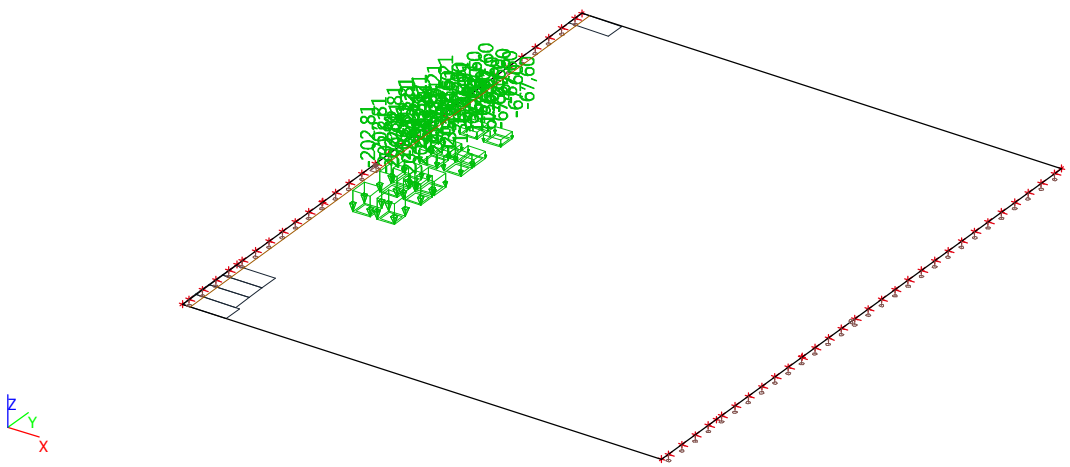

19. Traffic lane

Name	Used nodes	Node	Use for calculation
TR2	2	Head	✓
		End	
TR1	2	Head	✓
		End	
TR3	2	Head	✓
		End	

20. Lane loads manager

Name	Traffic Loads	Traffic lane	Load group	Load case name	Step [m]
LL1	LP2	TR1	LG3	TR1/LP2	0,500
LL2	LP1	TR1	LG3	TR1/LP1	0,500
LL3	LP3	TR2	LG3	TR2/LP3	0,500
LL4	LP1	TR3	LG3	TR3/LP1	0,500

21. Load pattern

Name	Type	Description	Force [kN/m²]	Position x1 [m] Repeat x (n) Position x2 [m] Repeat y (n)	Position y1 [m] Delta x [m]	Position y2 [m] Delta y [m]
LP1	Rectangle	TS AT	-202,81	0,000	0,000	0,860
	Rectangle		-135,21	0,000	3,000	3,860
	Rectangle		-67,60	0,000	6,000	6,860
				2	1,200	2,000
				2	1,200	2,000
				2	1,200	2,000
				0,860		
				0,860		
				0,860		
				2		
				2		
				2		
LP2	Rectangle	TS PT	-202,81	0,000	0,000	0,860
				2	1,200	2,000
				0,860		
				2		
LP3	Rectangle	Tram Load	-211,47	0,000	0,000	0,380
	Rectangle		-211,47	11,000	0,000	0,380
	Rectangle		-211,47	22,000	0,000	0,380
	Rectangle		-211,47	0,000	3,000	3,380
	Rectangle		-211,47	11,000	3,000	3,380
	Rectangle		-211,47	22,000	3,000	3,380
				2	1,800	1,435
				2	1,800	1,435
				2	1,800	1,435
				2	1,800	1,435

Name	Type	Description	Force [kN/m²]	Position x1 [m]	Position y1 [m]	Position y2 [m]
				Repeat x (n)	Delta x [m]	Delta y [m]
				Position x2 [m]		
				Repeat y (n)		
				2	1,800	1,435
				2	1,800	1,435
				0,560		
				11,560		
				22,560		
				0,560		
				11,560		
				22,560		
				2		
				2		
				2		
				2		
				2		
				2		

22. Load groups

Name	Load	Relation	Type
LG1	Permanent		
LG2	Variable	Standard	Cat A : Domestic
LG3	Variable	Exclusive	Cat G : Vehicle >30kN

23. Combinations

Name	Description	Type	Load cases	Coeff. [-]
BC1	1. ULS| PT| Vehicle governing	Envelope - ultimate	LC2 - Dead Load	1,20
			LC3 - Edge Load	1,20
			LC4 - Traffic load| P.T| UDL	1,35
			LC9 - Pedestrian Loading on des. loc.	1,08
			LC11 - TR1/LP20,000 m	1,35
			LC12 - TR1/LP20,500 m	1,35
			LC13 - TR1/LP21,000 m	1,35
			LC14 - TR1/LP21,500 m	1,35
			LC15 - TR1/LP22,000 m	1,35
			LC16 - TR1/LP22,500 m	1,35
			LC17 - TR1/LP23,000 m	1,35
			LC18 - TR1/LP23,500 m	1,35
			LC19 - TR1/LP24,000 m	1,35
			LC20 - TR1/LP24,500 m	1,35
			LC21 - TR1/LP25,000 m	1,35
			LC22 - TR1/LP25,500 m	1,35
			LC23 - TR1/LP26,000 m	1,35
			LC24 - TR1/LP26,500 m	1,35
			LC25 - TR1/LP27,000 m	1,35
			LC26 - TR1/LP27,500 m	1,35
			LC27 - TR1/LP28,000 m	1,35
			LC28 - TR1/LP28,500 m	1,35
			LC29 - TR1/LP29,000 m	1,35
			LC30 - TR1/LP29,500 m	1,35
			LC31 - TR1/LP210,000 m	1,35
			LC32 - TR1/LP210,500 m	1,35
			LC33 - TR1/LP211,000 m	1,35
			LC34 - TR1/LP211,500 m	1,35
			LC35 - TR1/LP212,000 m	1,35
			LC36 - TR1/LP212,500 m	1,35
			LC37 - TR1/LP213,000 m	1,35
			LC38 - TR1/LP213,500 m	1,35
			LC39 - TR1/LP214,000 m	1,35
			LC40 - TR1/LP214,500 m	1,35
			LC41 - TR1/LP215,000 m	1,35
			LC42 - TR1/LP215,500 m	1,35
			LC43 - TR1/LP216,000 m	1,35
			LC44 - TR1/LP216,500 m	1,35
			LC45 - TR1/LP217,000 m	1,35
			LC46 - TR1/LP217,500 m	1,35
			LC47 - TR1/LP218,000 m	1,35
			LC48 - TR1/LP218,500 m	1,35
			LC49 - TR1/LP219,000 m	1,35
			LC50 - TR1/LP219,500 m	1,35

Name	Description	Type	Load cases	Coeff. [-]
			LC51 - TR1/LP220,000 m	1,35
			LC52 - TR1/LP220,500 m	1,35
			LC53 - TR1/LP221,000 m	1,35
			LC54 - TR1/LP221,500 m	1,35
			LC55 - TR1/LP222,000 m	1,35
			LC56 - TR1/LP222,500 m	1,35
			LC57 - TR1/LP223,000 m	1,35
			LC58 - TR1/LP223,500 m	1,35
			LC59 - TR1/LP224,000 m	1,35
			LC109 - TR2/LP30,000 m	1,16
			LC110 - TR2/LP30,500 m	1,16
			LC111 - TR2/LP31,000 m	1,16
			LC112 - TR2/LP31,500 m	1,16
			LC113 - TR2/LP32,000 m	1,16
			LC114 - TR2/LP32,500 m	1,16
			LC115 - TR2/LP33,000 m	1,16
			LC116 - TR2/LP33,500 m	1,16
			LC117 - TR2/LP34,000 m	1,16
			LC118 - TR2/LP34,500 m	1,16
			LC119 - TR2/LP35,000 m	1,16
			LC120 - TR2/LP35,500 m	1,16
			LC121 - TR2/LP36,000 m	1,16
			LC122 - TR2/LP36,500 m	1,16
			LC123 - TR2/LP37,000 m	1,16
			LC124 - TR2/LP37,500 m	1,16
			LC125 - TR2/LP38,000 m	1,16
			LC126 - TR2/LP38,500 m	1,16
			LC127 - TR2/LP39,000 m	1,16
			LC128 - TR2/LP39,500 m	1,16
			LC129 - TR2/LP310,000 m	1,16
			LC130 - TR2/LP310,500 m	1,16
			LC131 - TR2/LP311,000 m	1,16
			LC132 - TR2/LP311,500 m	1,16
			LC133 - TR2/LP312,000 m	1,16
			LC134 - TR2/LP312,500 m	1,16
			LC135 - TR2/LP313,000 m	1,16
			LC136 - TR2/LP313,500 m	1,16
			LC137 - TR2/LP314,000 m	1,16
			LC138 - TR2/LP314,500 m	1,16
			LC139 - TR2/LP315,000 m	1,16
			LC140 - TR2/LP315,500 m	1,16
			LC141 - TR2/LP316,000 m	1,16
			LC142 - TR2/LP316,500 m	1,16
			LC143 - TR2/LP317,000 m	1,16
			LC144 - TR2/LP317,500 m	1,16
			LC145 - TR2/LP318,000 m	1,16
			LC146 - TR2/LP318,500 m	1,16
			LC147 - TR2/LP319,000 m	1,16
			LC148 - TR2/LP319,500 m	1,16
			LC149 - TR2/LP320,000 m	1,16
			LC150 - TR2/LP320,500 m	1,16
			LC151 - TR2/LP321,000 m	1,16
			LC152 - TR2/LP321,500 m	1,16
			LC153 - TR2/LP322,000 m	1,16
			LC154 - TR2/LP322,500 m	1,16
			LC155 - TR2/LP323,000 m	1,16
			LC156 - TR2/LP323,500 m	1,16
			LC157 - TR2/LP324,000 m	1,16
BC2	2. ULS| PT| Tram governing	Envelope - ultimate	LC2 - Dead Load	1,20
			LC3 - Edge Load	1,20
			LC4 - Traffic load| P.T| UDL	1,35
			LC9 - Pedestrian Loading on des. loc.	1,08
			LC11 - TR1/LP20,000 m	1,08
			LC12 - TR1/LP20,500 m	1,08
			LC13 - TR1/LP21,000 m	1,08
			LC14 - TR1/LP21,500 m	1,08
			LC15 - TR1/LP22,000 m	1,08
			LC16 - TR1/LP22,500 m	1,08
			LC17 - TR1/LP23,000 m	1,08
			LC18 - TR1/LP23,500 m	1,08
			LC19 - TR1/LP24,000 m	1,08
			LC20 - TR1/LP24,500 m	1,08
			LC21 - TR1/LP25,000 m	1,08
			LC22 - TR1/LP25,500 m	1,08
			LC23 - TR1/LP26,000 m	1,08
			LC24 - TR1/LP26,500 m	1,08

Name	Description	Type	Load cases	Coeff. [-]
			LC25 - TR1/LP27,000 m	1,08
			LC26 - TR1/LP27,500 m	1,08
			LC27 - TR1/LP28,000 m	1,08
			LC28 - TR1/LP28,500 m	1,08
			LC29 - TR1/LP29,000 m	1,08
			LC30 - TR1/LP29,500 m	1,08
			LC31 - TR1/LP210,000 m	1,08
			LC32 - TR1/LP210,500 m	1,08
			LC33 - TR1/LP211,000 m	1,08
			LC34 - TR1/LP211,500 m	1,08
			LC35 - TR1/LP212,000 m	1,08
			LC36 - TR1/LP212,500 m	1,08
			LC37 - TR1/LP213,000 m	1,08
			LC38 - TR1/LP213,500 m	1,08
			LC39 - TR1/LP214,000 m	1,08
			LC40 - TR1/LP214,500 m	1,08
			LC41 - TR1/LP215,000 m	1,08
			LC42 - TR1/LP215,500 m	1,08
			LC43 - TR1/LP216,000 m	1,08
			LC44 - TR1/LP216,500 m	1,08
			LC45 - TR1/LP217,000 m	1,08
			LC46 - TR1/LP217,500 m	1,08
			LC47 - TR1/LP218,000 m	1,08
			LC48 - TR1/LP218,500 m	1,08
			LC49 - TR1/LP219,000 m	1,08
			LC50 - TR1/LP219,500 m	1,08
			LC51 - TR1/LP220,000 m	1,08
			LC52 - TR1/LP220,500 m	1,08
			LC53 - TR1/LP221,000 m	1,08
			LC54 - TR1/LP221,500 m	1,08
			LC55 - TR1/LP222,000 m	1,08
			LC56 - TR1/LP222,500 m	1,08
			LC57 - TR1/LP223,000 m	1,08
			LC58 - TR1/LP223,500 m	1,08
			LC59 - TR1/LP224,000 m	1,08
			LC109 - TR2/LP30,000 m	1,45
			LC110 - TR2/LP30,500 m	1,45
			LC111 - TR2/LP31,000 m	1,45
			LC112 - TR2/LP31,500 m	1,45
			LC113 - TR2/LP32,000 m	1,45
			LC114 - TR2/LP32,500 m	1,45
			LC115 - TR2/LP33,000 m	1,45
			LC116 - TR2/LP33,500 m	1,45
			LC117 - TR2/LP34,000 m	1,45
			LC118 - TR2/LP34,500 m	1,45
			LC119 - TR2/LP35,000 m	1,45
			LC120 - TR2/LP35,500 m	1,45
			LC121 - TR2/LP36,000 m	1,45
			LC122 - TR2/LP36,500 m	1,45
			LC123 - TR2/LP37,000 m	1,45
			LC124 - TR2/LP37,500 m	1,45
			LC125 - TR2/LP38,000 m	1,45
			LC126 - TR2/LP38,500 m	1,45
			LC127 - TR2/LP39,000 m	1,45
			LC128 - TR2/LP39,500 m	1,45
			LC129 - TR2/LP310,000 m	1,45
			LC130 - TR2/LP310,500 m	1,45
			LC131 - TR2/LP311,000 m	1,45
			LC132 - TR2/LP311,500 m	1,45
			LC133 - TR2/LP312,000 m	1,45
			LC134 - TR2/LP312,500 m	1,45
			LC135 - TR2/LP313,000 m	1,45
			LC136 - TR2/LP313,500 m	1,45
			LC137 - TR2/LP314,000 m	1,45
			LC138 - TR2/LP314,500 m	1,45
			LC139 - TR2/LP315,000 m	1,45
			LC140 - TR2/LP315,500 m	1,45
			LC141 - TR2/LP316,000 m	1,45
			LC142 - TR2/LP316,500 m	1,45
			LC143 - TR2/LP317,000 m	1,45
			LC144 - TR2/LP317,500 m	1,45
			LC145 - TR2/LP318,000 m	1,45
			LC146 - TR2/LP318,500 m	1,45
			LC147 - TR2/LP319,000 m	1,45
			LC148 - TR2/LP319,500 m	1,45
			LC149 - TR2/LP320,000 m	1,45

Name	Description	Type	Load cases	Coeff. [-]
			LC150 - TR2/LP320,500 m	1,45
			LC151 - TR2/LP321,000 m	1,45
			LC152 - TR2/LP321,500 m	1,45
			LC153 - TR2/LP322,000 m	1,45
			LC154 - TR2/LP322,500 m	1,45
			LC155 - TR2/LP323,000 m	1,45
			LC156 - TR2/LP323,500 m	1,45
			LC157 - TR2/LP324,000 m	1,45
BC3	3. ULS| AT	Envelope - ultimate	LC2 - Dead Load	1,20
			LC3 - Edge Load	1,20
			LC6 - Traffic load| A.T| UDL	1,35
			LC9 - Pedestrian Loading on des. loc.	1,08
			LC60 - TR1/LP10,000 m	1,35
			LC61 - TR1/LP10,500 m	1,35
			LC62 - TR1/LP11,000 m	1,35
			LC63 - TR1/LP11,500 m	1,35
			LC64 - TR1/LP12,000 m	1,35
			LC65 - TR1/LP12,500 m	1,35
			LC66 - TR1/LP13,000 m	1,35
			LC67 - TR1/LP13,500 m	1,35
			LC68 - TR1/LP14,000 m	1,35
			LC69 - TR1/LP14,500 m	1,35
			LC70 - TR1/LP15,000 m	1,35
			LC71 - TR1/LP15,500 m	1,35
			LC72 - TR1/LP16,000 m	1,35
			LC73 - TR1/LP16,500 m	1,35
			LC74 - TR1/LP17,000 m	1,35
			LC75 - TR1/LP17,500 m	1,35
			LC76 - TR1/LP18,000 m	1,35
			LC77 - TR1/LP18,500 m	1,35
			LC78 - TR1/LP19,000 m	1,35
			LC79 - TR1/LP19,500 m	1,35
			LC80 - TR1/LP110,000 m	1,35
			LC81 - TR1/LP110,500 m	1,35
			LC82 - TR1/LP111,000 m	1,35
			LC83 - TR1/LP111,500 m	1,35
			LC84 - TR1/LP112,000 m	1,35
			LC85 - TR1/LP112,500 m	1,35
			LC86 - TR1/LP113,000 m	1,35
			LC87 - TR1/LP113,500 m	1,35
			LC88 - TR1/LP114,000 m	1,35
			LC89 - TR1/LP114,500 m	1,35
			LC90 - TR1/LP115,000 m	1,35
			LC91 - TR1/LP115,500 m	1,35
			LC92 - TR1/LP116,000 m	1,35
			LC93 - TR1/LP116,500 m	1,35
			LC94 - TR1/LP117,000 m	1,35
			LC95 - TR1/LP117,500 m	1,35
			LC96 - TR1/LP118,000 m	1,35
			LC97 - TR1/LP118,500 m	1,35
			LC98 - TR1/LP119,000 m	1,35
			LC99 - TR1/LP119,500 m	1,35
			LC100 - TR1/LP120,000 m	1,35
			LC101 - TR1/LP120,500 m	1,35
			LC102 - TR1/LP121,000 m	1,35
			LC103 - TR1/LP121,500 m	1,35
			LC104 - TR1/LP122,000 m	1,35
			LC105 - TR1/LP122,500 m	1,35
			LC106 - TR1/LP123,000 m	1,35
			LC107 - TR1/LP123,500 m	1,35
			LC108 - TR1/LP124,000 m	1,35
BC4	4. ULS| Crowd	Envelope - ultimate	LC2 - Dead Load	1,20
			LC3 - Edge Load	1,20
			LC10 - Crowd Loading	1,35
BC8	4. SLS| Crowd	Envelope - serviceability	LC2 - Dead Load	1,00
			LC3 - Edge Load	1,00
			LC10 - Crowd Loading	1,00
BC5	1. SLS| PT| Vehicle governing	Envelope - serviceability	LC2 - Dead Load	1,00
			LC3 - Edge Load	1,00
			LC4 - Traffic load| P.T| UDL	1,00
			LC9 - Pedestrian Loading on des. loc.	0,80
			LC11 - TR1/LP20,000 m	1,00
			LC12 - TR1/LP20,500 m	1,00
			LC13 - TR1/LP21,000 m	1,00
			LC14 - TR1/LP21,500 m	1,00

Name	Description	Type	Load cases	Coeff. [-]
			LC15 - TR1/LP22,000 m	1,00
			LC16 - TR1/LP22,500 m	1,00
			LC17 - TR1/LP23,000 m	1,00
			LC18 - TR1/LP23,500 m	1,00
			LC19 - TR1/LP24,000 m	1,00
			LC20 - TR1/LP24,500 m	1,00
			LC21 - TR1/LP25,000 m	1,00
			LC22 - TR1/LP25,500 m	1,00
			LC23 - TR1/LP26,000 m	1,00
			LC24 - TR1/LP26,500 m	1,00
			LC25 - TR1/LP27,000 m	1,00
			LC26 - TR1/LP27,500 m	1,00
			LC27 - TR1/LP28,000 m	1,00
			LC28 - TR1/LP28,500 m	1,00
			LC29 - TR1/LP29,000 m	1,00
			LC30 - TR1/LP29,500 m	1,00
			LC31 - TR1/LP210,000 m	1,00
			LC32 - TR1/LP210,500 m	1,00
			LC33 - TR1/LP211,000 m	1,00
			LC34 - TR1/LP211,500 m	1,00
			LC35 - TR1/LP212,000 m	1,00
			LC36 - TR1/LP212,500 m	1,00
			LC37 - TR1/LP213,000 m	1,00
			LC38 - TR1/LP213,500 m	1,00
			LC39 - TR1/LP214,000 m	1,00
			LC40 - TR1/LP214,500 m	1,00
			LC41 - TR1/LP215,000 m	1,00
			LC42 - TR1/LP215,500 m	1,00
			LC43 - TR1/LP216,000 m	1,00
			LC44 - TR1/LP216,500 m	1,00
			LC45 - TR1/LP217,000 m	1,00
			LC46 - TR1/LP217,500 m	1,00
			LC47 - TR1/LP218,000 m	1,00
			LC48 - TR1/LP218,500 m	1,00
			LC49 - TR1/LP219,000 m	1,00
			LC50 - TR1/LP219,500 m	1,00
			LC51 - TR1/LP220,000 m	1,00
			LC52 - TR1/LP220,500 m	1,00
			LC53 - TR1/LP221,000 m	1,00
			LC54 - TR1/LP221,500 m	1,00
			LC55 - TR1/LP222,000 m	1,00
			LC56 - TR1/LP222,500 m	1,00
			LC57 - TR1/LP223,000 m	1,00
			LC58 - TR1/LP223,500 m	1,00
			LC59 - TR1/LP224,000 m	1,00
			LC109 - TR2/LP30,000 m	0,80
			LC110 - TR2/LP30,500 m	0,80
			LC111 - TR2/LP31,000 m	0,80
			LC112 - TR2/LP31,500 m	0,80
			LC113 - TR2/LP32,000 m	0,80
			LC114 - TR2/LP32,500 m	0,80
			LC115 - TR2/LP33,000 m	0,80
			LC116 - TR2/LP33,500 m	0,80
			LC117 - TR2/LP34,000 m	0,80
			LC118 - TR2/LP34,500 m	0,80
			LC119 - TR2/LP35,000 m	0,80
			LC120 - TR2/LP35,500 m	0,80
			LC121 - TR2/LP36,000 m	0,80
			LC122 - TR2/LP36,500 m	0,80
			LC123 - TR2/LP37,000 m	0,80
			LC124 - TR2/LP37,500 m	0,80
			LC125 - TR2/LP38,000 m	0,80
			LC126 - TR2/LP38,500 m	0,80
			LC127 - TR2/LP39,000 m	0,80
			LC128 - TR2/LP39,500 m	0,80
			LC129 - TR2/LP310,000 m	0,80
			LC130 - TR2/LP310,500 m	0,80
			LC131 - TR2/LP311,000 m	0,80
			LC132 - TR2/LP311,500 m	0,80
			LC133 - TR2/LP312,000 m	0,80
			LC134 - TR2/LP312,500 m	0,80
			LC135 - TR2/LP313,000 m	0,80
			LC136 - TR2/LP313,500 m	0,80
			LC137 - TR2/LP314,000 m	0,80
			LC138 - TR2/LP314,500 m	0,80
			LC139 - TR2/LP315,000 m	0,80

Name	Description	Type	Load cases	Coeff. [-]
			LC140 - TR2/LP315,500 m	0,80
			LC141 - TR2/LP316,000 m	0,80
			LC142 - TR2/LP316,500 m	0,80
			LC143 - TR2/LP317,000 m	0,80
			LC144 - TR2/LP317,500 m	0,80
			LC145 - TR2/LP318,000 m	0,80
			LC146 - TR2/LP318,500 m	0,80
			LC147 - TR2/LP319,000 m	0,80
			LC148 - TR2/LP319,500 m	0,80
			LC149 - TR2/LP320,000 m	0,80
			LC150 - TR2/LP320,500 m	0,80
			LC151 - TR2/LP321,000 m	0,80
			LC152 - TR2/LP321,500 m	0,80
			LC153 - TR2/LP322,000 m	0,80
			LC154 - TR2/LP322,500 m	0,80
			LC155 - TR2/LP323,000 m	0,80
			LC156 - TR2/LP323,500 m	0,80
			LC157 - TR2/LP324,000 m	0,80
BC6	2. SLS| PT| Tram governing	Envelope - serviceability	LC2 - Dead Load	1,00
			LC3 - Edge Load	1,00
			LC4 - Traffic load| P.T| UDL	0,80
			LC9 - Pedestrian Loading on des. loc.	0,80
			LC11 - TR1/LP20,000 m	1,08
			LC12 - TR1/LP20,500 m	1,08
			LC13 - TR1/LP21,000 m	1,08
			LC14 - TR1/LP21,500 m	1,08
			LC15 - TR1/LP22,000 m	1,08
			LC16 - TR1/LP22,500 m	1,08
			LC17 - TR1/LP23,000 m	1,08
			LC18 - TR1/LP23,500 m	1,08
			LC19 - TR1/LP24,000 m	1,08
			LC20 - TR1/LP24,500 m	1,08
			LC21 - TR1/LP25,000 m	1,08
			LC22 - TR1/LP25,500 m	1,08
			LC23 - TR1/LP26,000 m	1,08
			LC24 - TR1/LP26,500 m	1,08
			LC25 - TR1/LP27,000 m	1,08
			LC26 - TR1/LP27,500 m	1,08
			LC27 - TR1/LP28,000 m	1,08
			LC28 - TR1/LP28,500 m	1,08
			LC29 - TR1/LP29,000 m	1,08
			LC30 - TR1/LP29,500 m	1,08
			LC31 - TR1/LP210,000 m	1,08
			LC32 - TR1/LP210,500 m	1,08
			LC33 - TR1/LP211,000 m	1,08
			LC34 - TR1/LP211,500 m	1,08
			LC35 - TR1/LP212,000 m	1,08
			LC36 - TR1/LP212,500 m	1,08
			LC37 - TR1/LP213,000 m	1,08
			LC38 - TR1/LP213,500 m	1,08
			LC39 - TR1/LP214,000 m	1,08
			LC40 - TR1/LP214,500 m	1,08
			LC41 - TR1/LP215,000 m	1,08
			LC42 - TR1/LP215,500 m	1,08
			LC43 - TR1/LP216,000 m	1,08
			LC44 - TR1/LP216,500 m	1,08
			LC45 - TR1/LP217,000 m	1,08
			LC46 - TR1/LP217,500 m	1,08
			LC47 - TR1/LP218,000 m	1,08
			LC48 - TR1/LP218,500 m	1,08
			LC49 - TR1/LP219,000 m	1,08
			LC50 - TR1/LP219,500 m	1,08
			LC51 - TR1/LP220,000 m	1,08
			LC52 - TR1/LP220,500 m	1,08
			LC53 - TR1/LP221,000 m	1,08
			LC54 - TR1/LP221,500 m	1,08
			LC55 - TR1/LP222,000 m	1,08
			LC56 - TR1/LP222,500 m	1,08
			LC57 - TR1/LP223,000 m	1,08
			LC58 - TR1/LP223,500 m	1,08
			LC59 - TR1/LP224,000 m	1,08
			LC109 - TR2/LP30,000 m	1,00
			LC110 - TR2/LP30,500 m	1,00
			LC111 - TR2/LP31,000 m	1,00
			LC112 - TR2/LP31,500 m	1,00
			LC113 - TR2/LP32,000 m	1,00

Name	Description	Type	Load cases	Coeff. [-]
			LC114 - TR2/LP32,500 m	1,00
			LC115 - TR2/LP33,000 m	1,00
			LC116 - TR2/LP33,500 m	1,00
			LC117 - TR2/LP34,000 m	1,00
			LC118 - TR2/LP34,500 m	1,00
			LC119 - TR2/LP35,000 m	1,00
			LC120 - TR2/LP35,500 m	1,00
			LC121 - TR2/LP36,000 m	1,00
			LC122 - TR2/LP36,500 m	1,00
			LC123 - TR2/LP37,000 m	1,00
			LC124 - TR2/LP37,500 m	1,00
			LC125 - TR2/LP38,000 m	1,00
			LC126 - TR2/LP38,500 m	1,00
			LC127 - TR2/LP39,000 m	1,00
			LC128 - TR2/LP39,500 m	1,00
			LC129 - TR2/LP310,000 m	1,00
			LC130 - TR2/LP310,500 m	1,00
			LC131 - TR2/LP311,000 m	1,00
			LC132 - TR2/LP311,500 m	1,00
			LC133 - TR2/LP312,000 m	1,00
			LC134 - TR2/LP312,500 m	1,00
			LC135 - TR2/LP313,000 m	1,00
			LC136 - TR2/LP313,500 m	1,00
			LC137 - TR2/LP314,000 m	1,00
			LC138 - TR2/LP314,500 m	1,00
			LC139 - TR2/LP315,000 m	1,00
			LC140 - TR2/LP315,500 m	1,00
			LC141 - TR2/LP316,000 m	1,00
			LC142 - TR2/LP316,500 m	1,00
			LC143 - TR2/LP317,000 m	1,00
			LC144 - TR2/LP317,500 m	1,00
			LC145 - TR2/LP318,000 m	1,00
			LC146 - TR2/LP318,500 m	1,00
			LC147 - TR2/LP319,000 m	1,00
			LC148 - TR2/LP319,500 m	1,00
			LC149 - TR2/LP320,000 m	1,00
			LC150 - TR2/LP320,500 m	1,00
			LC151 - TR2/LP321,000 m	1,00
			LC152 - TR2/LP321,500 m	1,00
			LC153 - TR2/LP322,000 m	1,00
			LC154 - TR2/LP322,500 m	1,00
			LC155 - TR2/LP323,000 m	1,00
			LC156 - TR2/LP323,500 m	1,00
			LC157 - TR2/LP324,000 m	1,00
BC7.	3. SLS| AT	Envelope - serviceability	LC2 - Dead Load	1,00
			LC3 - Edge Load	1,00
			LC6 - Traffic load| A.T| UDL	1,00
			LC9 - Pedestrian Loading on des. loc.	0,80
			LC60 - TR1/LP10,000 m	1,00
			LC61 - TR1/LP10,500 m	1,00
			LC62 - TR1/LP11,000 m	1,00
			LC63 - TR1/LP11,500 m	1,00
			LC64 - TR1/LP12,000 m	1,00
			LC65 - TR1/LP12,500 m	1,00
			LC66 - TR1/LP13,000 m	1,00
			LC67 - TR1/LP13,500 m	1,00
			LC68 - TR1/LP14,000 m	1,00
			LC69 - TR1/LP14,500 m	1,00
			LC70 - TR1/LP15,000 m	1,00
			LC71 - TR1/LP15,500 m	1,00
			LC72 - TR1/LP16,000 m	1,00
			LC73 - TR1/LP16,500 m	1,00
			LC74 - TR1/LP17,000 m	1,00
			LC75 - TR1/LP17,500 m	1,00
			LC76 - TR1/LP18,000 m	1,00
			LC77 - TR1/LP18,500 m	1,00
			LC78 - TR1/LP19,000 m	1,00
			LC79 - TR1/LP19,500 m	1,00
			LC80 - TR1/LP110,000 m	1,00
			LC81 - TR1/LP110,500 m	1,00
			LC82 - TR1/LP111,000 m	1,00
			LC83 - TR1/LP111,500 m	1,00
			LC84 - TR1/LP112,000 m	1,00
			LC85 - TR1/LP112,500 m	1,00
			LC86 - TR1/LP113,000 m	1,00
			LC87 - TR1/LP113,500 m	1,00

Name	Description	Type	Load cases	Coeff. [-]
			LC88 - TR1/LP114,000 m	1,00
			LC89 - TR1/LP114,500 m	1,00
			LC90 - TR1/LP115,000 m	1,00
			LC91 - TR1/LP115,500 m	1,00
			LC92 - TR1/LP116,000 m	1,00
			LC93 - TR1/LP116,500 m	1,00
			LC94 - TR1/LP117,000 m	1,00
			LC95 - TR1/LP117,500 m	1,00
			LC96 - TR1/LP118,000 m	1,00
			LC97 - TR1/LP118,500 m	1,00
			LC98 - TR1/LP119,000 m	1,00
			LC99 - TR1/LP119,500 m	1,00
			LC100 - TR1/LP120,000 m	1,00
			LC101 - TR1/LP120,500 m	1,00
			LC102 - TR1/LP121,000 m	1,00
			LC103 - TR1/LP121,500 m	1,00
			LC104 - TR1/LP122,000 m	1,00
			LC105 - TR1/LP122,500 m	1,00
			LC106 - TR1/LP123,000 m	1,00
			LC107 - TR1/LP123,500 m	1,00
			LC108 - TR1/LP124,000 m	1,00
BC9	5. ULS| my max	Envelope - ultimate	LC2 - Dead Load	1,20
			LC3 - Edge Load	1,20
			LC9 - Pedestrian Loading on des. loc.	1,08
			LC158 - UDL for max my	1,35
			LC160 - TR3/LP10,000 m	1,35
			LC161 - TR3/LP10,500 m	1,35
			LC162 - TR3/LP11,000 m	1,35
			LC163 - TR3/LP11,500 m	1,35
			LC164 - TR3/LP12,000 m	1,35
			LC165 - TR3/LP12,500 m	1,35
			LC166 - TR3/LP13,000 m	1,35
			LC167 - TR3/LP13,500 m	1,35
			LC168 - TR3/LP14,000 m	1,35
			LC169 - TR3/LP14,500 m	1,35
			LC170 - TR3/LP15,000 m	1,35
			LC171 - TR3/LP15,500 m	1,35
			LC172 - TR3/LP16,000 m	1,35
			LC173 - TR3/LP16,500 m	1,35
			LC174 - TR3/LP17,000 m	1,35
			LC175 - TR3/LP17,500 m	1,35
			LC176 - TR3/LP18,000 m	1,35
			LC177 - TR3/LP18,500 m	1,35
			LC178 - TR3/LP19,000 m	1,35
			LC179 - TR3/LP19,500 m	1,35
			LC180 - TR3/LP110,000 m	1,35
			LC181 - TR3/LP110,500 m	1,35
			LC182 - TR3/LP111,000 m	1,35
			LC183 - TR3/LP111,500 m	1,35
			LC184 - TR3/LP112,000 m	1,35
			LC185 - TR3/LP112,500 m	1,35
			LC186 - TR3/LP113,000 m	1,35
			LC187 - TR3/LP113,500 m	1,35
			LC188 - TR3/LP114,000 m	1,35
			LC189 - TR3/LP114,500 m	1,35
			LC190 - TR3/LP115,000 m	1,35
			LC191 - TR3/LP115,500 m	1,35
			LC192 - TR3/LP116,000 m	1,35
			LC193 - TR3/LP116,500 m	1,35
			LC194 - TR3/LP117,000 m	1,35
			LC195 - TR3/LP117,500 m	1,35
			LC196 - TR3/LP118,000 m	1,35
			LC197 - TR3/LP118,500 m	1,35
			LC198 - TR3/LP119,000 m	1,35
			LC199 - TR3/LP119,500 m	1,35
			LC200 - TR3/LP120,000 m	1,35
			LC201 - TR3/LP120,500 m	1,35
			LC202 - TR3/LP121,000 m	1,35
			LC203 - TR3/LP121,500 m	1,35
			LC204 - TR3/LP122,000 m	1,35
			LC205 - TR3/LP122,500 m	1,35
			LC206 - TR3/LP123,000 m	1,35
			LC207 - TR3/LP123,500 m	1,35
			LC208 - TR3/LP124,000 m	1,35
BC10	5. SLS| my max	Envelope - serviceability	LC2 - Dead Load	1,00
			LC3 - Edge Load	1,00

Name	Description	Type	Load cases	Coeff. [-]
			LC9 - Pedestrian Loading on des. loc.	0,80
			LC158 - UDL for max my	1,00
			LC160 - TR3/LP10,000 m	1,00
			LC161 - TR3/LP10,500 m	1,00
			LC162 - TR3/LP11,000 m	1,00
			LC163 - TR3/LP11,500 m	1,00
			LC164 - TR3/LP12,000 m	1,00
			LC165 - TR3/LP12,500 m	1,00
			LC166 - TR3/LP13,000 m	1,00
			LC167 - TR3/LP13,500 m	1,00
			LC168 - TR3/LP14,000 m	1,00
			LC169 - TR3/LP14,500 m	1,00
			LC170 - TR3/LP15,000 m	1,00
			LC171 - TR3/LP15,500 m	1,00
			LC172 - TR3/LP16,000 m	1,00
			LC173 - TR3/LP16,500 m	1,00
			LC174 - TR3/LP17,000 m	1,00
			LC175 - TR3/LP17,500 m	1,00
			LC176 - TR3/LP18,000 m	1,00
			LC177 - TR3/LP18,500 m	1,00
			LC178 - TR3/LP19,000 m	1,00
			LC179 - TR3/LP19,500 m	1,00
			LC180 - TR3/LP110,000 m	1,00
			LC181 - TR3/LP110,500 m	1,00
			LC182 - TR3/LP111,000 m	1,00
			LC183 - TR3/LP111,500 m	1,00
			LC184 - TR3/LP112,000 m	1,00
			LC185 - TR3/LP112,500 m	1,00
			LC186 - TR3/LP113,000 m	1,00
			LC187 - TR3/LP113,500 m	1,00
			LC188 - TR3/LP114,000 m	1,00
			LC189 - TR3/LP114,500 m	1,00
			LC190 - TR3/LP115,000 m	1,00
			LC191 - TR3/LP115,500 m	1,00
			LC192 - TR3/LP116,000 m	1,00
			LC193 - TR3/LP116,500 m	1,00
			LC194 - TR3/LP117,000 m	1,00
			LC195 - TR3/LP117,500 m	1,00
			LC196 - TR3/LP118,000 m	1,00
			LC197 - TR3/LP118,500 m	1,00
			LC198 - TR3/LP119,000 m	1,00
			LC199 - TR3/LP119,500 m	1,00
			LC200 - TR3/LP120,000 m	1,00
			LC201 - TR3/LP120,500 m	1,00
			LC202 - TR3/LP121,000 m	1,00
			LC203 - TR3/LP121,500 m	1,00
			LC204 - TR3/LP122,000 m	1,00
			LC205 - TR3/LP122,500 m	1,00
			LC206 - TR3/LP123,000 m	1,00
			LC207 - TR3/LP123,500 m	1,00
			LC208 - TR3/LP124,000 m	1,00

24. Result classes

Name	Description	List
RC1	ULS	BC1 - Envelope - ultimate
		BC2 - Envelope - ultimate
		BC3 - Envelope - ultimate
		BC4 - Envelope - ultimate
		BC9 - Envelope - ultimate
RC2	SLS	BC5 - Envelope - serviceability
		BC6 - Envelope - serviceability
		BC7. - Envelope - serviceability
		BC8 - Envelope - serviceability
		BC10 - Envelope - serviceability

25. Line force on 2D member edge

Name	2D member	Type	Dir	Value - P_1 [kN/m]	Pos x_1	Loc	Edge
	Load case	System	Distribution	Value - P_2 [kN/m]	Pos x_2	Coor	Orig
LFS1	E1	Force	Z	-2,00	0.000	Length	1
	LC3 - Edge Load	LCS	Uniform		1.000	Rela	From start
LFS2	E1	Force	Z	-2,00	0.000	Length	3
	LC3 - Edge Load	LCS	Uniform		1.000	Rela	From start

26. 2D member - Internal forces

Linear calculation, Extreme : Global
Selection : All
Class : RC1
Elementary design magnitudes. In nodes, avg. on macro.

Member	elem	Case	mxD+ [kNm/m]	myD+ [kNm/m]	mxD- [kNm/m]	myD- [kNm/m]	nxD [kN/m]	nyD [kN/m]
E1	180	RC1	**-1,33**	0,00	0,69	11,33	**0,00**	**0,00**
E1	61	RC1	**166,22**	**432,51**	-12,48	**0,00**	0,00	0,00
E1	2310	RC1	0,00	**-100,02**	373,90	17,54	0,00	0,00
E1	120	RC1	25,46	74,09	**-79,54**	0,00	0,00	0,00
E1	147	RC1	0,00	-4,26	**1712,15**	91,88	0,00	0,00
E1	1	RC1	0,00	26,97	54,57	0,00	0,00	0,00
E1	1195	RC1	0,00	217,40	737,57	**332,06**	0,00	0,00
E1	1	RC1	0,00	-11,02	119,02	77,94	0,00	0,00

27. 2D member - Internal forces

Linear calculation, Extreme : Global
Selection : All
Class : RC1
Basic magnitudes. In nodes, avg. on macro.

Member	elem	Case	mxy [kNm/m]
E1	1196	RC1	**-317,16**
E1	1144	RC1	**317,09**

28. 2D member - Internal forces; mxD-

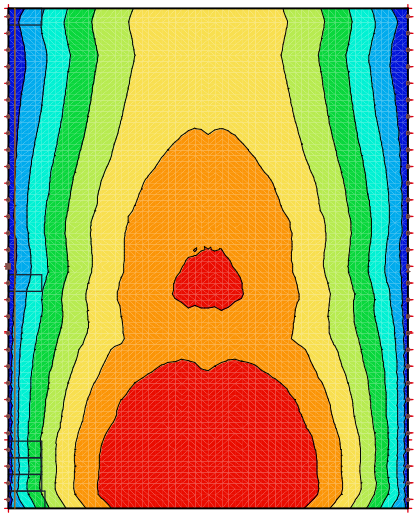

29. 2D member - Internal forces; myD-

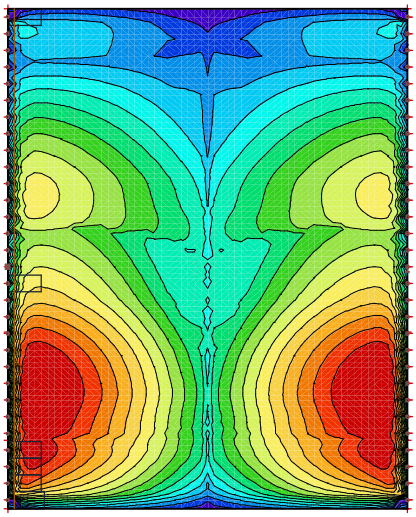

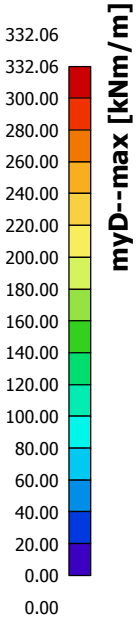

30. 2D member - Internal forces; mxy

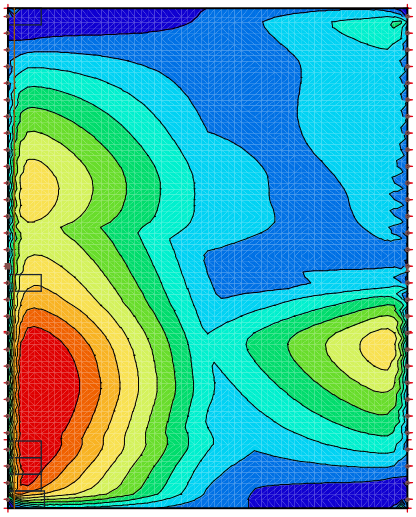

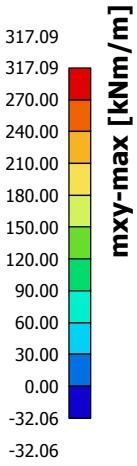

31. Section on plate

Name	Draw	Direction of cut
Snede1	Z direction	0,000[m] / 0,000[m] / 1,000[m]

32. Averaging strip

Name	2D member	Type	Direction	Width [m]	Coord X [m]	Coord Y [m]	Coord Z [m]	Coord x [m]	Coord y [m]	Coord z [m]
Strook1	E1	Strip	perpendicular	2,200	1,100	0,000	0,000	1,100	0,000	0,000
					1,100	1,000	0,000	1,100	1,000	0,000
Strook2	E1	Strip	perpendicular	2,000	1,000	1,000	0,000	1,000	1,000	0,000
					1,000	2,000	0,000	1,000	2,000	0,000
Strook4	E1	Strip	perpendicular	2,000	1,000	2,000	0,000	1,000	2,000	0,000
					1,000	3,000	0,000	1,000	3,000	0,000
Strook5	E1	Strip	perpendicular	2,000	1,000	30,000	0,000	1,000	30,000	0,000
					1,000	29,000	0,000	1,000	29,000	0,000
Strook6	E1	Strip	perpendicular	2,000	1,000	3,000	0,000	1,000	3,000	0,000
					1,000	4,000	0,000	1,000	4,000	0,000
Strook7	E1	Strip	perpendicular	2,000	1,000	13,000	0,000	1,000	13,000	0,000
					1,000	14,000	0,000	1,000	14,000	0,000

Explanations of symbols	
2D member	2D member E1

33. 2D member - Internal forces

Linear calculation, Extreme : Global
Selection : Snede1,E1
Class : RC1
Basic magnitudes. In nodes, avg. on macro.

Section	elem	Case	vx [kN/m]	vy [kN/m]
Snede1	4981	RC1	**31,53**	-44,42
Snede1	1	RC1	**584,56**	**374,64**
Snede1	1681	RC1	44,83	**-175,45**

34. 2D member - Internal forces; vx

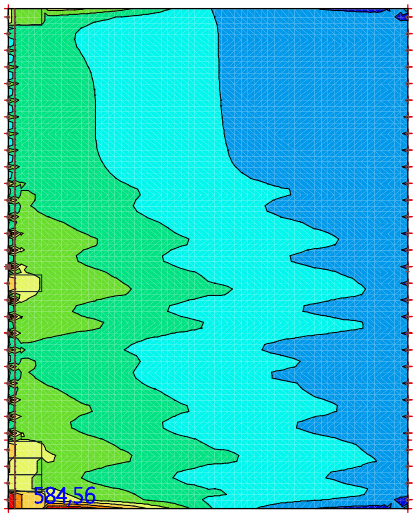

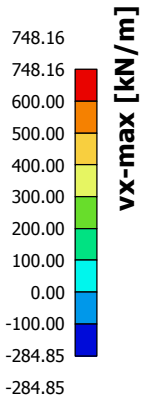

F. High strength fibre reinforced concrete

F.1 General

In the following the calculations are presented for the HPC C90/105 design. These calculations serve the purpose to back up the results given in the main part of the report. This calculation will have the same amount of detail as the UHPC calculation. First the cross-sectional and material properties are specified. Then the loads are defined. Afterwards a SCIA model is presented. With this model the forces caused by the loads is determined. Then with these results a design calculation is performed in both ULS (moment and shear capacity) and SLS (crack width, deflection and fatigue).

F.2 Material properties

The concrete and steel material properties are shown Table F-1. The values are based on NEN-EN-1992-1-1. The steel fibre volume will be 2.15% just as with the UHPC design.

Table F-1: Concrete and steel material properties

Concrete C90/105		
ρ_c		2500 kg/m3
f_{ck}		90 N/mm^2
f_{cm}	f_{ck}+8	98 N/mm^2
f_{ctk}		3.5 N/mm^2
γ_c		1.5
α_{cc}		1.0
K_{glob}		1.25
K_{loc}		1.75
f_{cd}	f_{ck}/γ_c	60 N/mm^2
$f_{ctd,1}$	f_{ctk}/γ_c	2.33 N/mm^2
E_{cm}		44000 N/mm^2
ε_{c3}		2.3 ‰
ε_{cu3}		2.6 ‰

Reinforcing steel B500		
ρ_s		7850 kg/m3
f_{yk}		500 N/mm^2
γ_s		1.15
f_{yd}	f_{yk}/γ_s	435 N/mm^2
E_s		210000 N/mm^2

Prestressing steel Y1860		
f_{pk}		1860 N/mm^2
$f_{p0.1k}$	0,9*f_{pk}	1674 N/mm^2
γ_s		1.1
f_{pd}	$f_{pk0.1}/\gamma_s$	1522 N/mm^2
σ_{pm0}	0.75*f_{pk}	1395 N/mm^2
E_p		195000 N/mm^2
A_p [ϕ_{strand}] (main direction)		139 mm^2 [15.2mm]
A_p [ϕ_{strand}] (transverse dir.)		150 mm^2 [15.7mm]

F.3 Cross sectional properties

The dimension and thus the cross sectional properties will be the same as for the C50/60 design. Because C90/105 has a lower strength it is wiser to keep the thicknesses of the flanges and webs the same as for the C50/60 design. Now there is a higher chance that the structure will meet the safety requirements. However the width will stay 1000mm instead of 1500mm. The cross section of the HPC girder is seen in Figure F-1.

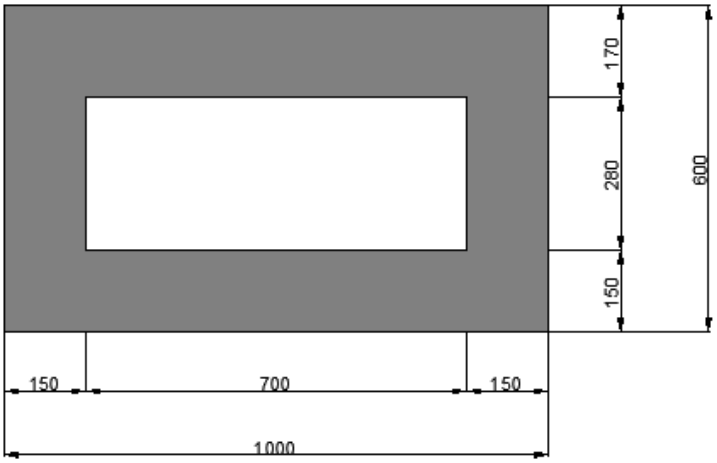

Figure F-1: Cross section UPHC box girder

In Table F-2 the dimensions and cross sectional properties of one girder are shown.

Table F-2: Dimensions and cross sectional properties of box girder

L	Span	24 m
H	Height girder	0.6 m
B	Width girder	1.0 m
b_{web}	Web thickness	0.15 m
$h_{top,fl}$	Top flange thickness	0.17 m
$h_{bot,fl}$	Bottom flange thickness	0.15 m
A_c	Cross sectional area	0.404 m^2
z_t	Distance top fibre to c.a.	0.295 m
z_b	Distance bottom fibre to c.a.	0.305 m
I_c	Moment of Inertia	0.0167 m^4
$W_{c,t}$	Section Modulus top fibre	0.0566 m^3
$W_{c,b}$	Section Modulus bottom fibre	0.0548 m^3

The values in the table are calculated as follows:

$A_c = B*H - (H - h_{top,fl} – h_{bot,fl}) *(B-2* b_{web})$

$z_t = \{B*H*0.5H – (H- h_{top,fl} – h_{bot,fl}) * (B-2* b_{web}) * 0.5*(H- h_{top,fl} – h_{bot,fl})+h_{top,fl})\}/ A_c$

$z_b = H - z_t$

$I_c = 2 * [(1/12)*b_{web}*H^3+b_{web}*H*(0,5*H-zt)^2] + [(1/12)*(B-2*b_{web})*h_{top,fl}^3+ (B -2*b_{web}) *h_{top,fl}* (z_t - 0,5*h_{top,fl})^2] + [(1/12)*(B-2*_{bweb})*h_{bot,fl}^3 + (B-2*b_{web})*h_{bot,fl}*(z_b-0,5*h_{bot,fl})]$

$W_{c,t} = I_c/z_t$

$W_{c,b} = I_c/z$

F.4 Exposure class and concrete cover

The exposure class and concrete cover are determined according to NEN-EN-1992-1-1 cl. 4.2 and cl. 4.4.1 respectively. For the outer perimeter of the box girder the exposure class is set to be XC4. For the inner perimeter of the box girder the exposure class is set to XC1, since the inside is not as exposed as the outside of the girder.

The nominal cover is $c_{nom} = c_{min} + \Delta c_{dev}$ (with $\Delta c_{dev} = 5$ mm)
The minimum cover is determined with:

- $c_{min} = \max \{c_{min,b}; c_{min,dur} + c_{dur,\gamma} - \Delta c_{dur,st} - \Delta c_{dur,add}; 10 \text{ mm}\}$
- $c_{min,b}$ = the minimum cover due to bond requirement. For pretensioned member: $c_{min,b} = \max(1.5*\varphi_{strand} ; d_{g,max})$. Since the maximum aggregate is small the governing value is $1.5*\varphi_{strand} = 22.8$ mm
- $c_{min,dur}$ is the minimum cover due to environmental conditions. So it has to be based on exposure class XC4. In the case for presressing steel and with structural class S4, $c_{min,dur}$ = 40mm (for XC1 $c_{min,dur}$= 25mm). In case of reinforcement with S4, $c_{min,dur}$ = 30mm (for XC1 $c_{min,dur}$= 15mm)
- $c_{min,p}$ = is the minimum cover due to the concrete placement conditions, which is $\max(1.5l_f; 1.5D_{max} ; \varphi_{strand})$. $c_{min,p} = 19.5$ mm
- $\Delta c_{dur,\gamma} = \Delta c_{dur,st} = \Delta c_{dur,add} = 0$mm
- Based on the determined values, the governing minimum cover is the one due to environmental conditions. So c_{nom} = 40+5 mm = **45 mm** for the outer perimeter and **30mm** for the inner perimeter of the box girder.

F.5 Load cases and load combinations

Before the SCIA Engineer model is presented, the loads have to be determined first. There are a lot of different loads that will work on the bridge. And these loads will not occur exclusively. Therefore it is important to determine all the load cases and load combinations for the bridge. The load cases and combinations are described more in detail in appendix B.

Basically the following load cases will occur on the bridge:

Permanent loads:	
LC1: Self-weight girders (not included in SCIA)	A_c*25 kN/m
LC2: Dead load	
– Pavement	4.6 kN/m^2
– Asphalt	4.8 kN/m^2
– Concrete filling around tram rails	3.5 kN/m^2
LC3: Steel railing and natural stone elements (Edge Load)	2.0 kN/m^2
Variable loads:	
LC4&5: Traffic loads with presence of trams (UDL & tandem axle)	Conform Load Model 1
LC6&7: Traffic loads with absence of trams (UDL & tandem axle)	Conform Load Model 1
LC8: Tram-axle loads (No UDL specified for tram loads)	Conform GVB
LC9: Pedestrian loads over whole width (crowd loading)	5.0 kN/m^2
LC10: Pedestrian loads on designed locations.	5.0 kN/m^2

In total there are five main load combinations:

- Combination 1: Traffic loads in the presence of tram loading, where the traffic loads are the leading variable load. (1 LM1 TS + 2 tram TS)
- Combination 2: Traffic loads in the presence of tram loading, where the tram loading is the leading variable load. (1 LM1 TS + 2 tram TS)
- Combination 3: Traffic loads in absence of tram loading. (3 LM1 TS)
- Combination 4: Crowd loading
- Combination 5: Governing transverse moment

F.6 Results SCIA Engineer

The same results that were used in the UHPC design will be used here as well. Even though the orthotropic parameters for HPC and UHPC are not the same, this will hardly have an influence on the results and both designs have the same amount of girders. So it is assumed that the same internal forces occur in the HPC design as in the UHPC design. This is allowed, because SCIA provides higher internal forces when the stiffness is higher. The stiffness of HPC is lower so SCIA would give slightly lower values. Furthermore the difference in these values is not high. Therefore as already said it is safe to use the results from the UHPC design.

F or bending moment resistance check:
mxD^-: 1712.15 kNm/m

For shear and [torsion + shear] safety check
mxy: 317.09 kNm/m (When torsion is governing)
116.75 kNm/m (When shear is governing)

vx: 235.94 kN/m (When torsion is governing)
584.56 kN/m (When shear is governing)
For transverse moment check
myD^-: 332.06 kNm/m
myD^+ 303.09 kNm/m

The presented values will be used for the safety checks. However these values are only based on the loads working on the bridge. Here no self-weight and no prestressing is included yet. These have to be added separately. This will be done in the following, where also the amount of prestressing will be determined.

F.7 Prestress tendon profile

The beams will consist of pre-tensioned strands, as the beams are prefabricated. The tendon profile is shown in Figure F-2. The tendon consists of straight and kinked strands. The kinked strands cause an upward force P_u at the deviation points. This point is at a distance 'a' from the support. The kinked strands are placed in the webs. In each web *4* strands are placed so in total there are *8* kinked profiles. The strands will be placed as high as possible to ensure a high upward force. This force slightly reduces the total shear force.

Assumed is that the kinked strands will be placed so that the gravity point of these strands is $z_b - h_{top} - 2*\varphi_{strand}$ = 94 mm above the centroid axis. Most of the strands will be placed in the bottom flange. This means that the fictitious tendon (or the gravity point) does not coincide with the neutral axis (dashed line). So these will create a moment at the heads due to eccentricity, so a capacity check at the support has to be made to make sure the structure can take the moments.

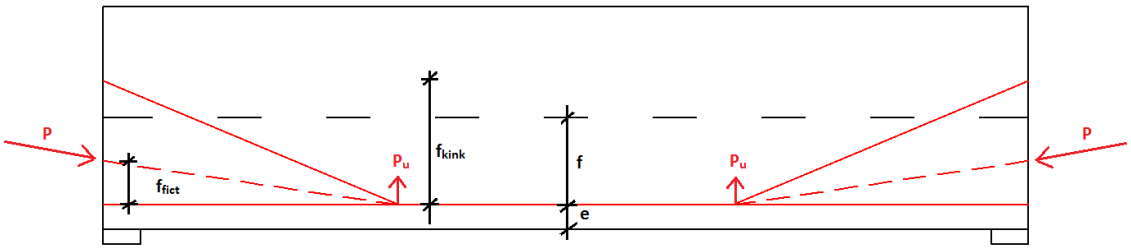

Figure F-2: Tendon profile pre-tensioned strands

The strands have a certain eccentricity in the mid span with reference to the bottom fibre. The minimum eccentricity (e) for the fictitious tendon with reference to the bottom fibre can be determined by taking the cover and strand spacing into account.
The nominal cover is 45mm. One strand has a diameter of 15.2mm and the gap between two strands vertically has to be $2*\varphi_{strand}$ which is 30.4 mm (here the maximum aggregate is not governing as only fine material is used. However the strands will not be placed directly underneath each other but in the way as done in the UHPC and C50/60 design. Therefore the distance is taken as $\varphi_{strands}$ instead. Expected is that some torsional reinforcement will be necessary, which also requires some stirrups.
So the eccentricity $e=c_{nom}+\varphi_{bar}+1.5\varphi_{strand}$ = 75.8 mm.
This results in a drape of: $f = z_b - e$ = 0.229m.
The kinks are at a distance of a = 8m from the support.

The upward force is calculated according to the drape of the kinked strands f_{kink} = f+0.094=0.323m. The drape of the fictitious tendon can be determined once the total amount of strands is determined. Then it will be known how much strands will go in the bottom flange. The rest of the values in the figure are:
$P_u = P_{kink} * \sin \alpha_{kink} \approx P_{kink} * (f_{kink}/a)$ or $P*(f_{fict}/a)$
$M_{p,mid} = P*f$

The prestress force is determined by taking a couple of requirements into account that concern stresses in the concrete. These requirements need to be applied in the governing cross section (cross section with highest bending moment). Here that is in the middle of the beam.

$$t = 0 \text{ at top fibre: } -\frac{P_{m0}}{A_c} + \frac{M_{p,0}}{W_{ct}} - \frac{M_g}{W_{ct}} \leq 0$$

$$t = 0 \text{ at bottom fibre: } -\frac{P_{m0}}{A_c} - \frac{M_{p,0}}{W_{cb}} + \frac{M_g}{W_{cb}} \geq -0.6 * f_{ck}$$

$$t = \infty \text{ at bottom fibre: } -\frac{P_{m\infty}}{A_c} - \frac{M_{p,\infty}}{W_{cb}} + \frac{M_{tot}}{W_{cb}} \leq 0$$

The first requirement states that at the construction of the bridge, when only dead loads are present, no tensile stresses are allowed which could be caused by the prestressing. The second requirement states that the compression stresses can't be too high at the bottom of the beam during construction. The third requirement states that during the use of the bridge, where all the loads are present, no tensile stresses are allowed at the bottom of the beam. Here $P_{m\infty}$ is used instead of P_{m0}. The difference is that immediate and time dependent losses are taken into account here.

Assumed is a total loss of 16% so $P_{m\infty} = 0.84*P_{m0}$. After the prestress force is determined with the three requirements, the actual losses (direct and time dependent losses) have to be determined and checked if the assumption of a 16% loss is on the safe side.

F.8 Required amount of prestressing strands

The required amount of prestressing strands in one beam is determined using the three requirements presented in paragraph F.7. To use these requirements the bending moments working on the beam need to be determined. To determine the total moments and the moments caused by the dead load. The result of mxD- in SCIA (paragraph F.6) has to be split apart. This means finding out what load cases contribute to the governing moment. This has been done by finding the node in SCIA, where the highest moment is located and writing down the results that SCIA gives in that node. The results are presented in Table F-3. The results are both in SLS and ULS. Also given are the resulting loads in kN/m.

Table F-3: Bending moments in one beam

mxD-	SLS			ULS	
	kNm (*1 beam*)	q [kN/m]	γ	kNm (*1 beam*)	q [kN/m]
dead load	294,83	4,095	1,2	353,80	4,914
edge load	13,98	0,194	1,2	16,776	0,233
AT| UDL	351,05	4,876	1,35	473,92	6,582
AT| TS	505,96	7,027	1,35	683,046	9,487
Pedestrian loads	170,94	2,374	1,08	184,62	2,564
TOTAL	**1336,76**	**18,566**		**1712,15**	**23,780**

In addition to these moments the moment due to self-weight needs to be determined as well. Assumed is that on each side a hammerhead of 1m long is located:
$q_{self} = (L-2)*A_c*\gamma_{conc} + 2*(H*B)*\gamma_{conc} = 10.508$ kN/m in SLS*1.2 = 12.61 kN/m in ULS
$M_{self} = (1/8)*q_{self}*L^2 = 756.6$ kNm
The moment due to all static loads now becomes:
$q_{perm} = q_{dead} + q_{edge} + q_{self} = 14.798$ kN/m in SLS and 17.757 kN/m in ULS
$M_g = 1065.41$ kNm
The moment due to the variable loads is:
$q_{var} = 14.28$ kN/m in SLS and 18.63 kN/m in ULS
$M_q = 1027.95$ kNm
This results in a total moment of:
$M_{tot} = 2093.36$ kNm

Now that the moments have been determined, the prestressing force can be calculated:

t=0: σ < 0	P_{m0} <	11960.326 kN
t=0: σ >-0,6*f_{ck}	P_{m0} <	11031.826 kN
t=∞: σ < 0	P_{m0} >	6835.73 kN

The minimum prestressing force has to be 6835.73 kN. This results in (σ_{pm0} = 1395MPa; $A_{p,strand}$ = 139mm^2): 6835.73/(1395*139) = 36 strands. These 36 strands have a cross sectional area of A_p = 5004 mm^2 in total, which results in a force of $P_{m0} = 6980.58$ kN.
The moment caused by the prestressing force is:
$M_p = P_{m\infty}*(f/a)*a = 1343.09$ kNm
The stress caused by the prestress force during t=∞ in the concrete is: $\sigma_{cp} = 0.84*P_{mo}/A_c = 14.51$ N/mm^2.

F.9 Prestressing Losses

The required amount of strands and also the resulting prestress force are determined. Now the actual losses have to be determined. The percentage of the total losses should be lower than the assumed losses of 16%, so that the determined prestress force is on the save side. If this is not the case the amount of strands has to be determined again with the correct percentage of losses.
The losses can be divided in direct and time dependent losses.

F.9.1 Direct losses

For pre-tensioned strands the elastic shortening is part of the direct losses. When the strands are released after tensioning the strands will shorten elastically. The result is that the stresses and forces in these strands decrease. Also occurring is concentrated friction at the kink points of the strands but these can be neglected when looking at the big picture.

F.9.1.1 Losses due to elastic deformation

The loss of force in one strand due to elastic shortening is (NEN-EN-1992-1-1 formula 5.44):

$$\Delta P_{el} = A_p * E_p * \frac{\Delta\sigma_c(t)}{E_{cm}(t)}$$

And $\Delta\sigma_c(t)$ being the variation of stress at the centre of gravity of the strands at time t:

$$\Delta\sigma_c(t) = \frac{P_{m0}}{A_c} * [1 + \frac{e_p^2 * A_c}{I_c}]$$

Here e_p is the distance of the neutral axis to the considered strand. In this case the governing strands are those in the bottom flange, because these provide the highest eccentricity.
For these strands e_p = f (drape) =241.1 mm.
The elastic deformation occurs after releasing the strands so at t=0.
For one strand: A_p = 139 mm^2 and $P_{m0} = A_p * \sigma pm0$ = 193.91kN.
$\Delta\sigma_c$ = 1.21N/mm^2. The loss of force in one strand now becomes: ΔP_{el} = 0.591 kN. The loss in force becomes 34*0.66 = 21.26 kN.

To compensate the loss in forces due to elastic shortening it is allowed to overstress the strands, provided that the stress stays under the maximum allowed stress $\sigma_{p,max}$ = min{k1*f_{pk};k2*$f_{p0,1k}$) = min{0.8*1860; 0.9*1674} = 1488 N/mm^2.
The extra stress per strand needed to compensate the loss is: $\sigma_{extra} = \Delta P_{el}/A_p$ = 4.25 N/mm^2. So the total stress applied becomes $\sigma_{pm0} + \sigma_{extra}$ = 1399.25 N/mm^2 which is far below the maximum allowed stress.

F.9.2 Time dependent losses

Certain losses appear during the life span of the structure. These are shrinkage and creep of the concrete and relaxation of the strands. All these losses can be combined in one formula which is given in NEN-EN-1992-1-1 formula 5.46:

$$\Delta P_{c+s+r} = A_p \Delta\sigma_{p,c+s+r} = A_p \frac{\varepsilon_{cs} E_p + 0{,}8\Delta\sigma_{pr} + \frac{E_p}{E_{cm}} \varphi(t,t_0).\sigma_{c,QP}}{1 + \frac{E_p}{E_{cm}} \frac{A_p}{A_c}(1 + \frac{A_c}{I_c} z_{cp}^2)[1 + 0{,}8\,\varphi(t,t_0)]}$$

In this formula the shrinkage strain, creep coefficient and the stress loss due to relaxation can be determined separately according to the Eurocode as will be explained later on.

F.9.2.1 Losses due to shrinkage

The total shrinkage of the concrete can be determined according to NEN-EN-1992-1-1 cl. 3.1.4(6). The total shrinkage is defined as:

$\varepsilon_{cs} = \varepsilon_{cd} + \varepsilon_{ca}$

Where

ε_{cs} is the total shrinkage

ε_{cd} is the drying shrinkage

ε_{ca} is the autogenous shrinkage

$\varepsilon_{cd}(t) = \varepsilon_{cd0} * k_h * \beta_{ds}(t,ts)$

Where

k_h is a coefficient depending on the notional size h_0 according to table 3.3 in NEN-EN-1992-1-1.

ε_{cd0} is the nominal unrestrained drying shrinkage, which is dependent on the strength class and relative humidity

$\beta_{ds}(t,ts)$ is a factor that takes the age of the concrete into account:

$$\beta_{ds}(t, t_s) = \frac{(t - t_s)}{(t - t_s) + 0.04\sqrt{h0^3}}$$

For C90/105 with RH=80%: $\varepsilon_{cd0} = 0.13*10^{-3}$.

$\beta_{ds}(t,ts)$ =1 for t=100 years

$h_0 = 2*A_c/u = 1000*2*0.404/3.2 = 252.5$ mm with interpolation between h_0 =200 and 300 mm for k_h is found: $k_h = 0.7975$.

So $\varepsilon_{cd} = 0.104*10^{-3}$

$\varepsilon_{ca}(t) = \beta_{as}(t)*\varepsilon_{ca}(\infty)$

Where

$\varepsilon_{ca}(\infty) = 2.5(f_{ck}-10)*10^{-6} = 0.2*10^{-3}$

$\beta_{as}(t) = 1-\exp(-0.2t^{0.5})$: For t=100 years $\beta_{as} = 1$

So $\varepsilon_{ca} = 0.2*10^{-3}$.

This results in a total shrinkage of: $\varepsilon_{cs} = 0.304*10^{-3}$

F.9.2.2 Losses due to creep

The creep coefficient φ(t,t0) can be determined by using figure 3.1 in NEN-EN-1992-1-1. Assuming outside conditions and t=100 days with a h_0 of 235,5mm:

φ(t,t0) = 0.8

F.9.2.3 Losses due to relaxation

The relaxation in the prestress steel can be determined with the following equation, which is given in NEN-EN-1992-1-1 formula 3.30:

$$\text{class 2: } \frac{\Delta\sigma_{pr}}{\sigma_{pi}} = 0.66 * \rho_{1000} * e^{(9.1*\mu)} * \left(\frac{t}{1000}\right)^{(0.75*(1-\mu)} * 10^{-5}$$

With:

Absolute value of initial prestress:	$\sigma_{pi} = P_{m0}/A_p = 1395$ N/mm^2
Value of relaxation loss at 1000 hours after tensioning: ρ_{1000}:	2.5%
Time after tensioning:	t=500.000 hours
μ:	σ_{pi}/f_{pk} =0.75

Filling everything in the equation gives: $\Delta\sigma_{pr}$ = 67.948N/mm^2. Shrinkage and creep reduce the relaxation. Therefore, when combining the three, the relaxation loss can be reduced with a factor 0.8. The loss in force due to relaxation becomes: $P_{pr} = 0.8 * \Delta\sigma_{pr} * A_p$ = 272 kN.

F.9.2.4 Total time dependent losses

The formula for the total time dependent losses was:

$$\Delta P_{c+s+r} = A_p \Delta\sigma_{p,c+s+r} = A_p \frac{\varepsilon_{cs} E_p + 0{,}8\Delta\sigma_{pr} + \frac{E_p}{E_{cm}} \varphi(t,t_0).\sigma_{c,QP}}{1 + \frac{E_p}{E_{cm}} \frac{A_p}{A_c}\left(1 + \frac{A_c}{I_c} z_{cp}^2\right)[1 + 0{,}8\,\varphi(t,t_0)]}$$

All values are determined except for $\sigma_{c,QP}$. This is the compressive stress in the concrete caused by the dead load, prestressing and quasi permanent actions:

$$\sigma_c = -\frac{P_{m0}}{A_c} - \frac{P_{m0} * f^2}{I_c} + \frac{M_g}{W_b} + \frac{\psi * M_q}{W_b}$$

The quasi permanent factor ψ_2 for LM1 and pedestrian loads is 0.4. This results in a compressive stress of:

$$\sigma_c = -\frac{6593}{0.404} - \frac{6593 * 0.229^2}{0.0167} + \frac{1065}{0.055} + \frac{0.4 * 712}{0.055} = -23.05\text{N/mm}^2$$

The losses have to be added up so the absolute value is taken:

$|\sigma_{c,QP|}$ = 21.48 N/mm^2

When all the parameters are filled in the main formula, the total stress loss due to time dependent losses becomes:

$\Delta\sigma_{p,c+s+r}$ = 135.7 N/mm^2.

This is 9.73% of σ_{pm0}, which is below the assumed loss of 16% so the assumption was on the safe side.

F.9.2.5 New amount of required prestress strands

Because the actual losses are smaller than the assumed loss, the losses will be set to 11%. Putting it to 11% results in a smaller amount of strands, while still taking unforeseen losses (such as friction at the deviators). With the losses being 11% the new minimum prestress force becomes:

Pm0 = 6451.7 kN.

The minimum required strands become 34 (instead of 36).

The total area of the strands is now: A_p = 4726 mm^2 (Pm0=6592.8 kN).

The prestress force delivers a vertical force at the deviators P_u, which is equal to: $P_{u0} = P_{m0} * (f_{fict}/a)$. The fictitious drape f_{fict} can be determined by finding the gravity point of all strands. There are 34 strands in total. With 8 strands in the webs the amount of strands in the bottom flange are 26. $F_{fict} = f_{kink} - (26A_p * f_{kink}/34A_p)$ = 0.076 m. This results in a P_{u0} = 62.64kN and P_u = 55.75 kN.

As can be expected the fictitious drape is very low because the gravity point is very close to the bottom flange, due to the high amount of strands there. The gravity point is at a distance of $f-f_{fict}$ = 0.153m from the neutral axis. This basically means the moment due to prestressing isn't zero anywhere.

F.10 Bending moment capacity

It is a requirement that the bending moment resistance is higher than the design bending moment: $M_{Rd} > M_{Ed}$.

$M_{Ed} = \gamma_g * M_g + \gamma_q * M_q - 1.0 * M_p$
Where:
$M_g(x) = 0.5 * q_g * x * (L-x)$
$M_q(x) = 0.5 * q_q * x * (L-x)$
$M_p(x) = P_u * a + P_m * (f - f_{fict})$ $0 \leq x < a$
$P_m * f$ $x \geq a$

The parameters are:

Load of self-weight (ULS):	$q_{self} =$ 12.61 kN/m
Permanent load (ULS):	$q_{perm} =$ 17.76 kN/m
Variable load (ULS):	$q_{var} =$ 18.63 kN/m
Prestress force at t=0:	$P_{m0} =$ 6592.77 kN
Prestress force at t=∞:	$P_{m\infty} =$ 5867.57 kN
Drape:	f = 0.229 m
Eccentricity of strands with regards to neutral axis:	$f - f_{fict} =$ 0.153m

It is possible that the eventual governing design bending moment is found at the construction stage (t=0) and perhaps at the support, because the prestressing causes a moment there.. So the bending moment will be determined for the whole span at multiple stages: These stages and the bending moments are:

- t=0 only self weight: $M_{Ed} = M_{self} - M_p$
- t=0 permanent loads: $M_{Ed} = M_{perm} - M_p$
- t=∞ all loads + torsion: $M_{Ed} = M_{perm} + M_{var} - M_p$

In Figure F-3 the moment lines are shown, for multiple stages. The governing M_{Ed} = 1276.1 kNm. The moment at the support is 1008.95 kNm. Technically right at the support the prestress force is also zero. The force has a certain transmission length, where after the force is fully transferred in the concrete.

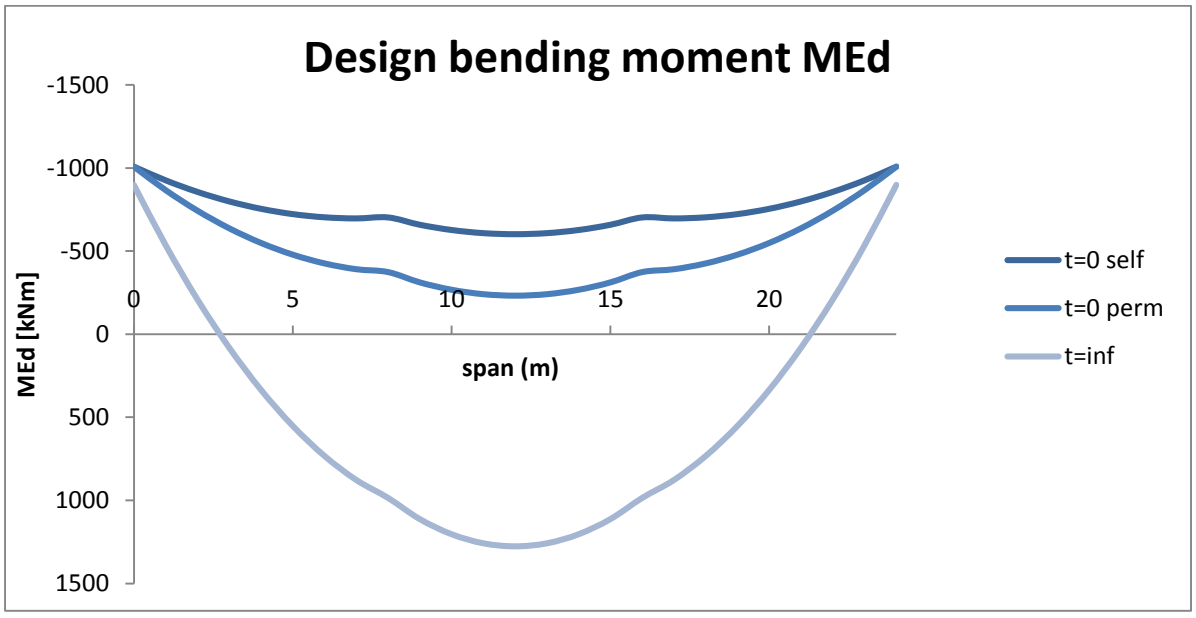

Figure F-3: Design bending moment at multiple stages

The moment capacity should be high enough to resist the determined $M_{Ed.}$. To determine the moment capacity, the same approach is used as with the UHPC design, since both consist of steel fibres so in the HPC design the tensile capacity may be taken into account as well.
The only difference here is that $f_{ctd2} = f_{cdt1}$, because it is not known what f_{ctd2} for HPC is, so this assumption neglects the hardening part, which makes it a safe assumption as the capacity is slightly underestimated. To determine M_{Rd} one has to assume equilibrium of internal forces in the cross section and with that assumption determine M_{Rd}. The general case of internal forces is seen in Figure F-4.

For equilibrium the following statement needs to hold true: $N_c - N_t = P_{m\infty} + \Delta N_p + N_s$. The last term N_s is removed, as there is no bending reinforcement applied.

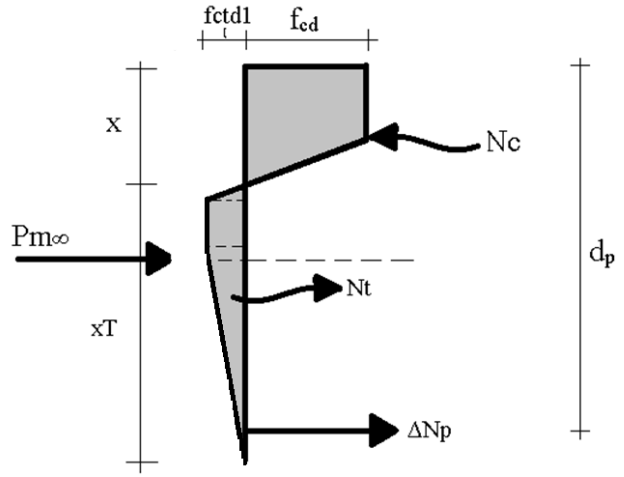

Figure F-4: Equilibrium of internal forces

Here unknowns are the height of the compressive (x) and tension (xT) zone. Because of the strain being assumed linear over the whole height, xT can be rewritten in terms of x. For a certain x there is equilibrium of forces. These forces can all be written in terms of x, making x the only unknown. However a box girder is used, which means that the width is not constant over the height. This will lead to multiple situations that can occur and thus different derivations (of internal forces) and results for the compressive zone height. These situations were already determined in the UHPC design and these situations can be applied here as well. The compressive strain limits are derived from the Eurocode and the tensile strain limits are derived according to the formulas in the AFGC Recommendations:
ε_{c3} = 2.3‰
ε_{cu3} = 2.6‰
$\varepsilon_{ct} = f_{ctd,1}/E_c$ =0.05303‰
$\varepsilon_{u0,3} = \varepsilon_{ct}$ + w0.3(=0.3mm)/ l_c(=2H/3) = 0.80303‰
$\varepsilon_{ctu} = l_f$ (=13mm)/4l_c = 8.125‰

For determining the moment capacity a maple sheet is used:

MAPLE SHEET: DETERMINATION OF Xu and MRd FOR HPC C90/105

Dimension

$restart;$
$H := 600 :$
$B := 1000 :$
$htop := 170 :$
$hbot := 150 :$
$bweb := 2 \cdot 150 :$
$Ac := H \cdot B - (H - htop - hbot) \cdot (B - bweb) :$
$ztop := \frac{1}{Ac}(H \cdot B \cdot 0.5 \cdot H - ((H - htop - hbot) \cdot (B - bweb) \cdot (htop + 0.5 \cdot (H - htop - hbot)))) :$

Concrete strength

$fck := 90 : \alpha c := 1 : fcd := \frac{\alpha c \cdot fck}{1.5} :$
$fctk := 3.5 :$
$\sigma 03 := 3.5 :$
$fctd1 := \frac{fctk}{1.5} : fctd2 := \frac{\sigma 03}{1.25 \cdot 1.5} :$
$E := 44000 :$

Concrete strains

$\varepsilon c3 := 2.3 \cdot 10^{-3} : \varepsilon cu3 := 2.6 \cdot 10^{-3} :$
$lf := 13 : \varepsilon ct := \frac{fctd1}{E} : \varepsilon u03 := \frac{0.3}{\frac{2}{3} \cdot H} + \varepsilon ct : \varepsilon ctu := \frac{lf}{\frac{4 \cdot 2}{3} \cdot H} :$

Prestressing

$n := 34 :$
$Ap := n \cdot 139 :$
$\sigma pt := 1265.597 : fpd := 1522 :$
$Ep := 195000 :$
$\varepsilon pd := \frac{1522}{Ep} :$
$e := 75.8 :$
$dp := H - e :$

Internal compressive force

$x1 := \frac{x \cdot (\varepsilon cu3 - \varepsilon c3)}{\varepsilon cu3} : x2 := x - x1 :$
$Nx1 := B \cdot fcd \cdot x1 : Nx2 := \frac{B \cdot (fcd)}{2} \cdot x2 :$
$Ncc := Nx1 + Nx2;$

$33461.53846\, x$

Internal tensile force

$$xT := H - x :$$

$$xT1 := \frac{xT \cdot \varepsilon ct}{\varepsilon ctu} : xT2 := htop - x - xT1 : xT3 := \frac{xT \cdot (\varepsilon u03 - \varepsilon ct)}{\varepsilon ctu}$$

$$- xT2 : xT4 := \frac{xT \cdot (\varepsilon ctu - \varepsilon u03)}{\varepsilon ctu} - hbot : xT5 := hbot :$$

$$Nt1 := 0.5 \cdot B \cdot fctd1 \cdot xT1 :$$

$$\sigma t1 := \frac{(fctd2 - fctd1)}{xT2 + xT3} \cdot xT2 + fctd1 : Nt2$$

$$:= \frac{B \cdot xT2 \cdot (\sigma t1 + fctd1)}{2} :$$

$$Nt3 := \frac{bweb \cdot xT3 \cdot (\sigma t1 + fctd1)}{2} :$$

$$\sigma t2 := \frac{(fctd2 \cdot hbot)}{xT4 + xT5} : Nt4 := \frac{bweb \cdot xT4 \cdot (fctd2 + \sigma t2)}{2} :$$

$$Nt5 := 0.5 \cdot B \cdot xT5 \cdot \sigma t2 :$$

$$Nt := Nt1 + Nt2 + Nt3 + Nt4 + Nt5;$$

$$4568.764568 - 7.614607615\, x + 500\, (166.0839161 - 0.9934731935\, x) \left(- \frac{0.466666666\, (166.0839161 - 0.9934731935\, x)}{55.3846154 - 0.0923076923\, x} + 4.666666666 \right) + 150\, (-110.6993007 + 0.9011655012\, x) \left(- \frac{0.466666666\, (166.0839161 - 0.9934731935\, x)}{55.3846154 - 0.0923076923\, x} + 4.666666666 \right) + 150\, (390.6993007 - 0.9011655012\, x) \left(1.866666667 + \frac{280.0000000}{540.6993007 - 0.9011655012\, x} \right) + \frac{2.100000000\, 10^{7}}{540.6993007 - 0.9011655012\, x}$$

Prestress force

$$\varepsilon p := \frac{\sigma pt}{Ep} + \varepsilon cu3 \cdot \left(\frac{dp}{x} - 1 \right) : \sigma pu := fpd + \left(\frac{(\varepsilon p - \varepsilon pd)}{(35 \cdot 10^{-3} - \varepsilon pd)} \right) \cdot (1691 - fpd) :$$

$$dNp := Ap \cdot (\sigma pu - \sigma pt) : P := Ap \cdot \sigma pt;$$

$$5.981211422\, 10^{6}$$

Solve compressive zone x

$$eq1 := Ncc = Nt + P + dNp$$

$$33461.53846\,x = 7.082563319\,10^{6} - 7.614607615\,x + 500\,(166.0839161 - 0.9934731935\,x)\left(-\frac{0.466666666\,(166.0839161 - 0.9934731935\,x)}{55.3846154 - 0.0923076923\,x} + 4.666666666\right) + 150\,(-110.6993007 + 0.9011655012\,x)\left(-\frac{0.466666666\,(166.0839161 - 0.9934731935\,x)}{55.3846154 - 0.0923076923\,x} + 4.666666666\right) + 150\,(390.6993007 - 0.9011655012\,x)\left(1.866666667 + \frac{280.0000000}{540.6993007 - 0.9011655012\,x}\right) + \frac{2.100000000\,10^{7}}{540.6993007 - 0.9011655012\,x} + \frac{4.002798891\,10^{7}}{x}$$

$$z := solve(eq1, x)$$

$$219.1739674,\ 600.0000000,\ 624.0892017,\ -5.226767101$$

$$xin := z[1]$$

$$219.1739674$$

Check if determined x is completety located in top flange

If a value is shown, proceed with determination of MRd. Otherwise determine x again.

if xin $<$ htop **then** xu $:=$ xin **else** $print(FIND\ NEW\ X)$ **end if**

FIND NEW X

Determination of x when xin $\geq$ htop

$$y := \frac{xin \cdot (\varepsilon cu3 - \varepsilon c3)}{\varepsilon cu3}$$

$$25.28930393$$

Maple function '*procedure*' is used to instantly determine the correct x for a given situation

SITUATION 1: y≤htop

$$
\begin{aligned}
it1 :=& \mathbf{proc}(B, bweb, htop, \varepsilon c3, \varepsilon cu3, fcd, Ap, \sigma pt, fpd, e, dp, Ep, \varepsilon pd, \\
& fctk, \sigma u03, fctd1, fctd2, lf, \varepsilon ct, \varepsilon u03, \varepsilon ctu, hbot)\mathbf{local}\ N1c, x11, \\
& x12, x13, N11, N12, N13, eq1, \sigma c, \varepsilon p, \sigma pu, dNp1, P1, xT10, xT11, \\
& xT12, xT13, xT14, Nt11, Nt12, Nt13, \sigma t2, Nt14, NT1, x; x11 \\
& := \frac{x\cdot(\varepsilon cu3 - \varepsilon c3)}{\varepsilon cu3}; x12 := htop - x11; x13 := x - htop; \sigma c \\
& := \frac{fcd\cdot(x13)}{x - x11}; N11 := B\cdot fcd\cdot x11; N12 := \frac{B\cdot(fcd + \sigma c)}{2}\cdot x12; \\
& N13 := bweb\cdot 0.5\cdot\sigma c\cdot x13; N1c := N11 + N12 + N13; xT10 := H \\
& - x; xT11 := \frac{xT10\cdot\varepsilon ct}{\varepsilon ctu}; xT12 := \frac{xT10\cdot(\varepsilon u03 - \varepsilon ct)}{\varepsilon ctu}; xT13 \\
& := \frac{xT10\cdot(\varepsilon ctu - \varepsilon u03)}{\varepsilon ctu} - hbot; xT14 := hbot; Nt11 := 0.5 \\
& \cdot bweb\cdot fctd1\cdot xT11; Nt12 := \frac{bweb\cdot xT12\cdot(fctd2 + fctd1)}{2}; \sigma t2 \\
& := \frac{(fctd2\cdot hbot)}{xT13 + xT14}; Nt13 := \frac{bweb\cdot xT13\cdot(\sigma t2 + fctd2)}{2}; Nt14 \\
& := 0.5\cdot B\cdot xT14\cdot\sigma t2; NT1 := Nt11 + Nt12 + Nt13 + Nt14; \varepsilon p \\
& := \frac{\sigma pt}{Ep} + \varepsilon cu3\cdot\left(\frac{dp}{x} - 1\right) : \sigma pu := fpd \\
& + \left(\frac{(\varepsilon p - \varepsilon pd)}{(35\cdot 10^{-3} - \varepsilon pd)}\right)\cdot(1691 - fpd) : dNp1 := Ap\cdot(\sigma pu \\
& - \sigma pt) : P1 := Ap\cdot\sigma pt : eq1 := N1c = P1 + dNp1 + NT1; x \\
& := solve(eq1, x); eval(x); \mathbf{end\ proc};
\end{aligned}
$$

```
proc(B, bweb, htop, εc3, εcu3, fcd, Ap, σpt, fpd, e, dp, Ep, εpd, fctk,
    σu03, fctd1, fctd2, lf, εct, εu03, εctu, hbot)
    local N1c, x11, x12, x13, N11, N12, N13, eq1, σc, εp, σpu, dNp1,
    P1, xT10, xT11, xT12, xT13, xT14, Nt11, Nt12, Nt13, σt2, Nt14,
    NT1, x;
    x11 := x*(εcu3 − εc3)/εcu3;
    x12 := htop − x11;
    x13 := x − htop;
    σc := fcd*x13/(x − x11);
    N11 := B*fcd*x11;
    N12 := 1/2*B*(fcd + σc)*x12;
    N13 := bweb*0.5*σc*x13;
    N1c := N11 + N12 + N13;
    xT10 := H − x;
    xT11 := xT10*εct/εctu;
    xT12 := xT10*(εu03 − εct)/εctu;
    xT13 := xT10*(εctu − εu03)/εctu − hbot;
    xT14 := hbot;
    Nt11 := 0.5*bweb*fctd1*xT11;
    Nt12 := 1/2*bweb*xT12*(fctd2 + fctd1);
    σt2 := fctd2*hbot/(xT13 + xT14);
    Nt13 := 1/2*bweb*xT13*(σt2 + fctd2);
    Nt14 := 0.5*B*xT14*σt2;
    NT1 := Nt11 + Nt12 + Nt13 + Nt14;
    εp := σpt/Ep + εcu3*(dp/x − 1);
    σpu := fpd + (εp − εpd)*(1691 − fpd)/(7/200 − εpd);
    dNp1 := Ap*(σpu − σpt);
    P1 := Ap*σpt;
    eq1 := N1c = P1 + dNp1 + NT1;
    x := solve(eq1, x);
    eval(x)
end proc
```

```
x := it1(B, bweb, htop, εc3, εcu3, fcd, Ap, σpt, fpd, e, dp, Ep, εpd,
    fctk, σu03, fctd1, fctd2, lf, εct, εu03, εctu, hbot)[1]
```

233.7253620

SITUATION 2: y≥ htop

$$
\begin{aligned}
it2 := \mathbf{proc}(&B, bweb, htop, \varepsilon c3, \varepsilon cu3, fcd, Ap, \sigma pt, fpd, e, dp, Ep, \varepsilon pd,\\
&fctk, \sigma u03, fctd1, fctd2, lf, \varepsilon ct, \varepsilon u03, \varepsilon ctu, hbot)\ \mathbf{local}\ x21, x22,\\
&x23, N21, N22, N23, eq2, N2c, \varepsilon p, \sigma pu, dNp2, P2, xT20, xT21,\\
&xT22, xT23, xT24, Nt21, Nt22, Nt23, \sigma t12, Nt24, NT2, z; x21\\
&:= htop; x22 := \frac{z\cdot(\varepsilon cu3 - \varepsilon c3)}{\varepsilon cu3} - htop; x23 := z\\
&- \frac{z\cdot(\varepsilon cu3 - \varepsilon c3)}{\varepsilon cu3}; N21 := B\cdot fcd\cdot x21; N22 := bweb\cdot fcd\cdot x22;\\
&N23 := bweb\cdot 0.5\cdot fcd\cdot x23; N2c := N21 + N22 + N23; xT20 := H\\
&- x; xT21 := \frac{xT20\cdot\varepsilon ct}{\varepsilon ctu}; xT22 := \frac{xT20\cdot(\varepsilon u03 - \varepsilon ct)}{\varepsilon ctu}; xT23\\
&:= \frac{xT20\cdot(\varepsilon ctu - \varepsilon u03)}{\varepsilon ctu} - hbot; xT24 := hbot; Nt21 := 0.5\\
&\cdot bweb\cdot fctd1\cdot xT21; Nt22 := \frac{bweb\cdot xT22\cdot(fctd2 + fctd1)}{2}; \sigma t12\\
&:= \frac{(fctd2\cdot hbot)}{xT23 + xT24}; Nt23 := \frac{bweb\cdot xT23\cdot(\sigma t12 + fctd2)}{2}; Nt24\\
&:= 0.5\cdot B\cdot xT24\cdot\sigma t12; NT2 := Nt21 + Nt22 + Nt23 + Nt24; \varepsilon p\\
&:= \frac{\sigma pt}{Ep} + \varepsilon cu3\cdot\left(\frac{dp}{z} - 1\right) : \sigma pu := fpd\\
&+ \left(\frac{(\varepsilon p - \varepsilon pd)}{(35\cdot 10^{-3} - \varepsilon pd)}\right)\cdot(1691 - fpd) : dNp2 := Ap\cdot(\sigma pu\\
&- \sigma pt) : P2 := Ap\cdot\sigma pt : eq2 := N2c = P2 + dNp2 + NT2; z\\
&:= solve(eq2, z); eval(z); \mathbf{end\ proc};
\end{aligned}
$$

```
proc(B, bweb, htop, εc3, εcu3, fcd, Ap, σpt, fpd, e, dp, Ep, εpd, fctk,
    σu03, fctd1, fctd2, lf, εct, εu03, εctu, hbot)
    local x21, x22, x23, N21, N22, N23, eq2, N2c, εp, σpu, dNp2, P2,
    xT20, xT21, xT22, xT23, xT24, Nt21, Nt22, Nt23, σt12, Nt24,
    NT2, z;
    x21 := htop;
    x22 := z*(εcu3 − εc3)/εcu3 − htop;
    x23 := z − z*(εcu3 − εc3)/εcu3;
    N21 := B*fcd*x21;
    N22 := bweb*fcd*x22;
    N23 := bweb*0.5*fcd*x23;
    N2c := N21 + N22 + N23;
    xT20 := H − x;
    xT21 := xT20*εct/εctu;
    xT22 := xT20*(εu03 − εct)/εctu;
    xT23 := xT20*(εctu − εu03)/εctu − hbot;
    xT24 := hbot;
    Nt21 := 0.5*bweb*fctd1*xT21;
    Nt22 := 1/2*bweb*xT22*(fctd2 + fctd1);
    σt12 := fctd2*hbot/(xT23 + xT24);
    Nt23 := 1/2*bweb*xT23*(σt12 + fctd2);
    Nt24 := 0.5*B*xT24*σt12;
    NT2 := Nt21 + Nt22 + Nt23 + Nt24;
    εp := σpt/Ep + εcu3*(dp/z − 1);
    σpu := fpd + (εp − εpd)*(1691 − fpd)/(7/200 − εpd);
    dNp2 := Ap*(σpu − σpt);
    P2 := Ap*σpt;
    eq2 := N2c = P2 + dNp2 + NT2;
    z := solve(eq2, z);
    eval(z)
end proc
```

```
z := it2(B, bweb, htop, εc3, εcu3, fcd, Ap, σpt, fpd, e, dp, Ep, εpd,
    fctk, σu03, fctd1, fctd2, lf, εct, εu03, εctu, hbot)
```

68.16703882, −58.49546299

The following statement determines which situation is at hand,based on y. Then it determines the right value for xu. If the first determined x was correct, than this value will be shown, otherwise it will be the result of situation 1 or 2.

if x ≤ htop **then** x := xin **elif** $x \geq htop$ **and** $y \leq htop$ **then** $x := it1(B, bweb, htop, \varepsilon c3, \varepsilon cu3, fcd, Ap, \sigma pt, fpd, e, dp, Ep, \varepsilon pd, fctk, \sigma u03, fctd1, fctd2, lf, \varepsilon ct, \varepsilon u03, \varepsilon ctu, hbot)[1]$ **elif** $x \geq htop$ **and** $y \geq htop$ **then** $x := it2(B, bweb, htop, \varepsilon c3, \varepsilon cu3, fcd, Ap, \sigma pt, fpd, e, dp, Ep, \varepsilon pd, fctk, \sigma u03, fctd1, fctd2, lf, \varepsilon ct, \varepsilon u03, \varepsilon ctu, hbot)[1]$ **end if**

233.7253620

$xu := x$

233.7253620

Determining Bending Moment resistance

There are three situations, which influence the determination of MRd. Situation A is used, when the first determined x is the correct one. Situation B is used, when the first determined x is higher than the top flange and y ≤ htop . Situation C is used when the first determined x is higher than the top flange and y ≥ htop.

SITUATION B: MRd when xu determined with iteration 1for y≤htop and x≥htop. **IGNORE SUBSECTION IF x ≤ htop OR y≥ htop!!**

Re-determination compressive and tensile forces and prestress force, due to change in variables during previous calculations.

$$x11 := \frac{x\cdot(\varepsilon cu3 - \varepsilon c3)}{\varepsilon cu3} : x12 := htop - x11 : x13 := x - htop : \sigma c := \frac{fcd\cdot(x13)}{x - x11} : N11 := B\cdot fcd\cdot x11 : N12 := \frac{B\cdot(fcd + \sigma c)}{2}\cdot x12 : N13 := bweb\cdot 0.5\cdot\sigma c\cdot x13 : N1c := N11 + N12 + N13;$$

$7.408348529\ 10^{6}$

$$xT10 := H - x : xT11 := \frac{xT10\cdot\varepsilon ct}{\varepsilon ctu} : xT12 := \frac{xT10\cdot(\varepsilon u03 - \varepsilon ct)}{\varepsilon ctu} : xT13 := \frac{xT10\cdot(\varepsilon ctu - \varepsilon u03)}{\varepsilon ctu} - hbot : xT14 := hbot : Nt11 := 0.5\cdot bweb\cdot fctd1\cdot xT11 : Nt12 := \frac{bweb\cdot xT12\cdot(fctd2 + fctd1)}{2} : \sigma t2 := \frac{(fctd2\cdot hbot)}{xT13 + xT14} : Nt13 := \frac{bweb\cdot xT13\cdot(\sigma t2 + fctd2)}{2} : Nt14 := 0.5\cdot B\cdot xT14\cdot\sigma t2 : NT1 := Nt11 + Nt12 + Nt13 + Nt14;$$

$1.590931878\ 10^{5}$

$$\varepsilon p := \frac{\sigma pt}{Ep} + \varepsilon cu3\cdot\left(\frac{dp}{x} - 1\right) : \sigma pu := fpd + \left(\frac{(\varepsilon p - \varepsilon pd)}{(35\cdot 10^{-3} - \varepsilon pd)}\right)\cdot(1691 - fpd) : dNp1 := Ap\cdot(\sigma pu - \sigma pt); P1 := Ap\cdot\sigma pt;$$

Check if equilibrium between internal forces

$$\frac{N1c - (dNp1 + P1 + NT1)}{1000};$$

0.0000032

Determination of distance of all forces to the rotation point. Rotation point on utmost top fibre.

$$armc11 := 0.5 \cdot x11 : armc12 := x11 + \frac{1}{3} \cdot x12 \cdot \left(\frac{(fcd + 2 \cdot \sigma c)}{(fcd + \sigma c)} \right) :$$

$$armc13 := x11 + x12 + \frac{x13}{3} :$$

$$armt11 := x + \frac{2 \cdot xT11}{3} : armt12 := x + xT11 + \frac{xT12}{3} \cdot \frac{(2 \cdot fctd2 + fctd1)}{fctd1 + fctd2} : armt13 := x + xT11 + xT12 + \frac{xT13}{3} \cdot \frac{(fctd2 + 2 \cdot \sigma t2)}{\sigma t2 + fctd2} : armt14 := x + xT11 + xT12 + xT13 + \frac{xT14}{3} :$$

Bending moment resistance

$$MRd2 := \frac{1}{1000000}(((Nt11 \cdot armt11 + Nt12 \cdot armt12 + Nt13 \cdot armt13 + Nt14 \cdot armt14) + (dNp1 \cdot dp) + \mathrm{P1} \cdot \mathrm{ztop}) - (N11 \cdot armc11 + N12 \cdot armc12 + N13 \cdot armc13));$$

1955.310088

FINAL RESULTS

Height of compressive zone

$xu;$

233.7253620

Height of tension zone

$xT;$

366.2746380

Bending moment resistance

if $x < htop$ **then** $MRd := MRd1$ **elif** $x \geq htop$ **and** $y \leq htop$ **then** $MRd := MRd2$ **else** $MRd := MRd3$ **end if**:

$MRd;$

1955.310088

Rotational capacity check

$$f := \frac{\left(\frac{1860}{1.1} - \sigma pt \right) \cdot Ap}{Ap};$$

425.3120910

$$g := 1 - \frac{f}{500 + f}; \frac{xu}{dp};$$

0.5403582260

0.4458705876

if $\frac{xu}{dp} \leq \mathrm{g}$ **then** $print(rotational\ capacity\ OK)$ **else** $print\ (rotaional\ capacity\ NOT\ OK)$ **end if**

rotational capacity OK

$$UC := \frac{xu}{dp \cdot g};$$

0.8251388915

$$\text{kappa} := \frac{\varepsilon cu3}{xu} \cdot 1000$$

0.01112416718

END MAPLE SHEET

The maple sheet results in a compressive height of:
x_u = 233.67 mm
The moment capacity is:
M_{Rd} = 1955.31 kNm

Unity Check: M_{Ed}/M_{Rd} = 1276.1/1955.31 = 0.652→ OK

F.11 Rotational capacity

The bending moment resistance suffices. But it is also important that the structure has enough rotational capacity in order to give enough warning before failure. For this the following requirement has to be met (NEN-EN-1992-1-1 Dutch NB cl.5.5):
$x / d \leq 500/(500+f)$ with $f= [(f_{pk}/\gamma_p - \sigma_{pm\infty})*A_p + f_{yd}*A_s]/(A_p + A_s)$ = (1860/1.1-1269)*4726/4726 = 425.31.

The requirement becomes: $x_u/d \leq 0.54$.
Filling in x = 233.73 mm and with d=h-e = 524.2 mm x/d becomes 0.446 < 0.54. So the structure has enough rotational capacity

F.12 Shear and torsion capacity

F.12.1 Shear

It is a requirement that the shear resistance is higher then the design shear force:
$V_{Rd} > V_d$
The design shear force is the sum of the shear force caused by bending moments and the shear force caused by torsional moments:
$V_d = V_{Ed} + V_{Td}$
Two cases have to be investigated, of which the most governing one will be used:

Situation 1. Location of highest torsional moment in structure
Situation 2. Location of highest shear force in structure

For both locations the internal forces were calculated and the results were presented in paragraph F.6. These were:
Mxy = TEd:

Situation 1. 317.09 kNm --> V_{Td} = 184.35 kN
Situation 2. 116.75 kNm --> V_{Td} = 67.88 kN

Vx (without self-weight and prestressing):

Situation 1. 235.94 kN
Situation 2. 584.56 kN

The shear force V_{Td} due to T_{Ed} is calculated with: $V_{Td} = h_m*T_{Ed}/(2*A_k)$.
$h_m = H-0.5*(h_{top,fl} + h_{bot,fl})$ = 0.6-0.5*(0.17+0.15) = 0.44 m
$b_m = B-2*0.5*b_{web}$ = 1.0-2*0.5*0.15=0.85 m
$A_k = b_m*h_m$ = 0.374 m^2

The governing total shear force taken from SCIA is the one where the sum of V_x and V_{Td} is the largest:

Situation 1. V_{Ed} =420.29 kN

Situation 2. V_{Ed} = 652.44 kN

So the governing situation for the shear resistance check wil be the location were the shear force is governing (situation 2). Furthermore the self-weight and prestressing also have to be taken into account with the result of V_{Ed} from SCIA. It is also possible that the eventual governing design shear force is found at the construction stage (t=0). So the shear force over the length of the beam needs to be determined at multiple stages. These stage and the shear forces are:

- t=0 only self weight: $V_{Ed} = V_{self} - P_{u0}$
- t=0 permanent loads: $V_{Ed} = V_{perm} - P_{u0}$
- t=∞ all loads + torsion: $V_{Ed} = V_{perm} + V_{var} - P_{u\infty}$

The upward force of the prestressing reduces the total shear force. But it only works between the support and the deviation point. The shear force is determined at the supports and just on each side of the deviation point. In general the shear force at these locations is determined as follows:

$V_{sup} = 0.5*q*L - P_u$

$V_{dev1} = 0.5*q*L - 0.5*q*a - P_u$

$V_{dev2} = 0.5*q*L - 0.5*q*a$

For t=∞ the shear force is added with V_{Td}. Assumed is that V_{Td} is constant over the length of the beam. The result are seen in Table F-4 with the shear force lines in Figure F-5.

The parameters are:

Load of self-weight (ULS):	q_{self} = 12.61 kN/m
Permanent load (ULS):	q_{perm} = 21.19 kN/m
Variable load (ULS):	q_{var} = 39.86 kN/m
Upward Prestress force at t=0:	P_{u0} = 62.64 kN
Upward Prestress force at t=∞:	$P_{u\infty}$ = 55.75 kN
Distance deviators to support:	a=8m

Table F-4: Results shear forces over length of beam

V [kN] at:	t=0 self	t=0 perm	t=inf
V_{sup}	88,679	177,219	748,807
V_{dev1}	-12,201	17,312	258,219
V_{dev2}	50,440	79,953	313,970

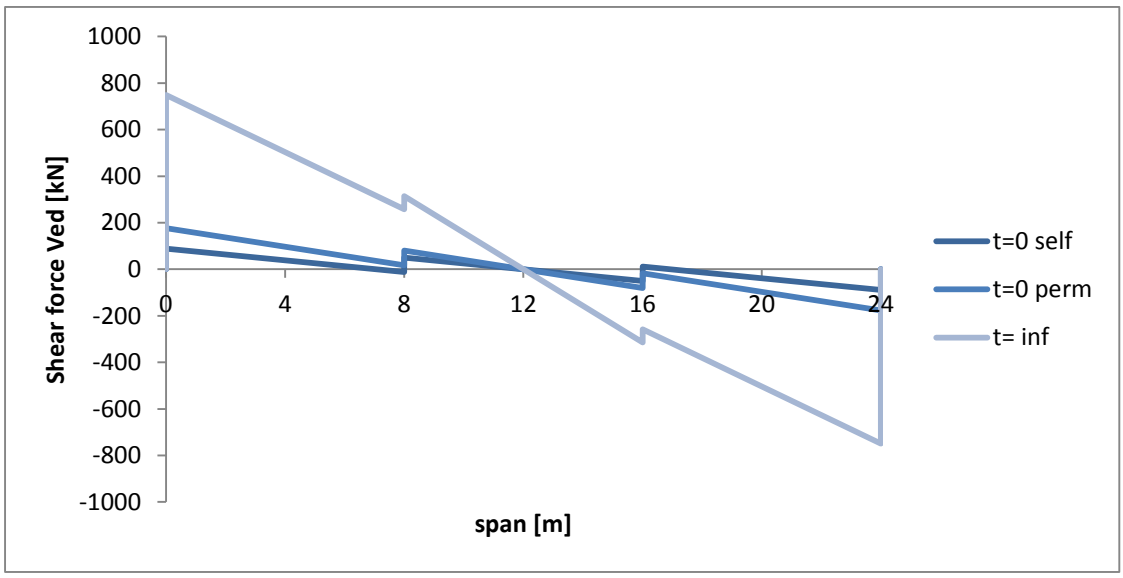

Figure F-5: Shear force line at multiple stages

The governing shear force V_{Ed} = 748.81 kN at t=∞. The shear resistance has to be high enough to resist this force.

The shear resistance for a HPC structure is determined in more or less the same way as a UHPC structure. This is because both contain steel fibres. The shear resistance is equal to:
$V_{Rd} = V_{Rd,F} + V_{Rd,s}$

Where:
$V_{Rd,F}$ = the contribution of the steel fibre reinforced concrete to the shear capacity
$V_{Rd,s}$ = the contribution of the shear reinforcement to the shear capacity

Because of the behaviour of the steel fibres in tension, it is allowed to view it separately from the concrete, as if it is serving as reinforcement. Shear reinforcement will not be applied (unless the shear capacity is not enough to resist the design shear force), so $V_{Rd} = V_{Rd,F}$.

The Eurocode has no method to determine the shear capacity, when steel fibres are present in the concrete. Therefore the Model Code MC2010 will be used to determine the shear capacity.
According to paragraph 7.7.3.2 of MC2010 the shear resistance is determined with:

$$V_{Rd,F} = \frac{1}{\gamma_F}\left(k_v\sqrt{f_{ck}} + k_f f_{Ftuk}\cot\theta\right) z * b_w$$

Where

$$k_v = \frac{0.4}{1 + 1500\varepsilon_x} * \frac{1300}{1000 + k_{dg} * z}$$

$k_{dg} = 32/(16+d_g)$. If d_g <16mm (which is the case here) then $k_{dg} = 1$
The term $k_v * \sqrt{f_{ck}}$ represents the contribution of the concrete and the term $k_f * f_{Ftuk} * \cot\theta$ represents the contribution of the steel fibres.
k_f=0.8

f_{Ftuk} is the ultimate residual tensile strength (formula 5.6-6 in MC2010):
$f_{Ftuk} = 0.45f_{R1} – (w_u/CMOD_3)(0.45f_{R1}-0.5f_{R3}+0.2f_{R1})$
where f_{R1} and f_{R3} are determined with experiments. Since it is not possible to perform experiments it is safe to assumed that $f_{Ftuk} = f_{ctk}$ if the concrete shows strain hardening behaviour.

ε_x is defined as (see also Figure F-6):

$$\varepsilon_x = \frac{\left(\frac{M_d}{z} + V_{Ed} + N_{Ed} * \frac{(z_p - e_p)}{z}\right)}{2 * \left(\frac{z_s}{z} E_s A_s + \frac{z_p}{z} E_p A_p\right)}$$

No steel reinforcement is used so $A_s = 0$ and $z = z_p = 0.9*d$
$M_d = M_{Ed} + M_{Pd} = 1276.1 + P_{m\infty} * \Delta e = 1276.1 + 6982.78 * (z_b – 0.5z+e_p) = 1316{,}2$ kNm
$N_{Ed} = -P_{m\infty} =$ -6982.78 kN
$V_{Ed} =$ 636.56 kN

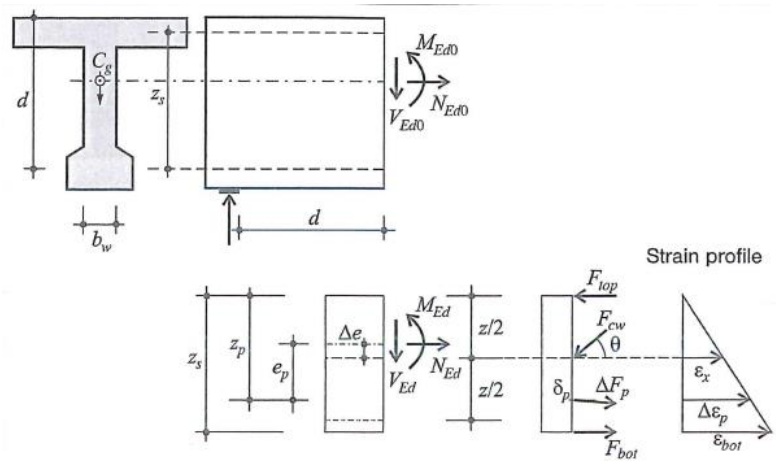

Figure F-6: Situation for determining ε_x

Filling all the unknown parameters results in:
$\varepsilon_x = 0.222*10^{-3}$.
This results in $k_v = 0.265$
$\theta_{min} = 29° + 7000\varepsilon_x = 30.94$ => assumed is 31°
$z = 0.9d = 471.78$ and $b_w = 2b_{web} = 300$ mm
If assumed is $f_{Ftuk} = f_{ctk} = 3.5$ N/mm^2 then the shear capacity becomes:
$V_{Rd,F} = 695.07$ kN.

The minimum shear resistance is determined with (same approach as the Eurocode):
$V_{min} = (v_{min} + k1*\sigma_{cp}) * b_w*z$.

Where
$V_{min} = 0.035*k*fck^{0.5}$
$b_w = 2*b_{web} = 300$ mm
$z = 0.9d = 471.78$ mm
$k = 1+(200/d)^{0.5} = 1.618$
$\sigma_{cp} = P_{m\infty}/A_c = 14.52$N/mm^2
The result is $V_{min} = 384.36$ kN. $V_{Rd,f}$ is higher so governing as well.

Unity Check: $V_{Ed}/V_{Rd,F} = 748.81/695.07 = 1.1$ → NOT OK

The structure has not enough shear capacity. So shear reinforcement is necessary. Because steel fibres are used the Total shear resistance may be set to:
$V_{Rd} = V_{Rd,f} + V_s$.
This means that the shear reinforcement needs to carry the remaining shear force of:
748.81 - 695.07 = 68.98 kN. With φ8 the spacing of the necessary stirrups is 600mm.
The maximum spacing, $s_{r,max} = 0.75d = 393.15$mm. Applied for minimum reinforcement is φ8-350 (A_s = 575mm^2). This will be applied instead of a spacing of 600mm. The resulting $\rho_w = 0.0055$. This is higher than $\rho_{w,min}$ (=$0.008*f_{ck}^{0.5}/f_{yk} = 0.0015$).

Remark: If the shear reinforcement needs to resist V_{Ed} alone, then 3700mm^2 would be necessary (ϕ12-125). At 1.13m of the supports the shear resistance becomes high enough to resist V_{Ed}. So only up to this point this amount of shear reinforcement is necessary. Also a hammerhead piece of 1m long is used at the supports and the hammerheads can easily resist V_{Ed}, since they are solid sections. So only a small part in the beam does not have sufficient shear capacity. The web thickness could be increased as well; If the web thickness is 170mm instead of 150mm, then UC = 0.99, which just enough capacity.

F.12.2 Torsion

There should be enough torsional resistance in the structure against working torsion moments:
$T_{Ed} \leq T_{Rd}$
If this is not the case reinforcement has to be applied. The torsion resistance can be determined with:
$T_{Rd} = f_{ctd,1} * t_{ef} * 2 * A_k$

Where
t_{ef} =A/u which is the effective wall thickness (in hollow sections upper limit is the real thickness) --> with A the total area of the cross section including hollow part and u as the circumference of the cross section:
t_{ef} = 0.6/3.2= 0.188m.
The smallest real thickness is 0.15 so this will be taken for t_{ef}.

The result is: T_{Rd} = 2.33*0.15*2*0.374= 261.8 kNm
Unity Check: T_{Ed}/T_{Rd} = 317.09/261.8=1.211
The torsional moment resistance (without taking the effect of the fibres into account) is not sufficient to resist the working torsional moments, so torsional reinforcement needs to be applied.

The required torsional reinforcement can be determined with (NEN-EN-1992-1-1 formula 6.28):
$\frac{\sum A_{sl} * f_{yd}}{u_k} = \frac{T_{Ed}}{2A_k} * \cot\theta$
The only unknown in the equation is A_{sl}. When everything is filled in the equation:
A_{sl} = 2828 mm^2. This has to be divided over the webs and flanges. Furthermore the reinforcement is divided in two layers in the webs and flanges:

The amount of reinforcement per flange: $A_s = T_{Ed}/(2*h_m*f_{yd})$ = 828 mm^2 → 6φ10 per layer (divided over the whole flange).

The amount of reinforcement per web: $A_s = T_{Ed}/(2*b_m*f_{yd})$ = 429 mm^2 → 3φ10 per layer (divided over the web, which is H – h_{top} – h_{bot}).

F.12.3 Shear + torsion

It is also required that the combination of shear forces and torsional moments is verified. The structure should be able to resist these forces. The requirement for this states that (NEN-EN-1992-1-1 cl. 6.3.2(4)):
$T_{Ed}/T_{Rd,max} + V_{Ed}/V_{Rd,max} \leq 1.0$
The requirement means that the capacity of the concrete struts has to be sufficient to resist the loads on the structure. Here the two previous situations (shear governing or torsion governing) are going to be investigated as well.
First $T_{Rd,max}$ and $V_{Rd,max}$ have to be determined according (to the Eurocode):
NEN-EN-1992-1-1 formula 6.30: $T_{Rd,max} = 2*\nu*\alpha_{cw}*f_{cd}*A_k*t_{ef}*\sin\theta\cos\theta$
NEN-EN-1992-1-1 formula 6.9: $V_{Rd,max} = \alpha_{cw}*b_w*z*\nu*f_{cd}/(\cot\theta+\tan\theta)$

where
$\nu = 0.9 - f_{ck}/200 = 0.46$
α_{cw}:
$(1 + \sigma_{cp}/f_{cd})$ for $0 < \sigma_{cp} \leq 0.25\ f_{cd}$
1.25 for $0.25\ f_{cd} < \sigma_{cp} \leq 0.5\ f_{cd}$
$2.5\ (1 - \sigma_{cp}/f_{cd})$ for $0.5\ f_{cd} < \sigma_{cp} < 1.0\ f_{cd}$
For this case α_{cw} = 1.25

$\theta=30°$
$t_{ef}=0.15m$
$b_w = 2b_{web} = 300$ mm
$z=0.9d = 486$ mm

Filling everything in the equations gives:
$T_{Rd,mac} = 1639.71$ kNm
$V_{Rd,max} = 2130.75$ kNm

Unity check:
Situation 1: 317.09/1639.71 + 518.04/2130.75 = 0.349
Situation 2: 116.75/1639.71 + 748.81/2130.75 = 0.390
For both situations the concrete struts suffice.

According to the Model Code $V_{Rd,max}$ is calculated as follows:
$V_{Rd,max} = k_c * f_{ck}/\gamma_c * b_w * z * \sin\theta\cos\theta$
Where
$k_c = k_\varepsilon * \eta_{fc}$
$k_\varepsilon = 1/(1.2+55\varepsilon_1)$ with $\varepsilon_1 = \varepsilon_x+(\varepsilon_x+0.002)\cot^2\theta$
$\eta_{fc} = (30/f_{ck})^{1/3}$
$\rightarrow k_c = 0.439$
This results in: $V_{Rd,max} = 1646.6$ kN
This value is lower than the value determined with the Eurocode. Most likely because the Eurocode uses α_{cw} which takes the compression stress caused by the prestressing into account.

F.13 Transverse direction (moments)

Transverse moments also occur in the structure. It is necessary to validate if the box girder can resist these moments. Transverse prestressing strands, which are placed in the top flange, can benefit the transverse moment capacity. These strands are also necessary to connect all the box girders together in order for the bridge to have transverse action. Only the top flange can contribute to the transverse moment capacity, together with the joints.

Assumed is that a tendon of 9φ15.7 strands with quality Y1860H are used which are placed with a centre spacing of 1000 mm.

The governing section is in the joint: The joint is not made of HPC and it has no other reinforcement in the concrete, except for the transverse prestressing. It has to be verified if the joint can resist the design transverse moment. Assumed is that the joint is made of C50/60. The joint will have a thickness of 260 mm.

Expected is for the highest transverse moment to be located right around the middle of the bridge. The highest moment should be found for the combination, where the loads are placed to give the highest transverse moments. In SCIA the result for the transverse moment myD^- was 322.06 kNm. However this (quite large) moment is found near the corners of the bridge. This can be explained by the fact that SCIA calculates myD^- by stating: $myD^- = my + |mxy|$. As the results showed in paragraph F.6, mxy = 317.09 kNm. This results in a high myD^-, which occurs in the same area as the highest torsional moment mxy. But the problem is that SCIA does not link the torsional moments with the given orthotropic parameters. For a box girder the stiffness is much higher in the longitudinal direction than in the transverse direction. So this also means that mxy ≠ myx. Therefore a factor K should be applied based on the orthotropy of a box girder:

$K_x = 2*D_{xy}/(D_{xy}+D_{yx})$
$K_y = 2*D_{yx}/(D_{xy}+D_{yx})$
This has been done in the Mathcad sheet for determining the orthotropic parameters. The resulting factors are:
$K_x = 1.948$
$K_y = 0.052$

To calculate myD^- the following is used: $myD^- = my + K_y*mxy$. Finding m_y in the same node as where the highest mxy is and then applying the factor will lead to myD^- = 34.53 kNm. This is much lower than the given value of 322.06 kNm. If this procedure would be applied all over the structure one would find the highest myD^- in the middle of the bridge as expected. Here m_y is the largest and mxy is very low in value.
SCIA gives a value of myD^- = 113.68 kNm/m. This is the value that will be used for determining if the transverse moment capacity ($M_{Rd,y}$) is sufficient. The moment on the box girder becomes:
$M_{Ed,y} = myD^-*B_{centre,spacing}$=113.68 kNm. This is the global transverse moment.
The global moment in the SLS state is: M_{SLS}=85.74 kNm.
Also necessary is to take into account the local transverse moment. For this Load Model 1 is turned into a single axle load where each wheel is 300 kN. To determine the local effect the transverse direction can be schematized as a continuous beam on multiple supports. The schematization is seen in Figure F-7. The point loads are spread until the heart line of the top flange and transformed into line loads. Each line load has a value of q_{wheel} = 300/ (2*0.080+2*0.150+0.4) = 348.84 kN/m. In combination with the dead load (assumed 4.8k N/m) a governing moment is found: $M_{Ed,local}$ = 46.84 kNm and $M_{SLS,local}$ = 26.05 kNm.

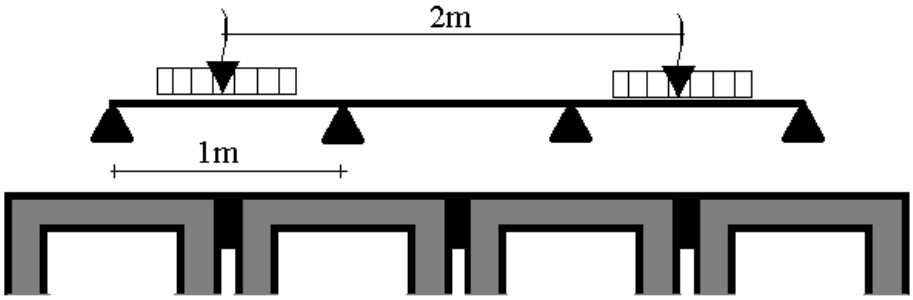

Figure F-7: Schematization for local effects

Because the placement of the axle loads for the local effects usually do not coincide with the placement of the axle loads for the global effects, the local effect may be reduced. A reduction of 25% is assumed. This results in a total transverse moment of:
ULS: $M_{Ed,tot}$ = 113.68+0.75*46.84 = 148.81 kNm
SLS: $M_{SLS,tot}$ = 85.74 +0.75*34.73 = 111.79 kNm

The transverse capacity is determined where the following equilibrium needs to hold true:
$N_c = P_{m\infty}$

Where
$N_c = \alpha * B * f_{cd} * x$
$P_{m\infty} = A_p * \sigma_{pm0} * 0.85$
With f_{cd} = 60 MPa and α=0.5577 the compression height is: x= 86.11
The moment capacity becomes: $M_{Rd,joint}$ = 161.6 kNm. UC=0.921 There is enough capacity.

For joints it is also important that there are no tensile stresses at the height of the prestressing strands. At this location the joint has to remain in compression at all times. This holds true for the SLS state. The stresses in the joints are ($-P_{m\infty}/A_{c,joint} \pm M_{SLS,local}/W_{c,b,joint}$)
At top fibre: -16.08 N/mm^2
At bottom fibre: +3.77 N/mm^2
At height of strands: -6.16 N/mm^2
The stress at the height of the strands is negative so there is compression.
So there is just enough capacity to resist the transverse moments. At the location of the duct the concrete has to be thickened internally to be able to fit the anchor and for enough space for the duct itself.

F.14 Capacity check of hammerhead

Because most of the strands are located in the bottom flange, the gravity point of strands will fall outside the neutral axis and cause an eccentric moment at the hammerheads. Since the moment due to static loading is very low close to the support it is necessary to see if there is enough capacity to resists the eccentric moment caused by the strands. The governing location is there where the strands have reached their full force and that is at the end of the transition at a distance of l_{pt} from the supports. The check should be performed at time of construction (t=0), as variable loads are not yet presented here to slightly counter balance the eccentric moment. Already was found that indeed at this stage the moment at the end support is the highest.
This transmission length is calculated according to EN 1992-1-1 cl. 8.10.2.2: l_{pt} = 767.38 mm.
$f_{ctd}(t)$ = $0.7*f_{ctm}/1.5$ = 2.333 N/mm^2
f_{bpt} = $f_{ctd}(t)*\eta_{p1}*\eta_p$ = 2.33*2.7*1 =6.3 N/mm^2
l_{pt} = $\alpha1*\alpha1*\phi_{strand}*\sigma_{pm0}/f_{bpt}$ = 639.49 mm
l_{pt1} = $0.8*l_{pt}$ = 511.59 mm
l_{pt2} = $1.2*l_{pt}$ = 767.38 mm

So for this calculation l_{pt} = 767.38 mm.

At l_{pt} the situation is as in Figure F-8 is presented. The compression zone is at the bottom side. The height of the compression zone has to be determined. Then the moment capacity can be calculated. The moment capacity $M_{Rd,head}$ should be higher than the design moment M_{Ed}.

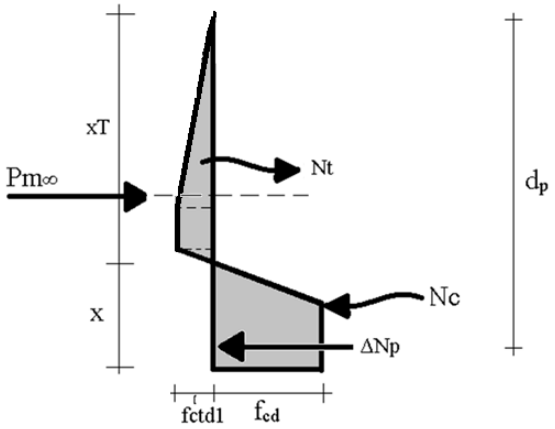

Figure F-8: Internal forces at hammerhead

The whole calculation including determining the design bending moment is done with a maple sheet that is shown in the following:

MAPLE SHEET: Capacity check hammerhead at lpt; HPC

$restart:\ H := 600 : B := 1000 : L := 24000;$

24000

$htop := 170 :$
$hbot := 150 :$
$bweb := 2 \cdot 150 :$
$Ac := H \cdot B - (H - htop - hbot) \cdot (B - bweb); qg := \frac{(H \cdot B \cdot 25 \cdot 2000 + Ac \cdot 25 \cdot (L - 2000))}{24 \cdot 1000000000} :$
$zb := H - \frac{1}{Ac}(H \cdot B \cdot 0.5 \cdot H - ((H - htop - hbot) \cdot (B - bweb) \cdot (htop + 0.5 \cdot (H - htop - hbot))));$

404000

304.8514851

$E := 44000; \varepsilon c3 := 2.3 \cdot 10^{-3} : \varepsilon cu3 := 2.6 \cdot 10^{-3} :$
$lf := 13 : \varepsilon ct := \frac{fctd1}{E} : \varepsilon u03 := \frac{0.3}{\frac{2}{3} \cdot H} + \varepsilon ct : \varepsilon ctu := \frac{lf}{\frac{4 \cdot 2}{3} \cdot H};$

$\frac{13}{1600}$

$fcd := 60 : fctd1 := 2.33333 : fctd2 := 2.33333 :$

Data from excel:

$lpt := 767.38 :$
$nstrands := 34 :$
$Apstr := 139 : Ap := Apstr \cdot nstrands : \sigma pm0 := 1395 : Pm0 := Ap \cdot \sigma pm0 :$
$a := 8000 : e := 75.8 : n1 := 4 : n2 := 4 : f := zb - e;$
$\mathrm{Mg} := 1.2 \cdot 0.5 \cdot \mathrm{qg} \cdot lpt \cdot (L - lpt);$
$1.124071032\,10^{8}$

$Pkink := (n1 + n2) \cdot Apstr \cdot \sigma pm0;$
1551240

$gravkink := (H - zb) - htop - 15.2 \cdot 2;$
94.7485149

$fkink := f + gravkink;$
323.8000000

$ffict := \frac{(n1 + n2) \cdot fkink}{nstrands};$
76.18823529

$Pufict := \frac{Pm0 \cdot ffict}{a};$
62786.43900

$Mp := Pufict \cdot lpt + Pm0 \cdot (f - ffict);$
$1.055973305\,10^{9}$

$Mpugt := 1.2 \cdot Mp;$
$1.267167966\,10^{9}$

$$MEd := \frac{(Mpugt - Mg)}{1000000};$$

1154.760863

Determination x

$$\alpha := \frac{((\varepsilon cu3 - \varepsilon c3) + 0.5\cdot\varepsilon c3)}{\varepsilon cu3};$$

0.5576923077

$$\beta := \frac{\left(\frac{\left(0.5\cdot(\varepsilon cu3 - \varepsilon c3)^2 + 0.5\cdot\varepsilon c3\cdot\left(\frac{\varepsilon c3}{3} + (\varepsilon cu3 - \varepsilon c3)\right)\right)}{(\varepsilon cu3 - \varepsilon c3) + 0.5\cdot\varepsilon c3}\right)}{\varepsilon cu3};$$

0.3373121133

$$Nc := \alpha\cdot B\cdot x\cdot fcd;$$

$33461.53846\,x$

$$xT := H - x:$$

$$xT1 := \frac{\varepsilon ct\cdot xT}{\varepsilon ctu}: Nt1 := 0.5\cdot xT1\cdot B\cdot fctd1:$$

$$xT2 := \frac{(\varepsilon u03 - \varepsilon ct)\cdot xT}{\varepsilon ctu}: Nt2 := 0.5\cdot B\cdot xT2\cdot(fctd1 + fctd2):$$

$$xT3 := \frac{(\varepsilon ctu - \varepsilon u03)\cdot xT}{\varepsilon ctu}: Nt3 := 0.5\cdot B\cdot xT3\cdot fctd2:$$

$$Nt := Nt1 + Nt2 + Nt3;$$

$$\sigma pu := 1606.36363: \Delta Np := Ap\cdot(\sigma pu - \sigma pm0);$$

$9.989045154\,10^5$

$$eq := Nc + \Delta Np = Nt + Pm0$$

$33461.53846\,x + 9.989045154\,10^5 = 7.357384292\,10^6 - 1274.357154\,x$

$$x := solve(eq, x);$$

183.0521328

$$armt1 := x(1 - \beta) + \frac{2\cdot xT1}{3}: armt2 := xT1 + x(1 - \beta) + \frac{xT2}{3}\cdot\frac{(2\cdot fctd1 + fctd2)}{fctd1 + fctd2}:$$

$$armt3 := xT1 + xT2 + x(1 - \beta) + \frac{xT3}{3}:$$

$$MRd := \frac{(Nt1\cdot armt1 + Nt2\cdot armt2 + Nt3\cdot armt3 + Pm0\cdot(zb - \beta\cdot x) + \Delta Np\cdot(\beta\cdot x - e))}{10^6};$$

1760.910492

$$MEd;$$

1154.760863

$$UC := \frac{MEd}{MRd};$$

0.6557748780

END MAPLE SHEET

The maple sheet result in a design bending moment of:

M_{Ed} = 1154.76 kNm

The moment capacity is:

M_{Rd} = 1760.91 kNm

Unity Check: M_{Ed}/M_{Rd} =1155/1761=0.66→ OK

F.15 Detailing

The pretress force in pre-tensioned steel is introduced by bonding. There is a certain transmission length (here l_{pt} = 532.91mm) where after the prestress force is fully transferred. Inside the transmission length the bond stresses can cause tensile stresses. In pre-tensioned steel three types of tensile stresses can occur (Figure F-9):

- Bursting stresses
- Splitting stresses
- Spalling stresses

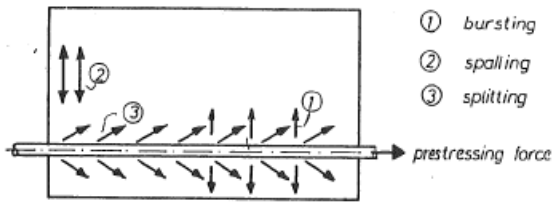

Figure F-9: Types of tensile stresses

The bursting and splitting stresses are prevented if the cover and distance between strands is at least 2φ. That is the case here so these two types of stresses are prevented. To determine the spalling stresses a graphical method by Den Uijl[1] can be used (Figure F-10).

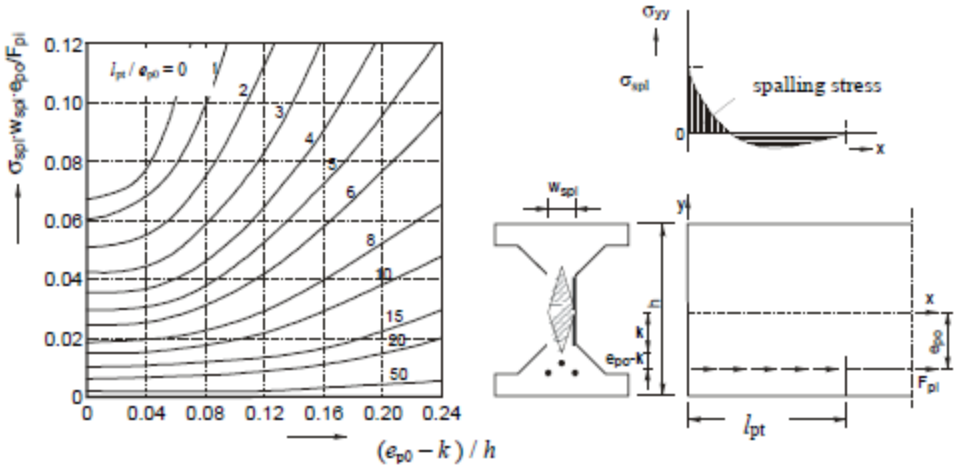

Figure F-10: Graphical method by Den Uijl for determining the spalling stresses

Starting from (e_{p0} - k) / h and l_{pt} / e_{p0} the value for $\sigma_{spl} \cdot w_{spl} \cdot e_{p0} / F_{pi}$ can be read from the diagram. After substitution of the known values for w_{spl}, e_{p0} and F_{pi}, the spalling stress σ_{spl} is obtained.

The values are:
l_{pt} = 639.5 mm. This means that the transfer of forces is completely in the hammerhead, which is a solid section.
$e_{p0} = f - f_{fict}$ = 153 mm
$k = W_b/A_c$ = 135.5 mm
h = 600mm
$(e_{p0}-k)/h$ = 0.0292
L_{pt}/e_{p0} = 4.18
With these values it can be read that $\sigma_{spl} \cdot w_{spl} \cdot e_{p0} / F_{pi}$ = 0.038

[1] Walraven, J.C., Braam, C.R. (2012) "Reader prestressed concrete", Delft University of Technology

W_{spl} = B = 1000mm (hammerhead)
F_{pi} = P_{m0} = 6592.77 kN
Filling everything in leads to:
σ_{spl} = 1.583 N/mm^2

The spalling stress is lower than the tensile strength (lower than both f_{ctd} and f_{ctk}), so no spalling reinforcement is needed in the structure.

F.16 Crack width verification

In order for a structure not to be verified for crack width, it is necessary that the maximum moments in SLS (M_{max}) do not exceed the cracking moment (M_{cr}). And it is also necessary that the tensile strength of the concrete is not exceeded anywhere in the structure. The maximum moment M_{max} can be determined by using paragraph F.8 and by using the value determined for the moment due to the prestressing force M_p. Only the frequent factor ψ1 has to be applied for the variable loads (is 0.8 for UDL, TS and pedestrian load). M_{max} becomes:
$M_{max} = M_g + M_q – M_p$ = 1065.4+1027.95-1343.9 = 543.8 kNm
The cracking moment M_{cr} is determined with:
$M_{cr} = W_b*(f_{ctm} + P_{m\infty}/A_c)$. For f_{ctm} is taken f_{ctk} instead, which is 3.5N/mm^2. With $P_{m\infty}/A_c$ = 14.5 N/mm^2:
M_{cr} = 0.055*(3.5+14.5)*10^3 = 986.78 kNm.

Unity Check: M_{max}/M_{cr} = 543.8/986.78 = 0.551→OK
The maximum moments in the SLS do not exceed the cracking moment.

Now the stresses in the structure in the SLS have to be checked. This is done with the same expressions used to determine the amount of strands:
$t = 0$ at top fibre: $\sigma_c = -\frac{P_{m0}}{A_c} + \frac{M_{p,0}}{W_{ct}} - \frac{M_g}{W_{ct}}$: σ_c = -2.99 N/mm^2
$t = 0$ at bottom fibre: $\sigma_c = -\frac{P_{m0}}{A_c} - \frac{M_{p,0}}{W_{cb}} + \frac{M_g}{W_{cb}}$: σ_c = -30.08 N/mm^2
$t = \infty$ at bottom fibre: $\sigma_c = -\frac{P_{m\infty}}{A_c} - \frac{M_{p,\infty}}{W_{cb}} + \frac{M_g+\psi 1*M_q}{W_{cb}}$: σ_c = -4.59 N/mm^2
The structure is in all three situations completely under compression. So crack formation is not possible. These results are expected, since the prestressing is determined with assuming a fully prestressed beam.

The cracking moment is not exceeded and no tensile stresses occur at the construction and user stage in the SLS. Furthermore the bridge is simply supported so imposed deformations are not restricted, which means that unexpected tensile stresses will not occur. So crack width verification is not necessary in this case.

F.17 Deflection

It is important for the structure that the deformations caused by the working loadings during service life are within acceptable limits. When determining the deformations it is important to distinguish the deformation in a cracked and uncracked section, because this has a big influence on the deflections (in the shape of a greatly reduced stiffness). In the case of the Leiden Bridge there are no cracked sections as already was concluded in paragraph F.16. So the structure is considered to be uncracked everywhere. The governing cross section is right in the middle of the beam, since here the highest deformations will occur, caused by the combination of the highest moments.
The occurring deflections have to satisfy a couple of limits given in NEN-EN-1992-1-1 in chapter 7:

- The camber may not exceed L/250 = -96 mm (L = 24000 mm)
- The sag may not exceed L/250 during serviceability = 96 mm
- If a chance exists of damaging adjacent parts then the sag may not exceed L/500 = 48mm

The camber is caused by prestressing. The sag should be limited to L/500, because underneath the bridge there is an unused intermediate pier.
Three load combinations will be investigated:

1. t=0; fabrication and erecting structure; self-weight + prestressing: $q_{self} - q_{pm0}$
2. t=0; after placing asphalt and such; Dead load + prestressing: $q_{self} + q_{dead} - q_{pm0}$
3. t=∞; user stage; All loads as quasi permanent combination: $q_{self} + q_{dead} + \psi_2 * q_{var} - q_{pm\infty}$

The Eurocode states that for traffic loads the following quasi-permanent factors ψ_2 have to be used:

- UDL: ψ_2 =0.4
- Tandem system: ψ_2=0.4
- Pedestrians: ψ_2=0.4

The deflection in the middle of the span is determined with: $w = \frac{5*q*L^4}{384*E_{c,eff}*Ic}$
$E_{c,eff} = E_{cm}/(1+\phi(\infty,t0))$ with $\phi(\infty,t0)$ = 0.8 being the creep coefficient.
This gives $E_{c,eff}$ = 24444.44 N/mm^2 respectively.
The case when no heat treatment is used is the governing one. The values of the loads are:
q_{self} = 10.508 kN/m
q_{dead} = 4.29 kN/m
q_{pm0} = 20.97 kN/m
$q_{pm\infty}$ = 18.67 kN/m
$\psi * q_{var}$ = 5.71 kN/m

Using these values in the three combinations and then filling q in the formula for w will results in (Table F-5):

Table F-5: Results deflection

	With $E_{c,eff2}$	Limit
Combination 1: w [mm]	-110,810	-96,0
Combination 2: w [mm]	-65,395	-96,0
Combination 3: w [mm]	19,503	-48,0

The results in Table F-5 show that the occurring deflections satisfy the limits. Only the camber is too high in combination 1. This means that in terms of deflection the prestressing force is too high. But the first situation (self-weight and prestressing force) is a situation that mostly occurs in the factory. In the factory this issue can easily be monitored and fixed. The camber limit is used when formwork is used during construction. But because prefabricated beams are used, there will be no formwork (except for small planks for the joints between the beams). So the - higher than the limit - deflection will not cause major issues. Eventually the beams are erected and connected and then the hardening layers are placed. Now combination 2 occurs and here the deflections are lower than the limit.

F.18 Vibration

The vibrations occurring on the structure may not cause discomfort during serviceability. This can be checked by determining the natural frequency of the structure. The natural frequency has to suffice according to the demands given by the Eurocode.
The natural frequency for the first (and governing) node is determined with:

$$n0 = \frac{C}{2\pi} * \sqrt{\frac{E_{cm} * I_c}{A_c * \rho_c * L^4}} \quad [Hz]$$

With C being the constraint factor (= 9.87 = π^2 for simply supported structures).
If all variables are filled in the formula then n0 = 2.33Hz.

The Leiden Bridge is used both by traffic, trams and pedestrians. So the vibrations caused by each should be considered.

Pedestrians
The NEN-EN-1991-2 states for pedestrian bridges that the natural frequency should at least be 5 Hz. Furthermore it states that frequencies caused by pedestrians fall between 1 and 3 Hz.
The determined natural frequency is lower than 5 Hz and it falls in the range of the pedestrian frequencies. So there would be a chance that pedestrians could cause a frequency equal to n0, which could lead to resonance and discomfort. However the natural frequency is actually determined for a single beam. Combining all the beams together will result in a higher mass, which means that the frequency from the pedestrians will hardly have any effect on the actual bridge. So a dynamical analysis is not required to precisely determine the frequencies exerted by pedestrians. This would not be the case if considered was a pedestrian bridge. These are usually smaller in size and lighter than traffic bridges and a lot more susceptible to vibrations. This was the case with the bridge projects that were discussed in the literature study. A lot of these bridges were pedestrian bridges and almost all required dampers to limit the vibrations caused by pedestrians. But this is not the case for the Leiden Bridge so no further attention is necessary here.

Trams
For vibrations caused by trams specifically there is nothing stated in the Eurocode. However the Eurocode gives guidelines for vibrations caused by trains so these could be used to give an estimation of the vibrations caused by trams. In figure 6.9 NEN-EN-1991-2 a flowchart is given to determine if a dynamical requirement is necessary.

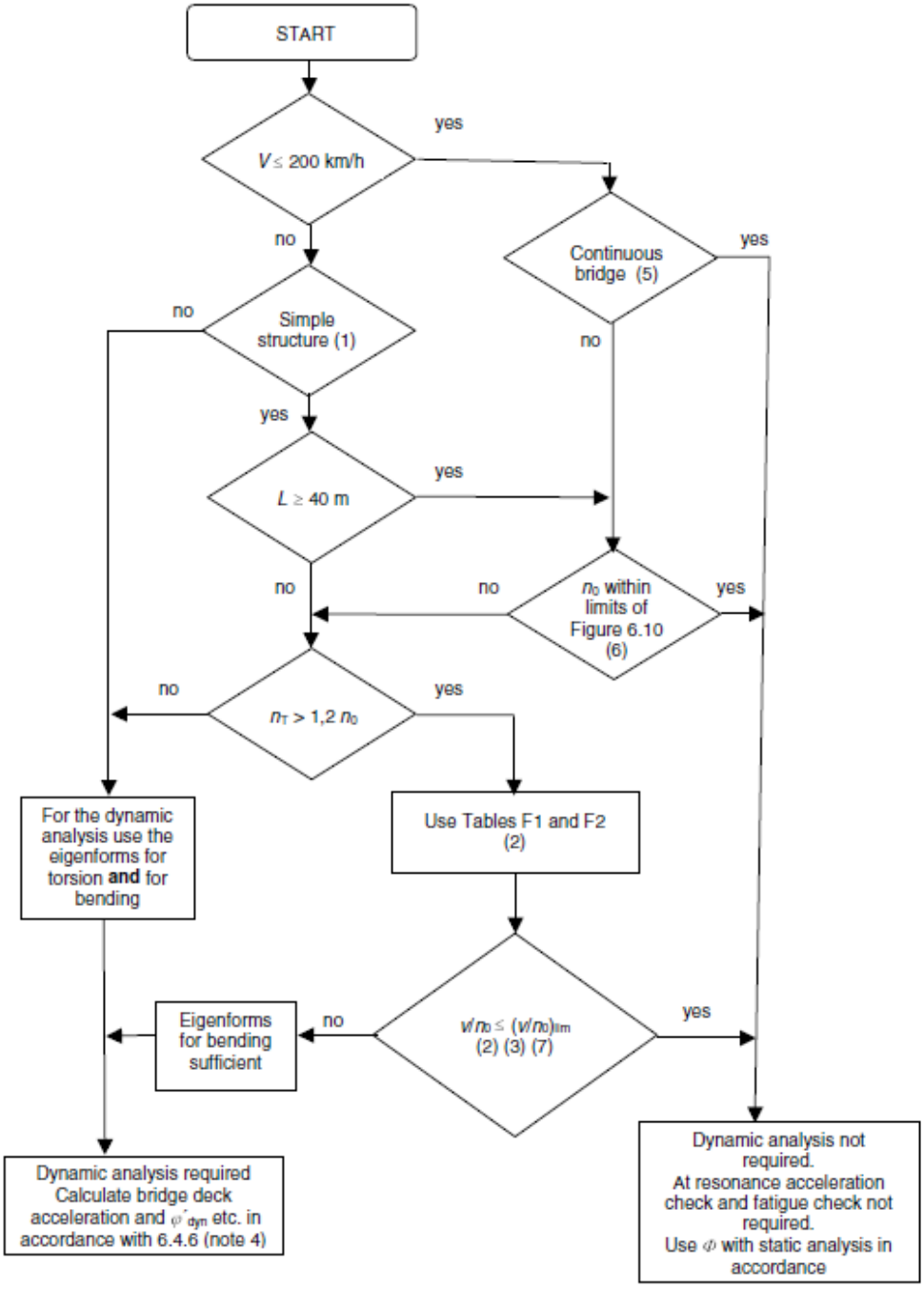

Figure 6.9 - Flow chart for determining whether a dynamic analysis is required

GVB (Amsterdam Public Transport) state that the tram has a maximum speed of 70km/h. The bridge is not continuous. Figure 6.10 in the code gives the upper and lower limits of the natural frequency with the length L=24m:

$n_{0,min} = 94.76*L^{-0.748} = 8.8$ Hz

$n_{0,max} = 23.58*L^{-0.592} = 3.6$ Hz

The upper limit of n_0 is governed by dynamic enhancements due to track irregularities and is given by :

$n_0 = 94{,}76L^{-0{,}748}$ (6.1)

The lower limit of n_0 is governed by dynamic impact criteria and is given by :

$n_0 = 80/L$
for $4\text{m} \le L \le 20\text{m}$
$n_0 = 23{,}58L^{-0{,}592}$
for $20\text{m} < L \le 100\text{m}$ (6.2)

where:

n_0 is the first natural frequency of the bridge taking account of mass due to permanent actions,
L is the span length for simply supported bridges or L_ϕ for other bridge types.

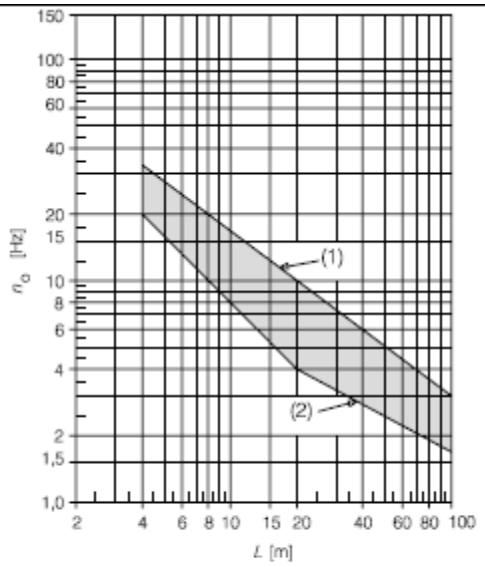

Key
(1) Upper limit of natural frequency
(2) Lower limit of natural frequency

Figure 6.10 - Limits of bridge natural frequency n_0 [Hz] as a function of L [m]

The natural frequency of the bridge (2.33 Hz) falls outside these limits, being lower than the minimum required frequency.

The natural torsional frequency n_T for a simply supported beam is determined with:

$$nT = \frac{\pi}{2\pi} * \sqrt{\frac{G*I_t}{I_p*\rho_c*L^2}}\ \text{Hz}$$

Where
G = E/(2(1+v) = 21740 MPa
I_t = torsional constant = 0.045m^4
I_p = Polar area of moment = I_z +I_y = 0.059 m^4

Filling the variables in the expression gives: nT = 53.6 Hz. This is higher than 1.2*n0.

Final step in the flow chart is to determine if v/n0 < $(v/n0)_{lim}$. In NEN-EN-1991-2 table F.1 the limits are given for v/n0, with v being the speed of the train (in this case tram). Assumed is that the acceleration of the tram is lower than 3.5m/s^2. The speed of the tram is 70/3.6 = 19.44 m/s. The bridge has a length of 24m. The mass of the total bridge is 30*A_c *ρ_c = 30.3*10^3 kg/m. This results in a $(v/n0)_{lim}$ of 14.17 m. The occurring v/n0 is 19.44/2.33 = 8.361, which is below the limit.

Table F.1 - Maximum value of $(v/n_0)_{lim}$ for a simply supported beam or slab and a maximum permitted acceleration of a_{max}< 3.50m/s^2.

Mass m 10^3 kg/m		≥5,0 <7,0	≥7,0 <9,0	≥9,0 <10,0	≥10,0 <13,0	≥13,0 <15,0	≥15,0 <18,0	≥18,0 <20,0	≥20,0 <25,0	≥25,0 <30,0	≥30,0 <40,0	≥40,0 <50,0	≥50,0 -
Span $L\in$ m [a]	ζ %	v/n_0 m	v/n_0 m	v/n_0 m	v/n_0 m	v/n_0 m	v/n_0 m	v/n_0 m	v/n_0 m	v/n_0 m	v/n_0 m	v/n_0 m	v/n_0 m
[5,00,7,50)	2	1,71	1,78	1,88	1,88	1,93	1,93	2,13	2,13	3,08	3,08	3,54	3,59
	4	1,71	1,83	1,93	1,93	2,13	2,24	3,03	3,08	3,38	3,54	4,31	4,31
[7,50,10,0)	2	1,94	2,08	2,64	2,64	2,77	2,77	3,06	5,00	5,14	5,20	5,35	5,42
	4	2,15	2,64	2,77	2,98	4,93	5,00	5,14	5,21	5,35	5,62	6,39	6,53
[10,0,12,5)	1	2,40	2,50	2,50	2,50	2,71	6,15	6,25	6,36	6,36	6,45	6,45	6,57
	2	2,50	2,71	2,71	5,83	6,15	6,25	6,36	6,36	6,45	6,45	7,19	7,29
[12,5,15,0)	1	2,50	2,50	3,58	3,58	5,24	5,24	5,36	5,36	7,86	9,14	9,14	9,14
	2	3,45	5,12	5,24	5,24	5,36	5,36	7,86	8,22	9,53	9,76	10,36	10,48
[15,0,17,5)	1	3,00	5,33	5,33	5,33	6,33	6,33	6,50	6,50	6,50	7,80	7,80	7,80
	2	5,33	5,33	6,33	6,33	6,50	6,50	10,17	10,33	10,33	10,50	10,67	12,40
[17,5,20,0)	1	3,50	6,33	6,33	6,33	6,50	6,50	7,17	7,17	10,67	12,80	12,80	12,80
[20,0,25,0)	1	5,21	5,21	5,42	7,08	7,50	7,50	13,54	13,54	13,96	14,17	14,38	14,38
[25,0,30,0)	1	6,25	6,46	6,46	10,21	10,21	10,21	10,63	10,63	12,75	12,75	12,75	12,75
[30,0,40,0)	1				10,56	18,33	18,33	18,61	18,61	18,89	19,17	19,17	19,17
≥40,0	1				14,73	15,00	15,56	15,56	15,83	18,33	18,33	18,33	18,33

[a] $L \in [a,b)$ means $a \le L < b$

NOTE 1 Table F.1 includes a safety factor of 1.2 on $(v/n_0)_{lim}$ for acceleration, deflection and strength criteria and a safety factor of 1,0 on the $(v/n_0)_{lim}$ for fatigue.

NOTE 2 Table F.1 includes an allowance of $(1+\varphi''/2)$ for track irregularities.

According to the flowchart there is no dynamical analysis needed concerning the vibrations caused by the tram.

F.19 Fatigue

The bridge is susceptible to cyclic loads coming from trams and traffic. In the demands for the new design it is given that there are 30 tram movements per track per hour over the bridge. That is equal to 788400 movements per year in total. Furthermore the bridge is assumed to be part of a main road with a low amount of heavy traffic. This means according to NEN-EN-1991-2 table 4.5 that there are $0.125*10^6$ vehicles per lane per year. So for a total of 100 years and 7 fictional lanes, this results in $87.5*10^6$ vehicles. So traffic is governing for the fatigue design.

In NEN-EN 1992-1 and NEN-EN 1992-2 it is described how to determine if a structure is safe concerning fatigue for both the concrete and prestressing steel. The procedures described there will be applied for Load Model 1. The fatigue resistance of both the concrete and prestressing steel will be determined separately.

F.19.1 Fatigue resistance concrete

The fatigue resistance of the concrete is checked at the mid span in both the top and bottom fibre of the cross section. To verify the fatigue resistance of concrete, cl. 6.8.7 of the Dutch National Annex of NEN-EN-1992-2 is used. This section state that the following expression must hold true:

$$N_i = 10^{\left[\frac{6}{1-0.57*k1*\left(1-\frac{f_{ck}}{250}\right)}*\frac{1-E_{cd,max,i}}{\sqrt{1-R_i}}\right]} > 10^6$$

Where:

$$R_{equ} = \frac{E_{cd,min,i}}{E_{cd,max,i}};\quad E_{cd,min,i} = \frac{\sigma_{cd,min,i}}{f_{cd} * (0.9 + \frac{logN_i}{60})};\quad E_{cd,max,i} = \frac{\sigma_{cd,max,i}}{f_{cd} * (0.9 + \frac{logN_i}{60})}$$

$\sigma_{cd,min,i}$ and $\sigma_{cd,max,i}$ are the lower and upper stresses of the damage equivalent stress spectrum with a number of cycles $N=10^6$. These are determined by using the following load combination:
For $\sigma_{c,max}$: $(\sum G_{k,j} + P + \psi_{1,1}Q_{k,1} + \psi_{2,j}Q_{k,j}) + Q_{fat}$
For $\sigma_{c,min}$: $(\sum G_{k,j} + P + \psi_{1,1}Q_{k,1} + \psi_{2,j}Q_{k,j})$
Q_{fat} is the fatigue load. In the governing situation traffic load model LM1 (when only vehicles are present) is the fatigue load. So the minimum and maximum stresses are determined when Q_{fat} is present and absent. For the fatigue calculation where LM1 is taken into account it is necessary according to NEN-EN 1991-2 cl. 4.6.2 to reduce the UDL with a factor 0.3 and the TS with a factor 0.7. The next and only other variable load is the pedestrian load so this one serves as $Q_{k,1}$
So the maximum minimum and permanent stresses are determined by:

$$t = \infty \text{ at top fibre: } \sigma_{c,max,equ} = -\frac{P_{m\infty}}{A_c} + \frac{M_{p,\infty}}{W_{ct}} - \frac{(M_{perm} + \psi_1 M_{peds} + M_{LM1,red})}{W_{ct}}$$

$$t = \infty \text{ at top fibre : } \sigma_{c,min,equ} = -\frac{P_{m\infty}}{A_c} + \frac{M_{p,\infty}}{W_{ct}} - \frac{(M_{perm} + \psi_1 M_{peds})}{W_{ct}}$$

$$t = \infty \text{ at bottom fibre: } \sigma_{c,max,equ} = -\frac{P_{m\infty}}{A_c} - \frac{M_{p,\infty}}{W_{cb}} + \frac{(M_{perm} + \psi_1 M_{peds} + M_{LM1,red})}{W_{cb}}$$

$$t = \infty \text{ at bottom fibre: } \sigma_{c,min,equ} = -\frac{P_{m\infty}}{A_c} - \frac{M_{p,\infty}}{W_{cb}} + \frac{(M_{perm} + \psi_1 M_{peds})}{W_{cb}}$$

The resulting stresses are:

	Top fibre	Bottom fibre
$\sigma_{cd,maxi}$:	-14,680	-22,754
$\sigma_{cd,min,i}$:	-6,555	-14,362

The absolute values of the stresses will be used in further calculations.

	Top fibre	Bottom fibre
$\sigma_{cd,maxi}$	14,680	22,754
$\sigma_{cd,min,i}$	6,555	14,362
$E_{cd,max,i}$	0,261	0,618
$E_{cd,min,i}$	0,124	0,231
$R_{c,equ}$	0,475	0,618

For the top fibre: $N_i = 4.32 * 10^9 > 10^6$
For the bottom fibre: $N_i = 3.62 * 10^9 > 10^6$
Both the top and bottom fibre in the mid span have enough fatigue resistance

F.19.2 Fatigue resistance prestressing steel

For the prestressing steel according to cl. 6.8.5 in NEN-EN-1992-1 it must hold true that:

$$\gamma_{F,fat} * \Delta\sigma_{S,equ}(N^*) \leq \frac{\Delta\sigma_{Risk}(N^*)}{\gamma_{s,fat}}$$

Where
$\Delta\sigma_{Risk}(N^*)$ is the stress range at N* cycles from the appropriate S-N curves given in figure 6.30 in NEN-EN-1992-1-1:

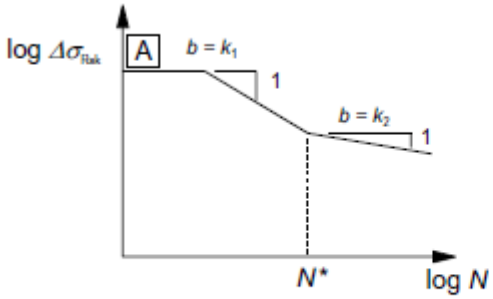

Figure 6.30: Shape of the characteristic fatigue strength curve (S-N-curves for reinforcing and prestressing steel)

For pre-tensioned steel:
$N^*=10^6$
k1=5
k2=9
$\Delta\sigma_{Risk}(N^*)$ = 185 MPa
$\Delta\sigma_{S,equ}(N^*)$ is the damage equivalent stress range for the steel considering N*.

Also allowed is to use a simpler approach by verifying (according to cl. 6.8.6 in NEN-EN-1992-1) that the stress range $\Delta\sigma_s$ should be lower than value k1, which is taken as 70 N/mm^2. If this holds true the verification stated earlier is not necessary to perform.
To determine $\Delta\sigma_s$ the maximum and minimum stress determined in paragraph F.19.1 are used to find the stress $\Delta\sigma_{c,p}$ at the height of the prestressing. This concrete stress is then transformed in a steel stress by: $\Delta\sigma_s = \Delta\sigma_{c,p} * (E_p/E_c)$.

The absolute concrete stresses with and without the presence of LM1 are:

	Top fibre	Bottom fibre
$\sigma_{cd,max}$ (with LM1):	14,680	22,754
$\sigma_{cd,min}$ (without LM1):	6,555	14,362

This results in:
$\sigma_{c,p,max}$ = (22.754-14.68)*(H-e)/H + 14.68 = 21.734 N/mm^2
$\sigma_{c,p,min}$ = (14.362-6.555)*(H-e)/H + 6.555 = 13.376 N/mm^2

The stress difference $\Delta\sigma_{c,p}$ =21.73-13.38 = 8.36 N/mm^2
This results in a steel stress range of:
$\Delta\sigma_s$ = 8.36*195000/50000 = 37.05 N/mm^2 which is well below 70 N/mm^2 (UC=0.529).
So the fatigue resistance of the prestesssing steel meets the requirements. Additional verifications are not necessary.

F.19.3 Conclusion fatigue

The concrete does not have enough fatigue resistance and the prestressing steel does have enough fatigue resistance to resist the variable cyclic loads that occur on the bridge. In order to suffice to the fatigue resistance the stiffness of the structure needs to be increased. This can be done the fastest by increasing the construction thickness. Increasing the height to 650 mm would provide in enough fatigue resistance.

F.20 Summary

Results if a thickness of 600 mm is used:

Amount of strands:	34ϕ15.2 strands	
Total losses in strands:	9.7%	
ULS		
Bending moment capacity, M_{Rd}:	M_{Rd} = 1955.31 kNm	UC = 0.652
Rotational capacity: x_u/d	x_u/d = 0.446	UC = 0.825
Shear capacity V_{Rd}:	V_{Rd} = 695.07 kNm	UC = 1.101
Shear reinforcement	A_{sw} = 575 mm^2 (min. reinf.)	
Torsional capacity T_{Rd}:	T_{Rd} =261.8 kNm	UC = 1.211
Torsion reinforcement:	A_s = 2828 mm^2	
Transverse moment capacity: $M_{Rd,y}$:	$M_{Rd,y}$ = 161.6 kNm	UC = 0.921
Capacity concrete at hammerhead:	$M_{Rd,head}$ = 1760.9 kNm	UC = 0.656
SLS		
Crack width verification:	M_{CR} = 986.78 kNm	UC= 0.551
Deflection:	w2 = 65.4mm < L/500	
	w3 = 19.5mm < L/250	
Fatigue:	Concrete: Top fibre:	UC = 0.580
	Bottom fibre:	UC = 0.859 but n_i/N_i>1
	Prestressing:	UC = 0.529

G. Results optimization process

G.1 General

In this appendix, the results from the optimization are presented. These are used to back up the claims and observations that were made in the main report.
The results are divided per optimization step:

- Optimization based on governing internal forces
  - Optimization of prestressing
  - Optimization of web thickness
  - Optimization of bottom flange
  - Optimization of construction height
- Sectional optimization
  - Sectional optimization first step
  - Sectional optimization final step

Also the SCIA engineering report for determining the deformations for the sectional optimized girder is found in this appendix.

G.2 Optimization based on governing internal forces

G.2.1 Results optimization of prestressing

Optimization of prestressing		Initial Design				Limited prestressing 1(<fctd1)				Limited prestressing 2 (<fctk)			
Requirements for type of prestressing	t=0 top fibre t=0 bottom fibre t=inf bottom fibre	σ < 0 σ >-0,6*fck σ < 0				σ < fctd1 σ >-0,6*fck σ < fctd1				σ < fctk σ >-0,6*fck σ <fctk			
Amount of strands	N	33				29				27			
Total area of strands	Ap	4587	mm2			4031	mm2			3753	mm2		
Total losses in strands		12,2	%			11,8	%			11,65	%		
ULS													
Bending moment capacity	MRd: Med:	2358,5 1259,6	kNm kNm	UC:	0,534	2107,1 1418	kNm	UC:	0,673	1997,8 1497	kNm	UC:	0,749
Rotational capacity	xu/d	0,365		UC:	0,734	0,242		UC:	0,493	0,229		UC:	0,466
Shear capacity	VRd: VEd:	1088,71 738,9	kN kN	UC:	0,679	1088,712 738.9	kN	UC:	0,598	1088,71 738.9	kN	UC:	0,607
Torsional capacity	TRd:	542,6	kNm	UC:	0,584	542,6	kNm	UC:	0,584	542,6	kNm	UC:	0,584
Transverse moment capacity	MRd,y:	76,75	kNm	UC:	0,96	76,75	kNm	UC:	0,96	76,75	kNm	UC:	0,96
Capacity concrete at hammerhead	MRd,head: Med,head:	2145,75 1190,45	kNm kNm	UC:	0,555	1960,6 964.11	kNm kNm	UC:	0,729	1865,9 799.94	kNm kNm	UC:	0,705
SLS													
Crack width verification	Mcr:	1162,86	kNm	UC:	0,461	1072,56	kNm	UC:	0,648	1027,4	kNm	UC:	0,753
Deflection	w2:	71	mm	UC:	0,74	46,38	mm	UC:	0,48	33,77	mm	UC:	0,35
	w3.1:	15	mm	UC:	0,31	37,96	mm	UC:	0,79	48,56	mm	UC:	1,01
	w3.2:			UC:	0,156			UC:	0,40			UC:	0,51
Vibrations	n0: v/n0:	2,52 7,705	Hz m			2,52 7,705	Hz m			2,52 7,705	Hz m		
Fatigue	Concr- Top Fibre: Concr - Bottom Fibre: Prestressing steel:			UC: UC: UC:	0,44 0,45 0,487			UC: UC: UC:	0,436 0,444 0,487			UC: UC: UC:	0,434 0,447 0,487

G.2.2 Results optimization web thickness

Optimization of web thickness													
Web thickness	bweb:	140	mm			130	mm			120	mm		
Total area of concrete	Ac	0,377	m2			0,371	m2			0,364	m2		
Self-weight	qself	9,885	kNm			9,743	kNm			9,601	kNm		
Amount of strands	n	29,000				29,000				28,000			
Total area of strands	Ap	4031,000	mm2			4031,000	mm2			3892,000	mm2		
Total losses in strands		11,800	%			11,800	%			11,790	%		
ULS													
Bending moment capacity	MRd:	2107,100	kNm	UC:	0,673	2100,000	kNm	UC:	0,668	2039,000	kNm	UC:	0,701
	MEd	1418,000				1403,831				1429,300			
Rotational capacity	xu/d	0,242		UC:	0,493	0,241		UC:	0,492	0,234		UC:	0,477
Shear capacity	VRd:	1088,712	kN	UC:	0,679	1010,900	kN	UC:	0,756	933,182	kN	UC:	0,816
	VEd	738,90				763,983				761,223			
Torsional capacity	TRd:	542,600	kNm	UC:	0,584	548,900	kNm	UC:	0,578	512,500	kNm	UC:	0,619
Transverse moment capacity:	MRd,y:	76,750	kNm	UC:	0,960	76,750	kNm	UC:	0,960	76,750	kNm	UC:	0,960
Capacity concrete at hammerhead	MRd,head	1960,600	kNm	UC:	0,492	1962,250	kNm	UC:	0,643	1917,260	kNm	UC:	0,630
	MEd,head	964,110	kNm			1262,270	kNm			1208,580	kNm		
SLS													
Crack width verification	Mcr	1072,560	kNm	UC:	0,648	1078,540	kNm	UC:	0,633	1061,620	kNm	UC:	0,669
Deflection	w2	46,380	mm	UC:	0,483	48,210	mm	UC:	0,502	43,687	mm	UC:	0,455
	w3.1	37,960	mm	UC:	0,791	36,460	mm	UC:	0,760	40,288	mm	UC:	0,839
	w3.2			UC:	0,395			UC:	0,380			UC:	0,420
Vibrations	n0	2,520	Hz			2,540	Hz			2,558	Hz		
	v/n0	7,705	m			7,654	m			7,602	m		
Fatigue	Concr- Top Fibre			UC:	0,436			UC:	0,436			UC:	0,436
	Concr - Bottom Fibre			UC:	0,444			UC:	0,445			UC:	0,446
	Prestressing steel			UC:	0,487			UC:	0,489			UC:	0,492

Web thickness	bweb:	110	mm			100	mm			90	mm		
Total area of concrete	Ac	0,358	m2			0,352	m2			0,346	m2		
Self-weight	qself	9,459	kNm			9,317	kNm			9,175	kNm		
Amount of strands	n	28,000				28,000				27,000			
Total area of strands	Ap	3892,000	mm2			3892,000	mm2			3753,000	mm2		
Total losses in strands		11,820	%			11,855	%			11,813	%		
ULS													
Bending moment capacity	MRd:	2032,120	kNm	UC:	0,696	2025,140	kNm	UC:	0,692	1963,432	kNm	UC:	0,726
	MEd	1415,100				1400,810				1426,386			
Rotational capacity:	xu/d	0,233		UC:	0,475	0,232		UC:	0,473	0,225		UC:	0,458
Shear capacity	VRd:	855,417	kN	UC:	0,887	777,652	kN	UC:	0,972	699,887	kN	UC:	1,076
	VEd	758,397				755,586				752,871			
Torsional capacity	TRd:	475,141	kNm	UC:	0,667	436,800	kNm	UC:	0,726	397,488	kNm	UC:	0,798
Transverse moment capacity:	MRd,y:	76,750	kNm	UC:	0,960	76,750	kNm	UC:	0,960	76,750	kNm	UC:	0,960
Capacity concrete at hammerhead	MRd,head	1919,430	kNm	UC:	0,632	1921,987	kNm	UC:	0,633	1876,550	kNm	UC:	0,621
	MEd,head	1213,050	kNm			1216,820	kNm			1164,488	kNm		
SLS													
Crack width verification	Mcr	1067,770	kNm	UC:	0,654	1074,163	kNm	UC:	0,638	1056,780	kNm	UC:	0,675
Deflection	w2	45,531	mm	UC:	0,474	47,399	mm	UC:	0,494	42,817	mm	UC:	0,446
	w3.1	38,776	mm	UC:	0,808	37,245	mm	UC:	0,776	41,132	mm	UC:	0,857
	w3.2			UC:	0,404			UC:	0,388			UC:	0,428
Vibrations	n0	2,575	Hz			2,594	Hz			2,612	Hz		
	v/n0	7,550	m			7,497	m			7,443	m		
Fatigue	Concr- Top Fibre			UC:	0,436			UC:	0,436			UC:	0,436
	Concr - Bottom Fibre			UC:	0,447			UC:	0,448			UC:	0,449
	Prestressing steel			UC:	0,494			UC:	0,496			UC:	0,498

G.2.3 Results optimization bottom flange

Optimization of bottom flange thickness									
Web thickness	bweb:	100	mm			100	mm		
Bottom flange thickness	hbot	130	mm			120	mm		
Eccentricity strands at bottom flange	e	65,8	mm			60	mm		
Total area of concrete	Ac	0,352	m2			0,344	m2		
Self-weight	qself	9,317	kNm			9,133	kNm		
Amount of strands	n	28,000				27,000			
Total area of strands	Ap	3892,000	mm2			3753,000	mm2		
Total losses in strands		11,855	%			11,864	%		
ULS									
Bending moment capacity	MRd:	2025,140	kNm	UC:	0,692	1955,710	kNm	UC:	0,706
	MEd	1400,810				1380,352			
Rotational capacity	xu/d	0,232		UC:	0,473	0,222		UC:	0,452
Shear capacity	VRd:	777,652	kN	UC:	0,972	786,095	kN	UC:	0,957
	VEd	755,586				752,529			
Torsional capacity	TRd:	436,800	kNm	UC:	0,726	441,600	kNm	UC:	0,718
Transverse moment capacity	MRd,y:	76,750	kNm	UC:	0,960	76,750	kNm	UC:	0,960
Capacity concrete at hammerhead	MRd,head	1921,987	kNm	UC:	0,633	1901,330	kNm	UC:	0,642
	MEd,head	1216,820	kNm			1220,680	kNm		
SLS									
Crack width verification	Mcr	1074,163	kNm	UC:	0,638	1032,126	kNm	UC:	0,647
Deflection	w2	47,399	mm	UC:	0,494	50,836	mm	UC:	0,530
	w3.1	37,245	mm	UC:	0,776	35,455	mm	UC:	0,739
	w3.2			UC:	0,388			UC:	0,369
Vibrations	n0	2,594	Hz			2,600	Hz		
	v/n0	7,497	m			7,478	m		
Fatigue	Concr- Top			UC:	0,436			UC:	0,439
	Concr - Bottom			UC:	0,448			UC:	0,455
	Prestressing steel			UC:	0,496			UC:	0,511

G.2.4 Results optimization construction thickness

Total height of beam	H	600	mm			590	mm			580	mm		
Web thickness	bweb:	100	mm			100	mm			100	mm		
Bottom flange thickness	hbot	120	mm			120	mm			120	mm		
Eccentricity strands at bottom flange	e	60	mm			60	mm			60	mm		
Total area of concrete	Ac	0,344	m2			0,344	m2			0,340	m2		
Self-weight	qself	9,133	kNm			9,067	kNm			9,000	kNm		
Amount of strands	n	27,000				28,000				28,000			
Total area of strands	Ap	3753,000	mm2			3892,000	mm2			3892,000	mm2		
ULS													
Bending moment capacity	MRd:	1955,710	kNm	UC:	0,706	1968,920	kNm	UC:	0,690	1928,000	kNm	UC:	0,714
	MEd	1380,352				1357,620				1376,420			
Rotational capacity:	xu/d	0,222		UC:	0,452	0,233		UC:	0,476	0,238		UC:	0,484
Shear capacity	VRd:	786,095	kN	UC:	0,957	773,142	kN	UC:	0,973	760,135	kN	UC:	0,990
	VEd	752,529				752,333				752,219			
Torsional capacity	TRd:	441,600	kNm	UC:	0,718	432,000	kNm	UC:	0,734	422,400	kNm	UC:	0,751
Transverse moment capacity	MRd,y:	76,750	kNm	UC:	0,960	76,750	kNm	UC:	0,960	76,750	kNm	UC:	0,960
Capacity concrete at hammerhead	MRd,head	1901,330	kNm	UC:	0,642	1906,410	kNm	UC:	0,658	1862,880	kNm	UC:	0,659
	MEd,head	1220,680	kNm			1253,570	kNm			1227,970	kNm		
SLS													
Crack width verification	Mcr	1032,126	kNm	UC:	0,647	1031,093	kNm	UC:	0,665	1006,586	kNm	UC:	0,661
Deflection	w2	50,836	mm	UC:	0,530	56,756	mm	UC:	0,591	55,692	mm	UC:	0,580
	w3.1	35,455	mm	UC:	0,739	33,921	mm	UC:	0,707	38,477	mm	UC:	0,802
	w3.2			UC:	0,369			UC:	0,353			UC:	0,401
Vibrations	n0	2,600	Hz			2,551	Hz			2,501	Hz		
	v/n0	7,478	m			7,623	m			7,775	m		
Fatigue	Concr- Top Fibre			UC:	0,439			UC:	0,444			UC:	0,449
	Concr - Bottom Fibre			UC:	0,455			UC:	0,463			UC:	0,470
	Prestressing steel			UC:	0,511			UC:	0,525			UC:	0,539

Total height of beam	H	570	mm			560	mm			550	mm		
Web thickness	bweb:	100	mm			100	mm			100	mm		
Bottom flange thickness	hbot	120	mm			120	mm			120	mm		
Eccentricity strands at bottom flange	e	60	mm			60	mm			60	mm		
Total area of concrete	Ac	0,338	m2			0,336	m2			0,334	m2		
Self-weight	qself	8,933	kNm			8,867	kNm			8,800	kNm		
Amount of strands	n	29,000				30,000				30,000			
Total area of strands	Ap	4031,000	mm2			4170,000	mm2			4170,000	mm2		
ULS													
Bending moment capacity	MRd:	1937,320	kNm	UC:	0,700	1943,810	kNm	UC:	0,688	1900,940	kNm	UC:	0,715
	MEd	1356,354				1338,069				1358,690			
Rotational capacity:	xu/d	0,249		UC:	0,507	0,261		UC:	0,531	0,266		UC:	0,542
Shear capacity	VRd:	747,074	kN	UC:	1,007	733,958	kN	UC:	1,024	720,787	kN	UC:	1,043
	VEd	752,105				751,910				751,797			
Torsional capacity	TRd:	412,800	kNm	UC:	0,768	403,200	kNm	UC:	0,786	393,600	kNm	UC:	0,806
Transverse moment capacity	MRd,y:	76,750	kNm	UC:	0,960	76,750	kNm	UC:	0,960	76,750	kNm	UC:	0,960
Capacity concrete at hammerhead	MRd,head	1864,960	kNm	UC:	0,674	1864,850	kNm	UC:	0,689	1819,930	kNm	UC:	0,690
	MEd,head	1257,900	kNm			1284,430	kNm			1256,250	kNm		
SLS													
Crack width verification	Mcr	1004,141	kNm	UC:	0,644	1000,740	kNm	UC:	0,629	975,363	kNm	UC:	0,667
Deflection	w2	61,779	mm	UC:	0,644	68,020	mm	UC:	0,709	68,750	mm	UC:	0,716
	w3.1	37,273	mm	UC:	0,777	36,190	mm	UC:	0,754	41,740	mm	UC:	0,870
	w3.2			UC:	0,388			UC:	0,377			UC:	0,435
Vibrations	n0	2,451	Hz			2,401	Hz			2,351	Hz		
	v/n0	7,933	m			8,098	m			8,271	m		
Fatigue	Concr- Top Fibre			UC:	0,455			UC:	0,461			UC:	0,467
	Concr - Bottom Fibre			UC:	0,479			UC:	0,491			UC:	0,497
	Prestressing steel			UC:	0,555			UC:	0,571			UC:	0,588

Total height of beam	H	540	mm			530	mm			520	mm		
Web thickness	bweb:	100	mm			100	mm			100	mm		
Bottom flange thickness	hbot	120	mm			120	mm			120	mm		
Eccentricity strands at bottom flange	e	60	mm			60	mm			60	mm		
Total area of concrete	Ac	0,332	m2			0,330	m2			0,328	m2		
Self-weight	qself	8,733	kNm			8,667	kNm			8,600	kNm		
Amount of strands	n	31,000				32,000				33,000			
Total area of strands	Ap	4309,000	mm2			4448,000	mm2			4587,000	mm2		
ULS													
Bending moment capacity	MRd:	1903,570	kNm	UC:	0,706	1903,420	kNm	UC:	0,698	1900,500	kNm	UC:	0,693
	MEd	1343,092				1329,279				1317,254			
Rotational capacity:	xu/d	0,278		UC:	0,567	0,291		UC:	0,594	0,305		UC:	0,622
Shear capacity	VRd:	707,561	kN	UC:	1,062	694,279	kN	UC:	1,082	680,941	kN	UC:	1,103
	VEd	751,603				751,491				751,379			
Torsional capacity	TRd:	384,000	kNm	UC:	0,826	374,400	kNm	UC:	0,847	364,800	kNm	UC:	0,869
Transverse moment capacity	MRd,y:	76,750	kNm	UC:	0,960	76,750	kNm	UC:	0,960	76,750	kNm	UC:	0,960
Capacity concrete at hammerhead	MRd,head	1816,800	kNm	UC:	0,704	1811,470	kNm	UC:	0,718	1803,920	kNm	UC:	0,731
	MEd,head	1278,950	kNm			1299,970	kNm			1318,430	kNm		
SLS													
Crack width verification	Mcr	970,549	kNm	UC:	0,656	964,779	kNm	UC:	0,646	958,053	kNm	UC:	0,639
Deflection	w2	73,130	mm	UC:	0,762	79,666	mm	UC:	0,830	86,340	mm	UC:	0,899
	w3.1	41,160	mm	UC:	0,858	40,815	mm	UC:	0,850	40,720	mm	UC:	0,848
	w3.2			UC:	0,429			UC:	0,425			UC:	0,424
Vibrations	n0	2,301	Hz			2,251	Hz			2,200	Hz		
	v/n0	8,451	m			8,640	m			8,838	m		
Fatigue	Concr- Top Fibre			UC:	0,474			UC:	0,481			UC:	0,489
	Concr - Bottom Fibre			UC:	0,510			UC:	0,526			UC:	0,543
	Prestressing steel			UC:	0,606			UC:	0,625			UC:	0,645

Total height of beam	H	510	mm			500	mm		
Web thickness	bweb:	100	mm			100	mm		
Bottom flange thickness	hbot	120	mm			120	mm		
Eccentricity strands at bottom flange	e	60	mm			60	mm		
Total area of concrete	Ac	0,326	m2			0,324	m2		
Self-weight	qself	8,533	kNm			8,467	kNm		
Amount of strands	n	34,000				35,000			
Total area of strands	Ap	4726,000	mm2			4865,000	mm2		
ULS									
Bending moment capacity	MRd:	1894,820	kNm	UC:	0,690	1886,400	kNm	UC:	0,688
	MEd	1307,021				1298,583			
Rotational capacity:	xu/d	0,320		UC:	0,651	0,335		UC:	0,682
Shear capacity	VRd:	667,547	kN	UC:	1,125	654,096	kN	UC:	1,148
	VEd	751,186				751,075			
Torsional capacity	TRd:	355,200	kNm	UC:	0,893	345,600	kNm	UC:	0,918
Transverse moment capacity	MRd,y:	76,750	kNm	UC:	0,960	76,750	kNm	UC:	0,960
Capacity concrete at hammerhead	MRd,head	1794,160	kNm	UC:	0,743	1782,180	kNm	UC:	0,756
	MEd,head	1333,490	kNm			1346,840	kNm		
SLS									
Crack width verification	Mcr	950,371	kNm	UC:	0,635	941,738	kNm	UC:	0,633
Deflection	w2	93,150	mm	UC:	0,970	100,090	mm	UC:	1,043
	w3.1	40,940	mm	UC:	0,853	41,520	mm	UC:	0,865
	w3.2			UC:	0,426			UC:	0,433
Vibrations	n0	2,150	Hz			2,099	Hz		
	v/n0	9,045	m			9,263	m		
Fatigue	Concr- Top Fibre			UC:	0,497			UC:	0,506
	Concr - Bottom Fibre			UC:	0,562			UC:	0,584
	Prestressing steel			UC:	0,666			UC:	0,689

G.3 Sectional optimization

G.3.1 Results first optimization step

Results sectional optimization 1st step		Section	1 & 22			Section	2 & 21			Section	3 & 20		
Total height of beam	H:	580	mm			580	mm			580	mm		
Web thickness	bweb:	100	mm			100	mm			100	mm		
Bottom flange thickness	hbot:	120	mm			120	mm			120	mm		
Eccentricity strands at bottom flange	e:	60	mm			60	mm			60	mm		
Total area of concrete	Ac:	0,340	m2			0,340	m2			0,340	m2		
Self-weight	qself:	8,500	kN/m			8,500	kN/m			8,500	kN/m		
Amount of strands:	n:	30,000				30,000				30,000			
Total area of strands	Ap:	4170,000	mm2			4170,000	mm2			4170,000	mm2		
ULS													
Bending moment capacity	MRd:	2030,024	kNm	UC:	0,020	2030,024	kNm	UC:	0,170	2030,024	kNm	UC:	0,276
	Med:	40,116	kNm			344,358	kNm			561,039	kNm		
Rotational capacity	xu/d:	0,251		UC:	0,512	0,251		UC:	0,512	0,251		UC:	0,512
Shear capacity	VRd:	760,135	kN	UC:	0,855	760,135	kN	UC:	0,802	760,135	kN	UC:	0,657
	Ved:	649,950	kN			609,278	kN			499,358	kN		
Torsional capacity	TRd:	422,400	kNm	UC:	0,743	422,400	kNm	UC:	0,743	422,400	kNm	UC:	0,705
	TEd:	314	kNm			314	kNm			298	kNm		
SLS													
Crack width verification	Mcr:	1051,624	kNm	UC:	0,269	1051,624	kNm	UC:	0,066	1051,624	kNm	UC:	0,071
	Mmax:	-283,034	kNm			-68,888	kNm			74,359	kNm		
Stresses in structure	σ at t=0 top:	2,377	N/mm2			1,434	N/mm2			0,655	N/mm2		
(Frequent combination)	σ at t=0 bottom:	-38,589	N/mm2			-37,55	N/mm2			-36,692	N/mm2		
	σ at t=inf bot:	-20,393	N/mm2			-15,837	N/mm2			-12,79	N/mm2		

		Section	4 & 19			Section	5 & 18			Section	6 & 17		
Total height of beam	H:	580	mm			580	mm			580	mm		
Web thickness	bweb:	100	mm			100	mm			100	mm		
Bottom flange thickness	hbot:	120	mm			120	mm			120	mm		
Eccentricity strands at bottom flange	e:	60	mm			60	mm			60	mm		
Total area of concrete	Ac:	0,340	m2			0,340	m2			0,340	m2		
Self-weight	qself:	8,500	kN/m			8,500	kN/m			8,500	kN/m		
Amount of strands:	n:	30,000				30,000				30,000			
Total area of strands	Ap:	4170,000	mm2			4170,000	mm2			4170,000	mm2		
ULS													
Bending moment capacity	MRd:	2030,024	kNm	UC:	0,350	2030,024	kNm	UC:	0,450	2030,024	kNm	UC:	0,517
	Med:	710,670	kNm			913,452	kNm			1049,429	kNm		
Rotational capacity	xu/d:	0,251		UC:	0,512	0,251		UC:	0,512	0,251		UC:	0,512
Shear capacity	VRd:	760,135	kN	UC:	0,557	760,135	kN	UC:	0,508	760,135	kN	UC:	0,462
	Ved:	423,212	kN			386,098	kN			350,914	kN		
Torsional capacity	TRd:	422,400	kNm	UC:	0,656	422,400	kNm	UC:	0,613	422,400	kNm	UC:	0,613
	TEd:	277	kNm			259	kNm			259	kNm		
SLS													
Crack width verification	Mcr:	1051,624	kNm	UC:	0,174	1051,624	kNm	UC:	0,300	1051,624	kNm	UC:	0,388
	Mmax:	182,906	kNm			315,752	kNm			407,899	kNm		
Stresses in structure	σ at t=0 top:	0,041	N/mm2			-0,409	N/mm2			-0,696	N/mm2		
(Frequent combination)	σ at t=0 bottom:	-36,015	N/mm2			-35,518	N/mm2			-35,202	N/mm2		
	σ at t=inf bot:	-10,481	N/mm2			-7,655	N/mm2			-5,694	N/mm2		

		Section	7 & 16			Section	8 & 15			Section	9 & 14		
Total height of beam	H:	580	mm			580	mm			580	mm		
Web thickness	bweb:	100	mm			100	mm			100	mm		
Bottom flange thickness	hbot:	120	mm			120	mm			120	mm		
Eccentricity strands at bottom flange	e:	60	mm			60	mm			60	mm		
Total area of concrete	Ac:	0,340	m2			0,340	m2			0,340	m2		
Self-weight	qself:	8,500	kN/m			8,500	kN/m			8,500	kN/m		
Amount of strands:	n:	30,000				30,000				30,000			
Total area of strands	Ap:	4170,000	mm2			4170,000	mm2			4170,000	mm2		
ULS													
Bending moment capacity	MRd:	2030,024	kNm	UC:	0,553	2030,024	kNm	UC:	0,583	2030,024	kNm	UC:	0,605
	Med:	1122,045	kNm			1182,842	kNm			1228,622	kNm		
Rotational capacity	xu/d:	0,251		UC:	0,512	0,251		UC:	0,512	0,251		UC:	0,512
Shear capacity	VRd:	760,135	kN	UC:	0,414	760,135	kN	UC:	0,379	760,135	kN	UC:	0,339
	Ved:	314,668	kN			287,881	kN			257,507	kN		
Torsional capacity	TRd:	422,400	kNm	UC:	0,481	422,400	kNm	UC:	0,419	422,400	kNm	UC:	0,355
	TEd:	203	kNm			177	kNm			150	kNm		
SLS													
Crack width verification	Mcr:	1051,624	kNm	UC:	0,433	1051,624	kNm	UC:	0,470	1051,624	kNm	UC:	0,504
	Mmax:	455,745	kNm			494,292	kNm			529,742	kNm		
Stresses in structure	σ at t=0 top:	-0,818	N/mm2			-0,777	N/mm2			-1,187	N/mm2		
(Frequent combination)	σ at t=0 bottom:	-35,068	N/mm2			-35,113	N/mm2			-34,661	N/mm2		
	σ at t=inf bot:	-4,676	N/mm2			-3,856	N/mm2			-3,102	N/mm2		

		Section	10 & 13			Section	11 & 12		
Total height of beam	H:	580	mm			580	mm		
Web thickness	bweb:	100	mm			100	mm		
Bottom flange thickness	hbot:	120	mm			120	mm		
Eccentricity strands at bottom flange	e:	60	mm			60	mm		
Total area of concrete	Ac:	0,340	m2			0,340	m2		
Self-weight	qself:	8,500	kN/m			8,500	kN/m		
Amount of strands:	n:	30,000				30,000			
Total area of strands	Ap:	4170,000	mm2			4170,000	mm2		
ULS									
Bending moment capacity	MRd:	2030,024	kNm	UC:	0,615	2030,024	kNm	UC:	0,617
	Med:	1247,522	kNm			1252,622	kNm		
Rotational capacity	xu/d:	0,251		UC:	0,512	0,251		UC:	0,512
Shear capacity	VRd:	760,135	kN	UC:	0,275	760,135	kN	UC:	0,205
	Ved:	208,805	kN			156,007	kN		
Torsional capacity	TRd:	422,400	kNm	UC:	0,289	422,400	kNm	UC:	0,223
	TEd:	122	kNm			94	kNm		
SLS									
Crack width verification	Mcr:	1051,624	kNm	UC:	0,519	1051,624	kNm	UC:	0,523
	Mmax:	545,492	kNm			549,742	kNm		
Stresses in structure	σ at t=0 top:	-1,433	N/mm2			-1,515	N/mm2		
(Frequent combination)	σ at t=0 bottom:	-34,39	N/mm2			-34,3	N/mm2		
	σ at t=inf bot:	-2,767	N/mm2			-2,677	N/mm2		

G.3.2 Results final step optimization

Results frame method optimization final step		Section	1 & 22			Section	2 & 21			Section	3 & 20		
Total height of beam	H:	500	mm			470	mm			460	mm		
Web thickness	bweb:	100	mm			100	mm			100	mm		
Bottom flange thickness	hbot:	120	mm			120	mm			120	mm		
Eccentricity strands at bottom flange	e:	60	mm			60	mm			60	mm		
Total area of concrete	Ac:	0,324	m2			0,318	m2			0,316	m2		
Self-weight	qself:	8,100	kNm			7,950	kNm			7,900	kNm		
Amount of strands:	n:	30,000				30,000				30,000			
Total area of strands	Ap:	4170,000	mm2			4170,000	mm2			4170,000	mm2		
ULS													
Bending moment capacity	MRd:	1688,980	kNm	UC:	0,116	1563,748	kNm	UC:	0,364	1522,329	kNm	UC:	0,586
	Med:	195,159	kNm			569,912	kNm			801,008	kNm		
Rotational capacity	xu/d:	0,294		UC:	0,600	0,315		UC:	0,642	0,322		UC:	0,657
Shear capacity	VRd:	654,096	kN	UC:	0,996	613,398	kN	UC:	0,997	599,720	kN	UC:	0,838
	Ved:	651,206	kN			611,600	kN			502,651	kN		
Torsional capacity	TRd:	345,600	kNm	UC:	0,909	316,800	kNm	UC:	0,991	307,200	kNm	UC:	0,970
	TEd:	314	kNm			314	kNm			298	kNm		
SLS													
Crack width verification	Mcr:	849,254	kNm	UC:	0,149	774,359	kNm	UC:	0,195	749,554	kNm	UC:	0,426
	Mmax:	-126,231	kNm			151,277	kNm			319,128	kNm		
Stresses in structure	σ at t=0 top:	2,51	N/mm2			1,052	N/mm2			-0,348	N/mm2		
(Frequent combination)	σ at t=0 bottom:	-40,278	N/mm2			-39,278	N/mm2			-37,959	N/mm2		
	σ at t=inf bot:	-18,512	N/mm2			-10,801	N/mm2			-5,474	N/mm2		
Governing for section was:		Shear force, VRd				Shear force, VRd				Torsional capacity, TRd			

		Section	4 & 19			Section	5 & 18			Section	6 & 17		
Total height of beam	H:	430	mm			470	mm			480	mm		
Web thickness	bweb:	100	mm			100	mm			100	mm		
Bottom flange thickness	hbot:	120	mm			120	mm			120	mm		
Eccentricity strands at bottom flange	e:	60	mm			60	mm			60	mm		
Total area of concrete	Ac:	0,310	m2			0,318	m2			0,320	m2		
Self-weight	qself:	7,750	kNm			7,950	kNm			8,000	kNm		
Amount of strands:	n:	30,000				30,000				30,000			
Total area of strands	Ap:	4170,000	mm2			4170,000	mm2			4170,000	mm2		
ULS													
Bending moment capacity	MRd:	1399,050	kNm	UC:	0,727	1563,748	kNm	UC:	0,730	1605,330	kNm	UC:	0,786
	Med:	1016,564	kNm			1142,069	kNm			1261,862	kNm		
Rotational capacity	xu/d:	0,348		UC:	0,709	0,315		UC:	0,642	0,308		UC:	0,627
Shear capacity	VRd:	539,745	kN	UC:	0,793	613,398	kN	UC:	0,636	627,022	kN	UC:	0,567
	Ved:	428,259	kN			390,400	kN			355,468	kN		
Torsional capacity	TRd:	278,400	kNm	UC:	0,995	316,800	kNm	UC:	0,818	326,400	kNm	UC:	0,794
	TEd:	277	kNm			259	kNm			259	kNm		
SLS													
Crack width verification	Mcr:	752,924	kNm	UC:	0,659	774,359	kNm	UC:	0,711	799,248	kNm	UC:	0,784
	Mmax:	495,929	kNm			550,309	kNm			626,282	kNm		
Stresses in structure	σ at t=0 top:	-2,102				-2,147	N/mm2			-2,513	N/mm2		
(Frequent combination)	σ at t=0 bottom:	-36,673				-35,808	N/mm2			-35,207	N/mm2		
	σ at t=inf bot:	1,677				1,239	N/mm2			2,964	N/mm2		
Governing for section was:		Torsional capacity, TRd				Amount of strands,n				Amount of strands,n			

		Section	7 & 16			Section	8 & 15			Section	9 & 14		
Total height of beam	H:	520	mm			530	mm			540	mm		
Web thickness	bweb:	100	mm			100	mm			100	mm		
Bottom flange thickness	hbot:	120	mm			120	mm			120	mm		
Eccentricity strands at bottom flange	e:	60	mm			60	mm			60	mm		
Total area of concrete	Ac:	0,328	m2			0,330	m2			0,332	m2		
Self-weight	qself:	8,200	kNm			8,250	kNm			8,300	kNm		
Amount of strands:	n:	30,000				30,000				30,000			
Total area of strands	Ap:	4170,000	mm2			4170,000	mm2			4170,000	mm2		
ULS													
Bending moment capacity	MRd:	1779,282	kNm	UC:	0,704	1815,670	kNm	UC:	0,713	1858,220	kNm	UC:	0,709
	Med:	1252,456	kNm			1294,508	kNm			1317,307	kNm		
Rotational capacity	xu/d:	0,282		UC:	0,575	0,276		UC:	0,563	0,271		UC:	0,552
Shear capacity	VRd:	680,941	kN	UC:	0,467	694,279	kN	UC:	0,413	707,561	kN	UC:	0,363
	Ved:	317,788	kN			286,681	kN			256,787	kN		
Torsional capacity	TRd:	364,800	kNm	UC:	0,556	374,400	kNm	UC:	0,473	384,000	kNm	UC:	0,391
	TEd:	203	kNm			177	kNm			150	kNm		
SLS													
Crack width verification	Mcr:	899,528	kNm	UC:	0,656	924,753	kNm	UC:	0,659	950,033	kNm	UC:	0,654
	Mmax:	589,996	kNm			609,333	kNm			621,227	kNm		
Stresses in structure	σ at t=0 top:	-1,902	N/mm2			-1,735	N/mm2			-1,973	N/mm2		
(Frequent combination)	σ at t=0 bottom:	-35,062	N/mm2			-35,044	N/mm2			-34,508	N/mm2		
	σ at t=inf bot:	0,121	N/mm2			0,221	N/mm2			0,137	N/mm2		
Governing for section was:		Amount of strands, n				Amount of strands, n				Amount of strands, n			

		Section	10 & 13			Section	11 & 12		
Total height of beam	H:	550	mm			550	mm		
Web thickness	bweb:	100	mm			100	mm		
Bottom flange thickness	hbot:	120	mm			120	mm		
Eccentricity strands at bottom flange	e:	60	mm			60	mm		
Total area of concrete	Ac:	0,334	m2			0,334	m2		
Self-weight	qself:	8,350	kNm			8,350	kNm		
Amount of strands:	n:	30,000				30,000			
Total area of strands	Ap:	4170,000	mm2			4170,000	mm2		
ULS									
Bending moment capacity	MRd:	1900,840	kNm	UC:	0,691	1900,840	kNm	UC:	0,694
	Med:	1313,731	kNm			1318,741	kNm		
Rotational capacity	xu/d:	0,266		UC:	0,542	0,266		UC:	0,542
Shear capacity	VRd:	720,787	kN	UC:	0,289	720,787	kN	UC:	0,216
	Ved:	208,445	kN			155,827	kN		
Torsional capacity	TRd:	393,600	kNm	UC:	0,310	393,600	kNm	UC:	0,239
	TEd:	122	kNm			94	kNm		
SLS									
Crack width verification	Mcr:	975,363	kNm	UC:	0,629	975,363	kNm	UC:	0,634
	Mmax:	613,846	kNm			618,021	kNm		
Stresses in structure (Frequent combination)	σ at t=0 top:	-2,024	N/mm2			-2,112	N/mm2		
	σ at t=0 bottom:	-34,328	N/mm2			-34,231	N/mm2		
	σ at t=inf bot:	-0,388	N/mm2			-0,291	N/mm2		
Governing for section was:		Amount of strands,n				Amount of strands,n			

SCIA ENGINEERING REPORT DEFORMATION OPTIMIZED BEAM

1. Project

Licence name	IBA
Project	Leiden Bridge
Part	Optimized C170/200 design
Description	deflection check
Author	-
Date	24. 11. 2014
Structure	Frame XZ
No. of nodes :	25
No. of beams :	24
No. of slabs :	0
No. of solids :	0
No. of used profiles :	12
No. of load cases :	6
No. of used materials :	1
Acceleration of gravity [m/s^2]	10,000
National code	EC - EN

2. Table of contents

3. Cross-sections

CS1		
Type	O asymmetrisch	
Detailed	1000; 100; 500; 120; 160	
Shape type	Thick-walled	
Item material	C170/200	
Fabrication	general	
A [m^2]	3,2400e-01	
Ay [m^2], Az [m^2]	2,4864e-01	1,2095e-01
AL [m^2/m], AD [m^2/m]	3,0000e+00	5,0400e+00
cYUCS [mm], cZUCS [mm]	-400	141
α [deg]	0,00	
Iy [m^4], Iz [m^4]	9,5982e-03	3,2280e-02
iy [mm], iz [mm]	172	316
Wely [m^3], Welz [m^3]	3,6794e-02	6,4560e-02
Wply [m^3], Wplz [m^3]	0,0000e+00	0,0000e+00
Mply+ [Nm], Mply- [Nm]	0,00e+00	0,00e+00
Mplz+ [Nm], Mplz- [Nm]	0,00e+00	0,00e+00
dy [mm], dz [mm]	0	8
It [m^4], Iw [m^6]	2,3529e-02	1,3051e-04
β y [mm], β z [mm]	-62	0

Picture

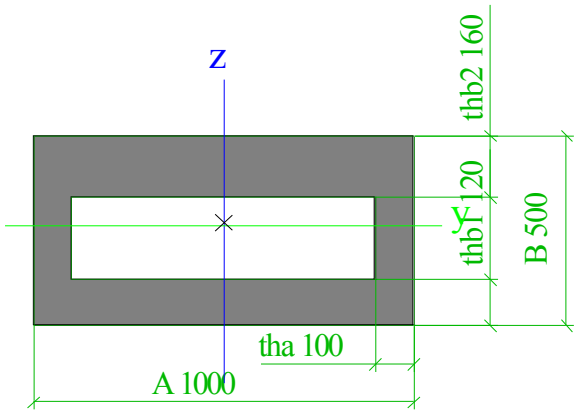

CS2		
Type	O asymmetrisch	
Detailed	1000; 100; 470; 120; 160	
Shape type	Thick-walled	
Item material	C170/200	
Fabrication	general	
A [m²]	3,1800e-01	
Ay [m²], Az [m²]	2,4726e-01	1,2059e-01
AL [m²/m], AD [m²/m]	2,9400e+00	4,9200e+00
cYUCS [mm], cZUCS [mm]	-400	125
α [deg]	0,00	
Iy [m⁴], Iz [m⁴]	8,1048e-03	3,1060e-02
iy [mm], iz [mm]	160	313
Wely [m³], Welz [m³]	3,3140e-02	6,2120e-02
Wply [m³], Wplz [m³]	0,0000e+00	0,0000e+00
Mply+ [Nm], Mply- [Nm]	0,00e+00	0,00e+00
Mplz+ [Nm], Mplz- [Nm]	0,00e+00	0,00e+00
dy [mm], dz [mm]	0	7
It [m⁴], Iw [m⁶]	2,0527e-02	1,3562e-04
β y [mm], β z [mm]	-56	0

Picture

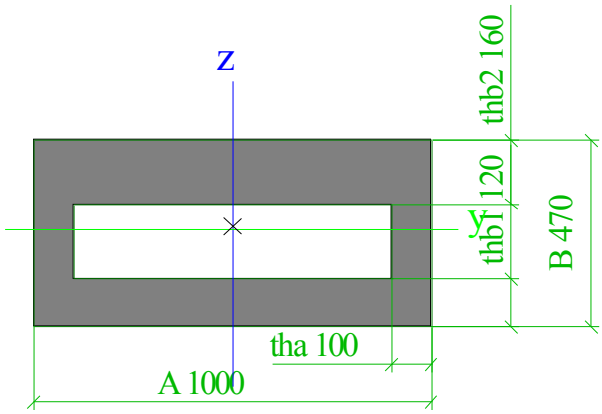

CS3		
Type	O asymmetrisch	
Detailed	1000; 100; 460; 120; 160	
Shape type	Thick-walled	
Item material	C170/200	
Fabrication	general	
A [m²]	3,1600e-01	
Ay [m²], Az [m²]	2,4653e-01	1,1450e-01
AL [m²/m], AD [m²/m]	2,9200e+00	4,8800e+00
cYUCS [mm], cZUCS [mm]	-400	119
α [deg]	0,00	
Iy [m⁴], Iz [m⁴]	7,6387e-03	3,0653e-02
iy [mm], iz [mm]	155	311
Wely [m³], Welz [m³]	3,1946e-02	6,1307e-02
Wply [m³], Wplz [m³]	0,0000e+00	0,0000e+00
Mply+ [Nm], Mply- [Nm]	0,00e+00	0,00e+00
Mplz+ [Nm], Mplz- [Nm]	0,00e+00	0,00e+00
dy [mm], dz [mm]	0	7
It [m⁴], Iw [m⁶]	1,9695e-02	1,3677e-04
β y [mm], β z [mm]	-54	0

Picture

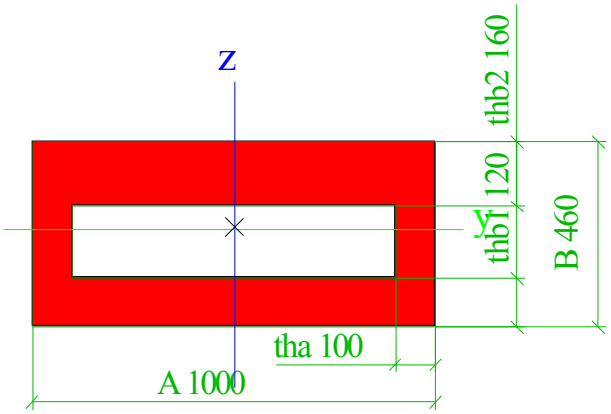

CS4		
Type	O asymmetrisch	
Detailed	1000; 100; 430; 120; 160	
Shape type	Thick-walled	
Item material	C170/200	
Fabrication	general	
A [m²]	3,1000e-01	
Ay [m²], Az [m²]	2,4476e-01	1,1854e-01
AL [m²/m], AD [m²/m]	2,8600e+00	4,7600e+00
cYUCS [mm], cZUCS [mm]	-400	103
α [deg]	0,00	
Iy [m⁴], Iz [m⁴]	6,3340e-03	2,9433e-02
iy [mm], iz [mm]	143	308
Wely [m³], Welz [m³]	2,8437e-02	5,8867e-02
Wply [m³], Wplz [m³]	0,0000e+00	0,0000e+00
Mply+ [Nm], Mply- [Nm]	0,00e+00	0,00e+00
Mplz+ [Nm], Mplz- [Nm]	0,00e+00	0,00e+00
dy [mm], dz [mm]	0	6
It [m⁴], Iw [m⁶]	1,6905e-02	1,3779e-04
β y [mm], β z [mm]	-48	0

Picture

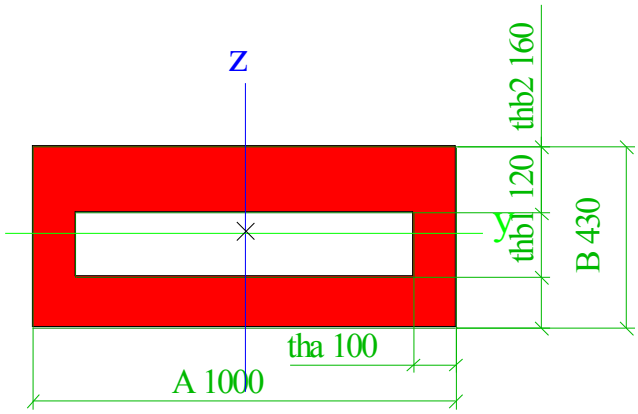

CS5		
Type	O asymmetrisch	
Detailed	1000; 100; 470; 120; 160	
Shape type	Thick-walled	
Item material	C170/200	
Fabrication	general	
A [m²]	3,1800e-01	
Ay [m²], Az [m²]	2,4726e-01	1,2059e-01
AL [m²/m], AD [m²/m]	2,9400e+00	4,9200e+00
cYUCS [mm], cZUCS [mm]	-400	125
α [deg]	0,00	
Iy [m⁴], Iz [m⁴]	8,1048e-03	3,1060e-02
iy [mm], iz [mm]	160	313
Wely [m³], Welz [m³]	3,3140e-02	6,2120e-02
Wply [m³], Wplz [m³]	0,0000e+00	0,0000e+00
Mply+ [Nm], Mply- [Nm]	0,00e+00	0,00e+00
Mplz+ [Nm], Mplz- [Nm]	0,00e+00	0,00e+00
dy [mm], dz [mm]	0	7
It [m⁴], Iw [m⁶]	2,0527e-02	1,3562e-04

β y [mm], β z [mm]	-56	0

Picture

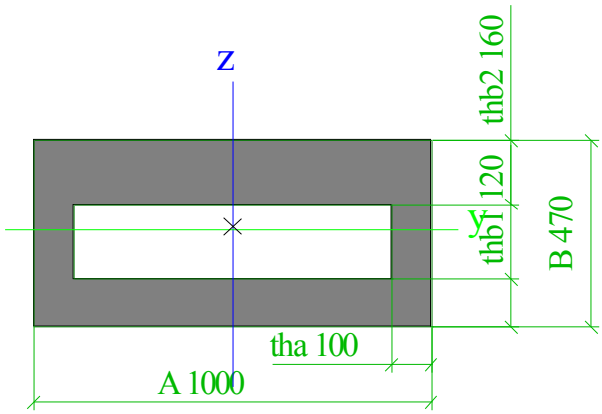

CS6		
Type	O asymmetrisch	
Detailed	1000; 100; 480; 120; 160	
Shape type	Thick-walled	
Item material	C170/200	
Fabrication	general	
A [m²]	3,2000e-01	
Ay [m²], Az [m²]	2,4795e-01	1,2050e-01
AL [m²/m], AD [m²/m]	2,9600e+00	4,9600e+00
cYUCS [mm], cZUCS [mm]	-400	130
α [deg]	0,00	
Iy [m⁴], Iz [m⁴]	8,5867e-03	3,1467e-02
iy [mm], iz [mm]	164	314
Wely [m³], Welz [m³]	3,4347e-02	6,2933e-02
Wply [m³], Wplz [m³]	0,0000e+00	0,0000e+00
Mply+ [Nm], Mply- [Nm]	0,00e+00	0,00e+00
Mplz+ [Nm], Mplz- [Nm]	0,00e+00	0,00e+00
dy [mm], dz [mm]	0	8
It [m⁴], Iw [m⁶]	2,1613e-02	1,3407e-04
β y [mm], β z [mm]	-58	0

Picture

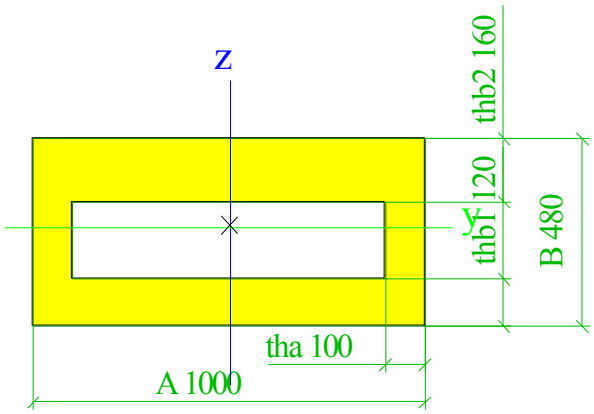

CS7		
Type	O asymmetrisch	
Detailed	1000; 100; 520; 120; 160	
Shape type	Thick-walled	
Item material	C170/200	
Fabrication	general	
A [m²]	3,2800e-01	
Ay [m²], Az [m²]	2,5005e-01	1,2194e-01
AL [m²/m], AD [m²/m]	3,0400e+00	5,1200e+00
cYUCS [mm], cZUCS [mm]	-400	152
α [deg]	0,00	
Iy [m⁴], Iz [m⁴]	1,0674e-02	3,3093e-02
iy [mm], iz [mm]	180	318
Wely [m³], Welz [m³]	3,9285e-02	6,6187e-02
Wply [m³], Wplz [m³]	0,0000e+00	0,0000e+00
Mply+ [Nm], Mply- [Nm]	0,00e+00	0,00e+00
Mplz+ [Nm], Mplz- [Nm]	0,00e+00	0,00e+00
dy [mm], dz [mm]	0	9

It [m⁴], Iw [m⁶]	2,5530e-02	1,2546e-04
β y [mm], β z [mm]	-65	0

Picture

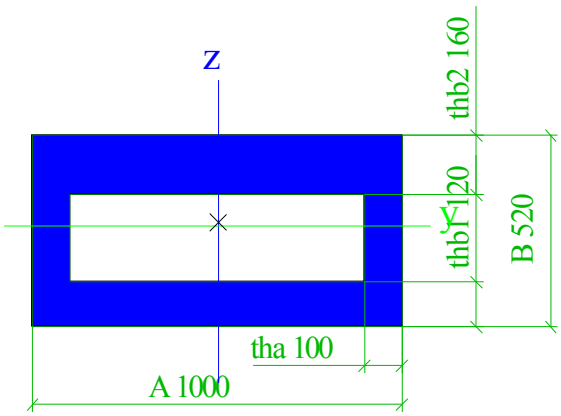

CS8		
Type	O asymmetrisch	
Detailed	1000; 100; 530; 120; 160	
Shape type	Thick-walled	
Item material	C170/200	
Fabrication	general	
A [m²]	3,3000e-01	
Ay [m²], Az [m²]	2,5021e-01	1,2043e-01
AL [m²/m], AD [m²/m]	3,0600e+00	5,1600e+00
cYUCS [mm], cZUCS [mm]	-400	157
α [deg]	0,00	
Iy [m⁴], Iz [m⁴]	1,1236e-02	3,3500e-02
iy [mm], iz [mm]	185	319
Wely [m³], Welz [m³]	4,0546e-02	6,7000e-02
Wply [m³], Wplz [m³]	0,0000e+00	0,0000e+00
Mply+ [Nm], Mply- [Nm]	0,00e+00	0,00e+00
Mplz+ [Nm], Mplz- [Nm]	0,00e+00	0,00e+00
dy [mm], dz [mm]	0	9
It [m⁴], Iw [m⁶]	2,6572e-02	1,2272e-04
β y [mm], β z [mm]	-67	0

Picture

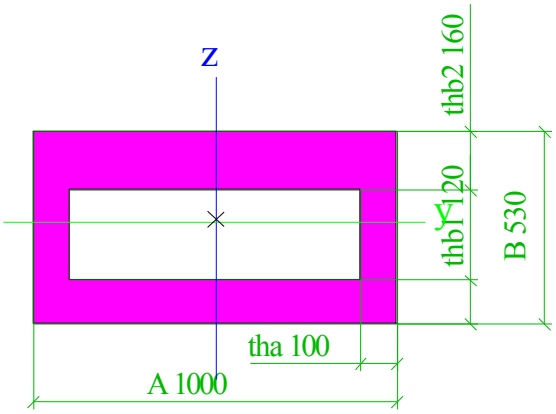

CS9		
Type	O asymmetrisch	
Detailed	1000; 100; 540; 120; 160	
Shape type	Thick-walled	
Item material	C170/200	
Fabrication	general	
A [m²]	3,3200e-01	
Ay [m²], Az [m²]	2,5090e-01	1,2579e-01
AL [m²/m], AD [m²/m]	3,0800e+00	5,2000e+00
cYUCS [mm], cZUCS [mm]	-400	163
α [deg]	0,00	
Iy [m⁴], Iz [m⁴]	1,1815e-02	3,3907e-02
iy [mm], iz [mm]	189	320
Wely [m³], Welz [m³]	4,1818e-02	6,7813e-02
Wply [m³], Wplz [m³]	0,0000e+00	0,0000e+00
Mply+ [Nm], Mply- [Nm]	0,00e+00	0,00e+00
Mplz+ [Nm], Mplz- [Nm]	0,00e+00	0,00e+00

dy [mm], dz [mm]	0	10
It [m⁴], Iw [m⁶]	2,7473e-02	1,1966e-04
β y [mm], β z [mm]	-68	0

Picture

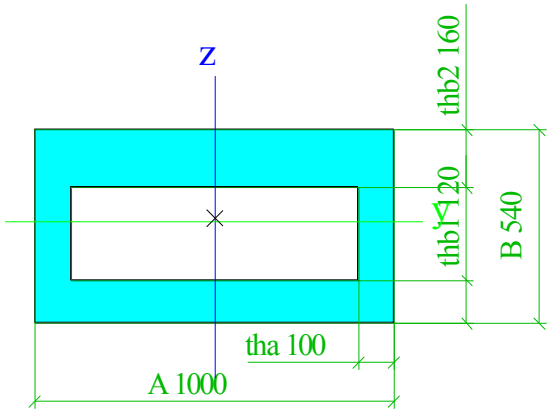

CS10		
Type	O asymmetrisch	
Detailed	1000; 100; 550; 120; 160	
Shape type	Thick-walled	
Item material	C170/200	
Fabrication	general	
A [m²]	3,3400e-01	
Ay [m²], Az [m²]	2,5064e-01	1,2651e-01
AL [m²/m], AD [m²/m]	3,1000e+00	5,2400e+00
cYUCS [mm], cZUCS [mm]	-400	168
α [deg]	0,00	
Iy [m⁴], Iz [m⁴]	1,2410e-02	3,4313e-02
iy [mm], iz [mm]	193	321
Wely [m³], Welz [m³]	4,3101e-02	6,8627e-02
Wply [m³], Wplz [m³]	0,0000e+00	0,0000e+00
Mply+ [Nm], Mply- [Nm]	0,00e+00	0,00e+00
Mplz+ [Nm], Mplz- [Nm]	0,00e+00	0,00e+00
dy [mm], dz [mm]	0	10
It [m⁴], Iw [m⁶]	2,8675e-02	1,1627e-04
β y [mm], β z [mm]	-70	0

Picture

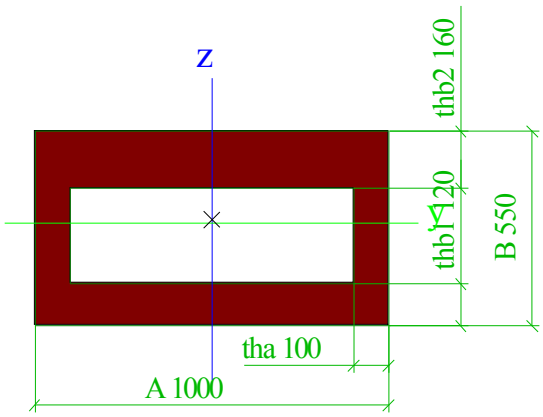

CS11		
Type	O asymmetrisch	
Detailed	1000; 100; 550; 120; 160	
Shape type	Thick-walled	
Item material	C170/200	
Fabrication	general	
A [m²]	3,3400e-01	
Ay [m²], Az [m²]	2,5064e-01	1,2651e-01
AL [m²/m], AD [m²/m]	3,1000e+00	5,2400e+00
cYUCS [mm], cZUCS [mm]	-400	168
α [deg]	0,00	
Iy [m⁴], Iz [m⁴]	1,2410e-02	3,4313e-02
iy [mm], iz [mm]	193	321
Wely [m³], Welz [m³]	4,3101e-02	6,8627e-02
Wply [m³], Wplz [m³]	0,0000e+00	0,0000e+00
Mply+ [Nm], Mply- [Nm]	0,00e+00	0,00e+00

Mplz+ [Nm], Mplz- [Nm]	0,00e+00	0,00e+00
dy [mm], dz [mm]	0	10
It [m^4], Iw [m^6]	2,8675e-02	1,1627e-04
β y [mm], β z [mm]	-70	0

Picture

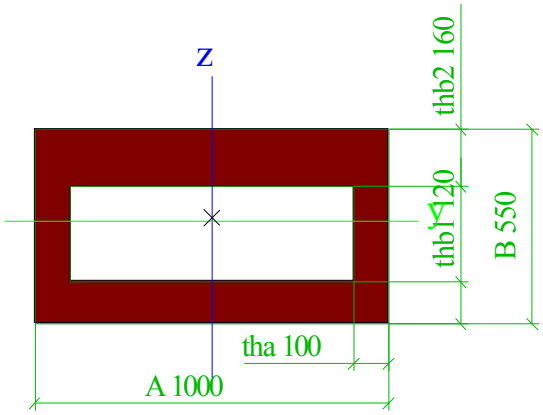

CS12		
Type	Rechthoek	
Detailed	500; 1000	
Shape type	Thick-walled	
Item material	C170/200	
Fabrication	concrete	
A [m^2]	5,0000e-01	
Ay [m^2], Az [m^2]	4,1667e-01	4,1667e-01
AL [m^2/m], AD [m^2/m]	3,0000e+00	3,0000e+00
cYUCS [mm], cZUCS [mm]	500	250
α [deg]	0,00	
Iy [m^4], Iz [m^4]	1,0417e-02	4,1667e-02
iy [mm], iz [mm]	144	289
Wely [m^3], Welz [m^3]	4,1667e-02	8,3333e-02
Wply [m^3], Wplz [m^3]	0,0000e+00	0,0000e+00
Mply+ [Nm], Mply- [Nm]	0,00e+00	0,00e+00
Mplz+ [Nm], Mplz- [Nm]	0,00e+00	0,00e+00
dy [mm], dz [mm]	0	0
It [m^4], Iw [m^6]	2,8533e-02	3,1354e-04
β y [mm], β z [mm]	0	0

Picture

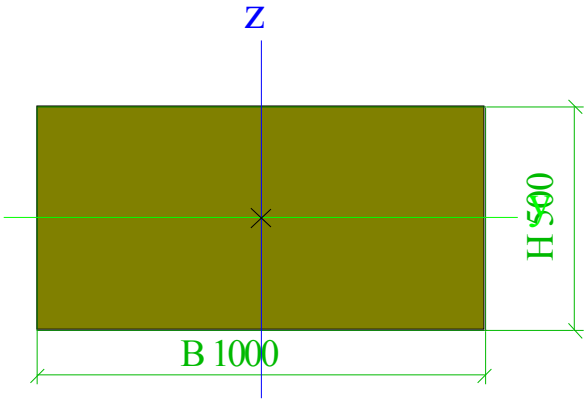

Explanations of symbols	
A	Area
Ay	Shear Area in principal y-direction - Calculated by 2D FEM analysis
Az	Shear Area in principal z-direction - Calculated by 2D FEM analysis
AL	Circumference per unit length
AD	Drying surface per unit length
cYUCS	Centroid coordinate in Y-direction of Input axis system
cZUCS	Centroid coordinate in Z-direction of Input axis system
IYLCS	Second moment of area about the YLCS axis
IZLCS	Second moment of area about the

Explanations of symbols	
	ZLCS axis
IYZLCS	Product moment of area in the LCS system
α	Rotation angle of the principal axis system
Iy	Second moment of area about the principal y-axis
Iz	Second moment of area about the principal z-axis
iy	Radius of gyration about the principal y-axis
iz	Radius of gyration about the principal z-axis
Wely	Elastic section modulus about the

Explanations of symbols	
	principal y-axis
Welz	Elastic section modulus about the principal z-axis
Wply	Plastic section modulus about the principal y-axis
Wplz	Plastic section modulus about the principal z-axis
Mply+	Plastic moment about the principal y-axis for a positive My moment
Mply-	Plastic moment about the principal y-axis for a negative My moment
Mplz+	Plastic moment about the principal z-axis for a positive Mz moment

Explanations of symbols	
Mplz-	Plastic moment about the principal z-axis for a negative Mz moment
dy	Shear center coordinate in principal y-direction measured from the centroid - Calculated by 2D FEM analysis
dz	Shear center coordinate in principal z-direction measured from the centroid - Calculated by 2D FEM analysis
It	Torsional constant - Calculated by 2D FEM analysis
Iw	Warping constant - Calculated by 2D FEM analysis
β y	Mono-symmetry constant about the principal y-axis
β z	Mono-symmetry constant about the principal z-axis

4. Nodes

Name	Coord X [m]	Coord Y [m]	Coord Z [m]
K1	0,000		0,000
K2	1,000		0,000
K3	2,000		0,000
K4	3,000		0,000
K5	4,000		0,000
K6	5,000		0,000
K7	6,000		0,000
K8	7,000		0,000
K9	8,000		0,000

Name	Coord X [m]	Coord Y [m]	Coord Z [m]
K10	9,000		0,000
K11	10,000		0,000
K12	11,000		0,000
K13	12,000		0,000
K14	13,000		0,000
K15	14,000		0,000
K16	15,000		0,000
K17	16,000		0,000
K18	17,000		0,000

Name	Coord X [m]	Coord Y [m]	Coord Z [m]
K19	18,000		0,000
K20	19,000		0,000
K21	20,000		0,000
K22	21,000		0,000
K23	22,000		0,000
K24	23,000		0,000
K25	24,000		0,000

5. Members

Name	CrossSection	Layer	Length [m]	Shape	Beg. node End node	Type FEM type
S1	CS11 - O asymmetrisch (1000; 100; 550; 120; 160)	Laag1	1,000	Line	K1 K2	general (0) standard
S2	CS1 - O asymmetrisch (1000; 100; 500; 120; 160)	Laag1	1,000	Line	K2 K3	general (0) standard
S3	CS2 - O asymmetrisch (1000; 100; 470; 120; 160)	Laag1	1,000	Line	K3 K4	general (0) standard
S4	CS3 - O asymmetrisch (1000; 100; 460; 120; 160)	Laag1	1,000	Line	K4 K5	general (0) standard
S5	CS4 - O asymmetrisch (1000; 100; 430; 120; 160)	Laag1	1,000	Line	K5 K6	general (0) standard
S6	CS5 - O asymmetrisch (1000; 100; 470; 120; 160)	Laag1	1,000	Line	K6 K7	general (0) standard
S7	CS6 - O asymmetrisch (1000; 100; 480; 120; 160)	Laag1	1,000	Line	K7 K8	general (0) standard
S8	CS7 - O asymmetrisch (1000; 100; 520; 120; 160)	Laag1	1,000	Line	K8 K9	general (0) standard
S9	CS8 - O asymmetrisch (1000; 100; 530; 120; 160)	Laag1	1,000	Line	K9 K10	general (0) standard
S10	CS9 - O asymmetrisch (1000; 100; 540; 120; 160)	Laag1	1,000	Line	K10 K11	general (0) standard
S11	CS10 - O asymmetrisch (1000; 100; 550; 120; 160)	Laag1	1,000	Line	K11 K12	general (0) standard
S12	CS11 - O asymmetrisch (1000; 100; 550; 120; 160)	Laag1	1,000	Line	K12 K13	general (0) standard
S13	CS11 - O asymmetrisch (1000; 100; 550; 120; 160)	Laag1	1,000	Line	K13 K14	general (0) standard
S14	CS10 - O asymmetrisch (1000; 100; 550; 120; 160)	Laag1	1,000	Line	K14 K15	general (0) standard
S15	CS9 - O asymmetrisch (1000; 100; 540; 120; 160)	Laag1	1,000	Line	K15 K16	general (0) standard
S16	CS8 - O asymmetrisch (1000; 100; 530; 120; 160)	Laag1	1,000	Line	K16 K17	general (0) standard
S17	CS7 - O asymmetrisch (1000; 100; 520; 120; 160)	Laag1	1,000	Line	K17 K18	general (0) standard
S18	CS6 - O asymmetrisch (1000; 100; 480; 120; 160)	Laag1	1,000	Line	K18 K19	general (0) standard
S19	CS5 - O asymmetrisch (1000; 100; 470; 120; 160)	Laag1	1,000	Line	K19 K20	general (0) standard
S20	CS4 - O asymmetrisch (1000; 100; 430; 120; 160)	Laag1	1,000	Line	K20	general (0)

Name	CrossSection	Layer	Length [m]	Shape	Beg. node	Type
					End node	FEM type
					K21	standard
S21	CS3 - O asymmetrisch (1000; 100; 460; 120; 160)	Laag1	1,000	Line	K21	general (0)
					K22	standard
S22	CS2 - O asymmetrisch (1000; 100; 470; 120; 160)	Laag1	1,000	Line	K22	general (0)
					K23	standard
S23	CS1 - O asymmetrisch (1000; 100; 500; 120; 160)	Laag1	1,000	Line	K23	general (0)
					K24	standard
S24	CS12 - Rechthoek (500; 1000)	Laag1	1,000	Line	K24	general (0)
					K25	standard

6. Nodal supports

Name	Node	System	Type	X	Z	Ry
Sn1	K1	GCS	Standard	Rigid	Rigid	Free
Sn2	K25	GCS	Standard	Free	Rigid	Free

7. Load cases

Name	Description	Action type	LoadGroup	Direction	Duration	Master load case
	Spec	Load type				
LC1	Self weight	Permanent	LG1	-Z		
		Self weight				
LC2	Dead load	Permanent	LG1			
		Standard				
LC3	UDL	Variable	LG2		Short	None
	Standard	Static				
LC4	TS	Variable	LG2		Short	None
	Standard	Static				
LC5	Pedestrian load	Variable	LG2		Short	None
	Standard	Static				
LC6	Prestress load qpm0	Permanent	LG1			
		Standard				

8. Line force

Name	Member	Type	Dir	Value - P_1 [kN/m]	Pos x_1	Coor	Orig	Ecc ey [m]
	Load case	System	Distribution	Value - P_2 [kN/m]	Pos x_2	Loc		Ecc ez [m]
Lijnlast1	S1	Force	Z	-4,29	0.000	Rela	From start	
	LC2 - Dead load	LCS	Uniform		1.000	Length		0,000
Lijnlast2	S2	Force	Z	-4,29	0.000	Rela	From start	
	LC2 - Dead load	LCS	Uniform		1.000	Length		0,000
Lijnlast3	S3	Force	Z	-4,29	0.000	Rela	From start	
	LC2 - Dead load	LCS	Uniform		1.000	Length		0,000
Lijnlast4	S4	Force	Z	-4,29	0.000	Rela	From start	
	LC2 - Dead load	LCS	Uniform		1.000	Length		0,000
Lijnlast5	S5	Force	Z	-4,29	0.000	Rela	From start	
	LC2 - Dead load	LCS	Uniform		1.000	Length		0,000
Lijnlast6	S6	Force	Z	-4,29	0.000	Rela	From start	
	LC2 - Dead load	LCS	Uniform		1.000	Length		0,000
Lijnlast7	S7	Force	Z	-4,29	0.000	Rela	From start	
	LC2 - Dead load	LCS	Uniform		1.000	Length		0,000
Lijnlast8	S8	Force	Z	-4,29	0.000	Rela	From start	
	LC2 - Dead load	LCS	Uniform		1.000	Length		0,000
Lijnlast9	S9	Force	Z	-4,29	0.000	Rela	From start	
	LC2 - Dead load	LCS	Uniform		1.000	Length		0,000
Lijnlast10	S10	Force	Z	-4,29	0.000	Rela	From start	
	LC2 - Dead load	LCS	Uniform		1.000	Length		0,000
Lijnlast11	S11	Force	Z	-4,29	0.000	Rela	From start	
	LC2 - Dead load	LCS	Uniform		1.000	Length		0,000
Lijnlast12	S12	Force	Z	-4,29	0.000	Rela	From start	
	LC2 - Dead load	LCS	Uniform		1.000	Length		0,000
Lijnlast13	S13	Force	Z	-4,29	0.000	Rela	From start	
	LC2 - Dead load	LCS	Uniform		1.000	Length		0,000
Lijnlast14	S14	Force	Z	-4,29	0.000	Rela	From start	
	LC2 - Dead load	LCS	Uniform		1.000	Length		0,000
Lijnlast15	S15	Force	Z	-4,29	0.000	Rela	From start	
	LC2 - Dead load	LCS	Uniform		1.000	Length		0,000
Lijnlast16	S16	Force	Z	-4,29	0.000	Rela	From start	
	LC2 - Dead load	LCS	Uniform		1.000	Length		0,000
Lijnlast17	S17	Force	Z	-4,29	0.000	Rela	From start	
	LC2 - Dead load	LCS	Uniform		1.000	Length		0,000
Lijnlast18	S18	Force	Z	-4,29	0.000	Rela	From start	

Name	Member	Type	Dir	Value - P_1 [kN/m]	Pos x_1	Coor	Orig	Ecc ey [m]
	Load case	System	Distribution	Value - P_2 [kN/m]	Pos x_2	Loc		Ecc ez [m]
	LC2 - Dead load	LCS	Uniform		1.000	Length		0,000
Lijnlast19	S19	Force	Z	-4,29	0.000	Rela	From start	
	LC2 - Dead load	LCS	Uniform		1.000	Length		0,000
Lijnlast20	S20	Force	Z	-4,29	0.000	Rela	From start	
	LC2 - Dead load	LCS	Uniform		1.000	Length		0,000
Lijnlast21	S21	Force	Z	-4,29	0.000	Rela	From start	
	LC2 - Dead load	LCS	Uniform		1.000	Length		0,000
Lijnlast22	S22	Force	Z	-4,29	0.000	Rela	From start	
	LC2 - Dead load	LCS	Uniform		1.000	Length		0,000
Lijnlast23	S23	Force	Z	-4,29	0.000	Rela	From start	
	LC2 - Dead load	LCS	Uniform		1.000	Length		0,000
Lijnlast24	S24	Force	Z	-4,29	0.000	Rela	From start	
	LC2 - Dead load	LCS	Uniform		1.000	Length		0,000
Lijnlast25	S2	Force	Z	-4,88	0.000	Rela	From start	
	LC3 - UDL	LCS	Uniform		1.000	Length		0,000
Lijnlast26	S3	Force	Z	-4,88	0.000	Rela	From start	
	LC3 - UDL	LCS	Uniform		1.000	Length		0,000
Lijnlast27	S4	Force	Z	-4,88	0.000	Rela	From start	
	LC3 - UDL	LCS	Uniform		1.000	Length		0,000
Lijnlast28	S5	Force	Z	-4,88	0.000	Rela	From start	
	LC3 - UDL	LCS	Uniform		1.000	Length		0,000
Lijnlast29	S6	Force	Z	-4,88	0.000	Rela	From start	
	LC3 - UDL	LCS	Uniform		1.000	Length		0,000
Lijnlast30	S7	Force	Z	-4,88	0.000	Rela	From start	
	LC3 - UDL	LCS	Uniform		1.000	Length		0,000
Lijnlast31	S8	Force	Z	-4,88	0.000	Rela	From start	
	LC3 - UDL	LCS	Uniform		1.000	Length		0,000
Lijnlast32	S9	Force	Z	-4,88	0.000	Rela	From start	
	LC3 - UDL	LCS	Uniform		1.000	Length		0,000
Lijnlast33	S10	Force	Z	-4,88	0.000	Rela	From start	
	LC3 - UDL	LCS	Uniform		1.000	Length		0,000
Lijnlast34	S11	Force	Z	-4,88	0.000	Rela	From start	
	LC3 - UDL	LCS	Uniform		1.000	Length		0,000
Lijnlast35	S12	Force	Z	-4,88	0.000	Rela	From start	
	LC3 - UDL	LCS	Uniform		1.000	Length		0,000
Lijnlast36	S13	Force	Z	-4,88	0.000	Rela	From start	
	LC3 - UDL	LCS	Uniform		1.000	Length		0,000
Lijnlast37	S14	Force	Z	-4,88	0.000	Rela	From start	
	LC3 - UDL	LCS	Uniform		1.000	Length		0,000
Lijnlast38	S15	Force	Z	-4,88	0.000	Rela	From start	
	LC3 - UDL	LCS	Uniform		1.000	Length		0,000
Lijnlast39	S16	Force	Z	-4,88	0.000	Rela	From start	
	LC3 - UDL	LCS	Uniform		1.000	Length		0,000
Lijnlast40	S17	Force	Z	-4,88	0.000	Rela	From start	
	LC3 - UDL	LCS	Uniform		1.000	Length		0,000
Lijnlast41	S18	Force	Z	-4,88	0.000	Rela	From start	
	LC3 - UDL	LCS	Uniform		1.000	Length		0,000
Lijnlast42	S19	Force	Z	-4,88	0.000	Rela	From start	
	LC3 - UDL	LCS	Uniform		1.000	Length		0,000
Lijnlast43	S20	Force	Z	-4,88	0.000	Rela	From start	
	LC3 - UDL	LCS	Uniform		1.000	Length		0,000
Lijnlast44	S21	Force	Z	-4,88	0.000	Rela	From start	
	LC3 - UDL	LCS	Uniform		1.000	Length		0,000
Lijnlast45	S22	Force	Z	-4,88	0.000	Rela	From start	
	LC3 - UDL	LCS	Uniform		1.000	Length		0,000
Lijnlast46	S23	Force	Z	-4,88	0.000	Rela	From start	
	LC3 - UDL	LCS	Uniform		1.000	Length		0,000
Lijnlast47	S24	Force	Z	-4,88	0.000	Rela	From start	
	LC3 - UDL	LCS	Uniform		1.000	Length		0,000
Lijnlast48	S1	Force	Z	-4,88	0.000	Rela	From start	
	LC3 - UDL	LCS	Uniform		1.000	Length		0,000
Lijnlast49	S1	Force	Z	-7,03	0.000	Rela	From start	
	LC4 - TS	LCS	Uniform		1.000	Length		0,000
Lijnlast50	S2	Force	Z	-7,03	0.000	Rela	From start	
	LC4 - TS	LCS	Uniform		1.000	Length		0,000
Lijnlast51	S3	Force	Z	-7,03	0.000	Rela	From start	
	LC4 - TS	LCS	Uniform		1.000	Length		0,000
Lijnlast52	S4	Force	Z	-7,03	0.000	Rela	From start	
	LC4 - TS	LCS	Uniform		1.000	Length		0,000
Lijnlast53	S5	Force	Z	-7,03	0.000	Rela	From start	
	LC4 - TS	LCS	Uniform		1.000	Length		0,000
Lijnlast54	S6	Force	Z	-7,03	0.000	Rela	From start	
	LC4 - TS	LCS	Uniform		1.000	Length		0,000
Lijnlast55	S7	Force	Z	-7,03	0.000	Rela	From start	

Name	Member	Type	Dir	Value - P_1 [kN/m]	Pos x_1	Coor	Orig	Ecc ey [m]
	Load case	System	Distribution	Value - P_2 [kN/m]	Pos x_2	Loc		Ecc ez [m]
	LC4 - TS	LCS	Uniform		1.000	Length		0,000
Lijnlast56	S8	Force	Z	-7,03	0.000	Rela	From start	
	LC4 - TS	LCS	Uniform		1.000	Length		0,000
Lijnlast57	S9	Force	Z	-7,03	0.000	Rela	From start	
	LC4 - TS	LCS	Uniform		1.000	Length		0,000
Lijnlast58	S10	Force	Z	-7,03	0.000	Rela	From start	
	LC4 - TS	LCS	Uniform		1.000	Length		0,000
Lijnlast59	S11	Force	Z	-7,03	0.000	Rela	From start	
	LC4 - TS	LCS	Uniform		1.000	Length		0,000
Lijnlast60	S12	Force	Z	-7,03	0.000	Rela	From start	
	LC4 - TS	LCS	Uniform		1.000	Length		0,000
Lijnlast61	S13	Force	Z	-7,03	0.000	Rela	From start	
	LC4 - TS	LCS	Uniform		1.000	Length		0,000
Lijnlast62	S14	Force	Z	-7,03	0.000	Rela	From start	
	LC4 - TS	LCS	Uniform		1.000	Length		0,000
Lijnlast63	S15	Force	Z	-7,03	0.000	Rela	From start	
	LC4 - TS	LCS	Uniform		1.000	Length		0,000
Lijnlast64	S16	Force	Z	-7,03	0.000	Rela	From start	
	LC4 - TS	LCS	Uniform		1.000	Length		0,000
Lijnlast65	S17	Force	Z	-7,03	0.000	Rela	From start	
	LC4 - TS	LCS	Uniform		1.000	Length		0,000
Lijnlast66	S18	Force	Z	-7,03	0.000	Rela	From start	
	LC4 - TS	LCS	Uniform		1.000	Length		0,000
Lijnlast67	S19	Force	Z	-7,03	0.000	Rela	From start	
	LC4 - TS	LCS	Uniform		1.000	Length		0,000
Lijnlast68	S20	Force	Z	-7,03	0.000	Rela	From start	
	LC4 - TS	LCS	Uniform		1.000	Length		0,000
Lijnlast69	S21	Force	Z	-7,03	0.000	Rela	From start	
	LC4 - TS	LCS	Uniform		1.000	Length		0,000
Lijnlast70	S22	Force	Z	-7,03	0.000	Rela	From start	
	LC4 - TS	LCS	Uniform		1.000	Length		0,000
Lijnlast71	S23	Force	Z	-7,03	0.000	Rela	From start	
	LC4 - TS	LCS	Uniform		1.000	Length		0,000
Lijnlast72	S24	Force	Z	-7,03	0.000	Rela	From start	
	LC4 - TS	LCS	Uniform		1.000	Length		0,000
Lijnlast73	S1	Force	Z	-2,37	0.000	Rela	From start	
	LC5 - Pedestrian load	LCS	Uniform		1.000	Length		0,000
Lijnlast74	S2	Force	Z	-2,37	0.000	Rela	From start	
	LC5 - Pedestrian load	LCS	Uniform		1.000	Length		0,000
Lijnlast75	S3	Force	Z	-2,37	0.000	Rela	From start	
	LC5 - Pedestrian load	LCS	Uniform		1.000	Length		0,000
Lijnlast76	S4	Force	Z	-2,37	0.000	Rela	From start	
	LC5 - Pedestrian load	LCS	Uniform		1.000	Length		0,000
Lijnlast77	S5	Force	Z	-2,37	0.000	Rela	From start	
	LC5 - Pedestrian load	LCS	Uniform		1.000	Length		0,000
Lijnlast78	S6	Force	Z	-2,37	0.000	Rela	From start	
	LC5 - Pedestrian load	LCS	Uniform		1.000	Length		0,000
Lijnlast79	S7	Force	Z	-2,37	0.000	Rela	From start	
	LC5 - Pedestrian load	LCS	Uniform		1.000	Length		0,000
Lijnlast80	S8	Force	Z	-2,37	0.000	Rela	From start	
	LC5 - Pedestrian load	LCS	Uniform		1.000	Length		0,000
Lijnlast81	S9	Force	Z	-2,37	0.000	Rela	From start	
	LC5 - Pedestrian load	LCS	Uniform		1.000	Length		0,000
Lijnlast82	S10	Force	Z	-2,37	0.000	Rela	From start	
	LC5 - Pedestrian load	LCS	Uniform		1.000	Length		0,000
Lijnlast83	S11	Force	Z	-2,37	0.000	Rela	From start	
	LC5 - Pedestrian load	LCS	Uniform		1.000	Length		0,000
Lijnlast84	S12	Force	Z	-2,37	0.000	Rela	From start	
	LC5 - Pedestrian load	LCS	Uniform		1.000	Length		0,000
Lijnlast85	S13	Force	Z	-2,37	0.000	Rela	From start	
	LC5 - Pedestrian load	LCS	Uniform		1.000	Length		0,000
Lijnlast86	S14	Force	Z	-2,37	0.000	Rela	From start	
	LC5 - Pedestrian load	LCS	Uniform		1.000	Length		0,000
Lijnlast87	S15	Force	Z	-2,37	0.000	Rela	From start	
	LC5 - Pedestrian load	LCS	Uniform		1.000	Length		0,000
Lijnlast88	S16	Force	Z	-2,37	0.000	Rela	From start	
	LC5 - Pedestrian load	LCS	Uniform		1.000	Length		0,000
Lijnlast89	S17	Force	Z	-2,37	0.000	Rela	From start	
	LC5 - Pedestrian load	LCS	Uniform		1.000	Length		0,000
Lijnlast90	S18	Force	Z	-2,37	0.000	Rela	From start	
	LC5 - Pedestrian load	LCS	Uniform		1.000	Length		0,000
Lijnlast91	S19	Force	Z	-2,37	0.000	Rela	From start	
	LC5 - Pedestrian load	LCS	Uniform		1.000	Length		0,000
Lijnlast92	S20	Force	Z	-2,37	0.000	Rela	From start	

Name	Member	Type	Dir	Value - P_1 [kN/m]	Pos x_1	Coor	Orig	Ecc ey [m]
	Load case	System	Distribution	Value - P_2 [kN/m]	Pos x_2	Loc		Ecc ez [m]
	LC5 - Pedestrian load	LCS	Uniform		1.000	Length		0,000
Lijnlast93	S21	Force	Z	-2,37	0.000	Rela	From start	
	LC5 - Pedestrian load	LCS	Uniform		1.000	Length		0,000
Lijnlast94	S22	Force	Z	-2,37	0.000	Rela	From start	
	LC5 - Pedestrian load	LCS	Uniform		1.000	Length		0,000
Lijnlast95	S23	Force	Z	-2,37	0.000	Rela	From start	
	LC5 - Pedestrian load	LCS	Uniform		1.000	Length		0,000
Lijnlast96	S24	Force	Z	-2,37	0.000	Rela	From start	
	LC5 - Pedestrian load	LCS	Uniform		1.000	Length		0,000
Lijnlast97	S1	Force	Z	18,46	0.000	Rela	From start	
	LC6 - Prestress load qpm0	LCS	Uniform		1.000	Length		0,000
Lijnlast98	S2	Force	Z	18,46	0.000	Rela	From start	
	LC6 - Prestress load qpm0	LCS	Uniform		1.000	Length		0,000
Lijnlast99	S3	Force	Z	18,46	0.000	Rela	From start	
	LC6 - Prestress load qpm0	LCS	Uniform		1.000	Length		0,000
Lijnlast100	S4	Force	Z	18,46	0.000	Rela	From start	
	LC6 - Prestress load qpm0	LCS	Uniform		1.000	Length		0,000
Lijnlast101	S5	Force	Z	18,46	0.000	Rela	From start	
	LC6 - Prestress load qpm0	LCS	Uniform		1.000	Length		0,000
Lijnlast102	S6	Force	Z	18,46	0.000	Rela	From start	
	LC6 - Prestress load qpm0	LCS	Uniform		1.000	Length		0,000
Lijnlast103	S7	Force	Z	18,46	0.000	Rela	From start	
	LC6 - Prestress load qpm0	LCS	Uniform		1.000	Length		0,000
Lijnlast104	S8	Force	Z	18,46	0.000	Rela	From start	
	LC6 - Prestress load qpm0	LCS	Uniform		1.000	Length		0,000
Lijnlast105	S9	Force	Z	18,46	0.000	Rela	From start	
	LC6 - Prestress load qpm0	LCS	Uniform		1.000	Length		0,000
Lijnlast106	S10	Force	Z	18,46	0.000	Rela	From start	
	LC6 - Prestress load qpm0	LCS	Uniform		1.000	Length		0,000
Lijnlast107	S11	Force	Z	18,46	0.000	Rela	From start	
	LC6 - Prestress load qpm0	LCS	Uniform		1.000	Length		0,000
Lijnlast108	S12	Force	Z	18,46	0.000	Rela	From start	
	LC6 - Prestress load qpm0	LCS	Uniform		1.000	Length		0,000
Lijnlast109	S13	Force	Z	18,46	0.000	Rela	From start	
	LC6 - Prestress load qpm0	LCS	Uniform		1.000	Length		0,000
Lijnlast110	S14	Force	Z	18,46	0.000	Rela	From start	
	LC6 - Prestress load qpm0	LCS	Uniform		1.000	Length		0,000
Lijnlast111	S15	Force	Z	18,46	0.000	Rela	From start	
	LC6 - Prestress load qpm0	LCS	Uniform		1.000	Length		0,000
Lijnlast112	S16	Force	Z	18,46	0.000	Rela	From start	
	LC6 - Prestress load qpm0	LCS	Uniform		1.000	Length		0,000
Lijnlast113	S17	Force	Z	18,46	0.000	Rela	From start	
	LC6 - Prestress load qpm0	LCS	Uniform		1.000	Length		0,000
Lijnlast114	S18	Force	Z	18,46	0.000	Rela	From start	
	LC6 - Prestress load qpm0	LCS	Uniform		1.000	Length		0,000
Lijnlast115	S19	Force	Z	18,46	0.000	Rela	From start	
	LC6 - Prestress load qpm0	LCS	Uniform		1.000	Length		0,000
Lijnlast116	S20	Force	Z	18,46	0.000	Rela	From start	
	LC6 - Prestress load qpm0	LCS	Uniform		1.000	Length		0,000
Lijnlast117	S21	Force	Z	18,46	0.000	Rela	From start	
	LC6 - Prestress load qpm0	LCS	Uniform		1.000	Length		0,000
Lijnlast118	S22	Force	Z	18,46	0.000	Rela	From start	
	LC6 - Prestress load qpm0	LCS	Uniform		1.000	Length		0,000
Lijnlast119	S23	Force	Z	18,46	0.000	Rela	From start	
	LC6 - Prestress load qpm0	LCS	Uniform		1.000	Length		0,000
Lijnlast120	S24	Force	Z	18,46	0.000	Rela	From start	
	LC6 - Prestress load qpm0	LCS	Uniform		1.000	Length		0,000

9. Load groups

Name	Load	Relation	Type
LG1	Permanent		
LG2	Variable	Standard	Cat G : Vehicle >30kN

10. Combinations

Name	Description	Type	Load cases	Coeff. [-]
w1		Linear - serviceability	LC1 - Self weight	1,00
			LC6 - Prestress load qpm0	1,00
w2		Linear - serviceability	LC1 - Self weight	1,00
			LC2 - Dead load	1,00
			LC6 - Prestress load qpm0	1,00
w3		Linear - serviceability	LC1 - Self weight	1,00

Name	Description	Type	Load cases	Coeff. [-]
			LC2 - Dead load	1,00
			LC3 - UDL	0,40
			LC4 - TS	0,40
			LC5 - Pedestrian load	0,40
			LC6 - Prestress load qpm0	0,84

11. Displacement of nodes

Linear calculation, Extreme : Node
Selection : All
Combinations : w1

Node	Case	Ux [mm]	Uz [mm]
K1	w1/2	**0,0**	**0,0**
K2	w1/2	0,0	17,0
K3	w1/2	0,0	33,8
K4	w1/2	0,0	49,7
K5	w1/2	0,0	64,6
K6	w1/2	0,0	77,7
K7	w1/2	0,0	88,9
K8	w1/2	0,0	98,2
K9	w1/2	0,0	105,8
K10	w1/2	0,0	111,6
K11	w1/2	0,0	115,8
K12	w1/2	0,0	118,3
K13	w1/2	0,0	**119,1**
K14	w1/2	0,0	118,3
K15	w1/2	0,0	115,7
K16	w1/2	0,0	111,6
K17	w1/2	0,0	105,7
K18	w1/2	0,0	98,2
K19	w1/2	0,0	88,8
K20	w1/2	0,0	77,6
K21	w1/2	0,0	64,5
K22	w1/2	0,0	49,7
K23	w1/2	0,0	33,7
K24	w1/2	0,0	17,0
K25	w1/2	0,0	0,0

12. Deformations on member

Linear calculation, Extreme : Global
Selection : All
Combinations : w1

Member	dx [m]	Case	ux [mm]	uz [mm]	fiy [mrad]	Resultant [mm]
S1	0,000	w1/2	**0,0**	0,0	**-17,0**	0,0
S12	1,000	w1/2	0,0	**119,1**	0,0	**119,1**
S24	1,000	w1/2	0,0	**0,0**	**17,0**	**0,0**

13. w1

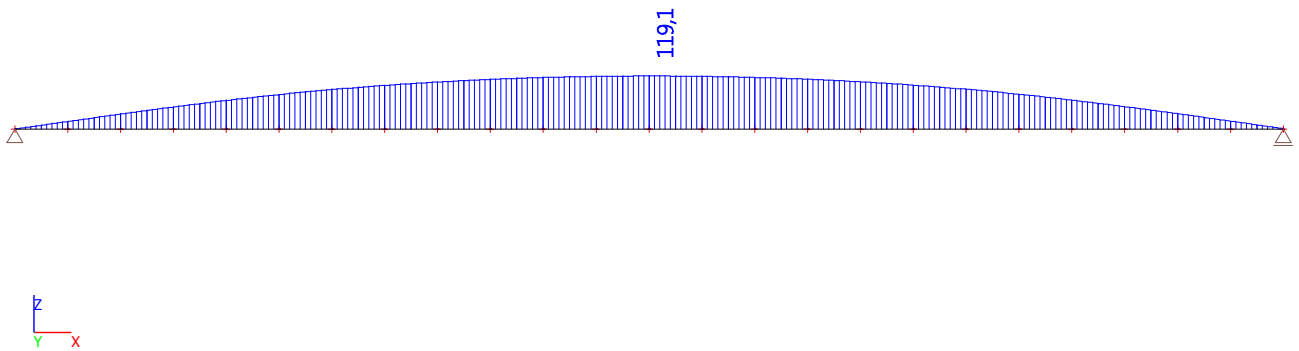

14. Displacement of nodes

Linear calculation, Extreme : Node
Selection : All
Combinations : w2

Node	Case	Ux [mm]	Uz [mm]
K1	w2/1	**0,0**	**0,0**
K2	w2/1	0,0	9,9
K3	w2/1	0,0	19,7
K4	w2/1	0,0	29,0
K5	w2/1	0,0	37,7
K6	w2/1	0,0	45,3
K7	w2/1	0,0	51,9
K8	w2/1	0,0	57,3
K9	w2/1	0,0	61,7
K10	w2/1	0,0	65,1
K11	w2/1	0,0	67,5
K12	w2/1	0,0	69,0
K13	w2/1	0,0	**69,4**
K14	w2/1	0,0	69,0
K15	w2/1	0,0	67,5
K16	w2/1	0,0	65,1
K17	w2/1	0,0	61,6
K18	w2/1	0,0	57,2
K19	w2/1	0,0	51,8
K20	w2/1	0,0	45,3
K21	w2/1	0,0	37,6
K22	w2/1	0,0	29,0
K23	w2/1	0,0	19,7
K24	w2/1	0,0	9,9
K25	w2/1	0,0	0,0

15. Deformations on member

Linear calculation, Extreme : Global
Selection : All
Combinations : w2

Member	dx [m]	Case	ux [mm]	uz [mm]	fiy [mrad]	Resultant [mm]
S1	0,000	w2/1	**0,0**	0,0	**-9,9**	0,0
S12	1,000	w2/1	0,0	**69,4**	0,0	**69,4**
S24	1,000	w2/1	0,0	**0,0**	**9,9**	**0,0**

16. w2

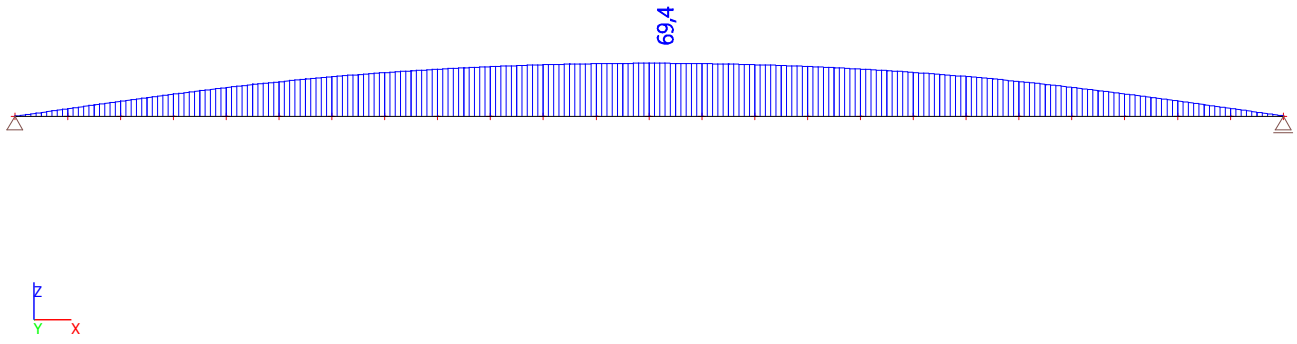

17. Displacement of nodes

Linear calculation, Extreme : Node
Selection : All
Combinations : w3

Node	Case	Ux [mm]	Uz [mm]
K1	w3/3	**0,0**	**0,0**
K2	w3/3	0,0	-4,4
K3	w3/3	0,0	-8,7
K4	w3/3	0,0	-12,8
K5	w3/3	0,0	-16,6
K6	w3/3	0,0	-20,0
K7	w3/3	0,0	-22,9
K8	w3/3	0,0	-25,4
K9	w3/3	0,0	-27,3
K10	w3/3	0,0	-28,9
K11	w3/3	0,0	-30,0
K12	w3/3	0,0	-30,6
K13	w3/3	0,0	**-30,8**
K14	w3/3	0,0	-30,6
K15	w3/3	0,0	-30,0
K16	w3/3	0,0	-28,9
K17	w3/3	0,0	-27,4
K18	w3/3	0,0	-25,4
K19	w3/3	0,0	-23,0
K20	w3/3	0,0	-20,1
K21	w3/3	0,0	-16,7
K22	w3/3	0,0	-12,9
K23	w3/3	0,0	-8,7
K24	w3/3	0,0	-4,4
K25	w3/3	0,0	0,0

18. Deformations on member

Linear calculation, Extreme : Global
Selection : All
Combinations : w3

Member	dx [m]	Case	ux [mm]	uz [mm]	fiy [mrad]	Resultant [mm]
S1	0,000	w3/3	**0,0**	**0,0**	**4,4**	**0,0**
S12	1,000	w3/3	0,0	**-30,8**	0,0	**30,8**
S24	1,000	w3/3	0,0	0,0	**-4,4**	0,0

19. w3

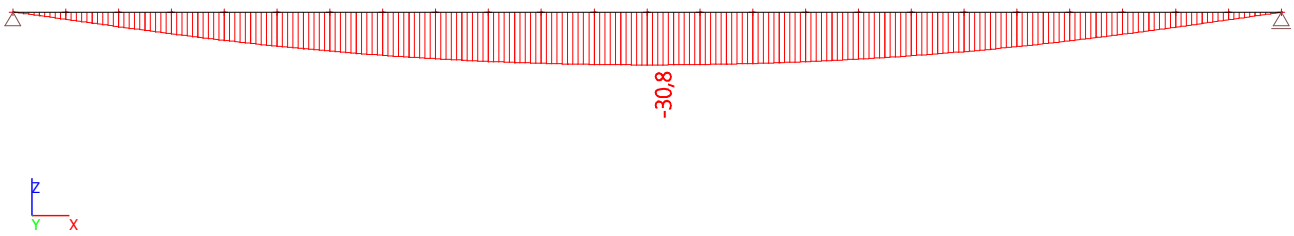

Determination height of compression and tension zone
For C170/200 UHPC Box-beam girder

Multiple situations can occur that cause different derivations and thus different results for $x_{u.}$ The reason different results will occur is because the box girder hasn't a constant width over the height of the cross section (width of the top flange versus width of the webs). Calculation will be based on the stress-strain diagram in the figure.

The situations for the compressive zone are:

Situation 1.1 $x_u \leq h_{top,fl}$

Situation 1.2 $x_u \geq h_{top,fl}$ and the height of the plastic area (named y) $\leq h_{top,fl}$

Situation 1.3 $x_u \geq h_{top,fl}$ and $y \geq h_{top,fl}$

The situations for the tension zone are:

Situation 2.1 The tension zone is located completely outside the top flange
This situation can only occur if $x_u \geq h_{top,fl}$, so with either situation 1.2 or 1.3.

Situation 2.2 Only the elastic part of the tension zone is partially located in the top flange
This situation can only occur when $x_u \leq h_{top,fl}$ (same goes for 2.3 and 2.4). However in most cases the elastic tensile part will fall completely in the top flange, when situation 1.1 occurs, as it is a very small area. Therefore situation 2.2 can often be neglected.

Situation 2.3 The whole elastic part of the tension zone and a part of the area between ε_{ct} and $\varepsilon_{u0.3}$ are located in the top flange.
If x_u is around the height of the top flange, situation 2.3 will most likely occur.

Situation 2.4 The area between ε=0 and $\varepsilon_{u0.3}$ is located in the top flange as well as a part of the area between ε_{ctu} and $\varepsilon_{u0.3}$.
This situation will occur is x_u is much smaller than the height of the top flange.

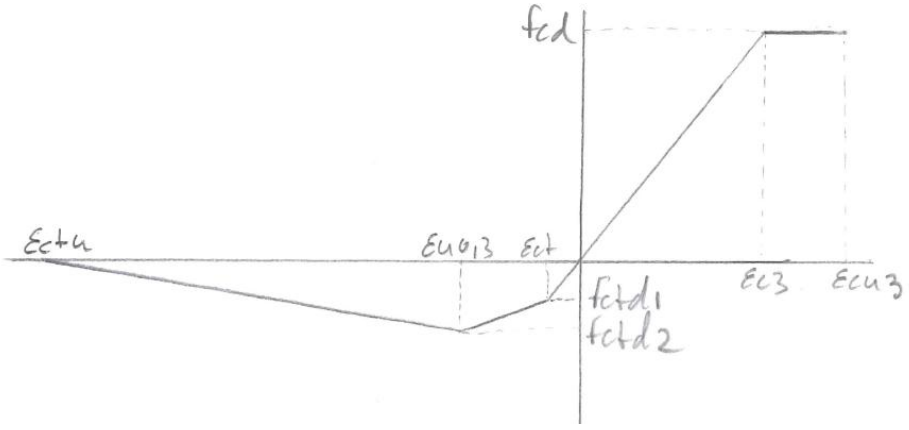

Figure: Stress diagram UHPC

For the determination of the bending moment resistance, the combination of situation 1.1 and 2.3 will be assumed first. So the height of the compressive zone is expected to be smaller than the height of the top flange, in such a way that the elastic part and a part of the area between ε_{ct} and $\varepsilon_{u0.3}$ are located in the top flange. If this proves not to be the case then the x_u will be calculated again using a different combination (1.2 with 2.4 or 1.3 with 2.4).

Derivation of the situations 1.1 - 1.3

Situation 1.1:

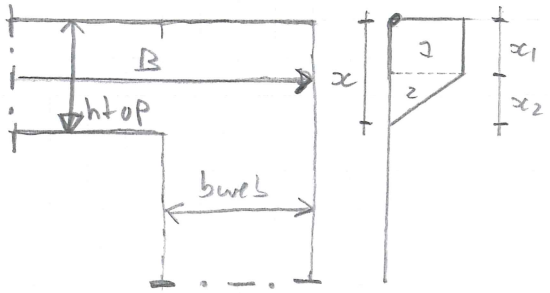

$$x_1 = \frac{x_c \cdot (\varepsilon_{cu3} - \varepsilon_{c3})}{\varepsilon_{cu3}}$$

$$x_2 = x - x_1$$

$$N_1 = B \cdot x_1 \cdot f_{cd} \qquad N_2 = \tfrac{1}{2} \cdot B \cdot x_2 \cdot f_{cd}$$

$$arm_1 = \tfrac{1}{2} \cdot x_1 \qquad arm_2 = x_1 + \tfrac{1}{3} x_2$$

Situation 1.2:

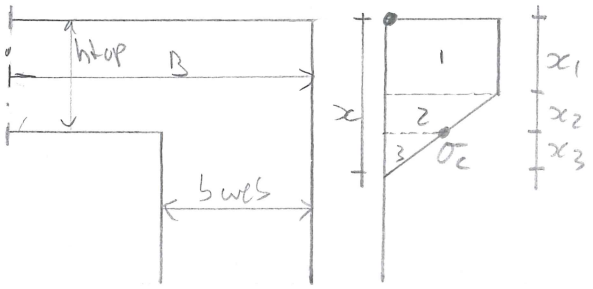

$$x_1 = \frac{x_c \cdot (\varepsilon_{cu3} - \varepsilon_{c3})}{\varepsilon_{cu3}}$$

$$x_2 = h_{top} - x_1 \qquad \sigma_c = \frac{f_{cd} \cdot x_3}{x_2 + x_3}$$

$$x_3 = x - h_{top}$$

$$N_1 = B \cdot x_1 \cdot f_{cd} \qquad N_2 = \tfrac{1}{2} B \cdot x_2 \cdot (f_{cd} + \sigma_c) \qquad N_3 = \tfrac{1}{2} \cdot b_{web} \cdot x_3 \cdot \sigma_c$$

$$arm_1 = \tfrac{1}{2} \cdot x_1 \qquad arm_2 = x_1 + \frac{1}{3} x_2 \frac{f_{cd} + 2\sigma_c}{f_{cd} + \sigma_c} \qquad arm_3 = x_1 + x_2 + \tfrac{1}{3} x_3$$

Situation 1.3:

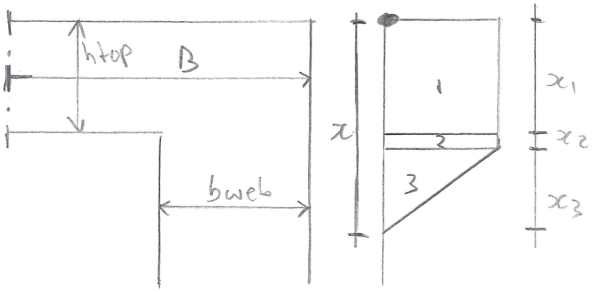

$$x_1 = h_{top}$$

$$x_2 = x_c \cdot \frac{(\varepsilon_{cu3} - \varepsilon_{c3})}{\varepsilon_{cu3}} - h_{top}$$

$$x_3 = x_c - x_c \cdot \frac{(\varepsilon_{cu3} - \varepsilon_{c3})}{\varepsilon_{cu3}}$$

$$N_1 = B \cdot x_1 \cdot f_{cd} \qquad N_2 = b_{web} \cdot x_2 \cdot f_{cd} \qquad N_3 = \tfrac{1}{2} \cdot b_{web} \cdot x_3 \cdot f_{cd}$$

$$arm_1 = \tfrac{1}{2} \cdot x_1 \qquad arm_2 = x_1 + \tfrac{1}{2} x_2 \qquad arm_3 = x_1 + x_2 + \tfrac{1}{3} x_3$$

In all situations x_c is supposed to be the only unknown variable.

Derivation of situations 2.1 - 2.4

Situation 2.1:

assume always: $x_T = H - x_c$

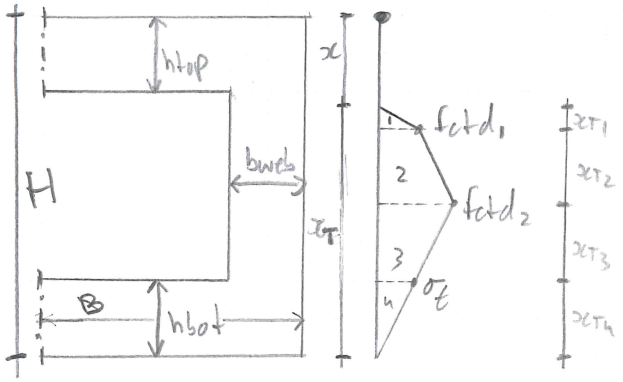

$$x_{T1} = x_T \cdot \frac{\varepsilon_{ct}}{\varepsilon_{ctu}}$$

$$x_{T2} = x_T \cdot \frac{\varepsilon_{uo,3} - \varepsilon_{ct}}{\varepsilon_{ctu}}$$

$$x_{T3} = x_T \cdot \frac{\varepsilon_{ctu} - \varepsilon_{uo,3}}{\varepsilon_{ctu}} - h_{bot}$$

$$x_{T4} = h_{bot}$$

$$\sigma_t = \frac{f_{ctd_2} \cdot x_{T4}}{x_{T3} + x_{T4}}$$

$$N_1 = \frac{1}{2} \cdot b_{web} \cdot x_{T1} \cdot f_{ctd_1} \qquad arm_1 = \frac{2}{3} x_{T1} + x$$

$$N_2 = b_{web} \cdot x_{T2} \cdot \frac{f_{ctd_1} + f_{ctd_2}}{2} \qquad arm_2 = x + x_{T1} + \frac{1}{3} x_{T2} \cdot \frac{2 f_{ctd_2} + f_{ctd_1}}{f_{ctd_2} + f_{ctd_1}}$$

$$N_3 = b_{web} \cdot x_{T3} \cdot \frac{f_{ctd_2} + \sigma_t}{2} \qquad arm_3 = x + x_{T1} + x_{T2} + \frac{1}{3} x_{T4} \cdot \frac{f_{ctd_2} + 2\sigma_t}{f_{ctd_2} + \sigma_t}$$

$$N_4 = \frac{1}{2} \cdot B \cdot x_{T4} \cdot \sigma_t \qquad arm_4 = H - \frac{2}{3} h_{bot}$$

Situation 2.2:

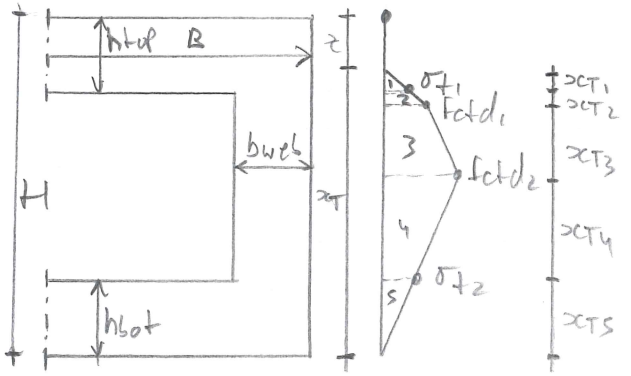

$$x_{T1} = h_{top} - x_c$$

$$x_{T2} = x_T \cdot \frac{\varepsilon_{ct}}{\varepsilon_{ctu}} - x_{T1}$$

$$x_{T3} = \frac{\varepsilon_{uo,3} - \varepsilon_{ct}}{\varepsilon_{ctu}} \cdot x_T$$

$$x_{T4} = x_T \cdot \frac{\varepsilon_{ctu} - \varepsilon_{uo,3}}{\varepsilon_{ctu}} - h_{bot}$$

$$x_{T5} = h_{bot}$$

$$\sigma_{t1} = \frac{f_{ctd_1} \cdot x_{T1}}{x_{T1} + x_{T2}} \qquad \sigma_{t2} = \frac{f_{ctd_2} \cdot x_{T5}}{x_{T4} + x_{T5}}$$

cont. on next page...

$N_1 = \frac{1}{2} \cdot B \cdot x_{cT_1} \cdot \sigma_{t_1}$ $\quad arm_1 = x + \frac{2}{3} x_{cT_1}$

$N_2 = b_{web} \cdot x_{cT_2} \cdot \frac{f_{ctd_1} + \sigma_{t_1}}{2}$ $\quad arm_2 = x + x_{cT_1} + \frac{1}{3} x_{cT_2} \cdot \frac{2 f_{ctd_1} + \sigma_{t_1}}{f_{ctd_1} + \sigma_{t_1}}$

$N_3 = b_{web} \cdot x_{cT_3} \cdot \frac{f_{ctd_1} + f_{ctd_2}}{2}$ $\quad arm_3 = x + x_{cT_1} + x_{cT_2} + \frac{1}{3} x_{cT_3} \cdot \frac{2 f_{ctd_2} + f_{ctd_1}}{f_{ctd_2} + f_{ctd_1}}$

$N_4 = b_{web} \cdot x_{cT_4} \cdot \frac{f_{ctd_2} + \sigma_{t_2}}{2}$ $\quad arm_4 = x + x_{cT_1} + x_{cT_2} + x_{cT_3} + \frac{1}{3} x_{cT_4} \cdot \frac{f_{ctd_2} + 2\sigma_{t_2}}{f_{ctd_2} + \sigma_{t_2}}$

$N_5 = \frac{1}{2} \cdot B \cdot x_{cT_5} \cdot \sigma_{t_2}$ $\quad arm_5 = H - \frac{2}{3} h_{bot}$

Situation 2.3:

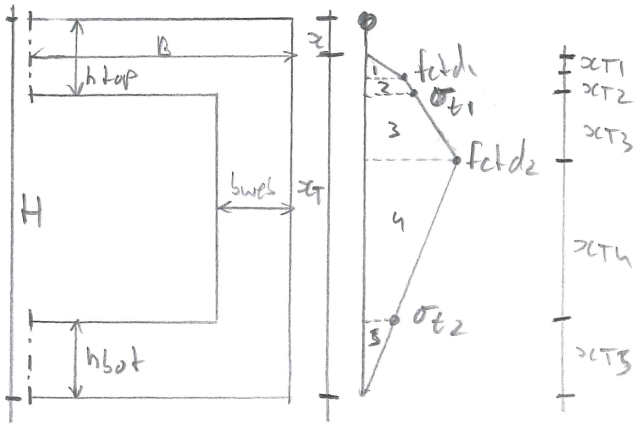

$x_{cT_1} = x_{cT} \cdot \frac{\varepsilon_{ct}}{\varepsilon_{ctu}}$

$x_{cT_2} = h_{top} - x - x_{cT_1}$

$x_{cT_3} = x_{cT} \cdot \frac{(\varepsilon_{uo_{1,3}} - \varepsilon_{ct})}{\varepsilon_{ctu}} - x_{cT_2}$

$x_{cT_4} = x_{cT} \cdot \frac{\varepsilon_{ctu} - \varepsilon_{uo_{1,3}}}{\varepsilon_{ctu}} - h_{bot}$

$x_{cT_5} = h_{bot}$

$\sigma_{t_1} = \frac{f_{ctd_2} - f_{ctd_1}}{x_{cT_2} + x_{cT_3}} \cdot x_{cT_2} + f_{ctd_1}$ $\quad \sigma_{t_2} = \frac{f_{ctd_2} \cdot h_{bot}}{x_{cT_4} + x_{cT_5}}$

$N_1 = \frac{1}{2} \cdot B \cdot x_{cT_1} \cdot f_{ctd_1}$ $\quad arm_1 = x + \frac{2}{3} x_{cT_1}$

$N_2 = B \cdot x_{cT_2} \cdot \frac{\sigma_{t_1} + f_{ctd_1}}{2}$ $\quad arm_2 = x + x_{cT_1} + \frac{1}{3} x_{cT_2} \cdot \frac{2\sigma_{t_1} + f_{ctd_1}}{\sigma_{t_1} + f_{ctd_1}}$

$N_3 = b_{web} \cdot x_{cT_3} \cdot \frac{\sigma_{t_1} + f_{ctd_2}}{2}$ $\quad arm_3 = x + x_{cT_1} + x_{cT_2} + \frac{1}{3} x_{cT_3} \cdot \frac{2 f_{ctd_2} + \sigma_{t_1}}{f_{ctd_2} + \sigma_{t_1}}$

$N_4 = b_{web} \cdot x_{cT_4} \cdot \frac{f_{ctd_2} + \sigma_{t_2}}{2}$ $\quad arm_4 = x + x_{cT_1} + x_{cT_2} + x_{cT_3} + \frac{1}{3} x_{cT_4} \cdot \frac{f_{ctd_2} + 2\sigma_{t_2}}{f_{ctd_2} + \sigma_{t_2}}$

$N_5 = \frac{1}{2} \cdot B \cdot x_{cT_5} \cdot \sigma_{t_2}$ $\quad arm_5 = H - \frac{2}{3} h_{bot}$

cont. on next page ...

situation 2.4:

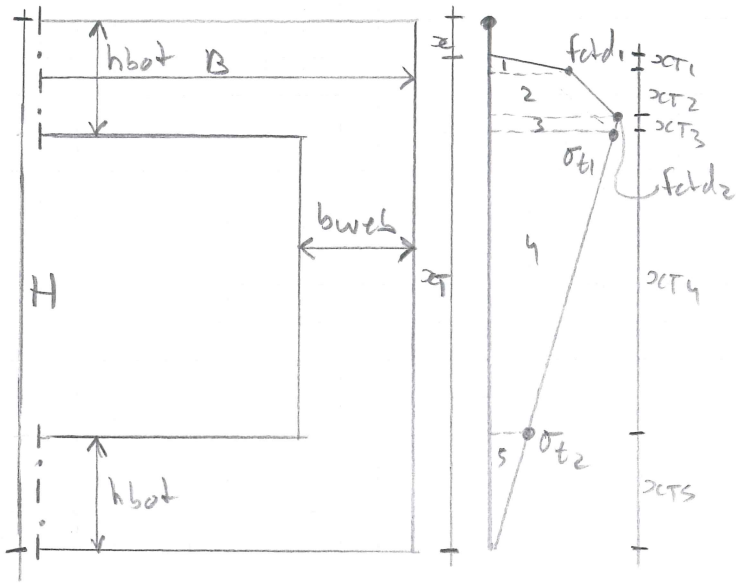

$x_{cT1} = x_{cT} \cdot \frac{\varepsilon_{ct}}{\varepsilon_{ctu}}$

$x_{cT2} = x_{cT} \cdot \frac{\varepsilon_{u0,3} - \varepsilon_{ct}}{\varepsilon_{ctu}}$

$x_{cT3} = h_{top} - x_c - x_{cT1} - x_{cT2}$

$x_{cT4} = x_T \cdot \frac{\varepsilon_{ctu} - \varepsilon_{u0,3}}{\varepsilon_{ctu}} - x_{cT3} - h_{bot}$

$x_{cT5} = h_{bot}$

$\sigma_{t1} = \frac{f_{ctd2} \cdot (x_{cT4} + x_{cT5})}{x_{cT3} + x_{cT4} + x_{cT5}}$ $\quad \sigma_{t2} = \frac{f_{ctd2} \cdot x_{T5}}{x_{cT4} + x_{cT5}}$

$N_1 = \frac{1}{2} B \cdot x_{cT1} \cdot f_{ctd1}$ $\quad arm_1 = x_c + \frac{2}{3} x_{cT1}$

$N_2 = B \cdot x_{cT2} \cdot \frac{f_{ctd1} + f_{ctd2}}{2}$ $\quad arm_2 = x_c + x_{cT1} + \frac{1}{3} x_{cT2} \cdot \frac{2 f_{ctd2} + f_{ctd1}}{f_{ctd2} + f_{ctd1}}$

$N_3 = B \cdot x_{cT3} \cdot \frac{\sigma_{t1} + f_{ctd2}}{2}$ $\quad arm_3 = x_c + x_{cT1} + x_{cT2} + \frac{1}{3} x_{cT3} \cdot \frac{f_{ctd2} + 2\sigma_{t1}}{f_{ctd2} + \sigma_{t1}}$

$N_4 = b_{web} \cdot x_{cT4} \cdot \frac{\sigma_{t1} + \sigma_{t2}}{2}$ $\quad arm_4 = x_c + x_{cT1} + x_{cT2} + x_{cT3} + \frac{1}{3} x_{cT4} \cdot \frac{\sigma_{t1} + 2\sigma_{t2}}{\sigma_{t1} + \sigma_{t2}}$

$N_5 = \frac{1}{2} \cdot B \cdot x_{cT5} \cdot \sigma_{t2}$ $\quad arm_5 = H - \frac{2}{3} x_{cT5}$

In all situations (2.1 - 2.4) x is the only unknown and $x_T = H - x$

TOP VIEW

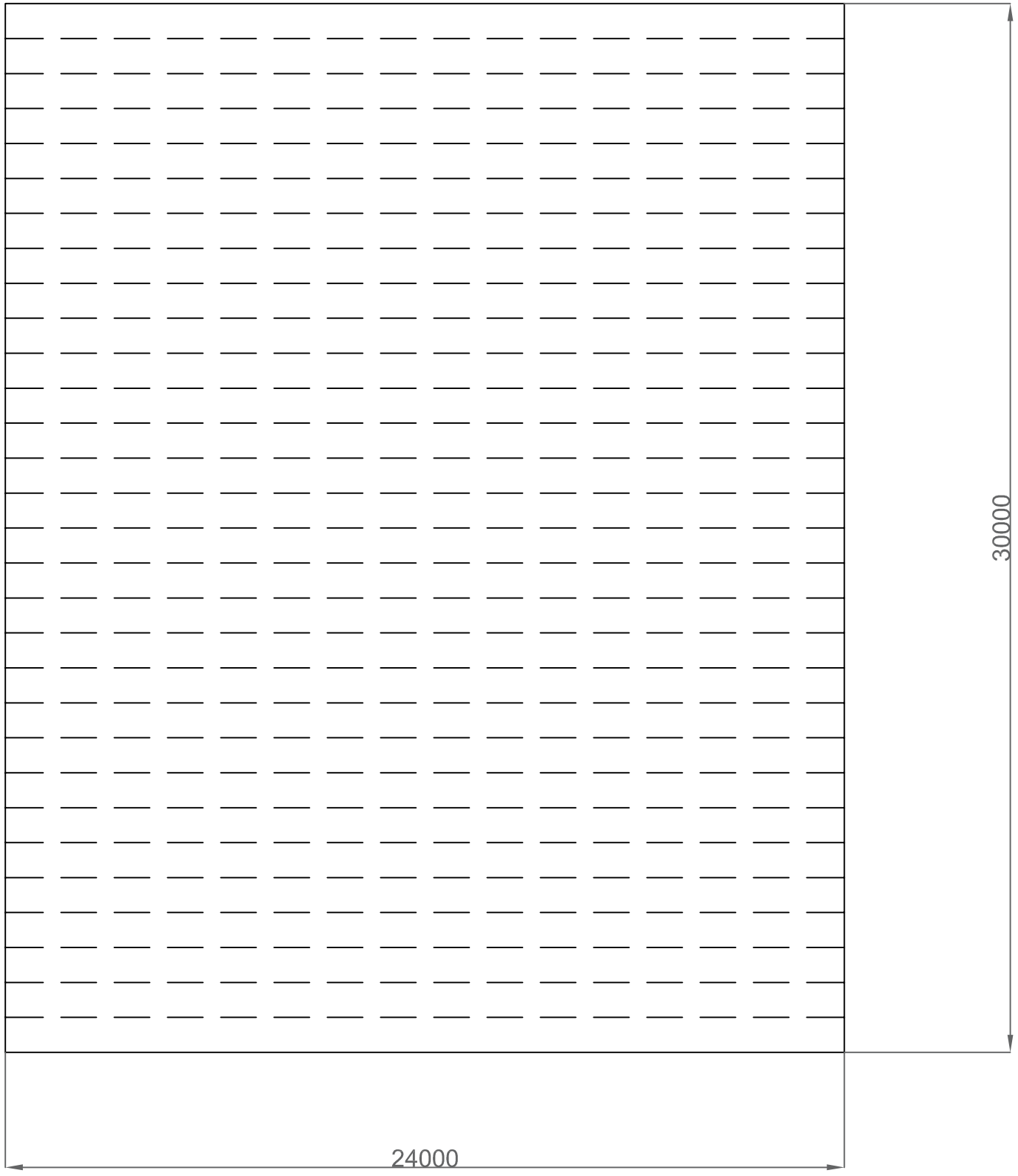

SIDE VIEW

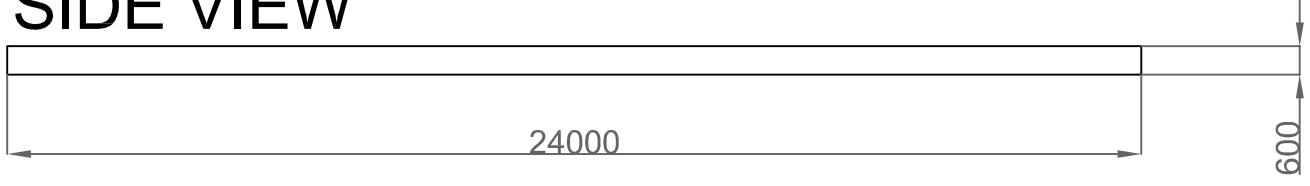

Scale			
Size A3	Unit mm		
Title: Global view of the new bridge (UHPC version)			
Date: 12/01/2015	TU Delft, Faculty of Civil Engineering and Geosciences		
Name: Antonio Paskvalin	Project: Master Thesis: Renovation Leiden Bridge		
drawing nr.			

Mid section

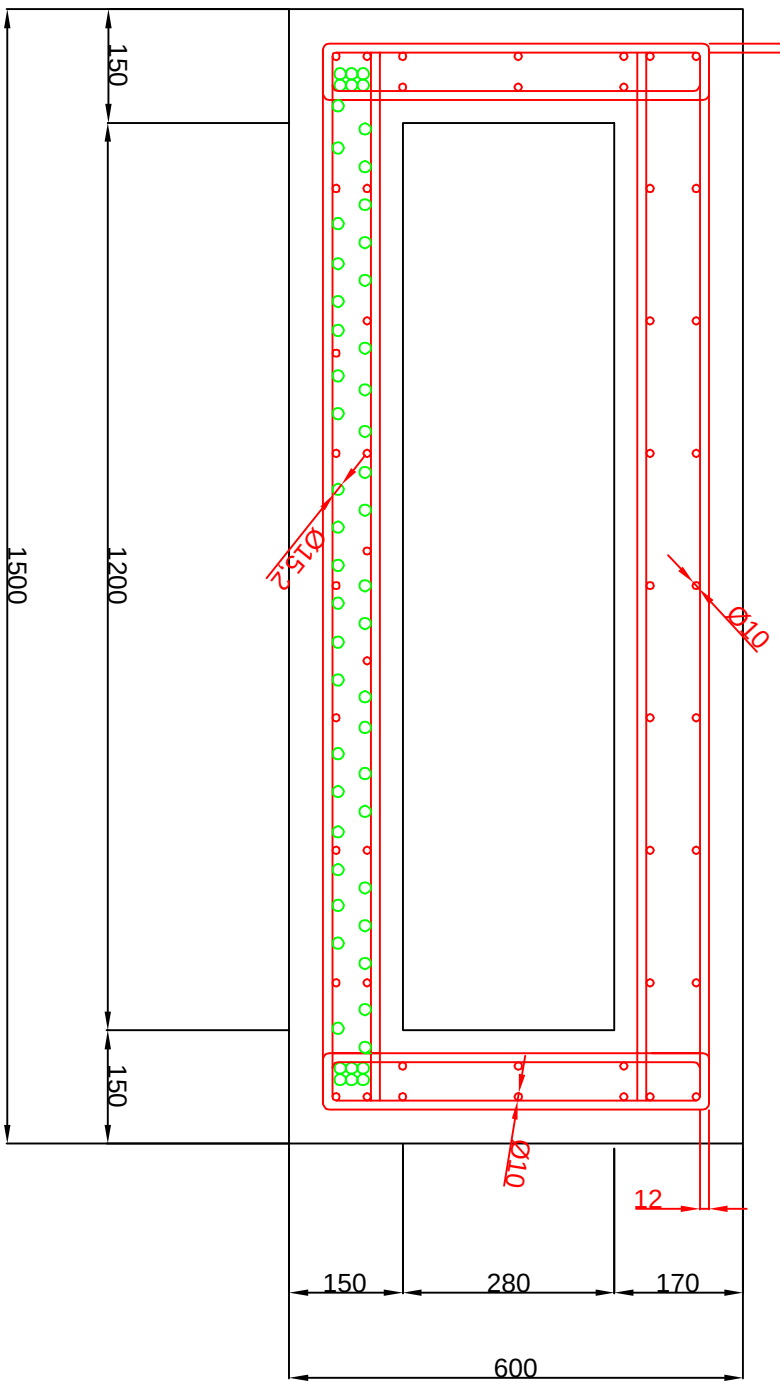

End section

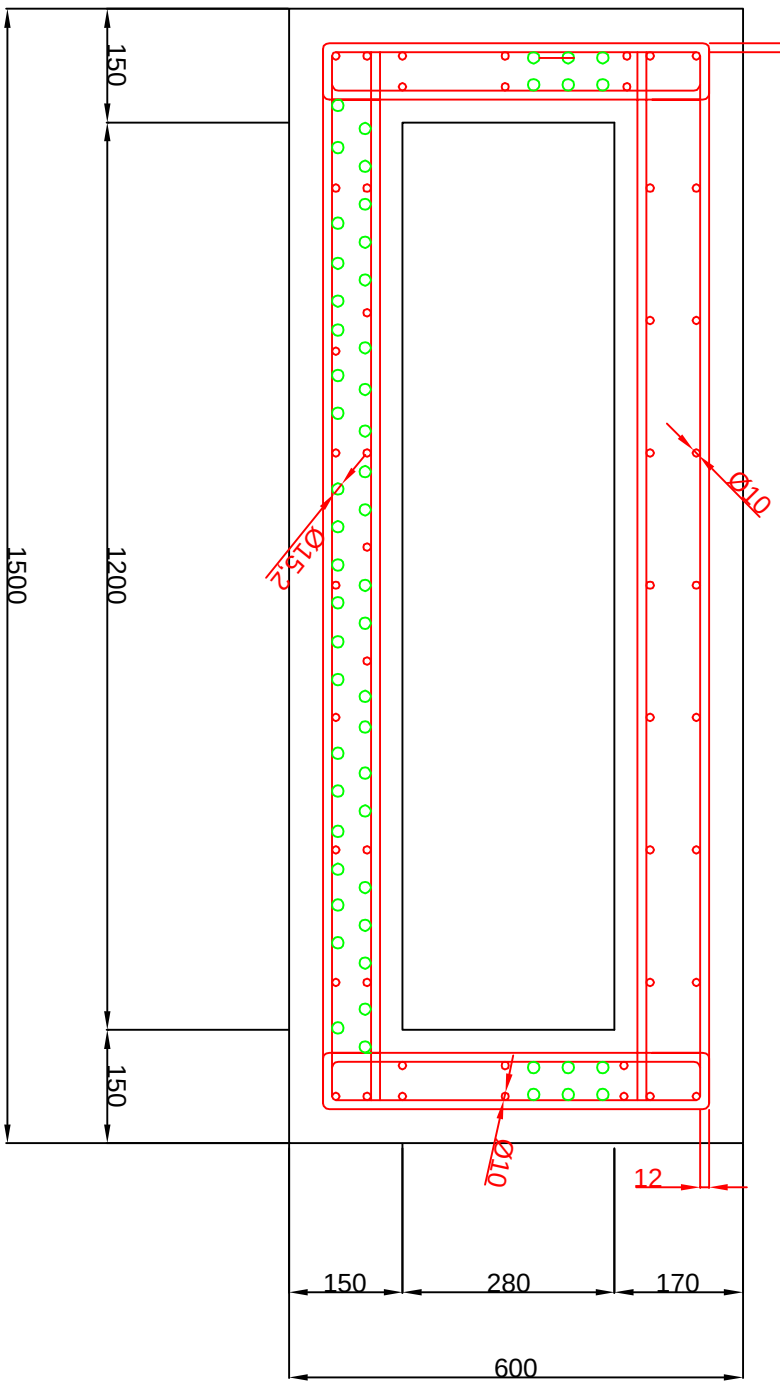

drawing nr.	Name	Date	Title	Size	Scale
	Antonio Paskvalin	12/01/2015	NSC Cross sections H=600mm	A3	1 : 10
	Project: Master Thesis: Renovation Leiden Bridge		TU Delft, Faculty of Civil Engineering and Geosciences	Unit: mm	

End section

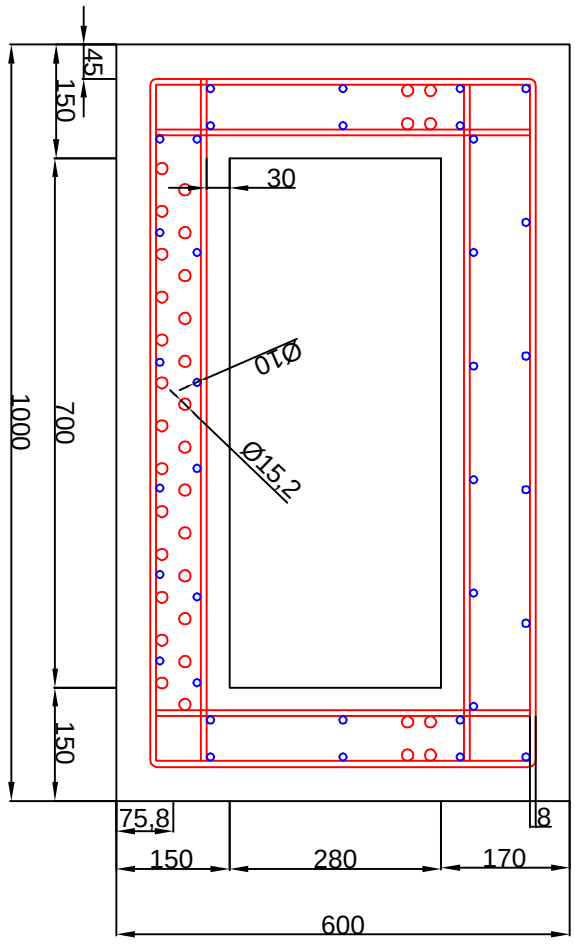

Mid section

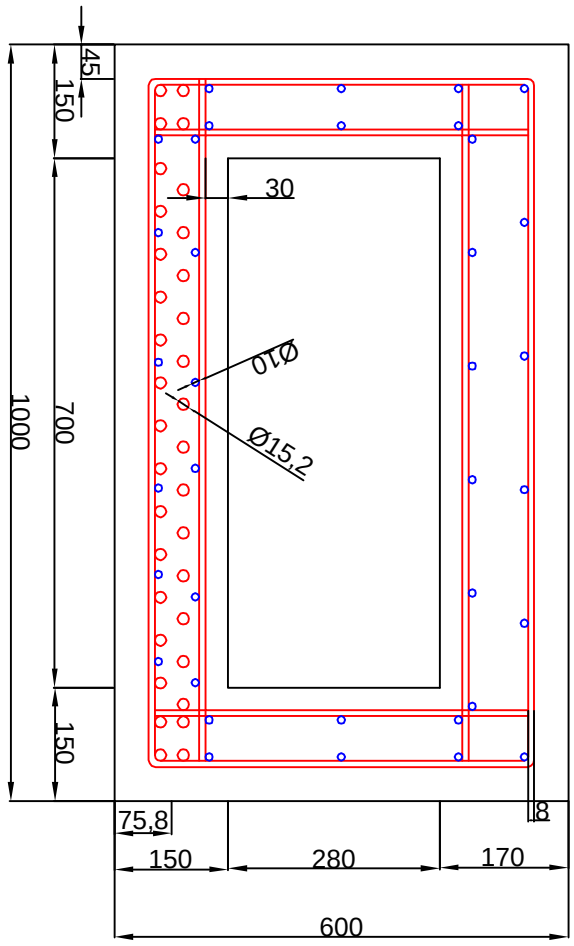

drawing nr.	Name	Date	Title	Size	Scale
	Antonio Paskvalin	12/01/2015	HPC Cross sections H=600mm	A3	1 ; 10
	Project: Master Thesis: Renovation Leiden Bridge		TU Delft, Faculty of Civil Engineering and Geosciences	Unit: mm	

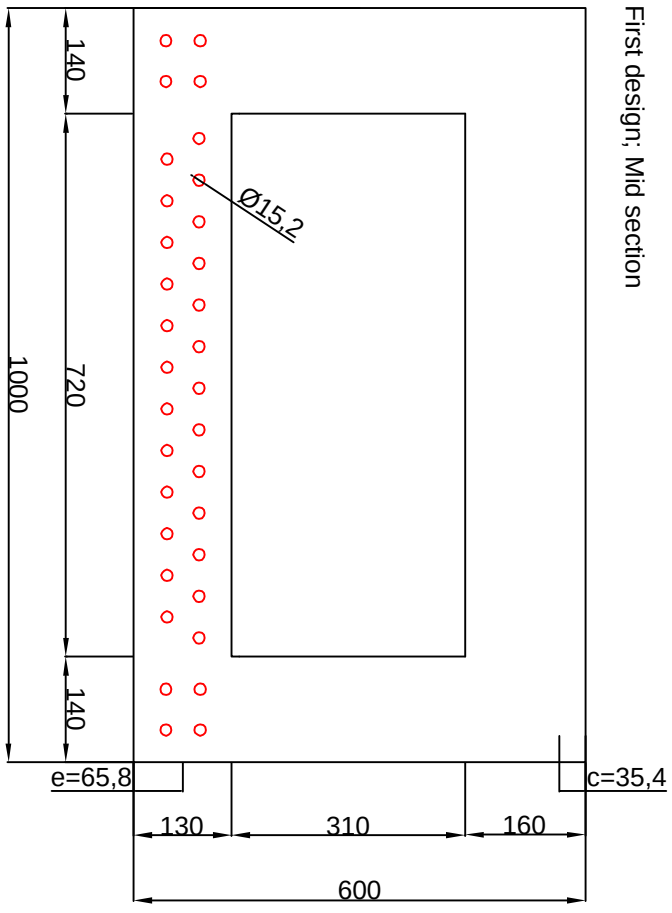

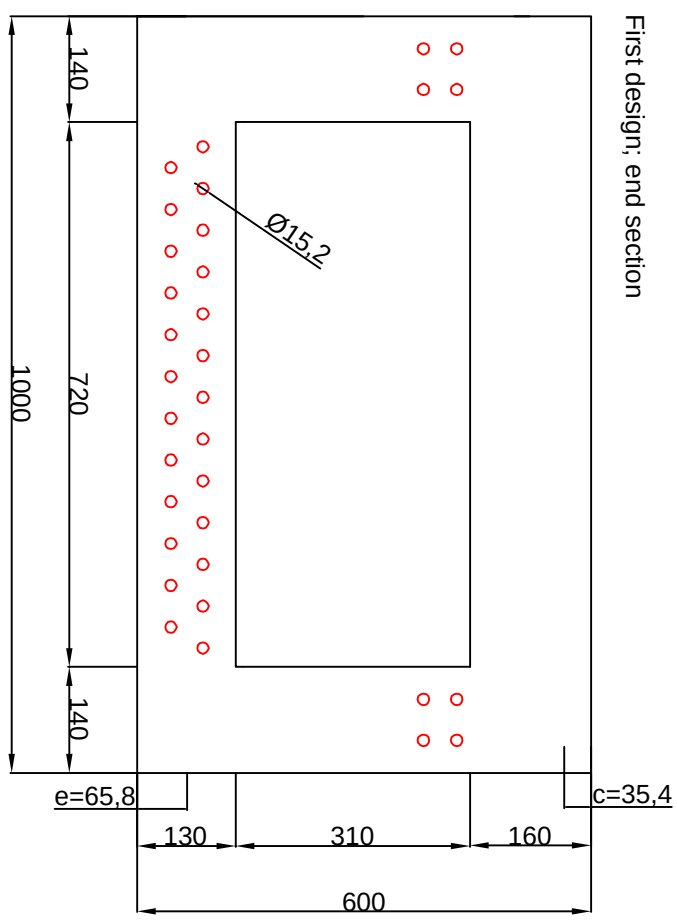

drawing nr.	Name	Date	Title	Size	Scale
	Antonio Paskvalin	12/01/2015	UHPC cross sections | initial design H=600mm	A3	1 ; 10
	Project: Master Thesis: Renovation Leiden Bridge		TU Delft, Faculty of Civil Engineering and Geosciences	Unit: mm	

1st optimized design; end section

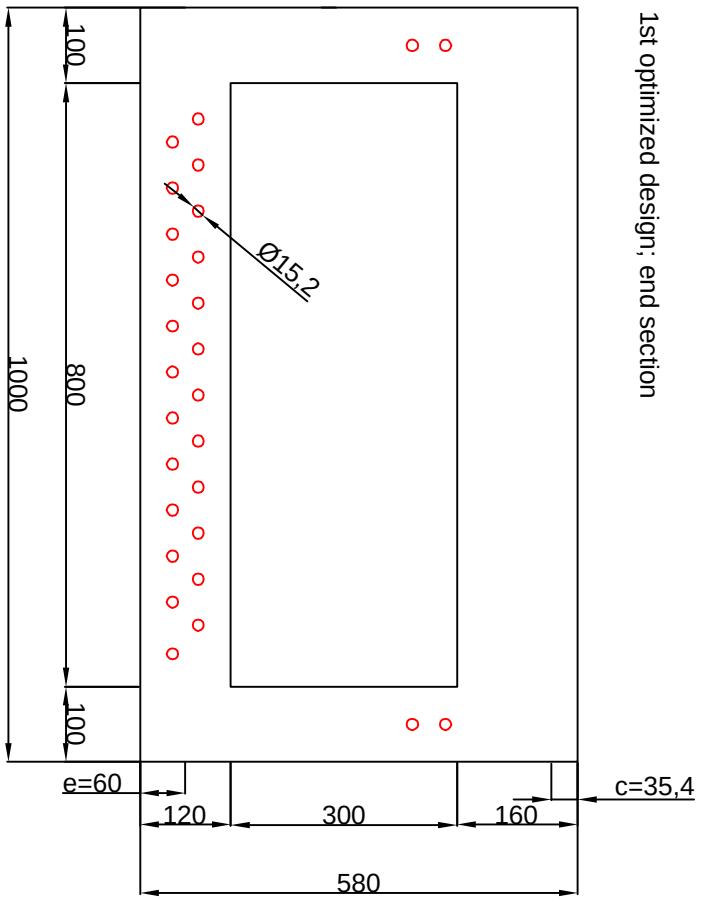

1st practical optimized design; end section

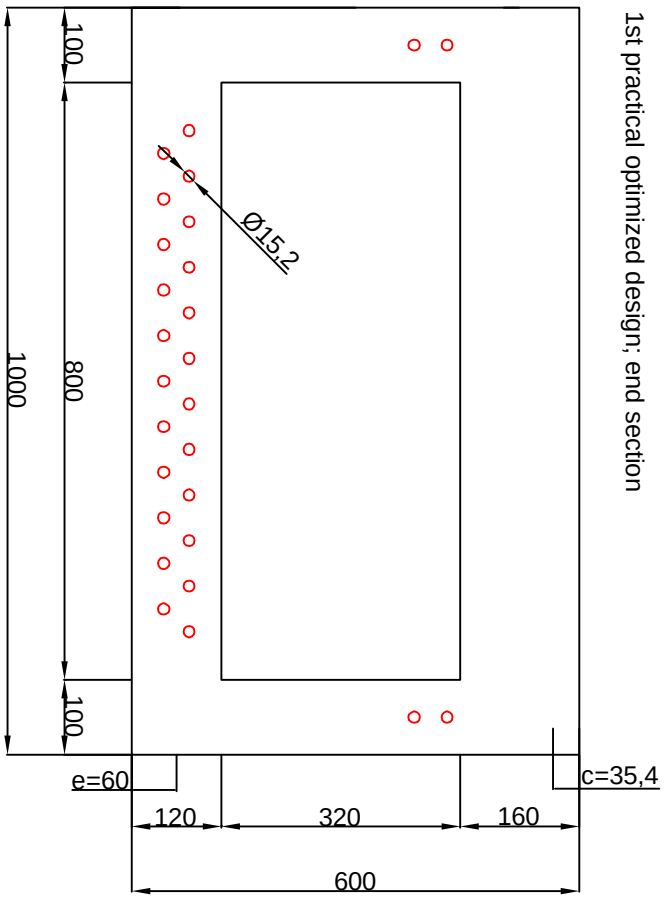

1st optimized design; Mid section

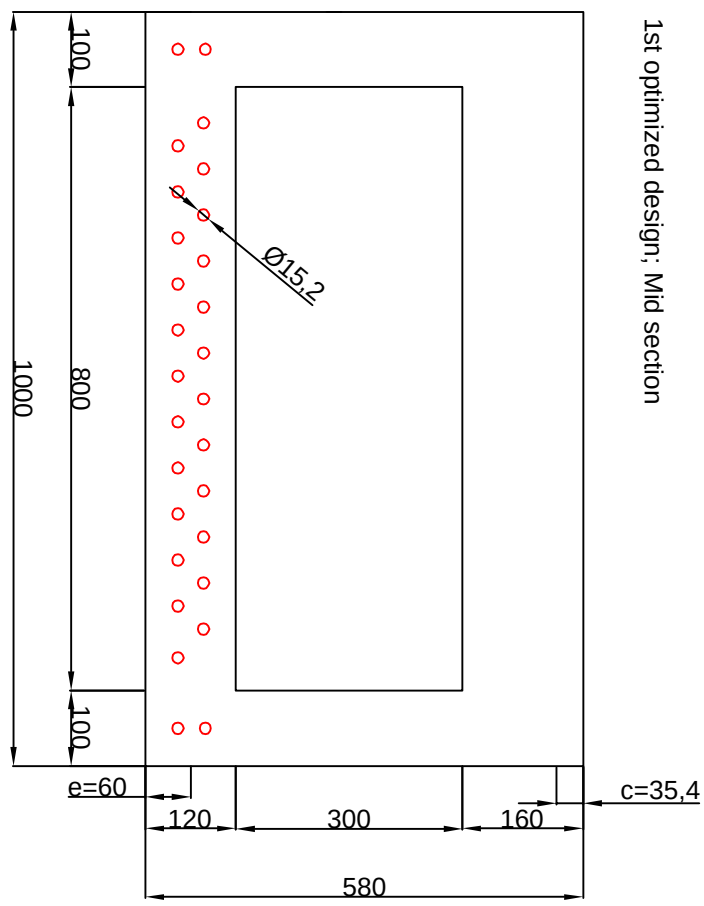

1st practical optimized design; Mid section

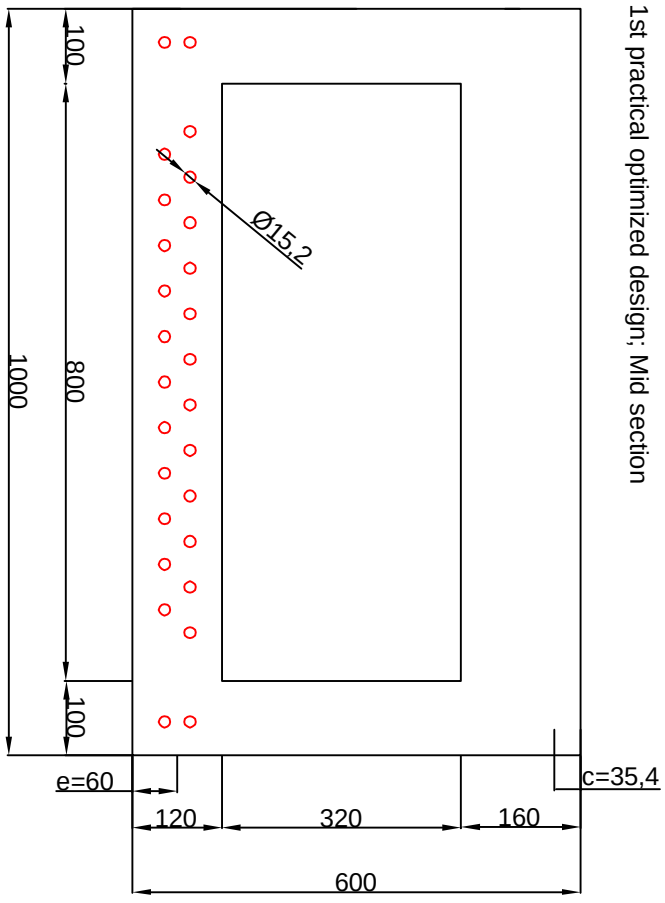

drawing nr.	Name	Date	Title	Size	Scale
	Antonio Paskvalin	12/01/2015	UHPC 1st optimized cross sections	A3	1 : 10
	Project: Master Thesis: Renovation Leiden Bridge		TU Delft, Faculty of Civil Engineering and Geosciences	Unit: mm	

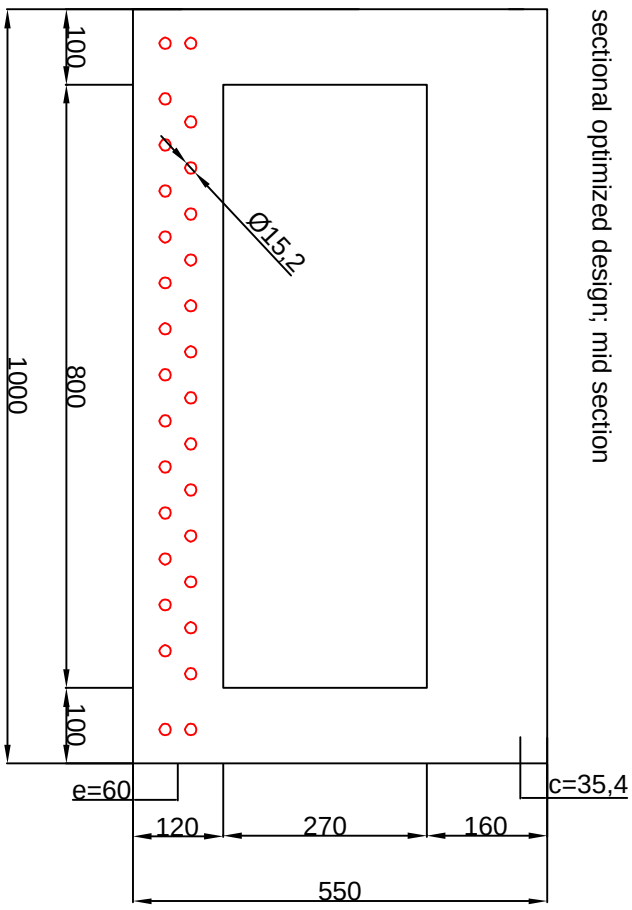

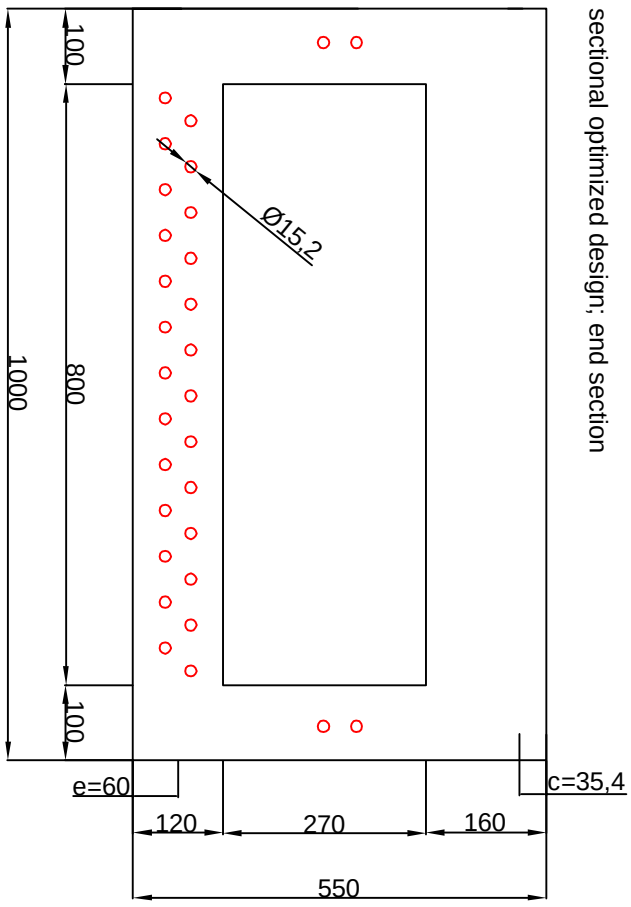

drawing nr.	Name	Date	Title	Size	Scale
	Antonio Paskvalin	12/01/2015	UHPC practical sectional optimized cross sections	A3	1 ; 10
	Project: Master Thesis: Renovation Leiden Bridge		TU Delft, Faculty of Civil Engineering and Geosciences	Unit: mm	